Empirical Validation of Building Simulation Software: Modelling of Double Facades
Final Report

Technical Report

IEA ECBCS Annex43/SHC Task 34
Validation of Building Energy Simulation Tools

Subtask E

O. Kalyanova
P. Heiselberg

SOLAR HEATING & COOLING PROGRAMME
INTERNATIONAL ENERGY AGENCY

AALBORG UNIVERSITY
Department of Civil Engineering

Aalborg University
Department of Civil Engineering
Indoor Environmental Engineering Research Group

DCE Technical Report No. 027

Empirical Validation of Building Simulation Software: Modelling of Double Facades Final Report

by

O. Kalyanova
P. Heiselberg

June 2009

Scientific Publications at the Department of Civil Engineering

Technical Reports are published for timely dissemination of research results and scientific work carried out at the Department of Civil Engineering (DCE) at Aalborg University. This medium allows publication of more detailed explanations and results than typically allowed in scientific journals.

Technical Memoranda are produced to enable the preliminary dissemination of scientific work by the personnel of the DCE where such release is deemed to be appropriate. Documents of this kind may be incomplete or temporary versions of papers—or part of continuing work. This should be kept in mind when references are given to publications of this kind.

Contract Reports are produced to report scientific work carried out under contract. Publications of this kind contain confidential matter and are reserved for the sponsors and the DCE. Therefore, Contract Reports are generally not available for public circulation.

Lecture Notes contain material produced by the lecturers at the DCE for educational purposes. This may be scientific notes, lecture books, example problems or manuals for laboratory work, or computer programs developed at the DCE.

Theses are monograms or collections of papers published to report the scientific work carried out at the DCE to obtain a degree as either PhD or Doctor of Technology. The thesis is publicly available after the defence of the degree.

Latest News is published to enable rapid communication of information about scientific work carried out at the DCE. This includes the status of research projects, developments in the laboratories, information about collaborative work and recent research results.

Acknowledgements

Preface

This report is a product of a joint effort between International Energy Agency Solar Heating and Cooling (IEA SHC) Task 34 and Energy Conservation in Buildings and Community Systems (ECBCS) Annex 43. Ron Judkoff of the National Renewable Energy Laboratory (NREL) was the Operating Agent for IEA 34/43 on behalf of the United States Department of Energy.

International Energy Agency

The International Energy Agency (IEA) was established in 1974 within the framework of the Organisation for Economic Co-operation and Development (OECD) to implement an international energy programme. A basic aim of the IEA is to foster co-operation among the twenty-four IEA participating countries and to increase energy security through energy conservation, development of alternative energy sources and energy research, development and demonstration (RD&D).

Solar Heating and Cooling Programme

The Solar Heating and Cooling Programme was one of the first IEA Implementing Agreements to be established. Since 1977, its members have been collaborating to advance active solar, passive solar and photovoltaic technologies and their application in buildings and other areas, such as agriculture and industry. Current members are:

Australia	Finland	Portugal
Austria	France	Spain
Belgium	Italy	Sweden
Canada	Mexico	Switzerland
Denmark	Netherlands	United States
European Commission	New Zealand	
Germany	Norway	

A total of 37 Tasks have been initiated, 26 of which have been completed. Each Task is managed by an Operating Agent from one of the participating countries. Overall control of the program rests with an Executive Committee comprised of one representative from each contracting party to the Implementing Agreement. In addition to the Task work, a number of special activities—Memorandum of Understanding with solar thermal trade organizations, statistics collection and analysis, conferences and workshops—have been undertaken.

The Tasks of the IEA Solar Heating and Cooling Programme, both underway and completed are as follows:

1. Current Tasks:

Task 27	*Performance of Solar Facade Components*
Task 29	*Solar Crop Drying*
Task 31	*Daylighting Buildings in the 21st Century*
Task 32	*Advanced Storage Concepts for Solar and Low Energy Buildings*
Task 33	*Solar Heat for Industrial Processes*
Task 34	*Testing and Validation of Building Energy Simulation Tools*
Task 35	*PV/Thermal Solar Systems*
Task 36	*Solar Resource Knowledge Management*
Task 37	*Advanced Housing Renovation with Solar & Conservation*

Completed Tasks:

Task 1	*Investigation of the Performance of Solar Heating and Cooling Systems*
Task 2	*Coordination of Solar Heating and Cooling R&D*
Task 3	*Performance Testing of Solar Collectors*
Task 4	*Development of an Insolation Handbook and Instrument Package*
Task 5	*Use of Existing Meteorological Information for Solar Energy Application*
Task 6	*Performance of Solar Systems Using Evacuated Collectors*
Task 7	*Central Solar Heating Plants with Seasonal Storage*

Task 8	*Passive and Hybrid Solar Low Energy Buildings*
Task 9	*Solar Radiation and Pyranometry Studies*
Task 10	*Solar Materials R&D*
Task 11	*Passive and Hybrid Solar Commercial Buildings*
Task 12	*Building Energy Analysis and Design Tools for Solar Applications*
Task 13	*Advance Solar Low Energy Buildings*
Task 14	*Advance Active Solar Energy Systems*
Task 16	*Photovoltaics in Buildings*
Task 17	*Measuring and Modeling Spectral Radiation*
Task 18	*Advanced Glazing and Associated Materials for Solar and Building Applications*
Task 19	*Solar Air Systems*
Task 20	*Solar Energy in Building Renovation*
Task 21	*Daylight in Buildings*
Task 22	*Building Energy Analysis Tools*
Task 23	*Optimization of Solar Energy Use in Large Buildings*
Task 24	*Solar Procurement*
Task 25	*Solar Assisted Air Conditioning of Buildings*
Task 26	*Solar Combisystems*
Task 28	*olar Sustainable Housing*

Completed Working Groups:
CSHPSS, ISOLDE, Materials in Solar Thermal Collectors, and the Evaluation of Task 13 Houses

To find more IEA Solar Heating and Cooling Programme publications or learn about the Programme visit our Internet site at **www.iea-shc.org** or contact the SHC Executive Secretary, Pamela Murphy, e-mail: pmurphy@MorseAssociatesInc.com.

Energy Conservation in Buildings and Community Systems

The IEA sponsors research and development in a number of areas related to energy. The mission of one of those areas, the ECBCS - Energy Conservation for Building and Community Systems Programme, is to facilitate and accelerate the introduction of energy conservation, and environmentally sustainable technologies into healthy buildings and community systems, through innovation and research in decision-making, building assemblies and systems, and commercialisation. The objectives of collaborative work within the ECBCS R&D program are directly derived from the on-going energy and environmental challenges facing IEA countries in the area of construction, energy market and research. ECBCS addresses major challenges and takes advantage of opportunities in the following areas:

- exploitation of innovation and information technology;
- impact of energy measures on indoor health and usability;
- integration of building energy measures and tools to changes in lifestyles, work environment alternatives, and business environment.

The Executive Committee
Overall control of the program is maintained by an Executive Committee, which not only monitors existing projects but also identifies new areas where collaborative effort may be beneficial. To date the following projects have been initiated by the executive committee on Energy Conservation in Buildings and Community Systems (completed projects are identified by (*)):

Annex 1:	Load Energy Determination of Buildings (*)
Annex 2:	Ekistics and Advanced Community Energy Systems (*)
Annex 3:	Energy Conservation in Residential Buildings (*)
Annex 4:	Glasgow Commercial Building Monitoring (*)
Annex 5:	Air Infiltration and Ventilation Centre
Annex 6:	Energy Systems and Design of Communities (*)
Annex 7:	Local Government Energy Planning (*)
Annex 8:	Inhabitants Behaviour with Regard to Ventilation (*)
Annex 9:	Minimum Ventilation Rates (*)
Annex 10:	Building HVAC System Simulation (*)

Participating countries in ECBCS:
Australia, Belgium, CEC, Canada, Czech Republic, Denmark, Finland, France, Germany, Greece, Israel, Italy, Japan, the Netherlands, New Zealand, Norway, Poland, Portugal, Sweden, Switzerland, Turkey, United Kingdom and the United States of America.

SHC Task 34 / ECBCS Annex 43: Testing and Validation of Building Energy Simulation Tools

Goal and Objectives

The goal of this Task/Annex is to undertake pre-normative research to develop a comprehensive and integrated suite of building energy analysis tool tests involving analytical, comparative, and empirical methods. These methods will provide for quality assurance of software, and some of the methods will be enacted by codes and standards bodies to certify software used for showing compliance to building energy standards. This goal will be pursued by accomplishing the following objectives:

- Create and make widely available a comprehensive and integrated suite of IEA Building Energy Simulation Test (BESTEST) cases for evaluating, diagnosing, and correcting building energy simulation software. Tests will address modeling of the building thermal fabric and building mechanical equipment systems in the context of innovative low energy buildings.
- Maintain and expand as appropriate analytical solutions for building energy analysis tool evaluation.
- Create and make widely available high quality empirical validation data sets, including detailed and unambiguous documentation of the input data required for validating software, for a selected number of representative design conditions.

Scope

This Task/Annex investigates the availability and accuracy of building energy analysis tools and engineering models to evaluate the performance of innovative low-energy buildings. Innovative low-energy buildings attempt to be highly energy efficient through use of advanced energy-efficiency technologies or a combination of energy efficiency and solar energy technologies. To be useful in a practical sense such tools must also be capable of modeling conventional buildings. The scope of the Task is limited to building energy simulation tools, including emerging modular type tools, and to widely used innovative low-energy design concepts. Activities will include development of analytical, comparative and empirical methods for evaluating, diagnosing, and correcting errors in building energy simulation software.

The audience for the results of the Task/Annex is building energy simulation tool developers, and codes and standards (normes) organizations that need methods for certifying software. However, tool users, such as architects, engineers, energy consultants, product manufacturers, and building owners and managers, are the ultimate beneficiaries of the research, and will be informed through targeted reports and articles.

Means

The objectives are to be achieved by the Participants in the following Projects.

Comparative and Analytical Verification Tests:
    Project A: Ground-Coupled Heat Transfer with respect to Floor Slab and Basement Constructions
    Project B: Multi-Zone Buildings and Air Flow
Empirical Validation and Comparative Tests:
    Project C: Shading/Daylighting/Load Interaction
    Project D: Mechanical Equipment and Controls
    Project E: Buildings with Double-Skin Facades
Other:
    Project G: Web Site for Consolidation of Tool Evaluation Tests

Participants

The participants in the task are Australia, Belgium, Canada, Czech Republic, Denmark, France, Germany, Japan, the Netherlands, Spain, Sweden, Switzerland, the United Kingdom, and the United States. The United States served as the Operating Agent for this Task, with Ron Judkoff of the National Renewable Energy Laboratory providing Operating Agent services on behalf of the U.S. Department of Energy.

This report documents work carried out under Project E: Buildings with Double-Skin Facades.

TABLE OF CONTENTS

EXECUTIVE SUMMARY

This report is an outcome of the empirical validation of building simulation software tools conducted within the Subtask E: Modelling of a Double Skin Façade of International Energy Agency (IEA), Annex 34, Task 43 by the Experts Group composed of experts from the Solar Heating and Cooling (SHC) Programme. The main objective of the Subtask E is for buildings with Double Skin Façade (DSF), to perform empirical validation and, in this way, to assess suitability and awareness of building energy analysis tools for predicting energy use, heat transfer, ventilation flow rates, solar protection effect and cavity air temperatures of double-skin façade.

The work carried out within the subtask is targeting a very narrow and specific topic in building simulation – the double-skin façade. This work, builds on already existing testing and validation studies. An extensive number of studies is already available and applied in practice. For more information about existing results of testing and validation work, please see references [1] and [2].

There are two different test cases defined in the empirical test case specification, these are: DSF100_e and DSF200_e. In the test case DSF100_e, all of the openings of the double-skin façade were closed (DSF functions in the transparent insulation mode). On the contrary, in the test case DSF200_e, the top and bottom openings of the DSF were open to the outside, thus the double-skin facade functioned in the external air curtain mode. The primary difference between these two cases is the mass exchange of the air between the cavity and outdoors in the test case DSF200_e caused by the natural driving forces, and no mass exchange in the cavity in the test case DSF100_e.

Results of the empirical exercises are compared between several building energy simulation programs and experiments. The following is the list of organisations which participated in the exercises and the simulation programs they used to perform the simulations.

Organisation		Program
VABI	VABI Software BV Delft The Netherlands	VA114
ESRU	Dept. of Mechanical Eng. University of Strathclyde Glasgow Scotland	ESP-r
TUD	Technical University of Dresden (TUD) Germany	TRNSYS-TUD
LTH	Division of Energy and Building Design Department of Architecture and Built Environment Lund Institute of Technology (LTH) Sweden	IDA
AAU	Dept. of Civil Engineering Aalborg University Denmark	BSim

Results of final IDA simulations are not included into this report, as due to circumstances, the experts didn't have a possibility to carry out the final iteration of simulations; however, a lot of work has been done by LTH experts during the iteration process of this subtask. In the report, some results from the earlier iterations include plots with IDA calculations.

Experimental data

The experiments were conducted in the full-scale outdoor test facility 'the Cube', located at the main campus of Aalborg University, Denmark. The test facility consists of two main thermal zones where the measurements were carried out: the double-skin façade cavity and the experiment room, being adjacent to the DSF cavity. The Double-Skin Façade, facing towards the South. The double skin façade had a height to depth ratio of approximately 10.

Duration of each experiment was approximately 2 weeks and started in the fall of 2006. Since the autumn/spring season represents the most complete spectrum of the DSF performance, the experiments were

carried out in autumn. Contrary to summer, climatic conditions in early autumn (or late spring) are more inconsistent, there are many periods with large cloud cover of the sky, while the solar radiation intensity with the clear sky can still be relatively strong, the temperature variation between day and night time is more considerable and, consequently, the day time periods may lead to significant solar heat gains, while the night time periods may lead to significant heat losses if the DSF performance has not been optimised.

The experiments were performed to collect information about the boundary conditions for the empirical validation and at the same time, the response of the whole building to these boundary conditions was measured in terms of energy use, mass flow rates, and surface and air temperatures. Existing experimental data sets have a benefit of rather varying solar radiation intensity, that allows to validate whether the models are able to cope with the frequent changes in solar radiation intensity.

Empirical validation and the results

Preliminary investigations

Prior to the empirical validation, a set of comparative test cases was defined, simulated, and analysed in the period of construction of the experimental test facility. Completion of the comparative test cases helped to point out the areas of modelling difficulties, the necessary empirical test cases for completing the subtask assignment and the important parameters to measure during the experiments.

Comparative exercises demonstrate some severe disagreements between the simulation tools when predicting the air flow rate in a naturally ventilated cavity, and thus demonstrate the necessity for the empirical exercises to complete the validation procedure. Only a limited number of comparative test cases were carried out, but these were sufficient to inform the experimental design and to appreciate the magnitude of differences between different simulation programs. As a result, the main emphasis of Subtask E was on the empirical tests to provide the reference against which modelling predictions could be compared.

Afterwards, the first empirical exercises were completed in the 'blind'-form, which means that the modellers received the experimental results only after submitting their results of simulations. All in all, there were three rounds of simulations in the empirical validation procedure. After the first round it became clear that the models had to be improved for better agreement with the actual conditions in the test facility during the measurements. Necessary improvements are explained below and were incorporated in the later rounds of simulations.

- The thermal bridge losses in the test facility were present in the test facility, but these were not included in the first round of simulations
- Fabric ducts placed on the floor of the test facility to generate a piston flow in the experiment room had not been considered when performed the first round of simulations.

Similar to the comparative test cases the first round of the empirical case studies has demonstrated a wide spread of results simulated with different tools, meanwhile, the diagnosis of reasons for disagreements between the experimental data and simulations were not easy, due to the complexity of the dynamic DSF-system and limitations in accuracy of the experimental data.

To diagnose the disagreements on a case by case basis, a set of additional test cases was defined and completed. These are:

- Steady state cases (SS)
- No solar case (NS)
- Surface film coefficient - sensitivity study test cases

Due to the additional case studies, the importance of assumptions made towards modelling of the longwave and convective heat transfer with the reference to the case DSF100_e was demonstrated. And, the overall summary of these studies show the directions for further improvements which are given below, but more studies are necessary if the guidelines for modelling of DSF are to be prepared.

- Combined treatment of surface film coefficients is too simple
- Application of fixed surface film coefficients together with the separate treatment is also insufficient, but more studies are needed to argue further on this issue.

Final results

First, an evaluation of the boundary conditions simulated by the different models was carried out. Sufficiently good agreement with the experimental data was achieved in computations of solar radiation striking the DSF surface for both of the test cases. Also, it was possible to demonstrate consistency in modelling the test cases and also to prove that the results of simulations are comparable with the experimental data.

Relatively small deviations were observed when calculating the transmitted solar radiation to the zones (first order of solar transmission). However, it was argued that the deviations are mainly caused by the minor differences in calculation of incident solar radiation, which became more pronounced in the transmitted solar radiation, due to the large window areas. This part of validation is comparative, as no empirical data are available to estimate the magnitude of transmitted solar radiation.

Performance of the models is evaluated, mainly using the global parameters, which are defined as:

- Air temperature and/or temperature raise in the DSF cavity compared to the outdoor air temperature
- Mass flow rate in the DSF cavity
- Cooling/heating power in the room adjacent to the DSF (zone 2) in order to maintain constant thermal conditions in that room as defined in the task specification

Because of the extremely high air change rates in the cavity in DSF200_e case, it is crucial for validation that the programs agree very well with the experiments when calculating the air temperature in the zone 1. For the high air change rates, the disagreements in the air temperature are unacceptable, as they may result in hundreds of watts of error in thermal balance.

The studies show that for the case DSF200_e, the models do not agree on the subject of air temperature in the zone 1. Even the models that perform best in terms of experimental results, still have an error of 1-5°C. Furthermore, the deviations from the experimental data in the periods with the peak solar radiation are much more significant. Only in the periods without solar radiation, a sufficient agreement is reached between the models and experiments. In the test case DSF100_e, which does not involve the mass transfer in the cavity, an approximation of the experimental data in the periods of peak solar loads is achieved for some models. Still, these models do not agree when other parameters like cooling/heating power, surface temperatures, etc. are compared.

Estimation of the mass flow rates is only relevant for the test case DSF200_e. Simulation and measurement of naturally induced flow rates are extremely difficult. Therefore, similarities in the shapes between the measurements and simulations for TRNSYS-TUD and ESP-r model show a great potential due to the fact that both of these programs take into the consideration the pressure difference coefficients for each opening. Still, the evaluation of the results against the empirical data is difficult, as there are two sets of the results available:

- Measured with the tracer gas method
- Measured with the velocity profile method

Estimation of the accuracy of these two methods is still the weak point in the validation procedure. The authors have pointed out all of the possible risks of error during the experiments and, for now, the final conclusion is left upon the reader.

The deviations between the measured and simulated cooling/heating power in the zone adjacent to the DSF (zone 2) have also became obvious when the results were compared. Most of the models underestimate the cooling power in the zone especially in the days with intensive solar irradiation, while at night the agreement is rather good. The difficulties with the simulation during the day time periods are the consequence of the greater deviations in predicted air temperature and magnitudes of the mass flow rates in the cavity.

The great deviation in the cooling/heating power to the zone is a result of interplay of many parameters, such as air flow rate, convection and radiation heat transfer, transmission of solar radiation etc. At the same time it is not possible to validate all of the inter-related parameters in this subtask, as many of those are the challenge for the whole field of building simulations. Therefore it is not easy to find a reason for the disagreements. However, the air flow rate is particularly interesting and influencing factor for the DSF performance, moreover, the air flow in the DSF is an unavoidable part of the whole DSF concept. Thus, the air flow rate was chosen as one of the main targets in the evaluation and validation of building simulation software for buildings with DSF. Therefore, the report includes a closer discussion of the mass flow models used in simulations.

C

At last, it is necessary to mention that this work concerns a very specific situation. However the empirical validation procedure should be used for software- and model- validation prior to simulation of any other DSF building. Repeating the steps of empirical validation procedure described in the report will allow other researchers to observe the performance of their model compared against already available results and experiments. This will allow users to allocate possible problems within the software or within the model. Model adjustments can be needed. The lessons learned within this subtask are described in the report and could serve a good background for the allocation of those problems.

Overview of the Subtask findings, conclusions and recommendations for future

Conclusions derived from the results of empirical validation exercise are summarised below.

- Good performance of the models in periods of lower solar intensity indicates that the thermal building simulation tools perform very well, but in the periods of higher solar intensity, more detailed calculations or models should be applied, as the presence of solar radiation is an essential element for the double skin facade operation (only the period with the moderate solar intensity was modelled in the empirical test cases) and there is often poor agreement between measurements and predictions at high solar intensities, especially in the natural ventilation configuration of the double façade.

- The results of this empirical validation should be regarded as an argument for further empirical and comparative validation, as most of the results do not allow deriving any solid conclusions, but designate mainly the directions to follow in search for improvements.

- In the report it is demonstrated that the application of commonly used combined fixed surface film coefficient is not sufficient enough.

- Modellers should consider application of separated variable surface film coefficients in order to obtain more realistic predictions during the peak loads of solar radiation. Especially, this involves the radiation surface film coefficients and internal convective film coefficients, otherwise the air temperatures in the cavity and also the cooling power in the zone 2 will be drastically underestimated.

- Also, the application of variable coefficients may not solve all of the disagreements, as the sensitivity study does not include any clear results, but only gives an indication of importance of assumptions towards the surface heat transfer.

- The difficulties are also expected when the variable convective surface film coefficient has to be defined, as there are no experimental data available to define the convective heat transfer processes in the cavity, and the rule of thumb does not apply for the double-skin facade constructions. Then, no knowledge base exists to rely on when attempting to calculate or fix the surface film coefficients in a simulation model.

- The set of experimental data has sources of error and compared to laboratory conditions, has relatively large uncertainties, but on the other hand these experimental results represent the full-scale outdoor measurements with well controlled and documented internal conditions. Moreover, the experimental data set includes 2 weeks of monitoring of the mass flow rate in the DSF cavity, induced by the natural driving forces. And, it is worse to mention, that these measurements are unique by nature and therefore they represent an exceptional source of information both in terms of natural ventilation and DSF performance.

- The night time ventilation of the DSF is mainly driven by wind, therefore the correspondence of the experimental results with the simulations in the night time periods, tells about proper estimation of the pressure difference coefficients in the empirical specification.

- An agreement was observed between experimentally and analytically estimated mass flow rate in the cavity, in conditions of pure buoyancy using the experimentally estimated discharge coefficients. This provides some level of confidence in the discharge coefficients determined experimentally in a wind tunnel.

- Conduction of the experiments led to a better insight into the double-skin façade phenomena and the occurrences that take place in the cavity. These can have a significant impact on the heat and mass transfer through the DSF cavity. Such occurrences as the reverse flow, wind washout effect and the recirculation flow in the cavity are discussed in the report together with their consequences on the set of the experimental data and simulation results.

In the future work it would be necessary to expand the sensitivity study and perform a number of tests where the convective and radiative heat transfer coefficients are extensively tested for application in a double-skin facade model.

Experimental study of the convective heat transfer in the cavity would allow to prepare some guidelines when defining the convective surface film coefficients in the cavity.

All in all, none of the models appeared to be consistent enough when comparing results of simulations with the experimental data: for every parameter considered – a different model seems to come closer to the experimental data. Meanwhile, every model has to demonstrate consistency of predictions for all parameters to be validated. So to say, all of the parameters for one model should have certain agreement with the experimental data. Since none of the models could fulfil this requirement, the main outcome of this report is the discussion of reasons for the disagreements, which are not straight forward. The disagreements between the models and experiments allow to indicate a problem, while further research is needed to solve these problems.

Another, important subject in the DSF modelling is modelling of shading device in the cavity. The predictions made for the double skin facade in the empirical test cases DSF100_e and DSF200_e do not include the shading device. Despite that fact, the complexity of the processes in the DSF appeared to be strict enough to result in deficient accuracy of simulations. Shading device is a distinctive element of DSF application and, in addition, it is an important contributor to the double skin facade physics. Its contribution to the DSF physics is expressed by means of an additional heat source in the DSF cavity and therefore more complex longwave radiation exchange, increased air temperature in the cavity and thus the increased buoyancy effect, etc. In view of these facts, modelling can become even more intricate. Therefore it is desirable to continue with the empirical validation of building simulation software, including the solar shading devices, their properties and positioning in the cavity.

Next, the empirical validation exercise was limited to a specific geometry and height/depth aspect ratio of approximately 10 in the double façade cavity. No steps for validation of models with other dimensions of the cavity were carried out. The aspect ratio of the cavity is often vital for the flow regime, which defines the convective heat transfer processes and consequently, the air temperature and the temperature gradients in the cavity. And finally, the spectral and thermal properties of glazing in the test facility 'the Cube' were used in validation, nevertheless, these will be different for any other building. Surface temperatures of the inner panes are critical for the comfort conditions in the room adjacent to a DSF and also the temperatures of the surfaces facing cavity are vital for the development of the boundary layer and the flow regime in the cavity. Such limitations of this validation task must be carefully considered if the validated model shall be transformed to simulate a DSF of different geometry and properties.

Identified difficulties, disagreements and improvements of the software for simulation of DSF performance

VA114
- Modelling of internal window was too simple in the previous version of the software. This is improved now
- The assumptions in the air flow model were revised according to the literature study

BSim
- Calculation of view factors for the longwave radiation exchange included a bug, which was corrected
- Weather data for solar radiation in form of [Global solar irradiation + Diffuse solar irradiation] causes an error in the calculation routine. The error is not corrected yet, but the following combination can be used [Normal direct solar irradiation + Diffuse solar irradiation on a horizontal surface]
- All solar radiation striking at the internal surfaces in the BSim models is fully absorbed (not yet corrected)
- Air temperature in thermal zone is now included as an option for the set-point in the systems control menu (was not possible in the previous versions of software, the operative air temperature was used instead)
- The thermal window model is combined with the optical model, which calculates the amount of solar radiation absorbed in the glass. This model is argued to be too simple and needs further improvements for simulation of DSF performance (no steps were made towards the improvement).

ESP-r
- None

TRNSYS-TUD
- A bug in the reporting routine was found and corrected
- A bug in the solar distribution model was found. The solar distribution model accounts for the calculation of solar radiation absorbed, reflected and transmitted (internal window) at the surfaces.

How to read this report?

With this report, the authors aimed to allow the reader to read it, without the necessity to look through all of the working documents attached in appendix. Therefore, the report includes a short summary of the test cases defined in the empirical test case specification and also the main requirements set for the models.

One of the main topics in the report is the empirical validation of the building simulation software and, therefore, the validation of empirical data set must take place along with the validation of models and software. It is impossible to make an opinion about the results of empirical validation and about the empirical data without the necessary information. In order to make the reader familiar with the main issues in the measurement set-up, measurement site or experimental procedures, one can go through the section *3. Short overview of the experiments*, where the main procedures are explained. Also here, the reader can find an overview of the main results and related discussions.

In the section *4. The Double Skin Facade Theory and Modelling of the Empirical Test Cases*, one can find an overview of the main difficulties when modelling a naturally ventilated cavity. Among the other things, here a summary of the assumptions made in the models towards the surface heat transfer coefficients and modelling the natural air flow is included.

Some work, included into this report involves studies of the phenomena of naturally induced flow in the cavity. The attention must be paid to the fact that all operations with the natural flow are done on the basis of the mass flow rates, which include air temperature, atmospheric pressure and moisture content. Still in the text, one can often meet an expression of 'air flow rate', which is applied only as a general expression, commonly used for the natural flow phenomena.

Carried out diagnosis of the models, together with limited sensitivity studies are explained in the section *5.Additional Test Cases*. This section is only an addition to the main work and the main results are mentioned in the later sections.

Final results of simulations are to be found in the section *6. Results from the Empirical Test Cases.* Here, a lot of references have been made comparing the results between the models and also against the experimental results. The attention is paid to the facts when the results from one or another model overestimate or underestimate a parameter compared to the experimental data. It is very important to stress that the attention to these occurrences is paid by the authors only to show the magnitude of differences between the simulations and experiments.

1. INTRODUCTION

1.1 Foreword

The main objective of the Subtask E is for buildings with Double Skin Facades (DSF) to assess suitability and awareness of building energy analysis tools for predicting energy consumption, heat transfer, ventilation flow rates, cavity air and surface temperatures and solar protection effect and interaction with building services systems.

The starting point of this subtask was to develop a set of empirical test cases for the experimental validation of building simulation software tools. From the literature review [3], it is clear that an identification of a double skin facade with a typical performance is not easy, as every double skin facade building is almost unique. Thus, considering the empirical validation of the double skin facade modelling, a number of questions appeared:

- What is the DSF construction to choose for the empirical validation (positioning of openings, type of glazing, dimension of the DSF cavity, application of shading device, partitioning of the cavity etc.)
- What is the operational principle for the DSF to choose for the empirical validation (naturally/mechanically ventilated, flow direction and origin of air flow)

In order to answer some of the questions, first, a set of comparative test cases was defined, simulated and analysed in the period of construction of the experimental test facility. Completion of the comparative test cases helped to point out the areas of modelling difficulties, the necessary empirical test cases for completing the subtask assignment and the important parameters to measure during the empirical test cases. Moreover useful feedback was obtained from the participants with comments on the test case specification, measurements and the review of the comparative/experimental results. Finally, the close collaboration made the authors familiar with the tools and approaches used in the software tools participating in the subtask exercises.

Comparative exercises demonstrate some severe disagreements between the simulation tools when predicting the air flow rate in a naturally ventilated cavity, and thus demonstrate the necessity for the empirical exercises to complete the validation procedure. Only a limited number of comparative test cases were defined, but these were sufficient to inform the experimental design and to appreciate the magnitude of differences between different simulation programs. As a result, the main emphasis of Subtask E was on the empirical tests to provide the reference against which modelling predictions could be compared.

The set of empirical test cases includes a case with the naturally induced flow in the DSF cavity when the outer openings open to the outside (external air curtain mode) and a case with all windows closed (thermal insulation mode). The third empirical case with the mechanically driven flow in the cavity was prepared, but not included into the subtask activity.

1.2 Participants in the empirical validation

Results of the empirical exercise are compared between several building energy simulation programs and experiments. The following is the list of organizations, which participated in the exercises and the simulation programs they used to perform the simulations.

Organisation		Program
VABI	VABI Software BV Delft The Netherlands	VA114
ESRU	Dept. of Mechanical Eng. University of Strathclyde Glasgow Scotland	ESP-r
TUD	Technical University of Dresden (TUD) Germany	TRNSYS-TUD
LTH	Division of Energy and Building Design Department of Architecture and Built Environment Lund Institute of Technology (LTH) Sweden	IDA
AAU	Dept. of Civil Engineering Aalborg University Denmark	BSim

Table 1. Organisations that performed the simulations and the simulation programs used.

2. FACTS ABOUT THE EMPIRICAL TEST CASE SPECIFICATION

2.1 Empirical test case specification. General

The empirical test case specification (Appendix II) was prepared for the outdoor test facility at Aalborg University, the 'Cube'. The geometry and the definition of the constructions, their properties in the specification are given according to the actual geometry and properties in the 'Cube'. Major part of the output parameters requested in the specification has a reference value among the empirical data. In the empirical specification, such parameters as air tightness, optical properties of the constructions etc. are defined according to the results of additional sets of measurements (see in [5])

As a result of discussion and evaluation of the results after each round of modelling, the empirical test case specification was changed a number of times by including additional output parameters, information, clarification and improvements to the defined test cases.

2.2 Test cases in the empirical test case specification

Case DSF100_e. All the openings are closed. There is no exchange of the zone air with the external or internal environment. The zone air temperature results from the conduction, convection and radiation heat exchange. The movement of the air in the DSF appears due to convective flows in the DSF. The test case is focused on assessment of the resulting cavity temperature in DSF and solar radiation transmitted through the DSF into adjacent zone.

Case DSF200_e. Openings are open to the outside. The DSF function is to remove the surplus solar heat gains by means of natural cooling. Temperature conditions and air flow conditions in the DSF should be examined together with the magnitude of natural driving forces.
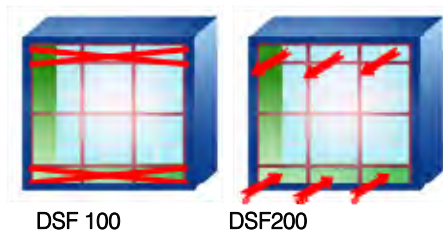
DSF 100   DSF200
Figure 1. Empirical test cases.

Test case	Solar shading	Driving force			Boundary conditions		Control of opening
		Buoyancy	Wind	Mechanical	Internal	External	
DSF100_e	No	-	-	-	constant	variable	-
DSF200_e	No	YES	YES	-	constant	variable	-

Table 2. Empirical test cases.

6

2.3　　　　Weather data

The weather data are provided for 1 hour time intervals and 10 minutes time intervals. Parameters given in the weather data files are as follows:

- External air temperature, $^{\circ}$C
- Global solar irradiation on horizontal surface, W/m^2
- Diffuse solar irradiation on horizontal surface W/m^2
- Wind direction, deg
- Wind speed, m/s, measured at 10 m above the ground
- Air relative humidity, %
- Atmospheric pressure, Pa

Period of the climate data is provided as following:

DSF100_e　　　　　　　　19.10.2006 - 06.11.2006 (both days are included)
DSF200_e　　　　　　　　01.10.2006 – 15.10.2006 (both days are included)

Besides the climate data, the ground temperature below the foundation in the experiment room is given as a boundary condition, together with the air temperature in neighbouring zones (instrument room and engine room).

2.4　　　　Test case objective

From the complexity point of view, the test case DSF100_e is twofold. In truth, the convective flows in the DSF cavity with the all openings closed can become very complex and very difficult to model. However, the building simulation tools are not always able to model the intricate convective flows. On many occasions, the convective models are simplified and then the test case becomes relatively easy to model. An application of the advanced convection modelling for this case may involve coupling of building simulation tool with CFD or involve superior models for evaluation of flow regime and convective heat transfer coefficients and, in that case, the modelling becomes more complex and time consuming.

Regarding the results of the comparative validation exercises [6], the differences between the air temperature in the DSF cavity calculated by different building simulation tools appeared to be significant: in the range of 10-15°C in the comparative test case corresponding to empirical case DSF100_e and 2-4°C for the comparative test case which corresponds to the empirical case DSF200_e. Also for the cooling power in the zone 2 the magnitude of differences is between the models is in the range of 1-2kW in the periods with the strong solar radiation. It is obvious, that there are different parameters that can cause these large deviations between the models. The convective heat transfer is one of the parameters that is likely to be significant, but, at the same time, it is not the task to perform the direct validation of the convective heat transfer, while the indirect validation is performed via global parameters, such as the air temperature, cooling/heating power, etc.

Availability of the experimental data for this and other test cases simplifies the level of assumption when assessing the model or its components such as flow element, convective heat transfer etc.

Looking upon the comparative test case DSF200_4, which corresponds to the empirical test case DSF200_e, the comparative results have demonstrated a great degree of deviations between the programs also when calculating the mass flow rate and the air temperature in the DSF cavity. As a result, the differences in predictions of cooling power in the experiment room appear reasonable. The fact that these are the test cases, which involve the phenomena of the natural air flow does not allow any further conclusions, as the naturally induced air flow has a complex nature and no model is experimentally validated for the application with the DSF. Therefore, the empirical test cases had to include the extensive measurements of the mass flow rate in the DSF cavity in order to be able to rely on the results of the empirical validation in the corresponding empirical test case DSF200_e. Finally, the objective of the empirical validation is to complete the validation procedure of the building simulation software for modelling buildings with DSF upon the experimental reference values.

2.5   Definition of zones

There are two main zones defined in the empirical test cases. Experts were asked to model a double skin facade as a separate zone – zone 1. The zone adjacent to the double skin facade is defined as zone 2, the experiment room. The heating and cooling system in zone 2 keeps the air temperature in the zone constant at apx. 22°C. The ability of building simulation tools to simulate the necessary energy use in zone 2, and the air temperature and mass flow in zone 1 are the main quantitative measures of the building simulation tool performance and its validation.
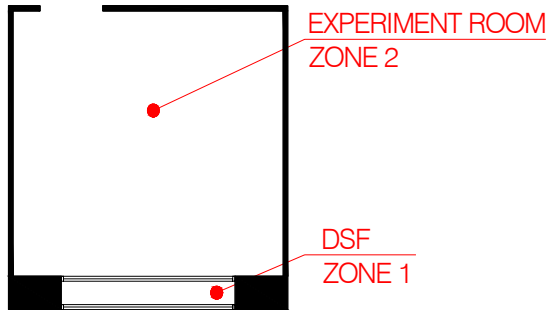
Figure 2. Definition of zones in the empirical test case specification.

2.6   Modelling requirements

Various building simulation software include different approaches and applications for modelling of the physical processes involved. Initially, it was desired that all case-models involve the same applications for the same parameters in every model and use the most detailed level of modelling allowed by simulation program being tested.

Cases specified for the modelling involve interaction of various processes; thus modelling may require different combinations of software applications and their options. For this reason, the building and its systems were specified in detail, but the way in which they were modelled was not prescribed. The design of the model had to be completed depending on the capability of the simulating software and the user's decision, but as close as possible to the specification.

In addition, it was requested that participants perform consistent modelling of the test cases. Modellers were asked to include in the modelling report, detailed documentation of any discrepancy between the test case specification and the model.

Finally, the participants were asked to perform a consistent modelling of the empirical test case in relation to the comparative once.

2.7   Output parameters

The output parameters are defined in the specification. The following are the output parameters shared for all test cases:

N	Output	Unit	Description
1	Direct solar irradiation on the window surface	W/m^2	Mean hourly value
2	Diffuse solar irradiation on the window surface	W/m^2	Mean hourly value
3	Total solar irradiation on the window surface	W/m^2	Mean hourly value
4	Total solar radiation received on the external window glass surface	kW	Mean hourly value
5	Solar radiation transmitted from the outside into zone1	kW	Mean hourly value
6	Solar radiation transmitted from zone 1 into zone2 (first order of solar transmission)	kW	Mean hourly value
7	Power used for cooling/heating in the zone 2	kW	Mean hourly value (with the '+'sign for heating and '-'sign for cooling)
8	Hour averaged surface temperature of external window surface facing external	ºC	Mean hourly value
9	Hour averaged surface temperature of external window surface facing zone1	ºC	Mean hourly value
10	Hour averaged surface temperature of internal window surface facing zone1,	ºC	Mean hourly value
11	Hour averaged surface temperature of internal window surface facing zone2	ºC	Mean hourly value
12	Hour averaged floor surface temperature in the zone 1	ºC	Mean hourly value
13	Hour averaged ceiling surface temperature in the zone 1	ºC	Mean hourly value
14	Hour averaged floor surface temperature in the zone 2	ºC	Mean hourly value
15	Hour averaged ceiling surface temperature in the zone 2	ºC	Mean hourly value
16	Hour averaged air temperature in the zone 1	ºC	Mean hourly value

Table 3. Output parameters shared for the all test cases.

In the test cases DSF100_e, the solar altitude in the middle of hour is included as a separate output parameter, in order to control calculation of solar radiation distribution in the models.
In the test case DSF200_e, the air flow rate is included as a separate output parameter.

3.   SHORT OVERVIEW OF THE EXPERIMENTS

3.1   Experimental test facility

'The Cube' is an outdoor test facility located at the main campus of Aalborg University. It has been built in the fall of 2005 with the purpose of detailed investigations of the DSF performance, development of the empirical test cases for validation and further improvements of various building simulation software for the modelling of buildings with double skin facades in the frame of IEA ECBCS ANNEX 43/SHC Task 34, Subtask E- Double Skin Facade.

The test facility is designed to be flexible for a choice of the DSF operational modes, natural or mechanical flow conditions, different types of shading devices etc. Moreover, the superior control of the thermal conditions in the room adjacent to the DSF and the opening control allow to investigate the DSF both as a part of a complete ventilation system and as a separate element of building construction.

The accuracy of these measurements is justified by the quality of the facility construction: 'the Cube' is very well insulated and tight. 'The Cube' consists of four domains, which are named as: Double Skin Facade, Experiment room, Instrument room and Engine room.
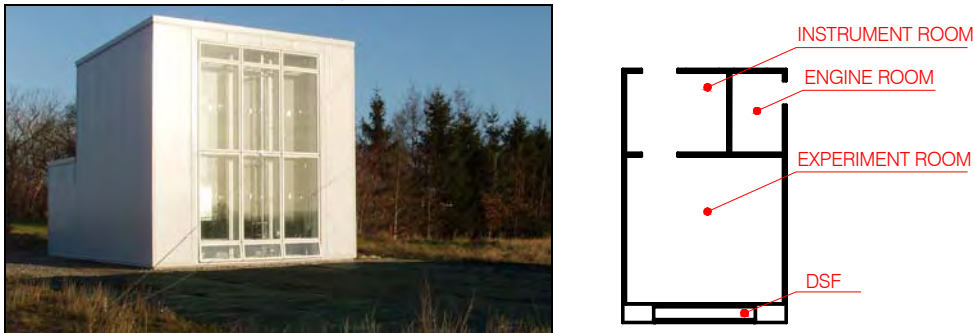
Figure 3. 'The Cube' (left). Rooms in 'the Cube' (right).

All openings of the double skin facade are controlled and can be operated separately. The combination of open openings defines the operative strategy of the DSF. Depending on the mode of DSF performance, it can function as a barrier for the solar heat gains, as an additional insulation, can preheat the air coming into the occupied zone, etc. In any of the above cases, the DSF affects the thermal conditions in the experiment room.

The temperature in the experiment room can be kept constant, as there is a cooling unit installed in the engine room and a ventilation system with the heating and cooling unit installed in the experiment room, Figure 4. In order to avoid temperature gradients in the experiment room, a recirculating piston flow with an air speed of approximately 0.2 m/s is used. This resulted in typical temperature gradient of approximately 0.02°C per meter height and maximum of 0.1°C per meter height. The air intake for recirculation is at the top of the room, after the intake the air passes through the preconditioning units of the ventilation system and then it is exhausted at the bottom of the room through the fabric ke-low impulse ducts. It is necessary to mention that the ducts affect the absorption of solar radiation on the floor surface. Also the temperature of the supply air in the ducts was different from the average air temperature in the zone. Therefore, the storage ability of the concrete floor was also affected by cooler or warmer air supplied through the ducts. Maximum power on cooling and heating unit is 10 kW and 2 kW, respectively.

Figure 4. KE-low impulse fabric ducts in the experiment room (left, centre), Ventilation system in the experiment room (right).

Knowledge of solar radiation is crucial for the task of these experiments. However, in non-laboratory conditions, the ground reflected solar radiation depends on the surrounding of the test facility and therefore, it can vary to a great extent. For this reason, a large carpet was fixed on the ground from the side of the southern facade of 'the Cube' to achieve uniform reflection from the ground. The size of the carpet ensured a view factor between the DSF and the ground of approximately 0.5. Achieving of a reasonably higher view factor would require to double-up the carpet size.

The fabric of the carpet was chosen so that it does not change reflectance property when it is wet due to its permeability and had reflectance property of apx. 0.1, close to the generally assumed reflectance property of the ground. The carpet is also seen in Figure 3.

Absorption, reflection and transmission properties of all the surfaces in the DSF, experiment room and windows were tested at the EMPA Materials Science & Technology Laboratory. This was also the case for the ground carpet. The information about the spectral properties of the surfaces is available as a function of the wavelength, in the wave length interval 250-2500nm.

3.2 Preliminary tests

A number of preliminary experiments were completed before the final experimental set-up. Preliminary experiments were focused on improvements and "calibration" of the test facility, improvements of measurement techniques and on best suitable positioning of equipment.

The air tightness of 'the Cube' was measured during construction, insulation and air tightening of the test facility, before and after installation of the experimental setup to ensure tightness. The final infiltration rate was 0.3 h^{-1} at 100 Pa. Transmission heat losses were estimated for two set points, when the difference between the air temperature in the test room and outdoors was 16°C and 21°C resulting in a heatloss of apx. 0.26 W/(m^{2}C). These tests have confirmed that 'the Cube' is extremely tight and well insulated.

3.3 Experimental data sets

3.3.1 Measurement conditions

Duration of each experiment was approximately 2 weeks and started in the fall of 2006. Since the autumn/spring season represents the most complete spectrum of the DSF performance, the experiments were carried out in autumn. Contrary to summer, climatic conditions in early autumn (or late spring) are more inconsistent, with frequent periods of large cloud cover of the sky, while the solar radiation intensity with the clear sky can still be relatively strong. The temperature variation between day and night time is more considerable and, consequently the day time periods may lead to significant solar heat gains, while the night time periods may lead to significant heat losses if the DSF performance has not been optimised.

The air temperature, air flow rate in the cavity and, correspondingly, the amount of surplus heat gains removed with the cavity air are the main measures of the double skin facade performance, and also it can be used as a measure for validation of a building simulation tool for modelling of a DSF performance. The air temperature in the experiment room of 'the Cube' was kept uniform and constant at approximately 22°C. to minimise the influence of the interior environment on DSF performance.

Both, the interior and exterior environment define the boundary conditions for the DSF, and the detailed knowledge of those was essential for further application of the experimental results and evaluation of the DSF performance.

The surplus solar gains into the experiment room were measured indirectly, by assessment of the total cooling power delivered to the experiment room in order to keep the air temperature constant. All of the equipment in the experiment room, which functioned as a heat source, was connected to the wattmeter to keep track of all loads and losses in the room.

3.3.2 Boundary conditions

3.3.2.1 Wind speed, wind direction and mean wind speed profile

The natural wind speed varies in time and space, the character of its variation is highly random and the wind flow is highly turbulent. At the same time, the wind speed is one of the main contributors to the natural ventilation flow.

The change of the mean wind velocity depending on height and intervening terrain is expressed through the mean wind speed profile. Once the mean wind speed profile is identified, based on a wide spectrum of wind velocities and wind directions with a substantial number of measurement points, then the wind profile turns to be one of the characteristics of the local environment.

Experimental data for the vertical wind speed profile covered a measurement period from 1st of June 2006 until 1st of January 2007. This period included various wind directions and wind speeds. Wind velocity and wind direction were measured in six points above the ground in order to build a vertical wind profile. Both 2D and 3D ultrasonic anemometers were placed on the mast in the centre line of the building, 12m away from its South facade (Figure 5). The sampling rate was 5 Hz.
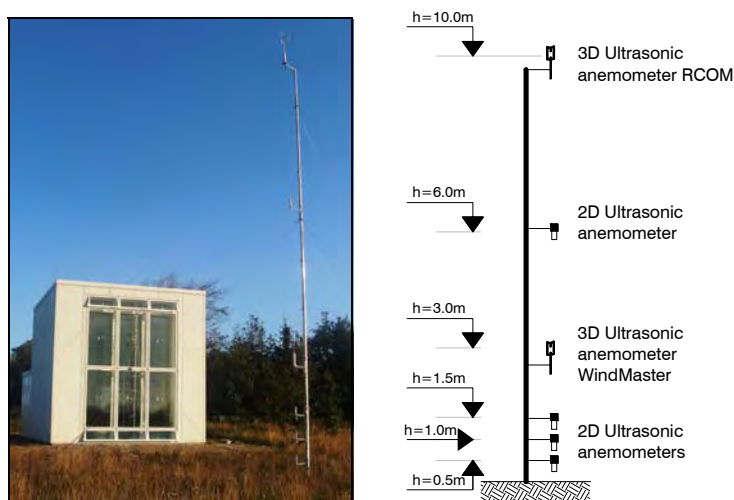
Figure 5. Wind mast in front of 'the Cube' (left). Positioning of equipment on the mast (right).

3.3.2.2 Outdoor air temperature, air humidity and solar radiation

Outdoor air temperature was measured using two thermocouples type K at the height of 2 m above ground. Air humidity of the outside air was measured continuously for completing the set of weather data parameters for building simulation tools. Outside air humidity was measured every 10 minutes.

For purpose of weather data assembling, two pyranometers were placed horizontally on the roof of 'the Cube'. BF3 pyranometer measures Global and Diffuse solar irradiation on the horizontal surface. Another pyranometer, Wilhelm Lambrecht, measures only Global solar irradiation on the horizontal surface and was placed on the roof for control of BF3-readings.

Primarily to the installation, all of the pyranometers were calibrated in reference with CM21, which was calibrated in sunsimulator and corrected by Kipp&Zonen B.V. The max errors appeared at the small angles of incidence, that meant that for most of the time the error was much less, see more in reference 5.

3.3.2.3 Air temperature and vertical temperature gradient in the DSF cavity

Direct solar radiation is an essential element for the facade operation, but it can heavily affect measurements of air temperature and may lead to errors of high magnitude using bare thermocouples. A number of tests were carried out preliminary to the experiments, where various techniques were investigated for their ability to shield thermocouples from direct irradiance, in order to achieve an accurate and reliable way to measure the air temperature reducing the error caused by radiation. As an outcome of these tests, all of the thermocouples placed free in the DSF cavity were protected: thermocouples were coated with silver, shielded from direct solar radiation by a silver-coated tube, which was continuously ventilated by a minifan, see Figure 6. The air

temperature in the DSF cavity was measured at six different heights in the centre line of the cavity. The measurements were carried out with the sampling frequency 5Hz and averaged for every 10 minutes.

The dimensionless air temperature was used to investigate the vertical temperature gradients in the DSF cavity, the definition of it is given in equation 1.

Figure 6. Experimental setup: testing of shielding techniques for air temperature measurements under direct solar access.

(●)	*all*	*- complete set of experimental data*
(o)	*$I_s>0$*	*- corresponds to the period with solar radiation*
(*)	*$I_s=0$*	*- corresponds to the period without solar radiation*
(▲)	*$I_s>I_{sm}$*	*- corresponds to the period with solar radiation higher than mean*
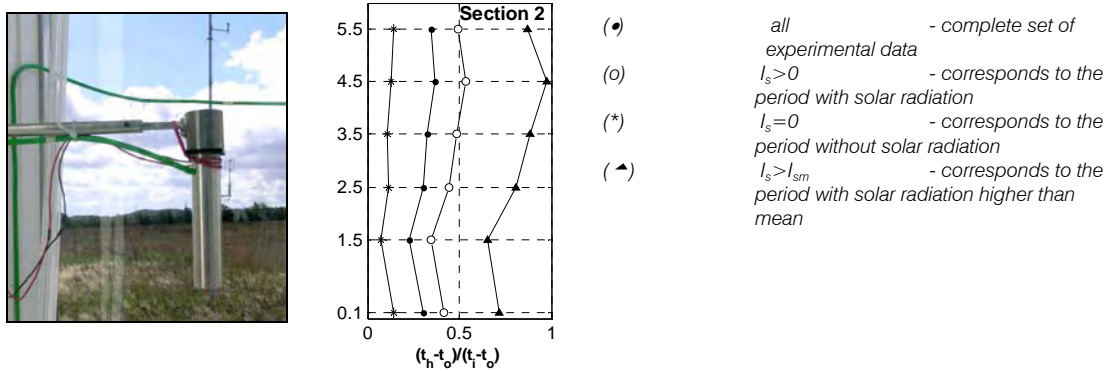
Figure 7. Silver coated ventilated tube for shielding a thermocouple from solar radiation (left). Dimensionless temperature gradient in the DSF cavity in the case DSF200_e (right).

Equation 3-1

$$t^h{}_{dim} = \frac{t_h - t_o}{t_i - t_o}$$

$t^h{}_{dim}$ - dimensionless air temperature in the DSF at the height h
t_h - temperature in the DSF cavity at the height h, °C
t_o - outdoor air temperature, °C
t_i - indoor air temperature (in the experiment room), °C

3.3.3 Surface temperature of the glazing

Measurement of glazing surface temperature was performed in the centre of a glazing pane for each large window section. The temperature was measured at: the internal surface of the inner window (ii), the external surface of the inner window (ei), and the internal surface of the outer windowpane (ie).

This measurement was conducted with sensors shaded from direct solar access. Continuous shading of the thermocouple sensor at the inner pane (ie) was ensured by a thin aluminium foil fixed around the sensor at the external surface. As a result, the foil shaded both a sensor at the external (ie) and internal (ii) surfaces. The thermocouple at the internal surface of the outer pane (ei) was shaded in a similar way by a piece of aluminium sticky tape on the external surface of the outer pain.

3.3.4 Mass flow rate in the DSF cavity

Assessment of the air change rate is crucial for the evaluation of indoor climate and the performance of a double skin facade. As a result, the air change rate repeatedly becomes a target for measurement, prediction and simulation. In the meantime, the air flow occurring in the naturally ventilated spaces is very intricate and extremely difficult to measure. The stochastic nature of wind and as a consequence non-uniform and dynamic flow conditions in combination with the assisting or opposing buoyancy force cause the main difficulties. There were three techniques used for the air flow measurements, but only two of them were successful. The third method (pressure difference method) was a failure as it's' accuracy was very sensitive to the location where the pressure difference is measured and also must be able to measure accurately in the range of 1-10 Pa. This method is rather young and there are no guidelines available for the procedure. In the experimental set-up the measurements of the pressure difference were not accurate enough.

Velocity profile method. This method requires a set of anemometers to measure a velocity profile in the opening, and then the shape of the determined velocity profile depends on the amount of anemometers installed. Instead of placing equipment directly in the opening in the case of the double skin facade, it can be placed in the DSF cavity, where the velocity profile can be measured in a few levels instead for one.

Accuracy of the velocity profile method depends on many factors (number of measurement points, positioning of equipment, and impact of boundary flow). Therefore, it is common to express it in accuracy of the measuring equipment. The hot sphere anemometers have been calibrated and had an accuracy of 0.01m/s.

Tracer gas method. This method requires the minimum amount of measurements and equipment, but it is characterised with frequent difficulties to obtain uniform concentration of the tracer gas, disturbances from the wind washout effects and finally with the time delay of signal caused by the time constant of gas analyzer. The constant injection method [15] was used in the experiments.

According to [17], the tracer gas theory assumes that the tracer gas concentration is constant throughout the measured zone. The expected error of tracer gas results is in the range of 5-10%, what greatly depends on the tracer gas mixing with the air in the DSF cavity.

Both of the measurement methods have sources of errors and comparing their outputs have some level of disagreement. However, the natural air flow phenomena is very complex and this results is the best approximation to the long time monitoring of natural air flow phenomena and can be used for experimental validation of numerical models of natural ventilation air flow.

Talking about the accuracy of these measurements, one can speak only of accuracy of equipment used for the measurement, as it is not possible to give estimation for the dataset accuracy for the whole measurement period. This is partly caused by the dynamics of the measured air flow, where the measurement accuracy will change along with the changes of boundary conditions. Another reason is simply the lack of information and experience for this kind of measurement in outdoor test facilities. Still, one can refer to the literature about the accuracy of the experimental method used.

Errors that may appear in the velocity profile method will also be discussed in the section 6.4.7 of this report.

3.3.5 Wind pressure, stack effect and their impact on a mass flow rate in the DSF cavity

The stack effect, known also as a buoyancy force, is the force that generates the flow motion between two or more zones with different air densities due to the differences in temperatures and/or moister content.

It is common to assume that the air flow in naturally ventilated cavities is buoyancy driven in summer, especially if a solar shading device is lowered in the cavity space. The solar radiation is then captured by the shading device, which emits the radiation in all directions and also releases it to the surrounding air by convection. Finally, the strength of the stack effect increases.

The kinetic energy of the wind changes into the potential energy (pressure) when meeting obstacles. The windward surfaces are submitted to positive and leeward surfaces to negative pressure. Natural ventilation by wind is the air exchange between zones, caused by wind-induced pressure differences on the building facades that propagate into the interior of the building. The distribution of the wind pressure on the building is described by the pressure difference coefficients C_p.

Figure 9, Figure 9, Figure 11 are given for an easy illustration of the different impact of the driving forces on the mass flow rate in the cavity. The wind force is expressed via the wind speed and the buoyancy force via the dimensionless air temperature in the cavity. Furthermore, the results of the mass flow rate for the night time period ($I_s=0$) and the period with the relatively strong solar radiation ($I_s>I_{sm}$) are split.

The dimensionless air temperature was used for the investigations, defined in the equation:
Equation 3-2

$$t_{dim} = \frac{t - t_o}{t_i - t_o}$$

t_{dim}	- dimensionless air temperature in DSF
t	- volume averaged air temperature in DSF, ^oC
t_o	- outdoor air temperature, ^oC
t_i	- indoor air temperature (in the experiment room), ^oC
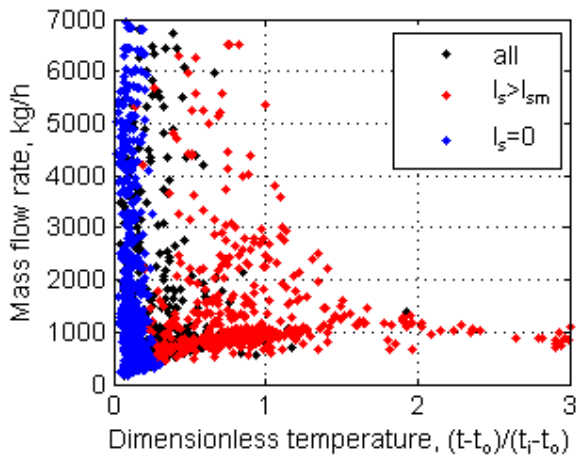
all	- data points for the whole set of data
I_s	- data points for the night time period (intensity of solar radiation is zero)
I_{sm}	- data points for the period with the relatively strong solar radiation (solar radiation intensity is above mean)

Figure 8. Correlation between dimensionless air temperature in the DSF cavity and mass flow rate in the cavity. Test case DSF200_e. Tracer gas method
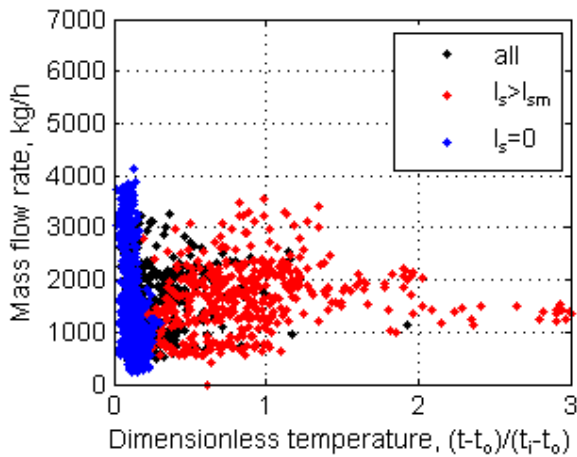
all   - data points for the whole set of data
I_s - data points for the night time period (intensity of solar radiation is zero)
I_{sm} - data points for the period with the relatively strong solar radiation (solar radiation intensity is above mean)

Figure 9. Correlation between dimensionless air temperature in the DSF cavity and mass flow rate in the cavity. Test case DSF200_e. Velocity profile method

In the tracer gas method, it is obvious that the empirical results include measurement errors, primarily caused by bad mixing of the tracer gas, flow reversal in the cavity or washout effects, while in the velocity profile method, the measurement errors cannot be observed directly.

Looking upon the plots in the Figure 9, it is evident that even for the higher air temperatures in the cavity, it is still difficult to observe the correlation between the mass flow in the cavity and the air temperature.

In case of pure buoyancy, the mass flow rate in the DSF can be calculated if the discharge coefficients are exact. In the preliminary experiments (see reference 5), these were estimated as 0.65 and 0.72 for the bottom and top opening, correspondingly. The mass flow rate for conditions of pure buoyancy is estimated in correspondence with experimental conditions and illustrated in the Figure 10. It is remarkable that the manual calculations are in good agreement with the lowest mass flow rates obtained experimentally. Still, the foremost part of experimental data available is located above the analytically obtained values for the buoyancy originated flow.

Another interesting matter to be pointed out is the choice of the discharge coefficients for the calculations in the Figure 10. An agreement between estimated and experimentally obtained data gives some level of confidence in achieving truthful results using the discharge coefficients determined experimentally in a wind tunnel.
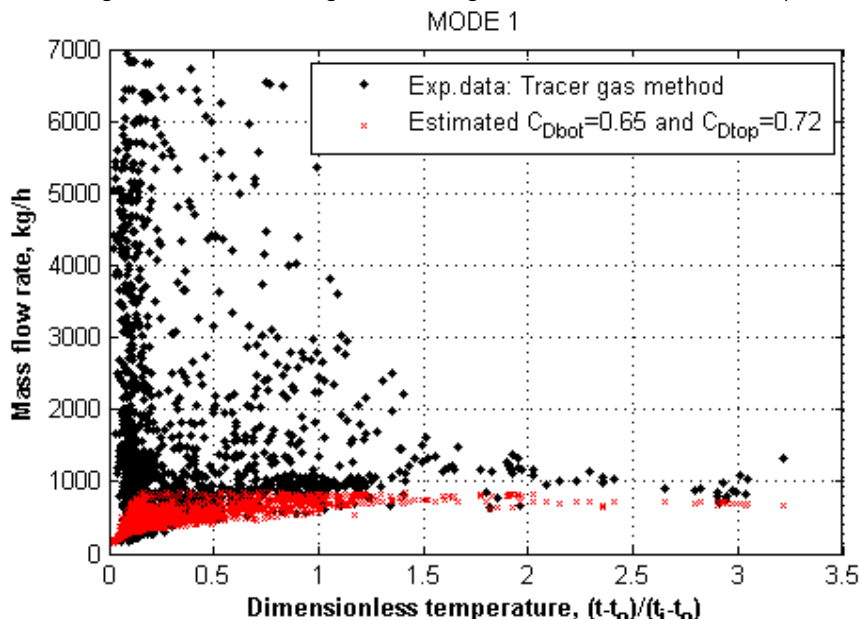
Figure 10. Estimated mass flow rate in the DSF cavity for pure buoyancy natural ventilation.

In both sets of the experimental results (tracer gas and the velocity profile methods), the high mass flow rates are characterized with the higher wind speed (Figure 11).
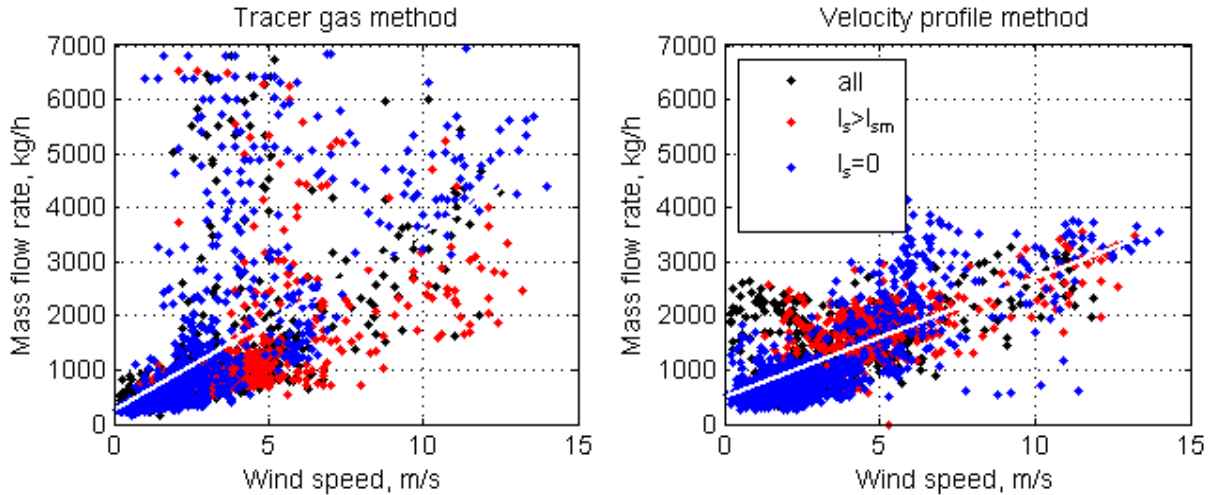
Figure 11. Correlation between mass flow rate in the in the DSF cavity and wind speed. DSF200_e case.

Here, the only conclusion can be drawn, that the greater part of the experimental data is available for the wind dominated natural ventilation or a combination of wind and buoyant forces. However, as demonstrated in Figure 10, it does not mean that there were no periods with the buoyancy dominated natural ventilation.

Further, in order to investigate strength of the buoyancy and strength of the wind driving forces separately, the mass flow rate is plotted as a function of the wind speed and dimensionless air temperature in the DSF cavity in Figure 12 and in Figure 13. The dimensionless air temperature in these figures is divided into three groups, in order to identify conditions for buoyancy dominated natural ventilation in the empirical results:

- Negative or low dimensionless temperature, $t_{dim}<0.3$
- Moderate temperature difference between the indoors and outdoors, $0.3\leq t_{dim}<0.8$
- Relatively high temperature difference between the indoors and outdoors, $t_{dim}>0.8$

From Figure 12 it is seen that for the low wind speed (0-2m/s) and high dimensionless temperatures ($t_{dim}>0.8$) the mass flow rate in the cavity is relatively constant. For the moderate wind speed (2-3m/s), more experimental errors are present. However, the range of the mean flow rate for the high dimensionless temperature is almost the same as for the low wind speed (apx. 900kg/h). Moreover, the mass flow rate is nearly constant and thus independent from the wind speed. In the last plot, with the higher range of wind velocities (4-14m/s), the mass flow rate has a scatter character and no consistency of the results can be observed.

Similar situation is observed for the velocity profile method (Figure 13), but it is still different, especially looking upon the spread of the flow rates for $t_{dim}\geq0.8$ and wind speed 0-4m/s. Meanwhile, for the wind speed above 4m/s, there is a clearer dependency between the mass flow rate and wind speed, which is not seen in tracer gas method plots.
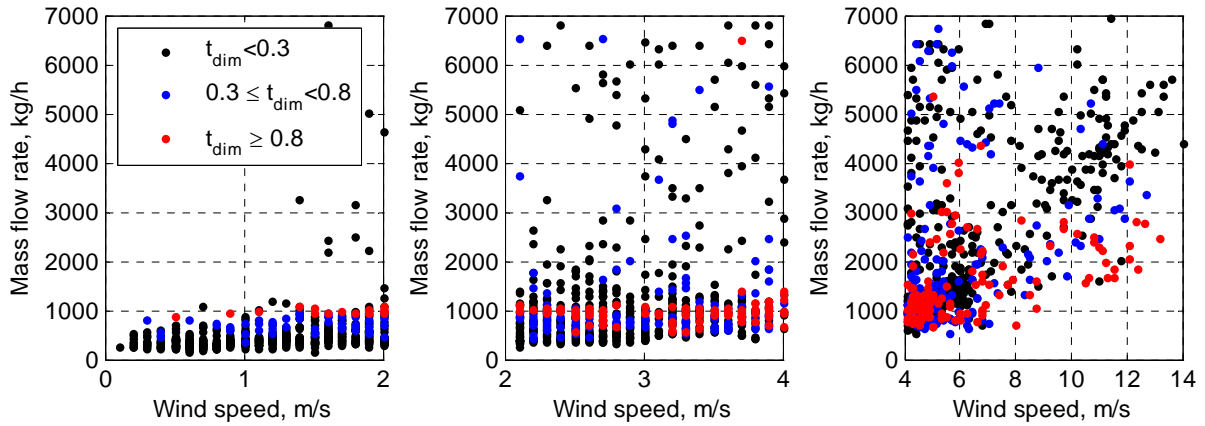
Figure 12. Effect of the wind speed and air temperature on the mass flow rate in DSF. Tracer gas method.
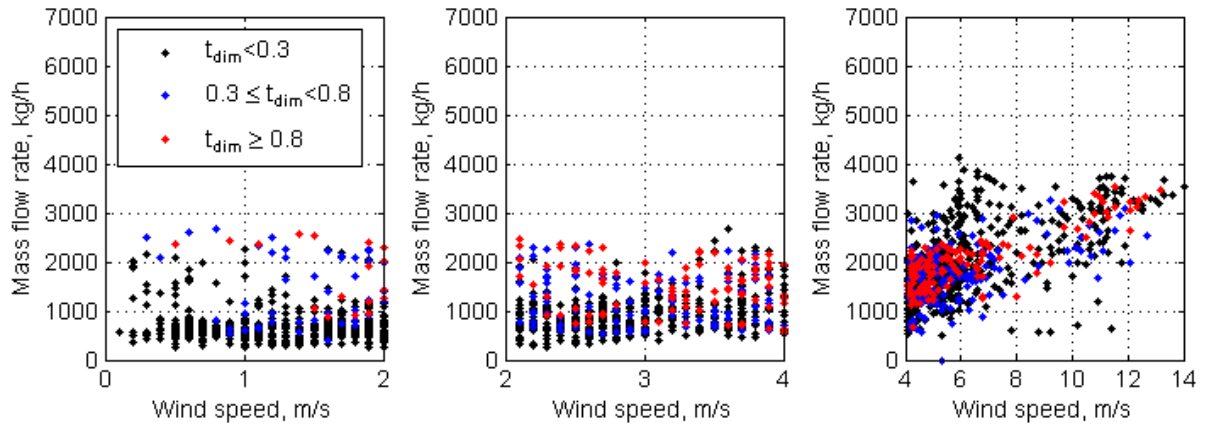
Figure 13. Effect of the wind speed and air temperature on the mass flow rate in DSF. Velocity profile method.

To outline Figure 12, it is necessary to draw an attention to the fact that the mass flow rate, plotted with the red spots ($t_{dim} \geq 0.8$) stays constant with the wind speed up to 4m/s. Consequently, these are the results obtained for the buoyancy dominated natural ventilation, while for the wind speed above 4m/s, the driving force in the cavity resulted from the wind forces or combined forces. And the greater part of the experimental data is available for the wind dominated or combined natural ventilation.

Similar observation was made by Larsen [16] in the wind-tunnel measurement results for the single sided ventilation through a single opening: with the increase of the wind speed up to 5m/s, the effect of the buoyant forces on the air flow rate through the opening was estimated as close to none-existing.

This outline, however, causes two reasons for disagreement. First one is an existing general assumption about the buoyancy driven natural ventilation in DSF. This disagreement, in the first place, is caused by the lack of a shading device in the DSF cavity, which normally functions as an additional heat source in the cavity and correspondingly helps to generate higher vertical temperature gradients.

The second one is the occurrence of the wind dominated or combined natural ventilation for the external air curtain mode in the double-skin facade (natural ventilation principle in this mode is categorised as single-sided natural ventilation on different levels) and the DSF openings are subjected to nearly the same wind generated pressure ($\Delta C_p \approx 0$).

In the Figure 14, it is demonstrated that the major part of the measurement errors is characteristic for approximately South wind direction (apx.180°, wind is directed to the DSF). The South wind directions are also characterised by the $\Delta C_p \approx 0$, thus the main reason for these measurement errors was probably the instability, when the smallest change in the wind pressure at the top or bottom opening could reverse the flow or cause multiple wash-outs.
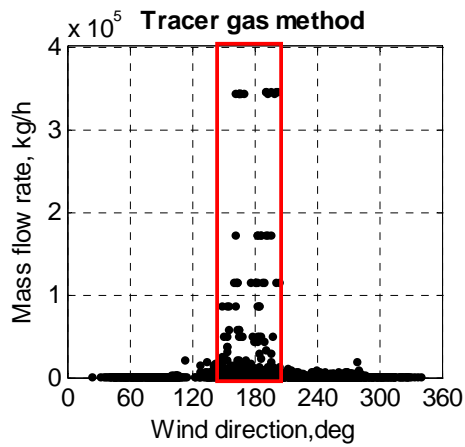
Figure 14. Effect of South wind direction on the mass flow rate in the DSF cavity. Tracer gas method. DSF200_e case.

Wind washout effect in DSF is the phenomenon, which causes an additional flow path in the double-skin façade cavity. Normally, wind washout effects exist together with the main flow. The washouts are originated when the wind blows in the direction of facade containing openings. Then the distribution of pressure on the façade's openings may vary a lot in a horizontal direction. And, in case of low flow resistances in the cavity, some small amount of air enters and leaves through the openings located on the same height above the ground, due to the differences in pressure distribution. For example: the air enters through the opening SOL1 and leaves through the opening SOL3 in the Figure 15.
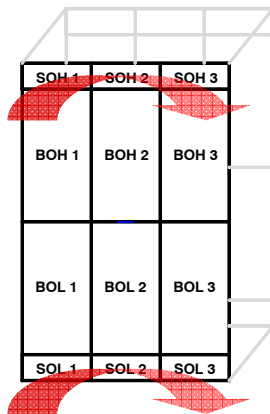
Figure 15. Illustration of wind wash out effect.

When the main flow in the DSF is low, then there is a higher probability for an error caused by wind washout effects, while for the high natural air flow rates in the cavity (such as in the test case DSF200_e) the magnitude of the main flow is rather high, that means that the façade resistance against the washout effects is also high.
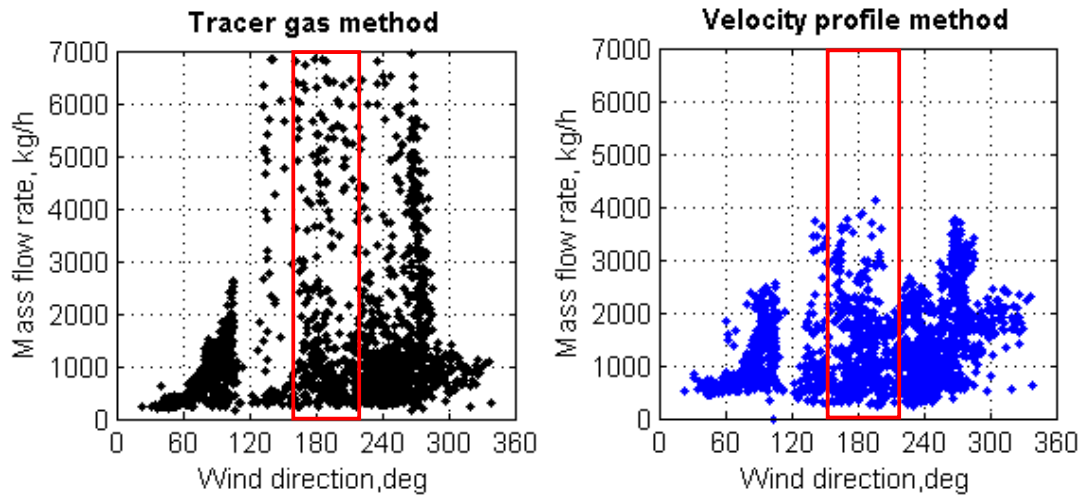
Figure 16. Effect of wind direction on the mass flow rate in the DSF cavity. Tracer gas method (left). Velocity profile method (right). DSF200_e case.

Considering that the air flow increases with the South wind directions, both in case of the velocity profile method and the tracer gas method, indicates that not only the measurement errors due to the wind washout take place for these wind directions, but actually, there is an increase of the flow rate for the Southern wind directions.

This, however, causes a disagreement with the commonly used theory of the wind pressure coefficients for calculation of the wind generated natural driving forces in a single-sided ventilation principle, as in many empirical models it is assumed that $\Delta C_p \approx 0$ and therefore, the wind forces have been disregarded in these models.

3.3.6 Cooling/heating power in the experiment room

One of the main targets of this experimental work was to accurately estimate solar gains and heat losses by the room adjacent to the double skin facade, as these parameters independently reflect the performance of the DSF cavity. Their independence was assured by the minimised influence of the experiment room on the DSF performance, as the thermal conditions in the room were kept constant, no regulation of the window openings was used and no shading devices were installed; the building was very well insulated and kept air tight, the transmission heat losses were estimated and all influencing climate parameters were measured.

Water was used in the cooling unit of the ventilation system. With the purpose to avoid the condensation on the surface of the surface of the cooling unit, the minimum water temperature was set to 12°C. The difference between the supply and return water temperature from the cooling unit in the experiment room was measured using one thermocouple type K with a maximum uncertainty of 0.1°C. The mass flow of the water supplied to the cooling unit was measured with a water flow meter MULTICAL from Kamstrup, which measures in a range from 0 to 1 kg/s and calibrated to an uncertainty of ±0.1% of the reading. Both the temperature difference and the water mass flow were collected by Helios data logger at a frequency 0.1 Hz.

The heating unit in the ventilation system was rarely activated, as in most cases, the additional heating load from the fan of the ventilation system in the experiment room ensured a sufficient cooling load. To keep a track of all loads to the experiment room, including the heating unit, all equipment in the room was connected to a wattmeter. The accuracy of the device was 0.1% of the reading (2.6 kW).

4. THE DOUBLE SKIN FACADE THEORY AND MODELLING OF THE EMPIRICAL TEST CASES

4.1 Modelling of the double skin facade

This chapter of the report is aimed to summarise the main issues when modelling DSF performance. The complexity of the DSF modelling is well known and there are no doubts about the necessity for the empirical exercises completed during the IEA Annex 34/43 activity. On the contrary, a general concern is expressed in the literature about the lack of the experimental data and validated software tools for the DSF buildings [3]. Moreover, there is literature available about the clarification *why* it is difficult to perform the modelling of the DSF performance. Looking upon these arguments, it is easy to understand why there is still an active hunt for a better model for the DSF modelling.

From another point of view, there is a number of well developed building simulation tools, able to perform calculations necessary for the DSF modelling. Then appear some questions:

- Does the claim that none of the simulation tools able to predict performance of a building with the DSF express the general difficulties for DSF modelling?
- Or is this claim caused by the lack of experience, knowledge or guidelines, when applying already existing building simulation tools or by the lack of knowledge about the suitable tool to use?
- Or is this just a call for a model that would simplify the modelling of the DSF?

In the literature review [3] the details about difficulties in DSF modelling are summarised. A classification is also made of the main elements in the DSF physics, these are the optical, heat transfer and air flow element. Earlier, the participants of the comparative and empirical exercises agreed that the optics and heat transfer elements are the common issues for the whole field of building simulations, then this report and whole activity of the subtask is focused on the investigations of the air flow element in modelling of the DSF performance, as its assessment is crucial for the indoor climate and evaluation of the performance of the double skin facade.

However, the convective flows in the DSF cavity can be very strong and can have a serious impact on a final result of simulation. At the same time the different building simulation software uses different models in calculation of surface heat transfer coefficients. In order to help the reader in the evaluation of performance of different simulation tools, this chapter includes a section with a short summary over the surface heat transfer coefficients used in different models, while even more details can be found in the modeller reports, which are included in Appendix VI.

4.2   Surface heat transfer coefficients. Convection

All of the models in the empirical validation exercises make a split between the convective and radiative surface heat transfer coefficients. A sensitivity study of the surface film coefficients for DSF modelling was also conducted (see more in section 5.4), where it is argued against the combined treatment of surface film coefficients for DSF modelling.

As it can be seen from the table below, all of the models use longwave radiation exchange with the sky and the ground, the details about it can be found in the modeller reports. When looking upon the level of detail in modelling of external longwave radiation exchange, all of the models include almost the same level of detail and therefore this will not be discussed further. However, it is not possible to do the same conclusion on the subject of convection heat transfer, as it is demonstrated in the table below. But first, the role of convective heat transfer in the specified empirical test cases is discussed.

The operational mode of the DSF can vary according to its function in one or another building, but the design of the DSF cavity is more or less the same: two layers of fenestration, separated with the air gap, which, in most of the cases, include shading device. No matter what is the operational strategy of the DSF, the air temperature in the gap is the result of the solar radiation absorbed by glazing and/or shading device. As a result, the air temperature in the DSF cavity is mainly the result of the convective heat transfer between the heated surfaces of glass and air. The floor or ceiling and side walls of the DSF rarely have any importance, as in a real life, the weight of their areas is very small compared to the area of fenestration and shading.

The convective heat transfer is relatively easier to estimate for the mechanically induced flow motion compared to the naturally driven flow, where the convection heat transfer depends on size, shape, orientation, flow regime, temperature etc.

The results of simulations can be very sensitive to the convective heat transfer coefficient in the models and the differences between the convection heat transfer coefficients in the models are important. The importance of the surface heat transfer coefficients is also investigated in the section 5.4, where a simple sensitivity study is used to demonstrate the consequences of the assumptions made towards the surface heat transfer. Below is the table of summary of the convection heat transfer coefficients used in models in the empirical exercises.

Software	BSim	VA114	ESP-r	TRNSYS-TUD
External heat transfer coefficient				
Convection	if $v_{wind} \leq 5\ m/s$ $h = 5.82 + 3.96\,v_{wind}$ else $h = \dfrac{7.68 \cdot v_{wind}}{\sqrt{v_{wind}}}$	18 W/(m²ºK)	$h = 2.8 + 3 \cdot V_{loc}$ V_{loc} -local wind speed, for which there are relationships with the climate wind speed and the difference between the surface azimuth and wind direction	25 W/(m²ºK) - set acc. to modellers opinion
Radiation (components)	sky, ground	sky, ground	sky, ground	sky, ground
Internal heat transfer coefficient				
Convection	for vertical surfaces: $if\ \Delta T \leq 9.5/L^3$ $h = 1.42\left(\dfrac{\Delta T}{L}\right)^{0.25}$ $if\ \Delta T > 9.5/L^3$ $h = 1.31(\Delta T)^{0.33}$	3 W/(m²ºK)	Buoyancy correlations of Alamdari and Hammond (1983) from [7] $h_c = \left\{ \left(a \cdot \left(\dfrac{\Delta T}{d}\right)^{p}\right)^{m} + \left(b(\Delta T)^{q}\right)^{m} \right\}^{\frac{1}{m}}$	4.4W/(m²ºK), except 3W/(m²ºK) for ceiling and floor (set acc. to modellers opinion)
Radiation	Linearised coefficients based on surface emissivity and view factors	Linearised coefficients based on surface emissivity and view factors	Linearised coefficients based on surface emissivity and view factors	Nonlinear treatment of radiation heat exchange

Table 4. Convection and radiation heat exchange at the surface.

4.3   Air (mass) flow models

This section deals with the models for calculation of the air flow rate in a naturally ventilated DSF cavity applied in the empirical validation exercise. The air flow in naturally ventilated spaces is induced by the pressure differences, which evoke from the wind pressure, wind fluctuations and buoyancy forces (the mechanical force is not discussed in this section). The determination of the buoyancy force is straight forward, while the main difficulties in the theory of the natural ventilation exist due to highly transient wind phenomenon.

There are a number of approaches used for calculations of air flow in a naturally ventilated (multizone) buildings, however, all of them have most of the following issues in common:

- Challenge to represent the wind speed reduction from the meteorological data to the local microclimate near the building
- Challenge in determination of the wind pressure coefficients
- Challenge to decide on appropriate discharge coefficients and pressure loss coefficients in general
- Challenge to agree on an appropriate relation between pressure loss and air flow rate through the opening (determination of coefficients in the relationships), etc.

Depending on external conditions and the double skin facade running mode the air flow rate in a ventilated cavity can have significant variation in order of magnitude and in occurrence of a reverse flow. In contrast, in a traditionally ventilated domain, the minimum air change rate is specified in requirements for the indoor air quality, while maximum is normally restricted by the energy savings considerations. In view of that, the great variations in the magnitude of the air flow rate are identified as the distinctive element of the cavity flow. The variation of the flow magnitude may result in variation of the flow regimes and will further complicate the situation.

The commonly used models for calculation of the natural air flow rates are:

- The network pressure model – is based on continuity equations to determine pressures in different zones of the network and then the air flow rates are determined on the basis of different relationships (orifice, power-law etc.)
- The loop pressure equation model – is method where the pressure loop equations are written for the whole air path loop, and the air flow rate is determined on the basis of those equations.
- The experimental method uses empirical relationships for the determination of the air flow rates depending on temperature, wind speed, wind pressure coefficients and the discharge coefficient.

The pressure network and the pressure loop method are very similar. Moreover, both of these methods can apply the orifice and the power-law relationships for determination of the air flow rate on the basis of pressure difference. However, an application of one or another relationship is a sensitive matter, as the classic orifice equation is more suitable for the large openings and fully developed turbulent flow. Meanwhile, the power-law equation is more flexible and can be adjusted to different conditions and opening sizes via the exponent *n* and coefficient *C.*

Equation 4-1

$$\Delta P = \frac{\rho \dot{V}^2}{2 \cdot C_D \cdot A^2}$$

Orifice equation

Equation 4-2

$$\Delta P = \left(\frac{\dot{V}}{C} \right)^{\frac{1}{n}}$$

Power-law equation

ΔP - pressure difference across the opening
ρ - air density
$\dot{V}$ - volume flow rate
C_D - discharge coefficient
A - opening area
n, C - exponent and flow coefficient

The experimental method is the simplified one, where the transient character of the wind is simplified and a relationship is shown below used for the calculation of air flow rates.

Equation 4-3

$$\dot{V} = \left| \frac{c_v}{|c_v|} \cdot (c_v \cdot V_{10})^2 + \frac{\Delta T}{|\Delta T|} \cdot (c_t \cdot |\Delta T|)^2 \right|^{1/2}$$

Equation 4-4

$$c_t = \sum_{j=1}^{n} c_{D,j} \cdot A_j \cdot \left(\frac{2 \cdot (H_o - H_j) \cdot g}{T_i} \right)^{1/2}$$

Equation 4-5

$$c_v = 0.03 \cdot A$$

$\dot{V}$ - volume flow rate
c_v, c_t - coefficient for the wind force and buoyancy respectively
V_{10} - the reference wind velocity at the height 10m
ΔT - temperature difference between two environments
n - number of openings
j - opening number
C_D - the discharge coefficient
A_j - area of the opening 'j'
H_o - height of the neutral plane
H_j - height of the opening 'j'
g - gravity force

The summary of the model used for the empirical exercises is done in the table below:

Software		BSim	VA114	ESP-r	TRNSYS-TUD
Influencing parameters in the flow model	wind force	x	x	x	x
	wind fluctuations	-	x	-	
	buoyancy	x	x	x	x
Air flow model*		experimental (explained above)	network	network	network
Pressure-Airflow relationship used			power-law	orifice	power-law
Discharge coefficient		0.65	0.61	as in spec. 0.65/0.72	0.65
Pressure difference coefficients		different from spec, ΔCp=0, but wind impact is included by application of C_v-coefficient	different from spec, ΔCp=0	as in spec	as in spec
Model for wind fluctuations		-	[11], [12]	-	-

* None uses the loop equations

Table 5. Comparison of air flow models used in the simulation tools.

Openings in the empirical exercises were specified, all of them had the same orientation and therefore the wind pressure component became less influencing or equal to zero (in VA114). In such a situation, the wind turbulence can generate a substantial flow rate. However, only VA114 considers the wind fluctuations.

In the empirical specification, the size of the openings is different for the top and the bottom openings. Consequently, the friction losses and contraction of the jet are different for the top and the bottom openings. This is specified via the discharge coefficients C_d for the openings on the basis of experiments; only ESP-r and BSim model have used this data.

The pressure coefficients given in the empirical test case specification are given for the wind velocity at the building height (6m), however, the wind velocity in the climate data file is given for the wind velocity at the 10m height. Besides the parameters included into the table above, the reduction of the wind speed to the local terrain next to the building can have some degree of influence on the calculations of the wind pressure magnitude and influence of the wind turbulence for the air flow calculations. Below is given the comparison of the wind speed reduction relationships used in different models and it demonstrates that the models use almost the same wind reduction relationship in the simulations.

Software:	BSim	VA114	ESP-r	TRNSYS-TUD
Reduction factor to the reference wind velocity at the height of 10m:	0.922	0.922	0.922	0.84

Table 6. Reduction factor to the reference wind velocity at the height of 10m in different models.

In the comparative exercises, the infiltration parameters were set to negligible minimum, while in the empirical exercises, this was specified, however not for the zone 1. According to the measurements, the experimental test facility has superior air tightness; therefore, the assumption of negligible infiltration in the empirical models is also satisfactory.

5. ADDITIONAL TEST CASES

5.1 Background

The initial goal of this subtask was to conduct the empirical validation of the building simulation software on its ability to simulate the performance of a DSF building. Accordingly, earlier versions of the model specifications were not strict and the experts were allowed to use the best suitable to their knowledge, approach to setup the model. First, in order to eliminate possible errors and complete a comparative validation of the models, a set of comparative test cases was defined and completed. The results from the comparative cases are available in a working document of the subtask, which demonstrated the magnitude of differences between the results obtained using different simulation tools and models.

Nearly the same conclusion was obtained with the first results of empirical case studies. Meanwhile, the diagnosis of reasons for disagreements between the experimental data and simulation results was not easy, due to the complexity of the dynamic DSF-system and limitations in accuracy of the experimental data.

There was a need for a step back and repetition of some simulations under the simplified conditions to diagnose disagreements on a case by case basis. First, the optical/thermal properties of the glazing were double-checked and corrected if necessary, in order to be identical in all of the models. Originally, in the specification, the optical properties of the glazing were given according to the product specification (see earlier versions of test case specification). However, experimentally obtained spectral properties of the glazing were also available. Spectral properties were used in WIS software to calculate the optical properties of the glazing (Appendix IV). The results were similar to the once from the product specifications. Finally, the optical properties for all models were chosen according to WIS-results (Table 7).

Incident angle	External window pane			Internal window pane			
	Transmission of external window	Reflection of external window FRONT/BACK	g-value of external window	Transmission of internal window	Reflection of internal window FRONT	Reflection of internal window BACK	g-value of internal window
0	0.763	0.076	0.8	0.532	0.252	0.237	0.632
10	0.763	0.076		0.531	0.252	0.237	0.632
20	0.76	0.076		0.529	0.251	0.237	0.631
30	0.753	0.078		0.524	0.252	0.239	0.627
40	0.741	0.084		0.513	0.258	0.245	0.618
50	0.716	0.103		0.488	0.277	0.264	0.595
60	0.663	0.149		0.435	0.326	0.309	0.542
70	0.55	0.259		0.331	0.436	0.405	0.433
80	0.323	0.497		0.163	0.638	0.579	0.244
90	0	1		0	1	1	0

Uvalue	5.67 W/m^{2}K	1.12 W/m^{2}K

Table 7. Optical properties in the models (acc. to WIS calculations).

Next, a number of additional test cases were specified for the diagnosis purposes. More information about the additional cases is included into the following sections of the report and also in the Appendix III.
The additional test cases are:

- Steady state cases (SS)
- No solar case (NS)
- Surface film coefficient - sensitivity study test cases

5.2   Steady state test cases

Earlier results of empirical validation have shown significant deviations between the models when calculating cooling or heating power. The deviations were obvious not only for a clear day, but also for the night time period, see Figure 17:
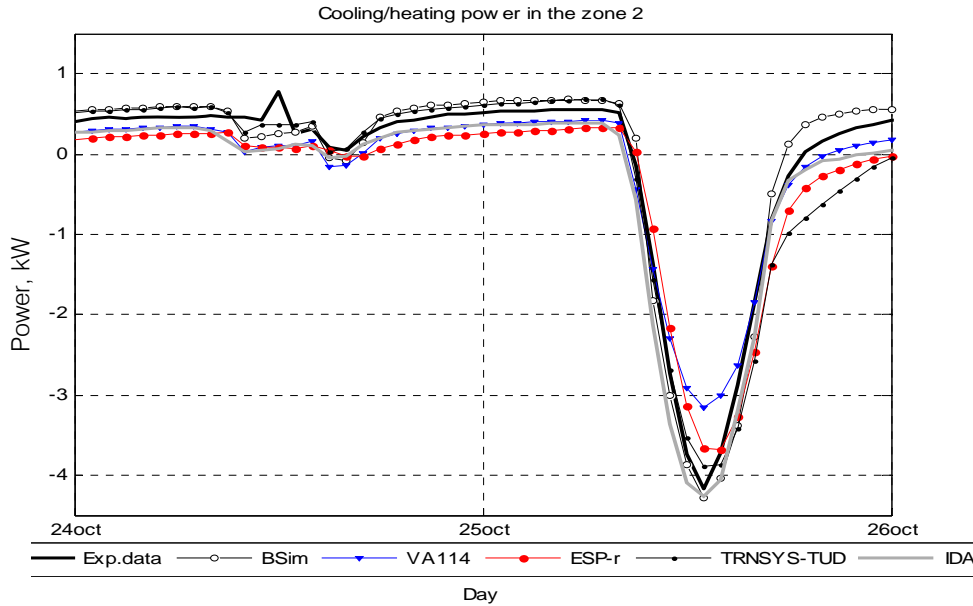
Figure 17. Example from earlier simulation results: Cooling/Heating power in the zone 2. Test case DSF100_e.

The main deviations in the night time heating power in the Figure 17 are caused by the lack of definitions for the thermal bridges in the specification and freedom left to the modellers when modelling the thermal bridge losses.

Also, there was a possibility for errors when setting-up the geometry and construction properties in the models. These deviations were minimised by the cross check of the models by a second person. This way, some small inconsistencies of the inputs, compared to the specification were found and corrected.

The steady state cases were defined in order to validate performance of the thermal models and, also, to agree on how to model the thermal bridge losses. The definition of the steady state cases was done according to experimental results (Appendix III). First, steady state simulations were performed with assumption that there are no thermal bridge losses in the 'Cube'. Results of the steady state cases were compared with the analytical calculations, using the U-values of the constructions in the test facility:
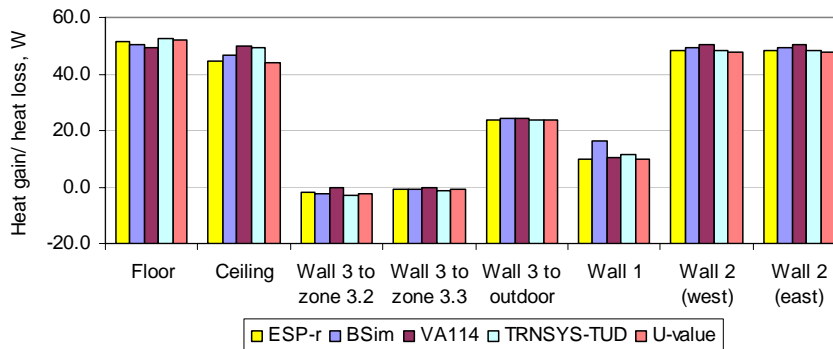
Figure 18. Heat fluxes in the zone 2. Steady State case.

Apparently, the results of SS case simulated by different software, in the above plot (Figure 18) are slightly different, due to the deviations between the models (Table 8). Also, it has been demonstrated in the example of ESP-r and BSim model that with application of variable film surface coefficients the heat losses from the zone 2 increase compared to application of fixed coefficients.

28

	BSim	VA114	ESP-r	TRNSYS-TUD
Convection internal, W/(m2.K)	Combined coef: 23 – for external 8 –for internal	3.00	Combined coef: 23 – for external 8 –for internal	3.00
Convection external, W/(m2.K)		18.0		15.0
Radiation internal, W/(m2.K)		based on view factors and emissivities		based on view factors and emissivities
Radiation external, W/(m2.K)				

* The table is valid only for the SS case

Table 8. Differences between the models in SS case.
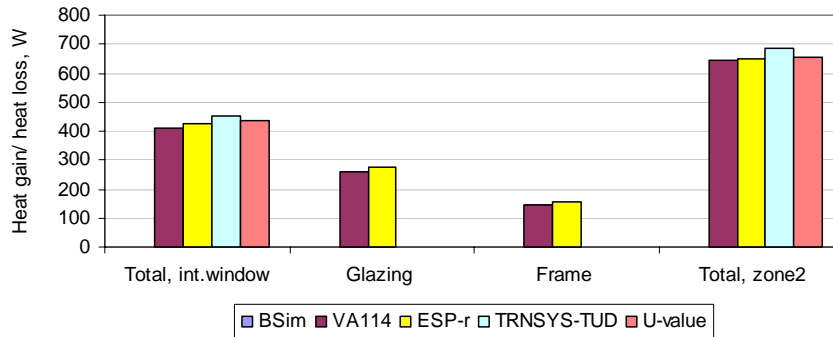
Figure 19. . Heat fluxes for the internal window surfaces facing zone 2. Steady State case.

The most significant deviations between the models were found for the window constructions (Figure 19). Therefore, the detailed energy balance for the internal windows was necessary for the diagnosis of these deviations. The energy balance was reported only for two models: TRNSYS-TUD and VA114. The main difference between these two models was the surface temperature of the outer glazing (7.18°C for TRNSYS-TUD and 8.15°C for VA114). This is explained by the different longwave radiation exchange at the surface.

During the SS simulations, the attention was also drawn to the fact that when dealing with the DSF in general, it is necessary to consider whether the U-values of the internal window glazing and frame have been corrected to the internal-internal surface film coefficients instead of conventionally used external-internal film coefficients. It must be mentioned that only one method is mathematically right when correcting the U-values, as there is a difference whether the overall U-value of the window or the separate values for the glazing and frames have been changed from external-internal film coefficient to internal-internal coefficients.

5.2.1   Comparison of the SS and empirical results

Results of SS cases were compared against the experimental data. Since the steady state simulations were ideal and did not include any thermal bridges – the deviations between the simulations and empirical results appeared to be significant (Figure 20):
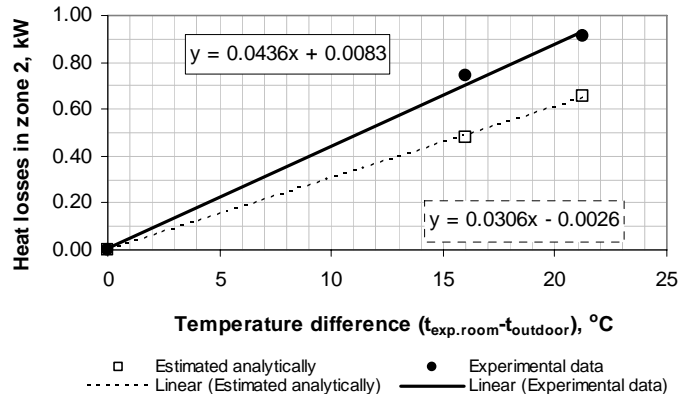
Figure 20. Comparison of steady state case results against the experimental data.

Next, the calibration of SS case models against the empirical results took place. Additional heat losses from the zone 2 (due to the thermal bridges) were evenly distributed to all constructions in the zone 2, except for the

windows. All of the models were identically modified, by increasing U-values of the constructions in the models, for more accurate prediction of the heat losses.
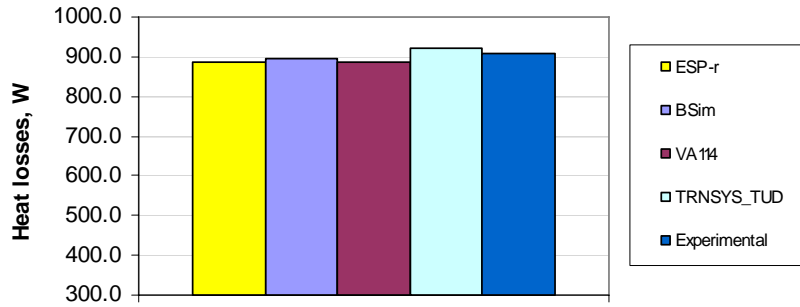
Figure 21.Total heat losses from the zone 2 in SS models, modified to count on thermal bridges.

After the modification of the models (Figure 21), only minor deviations can be seen between the models. Identical modifications have been made to all of the models in the DSF100_e and DSF200_e test cases.

5.3   No-solar test case based on DSF100_e

The main reason for the definition of 'no solar' (NS) case was that even with the calibration of the thermal models against each other and against the experimental results, still, there were many disagreements between the results in the later DSF100_e and DSF200_e models, while the prediction of the heating power has improved.

In the earlier simulations (Figure 22) and also after the calibration of the models, it was observed that the results are very sensitive to solar radiation. In addition, much better agreement of the glass surface temperatures for TRNSYS-TUD and VA114 was achieved in the SS results compared to the test case DSF100_2 and DSF200_2: difference 0.1 °C in SS case and more than 1°C in the other cases. Accordingly, in order to complete the diagnosis, the dynamic simulations were simplified by removing the impact of solar radiation and defining the 'non-solar' case, where the total, direct and diffuse solar radiation were set to zero.
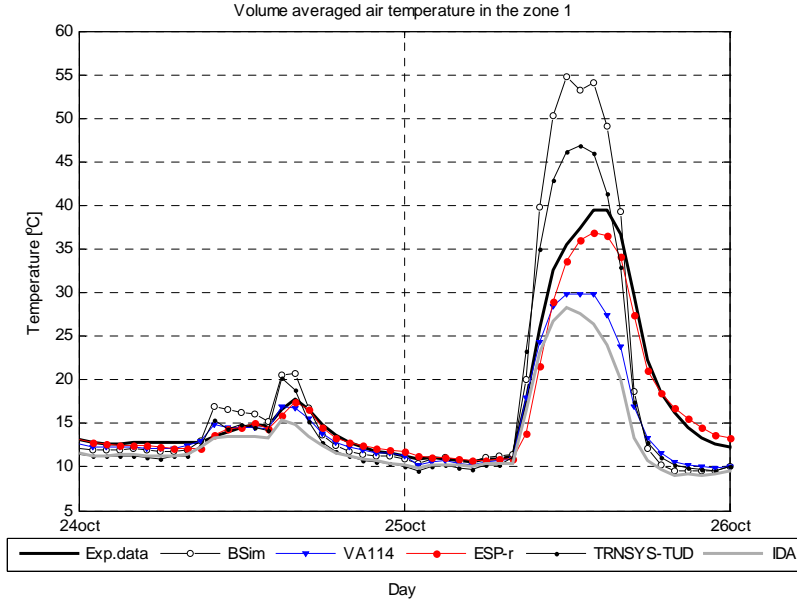
Figure 22. Air temperature in zone 1 in earlier case DSF_100e.
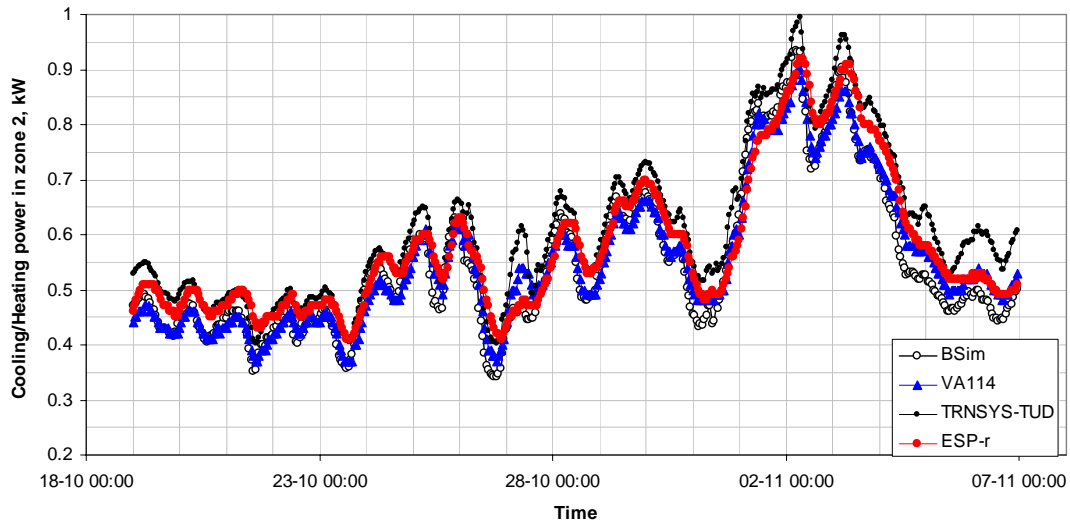
Figure 23. Cooling/Heating power in zone 2 in NS case.
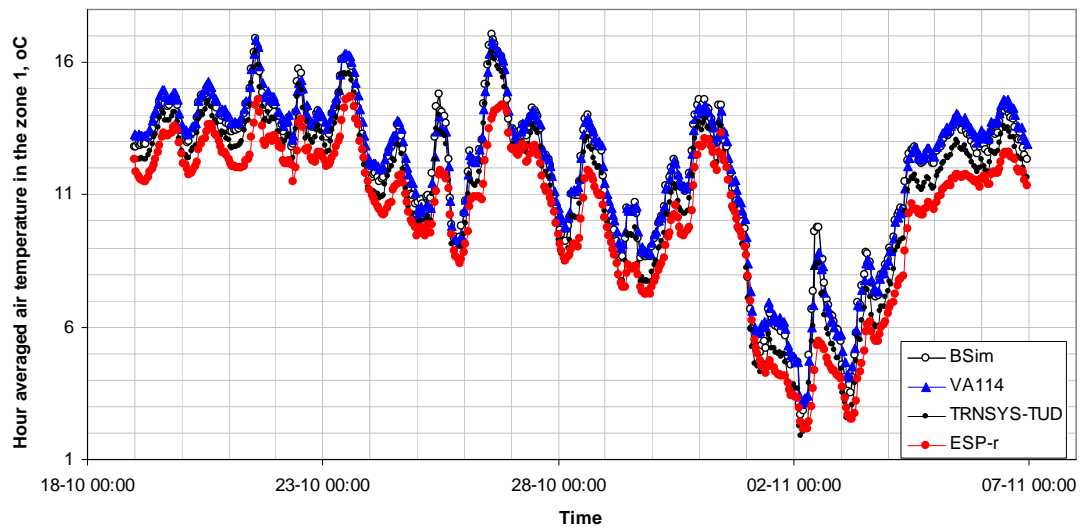
Figure 24. Hour averaged air temperature in zone 1, in NS case.

In NS case, better agreement was observed between the models if compared with the earlier results for DSF100_e, especially regarding the cooling/heating power in zone 2 (compare Figure 17 and Figure 23). Reasonably good agreement was observed for the air temperature predictions in zone 1 (2-6°C difference in the NS case and up to 30°C difference between the models in the earlier version of DSF_100e case, compare Figure 24 and Figure 22).

Also, it is interesting to consider the change in dynamics of air temperature in the DSF cavity when calculated with and without solar loads. It is clear that in the Figure 24, all of the models predict temperature dynamics in the same way. While, in the Figure 22, where the solar radiation is present, the ESP-r results differ most of all. In addition, ESP-r seems to be best to calculate the temperature dynamics in the cavity in the presence of solar radiation.

There is a comparison made for the surface temperature of the window frame and glass for the NS case results obtained with VA114 model. According to the comparison, the differences are small (in the order of 0-2°C), see Figure 25.
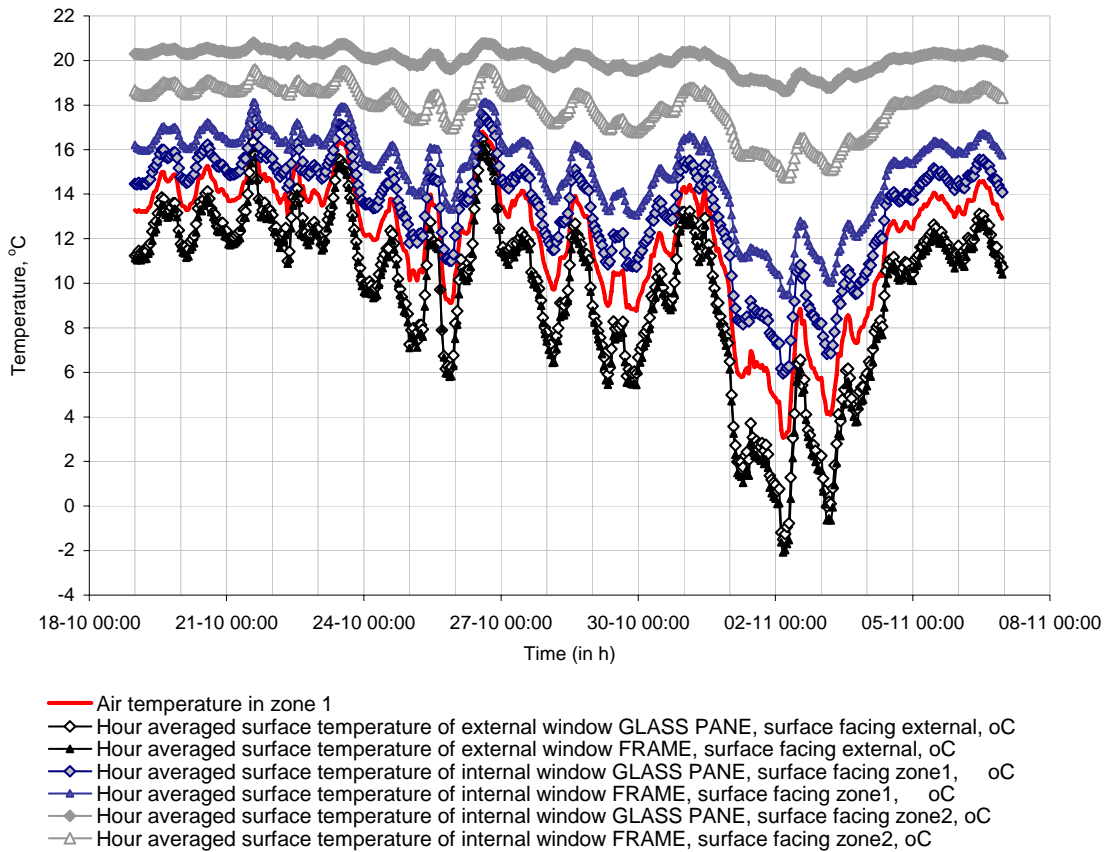
Figure 25. Comparison of the glass and frame surface temperatures in the NS case for VA114 model.

The most significant deviations between the models in the NS case results were observed only for the surface temperatures of the glazing, for the surfaces, which face the DSF cavity and also for the floor/ceiling surface temperatures in the DSF and in the zone 2.The differences in the glass surface temperatures for the surfaces facing DSF (zone 1) are explained by the differences in calculation of the convective/radiative heat transfer.

Some of the software-routine errors were detected and corrected, but no significant improvement has been made towards the solar cases.

5.4   Sensitivity study - impact of surface film coefficients

Both in SS case and NS case results, it was noted that the approach for modelling surface film coefficients can be very important for the final results of simulations. And, even though, that the validation of the convective and radiative heat transfer is not a part of the task, closer look into the surface film coefficients is necessary in order to answer at least some of the questions regarding the spread of the results calculated with different models.

Simple sensitivity study was performed using VA114 and ESP-r model. The sensitivity study included test cases based on NS case and DSF100_e case (Table 9). In the table, most of the cases are organised so that the lower the number of the test case – the more detailed modelling of the surface heat transfer used.

It must be mentioned that the case 1 for ESP-r and the case 2a for VA114 – are the reference cases, as the convection and longwave radiation heat transfer properties, as defined for these cases are used in the final results for ESP-r and VA114 correspondingly.

Case	Convection coef.		Radiation coef.		Combined coef.		Radiation ΔT		Model	Comment/ conclusion
	Int	Ext	Int	Ext	Int	Ext	Surf-surf using view factors	Surf-air		
1	vary	vary	vary	vary			yes		ESP-r for NS case and DSF100_e	Reference for ESP-r
2a	3.0	18	pc*	pc*			yes		VA114 for DSF100_e	Reference for VA114
2b	3.0	12	pc *	pc *			yes		VA114 for DSF100_e	Ext.conv is not important
2c	2.0	18	pc *	pc *			yes		VA114 for DSF100_e	Int.conv is very iportant
2d	2.0	12	pc *	pc *			yes		VA114 for DSF100_e	
4					8	23		yes	VA114 for DSF100_e	Combining coef. is not good, Int. longwave might be important
4a					7.7**	25		yes	ESP-r for NS case and DSF100_e	
5	vary		vary			25	yes (int)	yes (ext)	ESP-r for NS case and DSF100_e	Ext longwave is very important

*pc - for VA114 models, coefficient for long-wave radiation means, that its value is precalculated, based on view factors, emissivity and surface temperature.

** Internal surface film coefficients were fixed only for the surfaces in the zone 2.

Table 9. Test cases for the sensitivity studies of surface film coefficients.

Only insignificant changes of the glass surface temperatures, air temperature in DSF and cooling/heating power in zone 2 were observed when comparing the results from the study cases 2a and 2b, 2c and 2d. Accordingly, the importance of convective heat transfer at the external surface was very small (Figure 26, Figure 27).
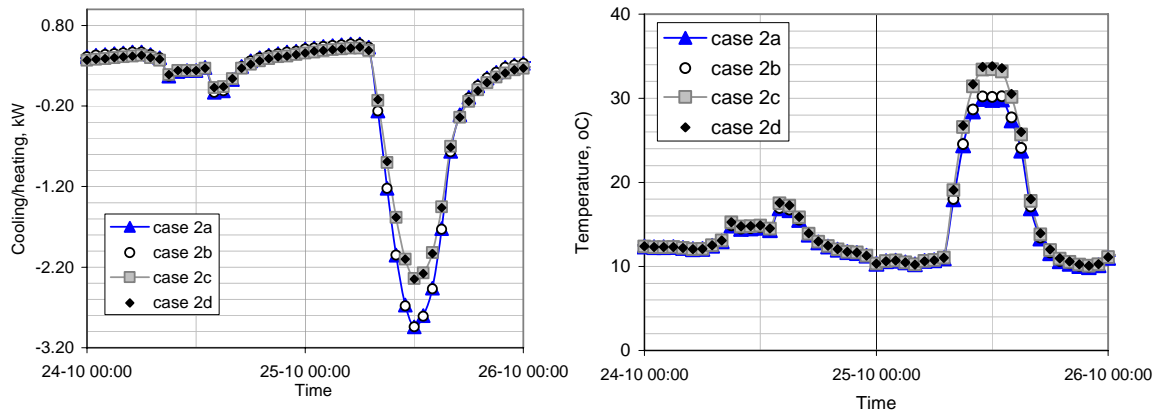
Figure 26. Cooling/heating power to zone 2 (left) , air temperature in the zone 1 (right), in the sensitivity study cases for DSF100_e, model VA114.
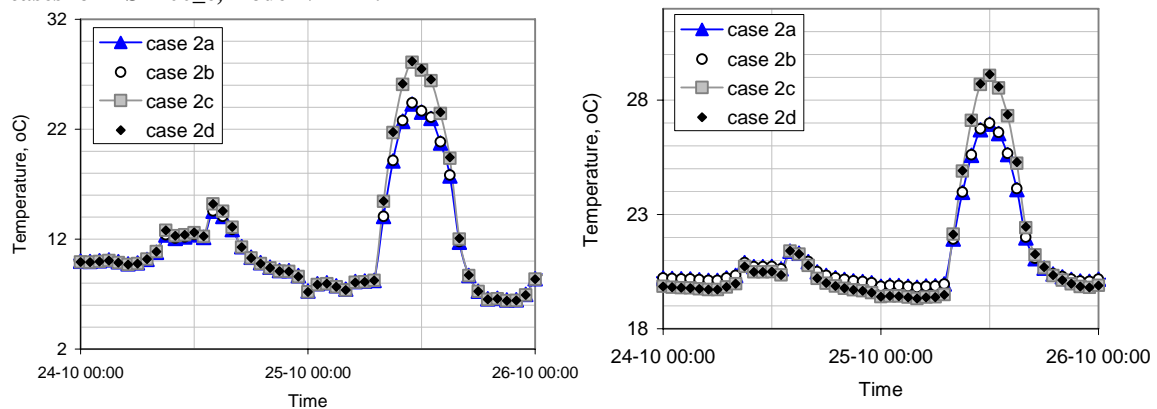
Figure 27. Temperature of the external window glass surface, facing outdoor (left). Temperature of the internal window glass surface, facing zone 2 (right) for DSF100_e, model VA114.

On the contrary, comparison of the cases 2a and 2c, 2b and 2d proves the importance of the convective heat transfer at the internal surfaces, but only at the day time period, when the solar radiation is present. Increase of the internal surface convective coefficient leads to the significant increase of the peak loads and has a big influence on the glass surface and air temperature in the DSF. In the night time, though, convective heat transfer at the internal surfaces is of minor importance (Figure 26, Figure 27).
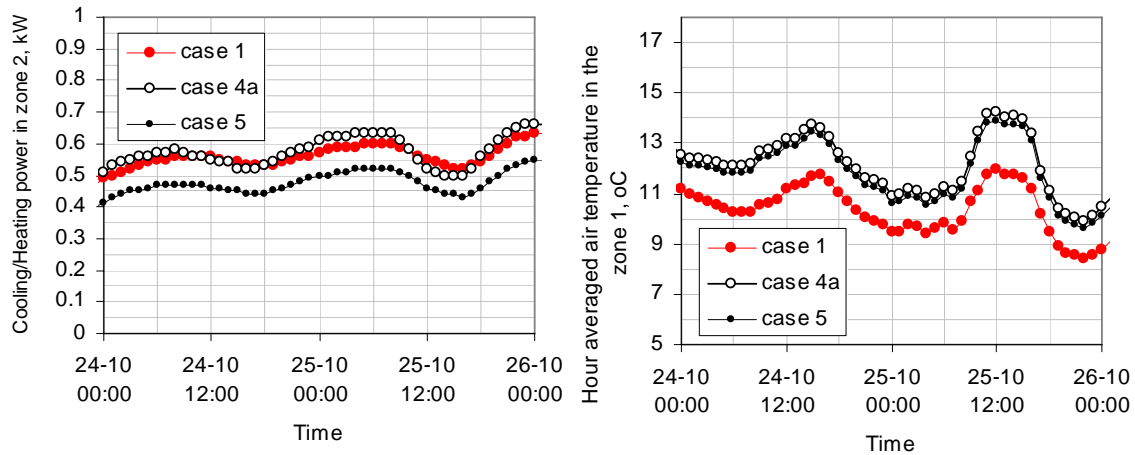
Figure 28. NS case with ESP-r results for sensitivity cases 1, 4a, 5.
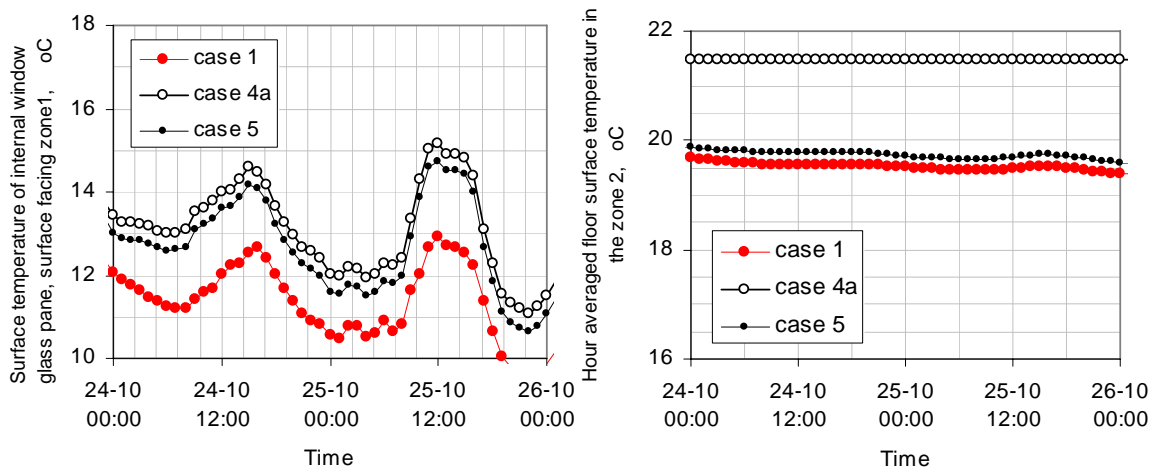
Figure 29. NS case with ESP-r results for sensitivity cases 1, 4a, 5.

By fixing the external surface film coefficient for the ESP-r model in NS case (compare cases: 1, 4a and 5 from the Table 9), the external glass surface temperatures increase with apx. 2°C for the case 4a compared to the case 1. Earlier, it was demonstrated for VA114 model that the external convection is of minor importance, thus the differences are caused by either the combined treatment of heat transfer or external longwave radiation.

ESP-r algorithms used for calculation of the surface heat transfer corresponded to those as in case 1, Table 9 and the results are illustrated in the Figure 24, Figure 23. By fixing the internal convection coefficient, the changes are especially seen for the internal surface temperatures (Figure 29). Yet the changes seem small in the above figures, but when ESP-r predictions for case 1, 4a and 5 are compared with the other models in NS case, and then the results for ESP-r change from lowest to highest for floor and ceiling temperatures in zone 2.

Still, the plots illustrated in the Figure 28 and Figure 29 belong to NS case and therefore the results are less sensitive to the surface film coefficients, as if the sensitivity study was done for a case with solar radiation present (Figure 30 - Figure 32 and Figure 33 - Figure 35). From the figures below it can be seen that there are major changes in the peak cooling loads and significant in the peak temperatures in the double-skin facade.

34
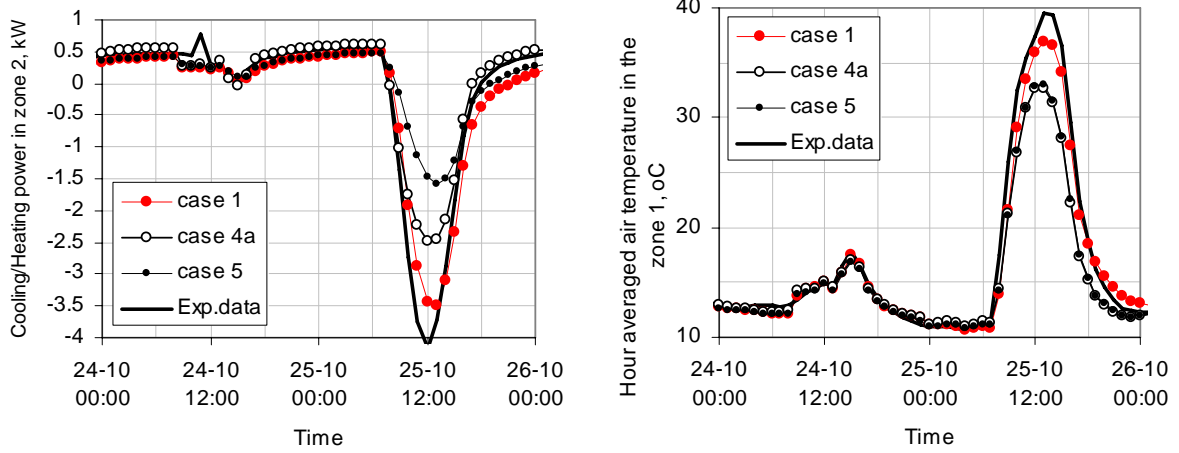
Figure 30. DSF100_e case with ESP-r results for sensitivity cases 1, 4a, 5.
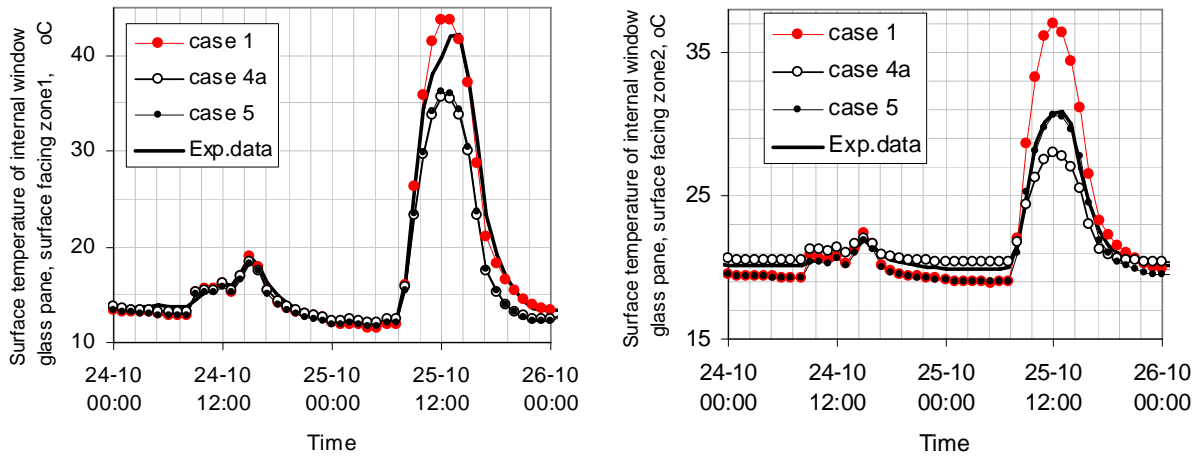
Figure 31. DSF100_e case with ESP-r results for sensitivity cases 1, 4a, 5.
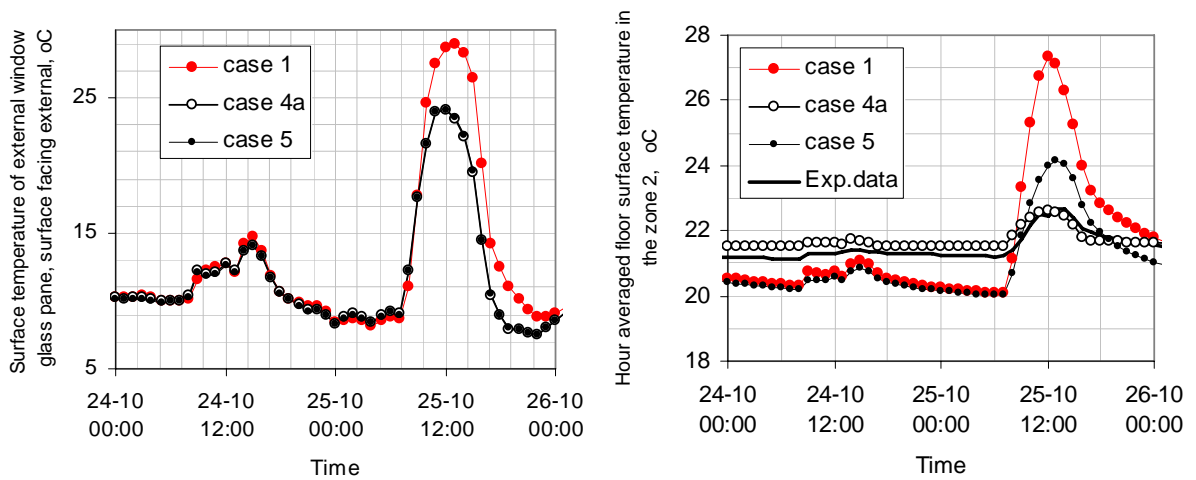
Figure 32. DSF100_e case with ESP-r results for sensitivity cases 1, 4a, 5.

35
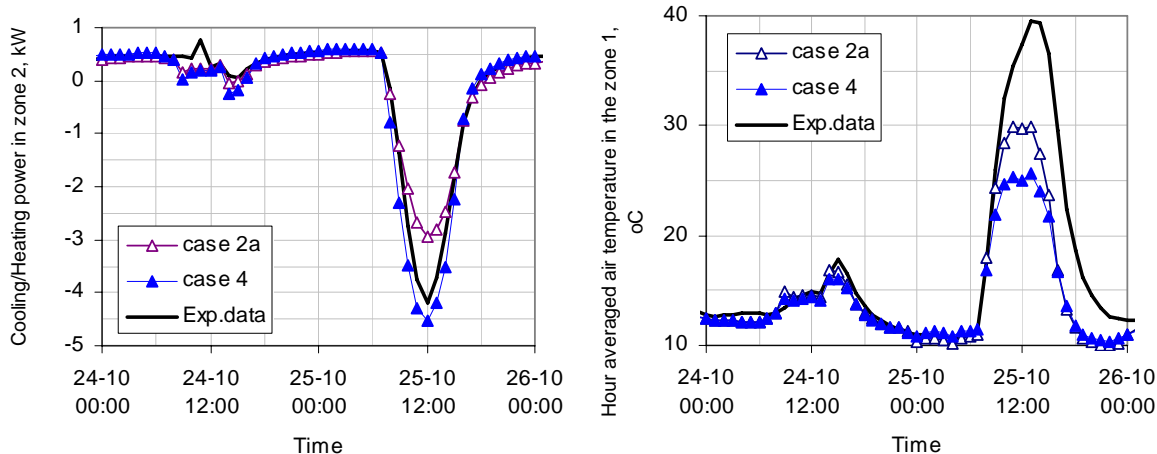
Figure 33. DSF100_e case with VA114 results for sensitivity cases 2a and 4.
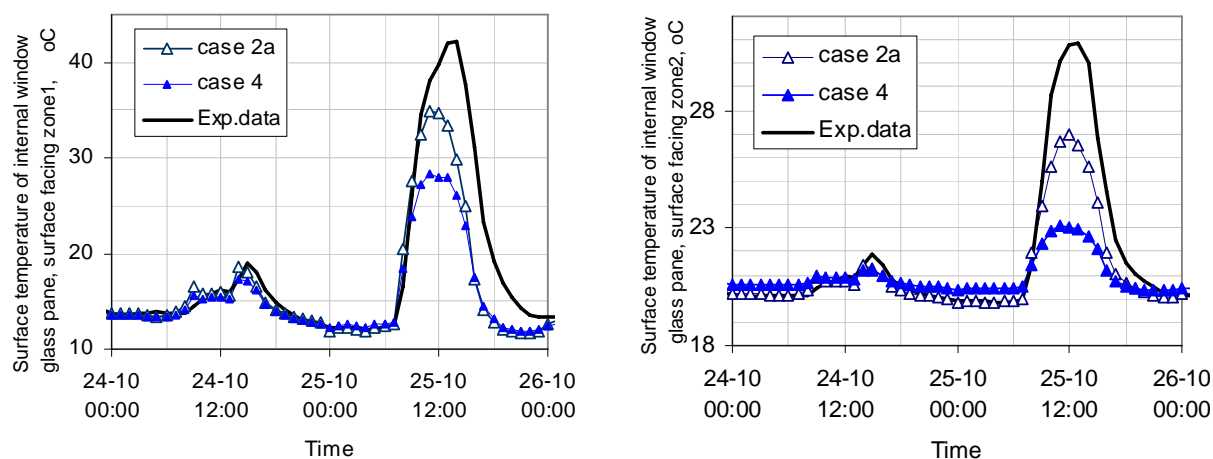
Figure 34. DSF100_e case with VA114 results for sensitivity cases 2a and 4.
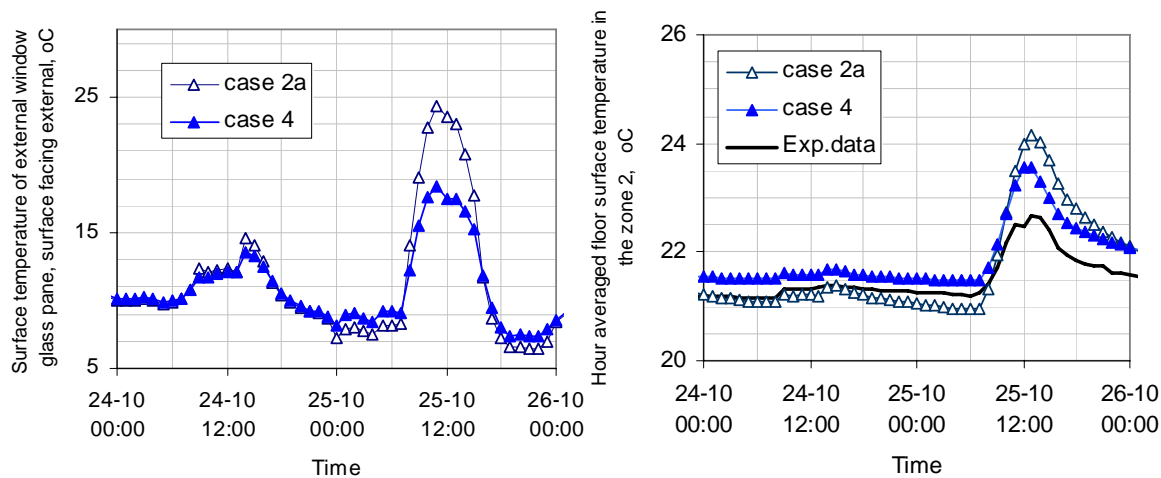
Figure 35. DSF100_e case with VA114 results for sensitivity cases 2a and 4.

When fixing the internal and external longwave radiation exchange in VA114 (as in case 4), the changes are very significant regarding all of the parameters: cooling/heating power (changed by apx. 1.5kW), surface

temperatures (changed by apx. 3-5°C) and air temperature in the DSF (Figure 33-Figure 35). The biggest impact is seen not only for the peak loads, but also the surface temperatures in the night time have changed.

By comparing the results from the case 1 and 5 for ESP-r model, it has already been demonstrated the importance of the external longwave radiation. The above figures confirm the same fact for the VA114 model. However in the case 4 for VA114, both the internal and external longwave radiation was fixed and there were major changes of the glass surface temperature facing zone 2.

It is necessary to mention that the case 4 and 4a were principally different, as in the case 4a, the internal film coefficients were fixed only in zone 2 and varied in the zone 1, while in the case 4 – all of the internal film coefficients were fixed.

5.5 Summary of sensitivity study

In the above studies, the importance of assumptions made towards modelling of the longwave and convective heat transfer was demonstrated with the reference to the case DSF100_e. It was observed that:

- The internal convective heat transfer is of the great importance
- The external convective heat transfer is of minor importance
- Internal longwave radiation heat exchange might be important
- External longwave radiation heat transfer is of the great importance
- The magnitude of changes of the results is huge for the peak cooling load, air temperature and surface temperatures when different assumptions are applied (combined/split treatment of surface heat transfer fixed/variable surface film coefficients)

These findings allow to draw a conclusion that the assumptions towards the surface heat transfer in the model can be crucial for simulation of buildings with double-skin facade. It is necessary to stress that the assumptions must be considered for two levels of detail:

- Separate or combined treatment of surface film transfer
- Fixed or variable surface film coefficients

More attention might be needed when modelling the internal convective heat transfer and longwave radiation heat exchange. Errors may appear in calculations of the peak loads if using fixed combined surface film coefficients. Finally, it is necessary to point out that the best performance, in regard to experimental results, is achieved for a model using split variable surface film coefficients, while the other models may perform well, but only for limited number of parameters.

Thus, the overall summary of these studies show the directions for further improvements which are given below, but more studies are necessary if the guidelines for modelling of DSF are to be prepared.

- Combined treatment of surface film coefficients is too simple and the separate treatment is required
- Application of fixed surface film coefficients together with the separate treatment is also insufficient, but further studies are needed to argue further on this issue.

6. RESULTS FROM THE EMPIRICAL TEST CASES

6.1 Foreword

Results of the empirical validation are reliant on the quality and accuracy in the experimental data. Besides, it was highly essential to obtain the experimental data for the global parameters, such as cooling/heating power in the experiment room, air flow and volume averaged air temperature in the double skin facade cavity.

The detailed description of the experimental test facility and the measurement procedure can be found in [5].

Similar to the comparative validation, the evaluation of the results from the empirical test cases will be performed in the following sections, separated for each test case, with application of three types of visualization:

1. Profiles with the results from the whole period of simulation
2. Profiles for a day with high and a day with low solar irradiation
3. Figure of the average, min and max values over the whole period of simulation

The first method of evaluation is very easy and visual: it gives an overview of the whole situation, and allows the identification of conditions when the model experiences difficulties etc. More details can be seen in the plots made for a day with the high and day low solar radiation. The final evaluation is supported with some statistical data and bar-plots for min, average and max values.

This time the results of simulations are plotted together with the empirical results, when the experimental data are available. Moreover, some statistical analysis is performed for the results of simulations in relation to the experiments.

Minimum	MIN	$Xmin=Min(X_t)$
Maximum	MAX	$Xmax=Max(X_t)$
Average	MEAN	$\overline{X} = \sum_{t=1}^{n} \frac{X_t}{n}$
Difference	DT	$D_t=X_t - M_t$
Difference 5%	DT95	$5\%percentile\ (D_t)$
Difference 95%	DT5	$95\%percentile\ (D_t)$
Average Difference	MEANDT	$\overline{D} = \sum_{t=1}^{n} \frac{D_t}{n}$
Absolute Average Difference	ABMEANDT	$\left|\overline{D}\right| = \sum_{t=1}^{n} \left|\frac{D_t}{n}\right|$
Root Mean Square Difference	RSQMEANDT	$\sqrt{D^2} = \sqrt{\sum_{t=1}^{n} \frac{D_t^{\,2}}{n}}$
Standard Error	STDERR	$\sigma = \sqrt{\frac{1}{n}\sum_{t=1}^{n}(D_t - \overline{D})}$

Where
X_t - predicted value at hour t
M   - measured value at hour t
n   - total hours in period of comparison.
Table 10. Definition of the statistical parameters.

The average values are calculated for the whole period of simulations, even if the average value for solar radiation intensity is considered.

6.2 Investigation of boundary conditions

In order to be able to compare results from the empirical test cases, first, it is necessary to look at the boundary conditions. These are the solar altitude, solar radiation on the double skin facade surface (direct, diffuse and total), solar radiation transmitted into the DSF and into the adjacent experiment room, air temperature in the neighbouring zones, etc. In the test case DSF100_e, the experts were asked to include the solar altitude as an output parameter and there were three programs able to give an access to this data. The comparison plots are included in the following chapters, separately for each test case. Here, the main principles of calculations in the models are discussed and summarised.

Modellers completed their simulations with the Perez model (1990 or 1987) and the circum solar radiation treated as diffuse. The choice of the Perez model was partly made on the basis of previous experience from the comparative validation exercises.

Calculation of the solar irradiation on a surface mainly depends on the solar model used in calculations. The differences between models are often expressed in different treatment of circum solar radiation and in calculations of the diffuse solar radiation, in general. The transmission of solar radiation depends on such factors in the model as:

- Calculation of solar path and path of solar radiation through the building (calculation of sunlit surfaces and surfaces in the shadow)
- Various treatment of diffuse and direct solar radiation (when calculating transmission of solar radiation)
- Level of detail in the window model
- Model for calculation of ground reflected solar radiation
- Incidence angle dependency
- etc.

6.2.1 Transmission of solar radiation

This section is focused on investigation of the window model used in different software. The reason for that is the variety of involved parameters and software limitations. Although the experimental data to characterise the spectral properties of the glazing are provided in the specification, it is seldom that the building simulation software is integrated with the routine for the advanced calculations of optical properties, such as incidence angle dependency of solar transmission, reflection and absorption. Some of the tools include only the intermediate complexity level of window model, using the fixed/default function of incidence in the program instead of provided in the specification glazing properties for normal angle of incidence. However, a number of programs allow manual definition of function of angle of incidence. In the latter case, the modellers have used optical properties as a function of angle of incidence using results of WIS calculations attached in Appendix IV.
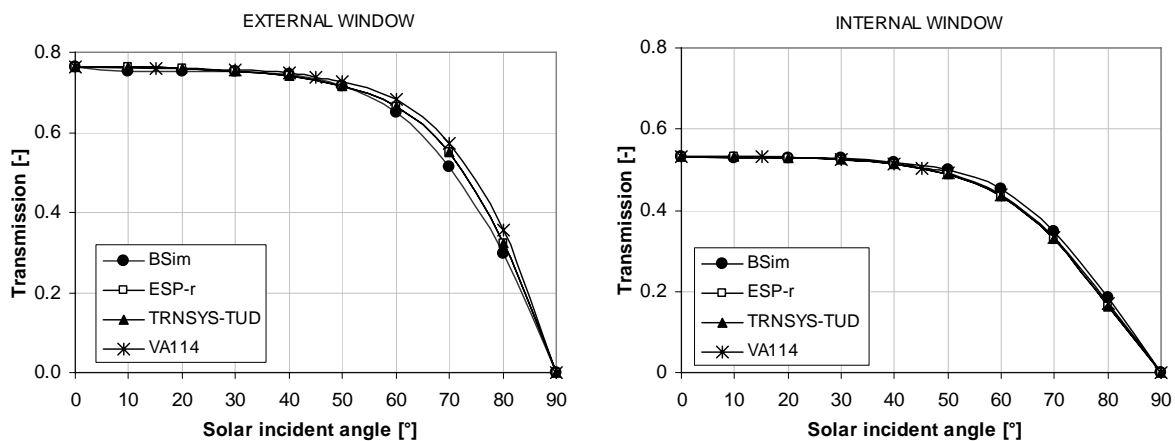
Figure 36. Transmission of direct solar radiation. External window (left). Internal window (right).

The transmission and reflection of solar radiation are user defined functions of solar incidence in TRNSYS-TUD and ESP-r. In the Figure 36, the input data in the models are compared, and a good agreement can be seen of the optical properties used in the models. Small deviations are present only for VA114 and BSim model, when described solar transmission property of the external window at the large angles of incidence, what is of minor importance.

Regarding VA114 and BSim, the g-value for the 45° and 90° angle of incidence, correspondingly, is used as input and then a default function is used to calculate the g-value, depending on the angle of incidence.

Another important issue in calculations of transmitted solar radiation is the form that the solar energy takes when passing the first bounce with the glass (direct or diffuse). This is not a physical question, as the form of solar energy in a software tool, direct or diffuse, depends purely on the assumptions in the mathematical model of simulation tool. Since various software tools treat the diffuse and direct solar radiation separately, when calculating the transmission or distribution of solar radiation (Table 11), then different calculation procedures are used. And, these procedures depend on whether the solar radiation is diffuse or direct. Therefore, the differences in predictions of transmitted or distributed solar radiation will depend on the level of detail in each of these calculations. As can be seen from the table, the solar radiation is treated identically in VA114 and BSim. In TRNSYS-TUD, the solar radiation is treated as diffuse after the second bounce with the glass and in ESP-r, it is treated as diffuse already after the first bounce. The differences in these assumptions may lead to disagreements when surface temperatures are calculated in the periods when the solar radiation is present.

EXTERNAL ENV.		ZONE 1	INTERNAL ENV.
BSim	direct solar	distributed to surfaces as direct	distributed to surfaces as direct
	diffuse solar	distributed to surfaces as diffuse	distributed to surfaces as diffuse
VA114	direct solar	distributed to surfaces as direct	distributed to surfaces as direct
	diffuse solar	distributed to surfaces as diffuse	distributed to surfaces as diffuse
ESP-r	direct solar	distributed to surfaces as direct	distributed to surfaces as direct
	diffuse solar	distributed to surfaces as diffuse	distributed to surfaces as diffuse
TRNSYS-TUD	direct solar	distributed to surfaces as direct	distributed to surfaces as diffuse
	diffuse solar	distributed to surfaces as diffuse	distributed to surfaces as diffuse

Table 11. Form of solar radiation after when passes through the glass.

Following Table 12 is prepared in order to make a clear picture of solar calculations in the models. Most of it has already been illustrated in Figure 36, except for assumptions towards the transmission of the diffuse solar radiation. In ESP-r model, the transmission of the diffuse solar through the external window will be approximately 9% and 3% higher than the once calculated by BSim and VA114 correspondingly.

Property	BSim	VA114	ESP-r	TRNSYS-TUD
Transmission of the direct solar radiation into the zone 1	$f(\alpha)$*	$f(\alpha)$*	$f(\alpha)$	$f(\alpha)$
Transmission of the direct solar radiation into the zone 2	$f(\alpha)$*	$f(\alpha)$*	$f(\alpha)$	$f(\alpha)$
Transmission of the diffuse solar radiation into the zone 1	$f(60°)$	$f(58°)$	$f(51°)$	$f(const)$

* - default function of incidence is used

α- an incidence angle

Table 12. Assumptions for solar transmission in the models.

The spectral data to evaluate the optical properties of the ground and internal constructions were provided in the empirical specification. However, due to the limitations in the programs, different values from the specification have been used (Table 13).

Comparison of the input parameters in the empirical models (Table 13) demonstrates that the ground reflectivity and longwave emissivity is almost identical for all of the models. Serious limitation is demonstrated for BSim, as all of solar radiation striking the internal surface is fully absorbed, this will lead to overestimation of solar gains in the zones and finally to overestimation of energy consumption for cooling.

Property	BSim	VA114	ESP-r	TRNSYS-TUD
Ground reflectivity	0.1	0.1	0.1	0.08
Shortwave reflectivity of constructions in zone 1	0*	0.66	0.66	0.66
Shortwave reflectivity of constructions in zone 2	0*	0.66	0.66	0.66
External shortwave reflectivity	0.6	0.6	0.6	0.6
Longwave emissivity of the internal surfaces	0.88	0.88	0.88	0.88
External longwave emissivity	0.88	0.88	0.88	0.88

* All solar radiation striking the surface is fully absorbed

Table 13. Summary of shortwave and longwave properties in the models.

Another issue that can have a significant impact on calculation of transmitted solar radiation in the models is the assumption made towards the geometry of windows in the model. It is common to simplify complex geometry when set-up the model. The geometry of the DSF in the empirical test case specification (Appendix II) is complex: there are 9 windows, containing transparent part (glazing) and nontransparent part (window frame). All of the modellers made their assumptions regarding the simplification of the geometry: the areas of the window frame and glazing were kept according to the specification, but the geometry definition had been changed (Figure 37). Since the solar path during the day is calculated in all of the models, then the distribution of shadow and the distribution of the direct solar radiation in all of the models will be different from the actual empirical case and, sometimes, can be overestimated.
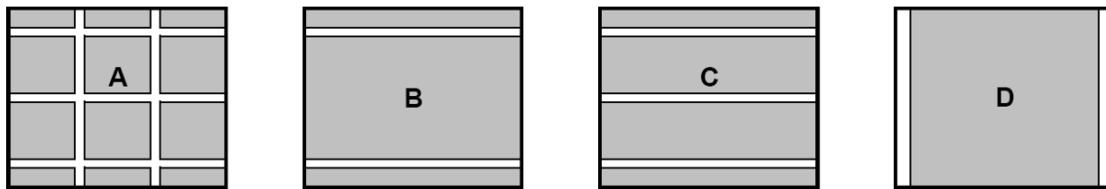
Figure 37. Schematics of assumptions made towards the geometry in the models. A - actual geometry in the specification. B - ESP-r model. C - BSim and TRNSYS-TUD model. D - VA114 model.

DSF100_e
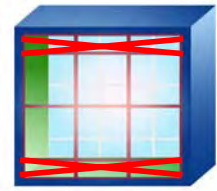
6.3   Test case DSF100_e

In this case, a complex convective flow field can develop in the DSF cavity, which can be significant for the final result. In order to assess the impact of such a complex cavity flow, the calculation tool may require an advanced convection model: model with the dynamic calculation of the convection heat transfer surface coefficients, calculations with more than one temperature node in the cavity, etc. The maximum level of detail can be obtained by CFD.

The experts in this empirical exercise have not used the CFD-calculations, their flow models are not able to count on the mass flow rate in the convective boundary layer and the calculation of the convective surface heat transfer coefficient is reasonably simplified. In the test case DSF100_e, the double skin facade acts as a thermal zone without the mass exchange. Still, the heat transfer processes are not straight forward, as it is seen from the examples in section 5.4, the long wave radiation heat flows and internal convective flows can be extremely important. Then the question is: how good performance of a simulation tool can be achieved using these common building simulation software tools?

6.3.1 Solar altitude
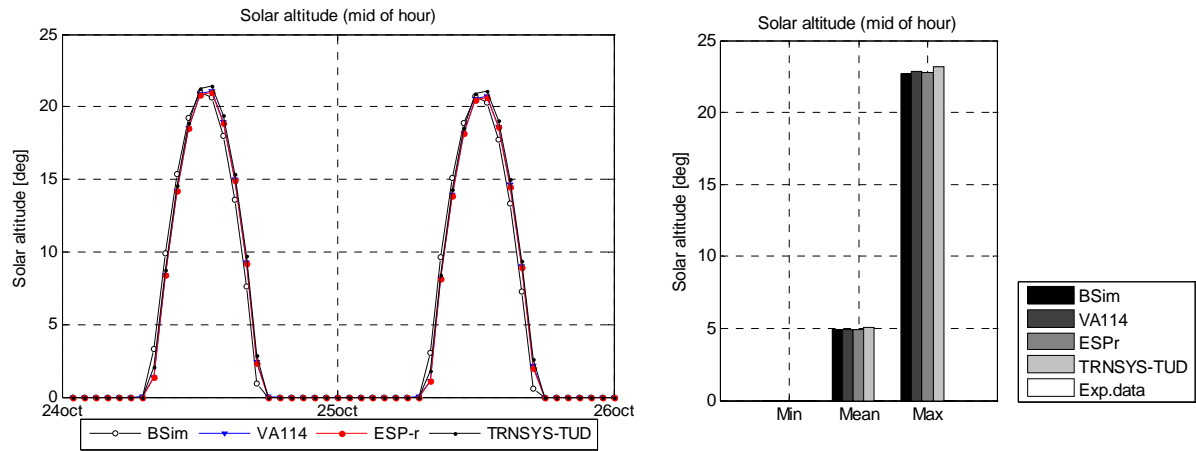
Figure 38. Solar altitude. Test case DSF100_e.

Solar altitude	BSim	VA114	ESP-r	TRNSYS-TUD
MIN, deg	-	0	0	0
MAX, deg	-	22.8	22.8	23.2
MEAN, deg	-	4.9	4.9	5.1

The solar height is available only for three programs: VA114, TRNSYS-TUD and ESP-r. From the above plots and the table, it is noticeable that there are minor differences in calculation of the solar height: TRNSYS-TUD predictions are slightly higher. Still, the instance of sunset and sunrise for TRNSYS-TUD is calculated the same as for VA114 and ESP-r.

6.3.2 Direct solar irradiation
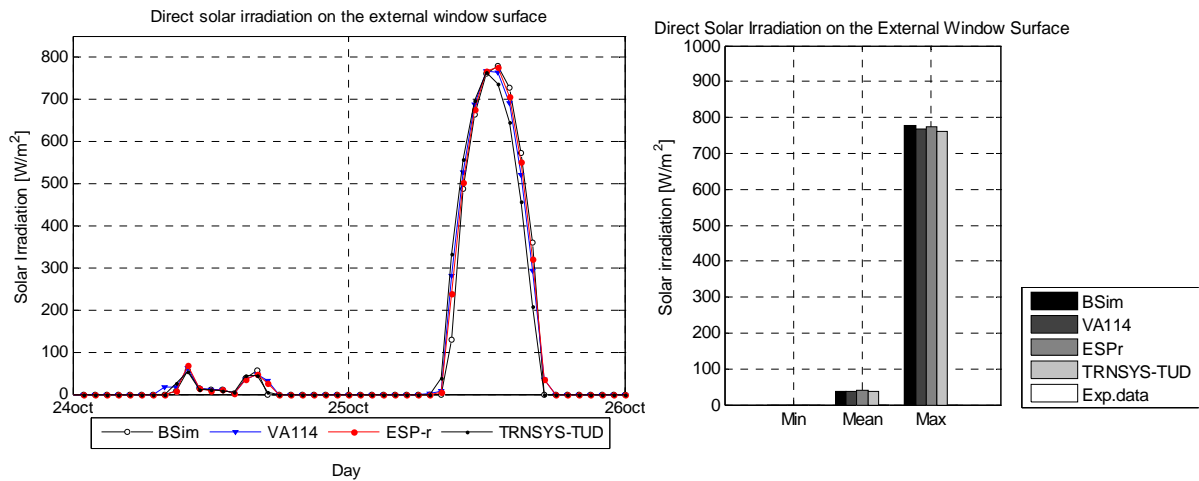
Figure 39. Direct solar irradiation on the external window surface. Test case DSF100_e.

Direct solar irradiation on ext window surface	BSim	VA114	ESP-r	TRNSYS-TUD
MIN, W/m^2	0	0	0	0
MAX, W/m^2	779	767	775	762
MEAN, W/m^2	37	39	40	38

Generally good agreement is seen between the models. It seems that the maximum of the direct solar radiation in TRNSYS-TUD is calculated for an hour earlier than in other models. This, however, is not a rule, as this episode does not repeat in the other days.

44

6.3.3   Diffuse solar irradiation
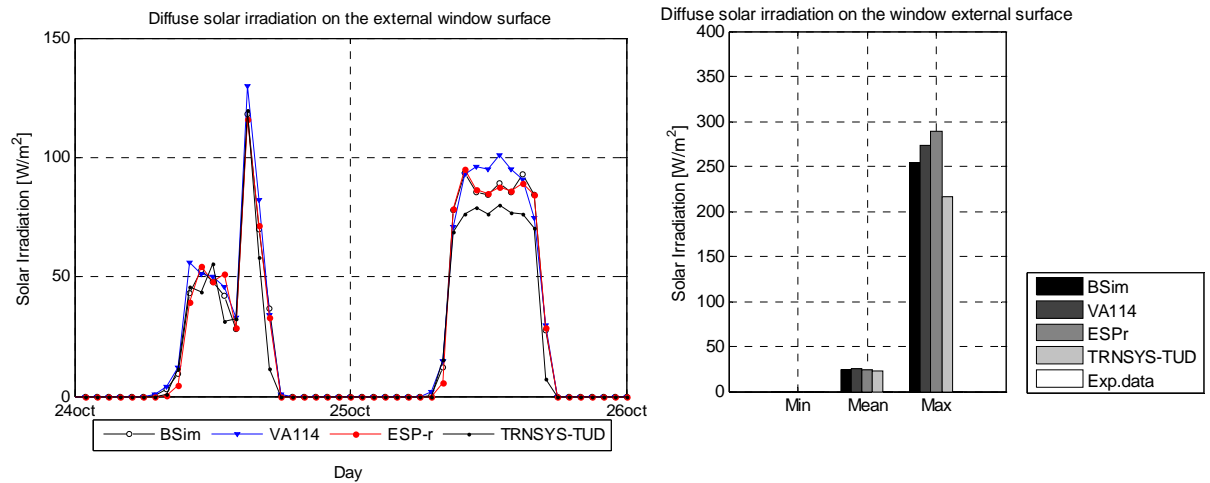
Figure 40. Diffuse solar irradiation on the external window surface. Test case DSF100_e.

Diffuse solar rad. on the window ext. surface	BSim	VA114	ESP-r	TRNSYS-TUD
MIN, W/m^2	0	0	0	0
MAX, W/m^2	254	274	290	217
MEAN, W/m^2	24	25	24	22

Prediction of the diffuse solar radiation also proves to be in agreement for the mean values. It is possible to see a certain tendency between the mean values, where ESP-r and BSim are very close, TRNSYS-TUD is slightly lower and VA114 is slightly higher than ESP-r and BSim. Looking upon the plot with the whole period of measurement, one can notice highly varying cloud distribution in the sky and, this can be a reason for disagreements between the programs when calculating the maximum values. Also, one should consider the limitations in modelling actual environment around the building that is important for the distribution of diffuse solar radiation on the building facades.

6.3.4   Total solar irradiation
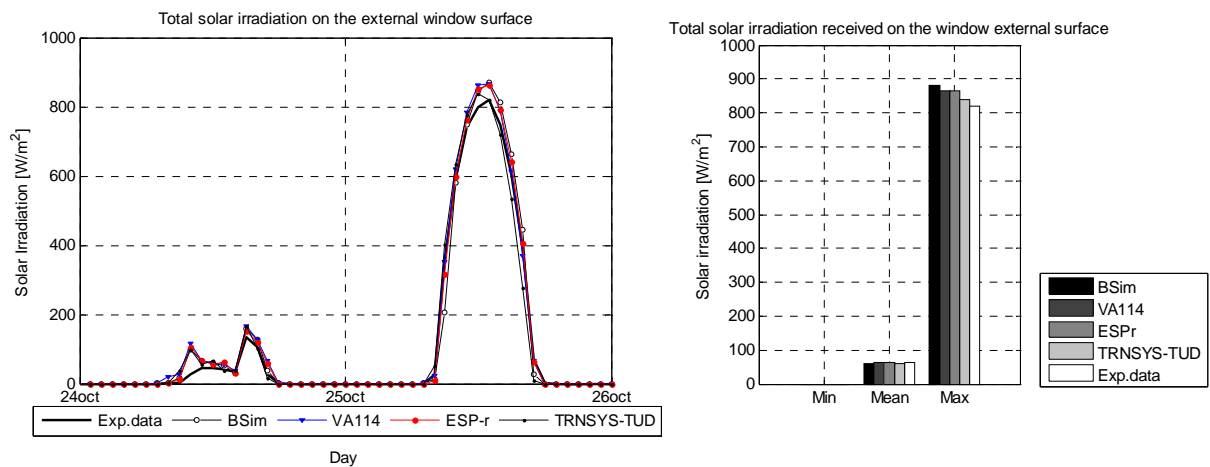
Figure 41. Total solar irradiation on the external window surface. Test case DSF100_e.

Total solar rad. on ext window surface	BSim	VA114	ESP-r	TRNSYS-TUD	Exp.
MIN, W/m^2	0	0	0	0	0
MAX, W/m^2	882	866	864	838	821
MEAN, W/m^2	61	64	63	61	65
DT95, W/m^2	-4	0	-7	-33	
DT5, W/m^2	44	45	44	50	
MEANDT, W/m^2	5	7	6	3	
ABMEANDT, W/m^2	8	9	9	11	
RSQMEANDT, W/m^2	21	19	21	27	
STDERR, W/m^2	20	18	20	27	

In general, one can say that the programs agree very well on calculation of the total solar radiation on the external window surface when comparing the mean values. TRNSYS-TUD has the widest spread of error, as DT5=50 W/m^2 and DT95=-33 W/m^2, what is less in the other models. Comparing the maximum values, the experimental data seem to be slightly lower and the disagreements are more pronounced. This is partly caused by differences in calculation of the diffuse solar radiation on the window surface and also due to the limitations in modelling actual environment around the building.

Talking about the experimental data, it is necessary to mention that only the total solar irradiation was measured, thus there is no access to the direct and diffuse components on the vertical surface of the DSF. At the same time, the ground reflection in the models was a fixed value, which can differ from the true experimental conditions, as only 0.5 of the DSF view factor was covered with the ground carpet. Moreover, the measurement accuracy can also have an impact, especially because of the often rain drops on the top of the pyranometer.

6.3.5 Solar radiation transmitted into the zone1 (first order of solar transmission)
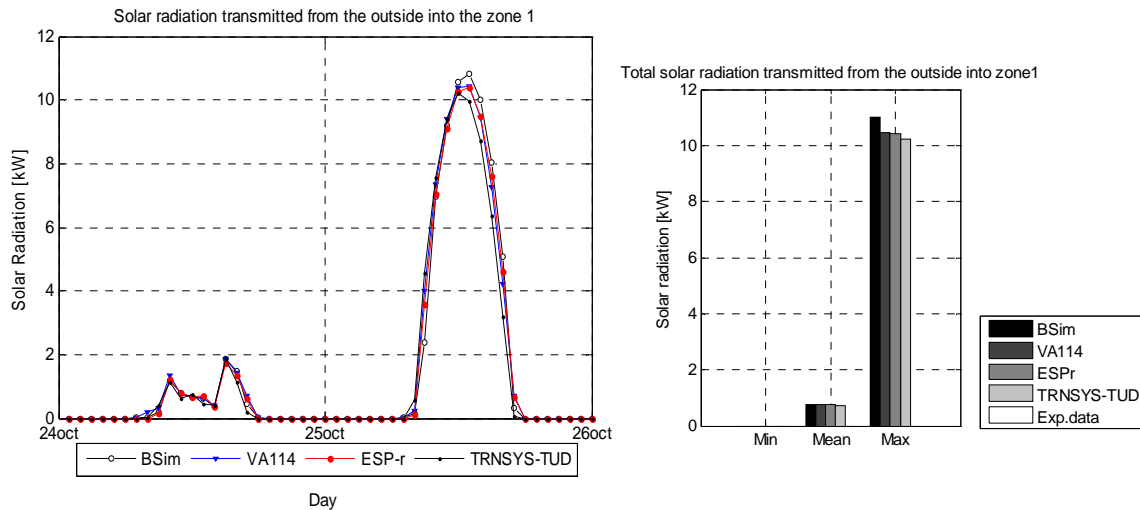
Figure 42. Solar radiation transmitted into the zone1 (first order of solar transmission). Test case DSF100_e.

Solar rad. transmitted into the zone 1	BSim	VA114	ESP-r	TRNSYS-TUD
MIN, kW	0	0	0	0
MAX, kW	11.02	10.45	10.42	10.21
MEAN, kW	0.74	0.75	0.74	0.71

Similar to calculations of the total solar radiation on the external surface of the DSF, the transmission of solar radiation into the DSF (zone 1) showed good correspondence of the mean values. Again, BSim calculates the maximum values, which are the consequence of calculated maximum incident solar radiation.

6.3.6 Solar radiation transmitted from zone 1 into the zone 2 (first order of solar transmission)
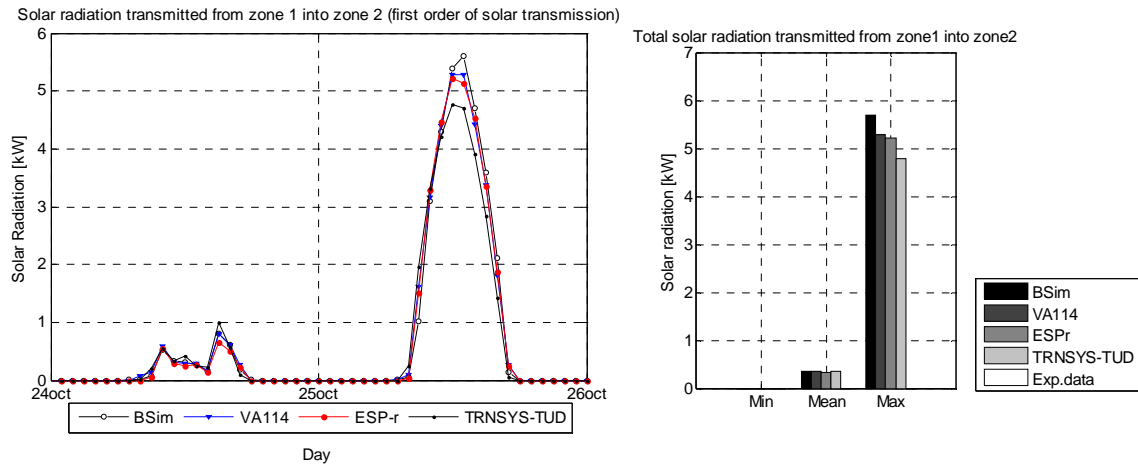
Figure 43. Solar radiation transmitted from zone 1 into the zone 2 (first order of solar transmission). Test case DSF100_e.

Solar rad. transmitted into the zone 2	BSim	VA114	ESP-r	TRNSYS-TUD
MIN, kW	0	0	0	0
MAX, kW	5.70	5.29	5.22	4.78
MEAN, kW	0.34	0.34	0.33	0.35

Comparative validation of the models is not a task of this exercise, but this is an important procedure when evaluating the modelling of the boundary conditions in a model. Transmission of the solar radiation is calculated with good agreement between the programs when comparing the mean values, while the disagreements in the maximum values are present. These are consistent with the calculations of the total incident solar radiation on the facade and also with solar radiation transmitted into the zone 1. Also the transmission/absorption property of the glazing was modelled almost identically.

So the main reasons of disagreements in the maximum values are, first of all tracked, from the differences in calculation of the incident solar radiation on the double-skin facade. Next the assumptions towards the distribution, absorption and reflection of solar radiation in the zone 2 are also a very important issue for the discrepancies in the maximum values (see section 6.2.1).

It is difficult to quantify the impact of one or another issue which was brought to attention in the section 6.2.1. However, the fact that in BSim model, all solar radiation striking the surfaces in the zone 1 and 2 is absorbed, will cause the overestimation of cooling loads not only in the zone 2, but especially in the peak loads.

47

6.3.7 Summary over simulation of boundary conditions

One of the most essential measures for the validation of simulation programs for buildings with the double skin facade is their ability to predict air temperature and air flow in the double facade cavity. The accuracy of these predictions is then reflected in the cooling/heating power in a neighbouring zone 2. Cooling/heating power in that zone is the main characteristic of the double-skin façade performance and also the consequence for the energy performance of the whole building. Therefore, the differences in the boundary conditions, such as solar radiation incident on the DSF surface, can be crucial. Glazing area of the double skin facade windows at the outer skin is 16.158m^2 and the differences in predictions of solar irradiation of ±100 W/m^2 will result in ±1.6 kW difference in received solar radiation on the glazing surface.

For the defined empirical test case DSF100_e, the solar altitude was verified. It was unfortunate that it was possible to assess it only for three programs (TRNSYS-TUD, ESP-r and VA114).

In further investigations, the direct and diffuse solar irradiation has demonstrated a degree of deviations in the maximum values, which are then traced through all of the results and became, probably, the main cause for the differences in solar loads to zones 1 and 2.

By any means, calculation of the incident, transmitted and distributed solar radiation is not the focus of these empirical exercises. However, the results of these calculations are the tool and the quality measure for completing the exercises. And, these were calculated with sufficient accuracy.

6.3.8 Air temperature in the double facade cavity
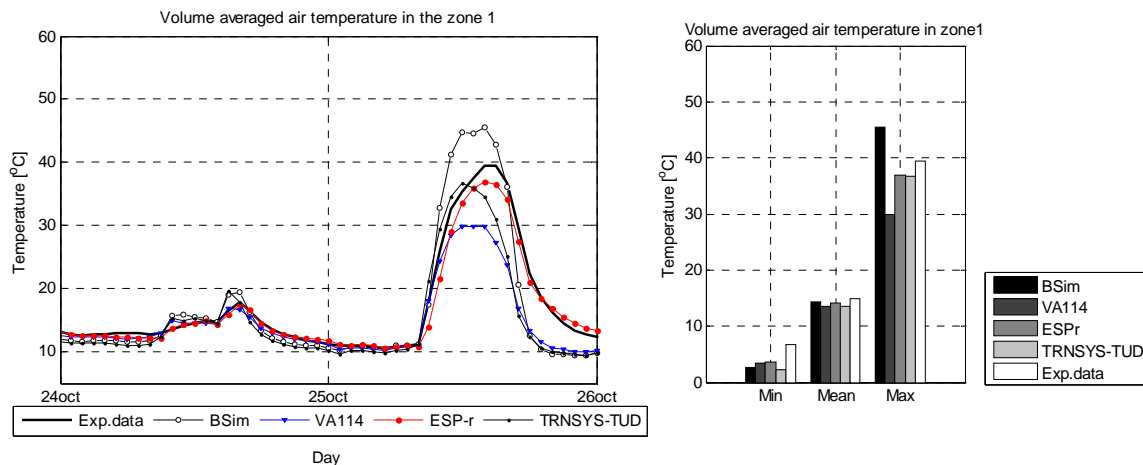
Figure 44. Volume averaged air temperature in the double facade cavity. Test case DSF100_e.

Volume averaged air temperature in zone 1	BSim	VA114	ESP-r	TRNSYS-TUD	Exp.
MIN, °C	2.72	3.32	3.55	2.23	6.73
MAX, °C	45.49	29.91	36.92	36.74	39.48
MEAN, °C	14.35	13.49	14.14	13.54	14.96
DT95, °C	-2.95	-5.21	-2.55	-4.26	
DT5, °C	5.15	0.61	0.98	3.01	
MEANDT, °C	-0.17	-0.92	-0.51	-0.90	
ABMEANDT, °C	1.57	1.13	0.82	1.78	
RSQMEANDT, °C	2.58	2.34	1.42	2.64	
STDERR, °C	2.58	2.16	1.32	2.49	
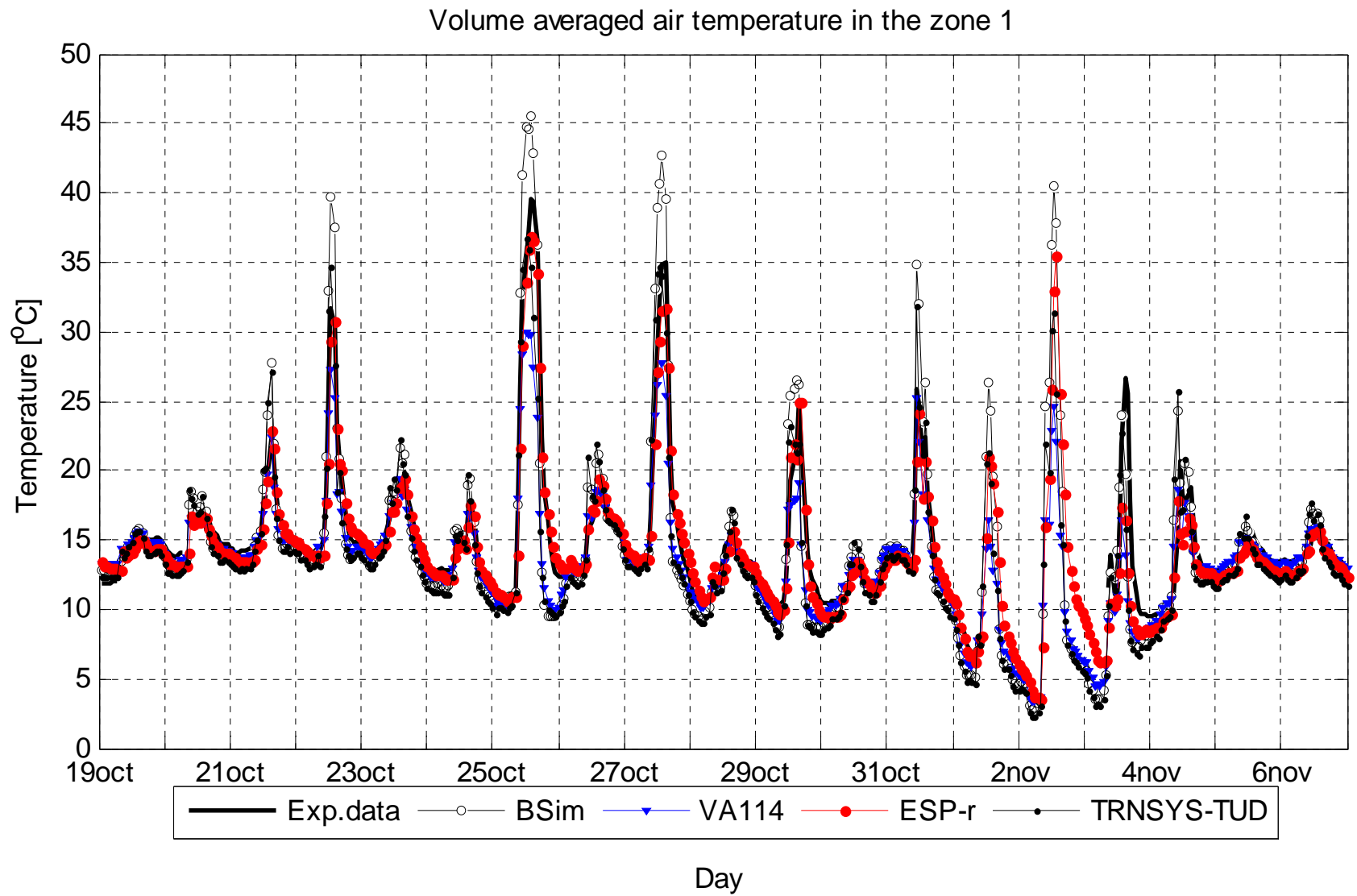
Figure 45. Volume averaged air temperature in the DSF cavity. Test case DSF100_e.

The bar-plot, Figure 44, demonstrates that the average values are in a satisfactory agreement between the calculations and experimental data. However, the maximum values are represented by three groups of the results [ESP-r, TRNSYS-TUD] in a good agreement with the experimental data, BSim with overestimated temperatures and VA114 with underestimated ones.

From the above plots, it is also obvious that solar radiation has a great impact on the air temperature, as all the results from all models fit well with the experiments in a cloudy day and have a spread of 10-20°C for a clear day. Remarkable is that ESP-r agrees very well with the dynamics of the air temperature measured in the cavity (also lowest STDERR), especially in the afternoons, while all of the other models show remarkable temperature drop. This cannot be caused by differences in assumptions regarding surface heat transfer, as according to the sensitivity study the shape of the temperature profile in ESP-r model is independent of that (see Figure 30). So, it is reasonable to assume that the time constant of zone 1 in ESP-r model differs from the other models.

Importance of the assumption made towards the heat transfer at the surface has already been investigated in section 5.4, which can, probably, explain the spread of the results. According to Table 4, all of the models split the convective and radiative heat transfer and include variable longwave radiation heat exchange at the surfaces, which depend on the surface temperature, emissivity of the constructions and geometry. Also, it was shown that the convective heat transfer at the surface facing external has a minor importance for calculation of DSF performance. Thus, the most significant difference between BSim, VA114, ESP-r and TRNSYS-TUD model (with regard to the heat transfer at the surface) is the assumption made towards the internal convective heat transfer coefficient. BSim and ESP-r use a variable convective heat transfer coefficient, which depends on the temperature difference. BSim and ESP-r result in the higher air temperatures in the periods of peak solar radiation. TRNSYS-TUD and VA114 use the fixed convective heat transfer coefficients ($4.4 W/m^2 K$ and $3 W/m^2 K$ correspondingly). Using higher convective heat transfer in the TRNSYS-TUD model compared to VA114, the air temperature in the zone 1 by TRNSYS-TUD fits well with the experimental data, while in the case without any solar radiation, all models are in a good agreement. Then the question is: what are the convective processes that take place in the DSF? Is it possible to develop any guidelines for the assessment of the convective processes in DSF?

The main difficulties experienced by the models are for the periods with the peak loads in solar radiation, and then the air temperature is underestimated by all of the models except for BSim.

With regard to the table of statistics, one can note that the mean error (MEANDT) is always with the minus sign, which denotes that the measured values are generally higher than the calculated ones. It is worth mentioning that glass surface temperatures are difficult to measure accurately because of the difficulty in completely excluding solar radiation effects on the sensors. The uncertainty of the measurement due to the solar radiation is minimised by shielding of the sensor explained in reference 5.

6.3.9 Temperature of the internal window glass surface facing zone 2
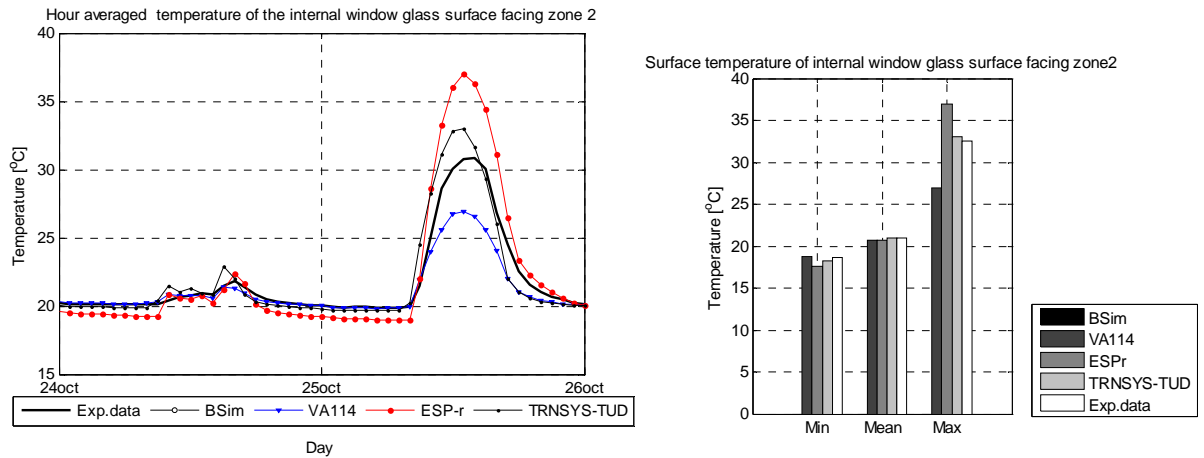
Figure 46. Temperature of the internal window glass surface facing zone 2. Test case DSF100_e.

Temperature of internal window glass surface facing zone 2	BSim	VA114	ESP-r	TRNSYS-TUD	Exp.
MIN, °C		18.76	17.57	18.26	18.61
MAX, °C		26.95	36.99	32.99	32.50
MEAN, °C		20.65	20.76	20.98	20.99
DT95, °C		-2.62	-1.02	-0.99	
DT5, °C		0.23	3.08	1.91	
MEANDT, °C		-0.34	-0.23	-0.01	
ABMEANDT, °C		0.44	0.92	0.53	
RSQMEANDT, °C		1.06	1.27	0.94	
STDERR, °C		1.00	1.25	0.94	

Temperature of the internal window glass surface faces the invented occupied zone and therefore had an impact on perception of comfort in the zone. From this point of view, this is an important parameter for empirical validation, as it is necessary that the building simulation tool is reliable when the comfort conditions in a building are evaluated.

Since the surface temperature of the glazing in a DSF building is very sensitive to the surface heat transfer coefficients used, then the issue of comfort can be difficult to deal with. According to the statistical data TRNSYS-TUD has the best, but not sufficient enough, agreement with the experimental data (error in peak loads is apx. 3°C).
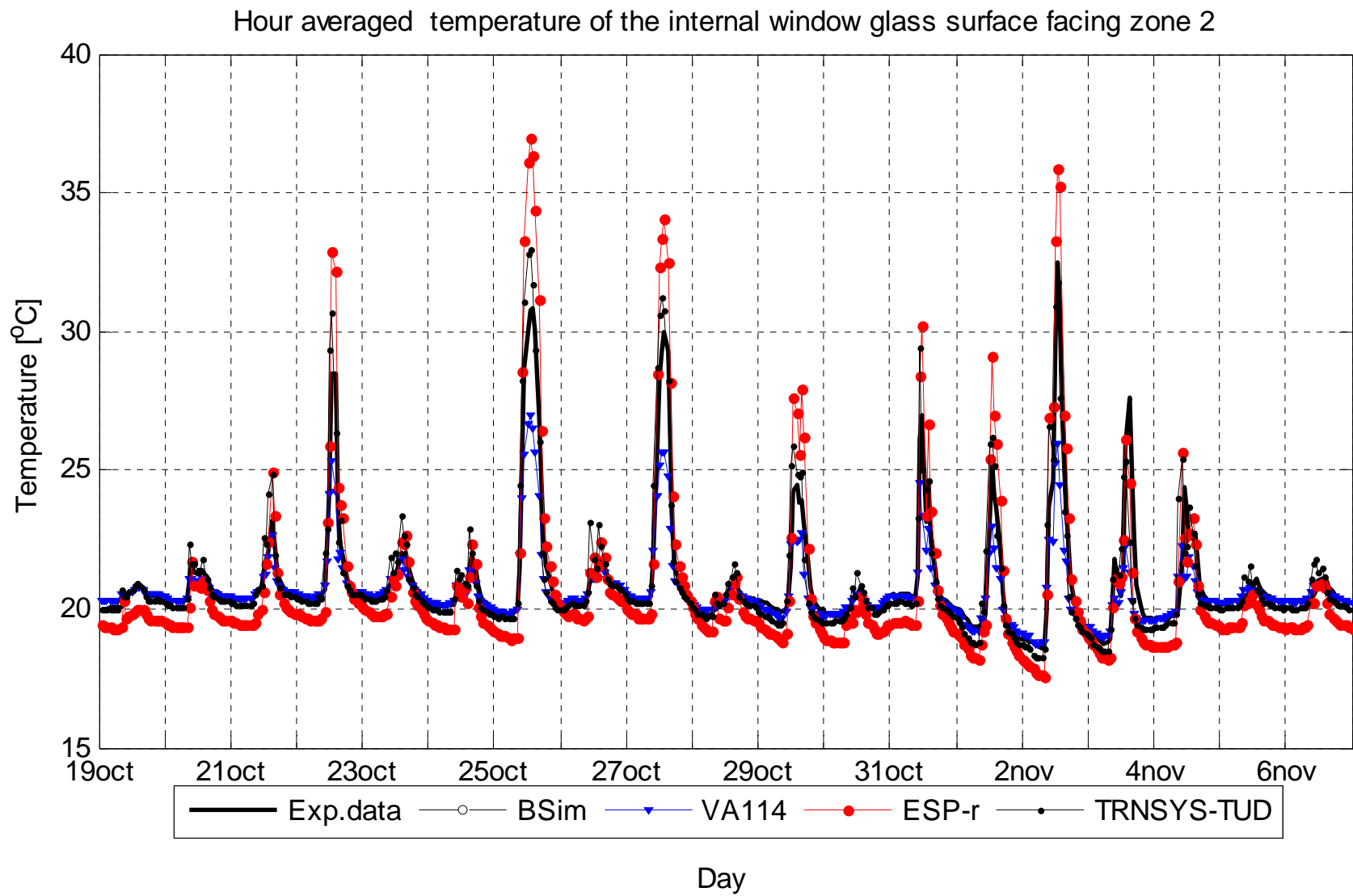
Figure 47. Temperature of the internal window glass surface facing zone 2. Test case DSF100_e.

6.3.10   Cooling/heating power in the zone 2
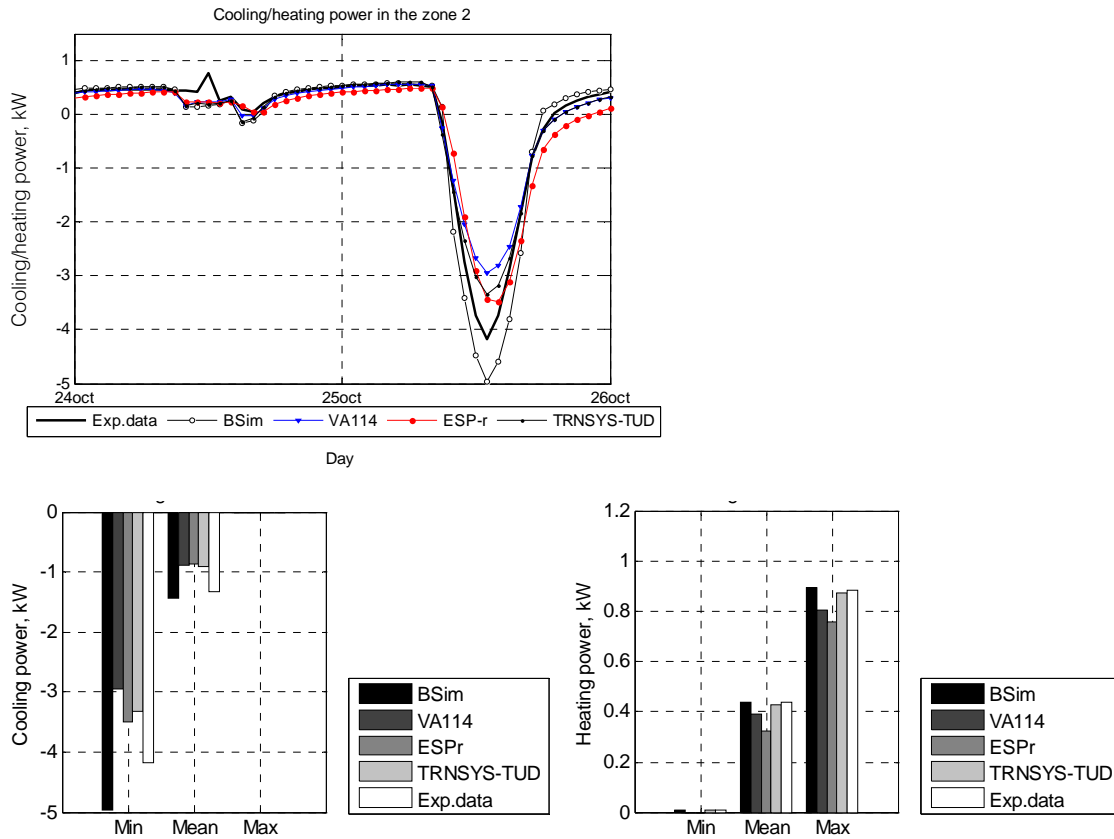
Figure 48. Cooling/heating power in zone 2. Test case DSF100_e.
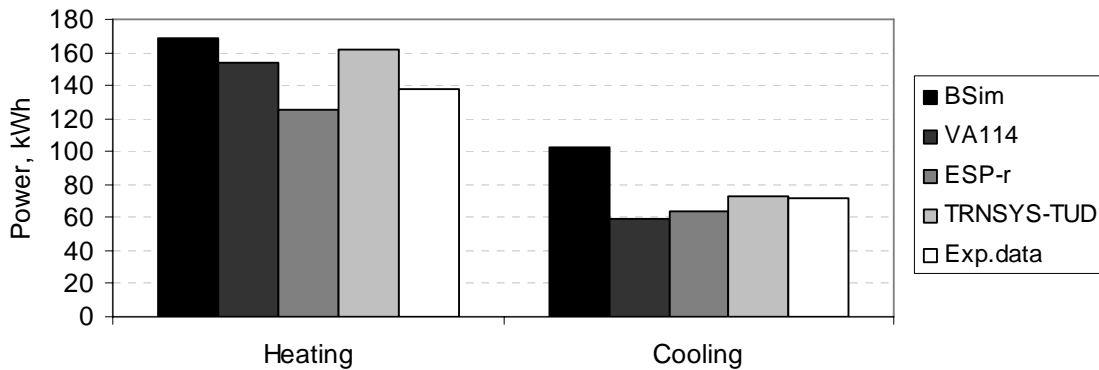
Figure 49. Total cooling/heating power in zone 2. Test case DSF100_e.

The above plot for the total cooling and heating is not exactly sufficient, as there were periods with the experimental data lacking, which resulted in the decreased total cooling/heating power in the experimental results, compared with simulations.

Cooling power in zone 2	BSim	VA114	ESP-r	TRNSYS-TUD	Exp.
MIN, kW	-4.97	-2.94	-3.49	-3.33	-4.18
MAX, kW	-0.02	0.00	0.00	-0.02	0.00
MEAN, kW	-1.44	-0.88	-0.86	-0.91	-1.33
DT95, kW	-0.92	-0.15	-0.49	-0.32	
DT5, kW	0.14	1.17	1.16	0.83	
MEANDT, kW	-0.45	0.32	0.26	0.13	
ABMEANDT, kW	0.47	0.37	0.43	0.27	
RSQMEANDT, kW	0.56	0.54	0.55	0.37	
STDERR, kW	0.35	0.44	0.49	0.35	

Considering the statistical analysis, most of the models underestimate the cooling power into the zone (positive MEANDT). It is characteristic that BSim predicts the highest cooling power, what is consistent with overestimation of the air temperature in the DSF cavity and, also, due to the fact that all solar radiation approaching the internal surfaces in the model is fully absorbed.

It is noticeable that the shape/slope of the ESP-r profile for cooling load in the afternoon of 25th of October is especially different from one for BSim and slightly different from one for TRNSYS-TUD and VA114 (see figure below). This behaviour of the plot is similar to the ESP-r temperature profile in the cavity for the same date. Once more these plots indicate a possibility of differences in the time constant between the models.

Heating power in zone 2	BSim	VA114	ESP-r	TRNSYS-TUD	Exp.
MIN, kW	0.01	0.00	0.00	0.01	0.01
MAX, kW	0.90	0.81	0.76	0.88	0.89
MEAN, kW	0.44	0.39	0.33	0.43	0.44
DT95, kW	-0.13	-0.13	-0.29	-0.15	
DT5, kW	0.12	0.03	0.04	0.08	
MEANDT, kW	0.00	-0.06	-0.12	-0.03	
ABMEANDT, kW	0.06	0.07	0.13	0.06	
RSQMEANDT, kW	0.09	0.09	0.16	0.09	
STDERR, kW	0.09	0.07	0.10	0.08	

A great improvement is seen in calculation of the heating power after the steady state simulation had been completed and all of the models were modified to include the thermal bridge losses.
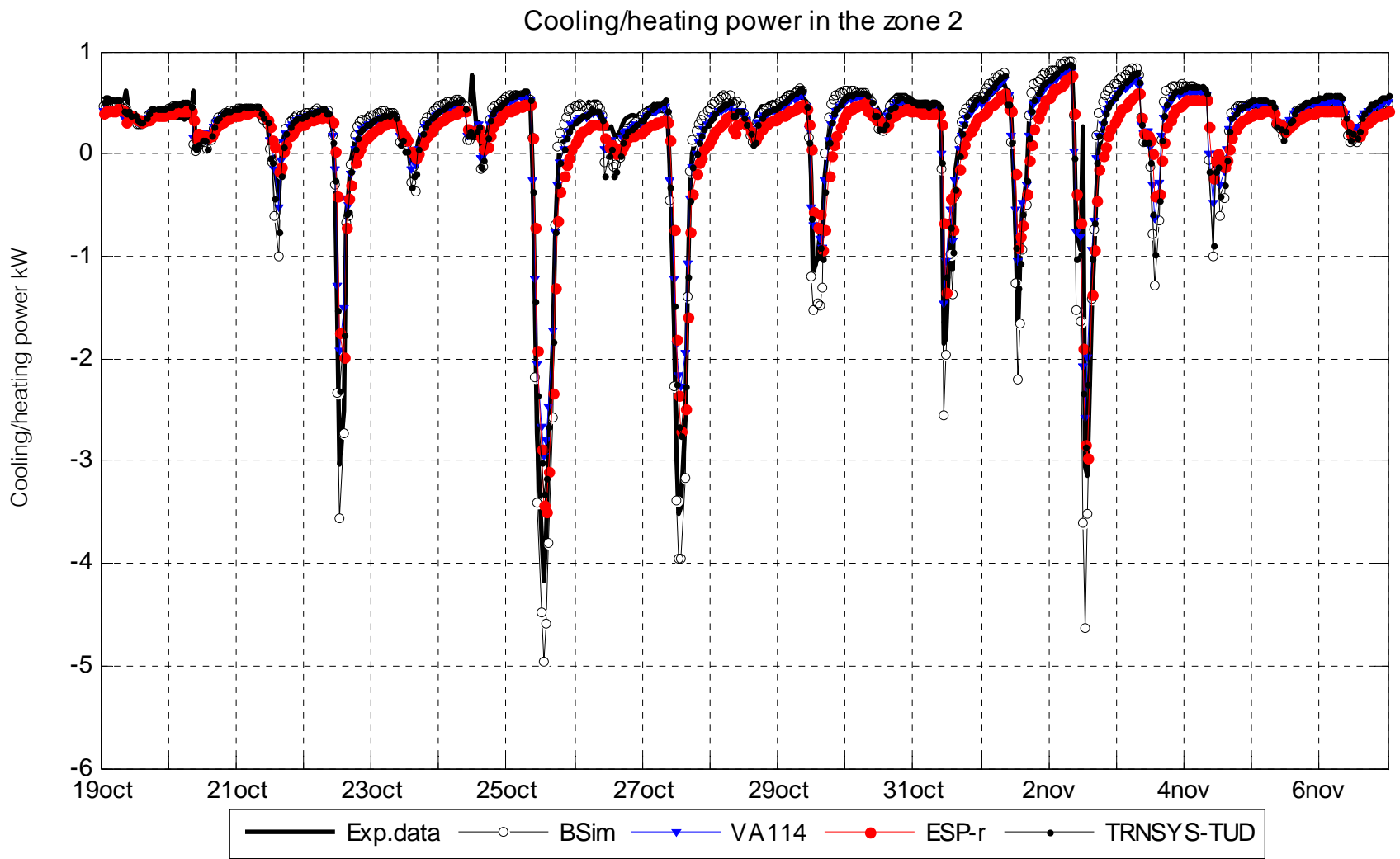
Figure 50. Figure 48. Cooling/heating power in zone 2. Test case DSF100_e.

DSF200_e

6.4   Test case DSF200_e

In this test case the most complex phenomenon of the double facade cavity is investigated – the naturally ventilated double skin facade, which includes impact both from the buoyancy and wind forces. The ventilation strategy in this test case belongs to the single sided ventilation with the openings at different levels.

6.4.1   Direct solar irradiation
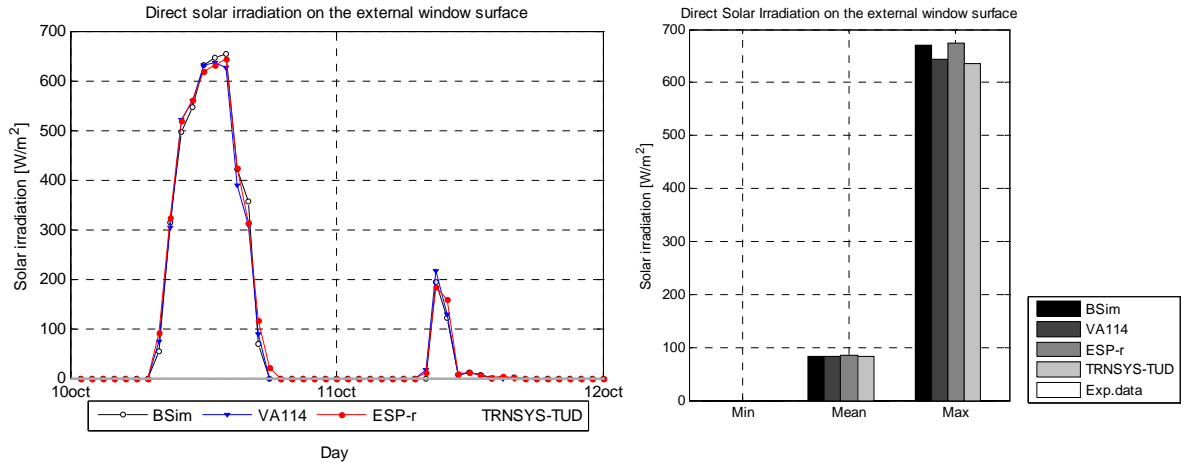
Figure 51. Direct solar irradiation on the external window surface. Test case DSF200_e.

Direct solar irradiation on ext window surface	BSim	VA114	ESP-r	TRNSYS-TUD
MIN, W/m^2	0	0	0	0
MAX, W/m^2	670	643	675	635
MEAN, W/m^2	83	84	84	82

6.4.2   Diffuse solar irradiation
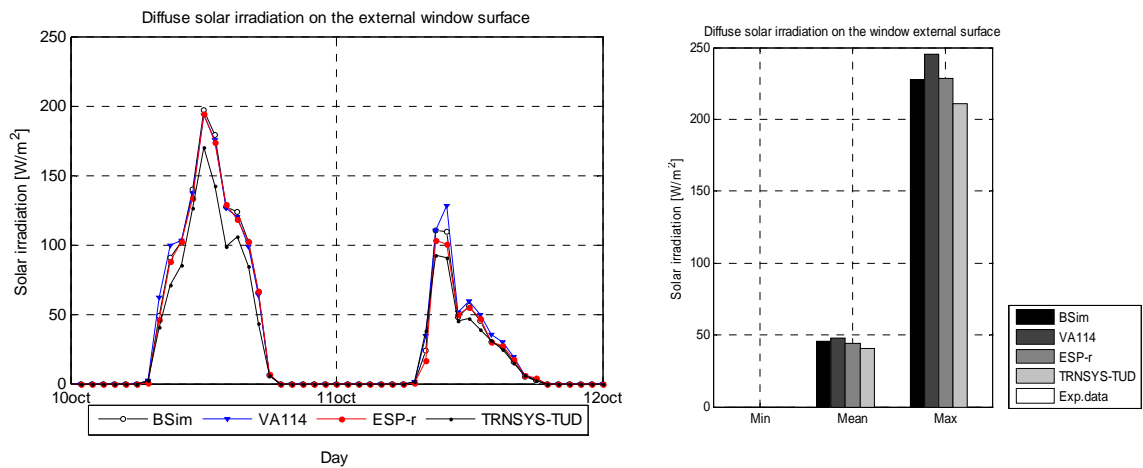
Figure 52. Diffuse solar irradiation on external window surface. Test case DSF200_e.

Diffuse solar irradiation on the window ext. surface	BSim	VA114	ESP-r	TRNSYS-TUD
MIN, W/m^2	0	0	0	0
MAX, W/m^2	228	245	229	211
MEAN, W/m^2	46	48	45	41

Perez model is used in all models for calculations of the diffuse solar radiation distribution.

6.4.3 Total solar irradiation
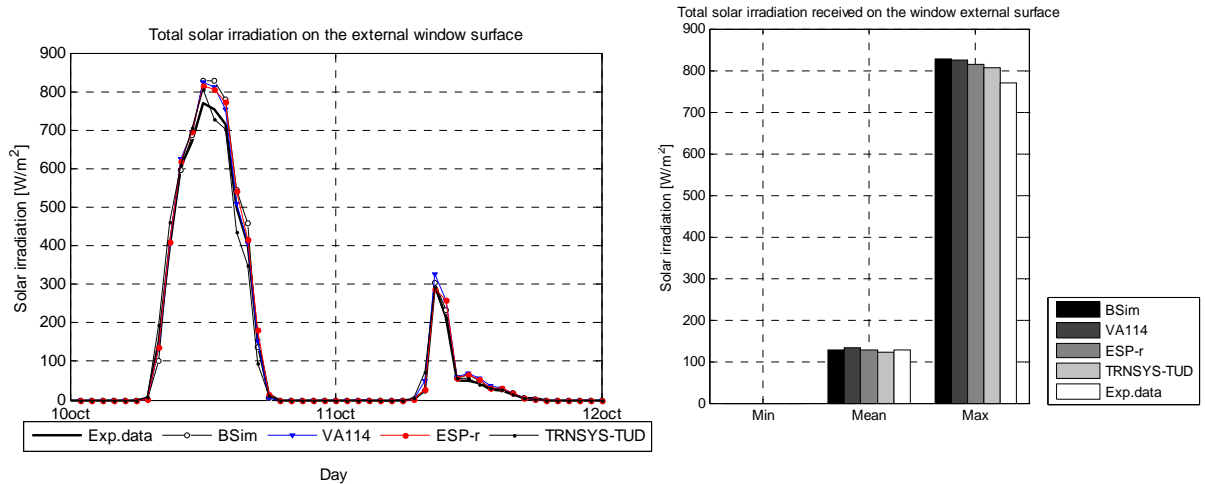
Figure 53. Total solar irradiation on the external window surface. Test case DSF200_e.

Total solar rad. on ext window surface	BSim	VA114	ESP-r	TRNSYS-TUD	Exp.
MIN, W/m²	0	0	0	0	0
MAX, W/m²	827	824	814	805	769
MEAN, W/m²	129	132	129	123	128
DT95, W/m²	-24	-9	-28	-63	
DT5, W/m²	49	39	41	36	
MEANDT, W/m²	3	6	3	-3	
ABMEANDT, W/m²	10	9	9	13	
RSQMEANDT, W/m²	19	17	18	27	
STDERR, W/m²	19	16	17	27	

6.4.4 Solar radiation transmitted into the zone1 (first order of solar transmission)
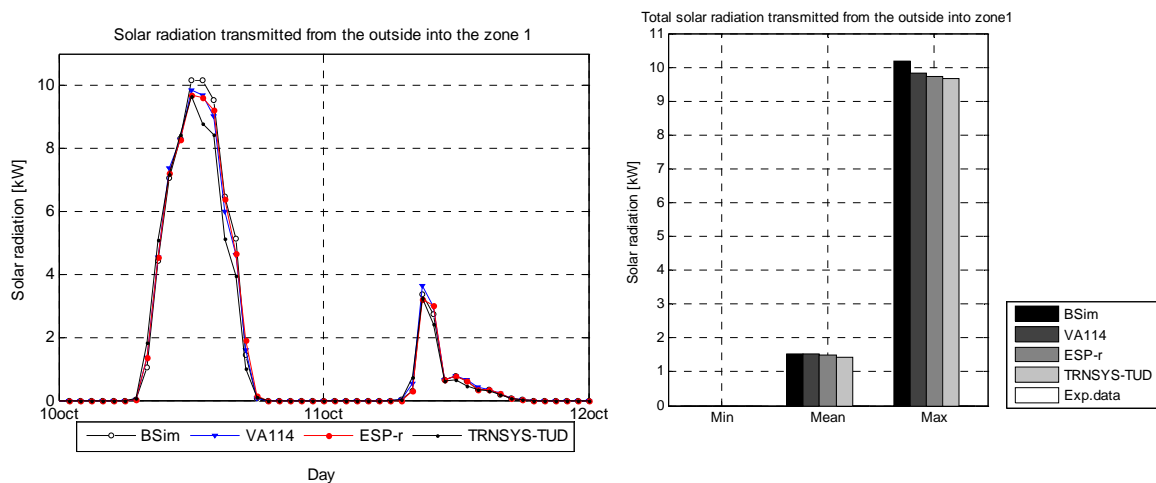
Figure 54. Solar radiation transmitted into the zone1 (first order of solar transmission). Test case DSF200_e.

Solar rad. transmitted into the zone 1	BSim	VA114	ESP-r	TRNSYS-TUD
MIN, kW	0	0	0	0
MAX, kW	10.17	9.83	9.72	9.66
MEAN, kW	1.53	1.52	1.49	1.42

6.4.5 Solar radiation transmitted into the zone2 (first order of solar transmission)
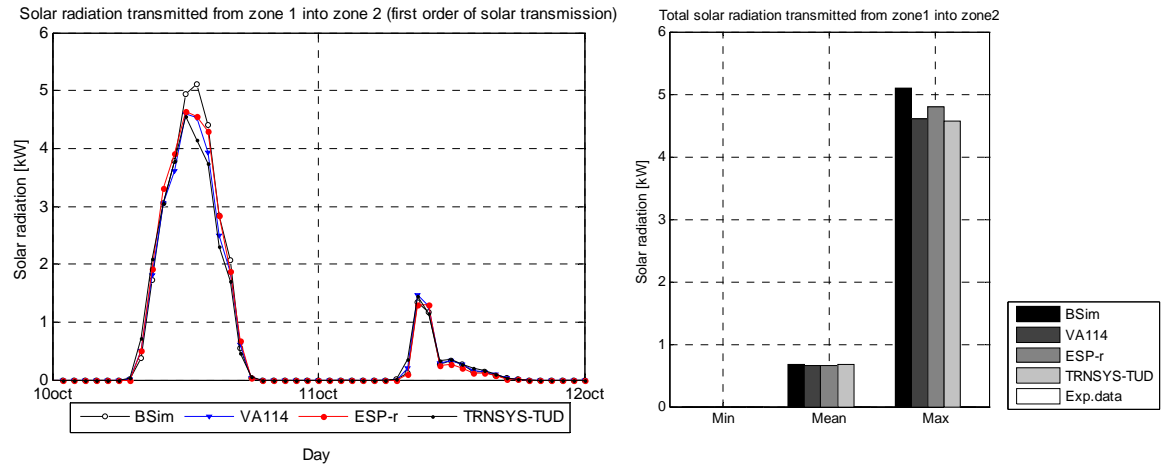
Figure 55. Solar radiation transmitted into the zone2 (first order of solar transmission). Test case DSF200_e.

Solar rad. transmitted into the zone 2	BSim	VA114	ESP-r	TRNSYS-TUD
MIN, kW	0	0	0	0
MAX, kW	5.10	4.60	4.80	4.56
MEAN, kW	0.68	0.66	0.65	0.67

The above plots of the direct, diffuse and total solar radiation on the external surface of the double-skin facade, as well as the solar radiation transmitted into the zone 1 and zone 2 have the same pattern as the results in the test case DSF100_e. This proves not only the consistency of modelling the test cases, but also once more illustrates the differences and limitations of the models to model the boundary conditions.

6.4.6 Air temperature in the double facade cavity
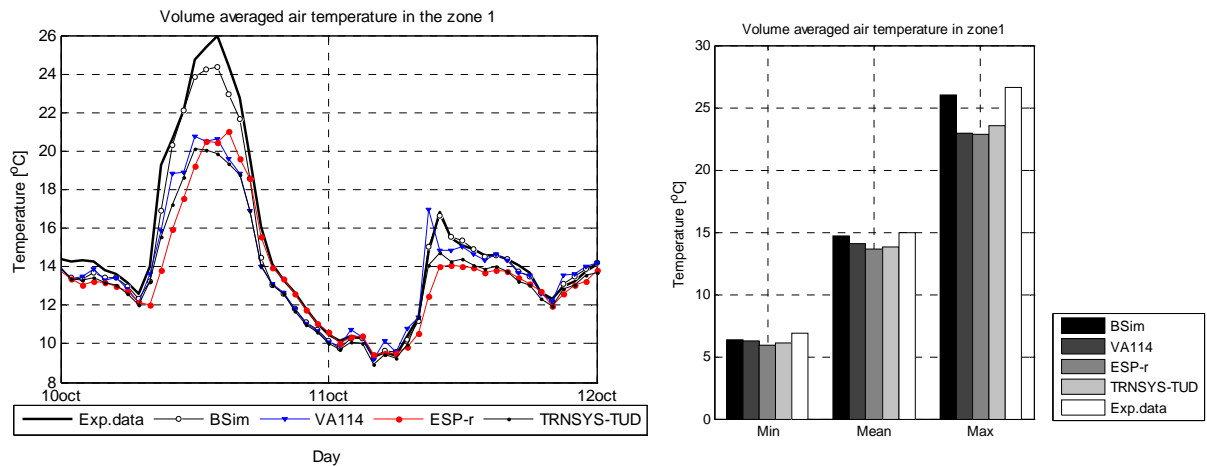
Figure 56. Volume averaged air temperature in the DSF cavity. Test case DSF200_e.

Volume averaged air temperature in zone 1	BSim	VA114	ESP-r	TRNSYS-TUD	Exp.
MIN, °C	6.35	6.23	5.96	6.08	6.91
MAX, °C	25.99	22.91	22.82	23.55	26.67
MEAN, °C	14.66	14.12	13.61	13.85	14.98
DT95, °C	-1.10	-3.63	-4.46	-3.60	
DT5, °C	1.15	0.30	-0.13	-0.04	
MEANDT, °C	-0.24	-0.80	-1.31	-1.07	
ABMEANDT, °C	0.55	0.89	1.31	1.10	
RSQMEANDT, °C	0.71	1.39	1.86	1.52	
STDERR, °C	0.67	1.14	1.33	1.09	

Besides the assumption regarding the convective/radiative heat transfer at the surfaces, the air temperature in the DSF cavity in this test case DSF200_e is also closely connected with the mass flow rate in the cavity.

In view of fact that the air flow rate in a double skin facade cavity is rather high compared to the temperature difference between the air in the cavity and outdoor, it is essential to perform the empirical validation of the air temperature predictions in the models via *'the temperature rise in the zone1'*. It is necessary to mention that an error in prediction of air temperature in the range of 1 degree Celsius can mean hundreds of watts of error in energy balance.
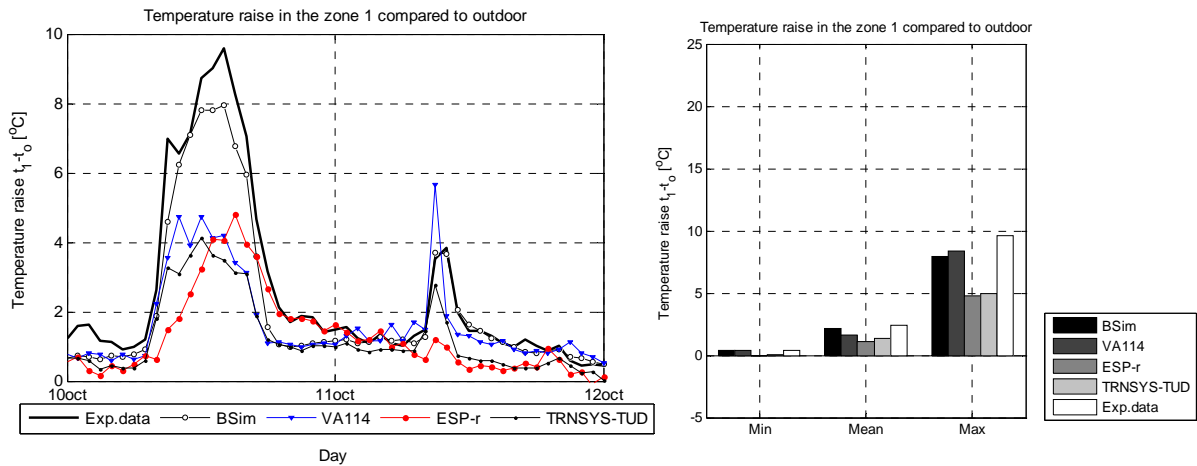
Figure 57. Temperature rise in the zone 1 compared to outdoor. Test case DSF200_e.

Temperature rise in the zone 1 compared to outdoor	BSim	VA114	ESP-r	TRNSYS-TUD	Exp.
MIN, °C	0.37	0.36	-0.08	0.02	0.40
MAX, °C	7.93	8.39	4.79	4.97	9.59
MEAN, °C	2.17	1.63	1.12	1.36	2.43
DT95, °C	-1.10	-3.63	-4.46	-3.60	
DT5, °C	1.15	0.30	-0.13	-0.04	
MEANDT, °C	-0.24	-0.80	-1.31	-1.07	
ABMEANDT, °C	0.55	0.89	1.31	1.10	
RSQMEANDT, °C	0.71	1.39	1.86	1.52	
STDERR, °C	0.67	1.14	1.33	1.09	

The statistical data in the table above demonstrate that all of the models underestimate the air temperature in the cavity, as all of the MEANDT values are negative. The absolute mean error varies between 0.5 and 1°C, what corresponds to energy transport with the mass flow of apx 0.2-0.3kW, when the mass flow is 1000kg/h. Certainly, the accuracy of the measurements becomes even more important here, since we deal with rather small temperature range.

From the 2-days plot it is seen that in a day with low solar intensity, the agreement between the experimental results and prediction is still limited: the experimental data are often higher, for most of the models. Also in the

night time periods, predictions underestimate the air temperature in the DSF by apx. 1°C. For the case DSF100_e, it was seen that using variable convective heat transfer coefficient ESP-r model was more successful to calculate the air temperatures in the zone 1. In the present case, DSF200_e, however, this is not the case. This time, the plot of the results differs a lot from the one for the test case DSF100_e: other programs get closer to the experimental data. Is this caused by the change in the flow regime and thus convection heat transfer in the cavity?

The air temperature in the cavity is the result of the heat exchange between the air and surfaces in the cavity. The underestimation of air temperature in the cavity can also happen if the convective heat transfer during the actual measurements is stronger than the one assumed in the models. Considering the surface temperature of the internal window glazing facing the zone 1 (Appendix I), one can observe that the surface temperature is greatly overestimated by ESP-r and TRNSYS-TUD model if compared against the experimental data. In view of that, one may consider the situation where the actual convective heat transfer in the cavity is much higher than the convective heat transfer in the models. Extremely high mass flow rate in the cavity might be a good reason for that. This hypothesis does not have a proof, but further investigation of the convective heat transfer in the DSF is inevitable for being able to predict their performance. To check this hypothesis, one may run an empirical validation of the model with using the convective surface film coefficients in the cavity as a function of air velocity and temperature difference.
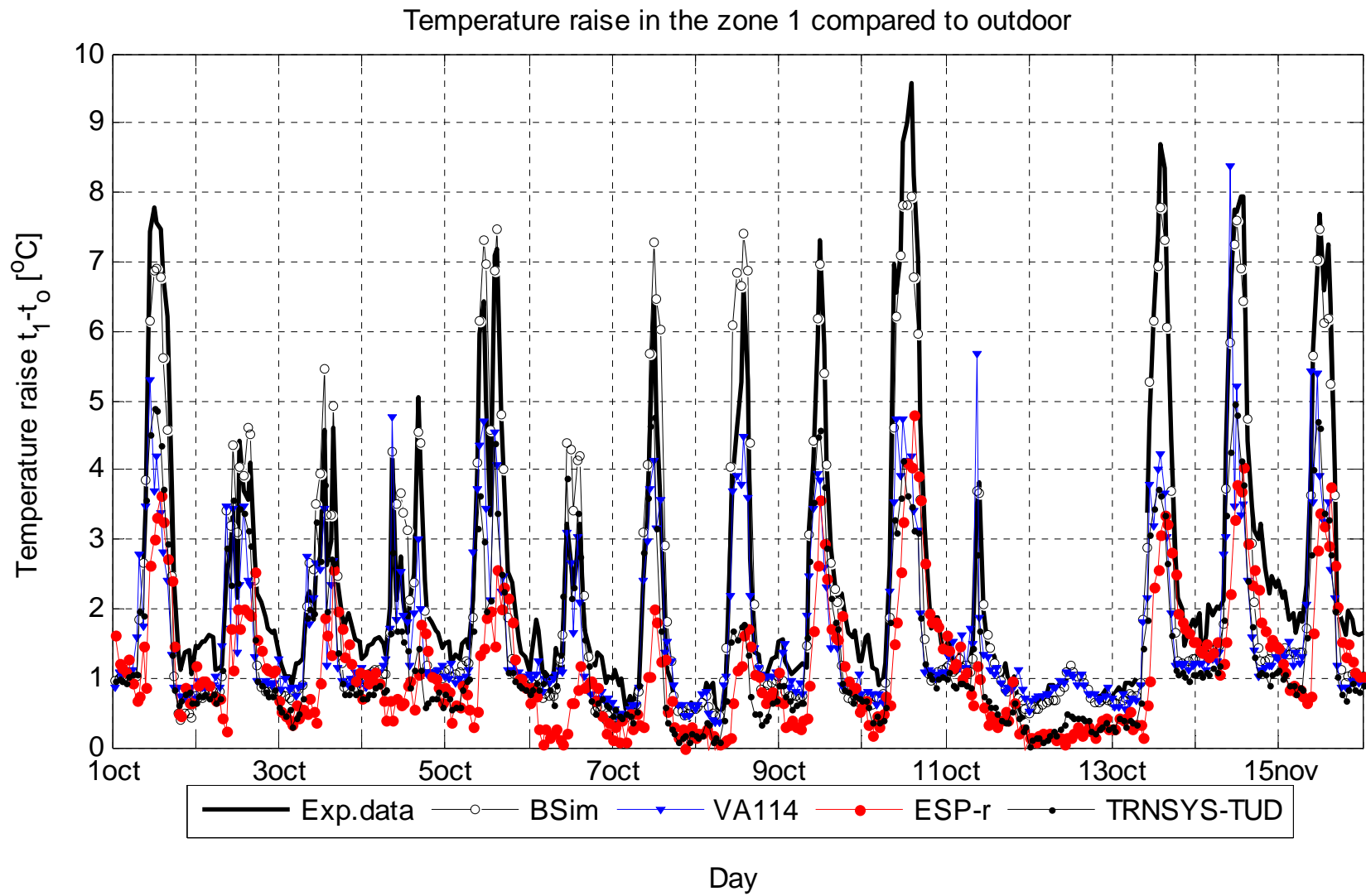
Figure 58. Temperature rise in the zone 1 compared to outdoor. Test case DSF200_e.

6.4.7   Temperature of the internal window glass surface facing zone 2
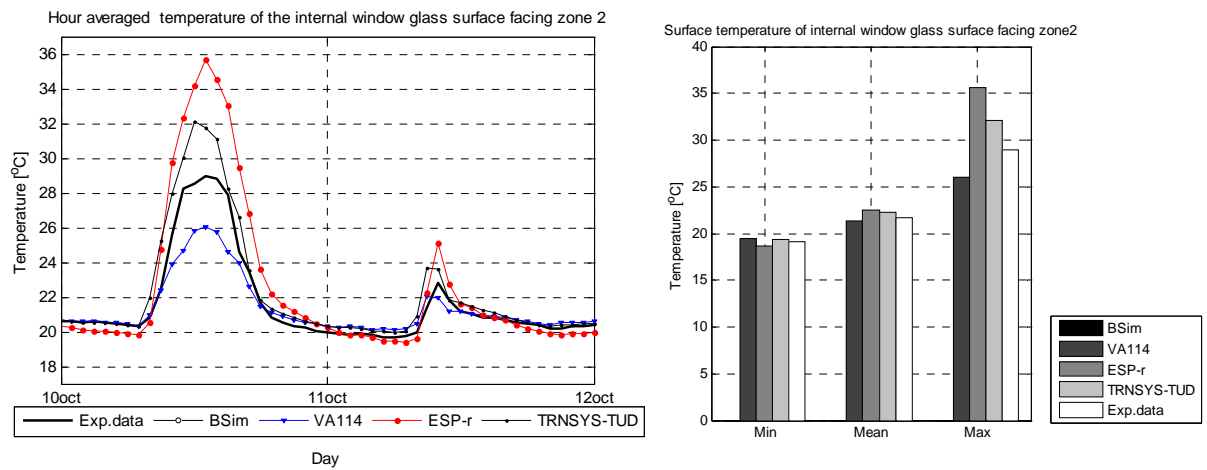
Figure 59. Temperature of the internal window glass surface facing zone 2. Test case DSF200_e.

Temperature of internal window glass surface facing internal	BSim	VA114	ESP-r	TRNSYS-TUD	Exp.
MIN, °C		19.52	18.70	19.39	19.11
MAX, °C		26.04	35.66	32.10	28.98
MEAN, °C		21.38	22.55	22.33	21.70
DT95, °C		-2.84	-0.59	-0.09	
DT5, °C		0.42	4.84	2.73	
MEANDT, °C		-0.32	0.86	0.63	
ABMEANDT, °C		0.58	1.22	0.65	
RSQMEANDT, °C		1.03	1.91	1.11	
STDERR, °C		0.98	1.71	0.92	

The models calculate a wide spread of temperatures and none of them is satisfactory with the empirical data. Predicted high surface temperatures could be a problem when dealing with issues of comfort since most of the other models considerably exceed the measured value.

If the issue of comfort should to be addressed in the calculations, then application of reliable convective/radiative surface heat transfer coefficients must be ensured. Otherwise, a sensitivity study will be necessary to prove the robustness of the results.
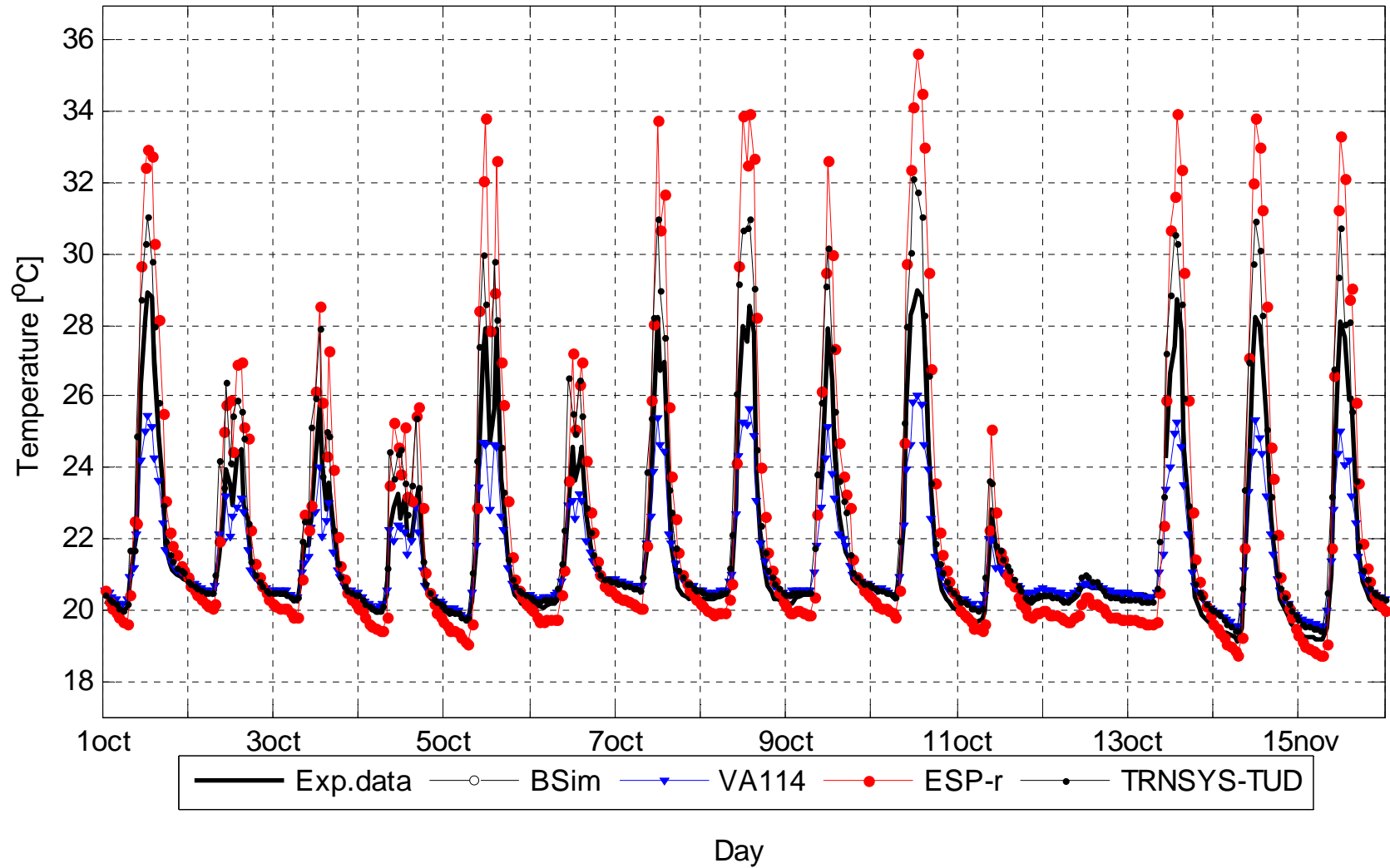
Figure 60. Temperature of the internal window glass surface facing zone 2. Test case DSF200_e.

6.4.8 Mass flow rate in the zone 1

Before assessment of the results with the experimental data, it is reasonable to start with the comparison of the results between the models. Earlier, in the comparative exercises, it was shown that the deviation of calculated airflows between the programs was significant. Then, due to the lack of the experimental data, conclusions have not been derived. Again, extreme spread of the results is obtained for this test case DSF200_e, see plots below.
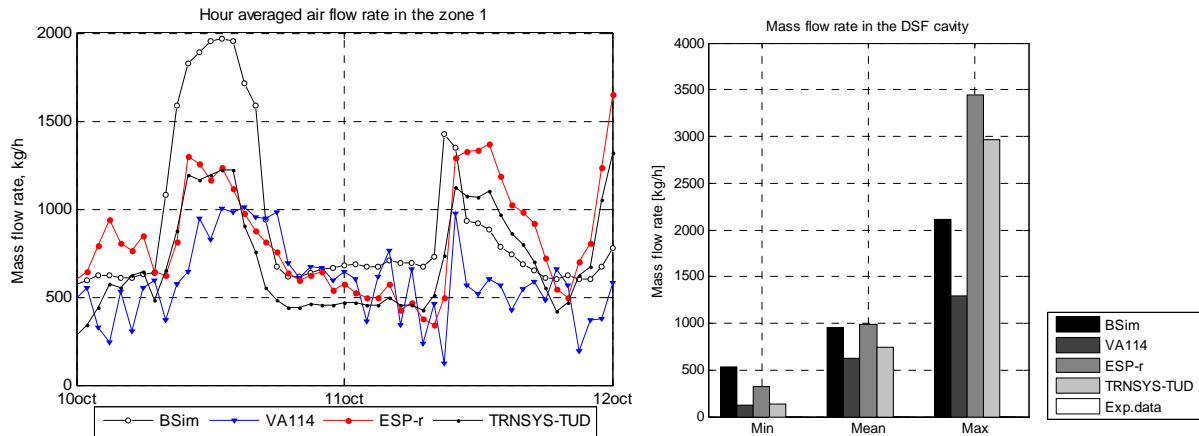
Figure 61. Predicted mass flow rate in the zone 1. Test case DSF200_e.
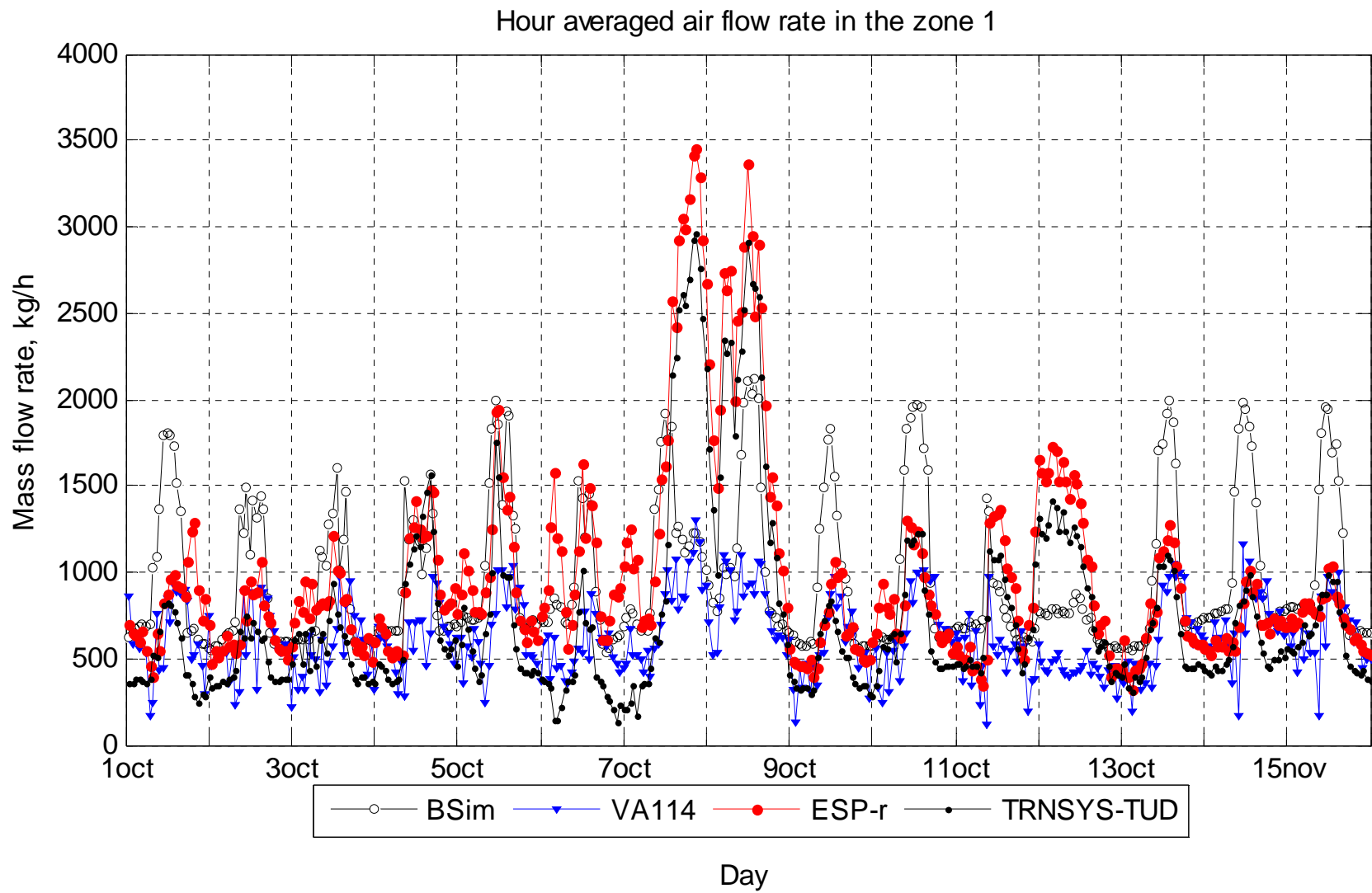
Figure 62. Predicted mass flow rate in the zone 1. Test case DSF200_e.

Next, the discussion of the experimental data should take place. The mass flow rate was measured with the three methods, explained in [5], however the results from only two of them are reported as reliable. As it is explained in [5], the measurement of the air flow rate is very difficult and although the accuracy of the equipment is rather good, different measurement errors may appear.

In the tracer gas method, the errors could appear when the tracer gas is not well mixed with the entrance air or in the case of wind wash-out effects and the reverse flow appearance. In the latter cases, the tracer gas is removed from the DSF cavity and, as a consequence, some measurement points are characterised with the air flow rate approximating the infinity.

The statistical analysis of this data is difficult and, sometimes, it can be unreliable for some statistical parameters, as it requires a flawless set of experimental data. Meanwhile, the exact periods of wash-out effect and reverse flow occurrence are not possible to recognise and therefore it is not possible to 'clean-up' the data properly. The authors have removed any points with the mass flow rate above 7000 kg/h that corresponds to the mean velocity in the DSF cavity above 0.85m/s and air change rate in the cavity above 500 1/h. This is rather high limit to choose for the mass flow rate, therefore most of the parameters in the table of statistics are affected and cannot be used for assessment. An option of the lower limit was not considered since this would be the data manipulation.

The occurrence of the reverse flow was experienced during the experiments, but it was not possible to visualise or record that phenomena. The detection of periods with the reverse flow from the experimental data can not be done accurately. However, it is worth mentioning that the greatest dilution of the tracer gas was noticed for the periods when the wind was of South direction (striking into the DSF openings).

In the velocity profile method, the errors are mainly caused by the approximation in the shape of the velocity profile and by the convection boundary flow at the heated glazed surfaces. Since, the velocity profiles were measured only in the central section of the DSF cavity, the assumption of equal flow conditions in all three sections of the DSF cavity could be applied, although there is little evidence that it was fulfilled during the experiments.

The application of the statistical analysis for the data obtained with the velocity profile is also difficult, as the measured air flow can include periodical errors, such as overestimation of the flow rate due to the measurement of increased air speed at the surfaces in the convective boundary flow. Periodical character of the errors (errors are distinctive for the periods with the strong solar irradiation) forbids an application of the mean values as meaningless.

Tables with the statistical data are included into this report, but they will be disregarded in the further discussion for both sets of empirical data. Therefore, the main discussion will be made taking into account the plots of simulated and measured mass flow rates.

For better visualisation of the results, the above plots are divided into three periods, with the scale that is suitable for each period.
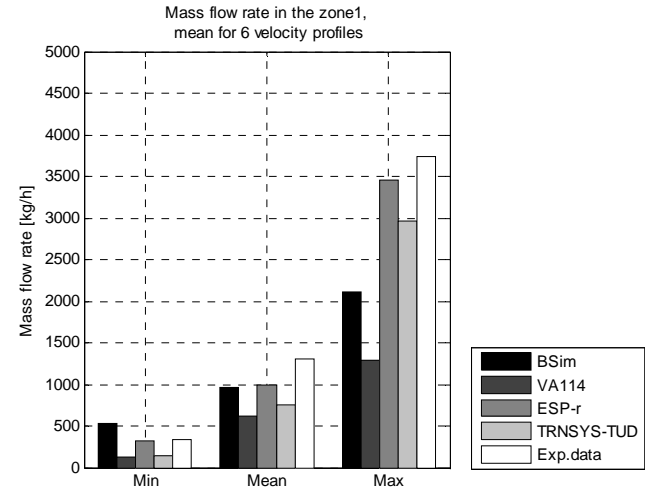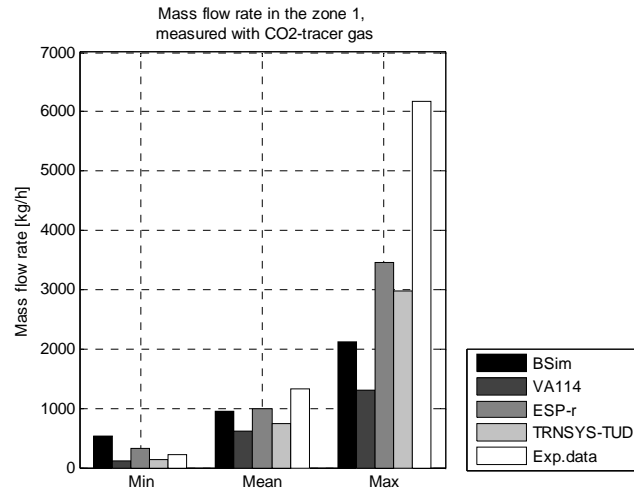
Figure 63.Predicted and measured mass flow rate in the zone 1, measured with the tracer gas method (left). Measured with the velocity profile (right).

Mass flow rate in the zone 1, CO_2 tracer gas method	BSim	VA114	ESP-r	TRNSYS-TUD	Exp.
MIN, kg/h	531	124	326	135	229
MAX, kg/h	2116	1298	3449	2968	6166
MEAN, kg/h	958	621	986	748	1324
DT95, kg/h	-3420	-3632	-2490	-2865	
DT5, kg/h	853	344	325	177	
MEANDT, kg/h	-335	-684	-304	-511	
ABMEANDT, kg/h					
STDERR, kg/h	791	815	524	595	

Mass flow rate in the zone 1, mean for 6 velocity profiles	BSim	VA114	ESP-r	TRNSYS-TUD	Exp.
MIN, kg/h	531	124	326	135	340
MAX, kg/h	2116	1298	3449	2968	3744
MEAN, kg/h	958	621	986	748	1299
DT95, kg/h	-1797	-2083	-1383	-1713	
DT5, kg/h	500	153	321	116	
MEANDT, kg/h	-339	-671	-301	-544	
ABMEANDT, kg/h					
STDERR, kg/h	530	707	412	583	
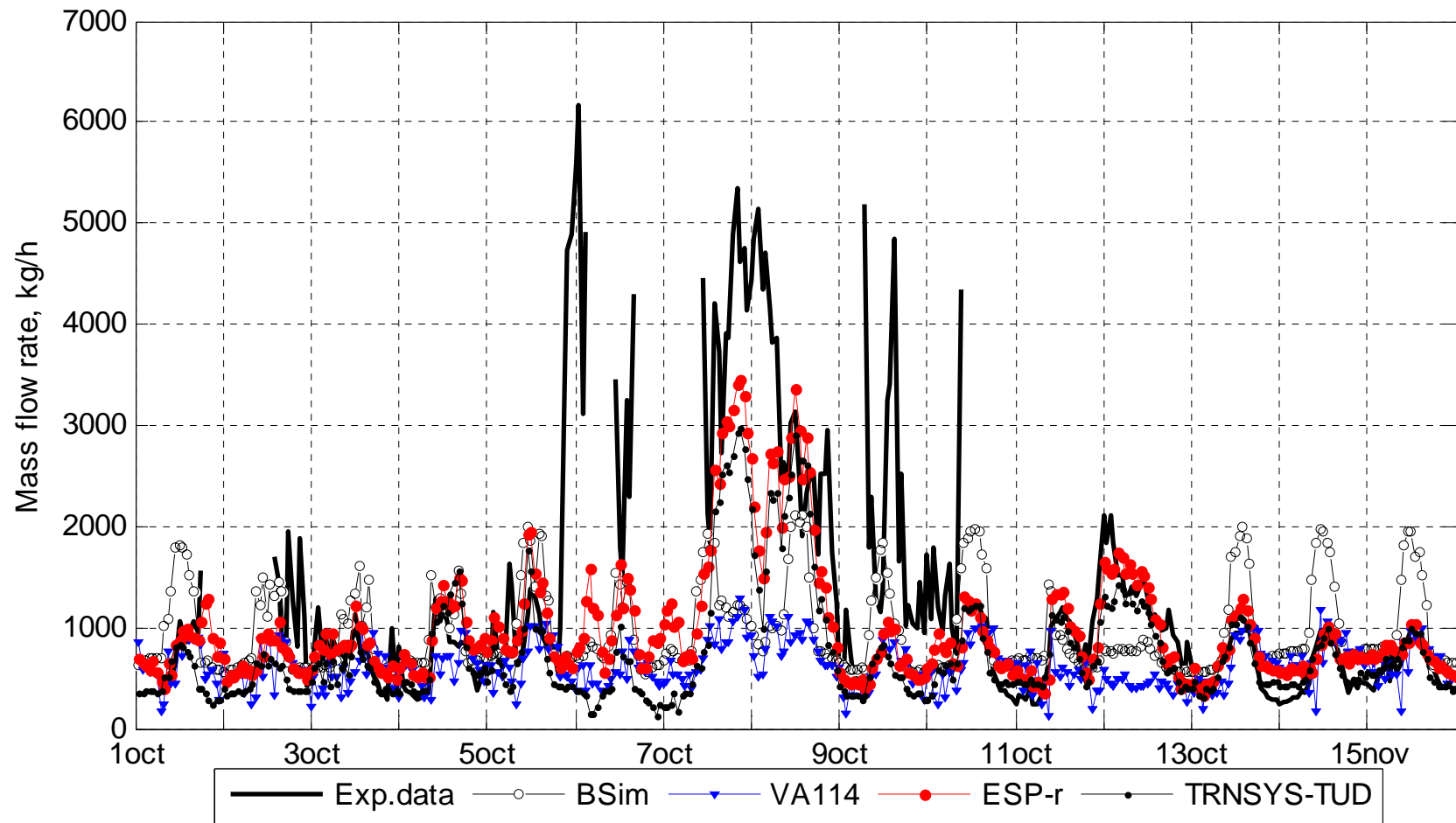
Figure 64. Hour averaged mass flow rate in the zone 1, measured with the tracer gas method. Test case DSF200_e.
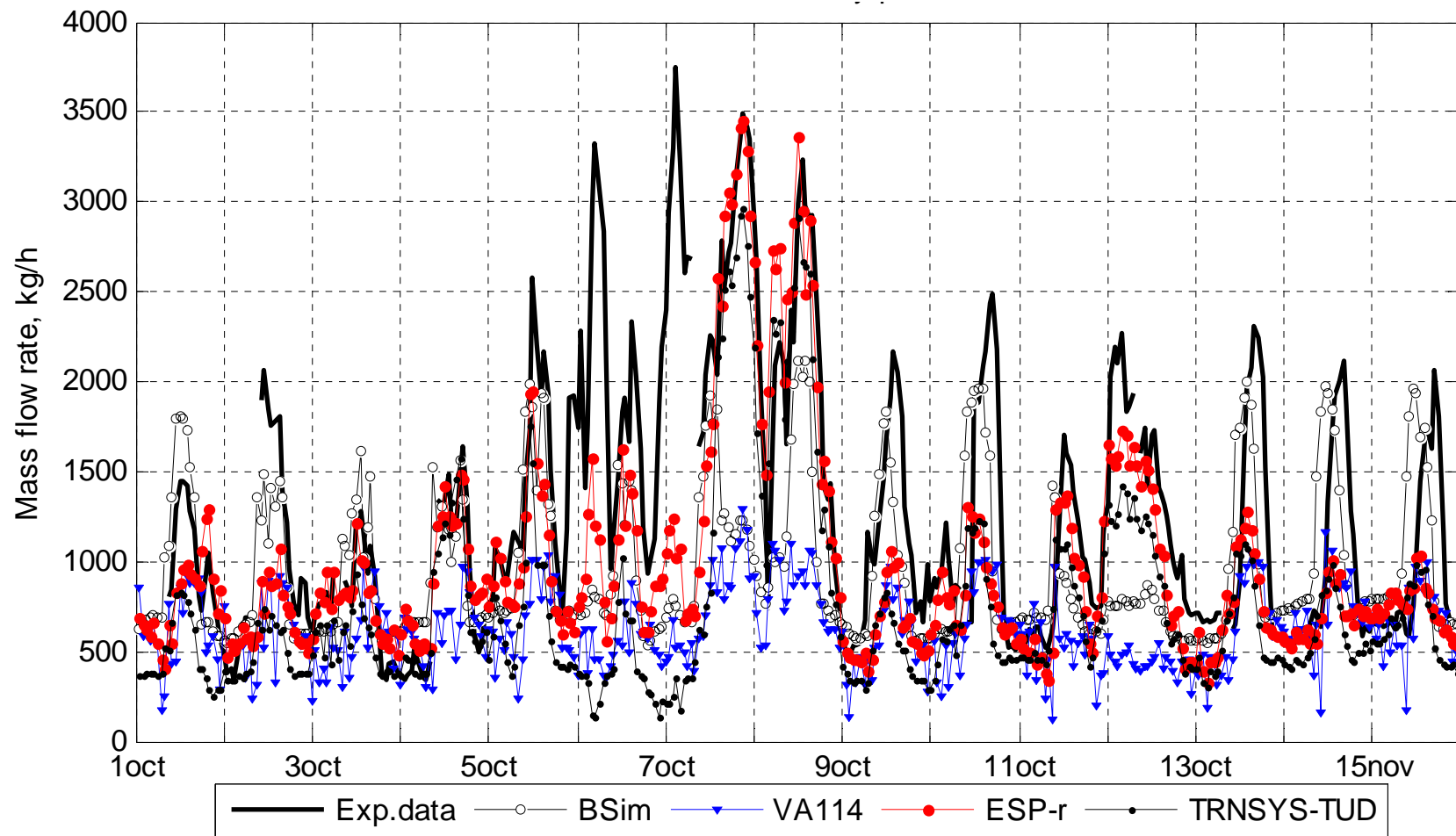
Figure 65.Hour averaged mass flow rate in the zone 1, measured with the velocity profile method - mean for 6 profiles. Test case DSF200_e.

Figure 66. Hour averaged mass flow rate in the zone 1, measured with the tracer gas method (PERIOD 1: 1 October – 6 October).

PERIOD 2: 6 October – 11 October
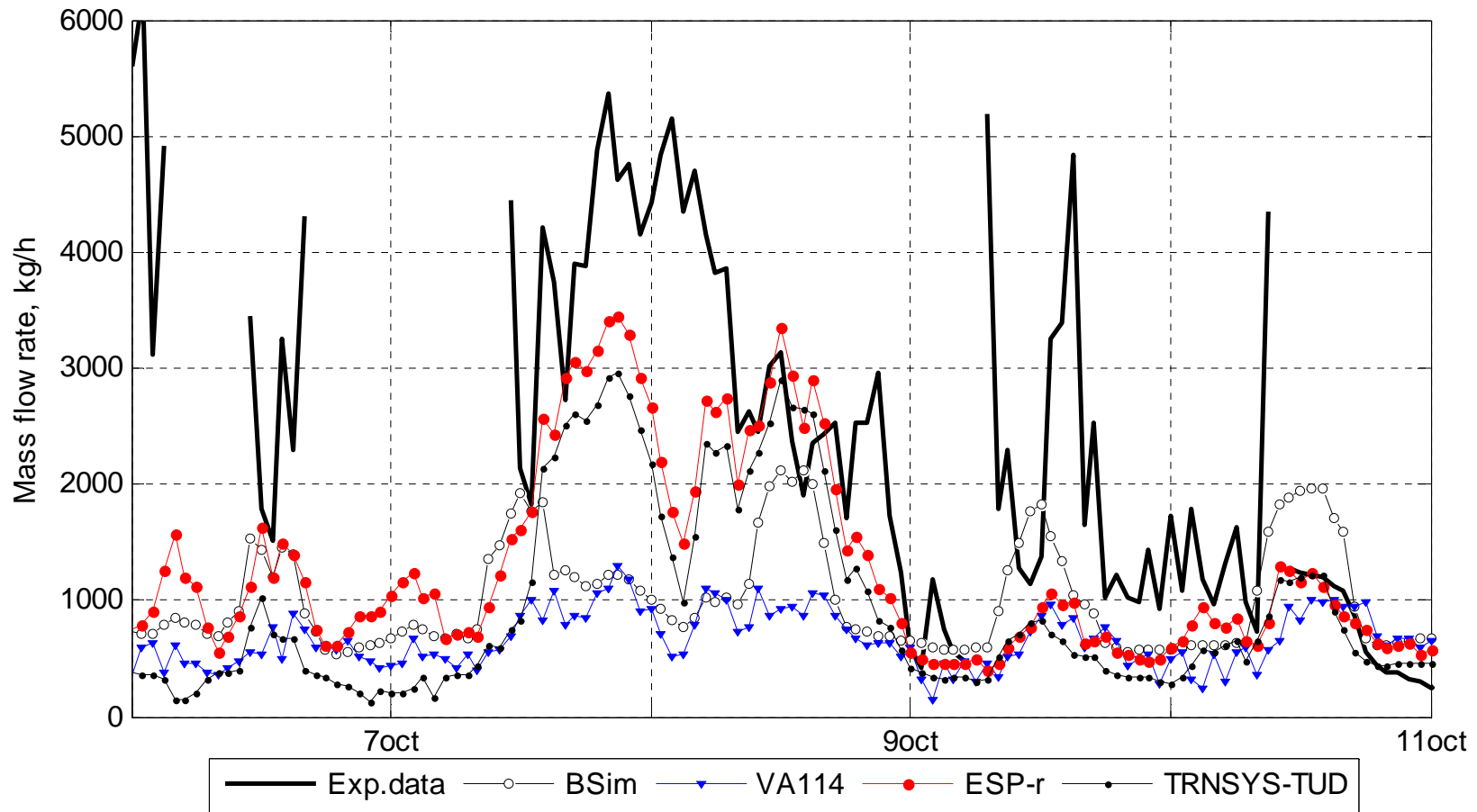
Figure 67. Hour averaged mass flow rate in the zone 1, measured with the tracer gas method (PERIOD 2: 6 October – 11 October).
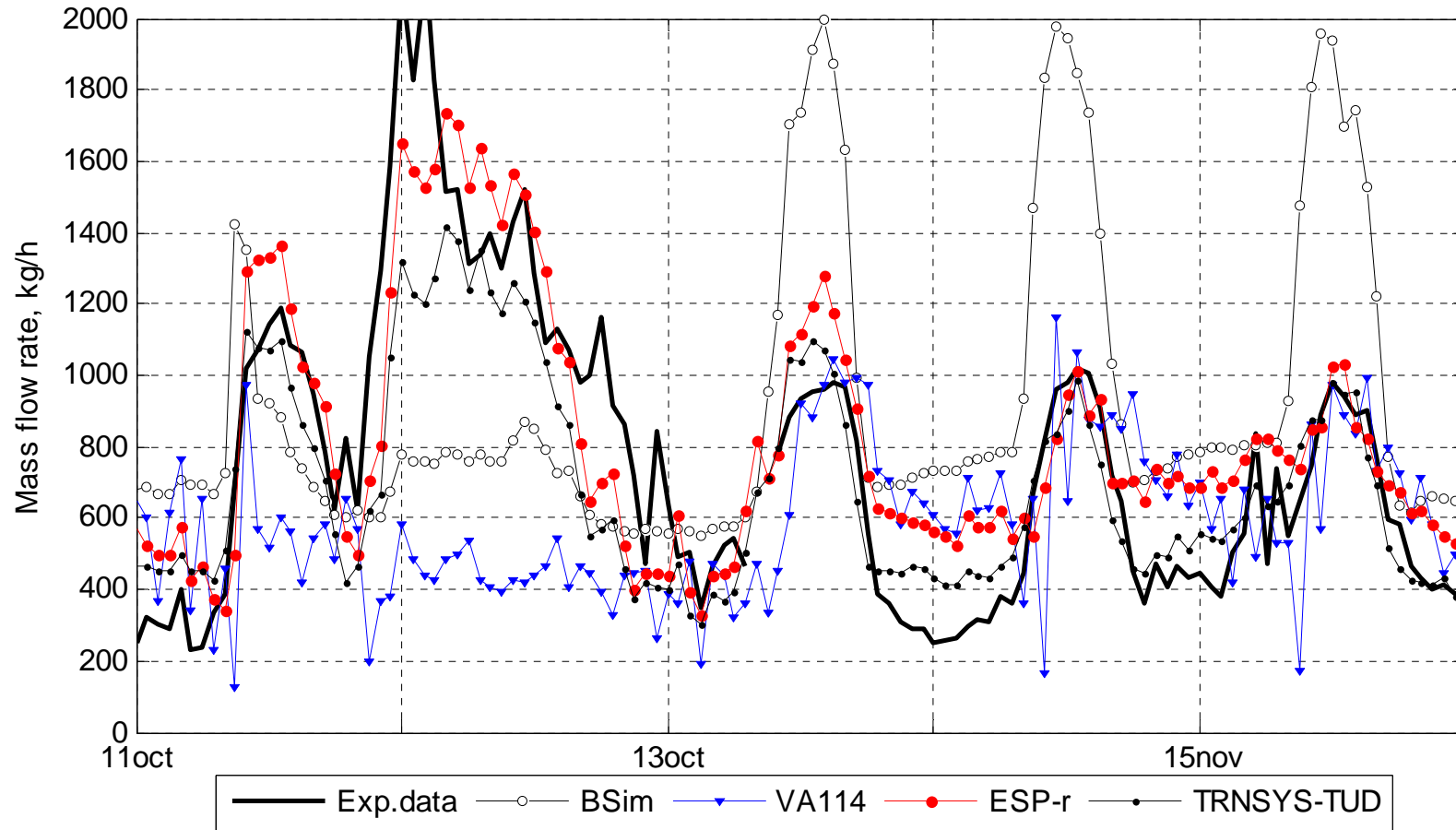
Figure 68. Hour averaged mass flow rate in the zone 1, measured with the tracer gas method (PERIOD 3: 11 October – 16 October).

Comparing the characteristics of expected errors in both experimental methods, it is necessary to note that the appearance of the reverse flow is periodical (South wind direction) and the periods are relatively easy to notice in the plots of the experimental results. The wind washout effect is also a wind generated phenomena, as the reverse flow, but its occurrence is more random and originated from the highly fluctuating wind nature. Washout is a short-term fluctuating phenomenon and therefore it does not have as much influence on the accuracy as the reverse flow. Finally, there is a third phenomenon that may take place in the DSF cavity; this is so called recirculating flow, which creates areas in the cavity with recirculating flow, generated due to the strength of the boundary layer flow (as explained later in this chapter).

Looking upon the bad mixing, it should be mentioned that it is not possible to evaluate the impact of this error, although a lot of effort was made during the experimental work to avoid this kind of error. With regard to the errors that could have appeared during the velocity profile measurement, the most significant of them is the impact of the boundary flow, as both in the days with the strong solar radiation or in the night time the boundary layer flow can result in overestimation of the air flow rate in the cavity and it is not possible to assess the degree of error.

First, the results of simulations are discussed upon the experimental data obtained with the tracer gas method. The result plots are subdivided into the three periods:
- 1October-6October
- 6October-11October
- 11October-16October

Results corresponding to the first two periods are very difficult to evaluate: both the results of simulations and experimental results seem to be very fluctuating and random, while in the third one it is easy to distinguish between the periods with the higher/lower solar irradiation, etc. It is likely that the haphazard air flow rate in the DSF cavity during the first two periods is caused by often variation in the wind directions between the South-East and South-West. Moreover the second period experienced high wind speed above 6m/s. More stable wind direction, relatively low wind velocity (below 6m/s), cooler outdoor temperature and less changeable solar irradiation have resulted in a more clear experimental data and simulation results. Therefore, the third period was further used for the assessment of the results.

The night time ventilation of the DSF is mainly driven by wind, therefore the correspondence of the experimental results with the simulations in the night time periods, tells about proper estimation of the pressure difference coefficients in the empirical specification.

Predictions of the air flow rate for TRNSYS-TUD and ESP-r are often of the same shape and have close values, although, these results are obtained with different flow models. TRNSYS-TUD air flow is often lower than in ESP-r model, this is probably caused by the application of the default discharge coefficient in TRNYS-TUD, while the discharge coefficient defined in the specification was used in ESP-r.

The night and day periods are less distinguished in VA114 model, this is partly due to the model which includes the impact of wind fluctuations on air flow rate in the cavity. At the same time, this model does not include the direct influence of the wind forces, as $\Delta C_p = 0$. In VA114, the mass flow rate is calculated based on the air temperature in the zone at the end of the previous time step, which causes calculation of somewhat more fluctuating mass flow rate.

BSim often overestimates the air flow rate, both during the day and night time, but during the period of strong wind speed, the air flow is underestimated, caused by the simplified empirical air flow model.

Similar to the tracer gas method, results of the velocity profile method are subdivided in the same periods, see figures below. There is a better agreement between experimental results and calculations, although the order of error is in the range of 500 kg/h. However, according to the velocity profile results, BSim predictions come into view with much better agreement, than compared against the tracer gas method results.

PERIOD 1: 1October - 6October
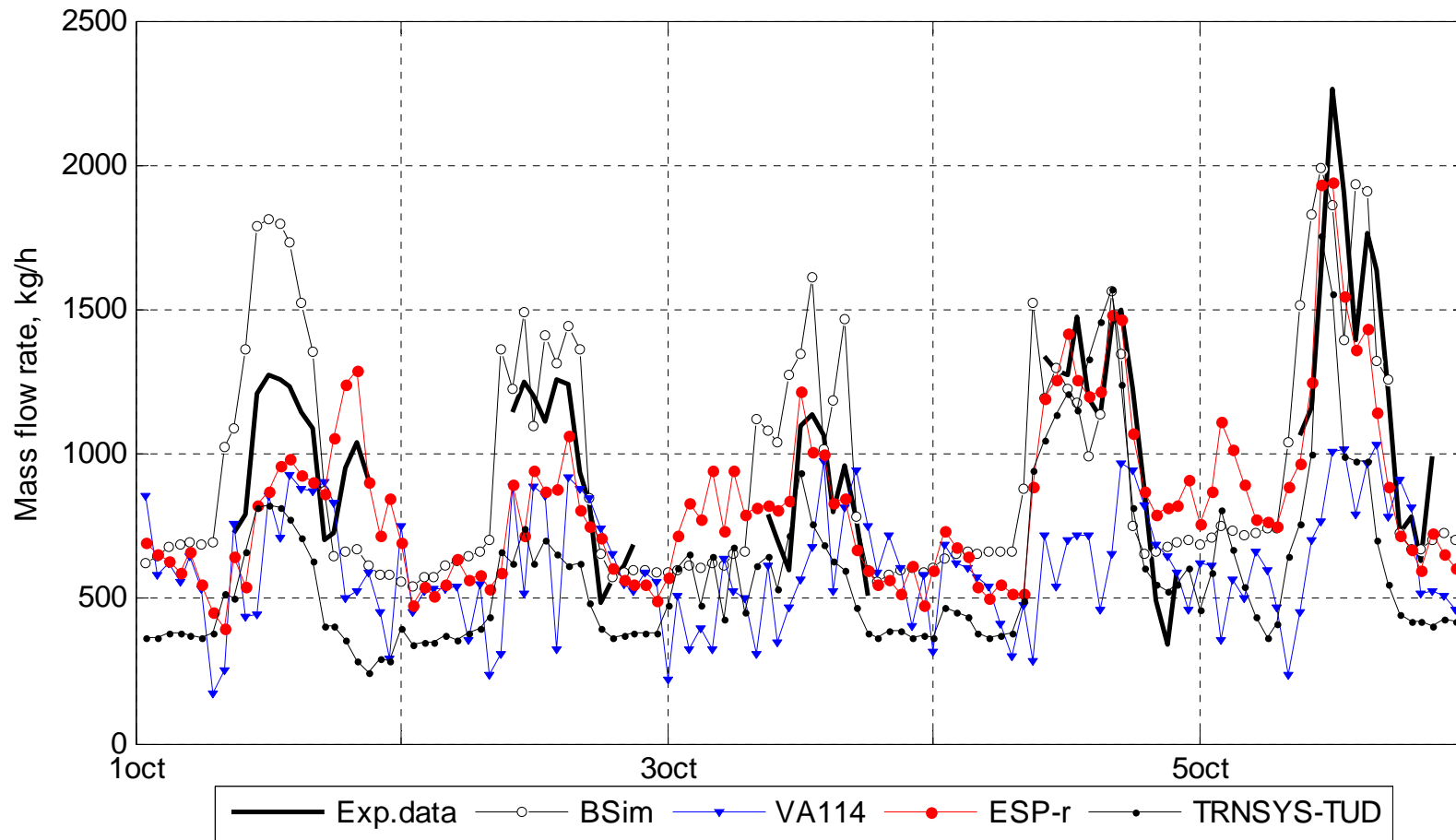
Figure 69. Hour averaged mass flow rate in the zone 1, measured with the velocity profile method. Velocity profile at h=1.91m (PERIOD 1: 1 October – 6 October).
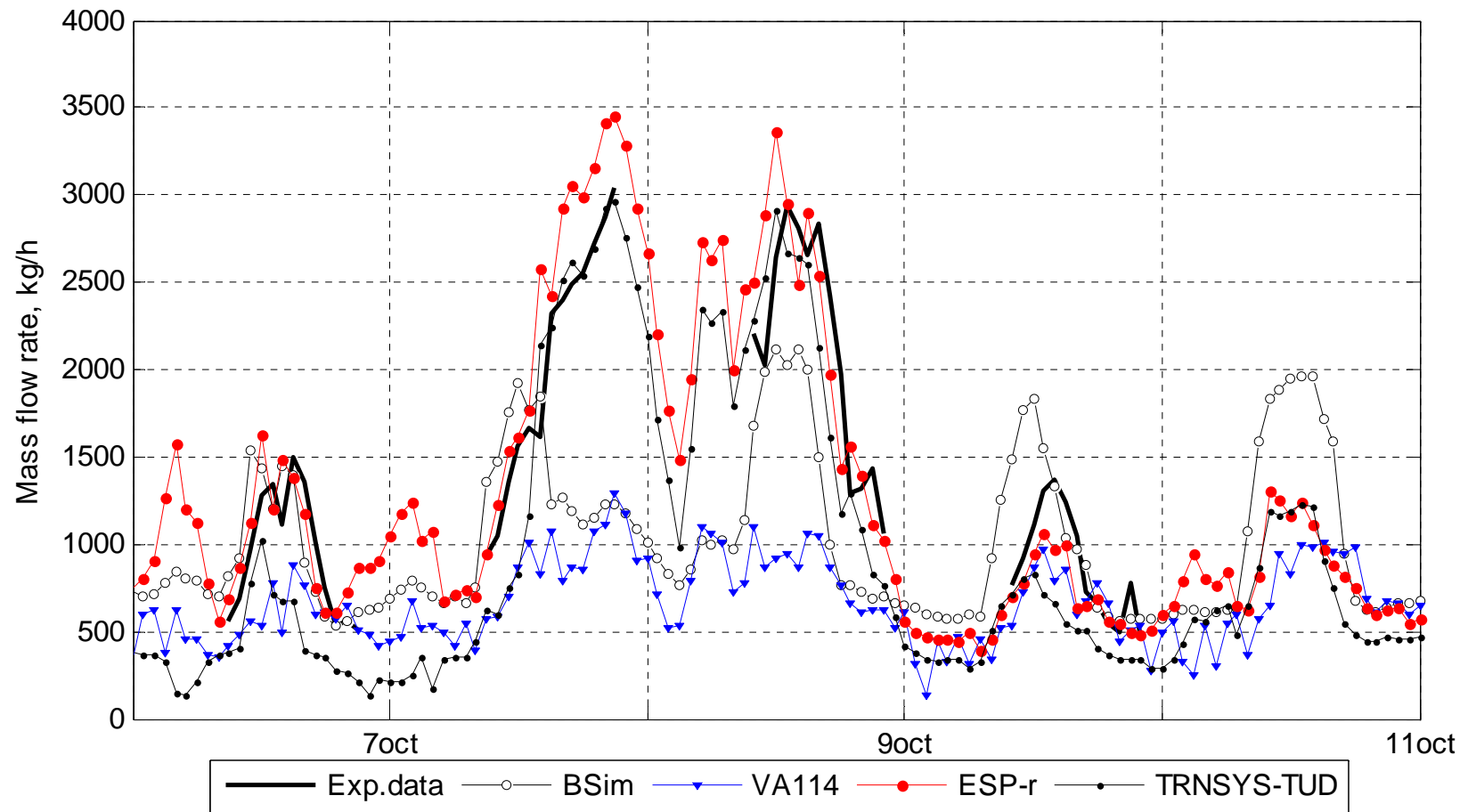
Figure 70. Hour averaged mass flow rate in the zone 1, measured with the velocity profile method. Velocity profile at h=1.91m (PERIOD 2: 6 October – 11 October).
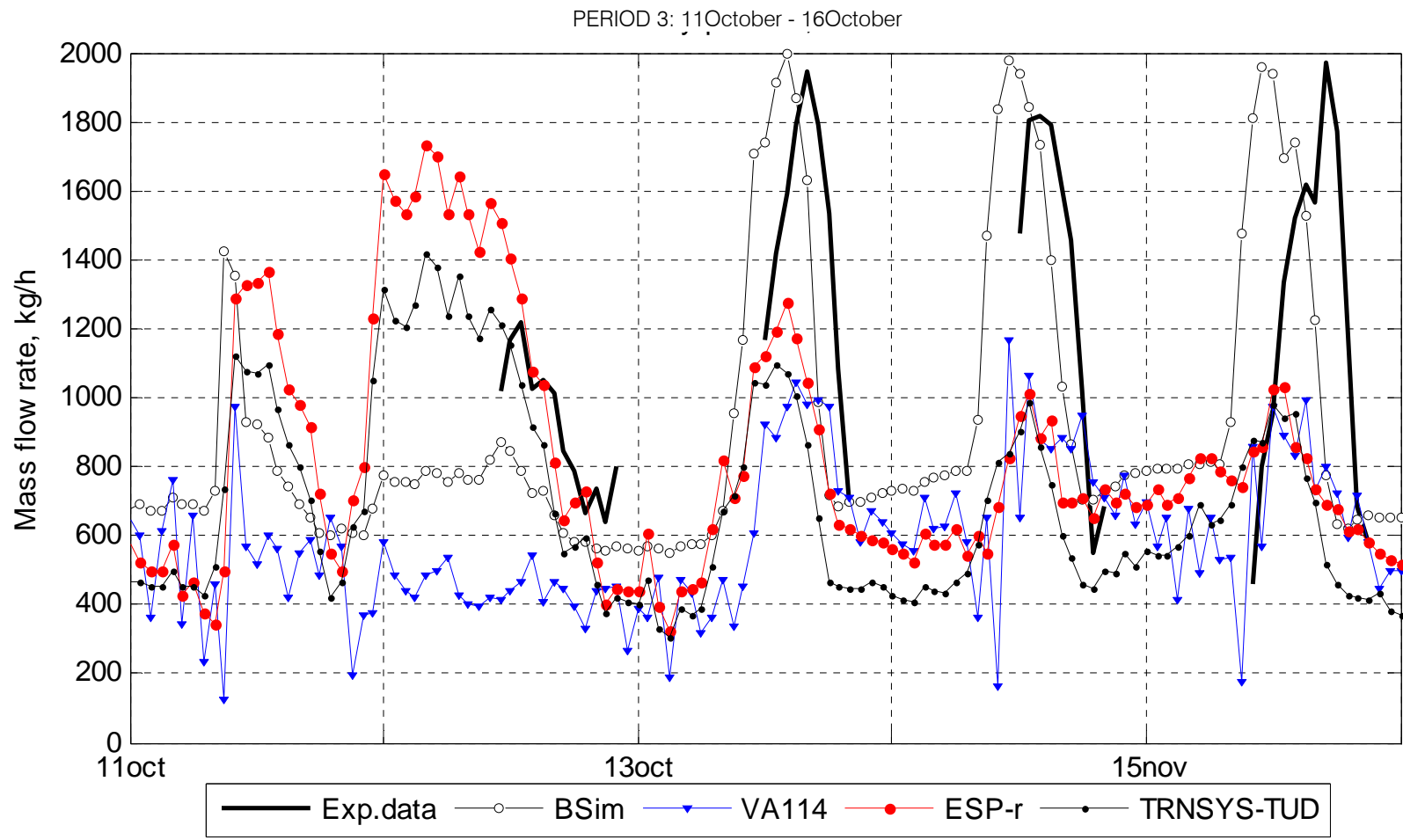
Figure 71. Hour averaged mass flow rate in the zone 1, measured with the velocity profile method. Velocity profile at h=1.91m (PERIOD 3: 11 October – 16 October).

The differences between the results obtained with the tracer gas method and the velocity profile method (mean value for all six velocity profiles) are evident: the air flow rates during the days with relatively high solar radiation are notably higher at noon compared to the results obtained with the tracer gas method. Also during the night time, the air flow rate in the cavity is higher for the velocity profile method. Meanwhile, the tracer gas method includes different periods with the enormous flow rates, which have not been removed from the data set.
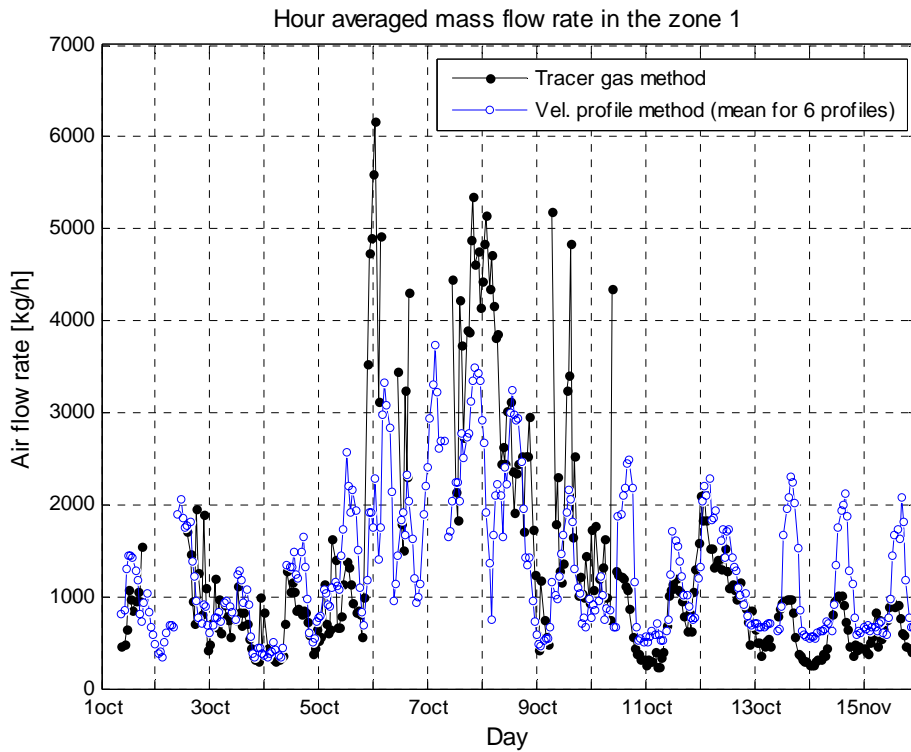
Figure 72. Hour averaged mass flow rate in the zone 1. The mass flow rate measured with the velocity profile method is plotted as mean for all 6 profiles.

The overestimation of the air flow rate can occur when using the velocity profile method, due to the boundary layer flow. Moreover, the boundary layer thickness increases with the distance from the origin and with increase of surface temperature. Since the velocity profiles in the DSF cavity were measured at six different heights, the error due to the convection at the boundary layer should increase with the height of the velocity profile measurement (see Figure 73).
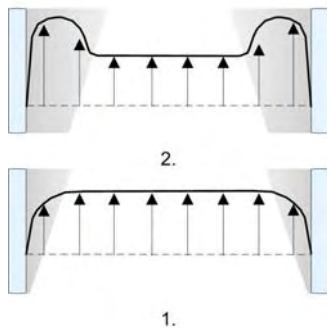
Figure 73. Simplified schema of velocity profile in the DSF cavity. 1 - at the entrance plane to the cavity. 2 – after some distance form the entrance plane.
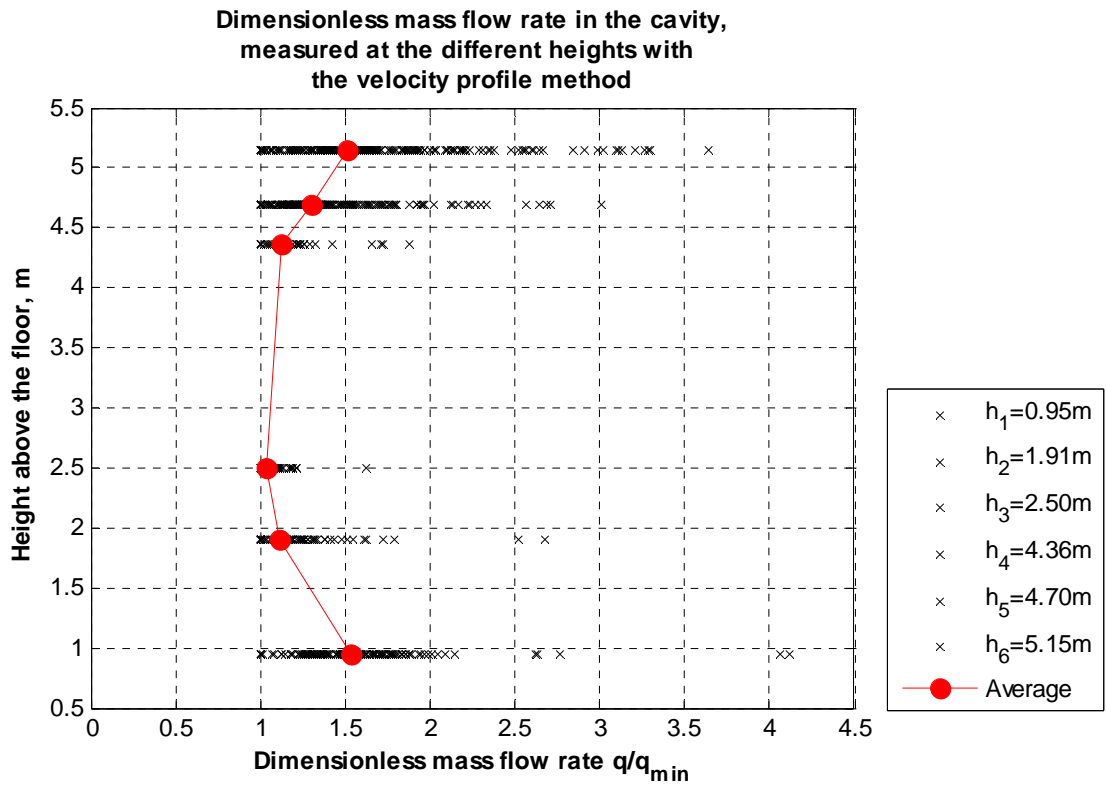
Figure 74. Dimensionless mass flow rate in the DSF cavity

In Figure 74, the mass flow rate in the cavity is dimensionless, where the value of 1 corresponds to the minimum air flow rate measured with one out of six velocity profiles. The figure demonstrates that actually the mass flow rate at the bottom of the cavity is not minimal; this is probably due to the bending of the jet when entering the cavity and wind washout effects. The dimensionless mass flow rate at the height of 2.5m and 4.36m is close to 1.This is probably due to the close location of the measurement points to the window frame, which destroys the boundary layer flow. Again, after passing the window frame, the development of the boundary layer should begin and this can be seen in the above figure for the height 4.70m ad 5.15m. As a consequence, in order to minimise the influence of the boundary flow, the mass flow rate in the DSF cavity should be calculated on the basis of the velocity profile at the height 1.91m, as there is a lack of measurements for the height 2.50m (min q/q_{min}).

Comparison of the experimental results obtained with the tracer gas and velocity profile method can be seen in Figure 75, for the velocity profile measured at a height 1.91m.

From the figure below it can be seen that from the 11th of October, the velocity profile method predicts higher air flow rates in the cavity during the daytime. For the night time periods, the mass flow rate for the velocity profile method at the height 1.91m is unavailable, as well as for many other periods. Thus the evaluation of the simulation results upon the experimental data is difficult, unless results from the measurements of velocity profile at other heights are used.
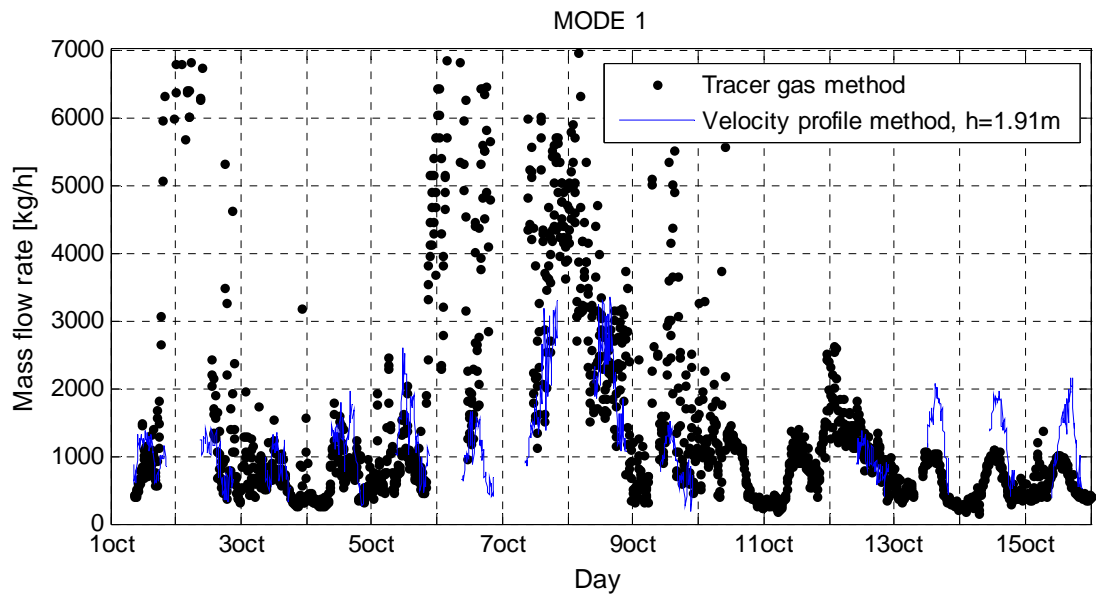
Figure 75. Hour averaged mass flow rate in the zone 1. The mass flow rate measured with the velocity profile method is plotted for the velocity profile measured at 1.91m height (Profile II).

6.4.9 Cooling/heating power in the zone 2
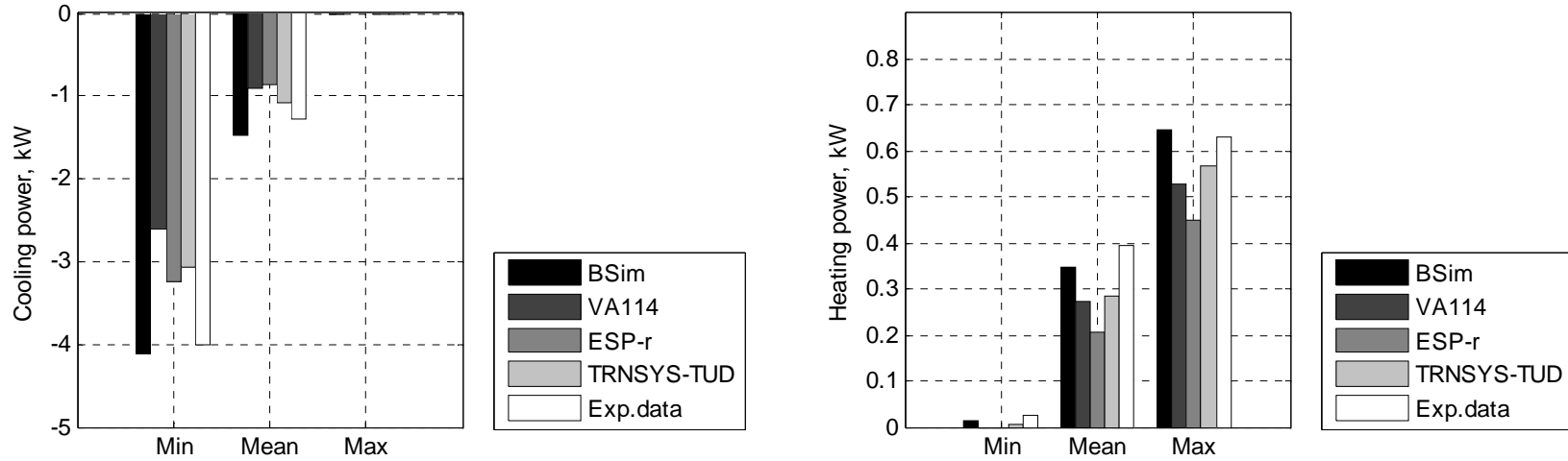
Figure 76. Cooling/heating power in the zone 2. Test case DSF200_e.

Cooling power in zone 2	BSim	VA114	ESP-r	TRNSYS-TUD	Exp.
MIN, kW	-4.12	-2.61	-3.25	-3.06	-4.00
MAX, kW	-0.01	0.00	0.00	0.00	-0.01
MEAN, kW	-1.47	-0.91	-0.86	-1.07	-1.28
DT95, kW	-0.58	-0.28	-0.61	-0.41	
DT5, kW	0.02	1.03	0.91	0.65	
MEANDT, kW	-0.24	0.19	0.12	-0.03	
ABMEANDT, kW	0.25	0.33	0.40	0.29	
RSQMEANDT, kW	0.30	0.46	0.47	0.34	
STDERR, kW	0.18	0.42	0.46	0.34	

Heating power in zone 2	BSim	VA114	ESP-r	TRNSYS-TUD	Exp.
MIN, kW	0.01	0.00	0.00	0.01	0.02
MAX, kW	0.65	0.53	0.45	0.57	0.63
MEAN, kW	0.35	0.27	0.21	0.28	0.40
DT95, kW	-0.13	-0.26	-0.37	-0.26	
DT5, kW	0.03	-0.06	-0.09	-0.02	
MEANDT, kW	-0.05	-0.15	-0.23	-0.14	
ABMEANDT, kW	0.06	0.15	0.23	0.14	
RSQMEANDT, kW	0.07	0.16	0.24	0.16	
STDERR, kW	0.04	0.06	0.09	0.07	
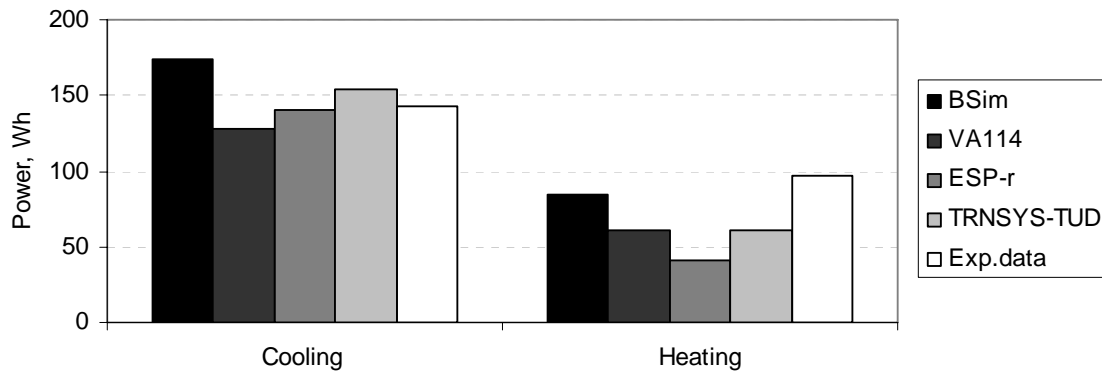
Figure 77. Total cooling/heating power in the zone 2. Test case DSF200_e.

The above plot for the total cooling and heating is not exactly sufficient, as there were periods with the experimental data lacking, which resulted in the decreased total cooling/heating power in the experimental results, compared with simulations.
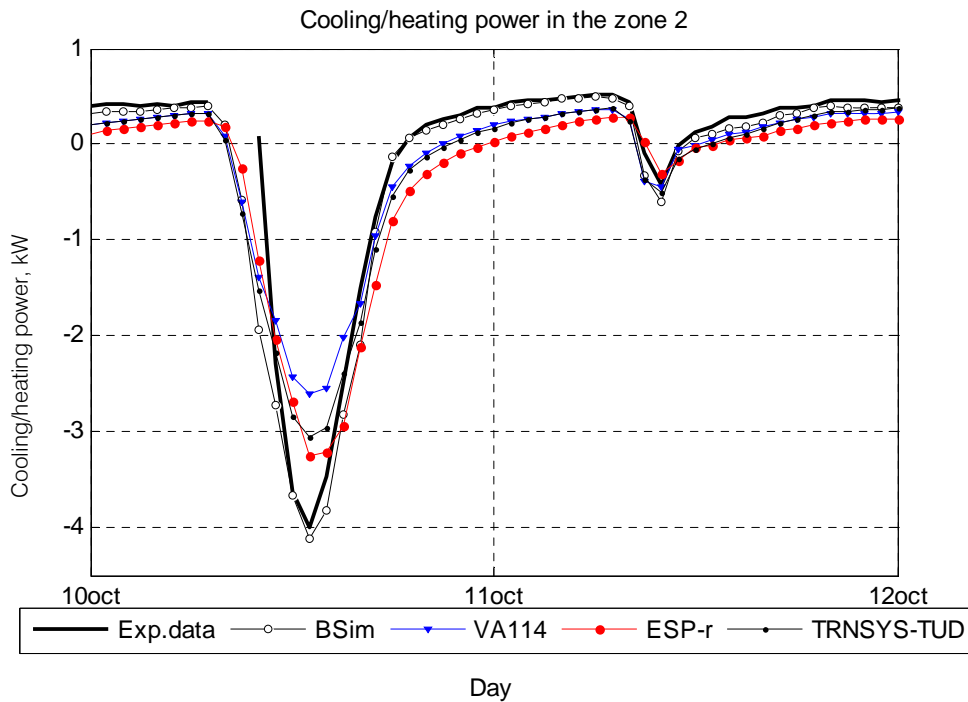
Figure 78. Cooling/heating power in zone 2. Test case DSF200_e.

In this test case, calculation of the heating power has also improved, since the models were modified to consider the thermal bridges. The cooling power in the zone 2 is mainly underestimated by all models, except for BSim, with results often exceeding the experimental data. The lowest values are obtained by VA114, while ESP-r and TRNSYS-TUD have similar results.

Again, it seems that the slope of the ESP-r profile in the afternoons differs from the others, indicating differences in the time constant of the models. Nevertheless, the cooling/heating power is the product of calculated air temperatures and mass flow rate in the double-skin facade cavity.
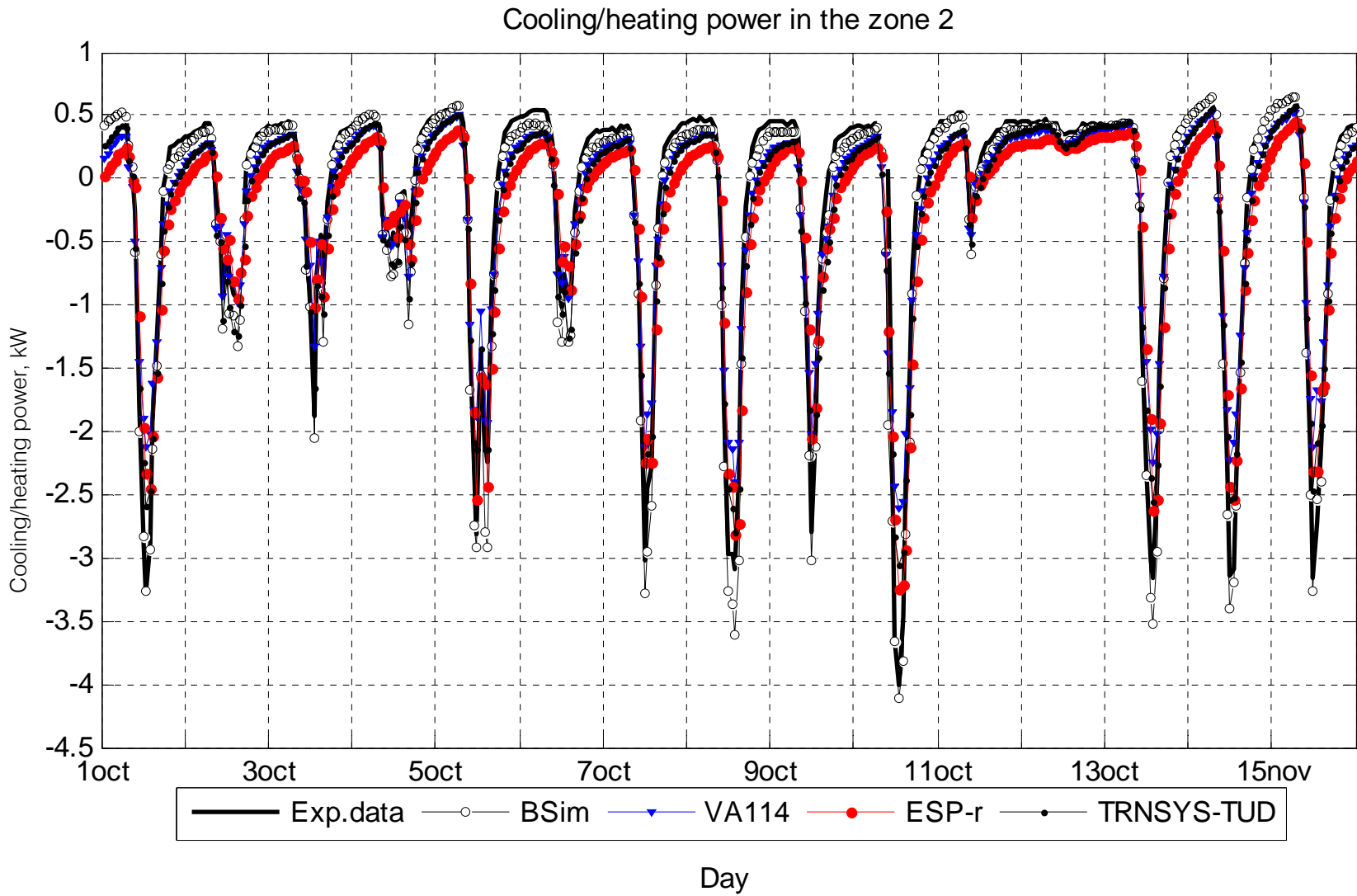
Figure 79. Cooling heating power in zone 2. Test case DSF200_e.

6.4.10   The other parameters in the empirical and simulation results

Besides the global parameters such as an air temperature, mass flow rate, energy load in a zone, modellers had to report the surface temperature of constrictions if possible. The surface temperatures of the constructions were measured during the experiments together with many other parameters. However, the plots of the results and their assessment are not included in the main report, but into the Appendix II.

Less attention is paid to these data, since the measurement of the surface temperatures of the constructions is very complex and the results can include errors, which are not possible to detect or assess. Moreover, the modelling of the surface temperatures is very sensitive to assumptions made towards the convective and radiative heat transfer at the surfaces. And, finally, it is not crucial to use these parameters for the empirical validation of building simulation software, since the assumptions vary from one tool to another, but the building simulation tools stay focused on the predictions of energy consumption and occupants' comfort and therefore the quantitative measure for the validation was chosen between the global parameters. However, it is desirable to point out a tool that is able not only to predict the energy consumption, but also to be able to provide a reasonable level of accuracy of other parameters, especially regarding the surface temperature of the inner window glazing, as a contributor to the operative air temperature in the zone 2 and thus a contributor to the general perception of comfort.

A measurement of the surface temperature requires a good junction between the surface and the temperature sensor and in case of a bad junction, a measurement error may occur, which is not possible to quantify. The risk of error during the measurements was minimised by means of thermal paste of high heat transmitting property, which was used to attach the sensors to a surface.

Measurement of the surface temperature of the glazing requires shielding of the thermal sensor from the solar radiation, as the solar absorption property for thermal sensor is considerably higher than for the glass. The details on shielding the sensors and on measurements of a surface temperature are given in [5].

The limitations in the experimental setup and correspondingly caused errors are normally described by the numerous cables, measurement devices and equipment placed in the test facility. Moreover, a number of errors can occur due to the experimental conditions, which, in many cases, are different from the situation in a real life. For example, the temperature in the test room was kept constant during the whole period of experiments. In order to fulfil that, four fabric ducts were placed on the floor of the zone 2. Since the air in the ducts was slightly cooler or warmer (depending on the temperature in the zone), the concrete floor in the zone was heated up or cooled down. Correspondingly, the measurement of the surface temperature in the zone 2 was affected by the air temperature in the ducts and therefore, it is not reliable to conduct any comparison between simulated and measured floor surface temperature in the zone 2 [5].

Moreover, the modellers had to take additional steps in order to model the actual situation in the zone 2, with the floor shadowed from the longwave and short wave radiation by the fabric ducts. As a consequence, in some models, an additional layer of insulation on the floor was used in order to simulate the effect of the ducts (ESP-r), in VA114, this was done via the definition between convective and radiative form of solar gains in to the zone (the convective part vas increased from 0 to 10%). The consequences of all these solutions are very unpredictable, and as a conclusion, it is necessary to state that the reported and measured floor temperature in the zone 2 is incomparable.

The situation is similar for the floor temperature measurements in the zone 1, as a big number of cables were placed on the floor of the DSF cavity and therefore, the measurement of this surface temperature was erroneous. [5].

6.5   Summary for the empirical validation test cases

6.5.1   Background

As explained in the literature review [3], the physics of the double skin facade involves complex processes and therefore requires detailed calculations of optics, flow regime, convection, natural air flow etc. Often, building simulation software is not able to perform such detailed level of computations. When the detailed computations are not possible, then the simplified models are used as an alternative and it can be difficult to validate the advanced physical processes, however, this is not the objective. The building simulation software must be validated *together with their limitations,* yet the best possible software performance must be achieved. Still, the results of modelling must be consistent and demonstrate reasonable agreement of all or nearly all simulated parameters with the experimental data.

Prior to empirical validation, the completed set of comparative exercises has demonstrated the magnitude of differences between different building simulation tools and has confirmed the complexity of the task to simulate building with a double skin facade. Certainly, the procedure of validation of a building simulation tool involves not only the program, but the modeller, his personal opinion, experience and time spent on modelling. The most important achievement in the comparative exercise was then the experience gained by the modellers in the DSF modelling, the justification of their models against each other and finally, the demonstration of how important it is to conduct the empirical validation for modelling of buildings with the DSF, and thus to provide reference against which modelling predictions could be compared.

The empirical exercises were completed in the 'blind'-form, which means that the modellers received the experimental results only after submitting their results of simulations.

In the empirical validation procedure, it is necessary to keep in mind that the validation procedure is actually two-sided, as not only the accuracy of the model is to be validated, but also the accuracy of the measurements and the material in the specification as well. Thus, in case of disagreement between the model and the experimental data, it is necessary to examine possible reasons of deviations, both if the software does not perform the proper calculations and also if the experimental data are inaccurate.

Prior to the empirical validation, a set of additional test cases was carried out. The results of these test cases verified whether the models are built according to the specification and whether their thermal models perform as anticipated. Sensitivity study of the assumptions towards the heat transfer coefficients was carried out for VA114 and ESP-r model. The main findings demonstrate that:

- The internal convective heat transfer is of great importance
- The external convective heat transfer is of minor importance (it must be verified for the windows whether the same conclusion applies for windows)
- External longwave radiation heat transfer is of great importance
- The magnitude of changes of the results is huge for the peak cooling loads, air temperature and surface temperatures when different assumptions are applied (combined/split treatment of surface heat transfer fixed/variable surface film coefficients)
- The magnitude of changes of the results is huge for the peak cooling loads, air temperature and surface temperatures

And, the overall summary of the sensitivity studies shows the directions for further improvements which are given below:

- Combined treatment of surface film coefficients is too simple and the separate treatment is required
- Application of fixed surface film coefficients together with the separate treatment is also insufficient, but further studies are needed to argue further on this issue.

Still, these directions are rather obscure, as the impact of the surface heat transfer in the DSF, first, must be studied separately from the zone 2. Also, the application of variable convective surface film coefficients puts few questions:

- What are the suitable expressions for convective heat transfer at the surfaces to use in the zone 2 and in the DSF?
- Is it necessary to use different expressions for the convective surface coefficients in the DSF cavity and zone 2?
- It is, also, reasonable to assume that application of different from the zone 2 expressions for the convective heat transfer in the cavity might be necessary due to different flow conditions in these two zones. If so, then different expressions might be needed for the DSF cavity in the different operational modes.

Most of results for the surface temperature are only included into the Appendix I. The reason for that is that the resulting surface temperatures, for example, depend on computations and assumptions in a model, such as distribution of solar radiation and shadow to the surfaces, level of detail in longwave radiation exchange, flow regime at the surface and assumptions made for calculation of the convective heat exchange at the surface etc. These computations and assumptions vary from one tool to another, but the building simulation tools stay focused on the predictions of energy consumption and occupants' comfort and therefore the quantitative measure for this empirical validation was chosen between the global parameters.

6.5.2   Overview of the results

Before comparing the global parameters, it was necessary to perform the verification of the boundary conditions, which was done in two steps:

- Evaluation of the boundary external conditions. Sufficiently good agreement with the experimental data was achieved in computations of solar radiation striking to the DSF surface for both of the test cases. Also, it was possible to demonstrate consistency in modelling the test cases and also to prove that the results of simulations are comparable with the experimental data.

- Validation of the boundary internal conditions. Relatively small deviations were observed when calculating the transmitted solar radiation to the zones (first order of solar transmission). However, it was argued that the deviations are mainly caused by the minor differences in calculation of incident solar radiation, which became more pronounced in the transmitted solar radiation, due to the large window areas. This part of validation is comparative, as no empirical data are available to estimate the magnitude of transmitted solar radiation. Another reason for disagreements between the models was explained by the different mathematical models and deviations in optical properties of constructions when calculate distribution, transmission and absorption of solar radiation.

The DSF is differently subdivided in ESP-r and TRNSYS-TUD models: there are three equal zones in ESP-r and 4 zones in TRNSYS-TUD (Figure 80), where two of the smaller zones were located at the bottom and at the top and two bigger ones were located in the middle of the cavity. The definition of zones in TRNSYS-TUD corresponds to the geometry of windows in the specification. Splitting up the cavity into a few zones stacked on the top of each other can highly improve the accuracy of simulation, but this solution is more suitable when it is necessary to count on the vertical temperature gradient only, as this does not solve the complexity of the local recirculation.
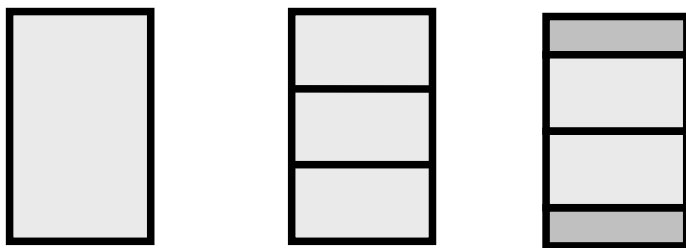
Figure 80. Illustration of zoning in the models. VA114 and BSim (left), ESP-r (center), TRNSYS-TUD (right).

When the results of simulations are compared against the experimental data, then the information about the measurement procedure and experimental set-up can be critical for evaluation of the measurement accuracy

and possibility for the error. On the whole, the main details of measurement procedure were mentioned in the report. Even more details about the experimental setup and experiments can be found in [5].

The air temperature in the DSF is evaluated via the temperature raise in the cavity compared to the outdoor air temperature. This is essential, especially for the test case DSF200_e, which is characterised by rather low temperature raise due to the high air change rate in the cavity. It is crucial for the validation that the programs agree very well with the experiments when calculating the air temperature in zone 1, as for the high air change rates, the disagreements in the air temperature are unacceptable, as they will result in hundreds of watts of error in thermal balance.

The studies show that the models do not agree on the subject of air temperature in the zone 1. Even the models that perform best in terms of experimental results, still have an error of 1-5°C (ABMEANDT), furthermore, the deviations from the experimental data in the periods with the peak solar radiation are much more significant. Only in the periods without solar radiation, a sufficient agreement is reached between the models and experiments.

In the test case DSF100_e, which does not involve the mass transfer in the cavity, the best approximation to the experimental data in the periods of peak solar loads is achieved for ESP-r model and TRNSYS –TUD model. Significant overestimation of the air temperature in the cavity is characteristic for BSim and underestimation for VA114.

Quite the opposite situation is seen for the air temperature predictions in zone 1 for the case DSF200_e. Here, all of the models, except BSim, are in agreement when compared against each other in the periods with the peak loads of solar radiation. The agreement is reached in the range of plus-minus 1 °C. Though, the experimental air temperature is 3-10°C higher than the calculated one. Meanwhile, all of the models calculate reasonably different mass flow rates in the cavity, which are very high. High flow rates can be a reason for a better agreement between the models in the test case DSF200_e compared against test case DSF100_e.

Finally, when discussing air temperature, it is important to draw an attention to the assumptions and their significance for the final result when defining the convective and radiative heat transfer at the surface in the models. As it was revealed in section 5.4 Sensitivity study - impact of surface film coefficients, right choice of the surface coefficients can become a focal point in the validation procedure.

According to the sensitivity study, by fixing an internal or external, convective or radiative coefficient or by combining the convective and radiative surface heat transfer coefficients, the performance of a model can change dramatically, however, using the separated variable convective and radiative heat transfer coefficients, the model is able to adjust better to the significant changes in solar radiation. Still, this might not solve all of the difficulties.

Regarding *the mass flow rate* in the DSF cavity, it was difficult to attain a final conclusion, due to the extreme complexity of the long time monitoring and measurement of the naturally induced air flow rate in the cavity. Although it is difficult to measure air flow in a naturally ventilated double skin facade cavity, as there is either no easy method or no accurate one exists, results obtained with the velocity profile method and the tracer gas method show reasonable agreement. However, due to the risk of error in each of the methods, the preference of one method to the other one can be given only upon personal opinion.
The authors have pointed out all of the possible risks of error during the experiments and, for now, the final conclusion is left upon the reader. At the same time it is important to point out that such conditions of experimental and simulation results argue for further experimental studies and empirical test case for validation of the building simulation software to conclude the subtask assignment.

The deviations between the measured and simulated *cooling/heating power in* the zone 2 are obvious. Most of the models underestimate the cooling loads to the zone especially in the days with intensive solar irradiation, while at night the agreement is rather good due to the modifications made to the models to count on thermal bridges. The difficulties with the simulation during the day time periods are the consequence of greater deviations in predicted air temperature and mass flow rates in the cavity. Also, the significance of surface heat transfer coefficients has already been pointed out.

The great deviation in the cooling/heating power in the zone is a result of interplay of many parameters, such as air flow rate, convection and radiation heat transfer, transmission of solar radiation etc. At the same time it is not possible to validate all of the inter-related parameters in this subtask, as many of those are the challenge for the whole field of building simulations. However, the air flow rate is particularly interesting and influencing factor for

the DSF performance, moreover, the air flow in the DSF is an unavoidable part of the whole DSF concept. Thus, the air flow rate was chosen as one of the main targets in evaluation and validation of building simulation software for buildings with DSF. Despite the fact that more empirical test cases are needed to complete the validation assignment, the discussion of the mass flow models upon the results of simulations and empirical results should be made.

All in all, none of the models is consistent enough when comparing results of simulations with the experimental data: for every parameter considered – a different model is closer to the experimental data. Thus, the models are still rough and may need further improvements.

6.5.3 Discussion of the air flow models and influencing matters in the air flow modelling.

It is well known that any model for calculations of natural air flow is very sensitive to a number of empirical parameters such as the discharge coefficient, the wind pressure coefficients, the terrain parameters, coefficients in the power-law equations etc. The situation is extremely rare when the experimental data for estimation of these coefficients exist for a particular building, which should to be modelled. In real life, the modelling takes part prior to construction and therefore a user of the simulation tool takes the decision upon different recommendations, standards and experience.

In order to avoid or minimise the sensitivity of the air flow models to the input parameters, these were specified in the empirical test case specification (discharge coefficient, pressure difference coefficients, tightness characteristics of the building and the function of the wind reduction according to the type of terrain). The discharge coefficients, the function of wind reduction and building tightness were obtained empirically for the experimental setup.

The pressure difference coefficients were specified on the basis of literature study for a building of the same shape as the experimental test facility. The sensitivity of the flow models to the pressure difference coefficients is very significant and therefore the truthfulness of the defined pressure difference coefficients is essential. This is verified via wind driven night time ventilation in the test case DSF200_e, for the models using the same pressure difference coefficients as in specification (TRNSYS-TUD, ESP-r), whose results demonstrate almost identical mass flow rate in the cavity as measured.

Experimentally obtained discharge coefficients are also verified using the manual calculation of the mass flow rate in the cavity caused by the buoyancy forces (Figure 10), with results of calculations being in a good agreement with the experimental results.

It is not always possible to use the specified data; therefore, the discharge and the pressure coefficients for the openings used in all models were also compared. In fact, the differences in input values for the discharge and pressure difference coefficients are noteworthy. Furthermore, they could have played a vital role in calculations and can be a reason for disagreements in predicted air flow rate due to the sensitivity of the air flow models to these parameters. As for example in VA114, the difference between the pressure coefficients is set to zero, and as a result, the wind pressure force is left out of consideration. In BSim, an empirically obtained relationship is used to calculate wind induced air flow rate. ESP-r and TRNSYS-TUD use the same pressure difference coefficients, but not the discharge coefficients, thus some differences in the flow magnitudes are observed while the shapes of their plots are often similar.

Earlier, it was mentioned that the application of the orifice model assumes the fully developed turbulent flow and in most of the cases, this assumption is valid as even the laminar flow regime turns to turbulent due to the opening size, sharp edges of the opening etc. However, the orifice equation is not accurate enough when the laminar flow or flow in transition to turbulent occurs. In this case the power-law model has the priority as it can be adjusted to one or another regime as long as it is known what flow regime one deals with. Yet, there is no empirical data available to verify the application of one or another relationship (orifice or power-law).

TRNSYS-TUD and VA114 use a power-low equation. It is known that the flow exponent of 1.5 is a user-defined parameter in VA114 model, which is normally used for very small openings and results in lower pressure loss through the openings if compared with orifice equation.

Another issue to discuss is the consideration of the wind turbulence effect on the air flow rates in the DSF cavity. Only one of the models in the empirical exercises considers the wind fluctuations as a contributor to the

total air flow rate in the cavity (VA114 uses the wind fluctuation model described in [11,12]). At the same time, the design of the DSF in many cases represents a construction with the openings at the different levels of the same surface. This is also the case in the comparative exercises. Although, the openings located at different levels (single-sided ventilation), the wind pressure, do not have as much effect on the air flow, as in case of cross ventilation. From this point of view, the wind fluctuation effect can have an increased importance and can influence the accuracy. Another expression for taking into account the wind fluctuations can be used, developed by Larsen [13], which it takes into consideration the location of the opening (windward/leeward side) and a combination of wind pressure and temperature differences.

Previously, it was explained that the air temperature in the DSF cavity is the result of the convective heat transfer between the glass surfaces and the cavity air. The surface temperature of the glass can become relatively high and as a part of convective heat transfer appears the boundary layer flow. The air flow rate in the boundary flow normally increases with the distance from the inlet opening and in some circumstances, it is likely that the air flow in the boundary layer can exceed the main flow rate in the cavity. This can cause the appearance of the reverse flow and even more intricate the flow field in the cavity.

At the moment, the network method and the loop method are the best suitable for the calculation of the dynamic air flow rate in a naturally ventilated space. The network method is also the one used for almost all models in the empirical exercise. However, one of the limitations of this method is that it is not suited to model the air flow patterns within the zone [14], such as reverse flow, local recirculation, etc.

6.6   Summary

Considering the topics of the discussion in the previous section, one can argue that the subject of naturally driven flow is complex and it is not easy to model the naturally driven flow in the DSF cavity. Moreover, taking into account the results of simulated and measured global parameters, one can note that the main difficulties experienced in predictions (or measurements) are characteristic for the periods with the intensive solar radiation, however the night time periods, or the days with the low solar intensity are relatively easy to model, both from the heat transfer and mass transfer point of view.

Good performance of the models in periods of lower solar intensity indicates that the building simulation tools perform very well, but in the periods of higher solar intensity, more detailed calculations or models should be applied, as the presence of solar radiation is an essential element for the double skin facade operation (only the period with the moderate solar intensity was modelled in the empirical test cases) and the models in the present validation task do not provide results of superior accuracy compared to empirical results.

Existing experimental data sets have a benefit of rather varying solar radiation intensity, which allows to validate whether the models are able to cope with the often changes in solar radiation intensity. On the other hand, rather limited solar radiation intensity in the dataset does not allow to completely explore the performance of the models.

In order to be able to deal with the double-skin facade buildings, modellers may consider application of separated variable surface film coefficients, as this would help to obtain more realistic predictions of the air temperature in the cavity during the peak loads of solar radiation. Especially, this involves the radiation surface film coefficients and internal convective film coefficients, otherwise the air temperatures in the cavity and also the cooling loads in the zone 2 will be drastically underestimated. This suggestion, however, requires some guidelines for definition of variable convective heat transfer coefficients. Also, the application of variable coefficients may not solve all of the disagreements, as the sensitivity study does not include any clear results, but only gives an indication of importance of assumptions towards the surface heat transfer.

Since there are no experimental data available about the convective heat transfer processes in the cavity, and the rule of thumb does not apply for the double-skin facade constructions, then there is no knowledge base exists to rely on when attempting to calculate or fix the surface film coefficients in a simulation model. Finally, the application of commonly used combined fixed surface film coefficient is not sufficient enough, as demonstrated in section 5.5.

In the future work it would be necessary to expand the sensitivity study and perform a number of tests where the convective and radiative heat transfer coefficients are extensively tested for application in a double-skin facade model, for different climates and geometry (preferably together with experimental data). Furthermore, some simple studies would be helpful to reveal the differences between and their impact on final result. These

could be simple test cases with the internal surface emissivity of 1; time constant of the constructions in zone 2 equal to 0; steady state simulation with presence of solar radiation.

If the issue of comfort should to be addressed in the calculations, then application of reliable convective/radiative surface heat transfer coefficients must be ensured. Otherwise, a sensitivity study will be necessary to prove the robustness of the results.

Another issue of modelling a double-skin facade building with naturally ventilated cavity is prediction of the mass flow rate in the cavity. This will certainly improve when the thermal model works without the flaws, but none of the existing models consider the recirculation flows in the cavity. The recirculation flows, however, may become very important, as they may generate an additional momentum at a certain level in the cavity, leading to the increased convective heat transfer and therefore the increased buoyancy force.

Certainly, the accuracy and quality of the experimental results must be also evaluated, as these are the main measures in empirical validation procedure. Most of the details about the accuracy and risk of error during the measurements are mentioned in the report, while more information is given in [5] It is apparent that the described measurement methods in [5] have sources of error and compared to laboratory conditions have relatively large uncertainties, but on the other hand these experimental results represent the full-scale outdoor measurements, with well controlled and measured internal conditions and with the measurement errors one can be aware of.

The results of the empirical validation can be regarded as arguments for further empirical and comparative validation, which should include some sensitivity studies of the parameters involved into the simulation of the DSF performance (or expanded number of the test cases), including wind pressure coefficients, discharge coefficients, spectral properties of the glazing along with the analysis of influence of the DSF-geometry *in the model* in means of partitioning the DSF in 2 or more zones stacked on the top of each other, equal and different size of these zones, application of shading device, etc.

Another, extremely important subject in the DSF modelling is modelling of shading device in the cavity (zone 1). The predictions made for the double skin facade in the empirical test cases DSF100_e and DSF200_e do not include the shading device, despite that fact, the complexity of the processes in the DSF appeared to be strict enough to result in deficient accuracy of simulations. Shading device is a distinctive element of DSF application and, in addition, it is an important contributor to the double skin facade physics. Its contribution to the DSF physics is expressed by means of an additional heat source in the DSF cavity and therefore more complex longwave radiation exchange, increased air temperature in the cavity and thus the increased buoyancy effect, etc. In view of these facts, the modelling can become even more intricate. Therefore it is desirable to continue with the empirical validation of building simulation software, including the solar shading devices, their properties and positioning in the cavity.

Completing of the validation procedure with the above suggestions would allow to finalize whether it is possible to perform the DSF modelling within the software tools available on the market, by means of improved model geometry and definitions, minimized error due to the model sensitivity to the input parameters and whether the solar shading device intricate the modelling procedure. And, finally, the additional test cases would clarify whether a new computation model is required to perform an accurate modelling of the double skin facade buildings and what are the improvements should be made in the new model compared to the existing ones.

LITERATURE

1.   Judkoff R. and Neymark, J.(2006). Model validation and testing: The methodological foundation of ASHRAE Standard 140, *ASHRAE Transactions* **112** (2) (2006), pp. 367–376

2.   *ASHRAE Handbook—Fundamentals*. (2005). Atlanta, GA: American Society of Heating, Refrigerating, and air-Conditioning Engineers. See Chapter 32, "Energy Estimating and Modeling Methods", section titled "Model Validation and Testing".

3.   Poirazis H. (2006). "Double Skin Facades for Office Buildings - Literature Review Report" (9.86MB). Division of Energy and Building Design, Department of Construction and Architecture, Lund Institute of Technology, Lund University, Report EBD-R—04

4.   Kalyanova, O., & Heiselberg, P. (2007). Empirical Test Case Specification: Test Cases DSF200_3 and DSF200_4 : IEA ECBCS Annex43/SHC Task 34 : Validation of Building Energy Simulation Tools. Aalborg: Aalborg University : Department of Civil Engineering.
ISSN 1901-726X DCE Technical Report No.033

5.   Kalyanova O. (2007). Experimental set-up and full-scale measurements in 'the Cube'.
Aalborg:Aalborg University: Department of Civil Engineering.
ISSN 1901-726X DCE Technical Report No.034.

6.   Kalyanova, O. & Heiselberg, P. (2007). Comparative validation of building simulation software: Modeling of Double Facades: REPORT. Aalborg: Aalborg University: Department of Civil Engineering. ISSN 1901-726X DCE Technical Report No.024.

7.   Clarke J.A. (1985). Energy Simulation in building design. Adam Hilger Ltd. Bristol and Boston.

8.   ASHRAE (1997) Handbook of fundamentals, Atlanta, 1997

9.   Perez R., Ineichen, P., Seals, R., Michalsky J. & Stewart, R. (1990) Modelling Daylight Availability and Irradiance Components from Direct and Global Irradiance, Solar Energy, Vol. 44, pp. 271-289

10.   Perez et al., (1987) R. Perez, R. Seals, P. Ineichen, R. Stewart and D. Menicucci, A new simplified version of the Perez diffuse irradiance model for tilted surfaces, Solar Energy 39 (1987) (3), pp. 221–232.

11.   Phaff et al., (1980). The ventilation of buildings. Investigation of the consequences of opening one window on the internal climate of the room, TNO report C448.

12.   Awbi, H.B. Ventilation of Buildings. Air infiltration and natural ventilation (chapter 3). F&FN Spon. ISBN 0-419-15690-9.

13.   Larsen, T.S. (2006). Natural Ventilation Driven by Wind and Temperature Difference. Aalborg : Department of Civil Engineering : Aalborg University, 2006. 140p.

14.   Walton G.N. (1989)Airflow Network Models for Element-Based Building Airflow Modeling. ASHRAE Transactions: 1989, Vol.95, Part 2, pp.611-620.

15.   Etheridge, D. & Sandberg, M. (1996). Building ventilation: theory and measurement. UK, Wiley, 1996, 724pp.

16.   Larsen, T S. 2006. Natural Ventilation Driven by Wind and Temperature Difference. Ph.D Thesis. Aalborg : Department of Civil Engineering : Aalborg University, 2006. 140 p.

17.   McWilliams J., (2002). Review of Airflow Measurement Techniques. Lawrence Berkeley National Laboratory, December 1, 2002

APPENDIX I. Results of empirical validation

Test case DSF100_e

Figures from the main report
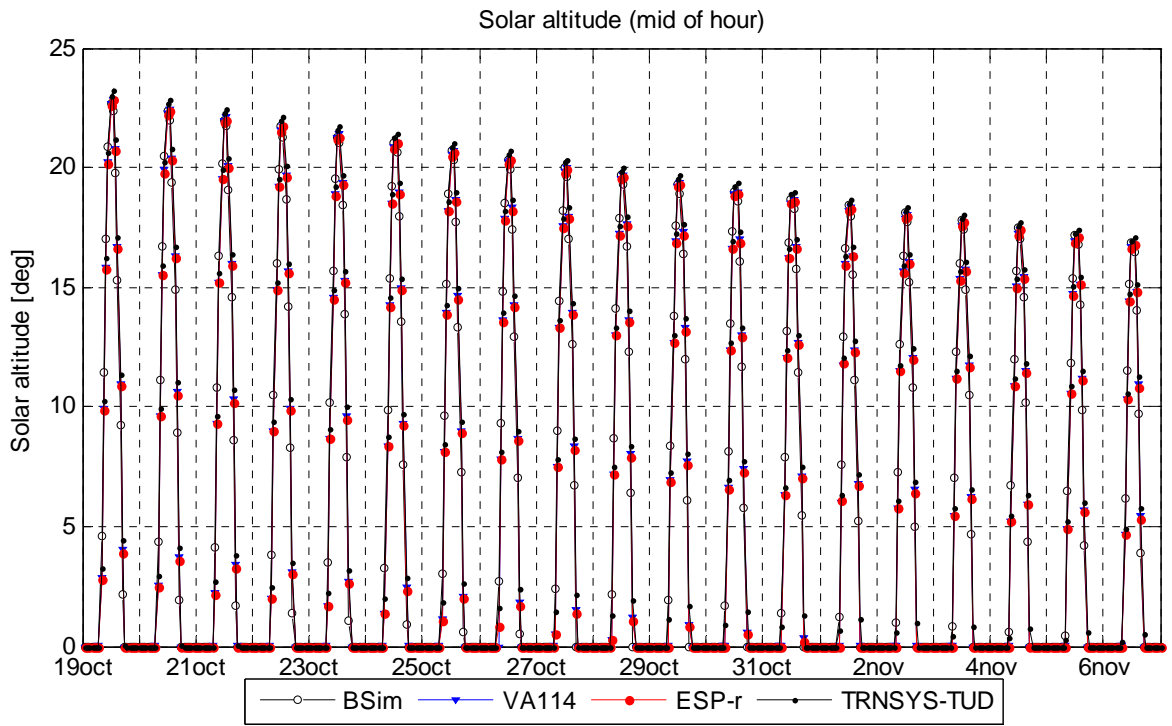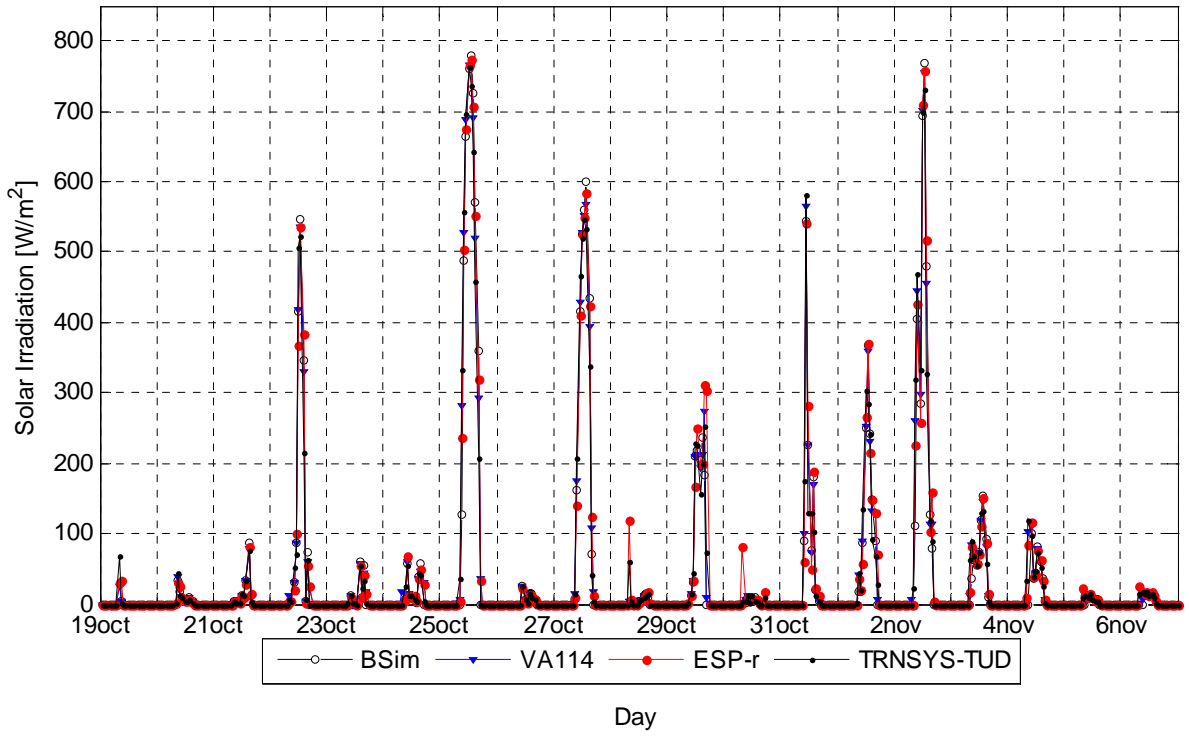
Solar altitude (mid of hour)

Direct solar irradiation on the external window surface

Diffuse solar irradiation on the external window surface

Total solar irradiation on the external window surface

Solar radiation transmitted from the outside into the zone 1

Solar radiation transmitted from zone 1 into zone 2 (first order of solar transmission)
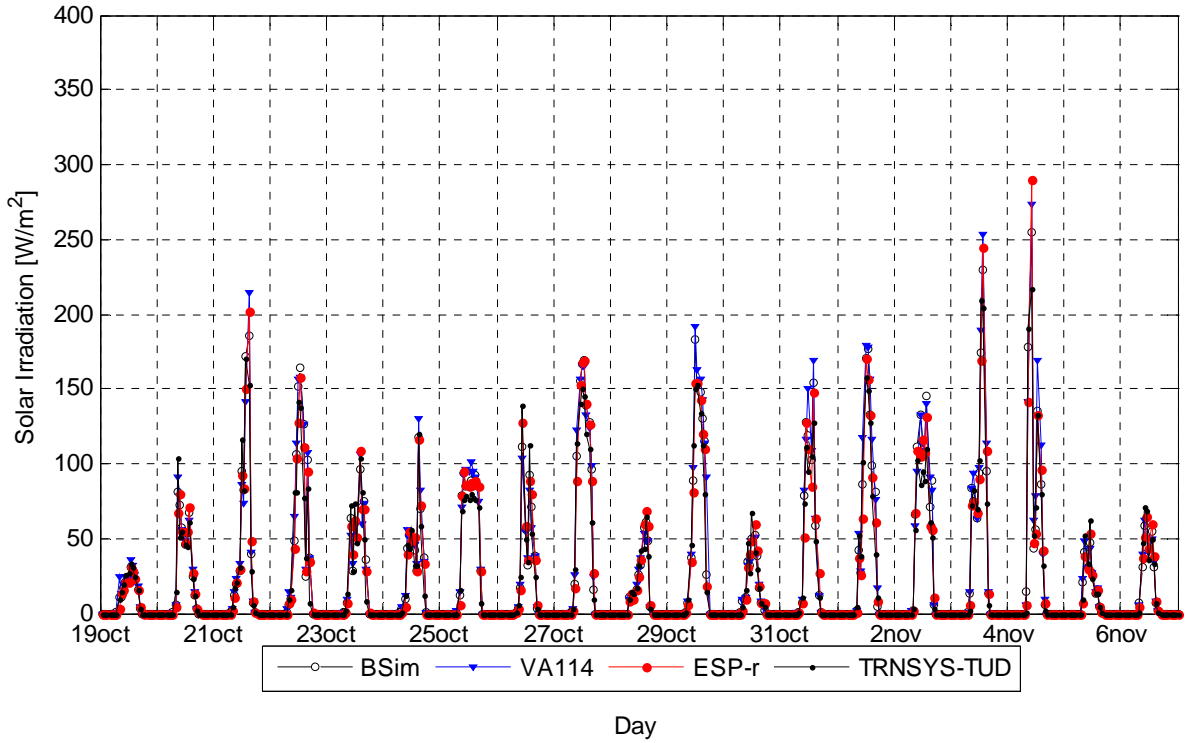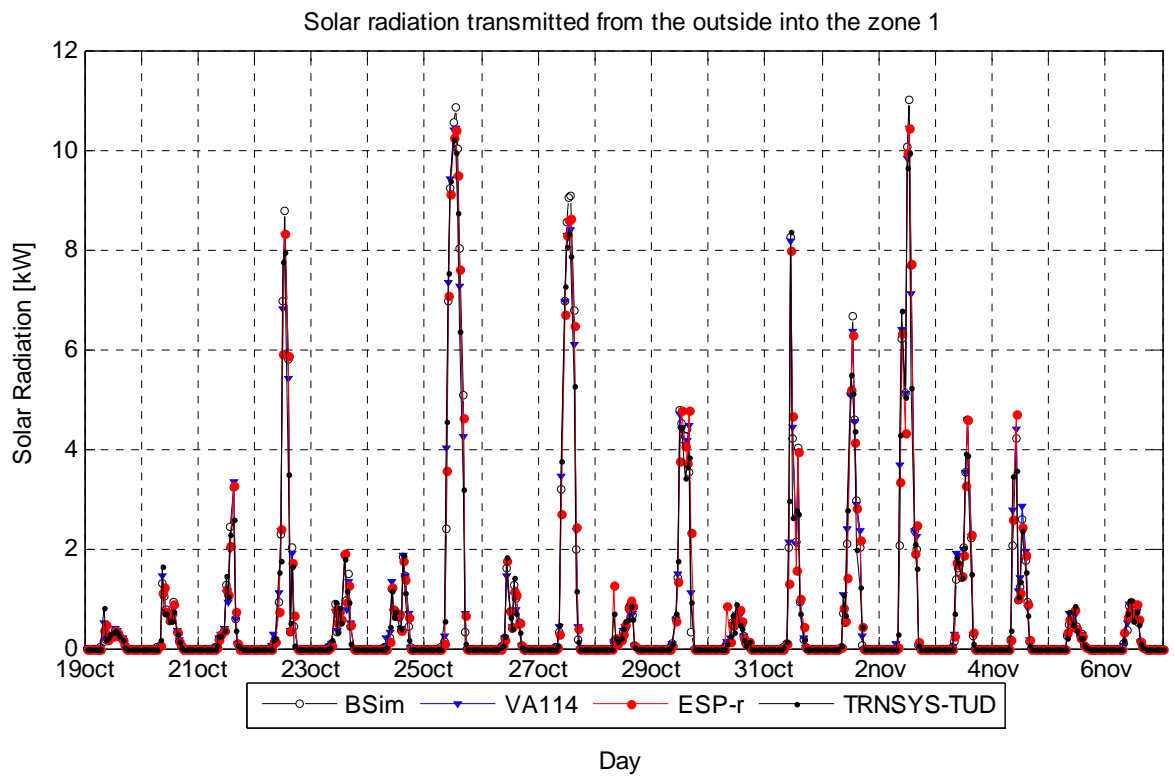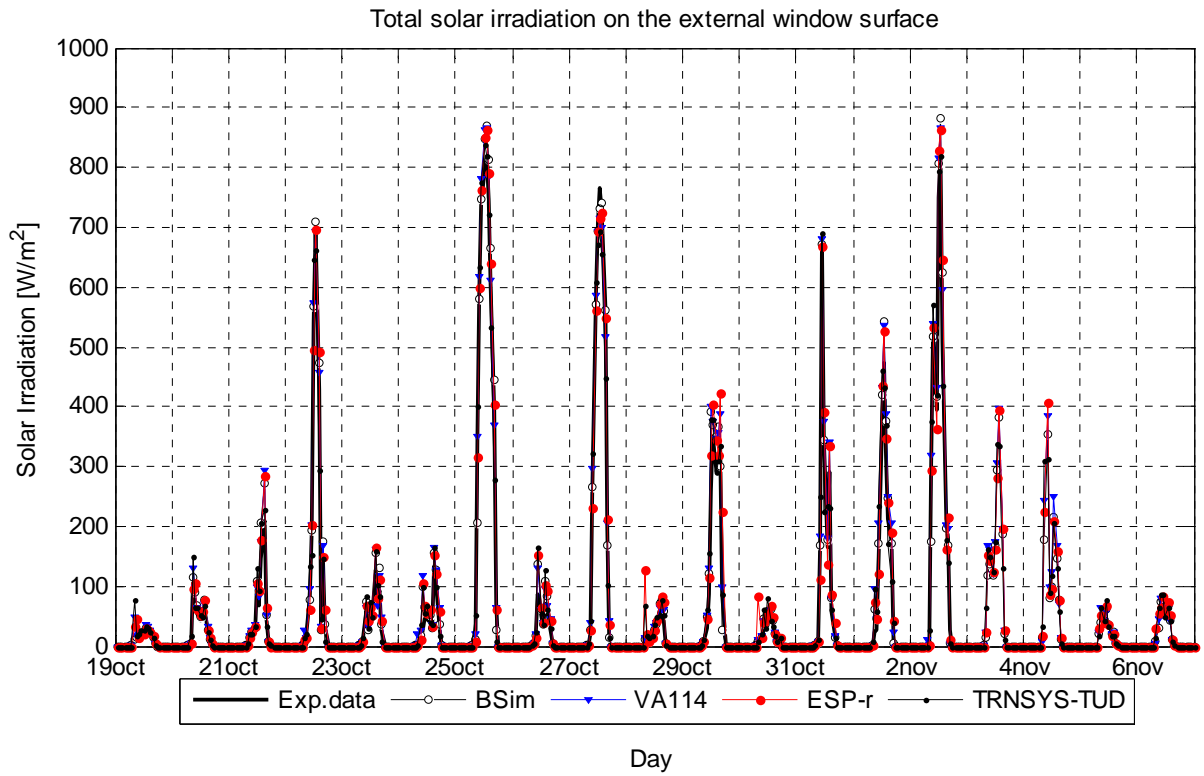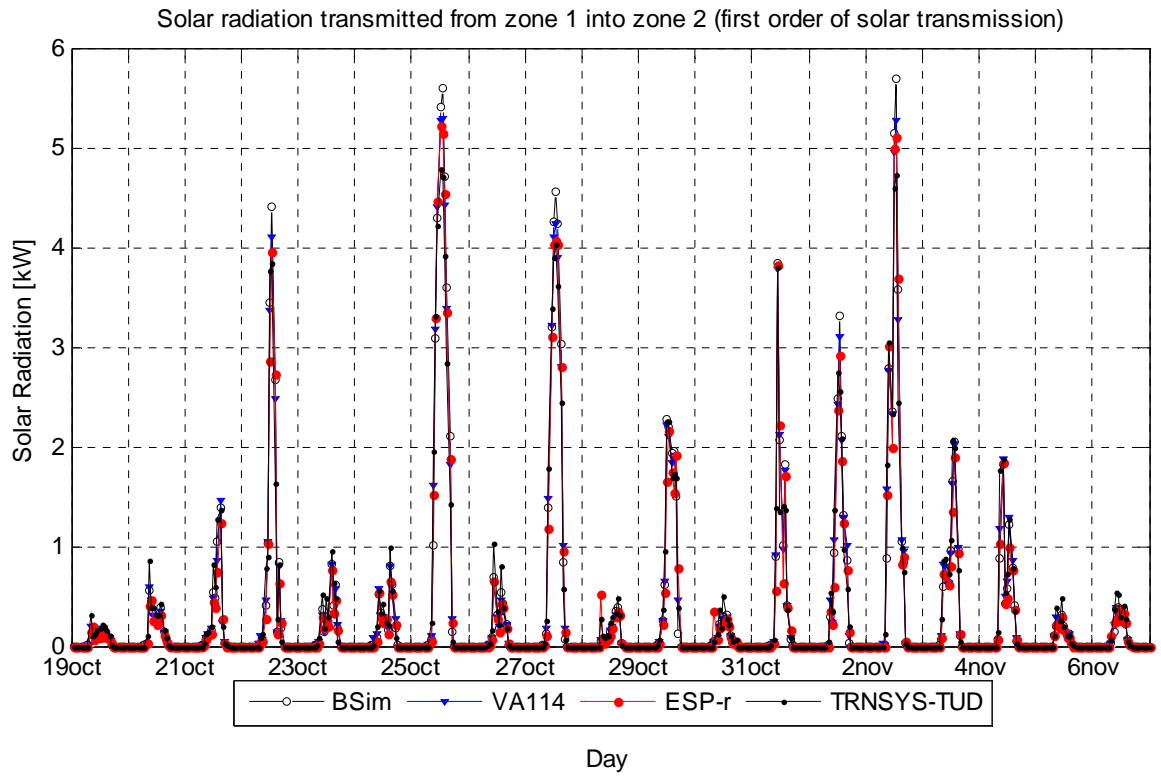
Surface temperature of the glazing
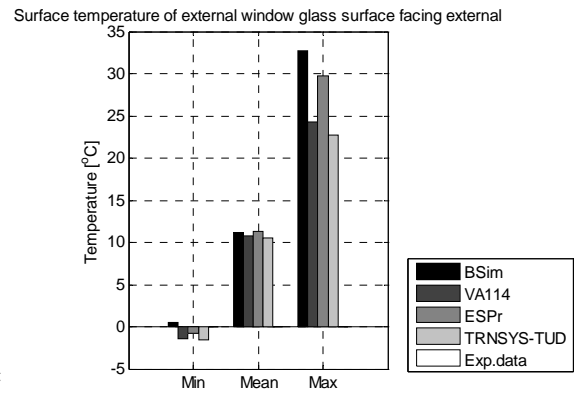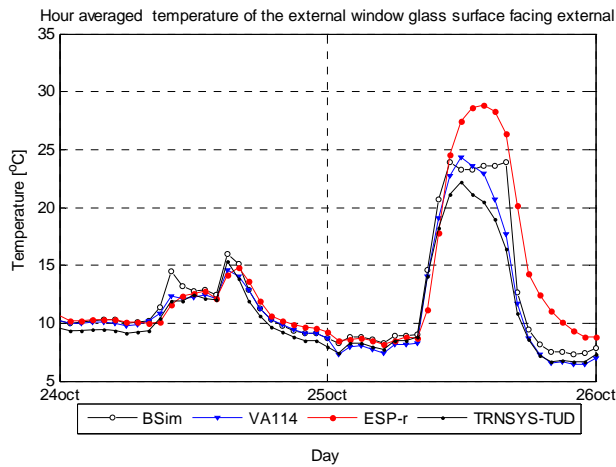
Temperature of external window glass surface facing external	BSim	VA114	ESP-r	TRNSYS-TUD	Exp.
MIN, °C	0.54	-1.42	-0.78	-1.61	-
MAX, °C	32.75	24.30	29.69	22.72	-
MEAN, °C	11.22	10.81	11.33	10.47	-

Hour averaged temperature of the external window glass surface facing external
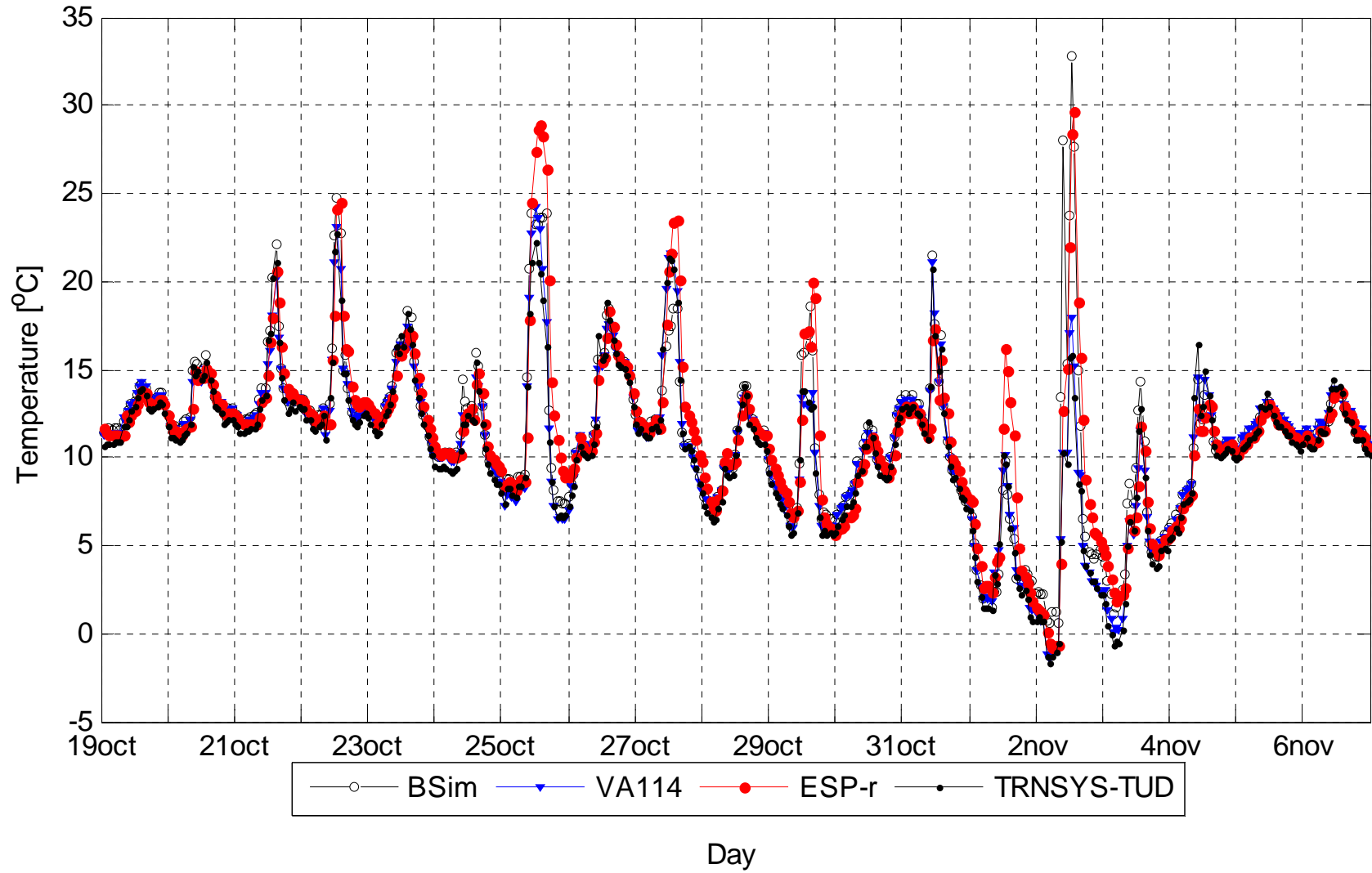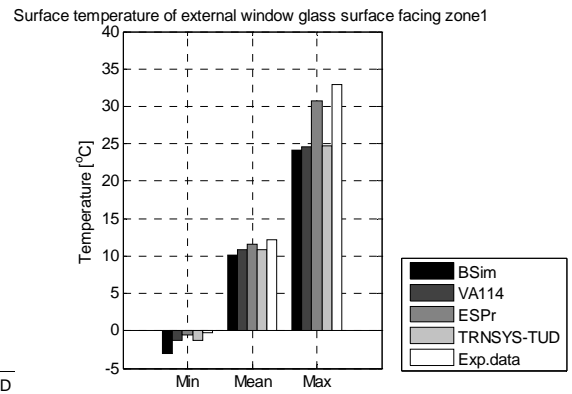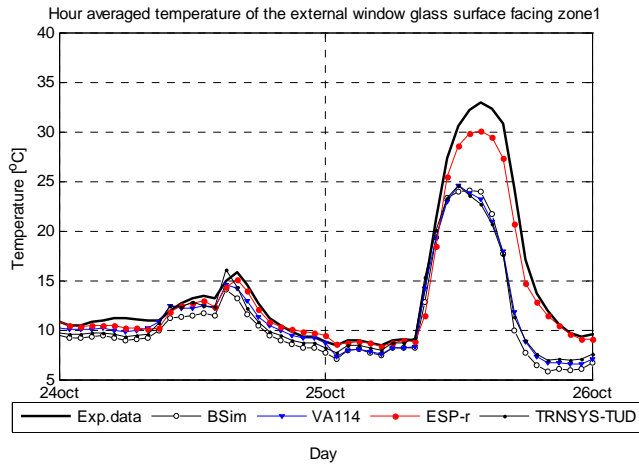
Hour averaged temperature of the external window glass surface facing zone1

Surface temperature of external window glass surface facing zone1

Temperature of external window glass surface facing zone 1	BSim	VA114	ESP-r	TRNSYS-TUD	Exp.
MIN, °C	-2.98	-1.33	-0.54	-1.21	-0.27
MAX, °C	24.16	24.58	30.70	24.72	32.97
MEAN, °C	10.17	10.88	11.54	10.86	12.17
DT95, °C	-6.52	-5.99	-2.53	-5.62	
DT5, °C	-0.28	0.10	0.94	1.01	
MEANDT, °C	-2.01	-1.30	-0.63	-1.31	
ABMEANDT, °C	2.03	1.37	0.91	1.59	
RSQMEANDT, °C	2.98	2.51	1.39	2.61	
STDERR, °C	2.21	2.15	1.24	2.25	

Hour averaged temperature of the external window glass surface facing zone1
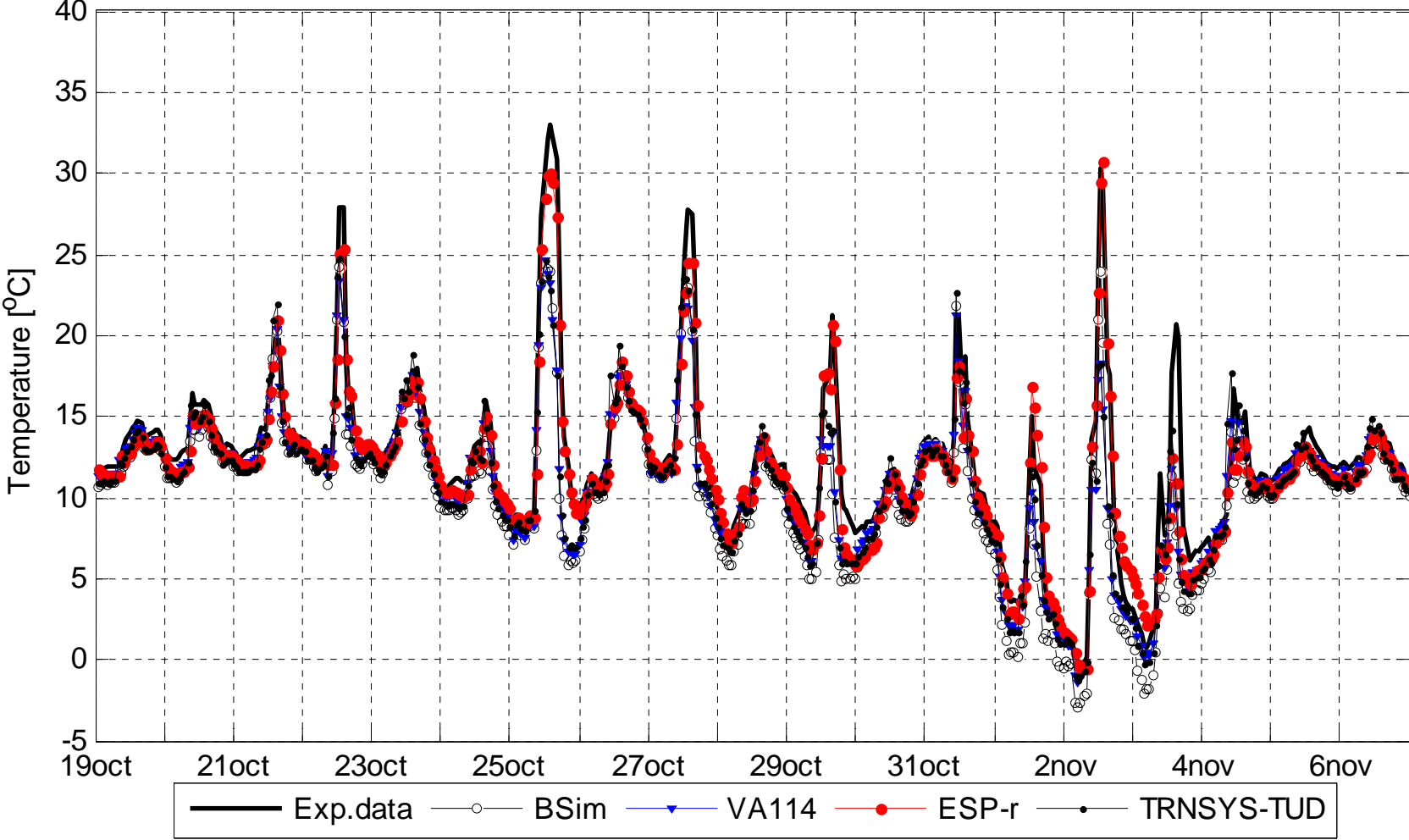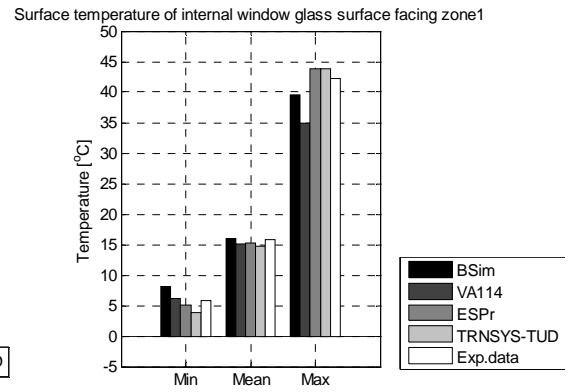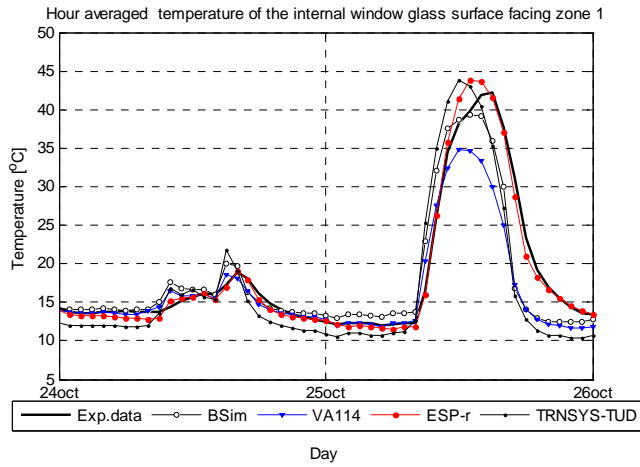
Hour averaged temperature of the internal window glass surface facing zone 1

Surface temperature of internal window glass surface facing zone1

Temperature of internal window glass surface facing zone 1	BSim	VA114	ESP-r	TRNSYS-TUD	Exp.
MIN, °C	8.09	6.14	5.12	3.86	5.72
MAX, °C	39.54	34.89	43.76	43.89	42.19
MEAN, °C	16.04	15.07	15.33	14.76	15.80
DT95, °C	-3.79	-5.34	-1.65	-4.86	
DT5, °C	3.13	1.17	1.65	5.72	
MEANDT, °C	0.24	-0.73	-0.46	-1.03	
ABMEANDT, °C	1.44	1.25	0.98	2.49	
RSQMEANDT, °C	2.50	2.57	1.51	3.52	
STDERR, °C	2.49	2.47	1.44	3.37	

Hour averaged temperature of the internal window glass surface facing zone 1

Hour averaged temperature of the internal window glass surface facing zone 2

Surface temperature of internal window glass surface facing zone2

Temperature of internal window glass surface facing zone 2	BSim	VA114	ESP-r	TRNSYS-TUD	Exp.
MIN, °C		18.76	17.57	18.26	18.61
MAX, °C		26.95	36.99	32.99	32.50
MEAN, °C		20.65	20.76	20.98	20.99
DT95, °C		-2.62	-1.02	-0.99	
DT5, °C		0.23	3.08	1.91	
MEANDT, °C		-0.34	-0.23	-0.01	
ABMEANDT, °C		0.44	0.92	0.53	
RSQMEANDT, °C		1.06	1.27	0.94	
STDERR, °C		1.00	1.25	0.94	

11

Hour averaged temperature of the internal window glass surface facing zone 2

Floor and ceiling surface temperature

Hour averaged floor surface temperature in the zone 1

Floor surface temperature in zone1

Floor surface temperature in zone 1	BSim	VA114	ESP-r	TRNSYS-TUD	Exp.
MIN, °C		7.16	7.91	8.02	7.02
MAX, °C		22.23	29.97	26.45	32.30
MEAN, °C		14.03	15.27	15.21	14.77
DT95, °C		-4.64	-0.77	-1.54	
DT5, °C		0.74	2.09	2.07	
MEANDT, °C		-0.75	0.50	0.44	
ABMEANDT, °C		1.05	0.80	0.97	
RSQMEANDT, °C		1.96	1.09	1.35	
STDERR, °C		1.82	0.97	1.28	

Hour averaged floor surface temperature in the zone 1

Hour averaged ceiling surface temperature in the zone 1

Ceiling surface temperature in zone1
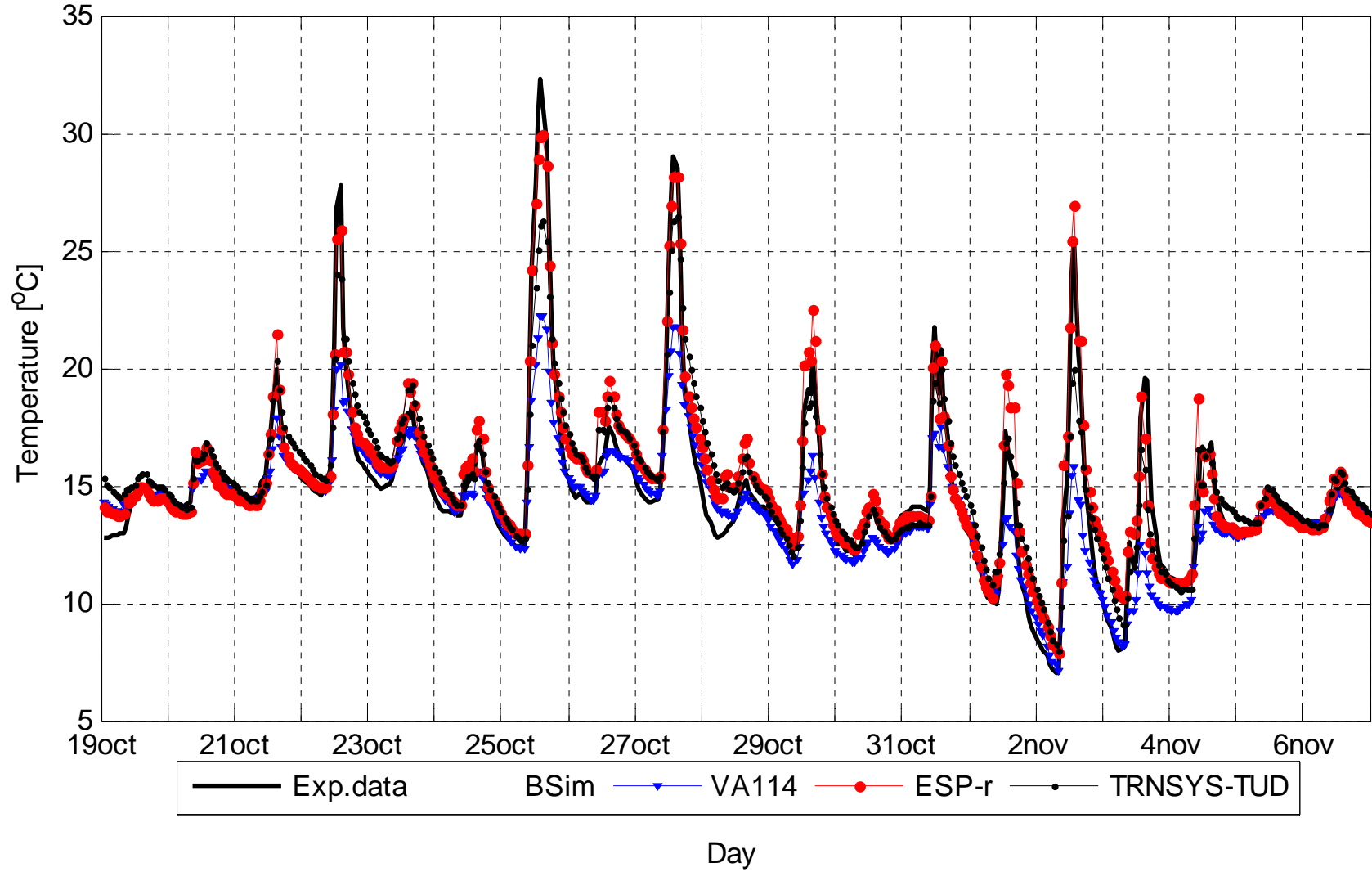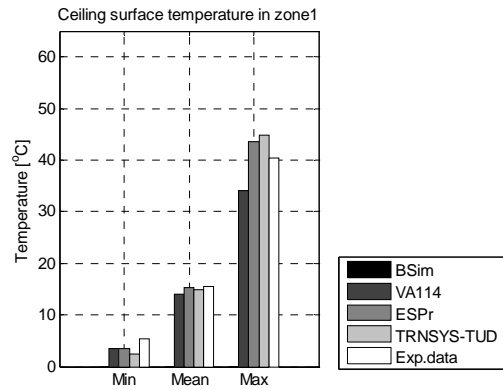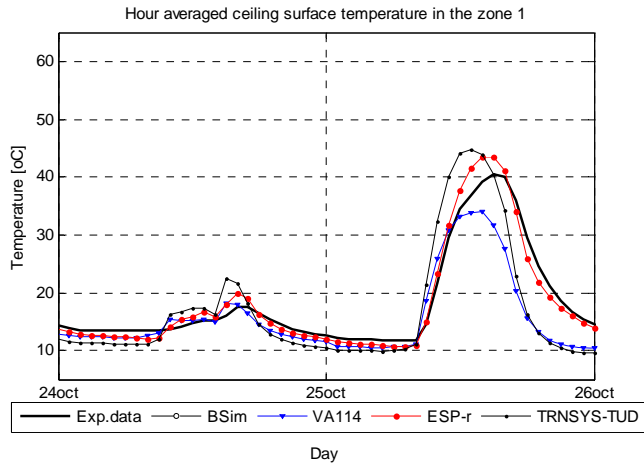
Ceiling surface temperature in zone 1	BSim	VA114	ESP-r	TRNSYS-TUD	Exp.
MIN, °C		3.54	3.44	2.38	5.45
MAX, °C		34.14	43.54	44.82	40.52
MEAN, °C		14.09	15.30	14.98	15.42
DT95, °C		-7.25	-2.01	-5.64	
DT5, °C		2.07	3.96	9.34	
MEANDT, °C		-1.33	-0.12	-0.44	
ABMEANDT, °C		1.92	1.38	3.21	
RSQMEANDT, °C		3.03	2.03	4.42	
STDERR, °C		2.72	2.03	4.40	

Hour averaged ceiling surface temperature in the zone 1
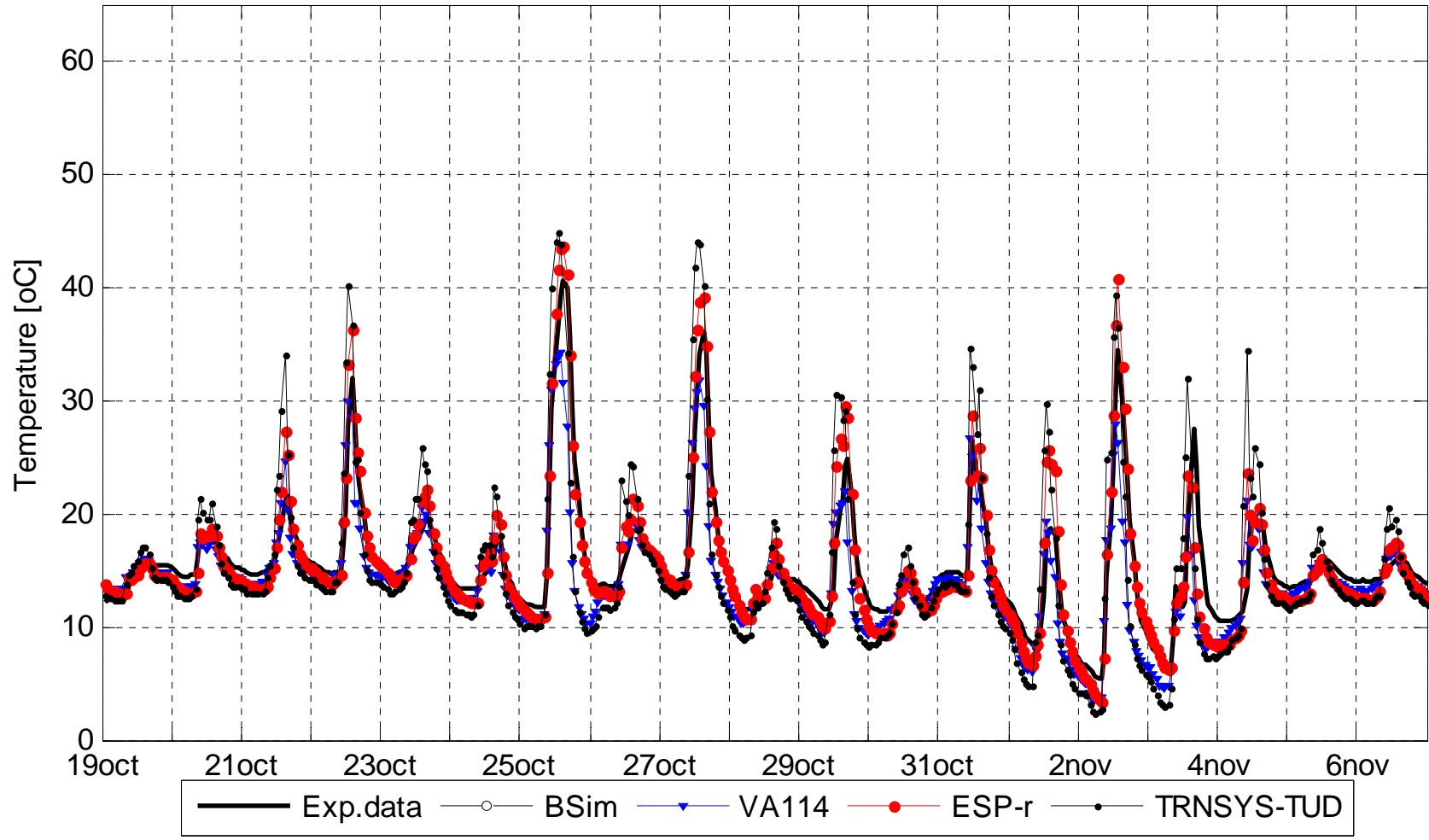
Hour averaged floor surface temperature in the zone 2

Floor surface temperature in zone2
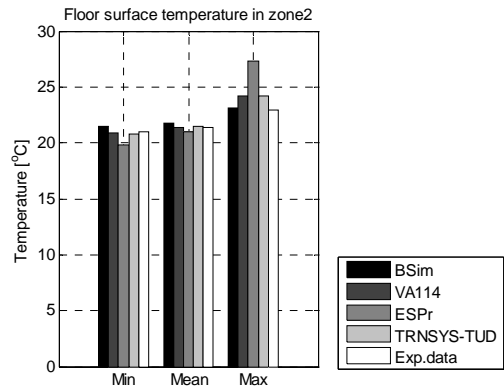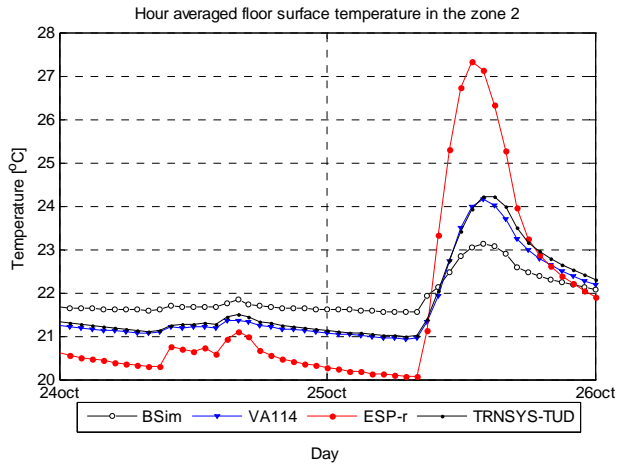
Floor surface temperature in zone 2	BSim	VA114	ESP-r	TRNSYS-TUD	Exp.
MIN, ^{o}C	21.51	20.86	19.84	20.79	21.03
MAX, ^{o}C	23.12	24.16	27.32	24.22	22.93
MEAN, ^{o}C	21.77	21.40	21.01	21.49	21.34
DT95, ^{o}C	0.28	-0.22	-1.17	-0.20	
DT5, ^{o}C	0.53	0.63	1.60	0.77	
MEANDT, ^{o}C	0.42	0.06	-0.33	0.14	
ABMEANDT, ^{o}C	0.42	0.18	0.80	0.22	
RSQMEANDT, ^{o}C	0.43	0.29	1.02	0.35	
STDERR, ^{o}C	0.09	0.28	0.96	0.31	

Hour averaged floor surface temperature in the zone 2

Exp.data · BSim · VA114 · ESP-r · TRNSYS-TUD

Day

Hour averaged ceiling surface temperature in the zone 2

Ceiling surface temperature in zone2
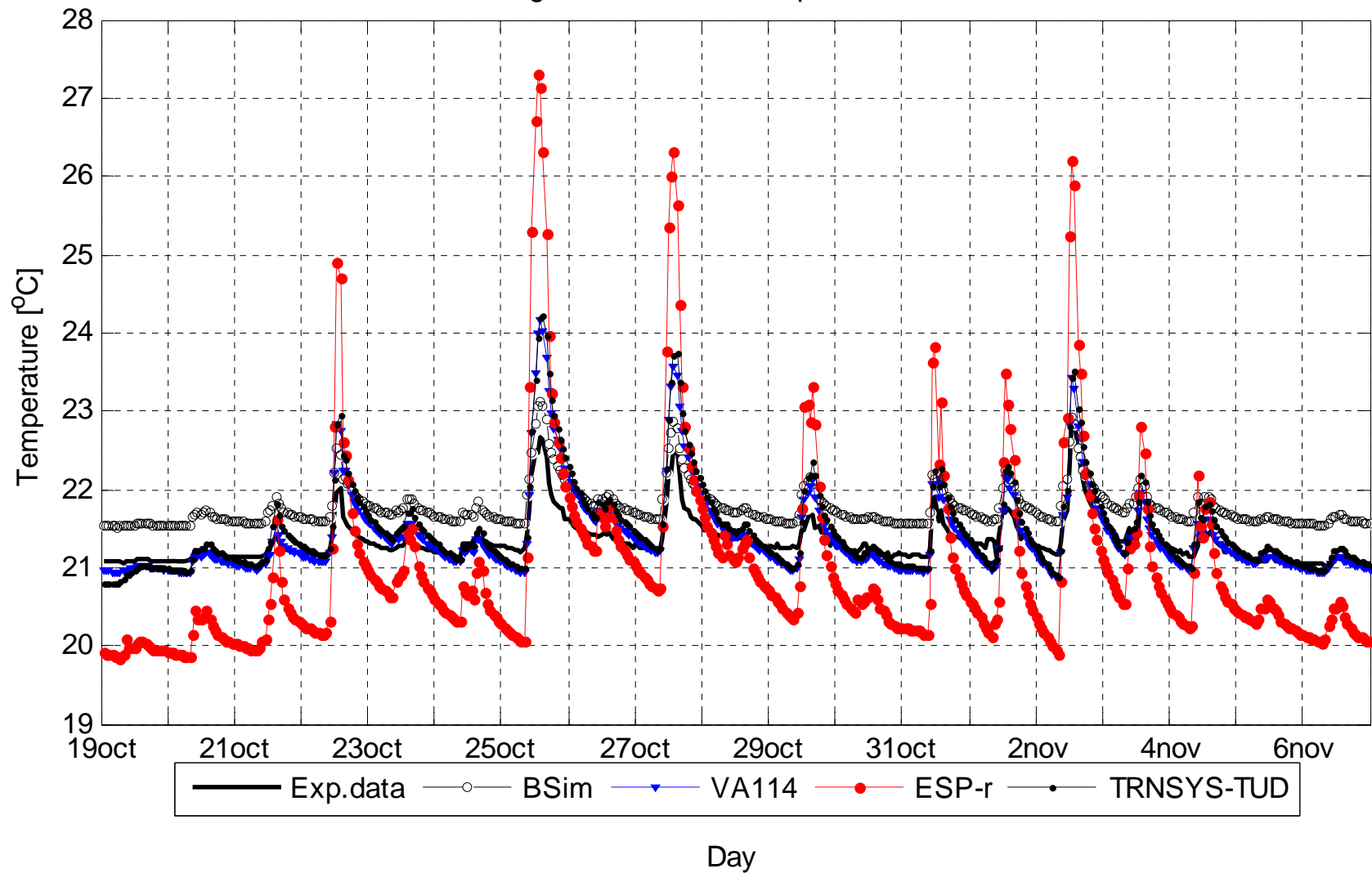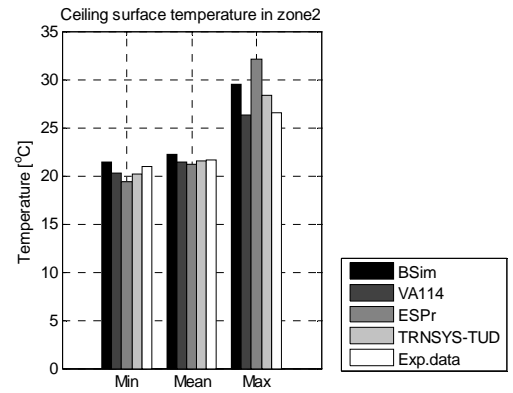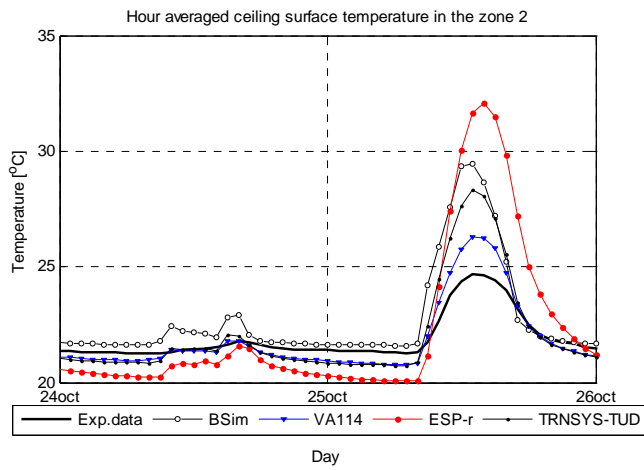
Ceiling surface temperature in zone 2	BSim	VA114	ESP-r	TRNSYS-TUD	Exp.
MIN, ºC	21.39	20.29	19.32	20.19	20.99
MAX, ºC	29.45	26.29	32.09	28.31	26.56
MEAN, ºC	22.19	21.41	21.25	21.50	21.61
DT95, ºC	0.06	-0.61	-1.25	-0.67	
DT5, ºC	2.24	0.59	2.59	1.36	
MEANDT, ºC	0.58	-0.20	-0.36	-0.10	
ABMEANDT, ºC	0.60	0.34	1.06	0.48	
RSQMEANDT, ºC	0.96	0.42	1.40	0.68	
STDERR, ºC	0.76	0.37	1.36	0.67	

Hour averaged ceiling surface temperature in the zone 2
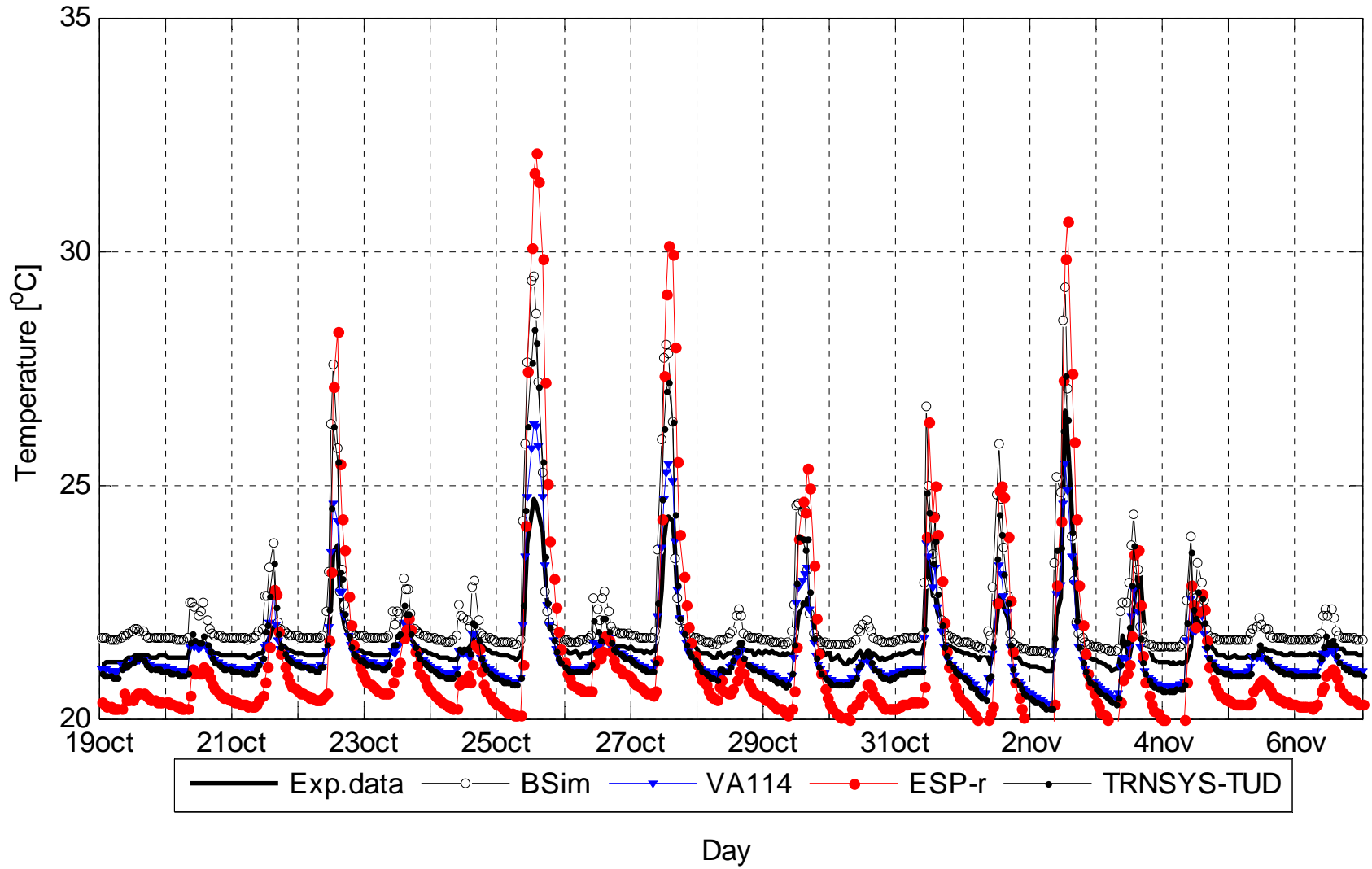
Direct solar irradiation on the external window surface

Diffuse solar irradiation on the external window surface

Total solar irradiation on the external window surface

Solar radiation transmitted from the outside into the zone 1

Solar radiation transmitted from zone 1 into zone 2 (first order of solar transmission)
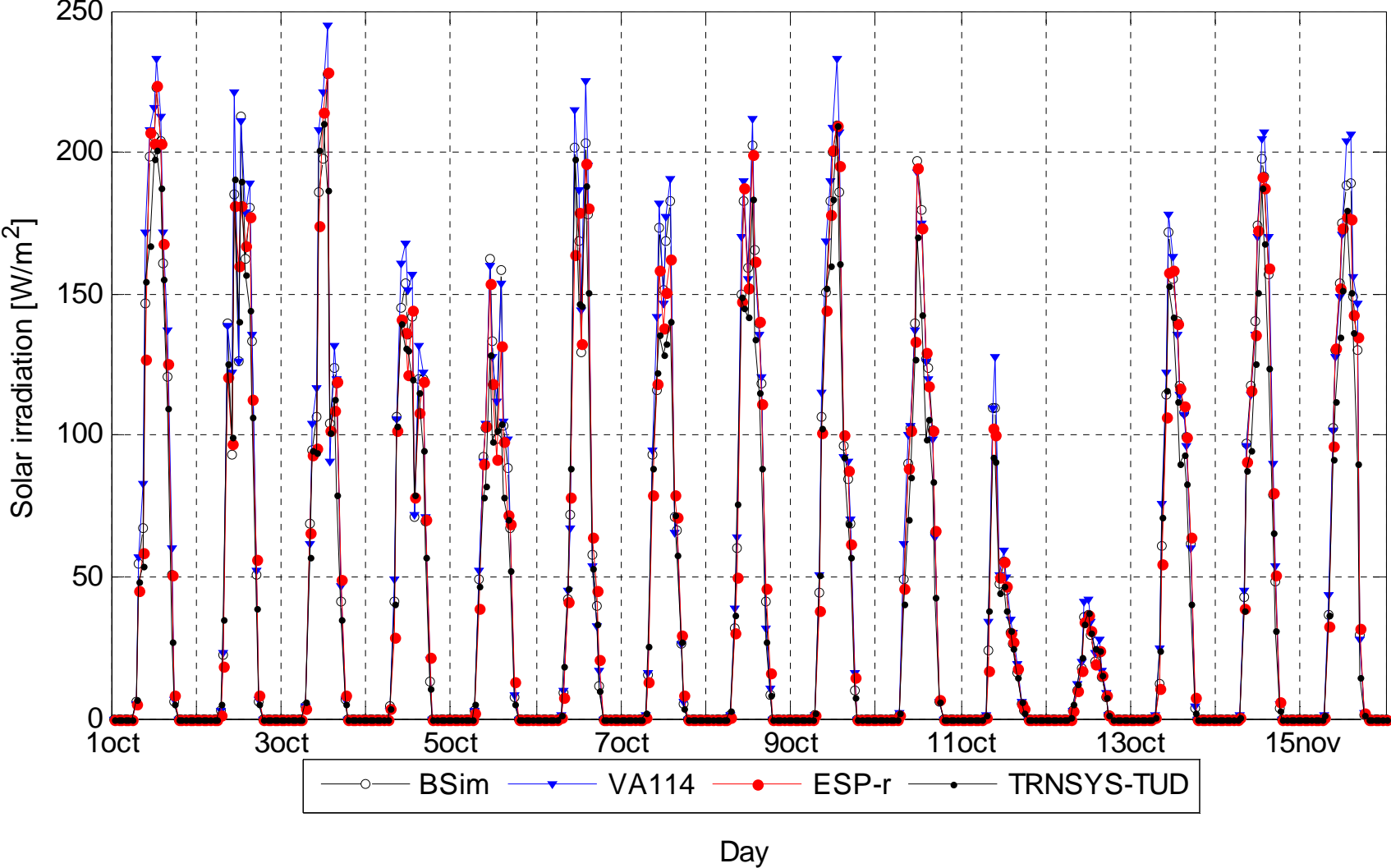
Surface temperature of the glazing

Hour averaged temperature of the external window glass surface facing external
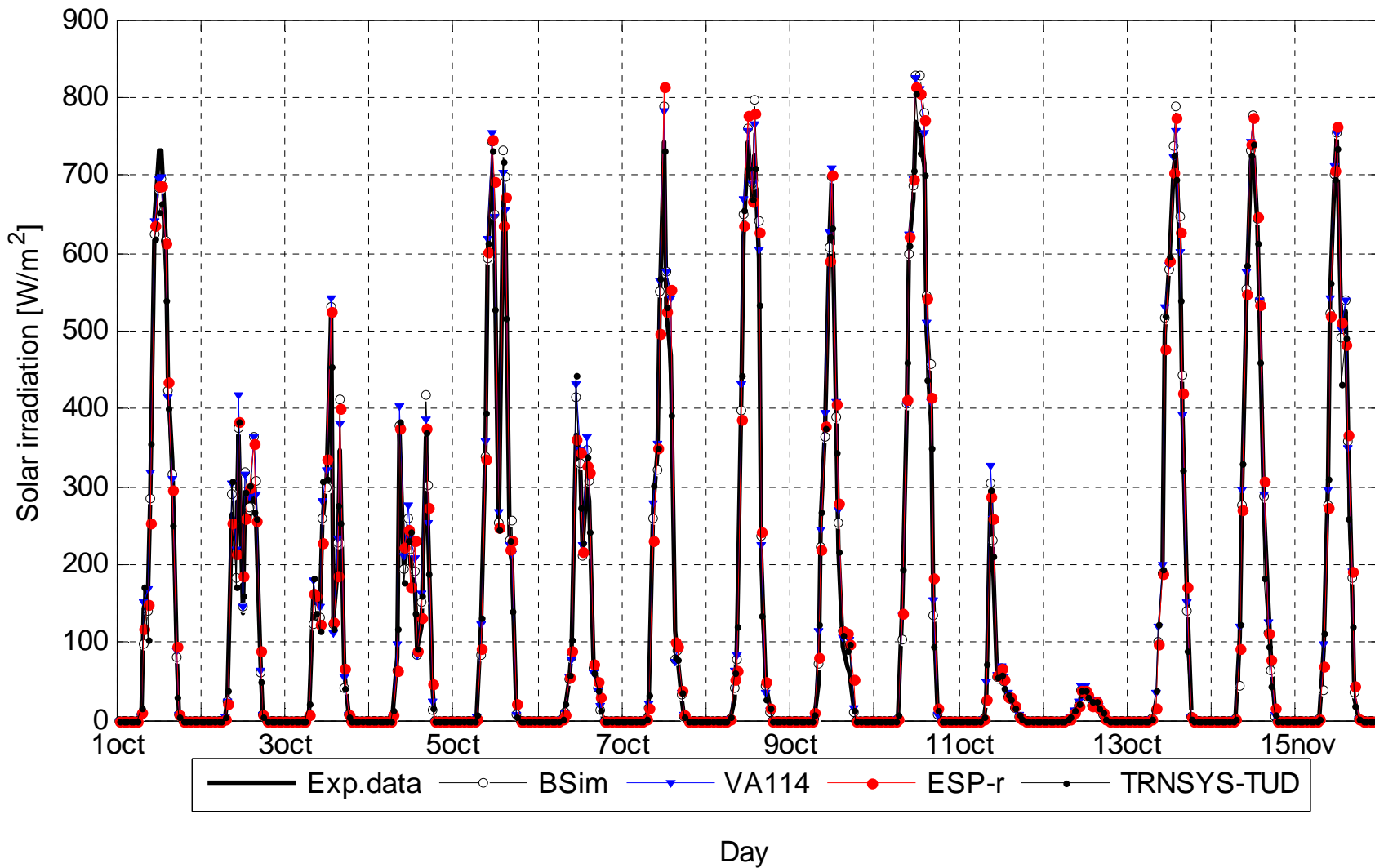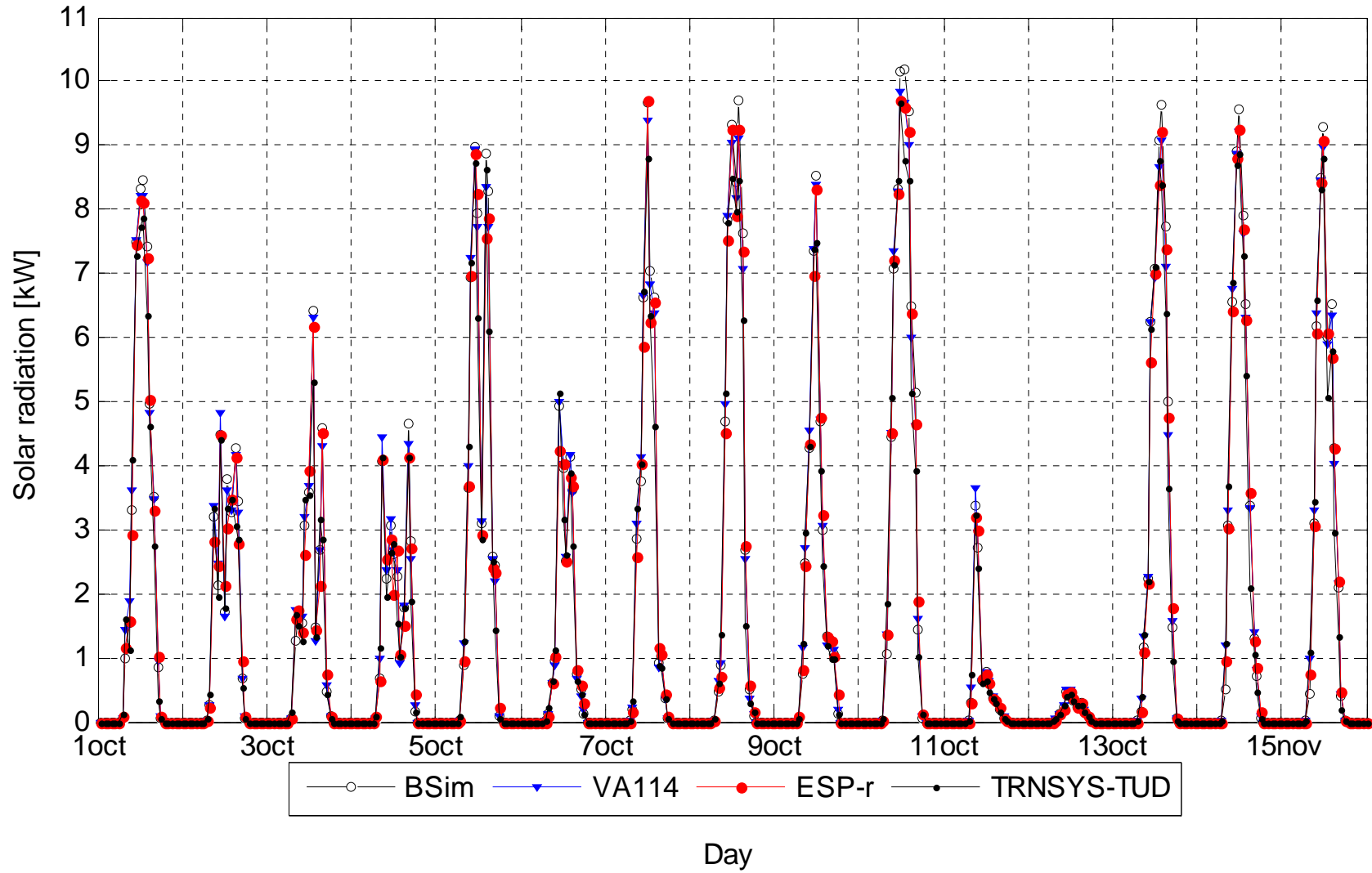
Surface temperature of external window glass surface facing external
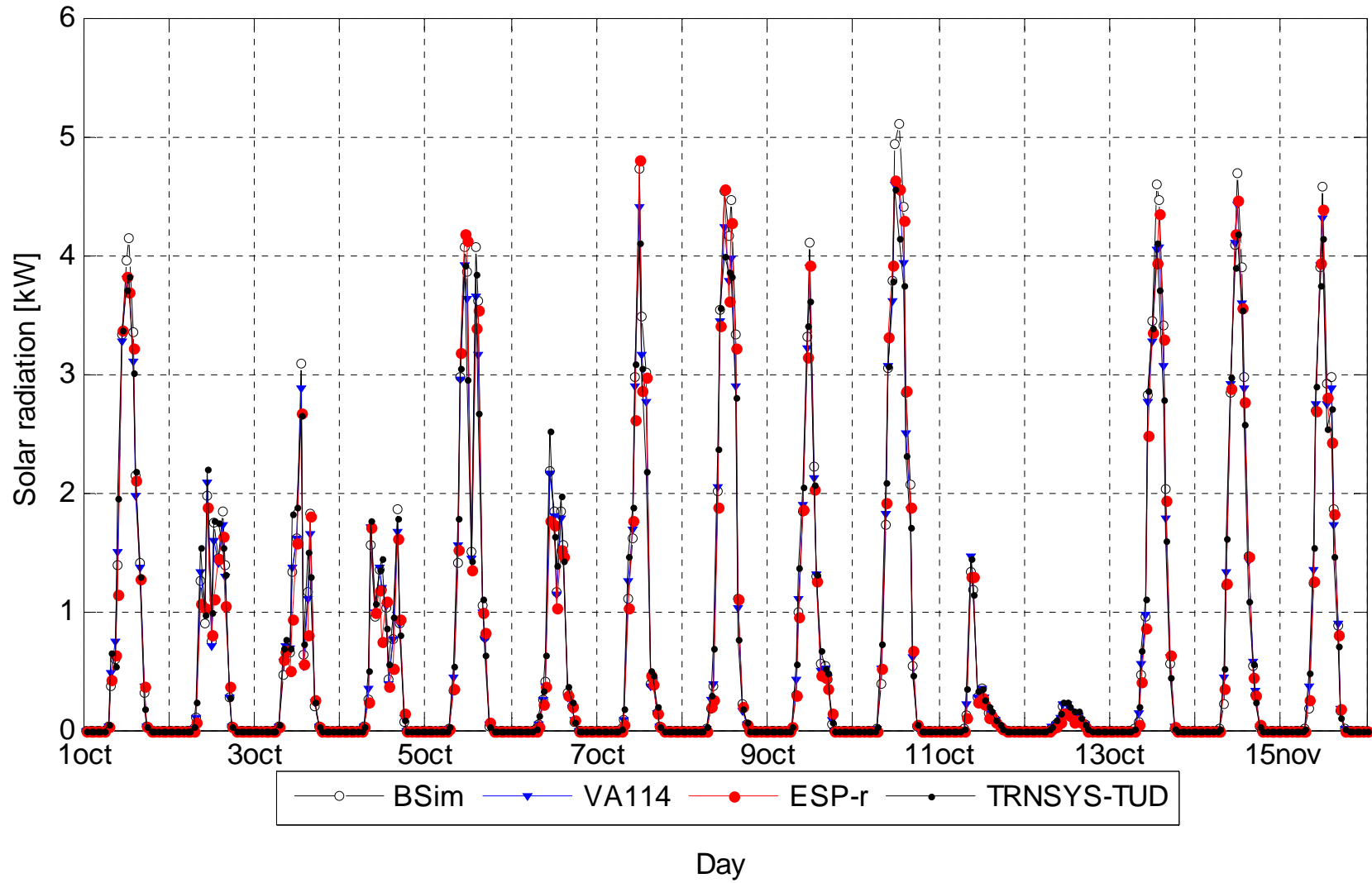
Temperature of external window glass surface facing external	BSim	VA114	ESP-r	TRNSYS-TUD
MIN, °C	5.44	4.88	5.36	4.92
MAX, °C	25.75	25.38	29.53	25.25
MEAN, °C	14.08	13.74	14.27	13.54

Hour averaged temperature of the external window glass surface facing external
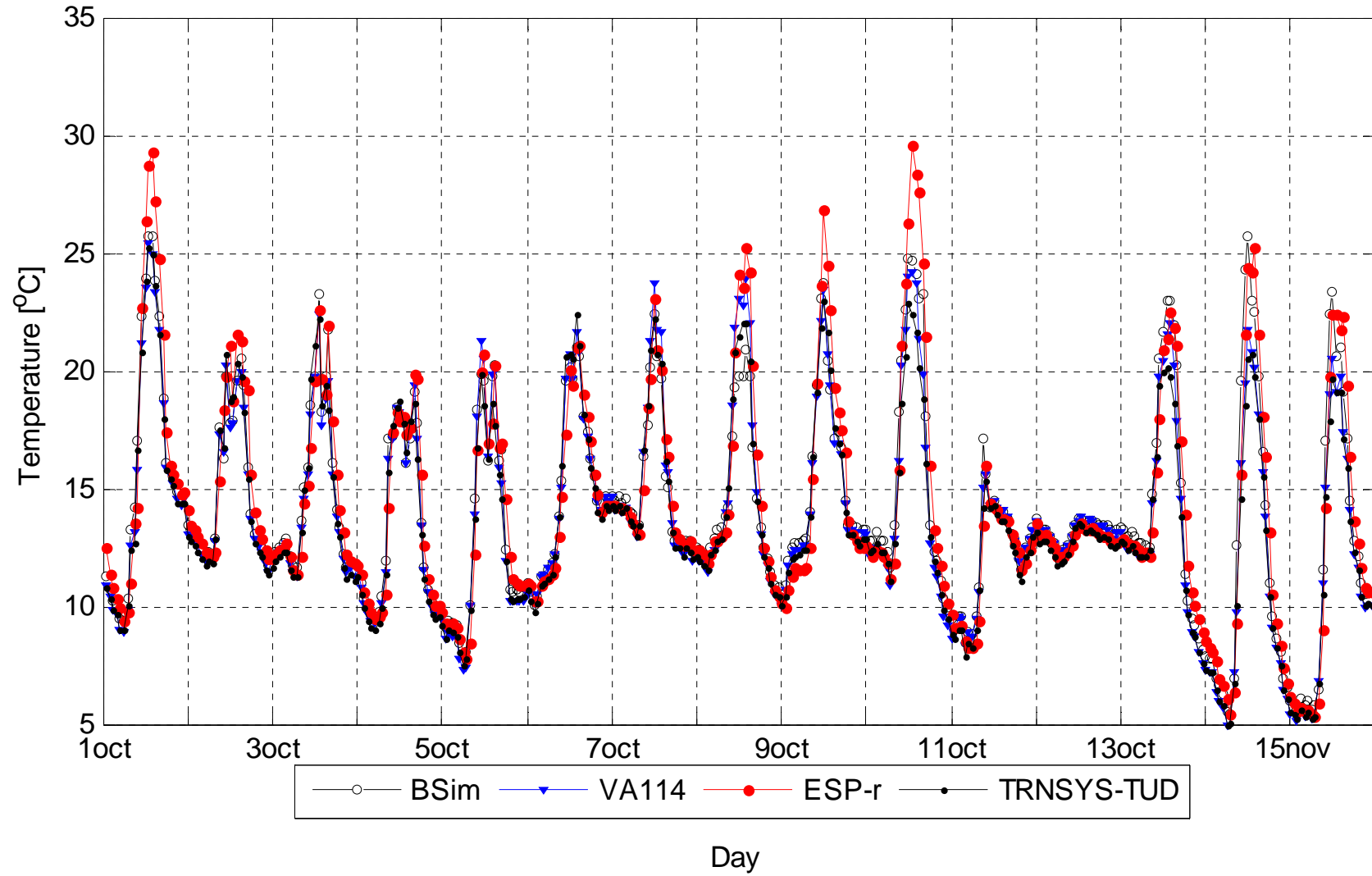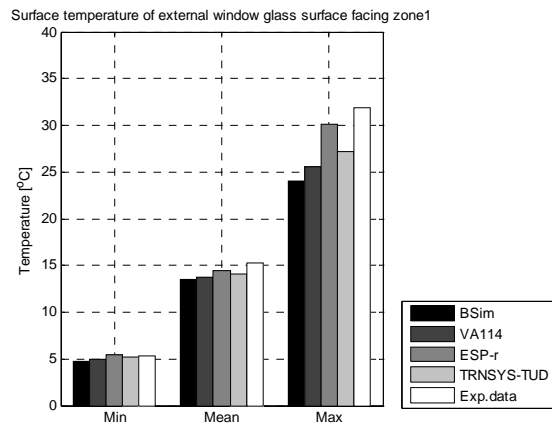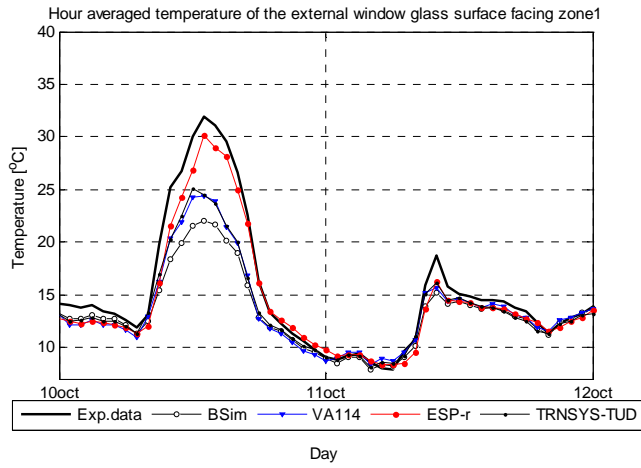
27

Hour averaged temperature of the external window glass surface facing zone1

Surface temperature of external window glass surface facing zone1

Temperature of external window glass surface facing zone1	BSim	VA114	ESP-r	TRNSYS-TUD	Exp.
MIN, °C	4.75	4.92	5.46	5.20	5.35
MAX, °C	24.05	25.53	30.13	27.19	31.90
MEAN, °C	13.48	13.80	14.45	14.05	15.27
DT95, °C	-7.38	-5.90	-3.54	-5.07	
DT5, °C	-0.13	0.01	0.68	0.52	
MEANDT, °C	-1.80	-1.49	-0.82	-1.24	
ABMEANDT, °C	1.81	1.52	0.98	1.39	
RSQMEANDT, °C	2.87	2.31	1.42	2.10	
STDERR, °C	2.23	1.77	1.16	1.70	

Hour averaged temperature of the external window glass surface facing zone1
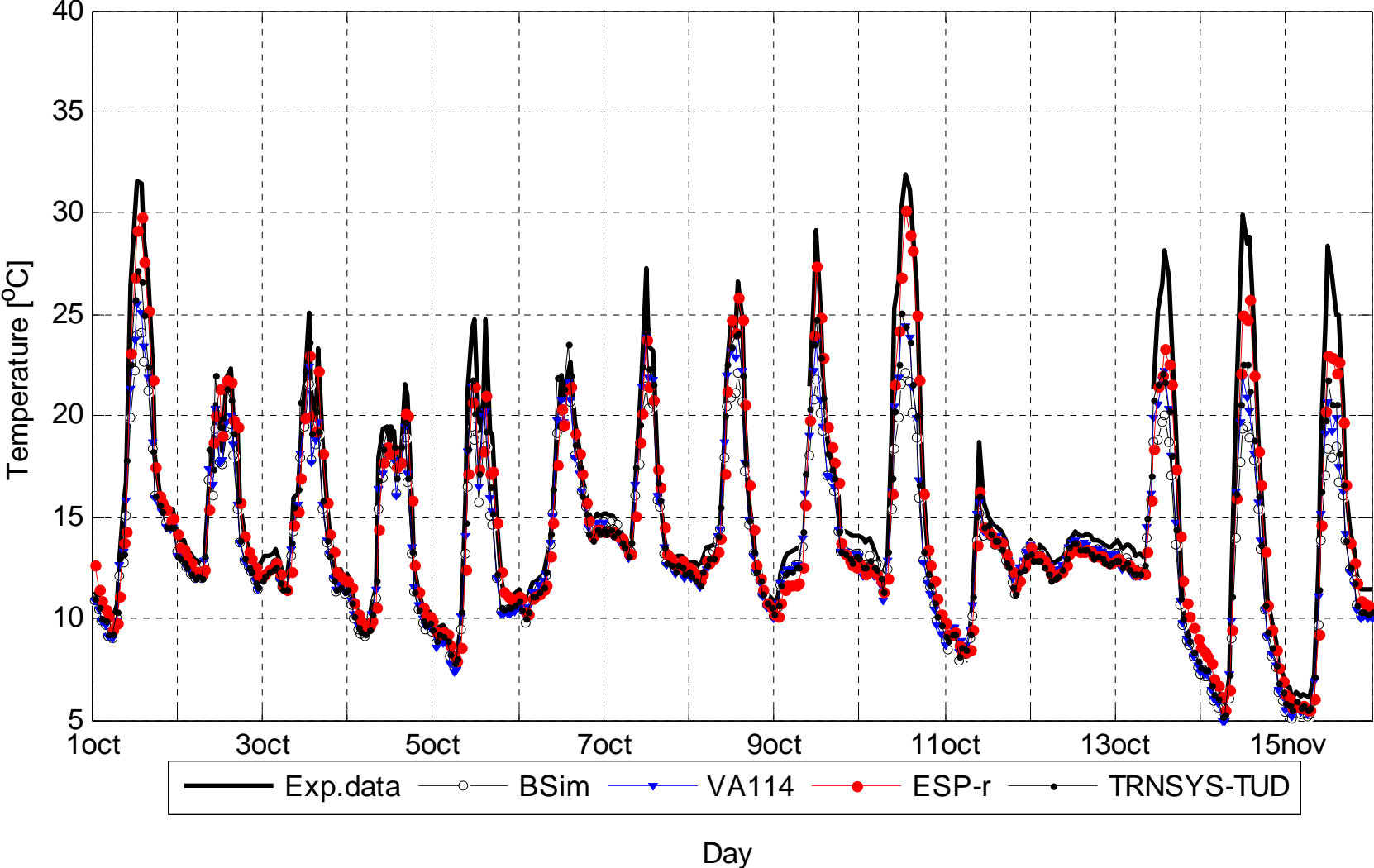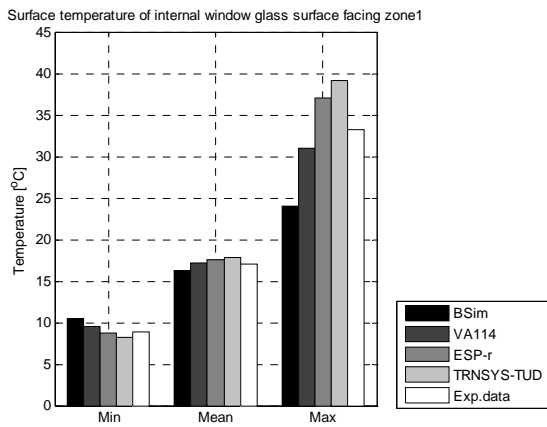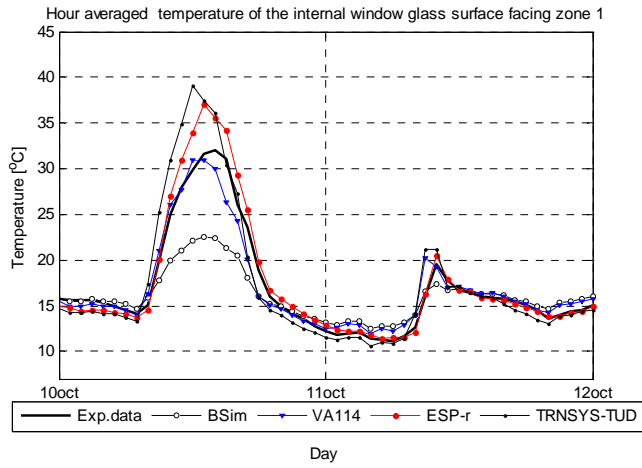
Legend: Exp.data — BSim — VA114 — ESP-r — TRNSYS-TUD

Hour averaged temperature of the internal window glass surface facing zone 1

Surface temperature of internal window glass surface facing zone1

Temperature of internal window glass surface facing zone1	BSim	VA114	ESP-r	TRNSYS-TUD	Exp.
MIN, °C	10.47	9.57	8.72	8.17	8.88
MAX, °C	23.97	30.97	37.06	39.10	33.16
MEAN, °C	16.22	17.20	17.57	17.82	17.10
DT95, °C	-7.41	-2.21	-0.68	-1.79	
DT5, °C	1.28	2.20	3.10	7.56	
MEANDT, °C	-0.89	0.09	0.48	0.69	
ABMEANDT, °C	1.73	0.87	0.82	2.00	
RSQMEANDT, °C	2.76	1.30	1.31	3.03	
STDERR, °C	2.62	1.30	1.22	2.95	

30

Hour averaged temperature of the internal window glass surface facing zone 1

Floor and ceiling surface temperature

Hour averaged floor surface temperature in the zone 1
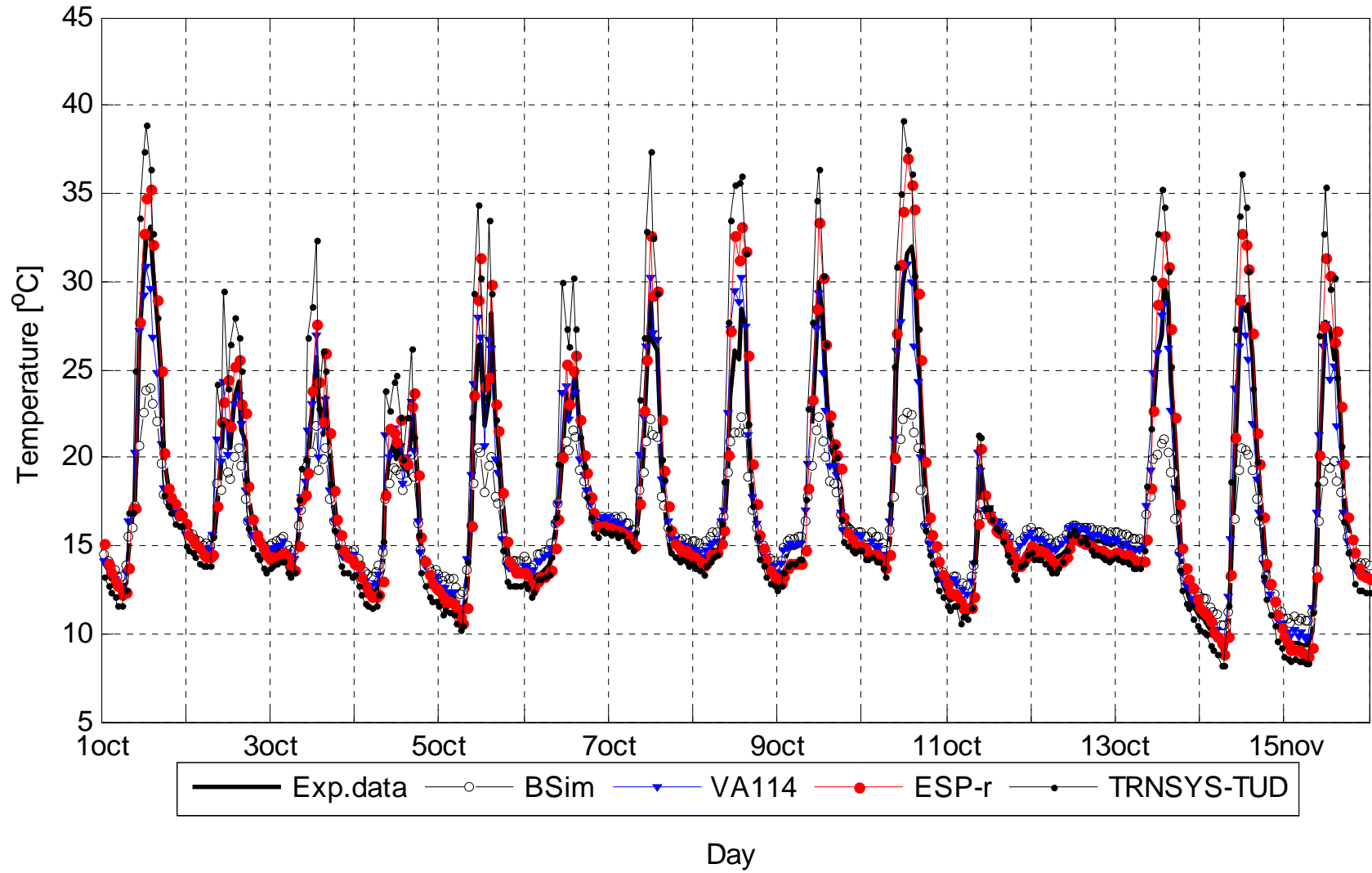
Floor surface temperature in zone1
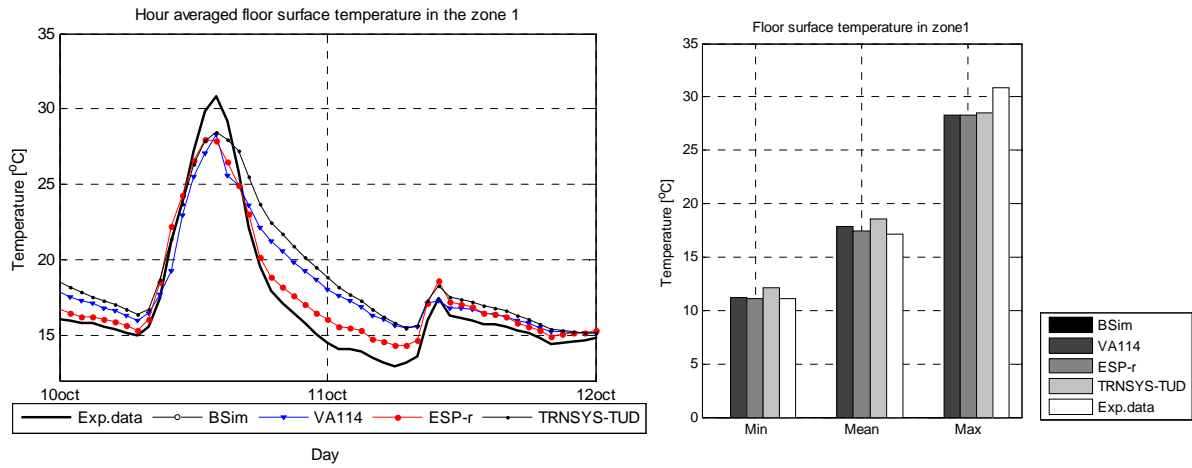
Floor surface temperature in zone 1	BSim	VA114	ESP-r	TRNSYS-TUD	Exp.
MIN, °C		11.25	11.08	12.13	11.11
MAX, °C		28.28	28.25	28.48	30.88
MEAN, °C		17.82	17.48	18.62	17.18
DT95, °C		-3.00	-1.29	-1.56	
DT5, °C		3.45	1.32	4.03	
MEANDT, °C		0.64	0.31	1.45	
ABMEANDT, °C		1.59	0.65	1.82	
RSQMEANDT, °C		2.11	0.86	2.16	
STDERR, °C		2.02	0.81	1.60	

Hour averaged floor surface temperature in the zone 1

Hour averaged ceiling surface temperature in the zone 1

Ceiling surface temperature in zone1
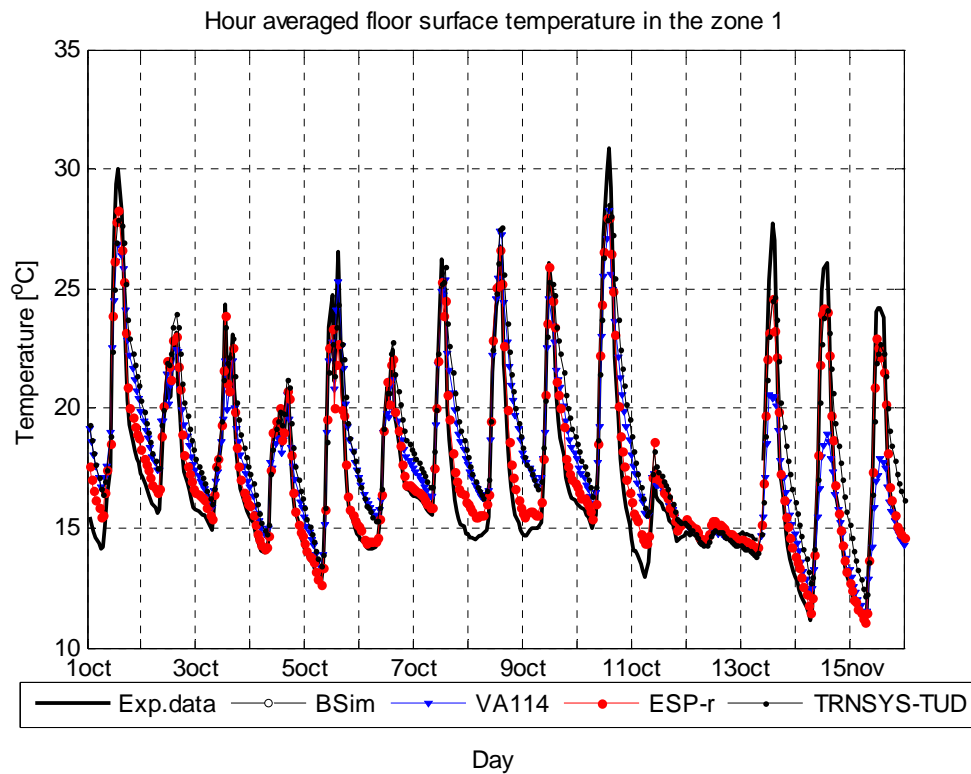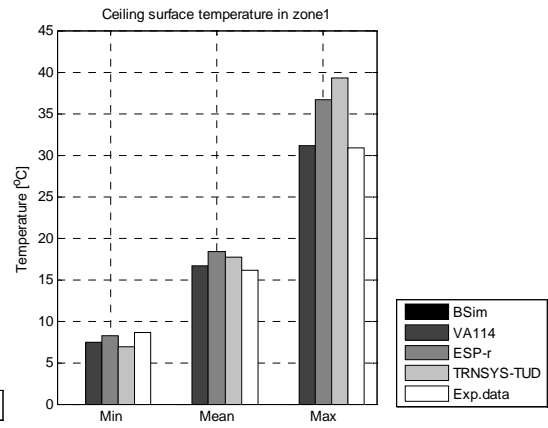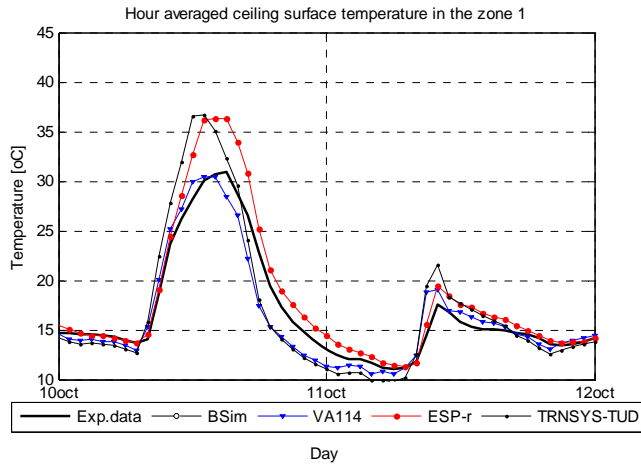
Ceiling surface temperature in zone 1	BSim	VA114	ESP-r	TRNSYS-TUD	Exp.
MIN, °C		7.43	8.16	6.91	8.62
MAX, °C		31.06	36.61	39.28	30.91
MEAN, °C		16.61	18.33	17.75	16.13
DT95, °C		-2.58	-0.33	-2.53	
DT5, °C		5.09	7.82	11.33	
MEANDT, °C		0.46	2.19	1.58	
ABMEANDT, °C		1.60	2.26	2.89	
RSQMEANDT, °C		2.29	3.29	4.41	
STDERR, °C		2.25	2.46	4.12	

Hour averaged ceiling surface temperature in the zone 1

Day

Hour averaged floor surface temperature in the zone 2

Floor surface temperature in zone2
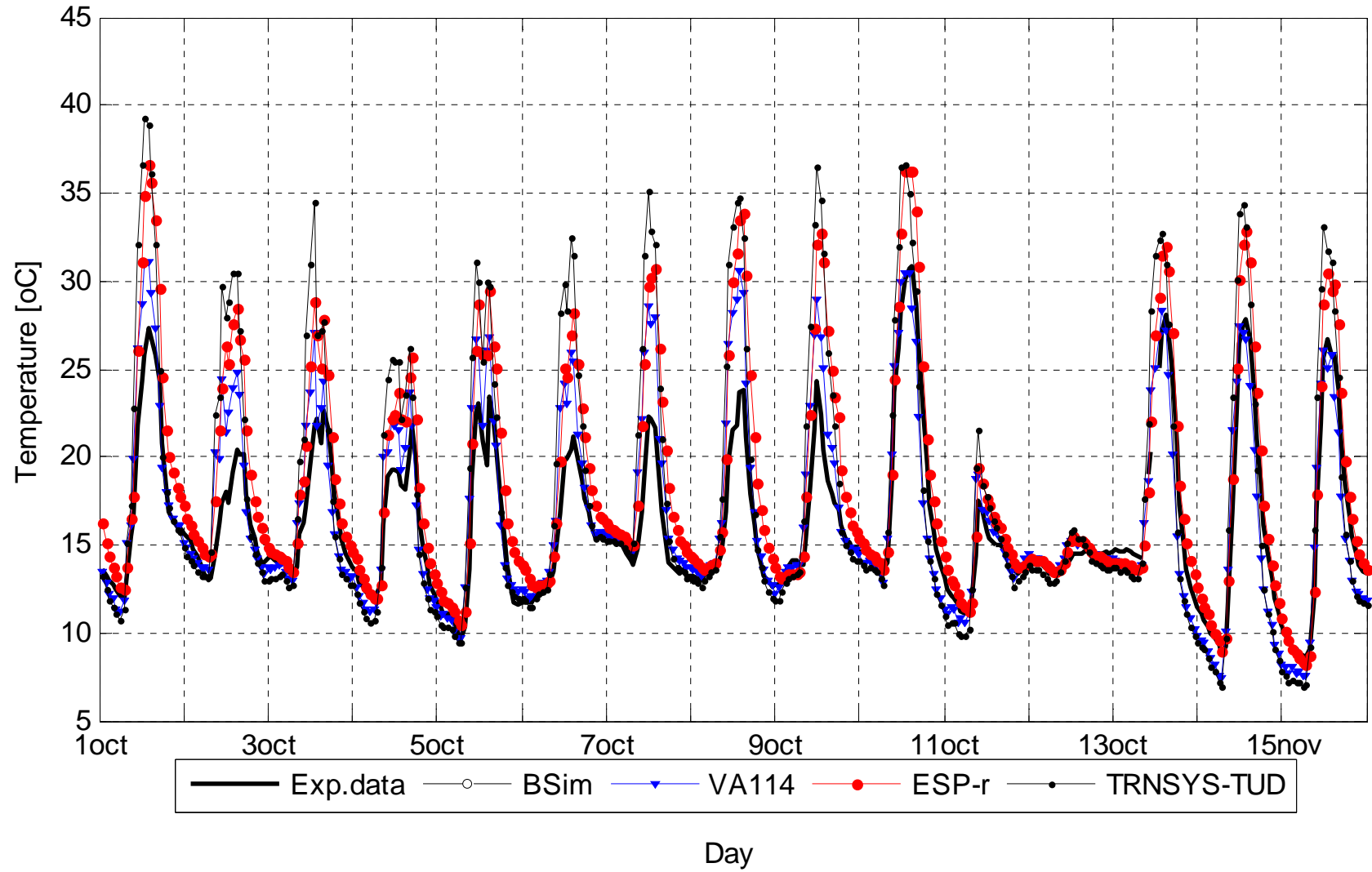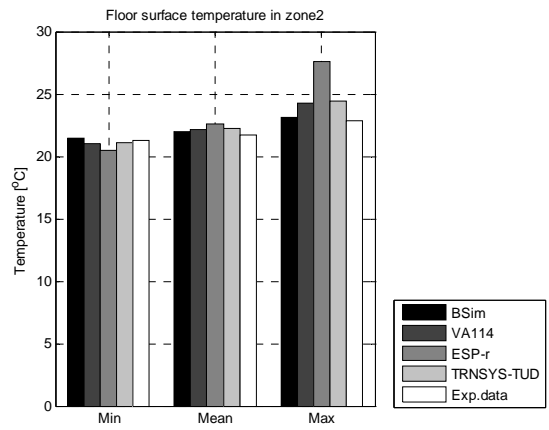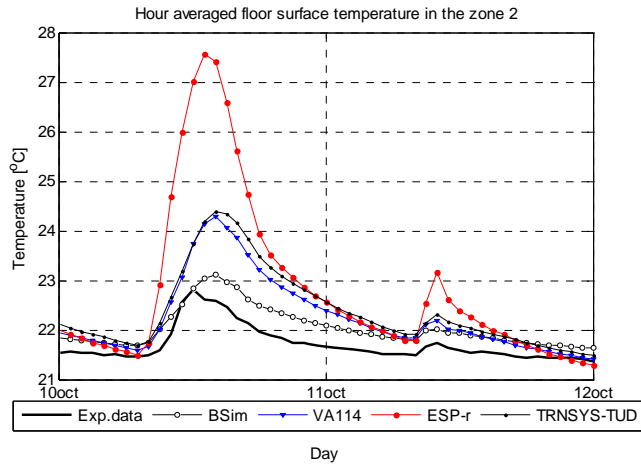
Floor surface temperature in zone 2	BSim	VA114	ESP-r	TRNSYS-TUD	Exp.
MIN, ºC	21.48	21.02	20.45	21.08	21.29
MAX, ºC	23.10	24.29	27.56	24.40	22.84
MEAN, ºC	21.97	22.12	22.56	22.23	21.70
DT95, ºC	0.10	-0.15	-0.45	-0.08	
DT5, ºC	0.50	1.17	3.51	1.33	
MEANDT, ºC	0.27	0.42	0.87	0.54	
ABMEANDT, ºC	0.27	0.46	1.00	0.56	
RSQMEANDT, ºC	0.30	0.58	1.46	0.68	
STDERR, ºC	0.13	0.39	1.17	0.42	

Hour averaged floor surface temperature in the zone 2

Hour averaged ceiling surface temperature in the zone 2

Ceiling surface temperature in zone2
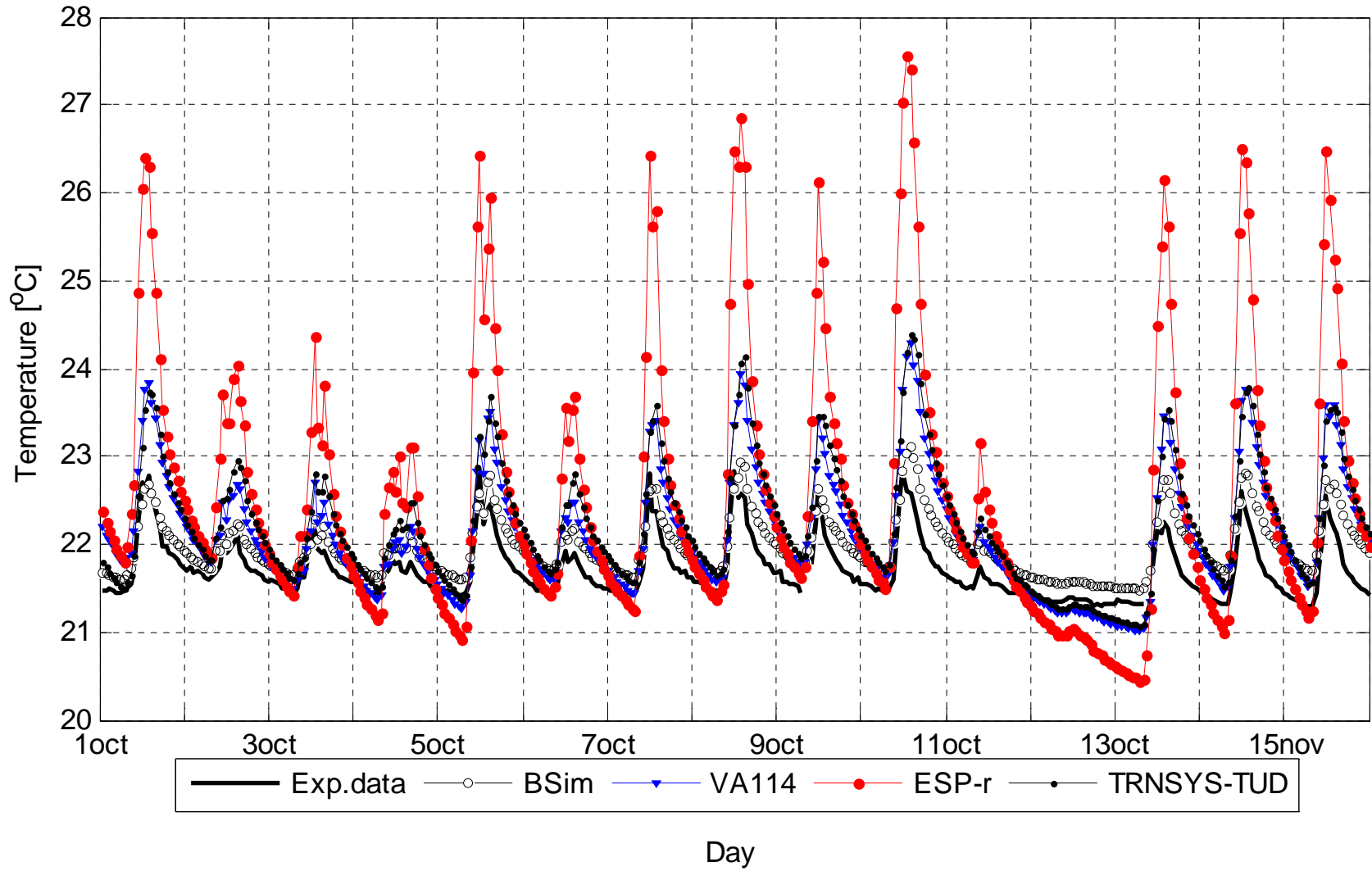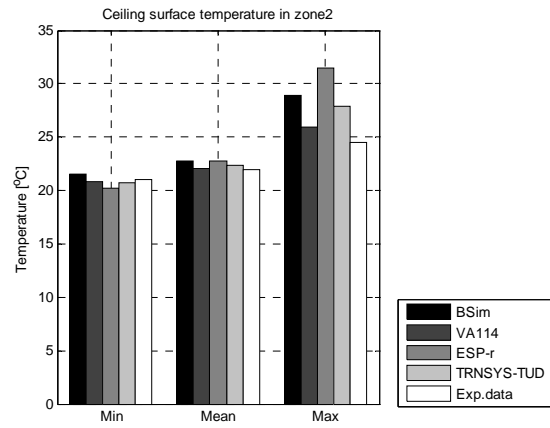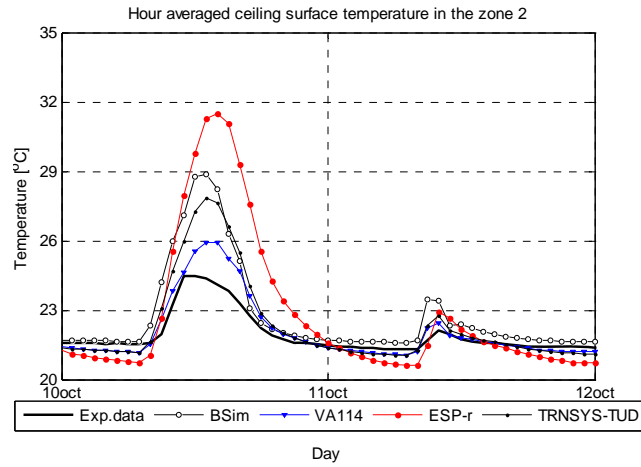
Ceiling surface temperature in zone 2	BSim	VA114	ESP-r	TRNSYS-TUD	Exp.
MIN, °C	21.50	20.79	20.19	20.73	21.05
MAX, °C	28.88	25.91	31.47	27.84	24.50
MEAN, °C	22.73	22.08	22.77	22.32	21.94
DT95, °C	0.10	-0.35	-0.87	-0.39	
DT5, °C	3.41	1.17	5.38	2.60	
MEANDT, °C	0.79	0.14	0.86	0.39	
ABMEANDT, °C	0.79	0.38	1.43	0.66	
RSQMEANDT, °C	1.34	0.52	2.15	1.02	
STDERR, °C	1.09	0.50	1.97	0.95	

Hour averaged ceiling surface temperature in the zone 2
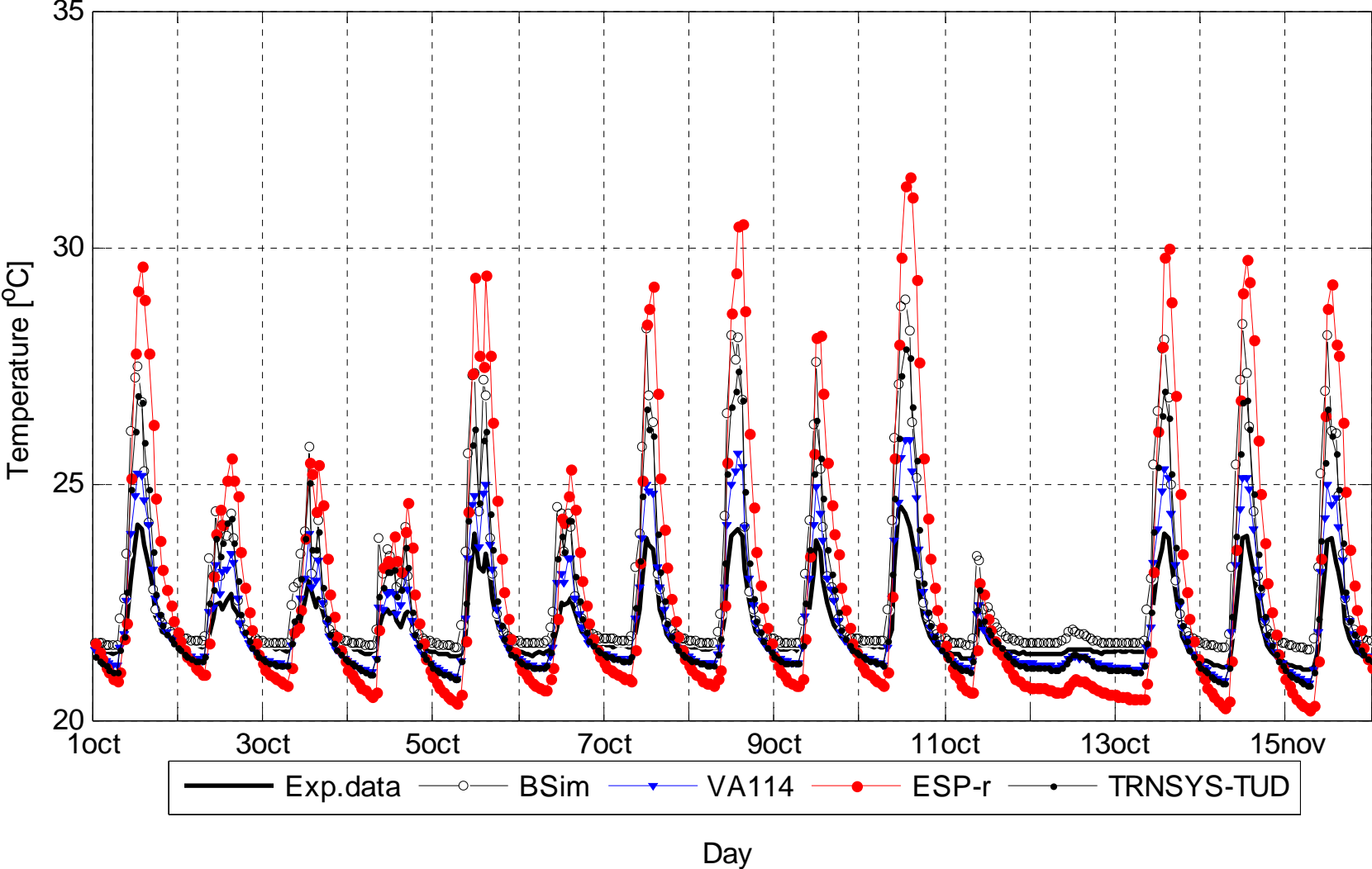
APPENDIX II.   Empirical test case specification

Final Empirical Test Case Specification

Test Case DSF200_e and DSF100_e
IEA ECBCS Annex43/SHC Task 34
Validation of Building Energy Simulation Tools

O. Kalyanova
P. Heiselberg

AALBORG UNIVERSITY

Department of Civil Engineering

Aalborg University
Department of Civil Engineering
Indoor Environmental Engineering Research Group

DCE Technical Report No. 033

Final Empirical Test Case Specification

Test Case DSF100_e and DSF200_e

by

O. Kalyanova
P. Heiselberg

June 2009

Scientific Publications at the Department of Civil Engineering

Technical Reports are published for timely dissemination of research results and scientific work carried out at the Department of Civil Engineering (DCE) at Aalborg University. This medium allows publication of more detailed explanations and results than typically allowed in scientific journals.

Technical Memoranda are produced to enable the preliminary dissemination of scientific work by the personnel of the DCE where such release is deemed to be appropriate. Documents of this kind may be incomplete or temporary versions of papers—or part of continuing work. This should be kept in mind when references are given to publications of this kind.

Contract Reports are produced to report scientific work carried out under contract. Publications of this kind contain confidential matter and are reserved for the sponsors and the DCE. Therefore, Contract Reports are generally not available for public circulation.

Lecture Notes contain material produced by the lecturers at the DCE for educational purposes. This may be scientific notes, lecture books, example problems or manuals for laboratory work, or computer programs developed at the DCE.

Theses are monograms or collections of papers published to report the scientific work carried out at the DCE to obtain a degree as either PhD or Doctor of Technology. The thesis is publicly available after the defence of the degree.

Latest News is published to enable rapid communication of information about scientific work carried out at the DCE. This includes the status of research projects, developments in the laboratories, information about collaborative work and recent research results.

TABLE OF CONTENTS

TABLE OF FIGURES

TABELS

1. General information

1.1. Introduction

This document includes the empirical specification on the IEA task of evaluation building energy simulation computer programs for the Double Skin Facades (DSF) constructions. There are two approaches involved in this procedure, one is the comparative approach and another is the empirical one. In the comparative approach (**Ref. 1**) the outcomes of different software tools are compared, while in the empirical approach the modelling results are compared with the results of experimental test cases.

Figure 1. The "Cube", outdoor test facility at Aalborg University.

The DSF Test Facility Building at Aalborg University (the "Cube") is the prototype for the specified model and the place for conducting the empirical test cases. Initially the DSF Test Facility Building is calibrated for air tightness and wind profile, further on these investigations will be followed with the heat transmission and time constants tests.

The empirical test cases cover three operational strategies of the DSF:

Case DSF100. All the openings are closed. There is no exchange of the zone air with the external or internal environment. The zone air temperature results from the conduction, convection and radiation heat exchange. The movement of the air in the DSF appears due to convective flows in the DSF. The test case is focused on assessment of the resulting cavity temperature in DSF and solar radiation transmitted through the DSF into zone.

Case DSF200. Openings are open to the outside. DSF function is to remove surplus solar heat gains by means of natural cooling. Temperature conditions and air flow conditions in the DSF are to be examined together with the magnitude of natural driving forces.
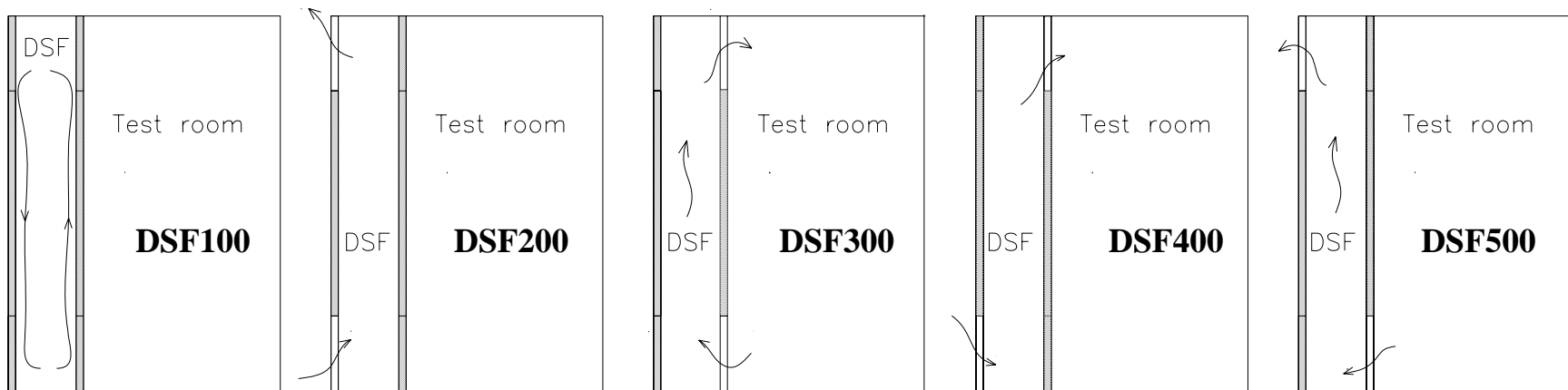
Figure 2. Test Cases. DSF100, DSF200, DSF300, DSF400, DSF500.

Case DSF100 - all openings are closed
Case DSF200 - openings are open to the outside
Case DSF300 - openings are open to the inside
Case DSF400 - bottom opening is open to the outside and the top opening is open to the inside (preheating mode)
Case DSF500 - top opening is open to the outside and the bottom opening is open to the inside (chimney/exhaust mode)

General test case	Empirical test case	Corresponding comparative test case	Solar shading		Driving force		Boundary conditions	Openings area
			Yes	No	Mechanical force	Combined natural forces	Internal=const External=floating	No control
DSF100	**DSF100_e**	**DSF100_2**		**X**			**X**	**All openings closed**
DSF200	**DSF200_e**	**DSF200_4**		**X**		**X**	**X**	**X**

Table 1. Summary table of modelling cases.

1.2. Test case DSF100_e objectives

The main interest in this test case is to ascertain the transmission of solar radiation into the room (zone 2), when there is no airflow between external and/or internal environment. Cooling system extracts the surplus heat from the zone and the cooling load to the zone 2 become the necessary parameter for estimation of the DSF influence. The heating system is installed to serve exactly the same needs as cooling – to keep constant temperature conditions in the room. The amount of heat supplied can be used as a criterion, similar to the cooling load.

Results of simulations will be compared with the experimental data from the outdoor test facility.

1.3. Test case DSF200_e objectives

The main objective of this test case is to test the building simulation software on its general ability to model the transmission of solar heat gains through the two layers of fenestration combined with naturally driven airflow through the DSF cavity. This time, the air movement exists only between the cavity and external, and the air temperatures in the cavity are mainly influenced by external environmental temperatures and solar radiation. The internal conditions remain constant; the Cooling/Heating system is introduced to the model to keep internal temperature in the zone 2 constant.

Results of simulations will be compared with the experimental data from the outdoor test facility.

1.4. Accompanying files for simulations

- Template for the output data
- Weather data files
- Data for ground temperature
- Temperature data for neighbouring zones
- Spectral data for opaque and transparent surfaces
- Files with additional documentation (*Drawing of window frames.pdf*)

2. Weather data description

2.1. General

The weather data is prepared for simulations in xls-file format as it is easy to transform into any other format. For each empirical test case, two weather data files are provided. For example for the test case DSF100_e:

wDSF100_e10.xls - provides average data for every 10 minutes. If the testing software tool is not able to perform calculation in this time interval, then 1-hour average data file can be used:

wDSF100_e60.xls - this data provides average data for every 1 hour, which is obtained by averaging 10 minutes-data.

It is assumed that parameters in the climate data are constant, for example:

>from 00:00 until 00:10 – for 10 min average data
>from 00:00 until 01:00 – for 1 hour average data

Parameters in the weather data files:

- External air temperature, ^{o}C
- Global solar irradiation on horizontal surface
- Diffuse solar irradiation on horizontal surface
- The wind direction in the data sheet is given in degrees from the North, so East corresponds to 90 degrees.
- Wind speed, m/s, measured at 10 m above the ground
- Air relative humidity, %
- Atmospheric pressure, Pa

Weather data for the empirical test cases are as follows:

DSF100_e	19.10.2006 - 06.11.2006 (both days are included)
DSF200_e	01.10.2006 – 15.10.2006 (both days are included)

2.2. Time plots of available weather data for the test case DSF100_e
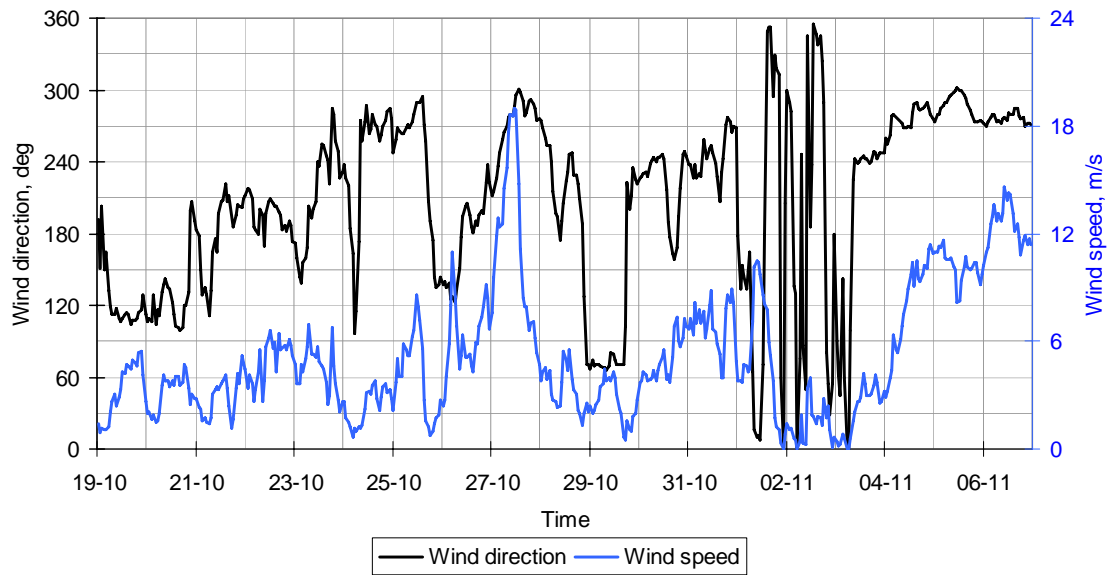
Figure 3. Wind direction and wind speed in weather data, test case DSF100_e.
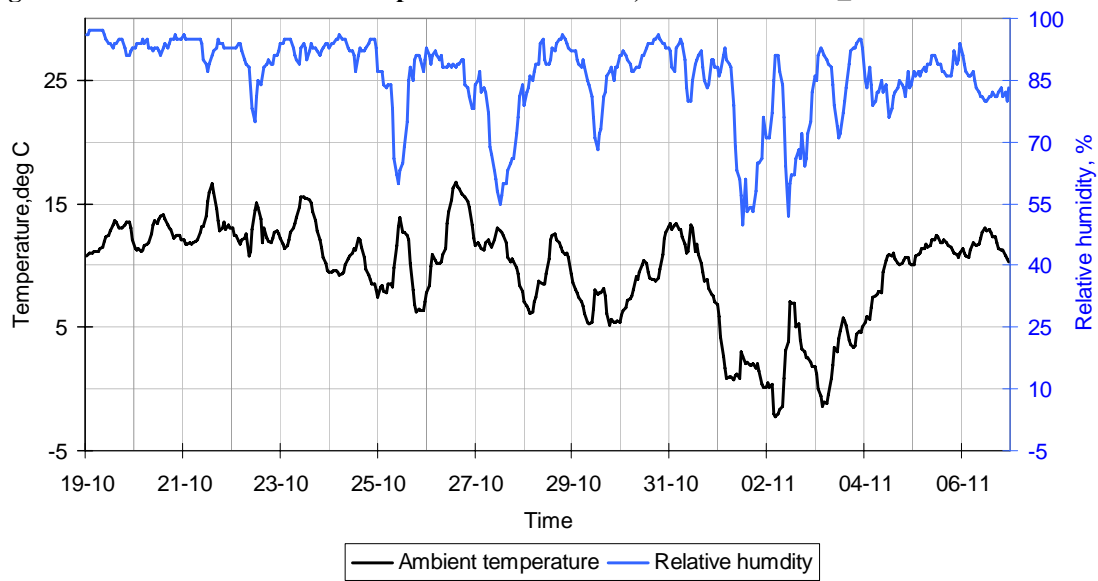
Figure 4. Air temperature and relative humidity in weather data, test case DSF100_e.
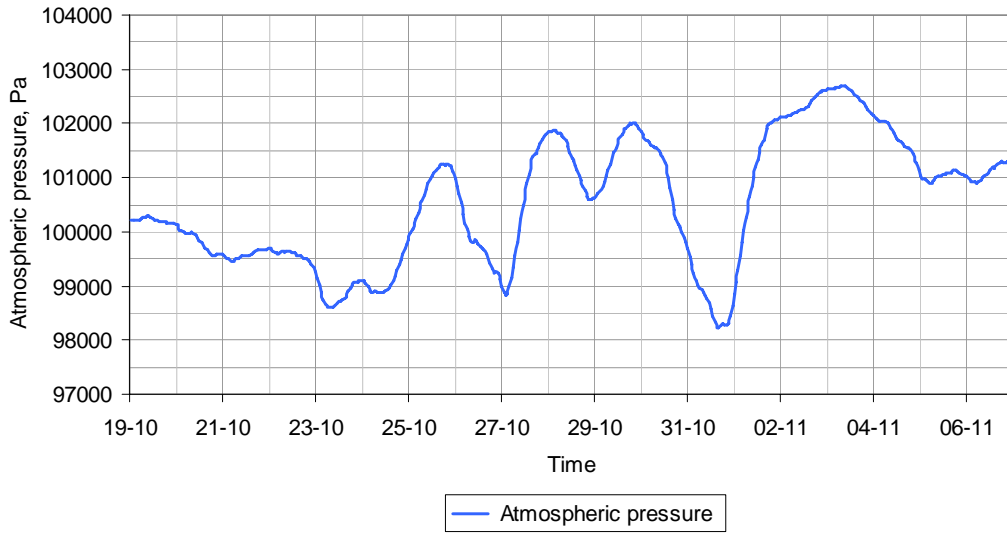
Figure 5. Atmospheric pressure in weather data, test case DSF100_e.
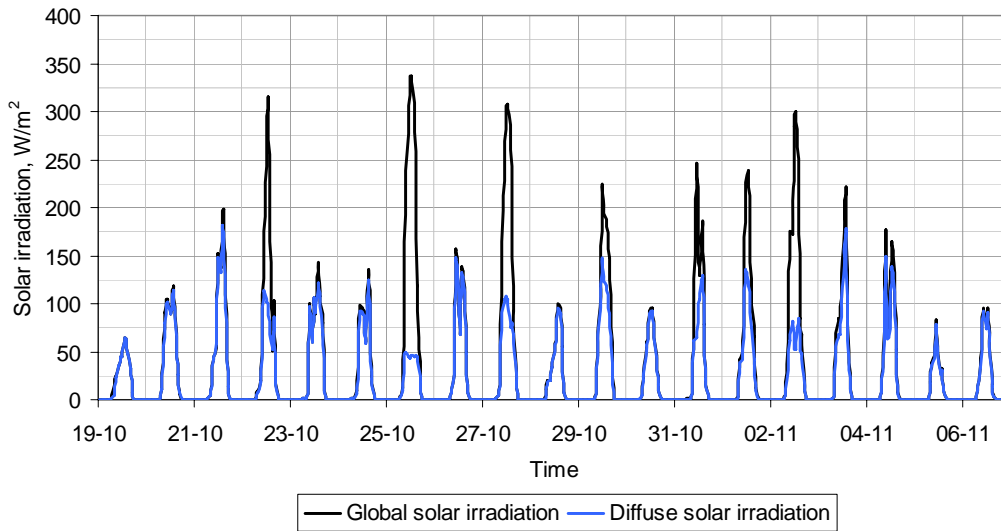
Figure 6. Global and diffuse solar irradiation on horizontal surface, test case DSF100_e.

2.3. Time plots of available weather data for the test case DSF200_e
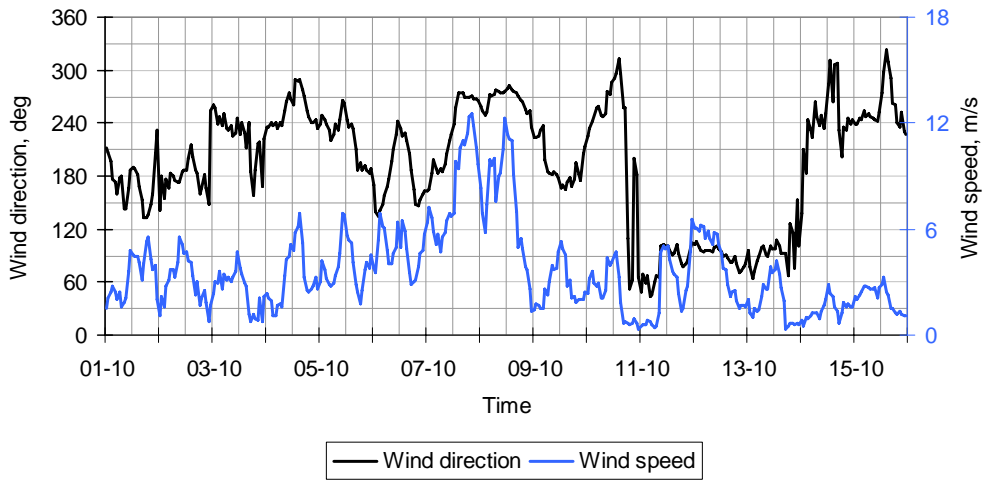
Figure 7. Wind direction and wind speed in weather data, test case DSF200_e.
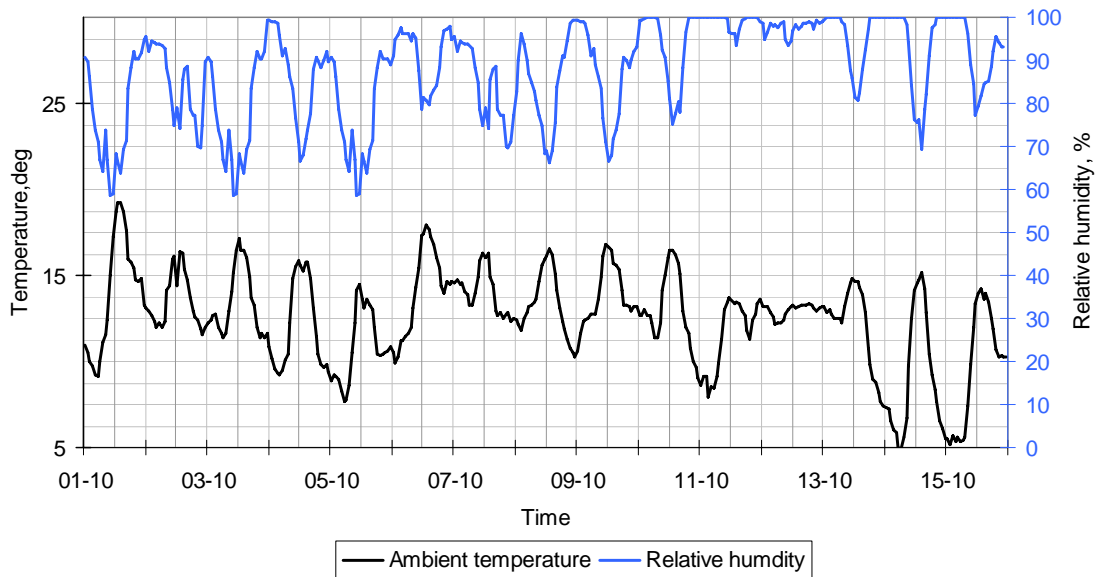
Figure 8. Air temperature and relative humidity in weather data, test case DSF200_e.
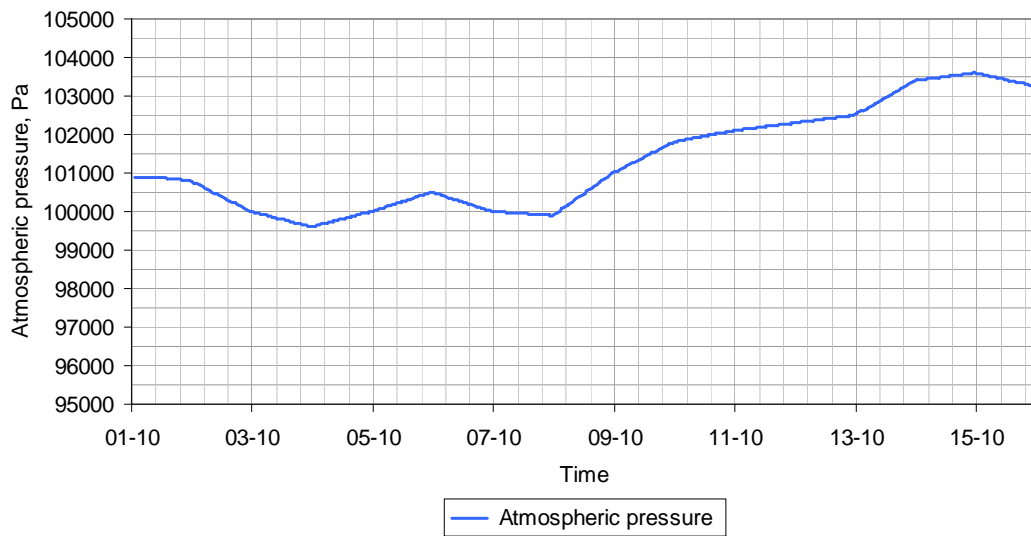
Figure 9. Atmospheric pressure in weather data, test case DSF200_e.
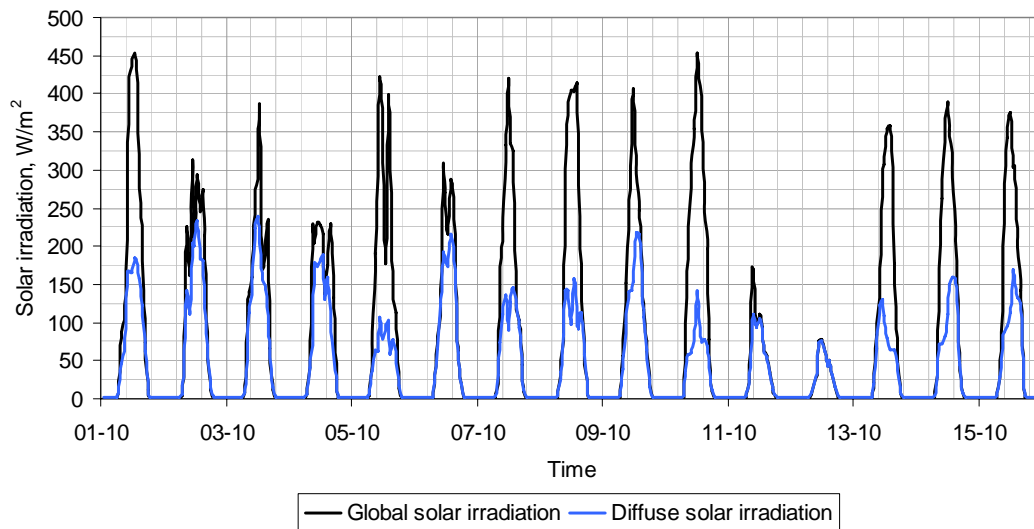
Figure 10. Global and diffuse solar irradiation on horizontal surface, test case DSF200_e.

15

2.4. Ground temperature

The ground temperature under the foundation was measured during the experiments and provided to the participants as an input parameter.

Ground temperature_DSF100_e10.xls - provides average data for every 10 minutes.
Ground temperature_DSF100_e60.xls - provides average data for every 1 hour.
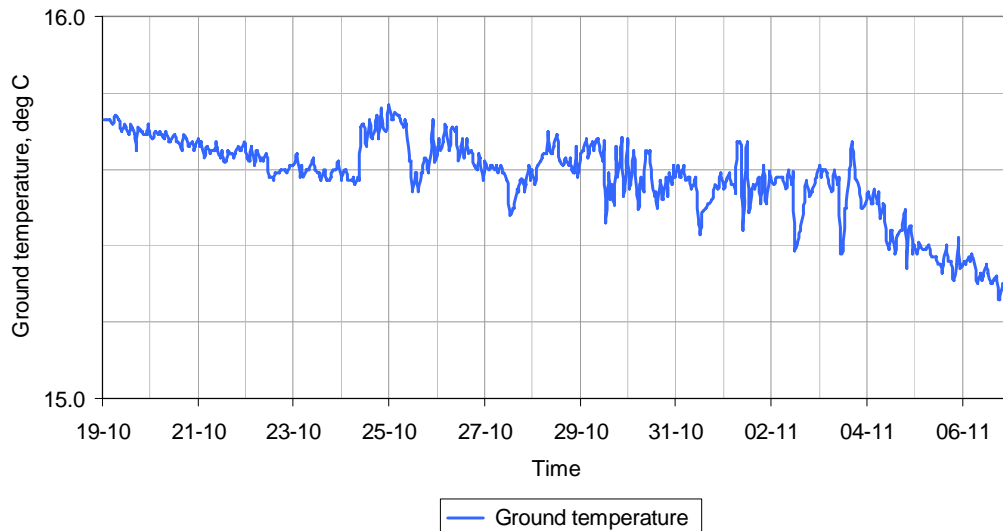
Figure 11. Ground temperature under foundation, test case DSF100_e
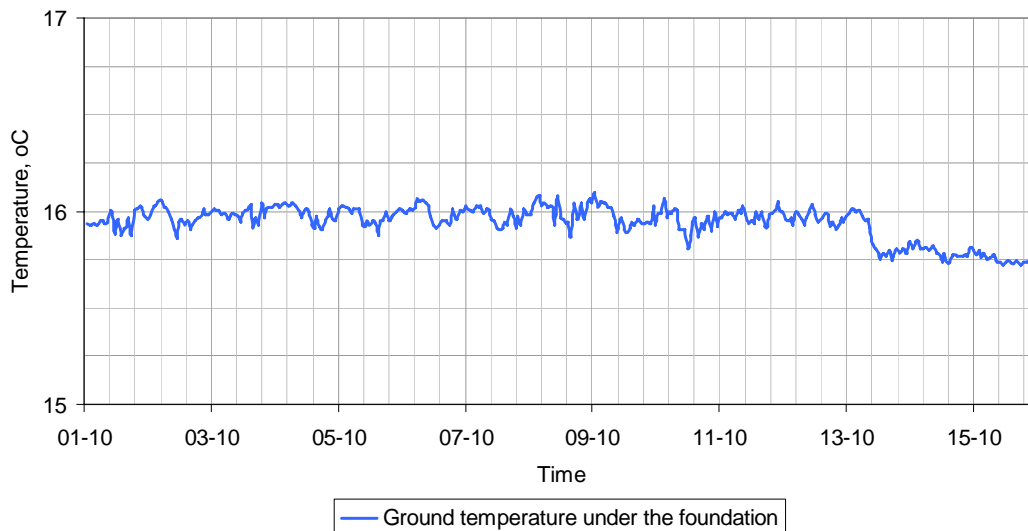
Figure 12. Ground temperature under foundation, test case DSF200_e

If the information about ground temperature can not be used in the software tool being tested, then use following values and note it in the report.

DSF100_e   15.6 ^{o}C
DSF200_e   16.0 ^{o}C

3. Rules for the modelling

3.1. Modelling methods

Various building simulation software include different approaches and applications for the modelling of the physical processes involved. Initially, it is desired that all case-models involve the same applications for the same parameters in every model and use the most detailed level of modelling allowed by simulation program being tested.

Cases specified for modelling involve interaction of various processes, thus modelling may require different combinations of software applications and their options. For this reason the requirements for the modelling are untied. Design of the model can be performed after the capability of the simulating software and user's decision, but as close as possible to the prescribed one in a physical and mathematical meaning and as close as possible to the specification and other cases modelled by the same task participant. The user is asked to notify whether and where differences exist. It is necessary to include the detailed documentation of changes into the report on modelling results in order to perform the overall comparison of the results.

3.2. Input parameters

In the specification for the test case modelling the input parameters are prescribed. These are to be used whether it is needed in the simulation software or to be used for approximate estimation of another parameter needed. When the specified parameter is found to be inapplicable for modelling the user may disregard that and continue modelling. The notification in modeller report is desirable.

3.3. Geometry parameters

In order to simplify the geometry input-parameters for all the building simulation software is involved into the Annex 43, the interior volume of zone 1 and 2 is specified. The definition of the zones and the geometrical details will be specified further in the document.

For zone 1 (DSF) the location of the windows is specified in the following figures, the interior volume is counted from the glass-pane surfaces, which are not symmetrical to the centre-line of the window frame. If it is not possible to specify the location of the glass-panes, please find a technique to keep the volume of zone 1, as close as possible to the prescribed one.

3.4. Simulation

When the simulation software allows the initialization process, then it begins the simulation with the zone air conditions equal to the outdoor air conditions.
If the simulation software allows the iterative simulation of an initial time period until temperature or fluxes, or both stabilize at initial value, then use this option.
The duration of the simulations for all the cases has to be complete, correspondingly to the provided weather data. The outputs are prescribed in section 9.

3.5. Time convention

The standard local time used (this is not the solar time!) is specified in section 4. The full day duration is 0:00-24:00. The duration of the first hour, for instance, is from 0:00 until 1:00. There is no daylight saving time to be considered.

3.6. Schedule/occupants

There are no occupants in the zones and no weekend or holiday schedules for the systems. All simulated days are considered to be equal.

3.7. Modifications of prescribed values

Some software may require modifications of values prescribed in this specification to be able to run the simulation. These modifications are undesired, but still might be necessary. The user has to make sure that the new values are obtained on the mathematical and physical bases and that these steps are documented in the modellers report.

3.8. Units

The specification is completed in SI-units, if you require conversion of units, use conversions of ASHRAE.

3.9. Shading by outdoor constructions

There are no outdoor constructions that shade the model.

4. Geography, site location

The modelling building is located close to the main campus of Aalborg University, Aalborg, Denmark. The following coordinates define the geographical location of the model:

Time zone	+1 hr MGT
Degrees of longitude	9°59'44.44"E
Degrees of latitude	57° 0'41.30"N
Altitude	19 m

Table 2. Geographical and site parameters for the model.

The orientation of the test facility is illustrated in Figure 14. Geometry

5. Model geometry

The model-building is subdivided into 2 zones, one of the zones represents the indoor environment in the ordinary room behind the DSF, named zone 2. To be able to attain the output results, it is necessary to identify DSF as a separate zone, named zone 1. It has been suggested to prescribe the interior volume of the zones as the first priority, the wall thickness may vary as long as the physical processes are correct (the user may need to perform the recalculation of the wall-thickness together with thermal properties of the wall). Zones and numbering of walls are defined in the Figure 14.

However, the actual Test Facility Building contains two supplementary rooms attached behind the Northern façade of the zone 2 (Figure 13). These two rooms are not to be modelled, but different heat transmission processes through Wall 3 are necessary to include into calculations. User shall build up the model with Wall 3, divided into three parts: one part faces external environment, and two others face the supplementary rooms. Air temperature in the supplementary rooms is given for every 10 minutes and 1 hour time intervals. For example for the test case DSF100_e

conditions 3_3 DSF100_e10.xls - provides average data for every 10 minutes.
conditions 3_2 DSF100_e10.xls- provides average data for every 10 minutes.

conditions 3_3 DSF100_e 60.xls- provides average data for every 1 hour.
conditions 3_2 DSF100_e60.xls- provides average data for every 1 hour.

Wall 3.3 and Wall 3.2 face different zones, the depth of both of these zones is 3 m.
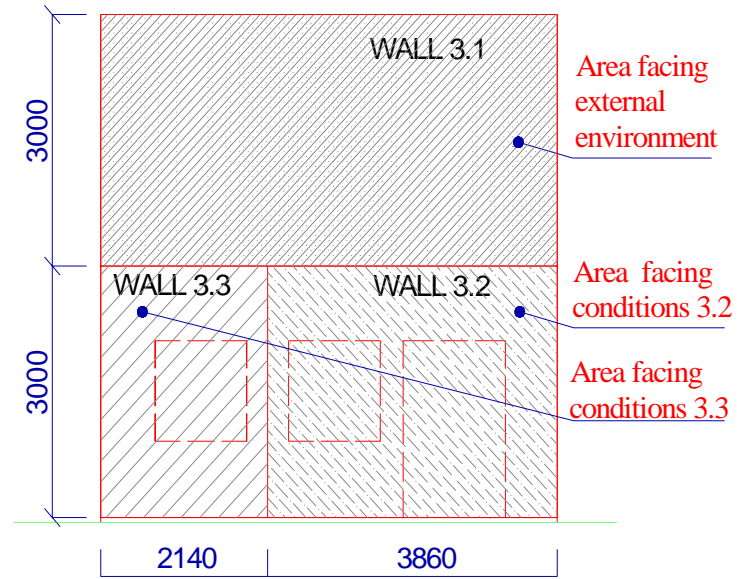
Figure 13. North Façade - left. Partitioning of the Wall 3 (view from the outside)-right.

Figure 14. Detailed plan and section of the model.

The prescribed interior volumes are (these dimensions are also specified on the previous figures):
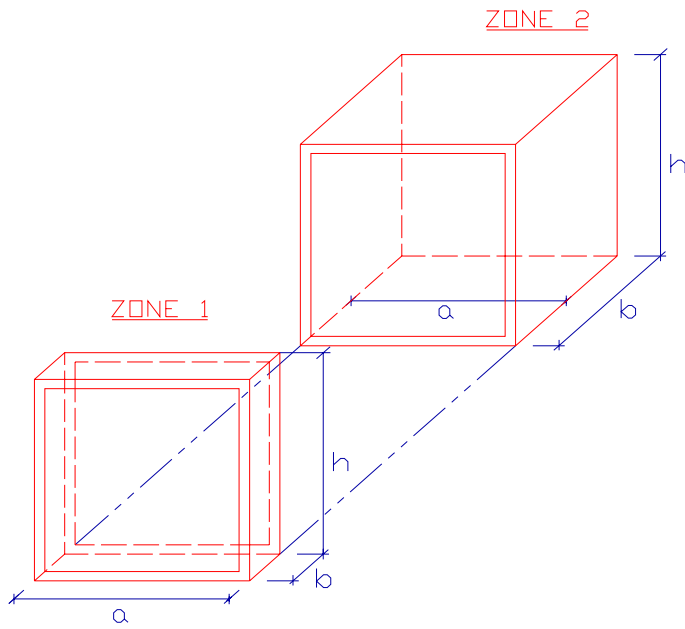
Figure 15. Internal dimensions .

Zone number	a, mm	b, mm	h, mm	Volume*, m^3
ZONE 1	3555	580	5450	11.24*
ZONE 2	5168	4959	5584	143.11*

Volume of Zone 1 and Zone 2 is calculated to the glass surfaces of the windows and NOT to the window frame
Table 3. Internal dimensions.
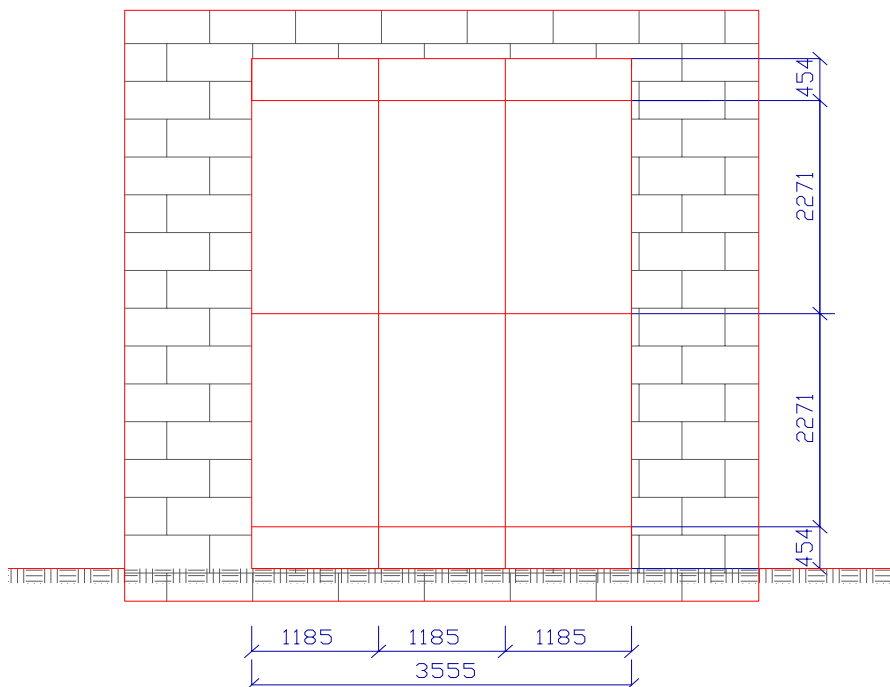
Figure 16. South facade. Dimensions of windows are inclusive frame.

Air temperature in zone 2 is constant and uniform due to a ventilation system installed in the zone. Thus, in order to avoid temperature gradients, the air was mixed, heated up or cooled down by the system. The recirculation of the air in the zone took place with the air intake at the top of the zone, its' preconditioning in the ventilation system and the exhaust at the bottom of the zone. In order to keep the exhaust velocities as low as possible the air is supplied through the FIBERTEX fabric ke-low impulse channels (Figure 17). The air motion caused by ventilation system results in the air velocity of apx. 0.2 m/s. As a consequence of this solution, only a part of the floor surface is exposed to the direct solar radiation. Moreover, air of different temperature than the ambient temperature is supplied to the zone trough the fabric channels, which results in different floor surface temperature underneath of the fabric channels. Finally, the weight of the ventilation system, located in the zone 1 is apx.750 kg, which acts as a thermal mass.

Figure 17. Ventilation recirculation system.

It has been agreed that the modellers will themselves find a solution how to model the floor in zone 2 and describe it in the report.
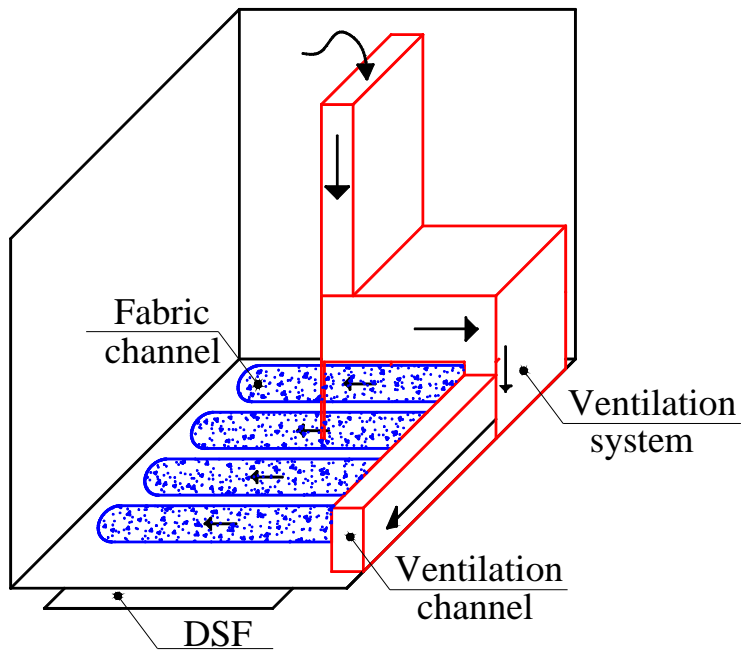
Figure 18. Schema of the ventilation recirculation system in zone 1.
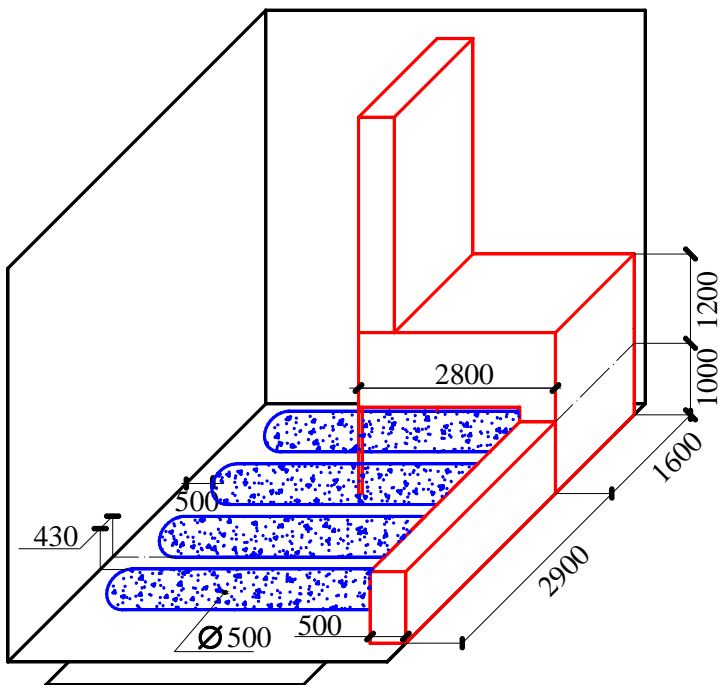
Figure 19. Dimensions of the ventilation system in the zone 1.

6. Windows geometry

It can be recognized six sections of the windows V1-V6 (Figure 20), the top and bottom sections of windows are operable and modelled as partly open in the test case DSF200_e.
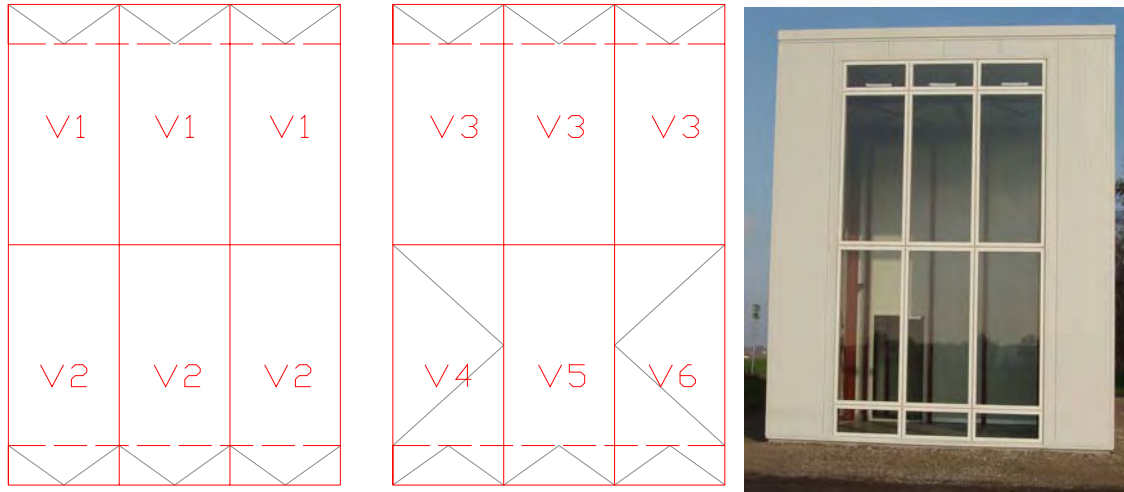
Figure 20. External window sections (left), Internal window section (centre), photo of the DSF from the outside (right).

The windows facing external environment are named as external windows and windows facing internal environment - as the internal ones. The dimensions given in Figure 16 are valid both for the internal and external windows. User must pay attention that the window constructions in Figure 20 have different typology, see Table 11.

Dimensions of window sections V1-V6 with the frames are given in Figure 21; the frame of 54 mm width encloses the glass panes.
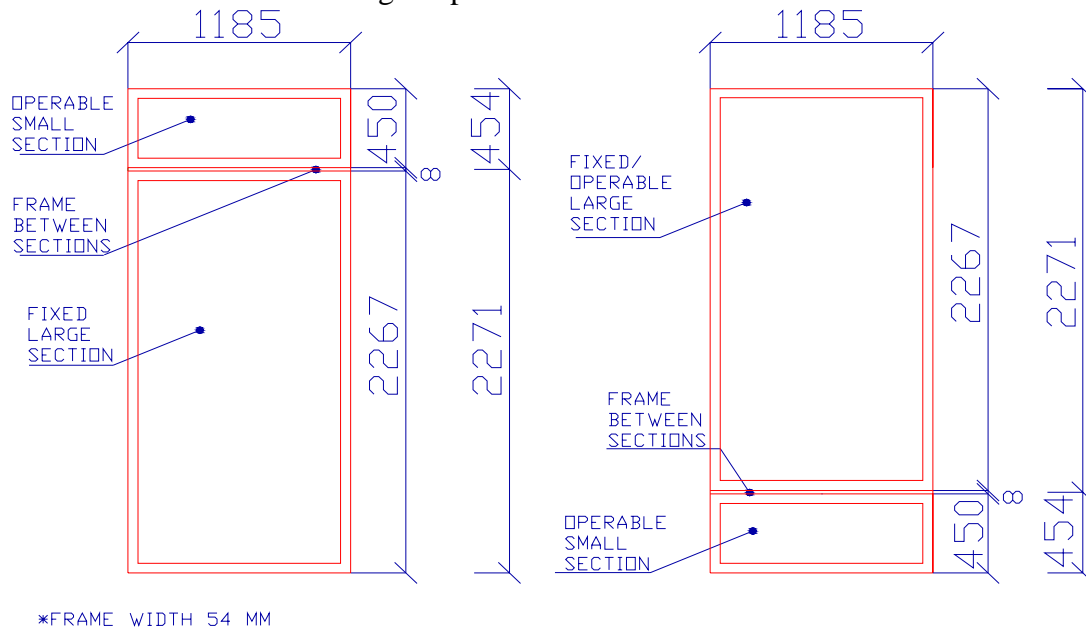
Figure 21. Dimensions of window sections with the operable top-opening (left) and bottom-opening (right).

The following table is combined as a summary for Figure 21:

Window section	Total area of visible glazing of window (large and small section), m²	Total frame area of window (large and small section), m²	Total area of window (large and small section), m²
V1-V6	2.693	0.536	3.229

Table 4. Glazing and frame areas for the window sections.

Detailed dimensions of the windows, including distances between the glass panes, thickness of the glass and cavity-gap are depicted.
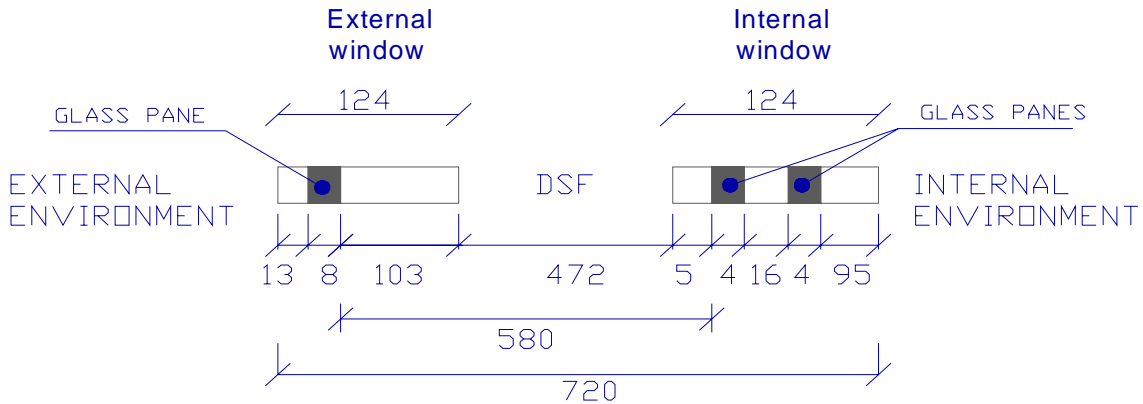
Figure 22. Distances between windows' surfaces in DSF (distances in mm).

As was explained before, the internal and external windows are of different type. The above figure demonstrates that the external window partitions consist of single 8mm-glazing, while the internal windows are double-glazed, filled with 90 % Argon.

In the file *Drawing of window frames.pdf* additional information about the window frames' construction is to be found if necessary. External part of window frame material is Aluminium and the material of the internal one is wood.

6.1. Opening degree

In the empirical test case DSF100_e all openings are closed.

In the empirical test case DSF200_e only the external top and bottom openings are open. The definition of free opening area as well as a drawing of top and bottom windows open is given below.
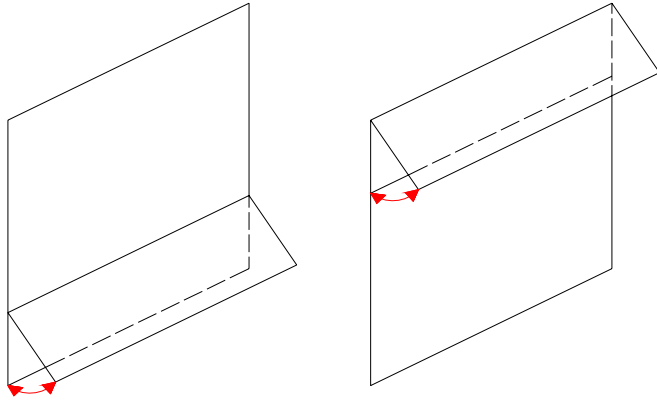
Figure 23. Direction of opening windows. Bottom window (left), top window (right).
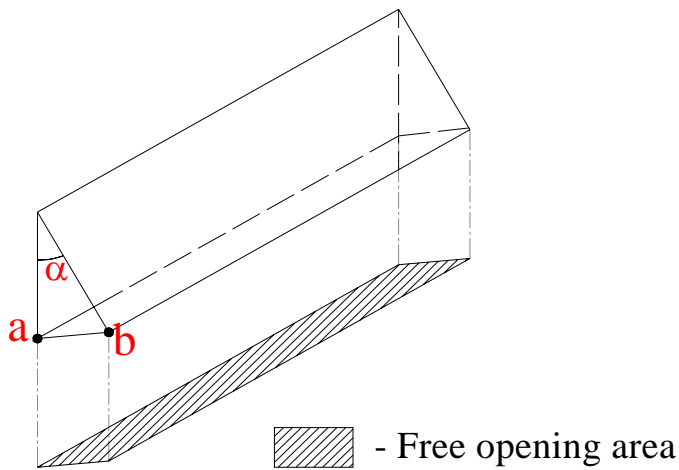
- Free opening area

Figure 24. Free opening area.

Following is the free opening areas for the empirical test case DSF200_e.

	Top opening	Bottom opening
Free opening area *of one operable opening*, m^2	0.11	0.13
Distance 'ab', m	0.09	0.110
Angle α, deg	11.5	14

Table 5. Free opening area.

It is expected that this information must be enough to complete the geometrical modelling of the window partitions.

7. Physical properties of the constructions

All constructions in the building are very well insulated. Constructions are subdivided into groups, which are:

- Wall 1- the South façade wall, comprise of external and internal windows
- Wall 2- the East and West façade walls, consist of the same materials.
- Wall 3- facing the North is divided into the three zones, as defined in the chapter 5.Model geometry
- Roof
- Floor

This grouping of the constructions is also depicted in the Figure 14. The material properties are prescribed in the following tables.

The data is given in separate tables for each of previously defined construction. The physical properties of the constructions are prescribed; these are required to keep unchanged.

The first layer in the table always denotes layer facing the internal environment of the model.

7.1. Walls' properties

Wall 1:

Material layer number	Material	Layer thickness, mm	Material density, kg/m^3	Thermal conductivity, W/mK	Specific heat capacity, J/kgK	Thermal resistance, m^2K/W
1	Plywood	16	544	0.115	1213	0.139
2	Rockwool M39	620	32	0.039	711	15.897
3	Isowand Vario	100	142	0.025	500	4

Table 6. Wall 1. Material properties.

Wall 2:

Material layer number	Material	Layer thickness, mm	Material density, kg/m^3	Thermal conductivity, W/mK	Specific heat capacity, J/kgK	Thermal resistance, m^2K/W
1	Plywood	16	544	0.115	1213	0.139
2	Rockwool M39	300	32	0.039	711	7.692
3	Isowand Vario	100	142	0.025	500	4

Table 7. Wall 2. Material properties.

Wall 3:

Material layer number	Material	Layer thickness, mm	Material density, kg/m^3	Thermal conductivity, W/mK	Specific heat capacity, J/kgK	Thermal resistance, m^{2}K/W
1	Plywood	16	544	0.115	1213	0.139
2	Rockwool M39	300	32	0.039	711	7.692
3	Isowand Vario	100	142	0.025	500	4

Table 8. Wall 3. Material properties.

Roof:

Material layer number	Material	Layer thickness, mm	Material density, kg/m^3	Thermal conductivity, W/mK	Specific heat capacity, J/kgK	Thermal resistance, m^{2}K/W
1	Plywood	16	544	0.115	1213	0.139
2	Rockwool M39	300	32	0.039	711	7.692
3	Isowand Vario	100	142	0.025	500	4

Table 9. Roof. Material properties.

Floor:
According to the DS 418, the ground resistance to the heat transmission is 1.5 m^{2}K/W.

Material layer number	Material	Layer thickness, mm	Material density, kg/m^3	Thermal conductivity, W/mK	Specific heat capacity, J/kgK	Thermal resistance, m^{2}K/W
1	Reinforced concrete, levelled and smoothed	150	2400	1.800	1000	0.639
2	Expanded Polystyrene	220	17	0.045	750	4.889

Table 10. Floor. Material properties.

7.2. Windows' properties

Grouping of window partitions and their dimensions were specified in the geometry-part. The physical properties of the windows are prescribed for the same groups.

Window	U-value of glazing W/m²K	U-value of frame W/m²K
V1,V2- External window partition	5.67	3.63
V3-V6 Internal window partition*	1.12	3.63

* U-values are given for standard conditions, using external-internal surface film coefficients and NOT internal-internal surface film coefficients.
Table 11. Windows. U-value.

7.3. Glazing

Windows V1-V6 consist of glazing, which has been tested and spectral properties are available for every sample. Samples are defined in the table:

Window	Sample number	
	Glass layer facing outside	*Glass layer facing inside*
External window sections V1, V2	Clear glass **Sample 1**	
Internal window sections V3- V6, filled with Argon, 90 %	Clear glass **Sample 2.1**	Glass with the coating attached to the front* surface. **Sample 2.2**

*The definition of front and back is given below
Table 12. Definition of samples for the glazing spectral data.

Front side always turned towards exterior, while back is turned towards the interior (zone 2).

The data from the spectral analyses for every sample is enclosed in file:
Glazing spectral data.xls

It includes following data in the wave length interval 250-2500 [nm]:
- Transmittance
- Reflectance (back and front)

The emissivity of the glass surfaces is following,

Window	Sample	Front	Back
External window sections V1, V2	Sample 1	0.84	
Internal window sections V3- V6, filled with Argon, 90 %	Sample 2.1	0.84	
	Sample 2.2	0.037	0.84

Table 13. Emissivity of glazing.

In case if the spectral data is inapplicable for the software tool, then the following data can be used:

Incident angle	External window pane			Internal window pane			
	Transmission of external window	Reflection of external window	g-value of external window	Transmission of internal window	Reflection of internal window FRONT	Reflection of internal window BACK	g-value of internal window
0	0.763	0.076	0.8	0.532	0.252	0.237	0.632
10	0.763	0.076		0.531	0.252	0.237	0.632
20	0.76	0.076		0.529	0.251	0.237	0.631
30	0.753	0.078		0.524	0.252	0.239	0.627
40	0.741	0.084		0.513	0.258	0.245	0.618
50	0.716	0.103		0.488	0.277	0.264	0.595
60	0.663	0.149		0.435	0.326	0.309	0.542
70	0.55	0.259		0.331	0.436	0.405	0.433
80	0.323	0.497		0.163	0.638	0.579	0.244
90	0	1		0	1	1	0

Table 14. Glazing properties according to spectral properties processed using WIS software.

7.4. Surface finishes

A carpet of known reflectance property was placed in front of the test facility in order to estimate solar radiation reflected from the ground. Spectral data of the carpet is given in the file:

Ground carpet spectral data.xls

If spectral data for ground reflectance can not be used by the software tool being tested then use ground reflectance of 10%, this has to be documented in the report.

Ceiling and wall surface finishing in Zone 1 and in Zone 2 were tested as well and the spectral data can be found in the following files:

Surface finish_zone1_ zone2_spectral data.xls

If spectral data for surface reflectance can not be used by the software tool being tested then use surface reflectance, as follows:

67% - for zone 2
65% - for zone 1

Properties of the floor surface in both of the zones and of the external surfaces can be assumed the same as for walls in zone 1.

Longwave emissivity	0.88
Surface roughness, mm	0.03

Table 15. Surface finish properties.

8. Other parameters and specifications

8.1. Infiltration

The overall tightness of the test facility measured with the blower door test in overpressure mode, with the assumption that the overpressure mode is equivalent to the underpressure mode.

Test case DSF100_e
The outer skin of the DSF kept closed during the blower door test. Results of the testing are given in the following figure and have to be included into the test case simulation (Figure 25. Overall air tightness characteristic of the "Cube" for the test case DSF100_e and DSF200_e.Figure 25).

Test case DSF200_e
The outer skin of the DSF kept open during the blower door test. Results of the testing are given in the following figure and have to be included into the test case simulation.
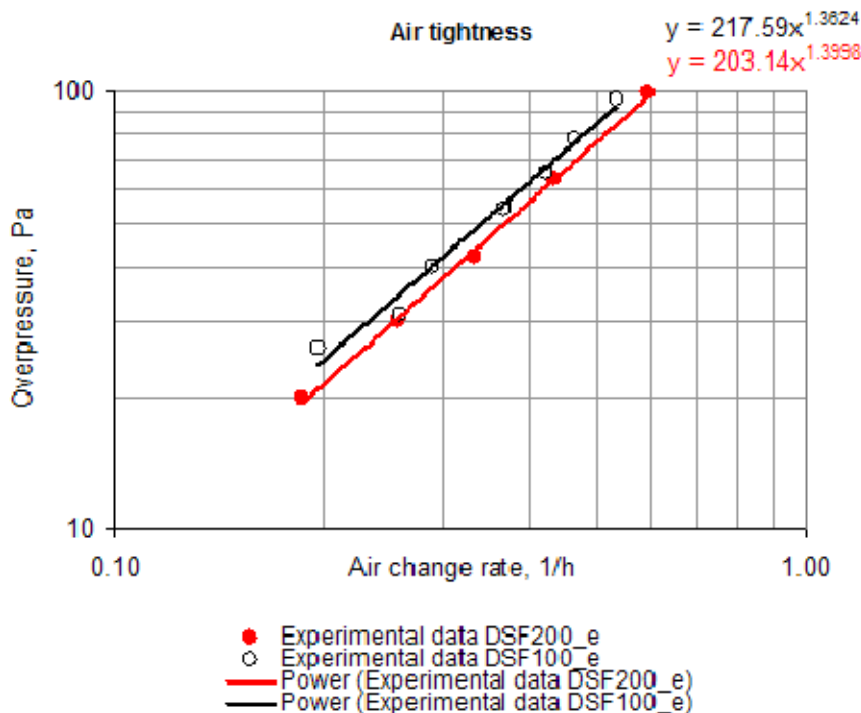
* Air change rate is calculated in correspondence with the dimensions of zone 2
Figure 25. Overall air tightness characteristic of the "Cube" for the test case DSF100_e and DSF200_e.

8.2. Discharge coefficient

Each opening is defined with two discharge coefficients. Discharge coefficient is set to 0.65 when opening is functioning as the supply opening. Another value of the discharge coefficient must be used if the air moves from inside towards the outside (opening is functioning as the exhaust opening), the discharge coefficient is set to 0.72.

8.3. Wind pressure coefficients

Wind pressure coefficients correspond to the wind velocity at the height of the roof of the building (6 m).
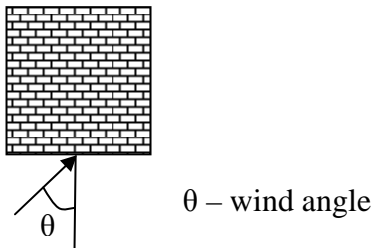
θ – wind angle

Location	Wind angle									
	0°	*45°*	**65°*	*90°*	*135°*	*180°*	*225°*	*270°*	**295°*	*315°*
Top openings	0.58	0.22	-0.2	-0.71	-0.5	-0.36	-0.5	-0.71	-0.2	0.22
Bottom openings	0.61	0.33	-0.06	-0.55	-0.5	-0.35	-0.5	-0.55	-0.06	0.33

* *Interpolated data*

Table 16. Wind pressure coefficients [Ref. 2].
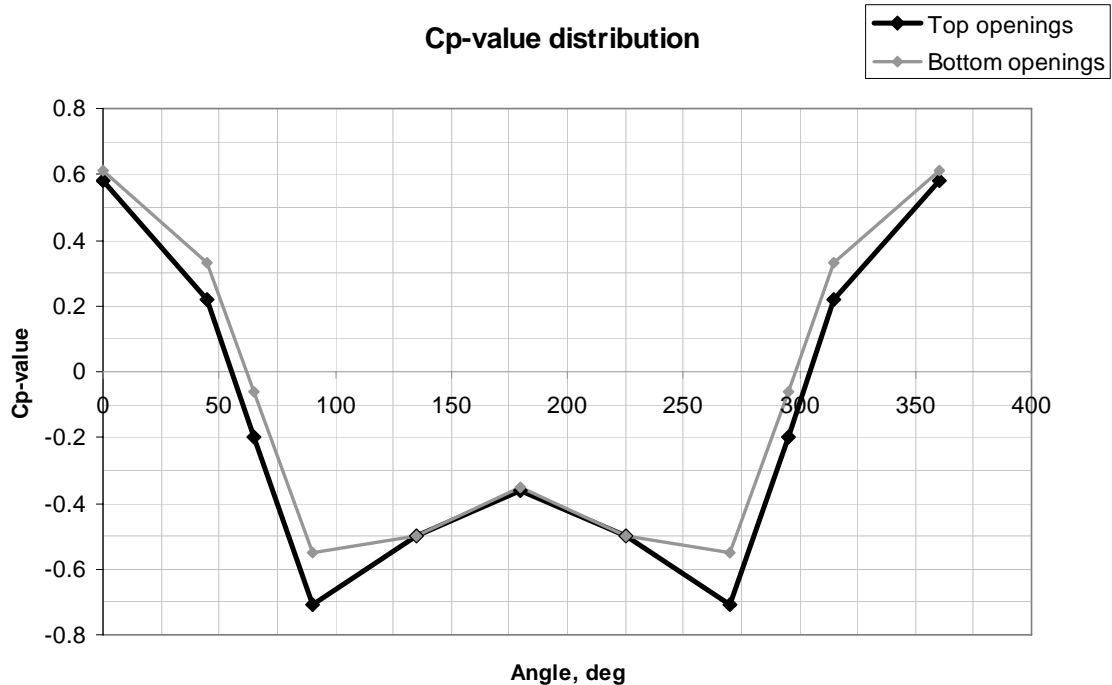
Figure 26. Distribution of wind pressure coefficients.

If the testing software tool does not allow manual definition of the wind pressure coefficients and values different from the above were used in the model, then the modeller report has to include detailed information about the values used.

8.4. Wind speed profile

Wind velocity profile is described by logarithmic low according to conducted measurements of horizontal velocity profile.
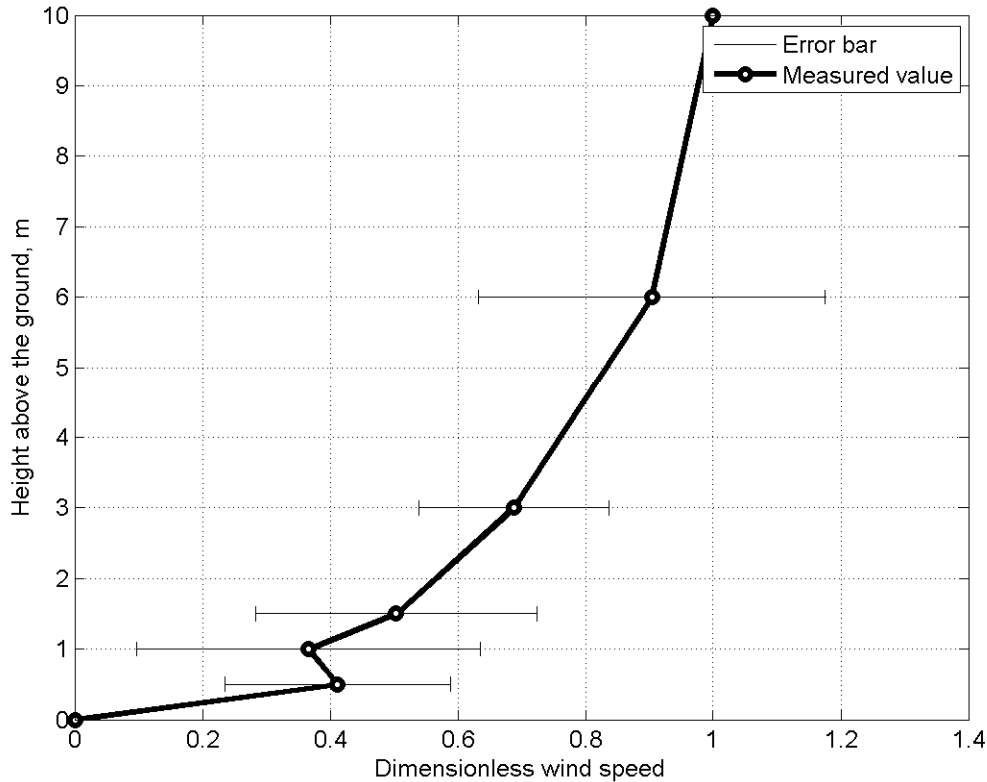
Figure 27. Dimensionless wind velocity profile at the measuring site.

General expression for the logarithmical wind velocity profile (**Ref. 3**)

$$V(h) = \frac{V_*}{K} \ln\left(\frac{h}{h_o}\right)$$

$V(h)$ – wind speed at height h
h – height above the ground
V_* – friction velocity
K – von Karman's constant
h_o – roughness height

Constants for the wind velocity profile at the measuring site are defined for the wind velocity provided in the weather data files.

Von Karman's constant is approximately 0.4.
Roughness height is 0.31
Friction velocity is the transient parameter and can be calculated from the experimental data as following:

$$V(h_{10}) = \frac{V_*}{0.4} \ln\left(\frac{h_{10}}{0.31}\right)$$

$$V_* = \frac{V(h_{10}) \cdot 0.4}{\ln\left(\dfrac{h_{10}}{0.31}\right)}$$

$V(h_{10})$ − wind speed at height 10 m
0.4 − von Karman's constant
h_{10} − 10 m height above the ground
0.31 − roughness height

8.5. Thermal bridges

The calculation of heat transmission through thermal bridges has to be included into the test cases.

Values for the overall heat transmission from the zones are given based on measurement results from calibration study on the test facility (**Ref. 5**), these are compared against the heat losses calculated manually, using the U-values and dimensions of the constructions in the "Cube", see Figure 28.
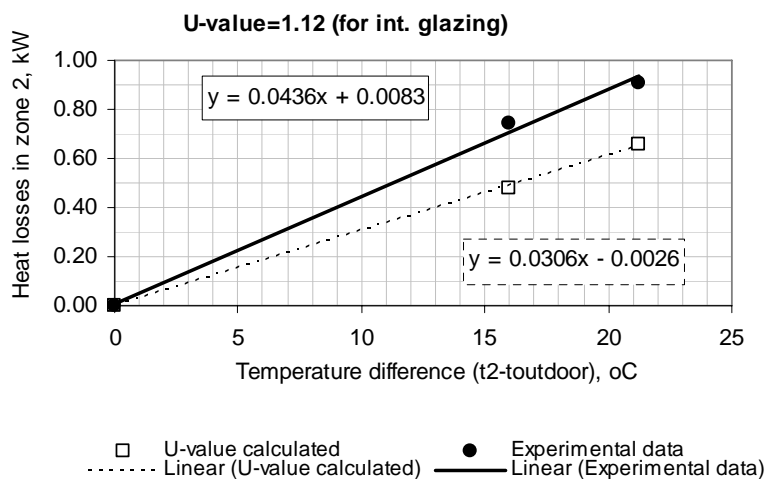
Figure 28. Heat transmission losses in the "Cube"

8.6. Driving force

In the test case DSF200_e thermal buoyancy is combined with the wind influence and has transient character.

8.7. Mixing in zone 2

Air in the zone 2 has been continuously mixed during the experiments.

8.8. Air temperature in zone 2

The air temperature in zone 2 is regarded to be uniform, with a fixed value of 21.8 $^{\circ}$C. In order to keep this temperature constant a control of cooling/heating system has to be included, as explained below.

8.9. Systems in zone 2

The zone 2 is provided with a mechanical heating/cooling system to provide constant zone air temperature. The energy has to be delivered to the zone air only by means of convection. The controlling sensor has to be located in the same zone. The schedule of the systems has to be *always,* during the simulation. System efficiency is set to 100%. Do not use Heat Recovery.

8.10. Operable openings control

There is no control of the openings. Area of the open openings is constant for the whole test case.

8.11. Distribution of solar radiation in a zone

Whether the software being tested allows the solar incidence to be distributed geometrically correct to surfaces (detailed analyses of the path of direct solar radiation through a building, thus calculating shadowing by constructions, etc.) then this option has to be used. When this is not possible, use the most accurate, physically correct option, able to handle solar radiation heat transmission. Approach for calculation of distribution of transmitted solar radiation to the surfaces has to be documented in the report.

8.12. Longwave radiation with external

If the software being tested allows the calculation of the longwave radiation exchange with the exterior, use this function, else note it in the report.

8.13. Longwave radiation with internal

If the software being tested allows the calculation of the longwave radiation exchange with the interior, use this function, and note in the report the approach that has been used.

8.14. Surface heat transfer coefficients

The computations of surface heat transfer coefficients for the empirical test cases are not prescribed. Every software tool should be able to present the best possible results of simulations.

It is required to notify the techniques for computations of surface heat transfer coefficients in the report.

8.15. Shading

No shading device defined for the empirical test cases.

8.16. Moisture transport

There is no moisture transport included into the simulations

9. Modeller report

This section includes the requirements to the contents and outline of the final modeller report, discussed and agreed on during the breakout session on March 26 in Colorado. The earlier requirements mentioned in the text of the specification are also summarized.

Besides completing the modeller report, participants are asked to fill in a questionnaire about the model and modelling approaches *for the test case DSF200_e*:

E_questionnaire_XXX.doc

XXX - name of the organization
E - corresponds to *Empirical* test cases

As a general requirement, the user is asked to notify whether and where differences exist between test case specification and the model. This includes:

- Disregarded parameters in specification
- Modification of parameters in specification
- Application of parameters not included in specification

The level of detail in the modeller report must allow anyone, using the same simulation tool, to repeat the model described in the report and achieve the same results.

The scope of this subtask is to perform a validation of the building simulation software for buildings with the double skin façade. As explained in the literature review (**Ref. 4**), the physics of the double skin façade involves complex processes and therefore require detailed calculations of optics, flow regime, convection, natural airflow etc. Often, the building simulation software is not able to perform such detailed level of computations. When the detailed computations are not possible, then the simplified models used as an alternative, as a result it is not always possible to validate the advance physical processes and this is not the main objective. The building simulations must be validated on their performance *together with their limitations.*

Although the validation of models for transmission of solar radiation, naturally driven flow, etc. is carried out by other subtasks, the complexity of the DSF physics results in difficulties for some of the simplified natural air flow models to predict accurately the airflow in the DSF cavity. In fact, results of the comparative test cases from the few rounds of simulations have shown large disagreements in the modelling of airflow rate in the DSF cavity. Therefore, the prediction and validation of the natural air flow in the DSF cavity have to be considered as a criterion and also as an objective for validation of building simulation tools for modelling DSF.

Because of importance of the airflow model used when modelling the test cases, participants are asked to include *detailed* description of the airflow model used.

Following is the summary of additionally requested information for the modeller report. However, it requires less detailed description than the air flow model does. All modellers are asked to:

- Notify what is the solar model used for simulations
- Describe the main assumptions used for calculation of transmitted and distributed solar radiation to the surfaces in the model (area weighted distribution of solar radiation or distribution according to the view factors; are there any differences when calculate transmitted direct or transmitted diffuse solar radiation?)
- Report on modelling windows (Is the glazing and frame modelled separate?)
- Include into the report the parameters about the glazing optical properties used for the modelling, especially if ones have been calculated on the basis of IGDB number. This information must be attached to the report as a separate Excel-file
- Notify the principle for calculation of the glazing temperature
- Explain assumptions (if there are any) for modelling the cavity air temperature: is there any temperature gradient, how is the temperature gradient defined?
- Describe what are the heat transfer coefficents used in the model, what is the background for calculation of convection heat transfer
- Describe how the floor in zone 2 is modelled

In the separate sections of the empirical test case specification the modellers are asked to report on several matters, depending on the design of their model compared to the specification. These requests are summarized below:

The user is asked to notify whether and where differences with the empirical test case specification exist. It is necessary to include the documentation of changes into the report.

The modifications to specification are undesired, but still might be necessary, must be included into the report.

When the parameter given in the specification is inapplicable for the modelling the user may disregard it and continue the modelling. The notification in modeller report is needed.

If the information about ground temperature, air temperature in the neighbouring zones, spectral data cannot be used in the software tool being tested, then note it in the report.

If the testing software tool does not allow manual definition of the wind pressure coefficients and values provided in the specification are different from the ones fixed within the code, then the modeller report has to include detailed information about the values used.

It is required to notify the techniques for computations of the surface heat transfer coefficients in the report.

It is requested to report on the glazing properties used/calculated in the model.

The report has to include the notation for the approach used for the calculation of transmitted direct and diffuse solar radiation.

If the software being tested allows the calculation of the longwave radiation exchange with the exterior, use this function, else note it in the report.

If the software being tested allows the calculation of the longwave radiation exchange with the interior, use this function, and note in the report the approach that has been used.

10. Output results

One of the main requirements for the modelling procedure is consistency: user is asked to use the same applications for the same parameters in every model and use the most detailed level of modelling allowed by simulation program being tested. Besides, user is asked to follow carefully the test case specification definitions. However this is not always possible and modelling report has to include documentation of all discrepancies between model and test case specification. Moreover, report has to include documentation of main principles for calculation of essential processes and any other factors which user might find important.

The list of the output results is specified for every test case separately. It is expected that the output results are compared to the experimental results and/or between the task participants. However, the first simulation of the empirical test case is blind (participants will receive empirical results only when submitted their results of modelling).

The template file for the output results is delivered in a separate file for each test case. For example for test case DSF100_e:

Output results DSF100_e60.xls - file for the output results for the comparative test case DSF100_e with 1 hour average data.

10.1. Output parameters for the test case DSF100_2

N	Output	Unit	Description
1	Direct solar irradiation on the window surface	W/m^2	Mean hourly value
2	Diffuse solar irradiation on the window surface	W/m^2	Mean hourly value
3	Total solar irradiation on the window surface	W/m^2	Mean hourly value
4	Total solar radiation received on the external window glass surface	kW	Mean hourly value
5	Solar radiation transmitted from the outside into zone 1	kW	Mean hourly value
6	Solar radiation transmitted from zone1 into zone2 (first order of solar transmission)	kW	Mean hourly value
7	Power used for cooling/heating in the zone 2	kW	Mean hourly value (with the '+'sign for heating and '-'sign for cooling)
8	Hour ave glass pane, raged surface temperature of external window surface facing external	^{o}C	Mean hourly value
9	Hour averaged surface temperature of external window glass pane, surface facing zone1	^{o}C	Mean hourly values
10	Hour averaged surface temperature of internal window glass pane, surface facing zone1,	^{o}C	Mean hourly value
11	Hour averaged surface temperature of internal window glass pane, surface facing zone2	^{o}C	Mean hourly value
12	Hour averaged floor surface temperature in the zone 1	^{o}C	Mean hourly value
13	Hour averaged ceiling surface temperature in the zone 1	^{o}C	Mean hourly value
14	Hour averaged floor surface temperature in the zone 2	^{o}C	Mean hourly value
15	Hour averaged ceiling surface temperature in the zone 2	^{o}C	Mean hourly value
16	Hour averaged air volume weighted temperature in the zone 1	^{o}C	Mean hourly value
17	Solar altitude angle	deg	In the middle of the hourly interval

Table 17. Required output parameters for the test case DSF100_2.

Depending on the software tool used for modelling and its accuracy, the minimum required outputs are defined in the above table. Besides that, a modeller is asked to report on the additional outputs, if this is possible:

- Solar radiation absorbed in the opaque surfaces in zone 1 and zone 2 (mean hourly values)
- Convective/ radiative heat fluxes at the glass surfaces (mean hourly values)
- Anyone using CFD, please provide vector plots together with the data sheets
- Report the air temperature in zone 1, as an air temperature for each stacked sub-zone. This must be reported in a separate Excel-file of free format.

10.2. Output parameters for the test case DSF200_e

N	Output	Unit	Description
1	Direct solar irradiation on the window surface	W/m^2	Mean hourly value
2	Diffuse solar irradiation on the window surface	W/m^2	Mean hourly value
3	Total solar irradiation on the window surface	W/m^2	Mean hourly value
4	Total solar radiation received on the external window glass surface	kW	Mean hourly value
5	Solar radiation transmitted from the outside into zone 1	kW	Mean hourly value
6	Solar radiation transmitted from zone 1 into zone2 (first order of solar transmission)	kW	Mean hourly value
7	Power used for cooling/heating in the zone 2	kW	Mean hourly value (with the '+'sign for heating and '-'sign for cooling)
8	Hour averaged surface temperature of external window glass pane, surface facing external	^{o}C	Mean hourly value
9	Hour averaged surface temperature of external window glass pane, surface facing zone1	^{o}C	Mean hourly value
10	Hour averaged surface temperature of internal window glass pane, surface facing zone1,	^{o}C	Mean hourly value
11	Hour averaged surface temperature of internal window glass pane, surface facing zone2	^{o}C	Mean hourly value
12	Hour averaged floor surface temperature in the zone 1	^{o}C	Mean hourly value
13	Hour averaged ceiling surface temperature in the zone 1	^{o}C	Mean hourly value
14	Hour averaged floor surface temperature in the zone 2	^{o}C	Mean hourly value
15	Hour averaged ceiling surface temperature in the zone 2	^{o}C	Mean hourly value
16	Hour averaged volume weighted air temperature in the zone 1	^{o}C	Mean hourly value
17	Mass flow rate in the zone 1	kg/h	Mean hourly value, including the sign convention: '+'sign for the upwards flow and '-'sign for the downwards flow

Table 18. Required output parameters for the test case DSF200_e

Depending on the software tool used for modelling and its accuracy the minimum required outputs defined in the above table. Besides that a modeller is asked to report on additional outputs, if this is possible:

- Solar radiation absorbed in the opaque surfaces in zone 1 and zone 2 (mean hourly values)
- Convective/ radiative heat fluxes at the glass surfaces (mean hourly values)
- Report the air temperature in zone 1, as an air temperature for each stacked sub-zone. This must be reported in a separate Excel-file of free format
- Anyone using CFD, please provide vector plots together with the data sheets

11. References

Ref. 1. Kalyanova O., Heiselberg P. (2005). Comparative Test Case Specification – Test Cases DSF100_2 and DSF400_3: Report for IEA ECBCS Annex 43/SHC Task 34 Validation of Building Energy Simulation Tools / Aalborg : Instituttet for Bygningsteknik, Aalborg Universitet.

Ref. 2. Straw M.P. (2000). Computation and Measurement of Wind Induced Ventilation: PhD thesis/ Nottingham University

Ref. 3. Allard F. (1998) Natural Ventilation in Buildings. A Design Handbook/James&James (Science Publishers) Ltd/ MPG Books Limited

Ref. 4. Poirazis H. (2006). "Double Skin Facades for Office Buildings - Literature Review Report" (9.86MB). Division of Energy and Building Design, Department of Construction and Architecture, Lund Institute of Technology, Lund University, Report EBD-R—04

Ref. 5 Kalyanova O. (2007). Experimental set-up and full-scale measurements in 'the Cube'. Aalborg:Aalborg University: Department of Civil Engineering.
ISSN 1901-726X DCE Technical Report No.034.

12. Weather data

12.1. Test case DSF100_e

12.1.1 Climate data, 1 hour average

Month	Date	Hour	Wind direction, deg	Wind speed*10, m/s	Diffus solar irradiation, W/m²	Global solar irradiation, W/m²	External air temperature*10, ºC	Relative humidity, %	Atmosferic pressure, Pa
10	19	1	192	14	0	0	108	96	100222
10	19	2	151	9	0	0	109	96	100212
10	19	3	203	11	0	0	111	97	100227
10	19	4	150	11	0	0	110	97	100212
10	19	5	165	11	0	0	111	97	100218
10	19	6	132	12	0	0	111	97	100253
10	19	7	119	21	1	2	111	97	100262
10	19	8	112	26	5	18	114	97	100282
10	19	9	112	30	23	24	115	97	100292
10	19	10	117	24	35	35	119	96	100292
10	19	11	109	29	45	45	123	95	100275
10	19	12	107	33	45	45	124	94	100242
10	19	13	109	43	65	65	128	94	100212
10	19	14	112	42	58	58	133	93	100203
10	19	15	114	47	47	47	136	94	100182
10	19	16	112	46	33	33	135	94	100193
10	19	17	104	45	8	8	131	95	100187
10	19	18	108	50	0	0	130	95	100180
10	19	19	108	48	0	0	131	95	100168
10	19	20	109	46	0	0	133	93	100150
10	19	21	114	54	0	0	135	91	100167
10	19	22	116	54	0	0	135	91	100162
10	19	23	129	41	0	0	130	92	100152
10	19	24	112	26	0	0	121	93	100120
10	20	1	107	20	0	0	114	93	100092
10	20	2	109	20	0	0	113	94	100035
10	20	3	106	16	0	0	113	94	100023
10	20	4	129	19	0	0	111	94	100002
10	20	5	104	15	0	0	112	95	99982
10	20	6	116	16	0	0	116	94	99967
10	20	7	111	20	1	1	117	95	99975
10	20	8	131	35	11	11	119	93	99987
10	20	9	137	41	80	91	125	93	99957
10	20	10	142	38	94	101	133	92	99935
10	20	11	135	38	101	105	136	93	99897
10	20	12	134	35	89	90	134	93	99843
10	20	13	122	38	100	102	137	92	99792
10	20	14	112	36	113	117	140	91	99748
10	20	15	103	41	53	54	141	93	99705
10	20	16	101	41	26	26	137	94	99657
10	20	17	99	36	7	6	132	93	99617

Month	Date	Hour	Wind direction, deg	Wind speed*10, m/s	Diffus solar irradiation, W/m²	Global solar irradiation, W/m²	External air temperature*10, °C	Relative humidity, %	Atmosferic pressure, Pa
10	20	18	102	37	0	0	130	94	99593
10	20	19	120	47	0	0	129	95	99562
10	20	20	120	45	0	0	123	95	99565
10	20	21	131	34	0	0	123	96	99587
10	20	22	199	25	0	0	125	95	99593
10	20	23	206	31	0	0	125	95	99595
10	20	24	191	28	0	0	121	95	99580
10	21	1	183	28	0	0	121	96	99553
10	21	2	178	23	0	0	117	95	99517
10	21	3	150	22	0	0	117	95	99498
10	21	4	129	15	0	0	118	95	99477
10	21	5	135	17	0	0	118	95	99460
10	21	6	129	15	0	0	119	95	99477
10	21	7	111	14	2	2	120	95	99502
10	21	8	132	17	5	5	121	95	99515
10	21	9	165	31	26	27	127	95	99528
10	21	10	176	33	41	42	132	94	99560
10	21	11	165	35	59	60	131	90	99560
10	21	12	197	33	146	151	140	89	99552
10	21	13	206	36	133	137	151	87	99557
10	21	14	208	38	181	194	159	89	99560
10	21	15	221	42	170	199	166	91	99587
10	21	16	207	34	54	57	159	92	99615
10	21	17	211	24	14	14	146	93	99633
10	21	18	194	12	1	2	136	95	99660
10	21	19	186	17	0	0	128	94	99670
10	21	20	196	34	0	0	131	94	99662
10	21	21	204	42	0	0	135	93	99660
10	21	22	203	37	0	0	129	93	99673
10	21	23	202	52	0	0	132	93	99678
10	21	24	209	48	0	0	131	93	99687
10	22	1	212	45	0	0	131	93	99665
10	22	2	218	34	0	0	124	93	99635
10	22	3	217	41	0	0	125	93	99625
10	22	4	209	36	0	0	120	94	99622
10	22	5	185	26	0	0	117	94	99592
10	22	6	183	33	0	0	121	92	99613
10	22	7	179	43	2	6	122	90	99647
10	22	8	200	56	8	9	125	89	99627
10	22	9	195	27	19	20	108	88	99630
10	22	10	170	38	71	82	111	83	99637
10	22	11	197	57	112	146	129	78	99638
10	22	12	207	62	102	269	145	75	99628
10	22	13	209	66	99	314	150	81	99617

Month	Date	Hour	Wind direction, deg	Wind speed*10, m/s	Diffus solar irradiation, W/m²	Global solar irradiation, W/m²	External air temperature*10, °C	Relative humidity, %	Atmosferic pressure, Pa
10	22	14	205	56	76	204	147	85	99567
10	22	15	203	59	53	54	137	84	99558
10	22	16	203	43	86	103	119	86	99568
10	22	17	198	64	23	26	130	88	99528
10	22	18	196	55	0	0	122	89	99500
10	22	19	183	56	0	0	120	90	99498
10	22	20	187	58	0	0	119	89	99467
10	22	21	182	55	0	0	122	89	99443
10	22	22	190	61	0	0	127	91	99388
10	22	23	187	57	0	0	128	91	99340
10	22	24	173	52	0	0	125	92	99263
10	23	1	172	47	0	0	122	94	99150
10	23	2	159	37	0	0	118	94	99022
10	23	3	144	37	0	0	114	95	98880
10	23	4	138	47	0	0	116	95	98747
10	23	5	156	43	0	0	121	95	98665
10	23	6	159	50	0	0	127	95	98613
10	23	7	168	57	1	2	130	93	98607
10	23	8	203	70	2	2	133	91	98598
10	23	9	193	53	16	16	138	90	98612
10	23	10	201	53	95	99	147	89	98643
10	23	11	206	51	60	60	155	93	98683
10	23	12	240	57	106	106	155	94	98713
10	23	13	236	49	91	91	154	93	98727
10	23	14	255	46	121	143	154	90	98743
10	23	15	253	44	105	108	153	92	98760
10	23	16	245	37	68	80	150	94	98803
10	23	17	241	25	22	24	143	93	98902
10	23	18	222	30	0	0	137	93	98958
10	23	19	284	67	0	0	128	92	99020
10	23	20	279	46	0	0	121	91	99067
10	23	21	257	37	0	0	115	92	99057
10	23	22	249	27	0	0	107	93	99080
10	23	23	227	20	0	0	102	94	99097
10	23	24	231	26	0	0	96	94	99103
10	24	1	237	26	0	0	94	93	99095
10	24	2	227	17	0	0	94	94	99040
10	24	3	220	15	0	0	95	94	98975
10	24	4	184	13	0	0	96	95	98897
10	24	5	163	7	0	0	94	95	98868
10	24	6	96	11	0	0	92	96	98893
10	24	7	115	10	1	1	93	95	98902
10	24	8	173	13	1	2	94	95	98877
10	24	9	275	12	6	10	100	95	98872

Month	Date	Hour	Wind direction, deg	Wind speed*10, m/s	Diffus solar irradiation, W/m²	Global solar irradiation, W/m²	External air temperature*10, °C	Relative humidity, %	Atmosferic pressure, Pa
10	24	10	257	13	43	63	105	93	98882
10	24	11	273	22	93	98	108	92	98888
10	24	12	287	31	90	94	110	92	98918
10	24	13	264	32	83	87	113	91	98925
10	24	14	267	31	60	61	113	87	98958
10	24	15	279	35	124	136	122	91	99020
10	24	16	271	38	63	75	120	93	99093
10	24	17	270	28	22	25	115	92	99187
10	24	18	257	22	1	1	107	92	99275
10	24	19	262	29	0	0	97	93	99390
10	24	20	270	35	0	0	92	94	99492
10	24	21	275	36	0	0	88	95	99592
10	24	22	282	32	0	0	85	95	99683
10	24	23	285	33	0	0	85	95	99790
10	24	24	276	28	0	0	80	93	99870
10	25	1	248	21	0	0	74	87	99975
10	25	2	258	37	0	0	82	87	100060
10	25	3	268	51	0	0	83	87	100147
10	25	4	266	41	0	0	80	84	100237
10	25	5	264	40	0	0	77	83	100350
10	25	6	263	58	0	0	85	84	100478
10	25	7	269	55	1	2	85	84	100577
10	25	8	271	52	10	12	83	78	100688
10	25	9	268	52	44	110	98	66	100788
10	25	10	273	62	49	217	117	62	100900
10	25	11	279	66	45	293	132	60	100973
10	25	12	289	86	43	334	138	63	101043
10	25	13	290	79	46	337	127	65	101088
10	25	14	290	72	44	296	127	69	101140
10	25	15	294	56	46	216	125	75	101157
10	25	16	271	27	45	118	121	85	101202
10	25	17	257	15	19	22	101	88	101242
10	25	18	206	12	0	0	81	85	101245
10	25	19	190	8	0	0	68	90	101232
10	25	20	175	10	0	0	62	91	101240
10	25	21	144	14	0	0	64	91	101233
10	25	22	135	18	0	0	63	90	101188
10	25	23	137	19	0	0	64	87	101103
10	25	24	143	27	0	0	70	90	100990
10	26	1	137	24	0	0	77	93	100843
10	26	2	140	27	0	0	83	91	100707
10	26	3	135	40	0	0	99	89	100547
10	26	4	139	58	0	0	109	91	100320
10	26	5	125	80	0	0	104	92	100155

Month	Date	Hour	Wind direction, deg	Wind speed*10, m/s	Diffus solar irradiation, W/m²	Global solar irradiation, W/m²	External air temperature*10, °C	Relative humidity, %	Atmosferic pressure, Pa
10	26	6	128	110	0	0	102	91	100040
10	26	7	123	85	0	0	101	90	99903
10	26	8	134	68	1	0	103	91	99820
10	26	9	151	45	8	8	109	88	99818
10	26	10	177	52	35	35	114	88	99857
10	26	11	194	64	146	155	134	88	99828
10	26	12	203	51	100	102	143	89	99775
10	26	13	205	51	68	69	153	88	99727
10	26	14	196	53	132	137	163	89	99693
10	26	15	186	46	100	104	168	88	99662
10	26	16	181	43	48	50	164	89	99583
10	26	17	191	59	8	8	162	89	99495
10	26	18	187	59	0	0	158	90	99412
10	26	19	195	69	0	0	157	90	99305
10	26	20	199	74	0	0	155	84	99245
10	26	21	197	79	0	0	152	83	99260
10	26	22	223	92	0	0	147	81	99235
10	26	23	238	84	0	0	132	78	99127
10	26	24	223	67	0	0	122	78	98978
10	27	1	212	76	0	0	116	84	98890
10	27	2	215	96	0	0	119	85	98823
10	27	3	227	118	0	0	116	87	98865
10	27	4	236	128	0	0	114	82	98982
10	27	5	248	124	0	0	113	83	99140
10	27	6	258	125	0	0	119	82	99348
10	27	7	265	145	1	1	121	77	99572
10	27	8	270	157	5	5	117	69	99800
10	27	9	277	177	31	34	115	67	100017
10	27	10	280	187	83	136	120	63	100235
10	27	11	278	185	104	253	126	61	100497
10	27	12	286	190	107	300	130	58	100688
10	27	13	296	189	105	307	128	55	100888
10	27	14	301	147	76	275	126	57	101057
10	27	15	298	111	80	202	125	60	101250
10	27	16	291	85	67	92	118	60	101392
10	27	17	278	79	18	19	107	63	101438
10	27	18	281	79	0	0	103	65	101458
10	27	19	291	66	0	0	105	66	101553
10	27	20	292	70	0	0	103	66	101642
10	27	21	288	71	0	0	99	72	101707
10	27	22	284	62	0	0	93	76	101768
10	27	23	275	54	0	0	84	81	101798
10	27	24	276	47	0	0	79	84	101838
10	28	1	275	38	0	0	71	79	101850

Month	Date	Hour	Wind direction, deg	Wind speed*10, m/s	Diffus solar irradiation, W/m²	Global solar irradiation, W/m²	External air temperature*10, °C	Relative humidity, %	Atmosferic pressure, Pa
10	28	2	268	43	0	0	67	82	101857
10	28	3	260	46	0	0	65	83	101872
10	28	4	254	39	0	0	61	86	101855
10	28	5	254	44	0	0	62	85	101833
10	28	6	240	31	0	0	70	87	101818
10	28	7	215	28	0	0	74	89	101773
10	28	8	197	27	5	11	87	89	101750
10	28	9	194	23	19	20	86	94	101678
10	28	10	175	24	20	20	85	95	101565
10	28	11	191	38	34	34	85	90	101470
10	28	12	205	55	54	55	93	89	101367
10	28	13	224	50	68	69	106	89	101295
10	28	14	231	44	96	100	120	90	101215
10	28	15	246	55	89	93	125	93	101133
10	28	16	247	39	52	55	126	92	101043
10	28	17	229	33	8	8	120	94	100945
10	28	18	229	30	0	0	118	95	100842
10	28	19	221	21	0	0	115	95	100747
10	28	20	209	20	0	0	111	96	100637
10	28	21	188	13	0	0	109	95	100585
10	28	22	127	20	0	0	110	94	100605
10	28	23	71	26	0	0	107	93	100618
10	28	24	70	21	0	0	93	92	100630
10	29	1	67	24	0	0	86	92	100695
10	29	2	74	20	0	0	81	92	100718
10	29	3	69	22	0	0	78	90	100762
10	29	4	71	25	0	0	74	89	100830
10	29	5	70	28	0	0	71	88	100927
10	29	6	69	35	0	0	67	90	101033
10	29	7	68	36	0	0	61	88	101145
10	29	8	68	44	1	1	54	85	101257
10	29	9	66	38	14	14	53	84	101353
10	29	10	69	40	56	60	54	81	101470
10	29	11	81	38	108	119	64	76	101547
10	29	12	79	43	148	222	81	71	101673
10	29	13	74	39	124	199	77	68	101732
10	29	14	70	31	119	184	78	72	101802
10	29	15	71	23	100	163	77	73	101905
10	29	16	70	20	90	148	82	81	101905
10	29	17	71	7	23	35	75	82	101962
10	29	18	103	5	0	0	62	86	102003
10	29	19	223	15	0	0	52	87	101997
10	29	20	200	11	0	0	56	88	102003
10	29	21	211	10	0	0	54	85	101998

Month	Date	Hour	Wind direction, deg	Wind speed*10, m/s	Diffus solar irradiation, W/m²	Global solar irradiation, W/m²	External air temperature*10, °C	Relative humidity, %	Atmosferic pressure, Pa
10	29	22	235	18	0	0	54	88	101948
10	29	23	225	20	0	0	55	88	101912
10	29	24	221	27	0	0	54	91	101845
10	30	1	226	37	0	0	60	91	101788
10	30	2	228	38	0	0	64	92	101725
10	30	3	230	43	0	0	66	91	101677
10	30	4	231	41	0	0	72	90	101655
10	30	5	228	38	0	0	73	89	101603
10	30	6	239	39	0	0	75	87	101570
10	30	7	241	40	1	1	80	87	101538
10	30	8	244	44	4	10	91	88	101542
10	30	9	240	38	20	21	89	88	101502
10	30	10	244	44	57	60	95	88	101450
10	30	11	244	47	64	66	100	91	101377
10	30	12	246	51	89	92	104	91	101275
10	30	13	242	55	93	96	101	93	101162
10	30	14	217	39	73	74	94	94	101013
10	30	15	189	42	36	37	90	94	100815
10	30	16	177	37	15	15	89	94	100585
10	30	17	163	51	5	5	88	95	100408
10	30	18	158	69	0	0	87	95	100248
10	30	19	168	74	0	0	89	96	100137
10	30	20	194	60	0	0	97	95	100067
10	30	21	218	57	0	0	109	94	99988
10	30	22	246	62	0	0	123	94	99895
10	30	23	249	73	0	0	127	93	99817
10	30	24	245	69	0	0	132	93	99693
10	31	1	238	67	0	0	134	92	99530
10	31	2	237	73	0	0	129	88	99392
10	31	3	226	63	0	0	132	87	99233
10	31	4	237	82	0	0	134	93	99105
10	31	5	226	71	0	0	129	94	99007
10	31	6	230	78	0	0	129	95	98967
10	31	7	228	70	0	1	123	94	98922
10	31	8	258	77	2	2	118	90	98872
10	31	9	250	62	16	16	110	83	98813
10	31	10	243	67	61	88	112	80	98770
10	31	11	251	80	65	245	133	80	98697
10	31	12	253	88	96	173	131	85	98593
10	31	13	247	67	104	129	111	89	98457
10	31	14	239	66	129	184	117	90	98342
10	31	15	228	58	74	79	109	91	98255
10	31	16	207	53	22	23	101	92	98238
10	31	17	231	39	1	1	95	88	98275

Month	Date	Hour	Wind direction, deg	Wind speed*10, m/s	Diffus solar irradiation, W/m²	Global solar irradiation, W/m²	External air temperature*10, °C	Relative humidity, %	Atmosferic pressure, Pa
10	31	18	243	40	0	0	87	85	98308
10	31	19	271	78	0	0	88	83	98292
10	31	20	277	86	0	0	81	84	98287
10	31	21	273	82	0	0	77	90	98320
10	31	22	265	89	0	0	75	90	98435
10	31	23	270	81	0	0	71	88	98630
10	31	24	269	49	0	0	68	88	98858
11	1	1	178	38	0	0	59	86	99070
11	1	2	134	38	0	0	42	87	99292
11	1	3	154	37	0	0	26	91	99563
11	1	4	145	47	0	0	17	93	99803
11	1	5	134	46	0	0	9	90	100030
11	1	6	148	43	0	0	10	89	100265
11	1	7	164	45	0	0	10	88	100477
11	1	8	64	71	3	3	7	79	100658
11	1	9	16	101	35	42	11	69	100830
11	1	10	10	105	45	50	13	63	101010
11	1	11	11	104	87	115	9	61	101183
11	1	12	8	97	134	218	31	57	101330
11	1	13	71	86	118	238	26	50	101473
11	1	14	180	81	104	177	21	61	101595
11	1	15	349	77	75	111	22	53	101687
11	1	16	353	59	42	66	20	54	101807
11	1	17	352	52	9	12	19	54	101912
11	1	18	294	38	0	0	21	53	101982
11	1	19	329	17	0	0	17	58	102023
11	1	20	318	13	0	0	20	65	102050
11	1	21	313	11	0	0	15	65	102060
11	1	22	59	3	0	0	4	66	102070
11	1	23	0	0	0	0	2	76	102095
11	1	24	205	9	0	0	1	71	102113
11	2	1	300	14	0	0	5	71	102120
11	2	2	290	11	0	0	2	71	102127
11	2	3	282	12	0	0	3	77	102132
11	2	4	136	6	0	0	-20	85	102138
11	2	5	130	5	0	0	-23	91	102150
11	2	6	0	0	0	0	-20	91	102182
11	2	7	75	4	0	1	-16	87	102193
11	2	8	246	19	4	4	-14	84	102213
11	2	9	86	3	39	81	9	76	102237
11	2	10	49	3	61	175	32	64	102248
11	2	11	345	34	82	173	39	52	102245
11	2	12	186	39	56	285	71	60	102255
11	2	13	237	19	52	300	70	62	102295

Month	Date	Hour	Wind direction, deg	Wind speed*10, m/s	Diffus solar irradiation, W/m²	Global solar irradiation, W/m²	External air temperature*10, °C	Relative humidity, %	Atmosferic pressure, Pa
11	2	14	355	18	85	226	69	62	102315
11	2	15	346	14	54	84	50	66	102367
11	2	16	338	18	48	68	53	68	102423
11	2	17	345	17	10	10	40	66	102468
11	2	18	324	13	0	0	32	72	102492
11	2	19	289	28	0	0	30	64	102525
11	2	20	80	17	0	0	25	66	102575
11	2	21	54	24	0	0	25	72	102592
11	2	22	29	11	0	0	22	75	102605
11	2	23	54	1	0	0	18	82	102622
11	2	24	179	7	0	0	18	86	102630
11	3	1	90	4	0	0	12	85	102638
11	3	2	62	2	0	0	0	91	102642
11	3	3	44	3	0	0	-6	93	102645
11	3	4	142	8	0	0	-14	92	102648
11	3	5	60	6	0	0	-11	91	102653
11	3	6	0	0	0	0	-12	90	102657
11	3	7	0	0	1	1	-4	89	102682
11	3	8	99	6	6	8	8	88	102705
11	3	9	225	16	49	62	19	84	102698
11	3	10	242	21	68	85	34	79	102672
11	3	11	239	26	67	84	30	74	102645
11	3	12	240	27	95	119	41	71	102613
11	3	13	243	29	151	189	46	72	102577
11	3	14	245	42	175	219	58	77	102540
11	3	15	243	37	83	104	56	80	102498
11	3	16	242	30	9	11	51	83	102463
11	3	17	239	30	0	0	40	89	102427
11	3	18	240	31	0	0	36	92	102390
11	3	19	249	36	0	0	34	93	102355
11	3	20	247	41	0	0	35	93	102308
11	3	21	242	37	0	0	44	94	102262
11	3	22	248	26	0	0	46	95	102213
11	3	23	248	27	0	0	46	95	102173
11	3	24	248	32	0	0	51	93	102145
11	4	1	260	29	0	0	53	85	102090
11	4	2	255	32	0	0	59	83	102062
11	4	3	262	39	0	0	57	88	102047
11	4	4	278	43	0	0	65	84	102035
11	4	5	279	63	0	0	74	79	102030
11	4	6	277	55	0	0	76	80	102037
11	4	7	276	53	0	0	77	82	102015
11	4	8	273	61	7	8	79	82	101948
11	4	9	272	69	79	94	78	85	101905

Month	Date	Hour	Wind direction, deg	Wind speed*10, m/s	Diffus solar irradiation, W/m²	Global solar irradiation, W/m²	External air temperature*10, °C	Relative humidity, %	Atmosferic pressure, Pa
11	4	10	268	75	150	177	94	82	101830
11	4	11	269	83	65	76	104	84	101753
11	4	12	270	89	80	94	107	80	101702
11	4	13	269	97	139	164	109	76	101685
11	4	14	281	104	100	117	108	78	101658
11	4	15	288	91	44	52	110	81	101623
11	4	16	289	105	6	7	106	82	101572
11	4	17	284	95	0	0	102	83	101562
11	4	18	283	94	0	0	101	85	101540
11	4	19	285	97	0	0	102	84	101517
11	4	20	286	102	0	0	104	83	101440
11	4	21	290	101	0	0	107	81	101343
11	4	22	284	111	0	0	106	87	101265
11	4	23	280	114	0	0	102	83	101130
11	4	24	276	109	0	0	101	84	101020
11	5	1	274	110	0	0	101	87	100985
11	5	2	280	110	0	0	108	86	100988
11	5	3	279	113	0	0	109	87	100952
11	5	4	285	113	0	0	110	86	100915
11	5	5	287	116	0	0	114	87	100890
11	5	6	289	106	0	0	114	88	100928
11	5	7	290	105	0	0	117	87	100958
11	5	8	294	105	17	18	115	89	101002
11	5	9	296	106	36	38	117	89	101027
11	5	10	298	102	46	49	120	91	101027
11	5	11	300	100	79	83	121	91	101032
11	5	12	302	82	48	51	125	90	101050
11	5	13	300	82	26	28	123	89	101070
11	5	14	299	94	31	33	119	89	101077
11	5	15	296	101	9	9	118	87	101083
11	5	16	293	108	2	2	121	87	101093
11	5	17	288	101	0	0	118	86	101137
11	5	18	283	100	0	0	116	86	101133
11	5	19	279	100	0	0	115	86	101107
11	5	20	274	104	0	0	112	88	101078
11	5	21	274	104	0	0	110	92	101058
11	5	22	273	98	0	0	109	89	101052
11	5	23	275	92	0	0	106	90	101037
11	5	24	274	98	0	0	110	94	101018
11	6	1	272	103	0	0	114	91	100965
11	6	2	270	110	0	0	110	89	100935
11	6	3	273	113	0	0	108	87	100935
11	6	4	277	125	0	0	107	86	100927
11	6	5	280	129	0	0	113	86	100900

Month	Date	Hour	Wind direction, deg	Wind speed*10, m/s	Diffus solar irradiation, W/m^2	Global solar irradiation, W/m^2	External air temperature*10, ^{o}C	Relative humidity, %	Atmosferic pressure, Pa
11	6	6	280	136	0	0	118	87	100913
11	6	7	274	127	0	0	117	85	100942
11	6	8	275	131	10	10	116	83	101008
11	6	9	272	127	34	35	117	82	101040
11	6	10	276	131	65	69	123	81	101058
11	6	11	277	146	92	96	127	81	101085
11	6	12	275	139	74	78	130	80	101130
11	6	13	281	143	91	95	128	80	101187
11	6	14	279	142	61	64	129	81	101165
11	6	15	280	132	14	15	126	81	101210
11	6	16	285	121	3	3	124	82	101238
11	6	17	285	125	0	0	124	81	101267
11	6	18	278	118	0	0	119	81	101297
11	6	19	276	108	0	0	113	82	101280
11	6	20	277	116	0	0	113	83	101287
11	6	21	270	119	0	0	113	81	101313
11	6	22	272	114	0	0	108	82	101283
11	6	23	272	117	0	0	105	80	101290
11	6	24	271	114	0	0	103	83	101282

12.1.2 Other boundary conditions, 1 hour average

Month	Date	Hour	Zone 3.2 Temperature*10, oC	Zone 3.3 Temperature*10, oC	Ground temperature under foundation*10, oC
10	19	1	192	130	157
10	19	2	192	130	157
10	19	3	193	130	157
10	19	4	193	130	157
10	19	5	193	131	157
10	19	6	193	130	157
10	19	7	193	129	157
10	19	8	183	127	157
10	19	9	188	130	157
10	19	10	193	131	157
10	19	11	194	135	157
10	19	12	195	138	157
10	19	13	195	139	157
10	19	14	195	139	157
10	19	15	196	142	157
10	19	16	196	142	157
10	19	17	196	142	157
10	19	18	196	139	157
10	19	19	196	139	157
10	19	20	196	141	157
10	19	21	196	142	157
10	19	22	196	141	157
10	19	23	196	139	157
10	19	24	196	137	157
10	20	1	196	133	157
10	20	2	195	133	157
10	20	3	195	133	157
10	20	4	195	131	157
10	20	5	195	133	157
10	20	6	195	133	157
10	20	7	195	134	157
10	20	8	195	135	157
10	20	9	197	138	157
10	20	10	197	142	157
10	20	11	197	143	157
10	20	12	198	144	157
10	20	13	198	144	157
10	20	14	198	147	157
10	20	15	199	149	157
10	20	16	199	147	157
10	20	17	198	145	157
10	20	18	198	143	157
10	20	19	198	141	157
10	20	20	198	135	157
10	20	21	197	136	157

Month	Date	Hour	Zone 3.2 Temperature*10, oC	Zone 3.3 Temperature*10, oC	Ground temperature under foundation*10, oC
10	20	22	197	142	157
10	20	23	197	144	157
10	20	24	197	142	157
10	21	1	197	140	157
10	21	2	197	139	157
10	21	3	197	136	156
10	21	4	197	136	157
10	21	5	197	135	157
10	21	6	196	136	156
10	21	7	196	138	157
10	21	8	196	138	157
10	21	9	196	141	157
10	21	10	197	145	157
10	21	11	198	146	156
10	21	12	198	153	157
10	21	13	199	161	156
10	21	14	200	166	156
10	21	15	201	172	157
10	21	16	201	172	156
10	21	17	200	166	156
10	21	18	200	162	156
10	21	19	199	153	156
10	21	20	199	150	157
10	21	21	198	152	157
10	21	22	198	150	157
10	21	23	198	149	157
10	21	24	198	146	157
10	22	1	198	146	156
10	22	2	198	144	156
10	22	3	197	143	157
10	22	4	197	141	156
10	22	5	197	140	156
10	22	6	197	141	157
10	22	7	197	141	156
10	22	8	197	143	156
10	22	9	197	135	156
10	22	10	197	133	156
10	22	11	198	143	156
10	22	12	198	147	156
10	22	13	197	156	156
10	22	14	197	156	156
10	22	15	197	152	156
10	22	16	198	146	156
10	22	17	197	147	156
10	22	18	197	140	156
10	22	19	196	138	156
10	22	20	196	137	156
10	22	21	196	138	156

Month	Date	Hour	Zone 3.2 Temperature*10, oC	Zone 3.3 Temperature*10, oC	Ground temperature under foundation*10, oC
10	22	22	196	141	156
10	22	23	196	142	156
10	22	24	196	141	156
10	23	1	196	139	156
10	23	2	195	136	156
10	23	3	195	132	156
10	23	4	195	128	156
10	23	5	195	132	156
10	23	6	195	138	156
10	23	7	195	141	156
10	23	8	195	145	156
10	23	9	196	152	156
10	23	10	197	160	156
10	23	11	198	164	156
10	23	12	194	165	156
10	23	13	188	164	156
10	23	14	189	166	156
10	23	15	189	167	156
10	23	16	188	165	156
10	23	17	187	163	156
10	23	18	186	158	156
10	23	19	186	154	156
10	23	20	185	152	156
10	23	21	184	143	156
10	23	22	184	137	156
10	23	23	183	132	156
10	23	24	183	127	156
10	24	1	182	125	156
10	24	2	182	125	156
10	24	3	181	127	156
10	24	4	181	127	156
10	24	5	181	126	156
10	24	6	181	125	156
10	24	7	181	126	156
10	24	8	181	124	156
10	24	9	181	127	156
10	24	10	192	130	157
10	24	11	187	135	157
10	24	12	185	137	157
10	24	13	172	139	157
10	24	14	183	139	157
10	24	15	184	142	157
10	24	16	185	144	157
10	24	17	186	141	157
10	24	18	185	137	157
10	24	19	185	131	157
10	24	20	185	128	158
10	24	21	184	126	157

Month	Date	Hour	Zone 3.2 Temperature*10, oC	Zone 3.3 Temperature*10, oC	Ground temperature under foundation*10, oC
10	24	22	184	125	157
10	24	23	184	124	157
10	24	24	184	122	158
10	25	1	183	116	157
10	25	2	183	118	157
10	25	3	183	118	158
10	25	4	183	117	157
10	25	5	183	115	157
10	25	6	183	115	157
10	25	7	182	116	157
10	25	8	182	117	157
10	25	9	182	122	157
10	25	10	180	130	156
10	25	11	180	139	156
10	25	12	178	141	155
10	25	13	178	140	156
10	25	14	177	140	156
10	25	15	177	141	155
10	25	16	179	142	156
10	25	17	180	132	156
10	25	18	181	121	156
10	25	19	181	115	156
10	25	20	181	110	156
10	25	21	182	107	157
10	25	22	182	103	157
10	25	23	181	100	156
10	25	24	182	99	157
10	26	1	182	103	157
10	26	2	182	106	157
10	26	3	182	114	157
10	26	4	183	119	157
10	26	5	182	116	157
10	26	6	182	114	157
10	26	7	183	113	157
10	26	8	184	117	157
10	26	9	183	120	157
10	26	10	182	127	157
10	26	11	182	138	156
10	26	12	184	148	157
10	26	13	185	159	157
10	26	14	185	166	156
10	26	15	187	173	157
10	26	16	186	172	156
10	26	17	186	172	157
10	26	18	186	169	156
10	26	19	186	167	156
10	26	20	186	165	156
10	26	21	186	163	156

Month	Date	Hour	Zone 3.2 Temperature*10, oC	Zone 3.3 Temperature*10, oC	Ground temperature under foundation*10, oC
10	26	22	186	159	156
10	26	23	186	146	156
10	26	24	186	138	156
10	27	1	185	131	156
10	27	2	184	130	156
10	27	3	184	127	156
10	27	4	184	123	156
10	27	5	184	124	156
10	27	6	184	128	156
10	27	7	184	131	156
10	27	8	184	128	156
10	27	9	183	126	156
10	27	10	181	130	156
10	27	11	180	133	156
10	27	12	179	135	156
10	27	13	177	138	155
10	27	14	177	141	155
10	27	15	178	142	155
10	27	16	179	139	156
10	27	17	180	130	155
10	27	18	180	127	156
10	27	19	180	131	156
10	27	20	181	133	155
10	27	21	181	131	156
10	27	22	181	126	156
10	27	23	181	123	156
10	27	24	181	119	156
10	28	1	180	115	156
10	28	2	180	113	156
10	28	3	180	108	156
10	28	4	180	105	156
10	28	5	180	104	156
10	28	6	180	104	156
10	28	7	181	106	156
10	28	8	182	113	157
10	28	9	180	116	157
10	28	10	181	116	156
10	28	11	181	116	157
10	28	12	181	120	157
10	28	13	181	124	157
10	28	14	182	132	156
10	28	15	182	138	156
10	28	16	183	139	156
10	28	17	183	138	156
10	28	18	183	137	156
10	28	19	183	135	156
10	28	20	183	136	156
10	28	21	182	134	156

Month	Date	Hour	Zone 3.2 Temperature*10, oC	Zone 3.3 Temperature*10, oC	Ground temperature under foundation*10, oC
10	28	22	183	136	157
10	28	23	182	135	156
10	28	24	182	128	156
10	29	1	182	128	157
10	29	2	181	122	157
10	29	3	182	124	157
10	29	4	181	121	156
10	29	5	181	116	157
10	29	6	181	110	157
10	29	7	181	102	157
10	29	8	181	98	157
10	29	9	181	94	157
10	29	10	180	94	157
10	29	11	179	92	156
10	29	12	180	96	157
10	29	13	177	99	155
10	29	14	178	101	156
10	29	15	178	105	155
10	29	16	178	108	156
10	29	17	178	111	155
10	29	18	179	109	157
10	29	19	179	102	156
10	29	20	179	102	156
10	29	21	179	102	157
10	29	22	178	100	155
10	29	23	179	99	156
10	29	24	179	98	157
10	30	1	178	95	156
10	30	2	179	96	156
10	30	3	180	97	157
10	30	4	180	100	156
10	30	5	179	102	155
10	30	6	179	102	155
10	30	7	180	106	156
10	30	8	179	108	155
10	30	9	180	112	157
10	30	10	181	115	156
10	30	11	180	119	157
10	30	12	180	122	156
10	30	13	180	121	155
10	30	14	180	119	155
10	30	15	180	117	155
10	30	16	180	117	156
10	30	17	180	111	155
10	30	18	181	103	155
10	30	19	181	103	156
10	30	20	181	114	155
10	30	21	181	123	156

Month	Date	Hour	Zone 3.2 Temperature*10, oC	Zone 3.3 Temperature*10, oC	Ground temperature under foundation*10, oC
10	30	22	181	134	156
10	30	23	181	140	156
10	30	24	182	142	156
10	31	1	182	144	156
10	31	2	182	142	156
10	31	3	182	142	156
10	31	4	182	143	156
10	31	5	183	140	156
10	31	6	183	139	156
10	31	7	183	137	156
10	31	8	183	136	156
10	31	9	182	132	156
10	31	10	182	132	156
10	31	11	181	139	155
10	31	12	179	138	154
10	31	13	180	130	155
10	31	14	180	131	155
10	31	15	180	126	155
10	31	16	180	124	155
10	31	17	181	123	155
10	31	18	181	120	155
10	31	19	181	120	155
10	31	20	181	117	156
10	31	21	181	113	156
10	31	22	181	106	156
10	31	23	181	104	156
10	31	24	180	113	156
11	1	1	179	124	156
11	1	2	178	111	156
11	1	3	176	104	156
11	1	4	174	103	156
11	1	5	173	95	156
11	1	6	173	95	155
11	1	7	175	93	157
11	1	8	174	92	157
11	1	9	176	92	157
11	1	10	171	91	154
11	1	11	172	84	157
11	1	12	170	102	157
11	1	13	167	103	155
11	1	14	168	106	156
11	1	15	169	98	156
11	1	16	170	98	156
11	1	17	172	95	156
11	1	18	173	87	156
11	1	19	173	95	155
11	1	20	174	90	156
11	1	21	173	91	155

Month	Date	Hour	Zone 3.2 Temperature*10, oC	Zone 3.3 Temperature*10, oC	Ground temperature under foundation*10, oC
11	1	22	174	81	155
11	1	23	175	71	156
11	1	24	174	67	156
11	2	1	174	69	156
11	2	2	175	68	156
11	2	3	175	69	156
11	2	4	174	59	156
11	2	5	174	53	156
11	2	6	174	50	156
11	2	7	174	49	156
11	2	8	174	49	156
11	2	9	173	51	156
11	2	10	170	61	156
11	2	11	169	72	156
11	2	12	175	86	154
11	2	13	171	99	154
11	2	14	167	108	154
11	2	15	170	102	154
11	2	16	169	96	155
11	2	17	171	98	155
11	2	18	172	90	156
11	2	19	172	102	155
11	2	20	173	102	155
11	2	21	172	105	155
11	2	22	173	97	156
11	2	23	173	82	156
11	2	24	174	77	156
11	3	1	173	76	156
11	3	2	174	68	156
11	3	3	173	64	156
11	3	4	173	57	156
11	3	5	173	53	156
11	3	6	172	54	155
11	3	7	173	56	156
11	3	8	173	55	156
11	3	9	173	60	156
11	3	10	171	70	156
11	3	11	150	67	154
11	3	12	164	75	154
11	3	13	138	80	155
11	3	14	131	83	155
11	3	15	156	85	156
11	3	16	165	86	156
11	3	17	171	83	157
11	3	18	173	79	156
11	3	19	174	78	156
11	3	20	174	76	156
11	3	21	173	79	155

Month	Date	Hour	Zone 3.2 Temperature*10, oC	Zone 3.3 Temperature*10, oC	Ground temperature under foundation*10, oC
11	3	22	173	85	155
11	3	23	174	87	155
11	3	24	174	89	155
11	4	1	174	92	155
11	4	2	174	97	155
11	4	3	175	94	155
11	4	4	175	100	156
11	4	5	175	103	155
11	4	6	176	106	155
11	4	7	176	108	155
11	4	8	177	110	155
11	4	9	177	107	155
11	4	10	177	111	154
11	4	11	177	118	154
11	4	12	177	121	154
11	4	13	178	123	154
11	4	14	177	123	154
11	4	15	176	127	154
11	4	16	177	127	154
11	4	17	178	125	154
11	4	18	178	123	154
11	4	19	179	124	155
11	4	20	178	124	153
11	4	21	179	129	154
11	4	22	179	127	155
11	4	23	179	123	154
11	4	24	179	121	154
11	5	1	179	120	154
11	5	2	180	124	154
11	5	3	180	125	154
11	5	4	180	127	154
11	5	5	180	130	154
11	5	6	180	132	154
11	5	7	180	134	154
11	5	8	180	137	154
11	5	9	180	139	154
11	5	10	179	142	154
11	5	11	180	144	154
11	5	12	180	150	154
11	5	13	180	150	154
11	5	14	180	149	153
11	5	15	180	147	154
11	5	16	180	142	154
11	5	17	180	139	154
11	5	18	180	136	154
11	5	19	180	133	153
11	5	20	180	131	153
11	5	21	181	128	154

59

Month	Date	Hour	Zone 3.2 Temperature*10, oC	Zone 3.3 Temperature*10, oC	Ground temperature under foundation*10, oC
11	5	22	181	127	154
11	5	23	181	127	153
11	5	24	181	128	154
11	6	1	181	130	154
11	6	2	181	128	154
11	6	3	181	127	154
11	6	4	181	127	154
11	6	5	181	129	154
11	6	6	181	132	154
11	6	7	181	131	153
11	6	8	181	130	153
11	6	9	181	131	153
11	6	10	181	134	153
11	6	11	182	136	153
11	6	12	182	139	154
11	6	13	182	140	153
11	6	14	182	141	153
11	6	15	182	139	153
11	6	16	182	138	153
11	6	17	181	139	153
11	6	18	181	136	153
11	6	19	181	131	153
11	6	20	181	131	153
11	6	21	181	129	153
11	6	22	181	127	153
11	6	23	181	125	153
11	6	24	181	124	153

12.2. Test case DSF200_e

12.2.1 Climate data, 1 hour average

Month	Date	Hour	Wind direction, deg	Wind speed*10, m/s	Diffus solar irradiation, W/m^2	Global solar irradiation, W/m^2	External air temperature*10, ^{o}C	Relative humidity, %	Atmosferic pressure, Pa
10	1	1	212	15	0	0	110	91	100900
10	1	2	207	21	0	0	105	90	100900
10	1	3	197	25	0	0	100	86	100900
10	1	4	177	28	0	0	98	79	100900
10	1	5	173	24	0	0	92	74	100900
10	1	6	161	20	0	0	91	71	100900
10	1	7	177	24	7	9	100	67	100900
10	1	8	181	16	46	88	111	64	100900
10	1	9	143	18	67	112	115	74	100899
10	1	10	144	21	165	246	124	67	100893
10	1	11	167	36	167	413	150	58	100886
10	1	12	187	48	166	440	172	59	100879
10	1	13	190	46	185	451	187	68	100872
10	1	14	188	44	171	397	192	67	100865
10	1	15	181	44	159	295	192	64	100858
10	1	16	169	42	122	215	187	69	100851
10	1	17	153	31	60	74	176	71	100844
10	1	18	132	40	12	12	160	84	100837
10	1	19	133	53	0	0	158	88	100830
10	1	20	136	55	0	0	155	92	100824
10	1	21	149	43	0	0	148	90	100817
10	1	22	159	37	0	0	146	90	100810
10	1	23	205	39	0	0	148	92	100803
10	1	24	231	20	0	0	133	95	100781
10	2	1	142	11	0	0	131	95	100747
10	2	2	179	22	0	0	129	92	100714
10	2	3	155	16	0	0	126	95	100681
10	2	4	176	28	0	0	123	94	100647
10	2	5	167	31	0	0	120	94	100614
10	2	6	184	37	0	0	122	94	100581
10	2	7	181	37	5	5	120	93	100547
10	2	8	175	33	41	42	124	93	100514
10	2	9	173	41	140	224	142	88	100481
10	2	10	173	55	112	164	144	85	100447
10	2	11	185	51	204	313	160	79	100414
10	2	12	186	46	200	211	161	75	100381
10	2	13	186	47	234	293	144	79	100347
10	2	14	199	42	185	245	164	74	100314
10	2	15	215	41	179	274	163	86	100281
10	2	16	202	34	133	214	154	88	100247
10	2	17	187	23	68	73	147	89	100214
10	2	18	184	31	12	12	137	79	100181

Month	Date	Hour	Wind direction, deg	Wind speed*10, m/s	Diffus solar irradiation, W/m^2	Global solar irradiation, W/m^2	External air temperature*10, ^{o}C	Relative humidity, %	Atmosferic pressure, Pa
10	2	19	159	17	0	0	129	77	100147
10	2	20	166	21	0	0	126	77	100114
10	2	21	182	25	0	0	124	70	100081
10	2	22	166	18	0	0	119	70	100047
10	2	23	148	8	0	0	115	75	100014
10	2	24	254	17	0	0	120	90	99990
10	3	1	260	23	0	0	122	91	99974
10	3	2	257	30	0	0	124	90	99957
10	3	3	239	30	0	0	126	86	99940
10	3	4	247	36	0	0	128	79	99924
10	3	5	237	26	0	0	120	74	99907
10	3	6	250	34	0	0	116	71	99890
10	3	7	234	31	6	8	114	67	99874
10	3	8	232	33	66	113	117	64	99857
10	3	9	238	31	114	139	129	74	99840
10	3	10	226	33	145	160	140	67	99824
10	3	11	229	36	225	266	152	58	99807
10	3	12	245	47	240	296	165	59	99790
10	3	13	228	38	218	383	171	68	99774
10	3	14	241	35	160	171	165	67	99757
10	3	15	229	30	143	197	165	64	99740
10	3	16	213	27	98	231	160	69	99724
10	3	17	241	12	63	66	149	71	99707
10	3	18	186	7	13	13	137	84	99690
10	3	19	157	12	0	0	132	88	99674
10	3	20	187	10	0	0	120	92	99657
10	3	21	216	9	0	0	114	90	99640
10	3	22	218	21	0	0	116	90	99624
10	3	23	168	7	0	0	113	92	99607
10	3	24	221	22	0	0	116	99	99610
10	4	1	236	24	0	0	108	99	99626
10	4	2	236	21	0	0	101	99	99643
10	4	3	241	19	0	0	96	99	99660
10	4	4	238	11	0	0	93	99	99676
10	4	5	240	11	0	0	92	96	99693
10	4	6	234	17	0	0	95	91	99710
10	4	7	240	18	5	6	101	93	99726
10	4	8	237	16	39	58	104	89	99743
10	4	9	254	34	85	227	123	86	99760
10	4	10	265	43	178	204	149	83	99776
10	4	11	275	45	174	232	155	76	99793
10	4	12	268	51	182	227	159	71	99810
10	4	13	261	48	189	217	156	67	99826
10	4	14	289	58	130	136	152	68	99843
10	4	15	288	62	159	175	157	72	99860
10	4	16	289	69	99	229	158	74	99876
10	4	17	278	52	56	132	148	78	99893
10	4	18	271	33	20	25	131	88	99910

Month	Date	Hour	Wind direction, deg	Wind speed*10, m/s	Diffus solar irradiation, W/m²	Global solar irradiation, W/m²	External air temperature*10, °C	Relative humidity, %	Atmosferic pressure, Pa
10	4	19	254	25	0	0	114	91	99926
10	4	20	247	25	0	0	105	90	99943
10	4	21	241	26	0	0	99	88	99960
10	4	22	241	28	0	0	96	90	99976
10	4	23	244	33	0	0	98	92	99993
10	4	24	233	26	0	0	94	90	100012
10	5	1	240	30	0	0	89	91	100033
10	5	2	249	42	0	0	92	90	100054
10	5	3	244	37	0	0	91	86	100075
10	5	4	240	32	0	0	90	79	100095
10	5	5	232	28	0	0	82	74	100116
10	5	6	220	28	0	0	77	71	100137
10	5	7	228	29	5	5	78	67	100158
10	5	8	238	34	38	64	86	64	100179
10	5	9	232	39	65	190	105	74	100200
10	5	10	243	46	63	324	122	67	100220
10	5	11	266	69	108	422	141	58	100241
10	5	12	263	68	77	355	145	59	100262
10	5	13	245	56	93	177	136	68	100283
10	5	14	235	54	102	394	131	67	100304
10	5	15	239	52	60	344	137	64	100325
10	5	16	234	41	77	138	133	69	100345
10	5	17	211	29	55	113	130	71	100366
10	5	18	187	24	14	14	120	84	100387
10	5	19	195	17	0	0	104	88	100408
10	5	20	186	25	0	0	104	92	100429
10	5	21	192	37	0	0	105	90	100450
10	5	22	186	42	0	0	105	90	100470
10	5	23	183	38	0	0	106	90	100491
10	5	24	189	45	0	0	109	89	100488
10	6	1	170	38	0	0	105	91	100467
10	6	2	139	35	0	0	99	95	100446
10	6	3	135	54	0	0	103	96	100425
10	6	4	141	69	0	0	112	98	100405
10	6	5	149	62	0	0	112	96	100384
10	6	6	158	61	0	0	115	96	100363
10	6	7	168	48	1	1	117	96	100342
10	6	8	177	40	19	19	120	94	100321
10	6	9	196	40	66	71	131	96	100300
10	6	10	210	47	121	127	143	95	100280
10	6	11	227	50	193	306	154	88	100259
10	6	12	242	64	186	271	173	79	100238
10	6	13	234	50	174	217	174	81	100217
10	6	14	225	64	216	288	180	81	100196
10	6	15	228	58	189	249	177	80	100175
10	6	16	220	49	97	100	173	82	100155
10	6	17	205	35	59	61	168	83	100134
10	6	18	187	29	19	20	161	84	100113

Month	Date	Hour	Wind direction, deg	Wind speed*10, m/s	Diffus solar irradiation, W/m²	Global solar irradiation, W/m²	External air temperature*10, °C	Relative humidity, %	Atmosferic pressure, Pa
10	6	19	164	30	0	0	155	88	100092
10	6	20	148	31	0	0	144	93	100071
10	6	21	146	39	0	0	140	97	100050
10	6	22	152	47	0	0	147	97	100030
10	6	23	160	48	0	0	145	98	100009
10	6	24	164	57	0	0	147	95	99998
10	7	1	163	64	0	0	145	95	99993
10	7	2	166	73	0	0	147	92	99989
10	7	3	183	67	0	0	144	95	99985
10	7	4	198	59	0	0	146	94	99981
10	7	5	189	51	0	0	140	94	99977
10	7	6	184	57	0	0	139	94	99973
10	7	7	188	47	2	1	133	93	99968
10	7	8	185	55	28	29	132	93	99964
10	7	9	194	58	74	154	139	88	99960
10	7	10	205	64	111	215	149	85	99956
10	7	11	221	69	136	332	158	79	99952
10	7	12	226	67	90	421	163	75	99948
10	7	13	238	69	126	334	161	79	99943
10	7	14	257	98	145	325	163	74	99939
10	7	15	275	95	120	125	149	86	99935
10	7	16	275	106	93	103	145	88	99931
10	7	17	274	110	41	44	129	89	99927
10	7	18	269	108	10	10	127	79	99923
10	7	19	269	115	0	0	129	77	99918
10	7	20	269	124	0	0	125	77	99914
10	7	21	270	125	0	0	128	70	99910
10	7	22	268	119	0	0	128	70	99906
10	7	23	268	106	0	0	123	71	99902
10	7	24	265	97	0	0	125	77	99927
10	8	1	259	84	0	0	124	83	99973
10	8	2	254	69	0	0	122	90	100018
10	8	3	249	58	0	0	118	96	100064
10	8	4	252	74	0	0	125	94	100110
10	8	5	273	99	0	0	129	90	100156
10	8	6	271	96	0	0	132	87	100202
10	8	7	273	100	2	2	133	85	100248
10	8	8	277	76	35	42	134	83	100293
10	8	9	275	90	83	91	136	81	100339
10	8	10	274	92	142	266	146	77	100385
10	8	11	274	105	143	382	156	75	100431
10	8	12	276	123	98	405	160	68	100477
10	8	13	279	113	157	402	161	69	100523
10	8	14	283	111	107	412	166	66	100568
10	8	15	277	111	92	318	162	69	100614
10	8	16	276	91	113	159	151	76	100660
10	8	17	274	70	58	59	141	84	100706
10	8	18	270	50	14	16	131	88	100752

Month	Date	Hour	Wind direction, deg	Wind speed*10, m/s	Diffus solar irradiation, W/m^2	Global solar irradiation, W/m^2	External air temperature*10, °C	Relative humidity, %	Atmosferic pressure, Pa
10	8	19	265	55	0	0	124	91	100798
10	8	20	264	49	0	0	119	91	100843
10	8	21	256	38	0	0	113	94	100889
10	8	22	251	37	0	0	107	99	100935
10	8	23	254	26	0	0	106	99	100981
10	8	24	235	14	0	0	102	99	101019
10	9	1	223	14	0	0	106	99	101053
10	9	2	224	17	0	0	117	99	101086
10	9	3	225	17	0	0	123	99	101119
10	9	4	233	15	0	0	125	99	101153
10	9	5	238	16	0	0	125	96	101186
10	9	6	198	26	0	0	127	91	101219
10	9	7	185	22	2	2	127	93	101253
10	9	8	184	30	39	57	128	89	101286
10	9	9	182	39	99	152	136	86	101319
10	9	10	185	37	141	246	149	83	101353
10	9	11	181	38	143	357	161	76	101386
10	9	12	178	47	154	405	168	71	101419
10	9	13	166	53	218	307	166	67	101453
10	9	14	170	49	215	246	165	68	101486
10	9	15	165	45	148	155	157	72	101519
10	9	16	174	28	107	116	156	74	101553
10	9	17	178	31	64	75	153	78	101586
10	9	18	169	21	16	19	142	88	101619
10	9	19	177	22	0	0	133	91	101653
10	9	20	195	19	0	0	133	90	101686
10	9	21	182	20	0	0	132	88	101719
10	9	22	174	20	0	0	129	90	101753
10	9	23	206	21	0	0	132	92	101786
10	9	24	214	24	0	0	132	93	101807
10	10	1	225	23	0	0	127	99	101820
10	10	2	233	32	0	0	127	99	101832
10	10	3	242	36	0	0	131	100	101845
10	10	4	247	29	0	0	127	100	101857
10	10	5	257	28	0	0	127	100	101870
10	10	6	260	29	0	0	122	100	101882
10	10	7	248	21	3	3	114	100	101895
10	10	8	247	21	37	70	114	100	101907
10	10	9	250	25	59	199	123	96	101920
10	10	10	275	44	61	299	141	92	101932
10	10	11	273	40	85	354	150	91	101945
10	10	12	285	41	140	452	160	85	101957
10	10	13	290	45	116	431	164	81	101970
10	10	14	296	47	74	379	164	75	101982
10	10	15	313	32	77	258	162	77	101995
10	10	16	296	18	68	197	157	80	102007
10	10	17	257	7	49	77	150	78	102020
10	10	18	258	8	10	11	129	88	102032

Month	Date	Hour	Wind direction, deg	Wind speed*10, m/s	Diffus solar irradiation, W/m²	Global solar irradiation, W/m²	External air temperature*10, °C	Relative humidity, %	Atmosferic pressure, Pa
10	10	19	109	6	0	0	120	97	102045
10	10	20	53	6	0	0	116	100	102057
10	10	21	63	7	0	0	108	100	102070
10	10	22	200	10	0	0	100	100	102082
10	10	23	182	7	0	0	96	100	102095
10	10	24	66	3	0	0	90	100	102105
10	11	1	49	5	0	0	86	100	102113
10	11	2	69	6	0	0	92	100	102122
10	11	3	59	6	0	0	92	100	102130
10	11	4	67	9	0	0	80	100	102138
10	11	5	44	8	0	0	85	100	102147
10	11	6	45	6	0	0	84	100	102155
10	11	7	61	4	2	1	91	100	102163
10	11	8	68	5	28	32	99	100	102172
10	11	9	66	13	89	173	113	100	102180
10	11	10	101	47	111	169	130	100	102188
10	11	11	103	50	93	96	135	100	102197
10	11	12	101	49	106	111	137	96	102205
10	11	13	101	51	91	94	135	96	102213
10	11	14	96	43	63	64	133	96	102222
10	11	15	90	36	55	55	135	93	102230
10	11	16	92	34	34	34	134	97	102238
10	11	17	102	33	12	11	129	99	102247
10	11	18	93	24	5	5	127	100	102255
10	11	19	81	13	0	0	118	100	102263
10	11	20	77	15	0	0	113	100	102272
10	11	21	81	25	0	0	124	100	102280
10	11	22	84	28	0	0	128	100	102288
10	11	23	97	47	0	0	133	100	102297
10	11	24	104	65	0	0	137	99	102305
10	12	1	103	60	0	0	132	99	102313
10	12	2	105	60	0	0	132	95	102322
10	12	3	99	59	0	0	132	97	102330
10	12	4	95	63	0	0	129	98	102338
10	12	5	95	61	0	0	126	98	102347
10	12	6	96	55	0	0	122	98	102355
10	12	7	95	59	0	0	122	98	102363
10	12	8	96	55	6	6	123	99	102372
10	12	9	95	51	22	21	124	99	102380
10	12	10	100	58	37	38	127	95	102388
10	12	11	102	57	75	76	130	93	102397
10	12	12	98	52	76	77	132	94	102405
10	12	13	95	46	62	62	133	97	102413
10	12	14	90	38	42	42	131	98	102422
10	12	15	91	37	50	50	132	97	102430
10	12	16	87	28	31	31	133	98	102438
10	12	17	82	22	16	16	133	99	102447
10	12	18	82	24	2	2	133	99	102455

Month	Date	Hour	Wind direction, deg	Wind speed*10, m/s	Diffus solar irradiation, W/m^2	Global solar irradiation, W/m^2	External air temperature*10, ^{o}C	Relative humidity, %	Atmosferic pressure, Pa
10	12	19	89	26	0	0	134	99	102463
10	12	20	80	20	0	0	133	99	102472
10	12	21	70	15	0	0	131	97	102480
10	12	22	73	17	0	0	129	99	102488
10	12	23	78	17	0	0	131	99	102497
10	12	24	80	16	0	0	132	99	102522
10	13	1	96	21	0	0	132	99	102559
10	13	2	77	12	0	0	128	100	102597
10	13	3	64	10	0	0	130	100	102634
10	13	4	72	15	0	0	128	100	102672
10	13	5	85	13	0	0	125	100	102709
10	13	6	89	14	0	0	125	100	102747
10	13	7	100	22	1	1	125	100	102784
10	13	8	100	29	20	22	122	99	102822
10	13	9	91	26	67	83	131	98	102859
10	13	10	89	26	123	156	140	94	102897
10	13	11	101	39	131	292	146	88	102934
10	13	12	97	35	110	308	148	86	102972
10	13	13	98	37	79	355	147	81	103009
10	13	14	107	42	63	359	147	81	103047
10	13	15	100	35	64	279	143	83	103084
10	13	16	92	26	65	178	139	88	103122
10	13	17	92	19	44	68	128	92	103159
10	13	18	92	3	7	7	108	97	103197
10	13	19	67	5	0	0	98	100	103234
10	13	20	127	6	0	0	90	100	103272
10	13	21	116	7	0	0	88	100	103309
10	13	22	76	6	0	0	82	100	103347
10	13	23	153	7	0	0	77	100	103384
10	13	24	101	6	0	0	74	100	103405
10	14	1	139	8	0	0	73	100	103413
10	14	2	211	5	0	0	73	100	103422
10	14	3	183	10	0	0	65	100	103430
10	14	4	243	9	0	0	61	100	103438
10	14	5	232	11	0	0	58	100	103447
10	14	6	224	12	0	0	50	100	103455
10	14	7	265	12	1	1	49	100	103463
10	14	8	247	13	31	46	56	100	103472
10	14	9	237	9	72	142	67	98	103480
10	14	10	249	14	71	263	98	94	103488
10	14	11	234	17	82	354	125	84	103497
10	14	12	251	20	112	390	142	76	103505
10	14	13	284	29	149	352	146	75	103513
10	14	14	311	24	160	310	147	76	103522
10	14	15	264	22	157	208	151	69	103530
10	14	16	306	16	91	104	142	79	103538
10	14	17	308	14	43	48	128	82	103547
10	14	18	232	7	7	8	105	91	103555

Month	Date	Hour	Wind direction, deg	Wind speed*10, m/s	Diffus solar irradiation, W/m^2	Global solar irradiation, W/m^2	External air temperature*10, ^{o}C	Relative humidity, %	Atmosferic pressure, Pa
10	14	19	202	13	0	0	92	98	103563
10	14	20	236	18	0	0	83	98	103572
10	14	21	232	16	0	0	77	100	103580
10	14	22	245	17	0	0	65	100	103588
10	14	23	238	16	0	0	61	100	103597
10	14	24	244	16	0	0	55	100	103591
10	15	1	239	22	0	0	55	100	103577
10	15	2	239	20	0	0	52	100	103562
10	15	3	246	22	0	0	57	100	103548
10	15	4	244	25	0	0	54	100	103533
10	15	5	254	27	0	0	56	100	103519
10	15	6	247	28	0	0	53	100	103504
10	15	7	250	27	1	1	54	100	103489
10	15	8	247	26	30	40	56	100	103475
10	15	9	246	26	77	143	74	96	103460
10	15	10	244	27	87	256	98	89	103446
10	15	11	242	21	96	343	120	84	103431
10	15	12	252	27	112	376	134	77	103416
10	15	13	275	29	167	303	140	79	103402
10	15	14	297	33	157	305	143	82	103387
10	15	15	324	24	133	213	137	85	103373
10	15	16	310	23	125	141	140	85	103358
10	15	17	291	15	31	34	135	85	103344
10	15	18	263	15	3	3	125	89	103329
10	15	19	261	13	0	0	119	92	103314
10	15	20	241	12	0	0	107	95	103300
10	15	21	235	13	0	0	102	94	103285
10	15	22	253	12	0	0	103	93	103271
10	15	23	231	11	0	0	103	93	103256
10	15	24	228	11	0	0	102	95	103241

12.2.2 Other boundary conditions, 1 hour average

Month	Date	Hour	Zone 3.2 temperature*10, oC	Zone 3.3 Temperature*10, oC	Ground temperature under foundation*10, oC
10	1	1	195	140	159
10	1	2	195	138	159
10	1	3	195	134	159
10	1	4	195	131	159
10	1	5	195	127	159
10	1	6	195	124	160
10	1	7	195	127	160
10	1	8	192	137	159
10	1	9	191	144	159
10	1	10	193	142	160
10	1	11	194	172	159
10	1	12	194	184	159
10	1	13	195	192	160
10	1	14	194	197	159
10	1	15	194	198	159
10	1	16	195	195	159
10	1	17	196	188	160
10	1	18	195	174	159
10	1	19	196	166	160
10	1	20	196	162	160
10	1	21	197	161	160
10	1	22	196	160	160
10	1	23	197	166	160
10	1	24	196	161	160
10	2	1	195	156	160
10	2	2	196	155	160
10	2	3	196	149	160
10	2	4	196	148	160
10	2	5	196	143	161
10	2	6	196	141	160
10	2	7	196	140	160
10	2	8	196	140	160
10	2	9	185	153	160
10	2	10	186	156	159
10	2	11	188	165	159
10	2	12	190	171	159
10	2	13	190	167	160
10	2	14	190	172	159
10	2	15	190	174	159
10	2	16	190	169	159
10	2	17	189	168	159
10	2	18	189	160	159
10	2	19	188	155	160
10	2	20	188	150	160
10	2	21	187	147	160

Month	Date	Hour	Zone 3.2 temperature*10, oC	Zone 3.3 Temperature*10, oC	Ground temperature under foundation*10, oC
10	2	22	187	146	160
10	2	23	186	141	160
10	2	24	186	147	160
10	3	1	186	149	160
10	3	2	186	151	160
10	3	3	186	148	160
10	3	4	185	148	160
10	3	5	185	146	160
10	3	6	184	142	160
10	3	7	184	138	160
10	3	8	184	139	160
10	3	9	186	150	160
10	3	10	185	154	160
10	3	11	181	160	159
10	3	12	173	173	160
10	3	13	181	178	160
10	3	14	184	177	160
10	3	15	185	179	160
10	3	16	185	176	159
10	3	17	185	172	160
10	3	18	184	165	159
10	3	19	184	158	160
10	3	20	183	152	160
10	3	21	183	146	160
10	3	22	182	145	160
10	3	23	182	141	160
10	3	24	182	141	160
10	4	1	182	139	160
10	4	2	181	131	160
10	4	3	181	131	160
10	4	4	180	130	160
10	4	5	179	128	160
10	4	6	179	129	160
10	4	7	179	131	160
10	4	8	179	134	160
10	4	9	180	147	160
10	4	10	181	164	160
10	4	11	182	171	160
10	4	12	184	175	160
10	4	13	184	171	160
10	4	14	184	173	159
10	4	15	184	175	159
10	4	16	185	177	160
10	4	17	184	171	159
10	4	18	184	163	159
10	4	19	184	151	160
10	4	20	183	140	160

Month	Date	Hour	Zone 3.2 temperature*10, oC	Zone 3.3 Temperature*10, oC	Ground temperature under foundation*10, oC
10	4	21	183	134	160
10	4	22	182	128	160
10	4	23	181	127	160
10	4	24	181	125	160
10	5	1	181	123	160
10	5	2	181	121	160
10	5	3	181	121	160
10	5	4	180	120	160
10	5	5	180	118	160
10	5	6	180	114	160
10	5	7	180	112	160
10	5	8	179	115	160
10	5	9	177	127	159
10	5	10	178	141	159
10	5	11	179	158	159
10	5	12	179	164	159
10	5	13	179	156	160
10	5	14	181	143	159
10	5	15	180	149	159
10	5	16	181	149	160
10	5	17	182	148	160
10	5	18	182	144	160
10	5	19	181	134	159
10	5	20	181	132	160
10	5	21	181	128	160
10	5	22	181	127	160
10	5	23	181	127	160
10	5	24	181	129	160
10	6	1	181	129	160
10	6	2	181	123	160
10	6	3	181	120	160
10	6	4	181	123	160
10	6	5	182	123	160
10	6	6	182	126	161
10	6	7	182	130	160
10	6	8	181	136	161
10	6	9	180	146	160
10	6	10	183	154	160
10	6	11	183	166	160
10	6	12	184	178	159
10	6	13	185	180	159
10	6	14	186	184	159
10	6	15	187	184	160
10	6	16	187	183	159
10	6	17	187	182	159
10	6	18	186	178	159
10	6	19	186	170	160

Month	Date	Hour	Zone 3.2 temperature*10, oC	Zone 3.3 Temperature*10, oC	Ground temperature under foundation*10, oC
10	6	20	186	161	160
10	6	21	186	153	160
10	6	22	186	157	160
10	6	23	186	158	160
10	6	24	186	160	160
10	7	1	186	159	160
10	7	2	186	158	160
10	7	3	186	159	160
10	7	4	186	160	160
10	7	5	186	157	160
10	7	6	186	155	160
10	7	7	186	151	160
10	7	8	186	149	160
10	7	9	186	154	160
10	7	10	186	161	160
10	7	11	186	166	160
10	7	12	186	172	159
10	7	13	186	169	159
10	7	14	185	171	159
10	7	15	186	166	159
10	7	16	186	162	159
10	7	17	186	151	160
10	7	18	185	146	160
10	7	19	184	144	159
10	7	20	184	142	160
10	7	21	183	142	159
10	7	22	183	142	160
10	7	23	182	140	160
10	7	24	182	141	160
10	8	1	182	140	160
10	8	2	183	140	160
10	8	3	183	138	161
10	8	4	183	142	161
10	8	5	183	147	160
10	8	6	184	148	160
10	8	7	184	148	160
10	8	8	184	151	160
10	8	9	184	152	160
10	8	10	184	164	159
10	8	11	185	173	161
10	8	12	183	174	160
10	8	13	182	173	160
10	8	14	182	176	159
10	8	15	183	173	159
10	8	16	183	167	159
10	8	17	184	161	160
10	8	18	184	158	160

Month	Date	Hour	Zone 3.2 temperature*10, oC	Zone 3.3 Temperature*10, oC	Ground temperature under foundation*10, oC
10	8	19	184	152	160
10	8	20	183	145	160
10	8	21	183	142	160
10	8	22	183	136	160
10	8	23	182	135	161
10	8	24	182	136	160
10	9	1	182	136	161
10	9	2	182	140	160
10	9	3	182	145	160
10	9	4	182	149	160
10	9	5	183	150	160
10	9	6	182	150	160
10	9	7	182	148	160
10	9	8	181	147	160
10	9	9	175	151	159
10	9	10	180	163	159
10	9	11	183	173	160
10	9	12	182	176	159
10	9	13	183	173	159
10	9	14	184	173	159
10	9	15	185	168	159
10	9	16	185	169	159
10	9	17	185	168	160
10	9	18	185	163	159
10	9	19	184	155	159
10	9	20	184	156	159
10	9	21	184	154	159
10	9	22	183	150	159
10	9	23	183	153	160
10	9	24	183	154	159
10	10	1	183	153	160
10	10	2	183	153	160
10	10	3	183	152	161
10	10	4	183	151	160
10	10	5	183	153	160
10	10	6	182	150	160
10	10	7	182	147	160
10	10	8	181	143	160
10	10	9	184	154	159
10	10	10	196	176	159
10	10	11	185	177	159
10	10	12	183	179	158
10	10	13	182	181	159
10	10	14	182	180	159
10	10	15	182	182	160
10	10	16	182	178	159
10	10	17	183	173	159

Month	Date	Hour	Zone 3.2 temperature*10, oC	Zone 3.3 Temperature*10, oC	Ground temperature under foundation*10, oC
10	10	18	183	159	159
10	10	19	183	150	159
10	10	20	182	145	160
10	10	21	182	140	159
10	10	22	182	134	160
10	10	23	181	131	159
10	10	24	180	126	160
10	11	1	180	124	160
10	11	2	180	126	160
10	11	3	180	126	160
10	11	4	180	121	160
10	11	5	179	121	160
10	11	6	179	121	160
10	11	7	179	124	160
10	11	8	180	127	160
10	11	9	180	136	160
10	11	10	180	146	160
10	11	11	181	144	159
10	11	12	181	144	159
10	11	13	182	144	159
10	11	14	182	144	160
10	11	15	182	146	160
10	11	16	182	146	160
10	11	17	181	144	159
10	11	18	181	143	159
10	11	19	181	139	160
10	11	20	181	136	160
10	11	21	181	140	160
10	11	22	181	141	161
10	11	23	181	142	160
10	11	24	181	143	160
10	12	1	181	139	160
10	12	2	181	139	160
10	12	3	181	140	160
10	12	4	181	138	159
10	12	5	181	136	160
10	12	6	181	133	160
10	12	7	181	133	160
10	12	8	181	133	159
10	12	9	180	134	160
10	12	10	181	136	160
10	12	11	182	137	160
10	12	12	182	140	160
10	12	13	182	143	159
10	12	14	182	144	159
10	12	15	182	144	160
10	12	16	182	146	160

Month	Date	Hour	Zone 3.2 temperature*10, oC	Zone 3.3 Temperature*10, oC	Ground temperature under foundation*10, oC
10	12	17	182	147	160
10	12	18	181	147	159
10	12	19	181	148	159
10	12	20	181	149	159
10	12	21	182	150	159
10	12	22	183	150	160
10	12	23	183	148	159
10	12	24	183	150	160
10	13	1	184	149	160
10	13	2	185	147	160
10	13	3	187	151	160
10	13	4	188	150	160
10	13	5	188	147	160
10	13	6	188	145	160
10	13	7	189	145	160
10	13	8	189	143	160
10	13	9	194	147	159
10	13	10	199	151	158
10	13	11	195	154	158
10	13	12	194	154	158
10	13	13	192	155	158
10	13	14	191	155	158
10	13	15	193	154	158
10	13	16	193	152	158
10	13	17	190	147	157
10	13	18	191	139	158
10	13	19	191	134	158
10	13	20	190	128	158
10	13	21	186	126	158
10	13	22	185	122	158
10	13	23	187	120	158
10	13	24	187	118	158
10	14	1	187	115	158
10	14	2	187	115	158
10	14	3	187	109	158
10	14	4	186	107	158
10	14	5	186	105	158
10	14	6	186	101	158
10	14	7	185	100	158
10	14	8	185	102	158
10	14	9	180	109	158
10	14	10	182	127	158
10	14	11	184	146	158
10	14	12	185	157	157
10	14	13	186	160	158
10	14	14	188	162	157
10	14	15	189	164	157

Month	Date	Hour	Zone 3.2 temperature*10, oC	Zone 3.3 Temperature*10, oC	Ground temperature under foundation*10, oC
10	14	16	191	162	158
10	14	17	191	153	158
10	14	18	191	139	158
10	14	19	190	130	158
10	14	20	189	125	158
10	14	21	188	120	158
10	14	22	188	113	158
10	14	23	187	110	158
10	14	24	187	106	158
10	15	1	186	104	158
10	15	2	186	101	158
10	15	3	186	102	158
10	15	4	186	100	158
10	15	5	185	102	157
10	15	6	185	101	158
10	15	7	185	100	158
10	15	8	184	100	158
10	15	9	185	110	157
10	15	10	185	122	157
10	15	11	186	138	157
10	15	12	186	149	157
10	15	13	187	155	157
10	15	14	189	158	157
10	15	15	189	158	157
10	15	16	190	159	157
10	15	17	191	155	157
10	15	18	191	151	157
10	15	19	191	144	157
10	15	20	191	138	157
10	15	21	190	134	157
10	15	22	190	133	158
10	15	23	190	132	157
10	15	24	190	132	157

APPENDIX III.   Additional Test Cases

Steady state (SS) test case

Steady state case corresponds to actual empirical conditions in the DSF and in the zone 2, during the heat transmission measurements. In this test case, all necessary weather data and volume averaged air temperature in the DSF and approximate air flow rate (which is important for modelling of the convective heat transfer coefficients in the DSF) are specified.

Conditions for the steady state cases	
Outdoor air temperature, °C	0.7
Wind direction	0
Wind speed , m/s	0
Diffuse solar radiation on horizontal, W/m²	0
Global solar radiation on horizontal, W/m²	0
Relative humidity , %	60
Atmospheric pressure, Pa	100000
Air temperature in the DSF , °C	5.3
Air temperatre in zone 3.3, °C	23.4
Air temperature in zone 3.2, °C	24.6
Air temperature in the zone 2, °C	21.95
Temperature under the foundation, °C	11.3
Air flow rate in DSF(supply from outside), m³/h	300

Modification of the U-values to the actual transmission heat losses

First steady state simulations were performed with assumption that there are no thermal bridge losses in the 'Cube'. Results of the steady state cases were compared with the empirical results, proving the existence of the thermal bridges. Accordingly the modifications of the construction properties had to be made to include the impact of thermal bridges.

Additional heat losses from the zone 2 (due to the thermal bridges) were evenly distributed to all constructions in the zone 2, except for the windows. All of the models were identically modified, by increasing U-values of the constructions in the models, for more accurate prediction of the heat losses.

Modified properties marked in bold, as following:

Wall	**1**		
Material	Plywood	Rockwool M39	Isovand vario
Thickness, m	0.016	0.62	0.1
Thermal conductivity W/(mK)	0.115	**0.11**	0.025

Wall	**2**		
Material	Plywood	Rockwool M39	Isovand vario
Thickness, m	0.016	0.3	0.1
Thermal conductivity W/(mK)	0.115	**0.19**	0.025

Wall	**3**		
Material	Plywood	Rockwool M39	Isovand vario
Thickness, m	0.016	0.3	0.1

Thermal conductivity W/(mK)	0.115	**0.19**	0.025

Wall	Roof		
Material	Plywood	Rockwool M39	Isovand vario
Thickness, m	0.016	0.3	0.1
Thermal conductivity W/(mK)	0.115	**0.19**	0.025

Wall	Floor	
Material	Reinforced concrete	Expanded polysterene
Thickness, m	0.15	0.22
Thermal conductivity W/(mK)	1.8	**0.1008**

APPENDIX IV. WIS results of glazing properties

DOUBLE PANE (INTERNAL WINDOW)

--- Basics (key thermal and solar properties) ---

```
 name transparent system          : aalborg_double
 U-value                          :    1.12 [W/(m2.K)]
 solar factor (g)                 :   0.632 [-]  (total solar energy transmittance)

 solar direct transmittance       :   0.532 [-]
 solar direct reflectance outdoor :   0.252 [-]
 solar direct reflectance indoor  :   0.237 [-]

 light transmittance              :   0.796 [-]
 light reflectance outdoor        :   0.129 [-]
 light reflectance indoor         :   0.128 [-]

 UV transmittance                 :   0.173 [-]
 UV reflectance outdoor           :   0.218 [-]
 UV reflectance indoor            :   0.127 [-]

 general colour rendering index (Ra) :   97.0 [-]
```

--- Split U-value ---

```
 Uconv                            :    0.437      [W/m2.K]
 Uir                              :    0.687      [W/m2.K]
 Uvent                            :    0.000      [W/m2.K]
                                       ---------------- +
 Utotal                           :    1.12       [W/m2.K]
```

--- Split all 'dark' heat flow coefficients into fractions (h-values) ---

```
 h_conv,indoor                    :    0.437      [W/m2.K]
 h_ir,indoor                      :    0.687      [W/m2.K]
 h_conv,outdoor                   :    0.892      [W/m2.K]
 h_ir,outdoor                     :    0.232      [W/m2.K]
 h_vent                           :    0.000      [W/m2.K]
                                       ---------------- +
 checksum (expected value = h_indoor - h_outdoor - h_vent = 0) :    0.000      [W/m2.K]
```

--- Split solar factor (g) into fractions ---

```
 solar direct transmittance               :    0.532      [-]
 solar factor convective          :    0.0387     [-]
 solar factor thermal radiative ir :    0.0620    [-]
 solar factor ventilation         :    0.000      [-]
                                       ---------------- +
 solar factor (g)                 :    0.632      [-]
```

--- Split solar gain coefficients to outdoor side into fractions ---

```
 solar fraction reflected to outdoor    :    0.252      [-]
 solar fraction convected to outdoor    :    0.0912     [-]
 solar fraction th. radiated to outdoor :    0.0243     [-]
 solar fraction ventilated to outdoor   :    0.000      [-]
                                            ---------------- +
 solar fraction to outdoor        :    0.368      [-]
```

--- Split all solar fractions, optical part ---

```
 solar direct transmittance       :    0.532      [-]
 solar direct reflectance         :    0.252      [-]
 solar absorption fraction layer 1 :   0.103      [-]
 solar absorption fraction layer 2 :   0.000      [-]
 solar absorption fraction layer 3 :   0.114      [-]

                                       ---------------- +
 checksum (expected value = 1)    :    1.00       [-]
```

--- Split all solar fractions, thermal part (a-values) ---

```
 solar absorbed                   :    0.216      [-]
 conv indoor                      :    0.0387     [-]
```

```
 ir indoor                                  :    0.0620          [-]
 conv outdoor                               :    0.0912          [-]
 ir outdoor                                 :    0.0243          [-]
 gap vent                                   :     0.000          [-]
                                                ---------------- +
 checksum (abs-others. expected value = 0) : 0.000          [-]



--- Short description conditions used for calculations ---

 For angular and diffuse properties estimated values are used (not very accurate) !!
 awaiting results from ongoing research

 Calculated using setting: No restrictions (expert level)
 Therefore results are calculated using user selected methods and settings



 For solar calculations in the total solar range, spectral properties are used

 For solar calculations in the visual range, spectral properties are used

 For solar calculations in the uv range, spectral properties are used

 The solar spectrum of EN 410 is used with air mass 1



--- Short system description ---

(from outdoor to indoor)

 layer 1 is a Pane named : aalborg_dg_outer with pane in original position.
 layer 2 is a Gap named : Air-Argon 10/90
 layer 3 is a Pane named : aalborg_double_inner with pane in original position.


 --- Detailed Thermal Solar Properties ---

abs x       : absorption fraction for each layer (layer = pane, gap, solar shading ...)

t_sol       : solar direct transmittance
r_sol_o     : solar direct reflectance on the outdoor side
r_sol_i     : solar direct reflectance on the indoor side

t_vis       : light transmittance
r_vis_o     : light reflectance outdoor side
r_vis_i     : light reflectance indoor side

t_uv        : UV transmittance
r_uv_o      : UV reflectance outdoor side
r_uv_i      : UV reflectance indoor side

g_val       : solar factor (total solar energy transmittance g)
diff        : diffuse (transmittance / reflectance)
```

prop		0	10	20	30	40	50	60	70	80	90	diff
abs	1	0.103	0.103	0.105	0.108	0.111	0.115	0.119	0.119	0.110	0.000	0.112
abs	2	0.000	0.000	0.000	0.000	0.000	0.000	0.000	0.000	0.000	0.000	0.000
abs	3	0.114	0.114	0.115	0.117	0.119	0.120	0.120	0.114	0.0889	0.000	0.116
t_sol		0.532	0.531	0.529	0.524	0.513	0.488	0.435	0.331	0.163	0.000	0.447
r_sol_o		0.252	0.252	0.251	0.252	0.258	0.277	0.326	0.436	0.638	1.00	0.325
r_sol_i		0.237	0.237	0.237	0.239	0.245	0.264	0.309	0.405	0.579	1.00	0.307
t_vis		0.796	0.795	0.793	0.787	0.772	0.735	0.653	0.490	0.239	0.000	0.668
r_vis_o		0.129	0.129	0.129	0.133	0.145	0.178	0.258	0.423	0.689	1.00	0.250
r_vis_i		0.128	0.128	0.128	0.131	0.142	0.173	0.247	0.399	0.642	1.00	0.240
t_uv		0.173	0.172	0.170	0.166	0.160	0.148	0.129	0.0933	0.0394	0.000	0.137
r_uv_o		0.218	0.217	0.217	0.217	0.221	0.234	0.269	0.355	0.550	1.00	0.271
r_uv_i		0.127	0.127	0.127	0.128	0.133	0.146	0.179	0.256	0.445	1.00	0.179
g_val		0.632	0.632	0.631	0.627	0.618	0.595	0.542	0.433	0.244	0.000	0.550

```
(Solar absorption assumed in center of layers)
```

```
--- temperatures ---

Outdoor air temperature      : 0.000
Outdoor radiant temperature  : 0.000

incidence angle              :    0    10    20    30    40    50    60    70    80    90   diff
Outdoor surface temperature  : 4.23  4.25  4.29  4.36  4.46  4.56  4.65  4.63  4.30  1.19  4.47
layer (center)            1 : 4.39  4.41  4.45  4.53  4.63  4.74  4.82  4.81  4.46  1.23  4.64
border                       : 4.45  4.46  4.51  4.59  4.69  4.79  4.88  4.87  4.51  1.28  4.70
layer (center)            2 : 14.0  14.0  14.1  14.2  14.3  14.4  14.4  14.2  13.4  9.14  14.2
border                       : 23.5  23.6  23.6  23.7  23.8  23.9  24.0  23.6  22.3  17.0  23.7
layer (center)            3 : 23.6  23.6  23.7  23.8  23.9  24.0  24.0  23.7  22.3  17.0  23.8
Indoor surface temperature   : 23.5  23.6  23.6  23.7  23.8  23.9  24.0  23.6  22.3  17.1  23.7

Indoor air temperature       : 20.0
Indoor radiant temperature   : 20.0


--- Network ---

Layer and node properties from outdoor side to indoor side

-- solar absorption fractions for layers [0-1]:

Solar absorption fraction of layer 1 : 0.103
Solar absorption fraction of layer 2 : 0.000
Solar absorption fraction of layer 3 : 0.114


-- conduction / convection heat transfer coefficients for layers:

IR and ventilation not included !

Heat transfer coeff of layer 1 : 250.
Heat transfer coeff of layer 2 : 1.32
Heat transfer coeff of layer 3 : 250.


Network of thermal coefficients (h) for perpendicular incidence angle

-- Total Network:

 hs are given between all nodes
 nodes are from outdoor to indoor
 all layers (including gaps) have 3 nodes of which 2 are joined with neighboring layers

 1      : node 1 (node at outdoor surface)
 2      : node 2 (center node of outdoor side layer) ...
 o_air  : outdoor air node
 o_rad  : outdoor radiant node
 i      : indoor node


                1       2       3       4       5       6       7    o_air   o_rad       i
     1    0.000    500.   0.000   0.000   0.000   0.000   0.000    15.0    3.97   0.000
     2     500.   0.000    500.   0.000   0.000   0.000   0.000   0.000   0.000   0.000
     3    0.000    500.   0.000    2.63   0.198   0.000   0.000   0.000   0.000   0.000
     4    0.000   0.000    2.63   0.000    2.63   0.000   0.000   0.000   0.000   0.000
     5    0.000   0.000   0.198    2.63   0.000    500.   0.000   0.000   0.000   0.000
     6    0.000   0.000   0.000   0.000    500.   0.000    500.   0.000   0.000   0.000
     7    0.000   0.000   0.000   0.000   0.000    500.   0.000   0.000   0.000    7.88
 o_air    15.0   0.000   0.000   0.000   0.000   0.000   0.000   0.000   0.000   0.000
 o_rad    3.97   0.000   0.000   0.000   0.000   0.000   0.000   0.000   0.000   0.000
     i    0.000   0.000   0.000   0.000   0.000   0.000    7.88   0.000   0.000   0.000


-- gap properties conduction/convection/ventilation :

 Layer : 2 is a gap with the following calculated properties :

 Nusselt_number : 1.18
 Prandtl_number : 0.683
```

```
 Grashof_number ; 1.53e+004


--- System description ---
(from outdoor to indoor for perpendicular incidence angle)

-- layer : 1 is a : Pane --

 name                            : aalborg_dg_outer
 id                              : 844
 thickness                       : 4.00 [mm]
 thermal conductance             : 1.00 [W/(m.K)]

 coating code                    : uu [-]

 IR transmittance                : 0.000 [-]
 IR emissivity outdoor           : 0.840 [-]
 IR emissivity indoor            : 0.840 [-]

 solar direct transmittance      : 0.840 [-]
 solar direct reflectance outdoor : 0.0817 [-]
 solar direct reflectance indoor  : 0.0817 [-]

 light transmittance             : 0.902 [-]
 light reflectance outdoor        : 0.0894 [-]
 light reflectance indoor         : 0.0894 [-]

 UV transmitance                 : 0.620 [-]
 UV reflectance outdoor           : 0.0833 [-]
 UV reflectance indoor            : 0.0833 [-]

 General colour rendering index (Ra) : 99.0 [-]   (0-100)

 component information




-- layer : 2 is a : Gap --

 name                   : Air-Argon 10/90
 gap width              : 16.0  [mm]
                             -10 oC          0 oC         10 oC         20 oC
 conduction            :       0.0166        0.0171        0.0177        0.0182
 dynamic viscosity     :    2.00e-005     2.06e-005     2.12e-005     2.19e-005
 density               :       1.78          1.68          1.65          1.59
 CP                    :       568.          568.          568.          568.




-- layer : 3 is a : Pane --

 name                            : aalborg_double_inner
 id                              : 847
 thickness                       : 4.00 [mm]
 thermal conductance             : 1.00 [W/(m.K)]

 coating code                    : cu [-]

 IR transmittance                : 0.000 [-]
 IR emissivity outdoor           : 0.0370 [-]
 IR emissivity indoor            : 0.840 [-]

 solar direct transmittance      : 0.609 [-]
 solar direct reflectance outdoor : 0.252 [-]
 solar direct reflectance indoor  : 0.198 [-]

 light transmittance             : 0.878 [-]
 light reflectance outdoor        : 0.0481 [-]
 light reflectance indoor         : 0.0585 [-]
```

```
UV transmitance                 : 0.211 [-]
UV reflectance outdoor          : 0.294 [-]
UV reflectance indoor           : 0.121 [-]

General colour rendering index (Ra) : 98.0 [-]   (0-100)

 component information
```

--- Environment ---

```
 name                           : Te/Ti=0/20 degrees; sun: 500
 id                             : 30

 radiant temperature outdoor    : 0.000 [oC]
 air temperature outdoor        : 0.000 [oC]
 radiant temperature indoor     : 20.0 [oC]
 air temperature indoor         : 20.0 [oC]

 Solar radiation                : 500. [W/m2]
 Convection coeff. outdoor      : 15.0 [W/(m2.K)]
 Convection coeff. indoor       : 3.00 [W/(m2.K)]
```

--- Disclaimer ---

SINGLE PANE (EXTERNAL WINDOW)

```
name                            : aalborg_sg
id                              : 842
thickness                       : 8 [mm]
thermal conductance             : 1 [W/(m.K)]

coating code                    : uu [-]

IR transmittance                : 0 [-]
IR emissivity outdoor           : 0.84 [-]
IR emissivity indoor            : 0.84 [-]

solar direct transmittance      : 0.763 [-]
solar direct reflectance outdoor : 0.0761 [-]
solar direct reflectance indoor  : 0.0761 [-]

light transmittance             : 0.882 [-]
light reflectance outdoor       : 0.0867 [-]
light reflectance indoor        : 0.0867 [-]

UV transmitance                 : 0.506 [-]
UV reflectance outdoor          : 0.0747 [-]
UV reflectance indoor           : 0.0747 [-]

General colour rendering index (Ra) : 97 [-]   (0-100)

component information
```

--- Angular Solar properties ---

```
angle     : incidence angle
T_tot     : solar direct transmittance
R_tot     : solar direct reflectance
T_vis     : light transmittance
R_vis     : light reflectance
T_uv      : UV transmittance
R_uv      : UV reflectance
diff      : diffusive (reflectance or transmittance)
```

angle	T_tot	R_tot	T_vis	R_vis	T_uv	R_uv
90	0.000	1.000	0.000	1.000	0.000	1.000
80	0.323	0.497	0.410	0.551	0.182	0.442
70	0.550	0.259	0.666	0.296	0.330	0.225
60	0.663	0.149	0.791	0.172	0.409	0.134
50	0.716	0.103	0.846	0.118	0.451	0.096
40	0.741	0.084	0.869	0.097	0.475	0.081
30	0.753	0.078	0.878	0.089	0.490	0.076
20	0.760	0.076	0.881	0.087	0.499	0.075
10	0.763	0.076	0.882	0.087	0.504	0.075
0	0.763	0.076	0.882	0.087	0.506	0.075
diff	0.679	0.144	0.802	0.163	0.431	0.132

--- Spectral Properties Total Solar ---
For perpendicular incidence angle
```
wavel      : wavelength [nm]
Reflec     : spectral reflectance
Transm     : spectral transmittance
```

Wavel	Transm	Reflec
300.0	0.000	0.063
320.0	0.008	0.059
340.0	0.382	0.064
360.0	0.775	0.087
380.0	0.798	0.087
400.0	0.876	0.092
420.0	0.871	0.091
440.0	0.872	0.090

```
 460.0  0.886  0.089
 480.0  0.893  0.089
 500.0  0.894  0.088
 520.0  0.895  0.088
 540.0  0.892  0.087
 560.0  0.887  0.087
 580.0  0.878  0.086
 600.0  0.868  0.085
 620.0  0.854  0.084
 640.0  0.840  0.083
 660.0  0.825  0.081
 680.0  0.808  0.080
 700.0  0.790  0.078
 720.0  0.773  0.077
 740.0  0.755  0.075
 760.0  0.735  0.074
 780.0  0.720  0.072
 800.0  0.705  0.070
 850.0  0.663  0.068
 900.0  0.653  0.070
 950.0  0.634  0.067
1000.0  0.623  0.064
1050.0  0.619  0.062
1100.0  0.619  0.061
1150.0  0.621  0.061
1200.0  0.626  0.061
1250.0  0.634  0.061
1300.0  0.647  0.061
1350.0  0.663  0.061
1400.0  0.678  0.061
1450.0  0.700  0.062
1500.0  0.721  0.063
1550.0  0.738  0.064
1600.0  0.751  0.064
1650.0  0.758  0.064
1700.0  0.761  0.064
1750.0  0.759  0.063
1800.0  0.756  0.060
1850.0  0.753  0.062
1900.0  0.749  0.054
1950.0  0.751  0.060
2000.0  0.748  0.059
2050.0  0.749  0.059
2100.0  0.751  0.057
2200.0  0.713  0.057
2300.0  0.729  0.055
2400.0  0.730  0.058
2500.0  0.697  0.052


--- Spectral Properties Light ---
For perpendicular incidence angle
wavel      : wavelength [nm]
Reflec     : spectral reflectance
Transm     : spectral transmittance

  Wavel  Transm Reflec
  380.0  0.798  0.087
  390.0  0.848  0.090
  400.0  0.876  0.092
  410.0  0.876  0.091
  420.0  0.871  0.091
  430.0  0.872  0.090
  440.0  0.872  0.090
  450.0  0.879  0.090
  460.0  0.886  0.089
  470.0  0.890  0.089
  480.0  0.893  0.089
  490.0  0.893  0.089
  500.0  0.894  0.088
  510.0  0.896  0.088
  520.0  0.895  0.088
  530.0  0.894  0.088
  540.0  0.892  0.087
```

```
550.0  0.890  0.087
560.0  0.887  0.087
570.0  0.883  0.087
580.0  0.878  0.086
590.0  0.873  0.086
600.0  0.868  0.085
610.0  0.861  0.084
620.0  0.854  0.084
630.0  0.847  0.083
640.0  0.840  0.083
650.0  0.833  0.082
660.0  0.825  0.081
670.0  0.817  0.080
680.0  0.808  0.080
690.0  0.799  0.079
700.0  0.790  0.078
710.0  0.782  0.077
720.0  0.773  0.077
730.0  0.763  0.076
740.0  0.755  0.075
750.0  0.745  0.074
760.0  0.735  0.074
770.0  0.727  0.073
780.0  0.720  0.072


--- Spectral Properties Uv ---
For perpendicular incidence angle
wavel      : wavelength [nm]
Reflec     : spectral reflectance
Transm     : spectral transmittance

  Wavel  Transm Reflec
  282.5  0.000  0.069
  287.5  0.000  0.067
  292.5  0.000  0.065
  297.5  0.000  0.064
  302.5  0.000  0.062
  307.5  0.000  0.061
  312.5  0.000  0.060
  317.5  0.002  0.059
  322.5  0.019  0.058
  327.5  0.070  0.058
  332.5  0.171  0.059
  337.5  0.308  0.062
  342.5  0.454  0.067
  347.5  0.581  0.074
  352.5  0.680  0.080
  357.5  0.750  0.085
  362.5  0.795  0.088
  367.5  0.821  0.090
  372.5  0.823  0.090
  377.5  0.804  0.088
```

--- Disclaimer ---

APPENDIX V. Questionnaires

Empirical

1	**Program name and version number**	**BSim 4.7.1.18**
2	**Name of organization performed the simulations**	**Aalborg University**
3	**Name of person performed simulations and contact information**	**Olena Kalyanova Ph.D. student, Aalborg University Sohngaardsholmsvej 57 DK-9000 tel. +45 9635 8587 ok@civil.aau.dk**

4   **Program status**

☐ Freeware
☒ Commercial
☐ Other, please specify

5   **Time convention for weather data: first interval in the weather input lasts 00:00-01:00, climate is assumed constant over the sampling interval**

☒ Yes
☐ No, please specify

CALCULATION OF BOUNDARY CONDITIONS

6   **Please specify the solar model for calculation of incident solar radiation**
Perez

7   **Transmission of the direct solar radiation into zone 1**

☐ Calculated with the constant solar heat gain coefficient (g-value)
☐ Calculated with the g-value as a function of incidence (function of incidence is fixed within code)
☒ Calculated with the g-value as a function of incidence (function of incidence is user defined)
☐ Other, please specify

8   **Transmission of the direct solar radiation into zone 2**

☐ Treated as diffuse solar radiation and calculated with the constant g-value
☐ Calculated with the g-value as a function of incidence (function of incidence is fixed within code)
☒ Calculated with the g-value as a function of incidence (function of incidence is user defined)
☐ Other, please specify

9   **Transmission of the diffuse solar radiation into zone 1**

☒ Calculated with the solar heat gain coefficient at the solar incidence 60°
☐ Other, please specify

10   **Distribution of solar radiation to the surfaces in the zone 1**

☐ Distributed equally to all surfaces
☐ Calculated according surface area weighting
☐ Calculated according to solar path and view factors
☐ Other, please specify: direct solar radiation is distributed according to the solar path, the diffuse solar radiation is area weighted

11   Distribution of solar radiation to the surfaces in the zone 2

☐ Distributed equally to all surfaces
☐ Calculated according surface area weighting
☐ Calculated according to solar path and view factors
☐ Other, please specify: direct solar radiation is distributed according to the solar path, the diffuse solar radiation is area weighted

MODEL DEFINITIONS

12   Air temperature in the zone 1 is calculated as:

☒ One node temperature
☐ Few zones are stacked on the top of each other and the air temperature in each of zones is calculated, please specify number of stacked zones
☐ Other, please specify

13   Air temperature in the zone 2 is calculated as:

☒ One node temperature
☐ Few zones are stacked on the top of each other and the air temperature in each of zones is calculated, please specify number of stacked zones
☐ Other, please specify

HEAT EXCHANGE WITH EXTERIOR

14   External heat transfer coefficients

☒ Split radiative/convective
☐ Combined radiative/ convective
☐ Other, please specify

15   External heat transfer coefficients are calculated with identical assumptions for all surfaces (window frame, window glazing, walls etc.)

☒ Yes
☐ No, please specify

16   External convection

☐ Constant coefficients fixed within code
☐ User-specified constant coefficients
☐ Calculated within code as a function of orientation
☒ Calculated within code as a function of wind speed
☐ Calculated within code as a function of wind speed and direction
☐ Other, please specify

17   External radiative heat exchange
☐ Assumed to be ambient temperature
☒ Assumed to be sky temperature
☐ Other, please specify

HEAT TRANSFER WITHIN ZONES

18   Internal heat transfer coefficients
☒ Split radiative/convection
☐ Combined radiative/ convective
☐ Other, please specify

19   Internal heat transfer coefficients are calculated with identical assumptions in all zones and for all surfaces (window frame, window glazing, walls etc.)

☒ Yes
☐ No, please specify

20   Internal convection

☐ Constant coefficients fixed within code
☐ User-specified constant coefficients
☒ Calculated within code as a function of orientation (vertical/horizontal)
☒ Calculated within code as a function of temperature difference
☐ Calculated within code as a function of air velocity in the zone
☐ Calculated within code as a function of surface finishes
☐ Other, please specify

21   Longwave radiation exchange within zone

☐ Constant linearized coefficients
☒ Linearized coefficients based on view factors
☐ Linearized coefficients based on surface emissivities
☐ Nonlinear treatment of radiation heat exchange
☐ Other, please specify

WINDOW

22   Window

☐ Window frame and glazing are modeled as separate elements of construction
☐ Window frame and glazing are modeled as separate elements of construction, but   the total U-value is calculated within the code
☐ Window frame and glazing are modeled as separate elements of construction, but   the total U-value and g-value are calculated within the code
☒ Other, please specify : Window frame and glazing are modelled as separate elements of construction, but   the total U-value is calculated within the code, but the g-value is calculated in the code on the basis of user defined solar transmission

23   Glazing temperature

☐ Calculated for 1 nodal point on the basis of fixed resistance
☐ Calculated dynamically, using the same scheme as for opaque elements
☒ Other, please specify: Calculated as a thermal ballance for the surface, depending on ammount of absorbed/reflected solar radiation and air temperature in the neighbouring zones

AIRFLOW MODEL

24   Discharge coefficient

☒ Fixed within the code
☐ User-specified fixed value
☐ Calculated by code, please specify what are the parameters involved in code calculations
☐ Other, please specify

25   Pressure difference coefficients
☒ Fixed within the code, identical for all openings sharing the same surface
☐ User-specified, identical for all openings sharing the same surface
☐ User-specified for every opening
☐ Other, please specify

26   Calculated mass flow rate in the model is a function of

☒ Buoyancy force
☒ Wind pressure
☐ Wind turbulence
☐ Other, please specify

GENERAL

Empirical

1   Program name and version number   **VA114 – version 2.25**

2   Name of organization performed the simulations   **VABI Software bv**

3   Name of person performed simulations and contact information   **A. Wijsman**

                                                                              Email: a.wijsman@vabi.nl

4   Program status

☐ Freeware
X Commercial
☐ Other, please specify

5   Time convention for weather data: first interval in the weather input lasts 00:00-01:00, climate is assumed constant over the sampling interval

X Yes
☐ No, please specify

CALCULATION OF BOUNDARY CONDITIONS

6   Please specify the solar model for calculation of incident solar radiation
See appendix D to this Modeler report

7   Transmission of the direct solar radiation into zone 1

☐ Calculated with the constant solar heat gain coefficient (g-value)
☐ Calculated with the g-value as a function of incidence (function of incidence is fixed within code)
☐ Calculated with the g-value as a function of incidence (function of incidence is user defined)
X Other, please specify: Calculated with Transmission (as a function of incidence – user defined) and Absorption in the pane;

8   Transmission of the direct solar radiation into zone 2

☐ Treated as diffuse solar radiation and calculated with the constant g-value
☐ Calculated with the g-value as a function of incidence (function of incidence is fixed within code)
☐ Calculated with the g-value as a function of incidence (function of incidence is user defined)
X Other, please specify: Calculated with Transmission and Absorption in the panes; properties at angle of incidence of 45 degree

9   Transmission of the diffuse solar radiation into zone 1

☐ Calculated with the solar heat gain coefficient at the solar incidence 60°
X Other, please specify: Calculated with Transmission (at solar incidence of 58°) and Absorption in the pane.

10   Distribution of solar radiation to the surfaces in the zone 1

☐ Distributed equally to all surfaces
☐ Calculated according surface area weighting
☐ Calculated according to solar path and view factors
X Other, please specify: Different treatment for Direct and Diffuse solar radiation. Distribution of Direct solar is calculated by solar path; partly absorbed and partly diffuse reflected at surfaces that are hit. Distribution of Diffuse solar and Diffuse reflected Direct solar is calculated by absorption factors (based on view factors and absorption coefficients of the surfaces that are hit)

11   Distribution of solar radiation to the surfaces in the zone 2

☐ Distributed equally to all surfaces
☐ Calculated according surface area weighting
☐ Calculated according to solar path and view factors
X Other, please specify: same as distribution in zone 1

MODEL DEFINITIONS

12   Air temperature in the zone 1 is calculated as:

X One node temperature
☐ Few zones are stacked on the top of each other and the air temperature in each of zones is calculated, please specify number of stacked zones
☐ Other, please specify

13   Air temperature in the zone 2 is calculated as:

X One node temperature
☐ Few zones are stacked on the top of each other and the air temperature in each of zones is calculated, please specify number of stacked zones
☐ Other, please specify

HEAT EXCHANGE WITH EXTERIOR

14   External heat transfer coefficients

X Split radiative/convective
☐ Combined radiative/ convective
☐ Other, please specify

15   External heat transfer coefficients are calculated with identical assumptions for all surfaces (window frame, window glazing, walls etc.)

☐ Yes
X No, please specify : External heat transfer coefficients are not calculated (see external convection and external radiative heat exchange)

16   External convection

☐ Constant coefficients fixed within code
X User-specified constant coefficients
☐ Calculated within code as a function of orientation
☐ Calculated within code as a function of wind speed
☐ Calculated within code as a function of wind speed and direction
☐ Other, please specify

17   External radiative heat exchange

☐ Assumed to be ambient temperature
X   Assumed to be sky temperature
☐ Other, please specify

HEAT TRANSFER WITHIN ZONES

18   Internal heat transfer coefficients

X   Split radiative/convection
☐ Combined radiative/ convective
☐ Other, please specify

19   Internal heat transfer coefficients are calculated with identical assumptions in all zones and for all surfaces (window frame, window glazing, walls etc.)

☐ Yes
☐ No, please specify : Ixternal heat transfer coefficients are not calculated (see internal convection and internal radiative heat exchange)

20   Internal convection

☐ Constant coefficients fixed within code
X   User-specified constant coefficients
☐ Calculated within code as a function of orientation (vertical/horizontal)
☐ Calculated within code as a function of temperature difference
☐ Calculated within code as a function of air velocity in the zone
☐ Calculated within code as a function of surface finishes
☐ Other, please specify

21   Longwave radiation exchange within zone

☐ Constant linearized coefficients
☐ Linearized coefficients based on view factors
X   Linearized coefficients based on view factors and surface emissivities
☐ Nonlinear treatment of radiation heat exchange
☐ Other, please specify

WINDOW

22   Window

X Window frame and glazing are modeled as separate elements of construction; properties are user defined
☐ Window frame and glazing are modeled as separate elements of construction, but   the total U-value is calculated within the code
☐ Window frame and glazing are modeled as separate elements of construction, but   the total U-value and g-value are calculated within the code
☐ Other, please specify

23   Glazing temperature

☐ Calculated for 1 nodal point on the basis of fixed resistance
X Calculated dynamically, using the same scheme as for opaque elements
☐ Other, please specify

AIRFLOW MODEL

24   Discharge coefficient

X Fixed within the code
☐ User-specified fixed value
☐ Calculated by code, please specify what are the parameters involved in code calculations
☐ Other, please specify

25   Pressure difference coefficients

☐ Fixed within the code, identical for all openings sharing the same surface
X User-specified, identical for all openings sharing the same surface
☐ User-specified for every opening
☐ Other, please specify

26   Calculated mass flow rate in the model is a function of

X Buoyancy force
X Wind pressure
X Wind fluctuations
☐ Other, please specify

GENERAL

empirical

1   **Program name and version number**   **ESP-r 11.3**

2   **Name of organization performed the simulations**   **ESRU,**
                                                                                     University of Strathclyde

3   **Name of person performed simulations and contact information**   **Paul Strachan**
                                                                                     paul@esru.strath.ac.uk
                                                                                     tel: +44 141 548 2041

4   **Program status**

☒ Freeware (Open Source)
☐ Commercial
☐ Other, please specify

5   **Time convention for weather data: first interval in the weather input lasts 00:00-01:00, climate is assumed constant over the sampling interval**

☐ Yes
☒ No, please specify: Solar data is hour centred (i.e. covers period 00:00-01:00) in these simulations. Linear interpolation is carried out for sub-hourly simulations

CALCULATION OF BOUNDARY CONDITIONS

6   **Please specify the solar model for calculation of incident solar radiation**
     See report. Perez 1990 is used for the anisotropic diffuse sky model.

7   **Transmission of the direct solar radiation into zone 1**

☐ Calculated with the constant solar heat gain coefficient (g-value)
☐ Calculated with the g-value as a function of incidence (function of incidence is fixed within code)
☐ Calculated with the g-value as a function of incidence (function of incidence is user defined)
☒ Other, please specify See report - transmittance is an input optical property as are layer absorptances. The convection and radiation are calculated explicitly at the glazing system boundaries. g-values are not used.

8   **Transmission of the direct solar radiation into zone 2**

☐ Treated as diffuse solar radiation and calculated with the constant g-value
☐ Calculated with the g-value as a function of incidence (function of incidence is fixed within code)
☐ Calculated with the g-value as a function of incidence (function of incidence is user defined)
☒ Other, please specify As above

9   **Transmission of the diffuse solar radiation into zone 1**

☐ Calculated with the solar heat gain coefficient at the solar incidence 60°
☒ Other, please specify As above; incident angle assumed to be 51 degrees

10   **Distribution of solar radiation to the surfaces in the zone 1**

☐ Distributed equally to all surfaces
☐ Calculated according surface area weighting
☒ Calculated according to solar path and view factors
☐ Other, please specify

11   **Distribution of solar radiation to the surfaces in the zone 2**

☐ Distributed equally to all surfaces
☐ Calculated according surface area weighting
☒ Calculated according to solar path and view factors
☐ Other, please specify

MODEL DEFINITIONS

12   Air temperature in the zone 1 is calculated as:

☒ One node temperature (for DSF100 case only)
☒ Few zones are stacked on the top of each other and the air temperature in each of zones is calculated, please specify number of stacked zones 3
☐ Other, please specify

13   Air temperature in the zone 2 is calculated as:

☒ One node temperature
☐ Few zones are stacked on the top of each other and the air temperature in each of zones is calculated, please specify number of stacked zones
☐ Other, please specify

HEAT EXCHANGE WITH EXTERIOR

14   External heat transfer coefficients

☒ Split radiative/convective
☐ Combined radiative/ convective
☐ Other, please specify

15   External heat transfer coefficients are calculated with identical assumptions for all surfaces (window frame, window glazing, walls etc.)

☒ Yes
☐ No, please specify

16   External convection

☐ Constant coefficients fixed within code
☐ User-specified constant coefficients
☐ Calculated within code as a function of orientation
☐ Calculated within code as a function of wind speed
☒ Calculated within code as a function of wind speed and direction
☐ Other, please specify

17   External radiative heat exchange

☐ Assumed to be ambient temperature
☐ Assumed to be sky temperature
☒ Other, please specify Sky and ground surface temperatures, depending on viewfactors

HEAT TRANSFER WITHIN ZONES

18   Internal heat transfer coefficients

☒ Split radiative/convection
☐ Combined radiative/ convective
☐ Other, please specify

19   Internal heat transfer coefficients are calculated with identical assumptions in all zones and for all surfaces (window frame, window glazing, walls etc.)

☒ Yes (with exception of mechanically ventilated case – see report)
☐ No, please specify

20   Internal convection

☐ Constant coefficients fixed within code
☐ User-specified constant coefficients
☐ Calculated within code as a function of orientation (vertical/horizontal)
☒ Calculated within code as a function of temperature difference
☐ Calculated within code as a function of air velocity in the zone
☐ Calculated within code as a function of surface finishes
☐ Other, please specify

21   Longwave radiation exchange within zone

☐ Constant linearized coefficients
☒ Linearized coefficients based on view factors
☒ Linearized coefficients based on surface emissivities
☐ Nonlinear treatment of radiation heat exchange
☐ Other, please specify

<u>WINDOW</u>

22   Window

☒ Window frame and glazing are modeled as separate elements of construction
☐ Window frame and glazing are modeled as separate elements of construction, but   the total U-value is calculated within the code
☐ Window frame and glazing are modeled as separate elements of construction, but   the total U-value and g-value are calculated within the code
☐ Other, please specify

23   Glazing temperature

☐ Calculated for 1 nodal point on the basis of fixed resistance
☒ Calculated dynamically, using the same scheme as for opaque elements
☐ Other, please specify

<u>AIRFLOW MODEL</u>

24   Discharge coefficient

☐ Fixed within the code
☒ User-specified fixed value
☐ Calculated by code, please specify what are the parameters involved in code calculations
☐ Other, please specify

25   Pressure difference coefficients

☐ Fixed within the code, identical for all openings sharing the same surface
☐ User-specified, identical for all openings sharing the same surface
☒ User-specified for every opening
☐ Other, please specify

26   Calculated mass flow rate in the model is a function of

☒ Buoyancy force
☒ Wind pressure
☐ Wind turbulence
☐ Other, please specify

GENERAL

Empirical

1   Program name and version number   **TRNSYS-TUD**

2   Name of organization performed the simulations   **Technical University of Dresden**

3   Name of person performed simulations and contact information

                                                                                           Clemens Felsmann
                                                                                           felsmann@itg-dresden.de

         Program status

         ☐ Freeware
         ☐ Commercial
         ☒ Other: The code was developed based on commercial TRNSYS for research purposes

5   Time convention for weather data: first interval in the weather input lasts 00:00-01:00, climate is assumed constant over the sampling interval

         ☐ Yes
         ☒ No: normally inputs change linearly but solar radiation is calculated using a special smoothing function..

   CALCULATION OF BOUNDARY CONDITIONS

6   Please specify the solar model for calculation of incident solar radiation
         Perez model

7   Transmission of the direct solar radiation into zone 1

         ☐ Calculated with the constant solar heat gain coefficient (g-value)
         ☐ Calculated with the g-value as a function of incidence (function of incidence is fixed within code)
         ☐ Calculated with the g-value as a function of incidence (function of incidence is user defined)
         ☒ Other: Calculated with the g-value as a function of incidence (function of incidence was calculated by WINFOW5 Software)

8   Transmission of the direct solar radiation into zone 2

         ☒ Treated as diffuse solar radiation and calculated with the constant g-value
         ☐ Calculated with the g-value as a function of incidence (function of incidence is fixed within code)
         ☐ Calculated with the g-value as a function of incidence (function of incidence is user defined)
         ☐ Other, please specify

9   Transmission of the diffuse solar radiation into zone 1

         ☐ Calculated with the solar heat gain coefficient at the solar incidence 60°
         ☒ Other: Calculated with the solar heat gain coefficient was calculated by WINFOW5 Software

10   Distribution of solar radiation to the surfaces in the zone 1

         ☒ Distributed equally to all surfaces: diffuse radiation
         ☐ Calculated according surface area weighting
         ☒ Calculated according to solar path and view factors: direct radiation
         ☐ Other, please specify

11   Distribution of solar radiation to the surfaces in the zone 2

☒ Distributed equally to all surfaces because all radiation was treated as diffuse radiation
☐ Calculated according surface area weighting
☐ Calculated according to solar path and view factors
☐ Other, please specify

MODEL DEFINITIONS

12   Air temperature in the zone 1 is calculated as:

☒ One node temperature was reported but…
☒ Few zones are stacked on the top of each other and the air temperature in each of zones is calculated, please specify number of stacked zones 4
☐ Other, please specify

13   Air temperature in the zone 2 is calculated as:

☒ One node temperature was reported but …
☒ Few zones are stacked on the top of each other and the air temperature in each of zones is calculated, please specify number of stacked zones 4
☐ Other, please specify

HEAT EXCHANGE WITH EXTERIOR

14   External heat transfer coefficients

☒ Split radiative/convective
☐ Combined radiative/ convective
☐ Other, please specify

15   External heat transfer coefficients are calculated with identical assumptions for all surfaces (window frame, window glazing, walls etc.)

☒ Yes
☐ No, please specify

16   External convection

☐ Constant coefficients fixed within code
☒ User-specified constant coefficients
☐ Calculated within code as a function of orientation
☐ Calculated within code as a function of wind speed
☐ Calculated within code as a function of wind speed and direction
☐ Other, please specify

17   External radiative heat exchange

☐ Assumed to be ambient temperature
☐ Assumed to be sky temperature
☒ Other: it depends on the orientation whether ambient or sky temperature will be used

HEAT TRANSFER WITHIN ZONES

18   Internal heat transfer coefficients

☒ Split radiative/convection
☐ Combined radiative/ convective
☐ Other, please specify

19   Internal heat transfer coefficients are calculated with identical assumptions in all zones and for all surfaces (window frame, window glazing, walls etc.)

☒ Yes
☐ No, please specify

20   Internal convection

☐ Constant coefficients fixed within code
☒ User-specified constant coefficients
☐ Calculated within code as a function of orientation (vertical/horizontal)
☐ Calculated within code as a function of temperature difference
☐ Calculated within code as a function of air velocity in the zone
☐ Calculated within code as a function of surface finishes
☐ Other, please specify

21   Longwave radiation exchange within zone

☐ Constant linearized coefficients
☐ Linearized coefficients based on view factors
☐ Linearized coefficients based on surface emissivities
☒ Nonlinear treatment of radiation heat exchange
☐ Other, please specify

WINDOW

22   Window

☐ Window frame and glazing are modeled as separate elements of construction
☐ Window frame and glazing are modeled as separate elements of construction, but   the total U-value is
    calculated within the code
☒ Window frame and glazing are modeled as separate elements of construction, but   the total U-value and g-
    value are calculated within the code
☐ Other, please specify

23   Glazing temperature

☒ Calculated for 1 nodal point on the basis of fixed resistance
☐ Calculated dynamically, using the same scheme as for opaque elements
☐ Other, please specify

AIRFLOW MODEL

24   **Discharge coefficient**

☐ Fixed within the code
☒ User-specified fixed value
☐ Calculated by code, please specify what are the parameters involved in code calculations
☐ Other, please specify

25   **Pressure difference coefficients**

☐ Fixed within the code, identical for all openings sharing the same surface
☐ User-specified, identical for all openings sharing the same surface
☒ User-specified for every opening
☐ Other, please specify

26   **Calculated mass flow rate in the model is a function of**

☒ Buoyancy force
☒ Wind pressure
☐ Wind turbulence
☐ Other, please specify

APPENDIX VI. Modeler reports

BSim Modeler Report

Empirical Validation of Building Simulation Software

Technical Report

IEA ECBCS Annex43/SHC Task 34
Validation of Building Energy Simulation Tools

Subtask E

O. Kalyanova
P. Heiselberg

AALBORG UNIVERSITY
Department of Civil Engineering

Aalborg University
Department of Civil Engineering
Indoor Environmental Engineering Research Group

DCE Technical Report No. 029

BSim Modeler Report
Empirical Validation of Building
Simulation Software

by

O. Kalyanova
P. Heiselberg

maj 2008

Scientific Publications at the Department of Civil Engineering

Technical Reports are published for timely dissemination of research results and scientific work carried out at the Department of Civil Engineering (DCE) at Aalborg University. This medium allows publication of more detailed explanations and results than typically allowed in scientific journals.

Technical Memoranda are produced to enable the preliminary dissemination of scientific work by the personnel of the DCE where such release is deemed to be appropriate. Documents of this kind may be incomplete or temporary versions of papers—or part of continuing work. This should be kept in mind when references are given to publications of this kind.

Contract Reports are produced to report scientific work carried out under contract. Publications of this kind contain confidential matter and are reserved for the sponsors and the DCE. Therefore, Contract Reports are generally not available for public circulation.

Lecture Notes contain material produced by the lecturers at the DCE for educational purposes. This may be scientific notes, lecture books, example problems or manuals for laboratory work, or computer programs developed at the DCE.

Theses are monograms or collections of papers published to report the scientific work carried out at the DCE to obtain a degree as either PhD or Doctor of Technology. The thesis is publicly available after the defence of the degree.

Latest News is published to enable rapid communication of information about scientific work carried out at the DCE. This includes the status of research projects, developments in the laboratories, information about collaborative work and recent research results.

INDEX

1. Introduction

Test cases DSF100_e and DSF200_e were simulated with the Danish Building simulating software BSim, version 4.7.1.18.

Statens Byggeforskningsinstitut
Danish Building and Urban Research
P.O.Box 119
DK-2970 Hørsholm.
Telephone: (+45) 45 86 5533
Telefax: (+45) 45 86 7535
E-mail   info@by-og-byg.dk
Web: http://www.by-og-byg.dk   (Danish)
                http://www.dbur.dk   (English)
                http://www.bsim.dk   (BSim homepage)

BSim (Building Simulation) is the integrated tool for projecting buildings and installations. The software consists of seven modules:

- SimView - Graphic user interface
- Tsbi5 - Indoor climate, thermal and moisture conditions
- Xsun - Sunlight and shadows
- SimLight - Daylight calculations
- BV98 - Danish Building regulations compliance checker
- SimDXF - Importing CAD drawings
- SimDB - Database with constructions and materials

Moreover there few advanced options available, these are:

- Advanced simulations of moisture transport in buildings and constructions
- Calculations of electrical energy yield from a building integrated solar cell (PV) system
- Simulation of indoor climate with natural ventilation in the building

2. Modelling approaches in BSim

Calculations in BSim performed in a steady state condition for the each time step. The software contains also accumulation of heat and moisture calculations. There are two or more time steps per hour.

Zones

A building consists of an arbitrary number of zones, which are limited by an arbitrary number of surfaces.

The zone air is represented in the building description as a nodal point, for which air temperature and water vapour content are calculated. It is assumed that the air in a zone is fully mixed. However, the temperature stratification in a zone can be modeled by means of Kappa-model, which is highly dependent on user assumptions/inputs.

External environment

This is so-called virtual zone, e.g. the outside air, the condition of which is not to be calculated, but is given by data from a file or a timetable, defined by user.

Transmission of solar radiation to the zone

XSun, which forms a part of the BSim software suite, can be used for the detailed analyses of the path of direct solar radiation through a building. It is possible to see where and when the sun strikes any face in the model. The direct solar radiation through the external and internal window will be distributed geometrically correct according to the solar path, while the diffuse solar radiation will be distributed according to surface area weighting.

Solar radiation

From the values given in the weather data file BSim is able to calculate the solar incidence on an arbitrarily oriented surface. Petersen's model is the default one for calculation of solar incidence in BSim. Available models for calculation of solar incidence in BSim are: Petersen's, Munier's, Lund's and Perez's.

Longwave radiation exchange between the model and ambient

Only the radiative exchange to the sky takes part in the simulation. There is thus no radiative exchange with eventual other buildings in the model and nor with eventual advanced parts of the building itself. The radiative heat exchange is thus only dependant on the temperature difference between any surface and the sky, respectively the ground and the tilt of the surface.

Internal longwave radiation exchange

It is only possible to simulate long-wave radiative exchange in tsbi5 in those rooms, which are convex, in order to enable calculation of view factors in BSim. When the internal longwave radiation exchange is to be calculated then the convective heat transfer coefficients are calculated separately for each surface, otherwise a combined value of convection and radiation is used.

The longwave radiation exchange from the surfaces of the glass and the surrounding surfaces with average emission coefficient (e = 0.94) is used for all surfaces made of glass.

Outdoor surface convection coefficient

Next to calculating the long wave radiation effects, the heat transfers coefficient between the outdoor air and the first node point on the exterior side of the construction is calculated as a function of wind speed.

Convective heat transfer coefficients

For vertical surfaces:
Laminar conditions, small surfaces ($\Delta T \leq 9.5/L^3$):
Equation 2-1

$$\alpha_c = 1.43 \left(\frac{\Delta T}{L} \right)^{0.25} \quad \text{W/m}^2\text{K}$$

Turbulent conditions, large surfaces ($\Delta T > 9.5/L^3$):
Equation 2-2

$$\alpha_c = 1.31 (\Delta T)^{0.33} \quad \text{W/m}^2\text{K}$$

For horizontal surfaces with upward heat flow (warm floors or cold ceilings):
Laminar conditions, small surfaces ($\Delta T \leq 0.19/L^3$):

Equation 2-3

$$\alpha_c = 1.32 \left(\frac{\Delta T}{L} \right)^{0.25} \ \text{W/m}^2\text{K}$$

Turbulent conditions, large surfaces ($\Delta T > 0.19/L^3$):
Equation 2-4

$$\alpha_c = 1.52 (\Delta T)^{0.33} \ \text{W/m}^2\text{K}$$

For horizontal surfaces with downward heat flow (cold floors or warm ceilings), only laminar conditions:
Equation 2-5

$$\alpha_c = 0.59 \left(\frac{\Delta T}{L} \right)^{0.25} \ \text{W/m}^2\text{K}$$

Glass temperature

In the model, different absorption and reflection at the two glass faces are used in the calculation of the absorbed amount of radiation in the glass. Then the temperature for the glass surfaces is calculated as a heat balance to the air temperature next to the glass surface, including the amount of absorbed energy in the glass face.

Heat balance for the zone air

The heat balance for the air in a zone does not make allowance for the heat capacity of the air which means that the air momentarily adjusts itself to alterations in the surroundings, includes:

-heat flows from adjoining constructions
-heat flows through windoors
-solar radiation through windoors (of which only a limited amount is assumed to be induced to the air)
-thermal contribution from various heat loads and systems
-air penetration from outdoor air (infiltration, venting)
-air supplied from ventilation systems
-air transferred by from other zones (mixing)

Heat transmission in the constructions

The constructions consist of one or more layers, which are assumed to be homogeneous, consisting of one material, which is characterized by thermal material values. The heat transmission internally in the constructions is described non-stationary, i.e. by making allowance for each individual layer's thermal capacity. Thick material layers are divided into several thinner layers (control volumes).

Heat transfer coefficients at the window surfaces are calculated in the same way as the heat transfer coefficients for the wall containing the window.

Air mass balance

If an un-balanced air-stream is introduced in any thermal zone, this will automatically be balanced with in- or exfiltration of air from the outdoors in the tsbi5 simulations. This happens even if the thermal zone has no direct connection (faces) to the outdoors.

Control

All systems in BSim are controlled on the basis of an operative temperature in the thermal zone to which they are attached. However, it is possible to adjust the control system for application of the air temperature instead for the operative air temperature.

3. Modelling assumptions

General

Weather data

The climate data is provided together with the specification, where it is advised to use global and diffuse solar radiation on the horizontal surface as input parameters. BSim is not able to use these parameters as inputs; therefore the Normal direct solar radiation and diffuse solar radiation were used instead for. Normal direct solar radiation was calculated manually on the basis of provided climate data.

Model geometry

Thermal zones in the model are defined according to the specification, thus zone 1 represents the DSF and zone 2 represents the room adjacent to the DSF.

WALL 1, shared by zone 1 and zone 2 was modeled as an adiabatic and relatively thin wall for each of the zones, see Figure 1a. The internal dimensions of the zone 1were kept unchanged according to the specification. Internal dimensions and shape of the zone 2 were changed, as following: left and right WALL 1 in the zone 2 was given a slope in order to activate the longwave radiation calculations (BSim limitation for the concave spaces). The length of the WALL 2 was changed to attain the same internal zone volume as in the specification (Figure 1) .

a.   b.
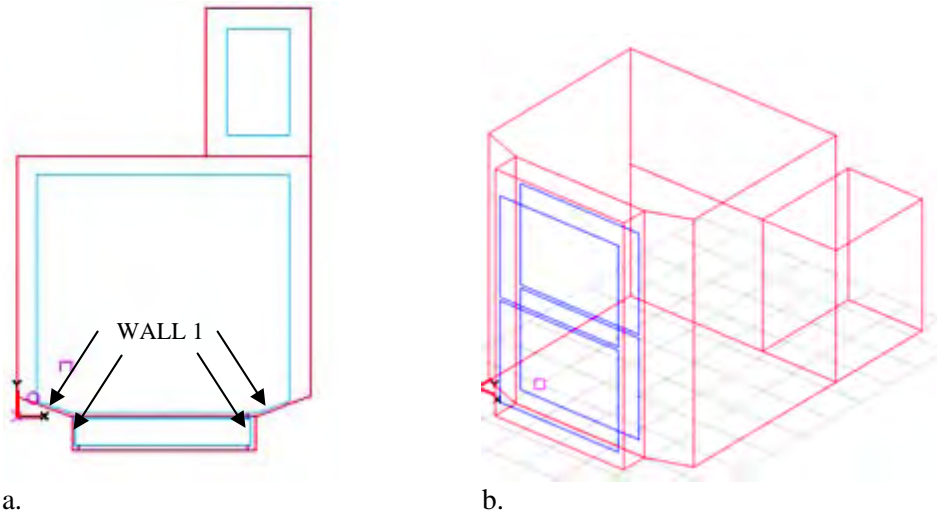
Figure 1. Geometry of BSim model. Plan (a). Model in 3D (b).
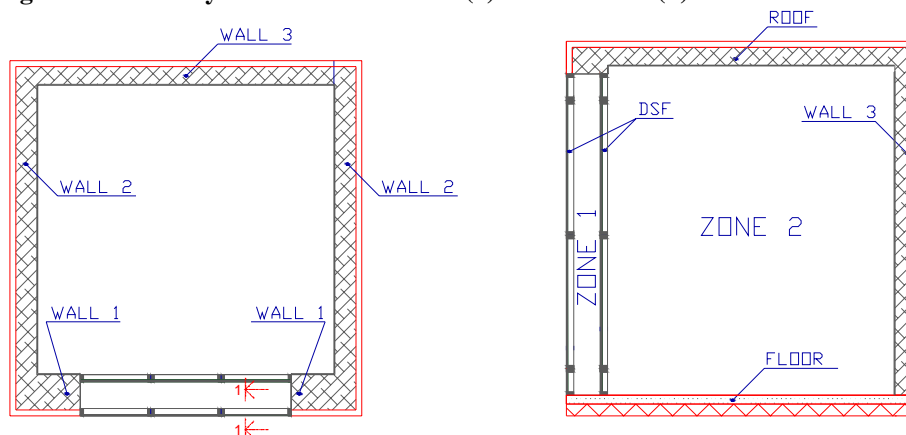
Figure 2. Definition of zones and walls in the specification. Plan (left) and section1-1 (right).

10

Opaque constructions

U-values for the constructions are calculated by BSim when the material properties of the constructions are defined by user. The U-value is calculated according to the Danish Norms DS 418. Material properties were defined according to the specification.

Transparent constructions (Windoors)

Following Figure 3 is included in the report to explain the modelling procedure for the DSF. Figure 3a corresponds to the original geometry definition in the test specification. First, all windows and wall of the external façade are replaced by a separate construction with the U-value equal to the U-value of the window frame (U= 3.86 W/m^2, Figure 3b). Then windows are added to the new construction (Figure 3c). Six sections of the external windows are replaced by 2 sections with the corresponding area of glazing.

It is necessary to leave some distance between the window frame and the edge of the construction in BSim. In the Figure 3c is shown area of 1.236 m^2, left around the windows (blue color), this area has the same U-value as the window frame. Total frame area of windows is 3.216 m^2. Remaining frame area will be:
A=3.216-1.236=1.98 m^2
This area 1.98m^2 was equally distributed between 2 windows (Figure 3c.)
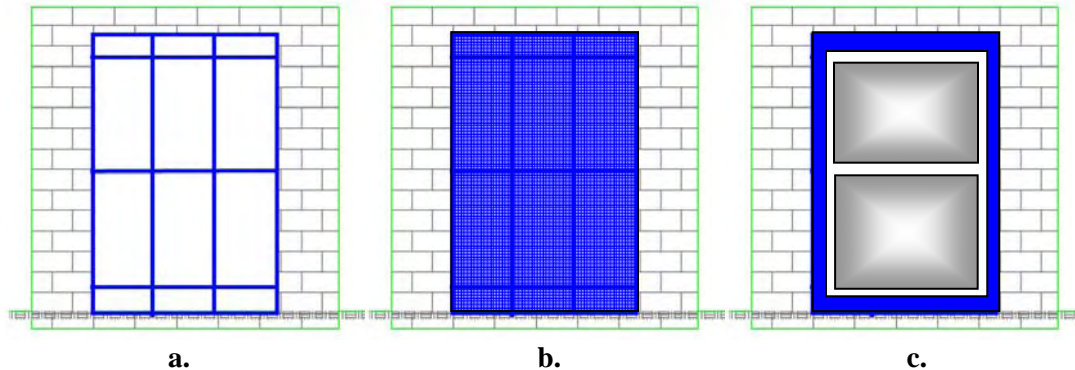
| **a.** | **b.** | **c.** |
Figure 3. South façade, defined in the test case specification and in the model

Same steps were repeated for the internal window sections.

These changes require adjustments in U-value of the windows, to fulfill a condition:

Equation 3-1

$$A_w \cdot U_w \cdot 6 \approx A_c \cdot U_f + A_w^* \cdot U_w^* \cdot 2$$

A_w – area of window section defined in the specification, m^2
U_w – U-value of the window section defined in the specification, W/m^2
6   – number of window sections
A_c – area (of new construction) left around the window, m^2
U_f – U-value of the frame defined in the specification, W/m^2
A_w^* – area of 1 out of 2 window sections (Figure 3c), m^2
U_w^* – adjusted U-value of window sections in Figure 3c, m^2
2   – number of window sections (Figure 3c)

Incident solar radiation

Perez model was used for the calculations

Transmission of solar radiation
The transmission of solar radiation as a function of angle of incidence is estimated on the basis of a default function in BSim:

Incident angle	Transmission of external window pane	Transmission of internal window panes
0	0.76	0.53
10	0.75	0.53
20	0.75	0.53
30	0.75	0.53
40	0.74	0.52
50	0.72	0.50
60	0.65	0.45
70	0.52	0.35
80	0.30	0.19
90	0.00	0.00

Solar heat transmittance (g-value) for the solar radiation normal to the glass surface is calculated f by BSim on the basis of glazing transmittance properties. Values used in simulations are according to the WIS calculations given in specification.

Program assumes heat transmittance for diffuse solar radiation (reflected from surroundings, i.e. neighbor buildings, ground, clouds etc.) equal to the transmittance for direct radiation at an angle of incidence of 60°.

Surface finishes

Solar radiation sticking the opaque external surfaces is absorbed according to the defined surface absorption property, however solar radiation sticking on the opaque internal surfaces is fully absorbed by the surface.

Glazing Surface temperatures

In BSim the model for calculation of the glazing surface temperatures is simplified, it accounts for the absorbed solar radiation in the glazing pan and the air temperature in the neighboring zones. However there it has a limitation: it is assumed that there are always two layers of glass and this model is not applicable for the glass with coatings. And therefore it can not be directly applied for the constructions defined in the specification.

Glazing emissivity

This is the default value in the BSim and equals 0.84

Air flow modelling

The airflow model for the case defined in the specification is described as 'Single Sided in Different Levels'. It is used when several pairs of openings in one face are located in different vertical levels with the uniform temperature distribution in the thermal zone. The airflow through the zone is described by general expression in Equation 3-2.

Equation 3-2

$$q = \left| \pm q_v^2 \pm q_t^2 \right|^{1/2} = \left| \frac{c_v}{|c_v|} \cdot \left(c_v \cdot V_{10} \right)^2 + \frac{\Delta T}{|\Delta T|} \cdot \left(c_t \cdot |\Delta T| \right)^2 \right|^{1/2}$$

Equation 3-3

$$c_t = \sum_{j=1}^{n} c_{D,j} \cdot A_j \cdot \left(\frac{2 \cdot \left(H_o - H_j \right) \cdot g}{T_i} \right)^{1/2}$$

Equation 3-4

$$c_v = 0.03 \cdot A$$

q   - air flow rate in the zone
q_v, q_t - airflow rate caused by wind forces and buoyancy correspondingly
c_v, c_t - coefficient for the wind force and buoyancy correspondingly
V_{10} - the reference wind velocity at the height 10m
ΔT - temperature difference between two environments
n   - number of openings
j   - opening number
c_D - the discharge coefficient
A_j - area of the opening 'j'
H_o - height of the neutral plan
H_j - height of the opening 'j'
g   - gravity force

Wind pressure coefficients

In BSim the wind pressure coefficients are the default values, determined as average values for the surfaces at the different wind incidence angles. BSim chooses the Cp-values from these standards based on the geometry of the building model. Comparison of the Cp values given in the specification and BSim-values is performed in Figure 4.

However, the BSim approach means that every surface is given only 1 value independently on number of openings in the surface and as consequence there is no pressure difference between the openings on the same surface caused by wind.
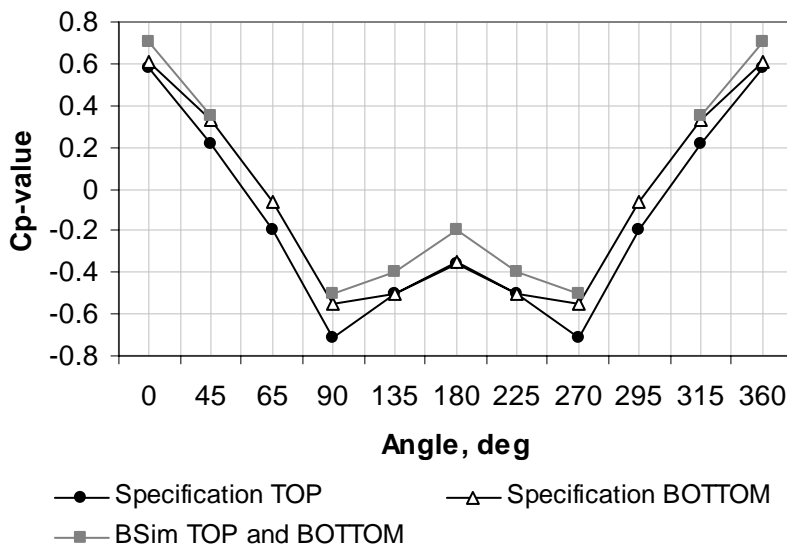
Figure 4. Comparison between Cp -values in the specification and BSim default.

Wind profile

The default function is used to describe the wind velocity profile. A function for the scattered wind breaks was used in the calculations and can be described as in Figure 5.
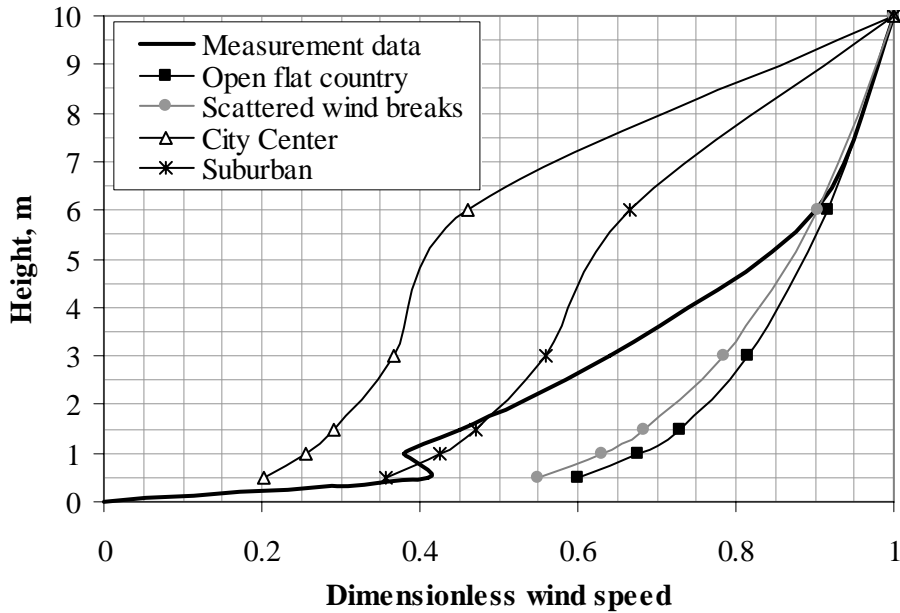
Figure 5. Wind profiles available in BSim.

$V_h = V_{10} k h^{\alpha}$

V_h is the wind velocity in height h [m/s]

V_{10} is the measured wind velocity 10 meters above the free terrain [m/s]

h is the actual height above terrain [m]

k is a factor dependant on the terrain

α is an exponent, dependant in the terrain

For the terrain with the scattered wind breaks the k and α coefficients are as following
$k=0.52$
$\alpha=0.20$
Thus the wind speed reduction coefficient for the height of 6m (roof of the building) is 0.744

Discharge coefficient

The discharge coefficient in BSim is used 0.65 and 0.72 for the bottom and top openings correspondingly to the specification.

Thermal bridges

Thermal bridges were included into the calculations by modification of the constructions in correspondence with the heat loss measurement, described in the specification.

Infiltration

Infiltration is not included into the calculations

Control and air temperature

In BSim systems are controlled according to the operative air temperature, however in the specification the control is performed true the air temperature only. I order to follow the

14

requirements in the specification the longwave radiation contribution on the calculations of the operative air temperature were deactivated.

Remaining parameters

Remaining parameters were modeled according to the test case specification

DSF100_e

Heating/cooling

Heating/Cooling system is introduced to *Zone 2*. The set point temperature for cooling is set to 21.8^{o}C and 21.7^{o}C for heating.
The proportion of the cooling output that is reckoned to be given off to the room air by convection is equal to 1. Heating/Cooling power provided to the *Zone 2* is unlimited to maintain the set point temperature of the room.

DSF200_e

Heating/cooling

Heating/Cooling system is introduced to *Zone 2*. The set point temperature for cooling is set to 21.8^{o}C and 21.7^{o}C for heating.
The proportion of the cooling output that is reckoned to be given off to the room air by convection is equal to 1. Heating/Cooling power provided to the *Zone 2* is unlimited to maintain the set point temperature of the room.

Natural ventilation

The natural ventilation is activated and calculated as described above

4.   Results

All results are given in tables:
Output results DSF100_e.xls
Output results DSF200_e.xls

5.   Remarks

Glass surface temperature needs investigations

6.   Corrected errors

Calculation of view factors for the large opposing glazed surfaces on a short distance from each other.

IEA SHC Task 34 / ECBCS Annex 43
Subtask E: Double Skin Facade

Double Skin Facade - Modeler Report

Empirical Test cases

VA114

VABI Software BV
P.O. Box 29
2600 AA Delft
The Netherlands

February 08, 2008 (third draft)
June 26, 2007 (second draft)
April 27, 2007 (first draft)

Report by A. Wijsman

Remark:
In April 2007 a first draft of the Modeller Report concerning the Empirical tests [6] was made: it contained a description of the model, its assumptions and the first results of the IEA-34/43 DSF Empirical tests.

The VA114 simulation program passed in earlier times the BESTEST [1], [2], [3]. Within this IEA-34/43 project it was already subjected to the IEA-34/43 DSF Comparative tests [4]. Results of these tests can be found in [5].

In June 2007, a second draft came ready. Two descriptions were added: a description of the VA114-submodel for air flow by wind fluctuations and a description of VA114's solar processor. A completed questionnaire for the program VA114 was added too. Reruns were done and results were reported.

Now, February 2008, a third draft (the final draft) is ready. Based on Steady State calculations and Steady State measurements the subtask concluded the presence of thermal bridges (cold bridges). The magnitude of these thermal bridges was determined. These thermal bridges have be taken into account. The U-value of the internal glazing changed slightly too. Reruns (the final runs) were done. Results are reported in this draft.

Heat exchange within a Zone and between Zones

1.   Introduction

The Building simulation program VA114 is developed and distributed by VABI Software bv. The current version is 2.25.

The program calculates the Demand, the Supply, the Distribution and the Generation of heat and cold for a building with its energy supply system. Moreover the internal comfort temperature and overheating are calculated.

VA114 is a multi-zone program (up to 30).

The time step applied in VA114 is 1 hour.

The boundary conditions, that are possible in VA114 are:
-        bounded to ambient
-        bounded to a neighbour zone
-        bounded to a mirror zone
-        bounded to the underground

The current program VA114 models:
-        heat exchange within a zone
-        heat exchange between zones by conduction
-        heat exchange between zones by airflow (ventilation)
-        solar gain and solar exchange between zones
-        solar shading
-        and other processes

The simulation program VA114 passed the BESTEST [1],[2],[3]. In 2005 the simulation program was subjected to the new IEA-34/43 tests of subtask B (Multi-zone Non air – tests MZ320, MZ340, MZ350, MZ355 and MZ360).

Within IEA-34/43 subtask E (Double Skin Façade) last year (2006) the program was subjected to the Comparative tests [4]. Tests were still under development and were repeated a few times. The last time was in June 2007. Results can be found in [5].

In April 2007, within the same subtask, the program was subjected to the Empirical tests [6]. Available were test results from the test facility in Aalborg, Denmark. In the first draft of the Modeler report all background information and the results of the tests (first round) were given.

In June 2007, a second draft of the Modeler report came ready. Two descriptions were: a description of the VA114-submodel for air flow by wind fluctuations (appendix AA) and a description of VA114's solar processor (appendix D). A completed questionnaire for the program VA114 was added too (Appendix E). After some iterations the reruns were done and results were reported [9].

Now, February 2008, a third draft (the final draft) is ready. Based on Steady State calculations and Steady State measurements the subtask concluded the presence of thermal bridges (cold bridges). The magnitude of these thermal bridges was determined. These thermal bridges have be taken into account. The U-value of the internal glazing changed slightly too. Reruns (the final runs) were done. Results are reported in this report.

Remark:
VABI Software bv is developing the simulation program VA114. A new version of VA114 was distributed to its users (about 200) in February 2006. Before the distribution of this new version it was tested extensively: by running the Bestest cases (1995), by running the Dutch EDR-tests and by running the new IEA-34/43-MZ-tests.

2.   Model description

The current program VA114 models:
-        heat exchange within a zone
-        heat exchange between zones by conduction
-        heat exchange between zones by airflow (ventilation)
-        solar gain and solar exchange between zones
-        solar shading
-        and other processes

In more detail:

-        heat exchange within a zone
The zone air is described by one node. Between this zone air node and the internal surfaces heat exchange takes place by convection. The convection coefficient is user given and can be specific for each surface.
Heat exchange between the surfaces happens by long wave radiation. This heat exchange is dependent on the view factors and emittance factor of the internal surfaces.
Remark: there is an option in the model the value of the convection coefficient can switch between two values.

-        heat exchange between zones by conduction
Internal and external walls are simulated by a number of nodes. Each with a heat capacity and with heat resistances in between.

-        heat exchange between zones by airflow (ventilation)
Air exchange takes place between ambient and the zone and between neighbouring zones. This air exchange can be user given or calculated according to a network node model.
In Appendix A detailed information is given about the modelling aspects of this process.

-        solar gain and solar exchange between zones
Solar radiation enters a zone by windows. This solar radiation is absorbed in the zone or can leave the zone through windows, to ambient or to a neighbouring zone.
In Appendix B detailed information is given about the modelling aspects of this process.
Incident solar radiation is calculated by VA114's solar processor (see Appendix D).

-        solar shading
Solar shading happens by surrounding buildings, by external façade parts, by own buildings parts and by setback of the window.
In Appendix C detailed information is given about the modelling aspects of this process.

-        and other processes
Like: internal heat production (by persons, equipment and lighting), mechanical ventilation, ….

3.   Modeling Assumptions

In this chapter the modeling assumptions are discussed. First in general and then specific per test case. See the corresponding paragraphs of the Test case specification [6]

Comments/assumptions with respect to the General information

DSF test cases
The DSF test cases are subdivided into 5 groups:
- DSF100: All openings are closed
- DSF200: Openings are open to the outside
- DSF300: Openings are open to the inside
- DSF400: Bottom opening is open to the outside and the top opening is open to the inside (pre-heating mode)
- DSF500: Top opening is open to the outside and the bottom opening is open to the inside (chimney/exhaust mode).

Geography, site location
Outdoor test facility the "Cube" at Aalborg University, Aalborg, Denmark:
- latitude 57,01 degree North
- longitude 10,00 degree East
- Altitude: 19 m above sea level

Weather data
The time on the tape is "standard local time". Total solar radiation on the horizontal and diffuse solar radiation on the horizontal are given; direct normal solar radiation is calculated from the 2 given components.
Wind velocity on the tape is the velocity in the open field at a height of 10 m.

Geometry
Four zones are specified:
- zone 1, the DSF
- zone 2, the zone behind the DSF
- zone 3, the left back zone
- zone 4, the right back zone

The inner dimensions were used to get the right volume. The depth of the zones 3 and 4 is 3,00 m. The wall in between zone 2 and 3 is not adiabatical; so is the wall in between zone 3 and 4.

Remark: with respect to the comparative tests cases the DSF is 20 mm deeper (internal window is moved that distance backwards)

The external and the internal window have an area of 19,37 m^2 (6 * 3,229 m^2): 16,16 m^2 is glazing (83,4%), 3,21 m^2 is frame.

Window properties

The <u>external window</u> has the following properties:

      U-value = 5,36 W/(m^2.K)   (glazing = 5,70 and frame = 3,63)
      g-value = 0,667   (glazing = 0,80 and frame = 0,00)
      C_f-value= 0,017   (glazing = 0,020 and frame = 0,00)

Angular Modifier (AM) of this single glazing:
```
Angle=   0.   15.   30.   40.   45.   50.   60.   70.   80.   90.
AM=    1.032 1.029 1.024 1.012 1.000 0.985 0.921 0.776 0.480 0.000
```
For diffuse solar radiation an incidence angle of 58° is applied.

<u>Remark:</u> above g-value is for perpendicular incident radiation (incident angle is 0°); AM is a multiplier for g-value at 45° incident angle. So as input g-45 has to be used:

      g-45 = 0,667 /1,032 = 0,646   (glazing = 0,775 and frame = 0,00)

The <u>internal window</u> has the following properties:

      U-value = 1,53 W/(m^{2}K)   (glazing = 1,12 and frame = 3,63)
      g-value = 0,525   (glazing = 0,63 and frame = 0,00)
      C_f-value=0,057   (glazing = 0,068 and frame = 0,00)

Angular Modifier (AM) of this double glazing:
```
Angle=   0.   15.   30.   40.   45.   50.   60.   70.   80.   90.
AM=    1.054 1.051 1.041 1.021 1.000 0.973 0.866 0.661 0.338 0.000
```
For diffuse solar radiation an incidence angle of 58° is applied.

<u>Remark:</u> above g-value is for perpendicular incident radiation (incident angle is 0°); AM is a multiplier for g-value at 45° incident angle. So as input g-45 has to be used:

      g-45 = 0,525 /1,054 = 0,498   (glazing = 0,598 and frame = 0,00)

The emissivity of the glazing is 0,84 on both the side to external and the side to internal.

<u>Remark:</u> C_f-value is determined by simulation and interpolation – at what C_f-value is for the given g-value the transmission as prescribed.

<u>Remark:</u> the standard AM's available in the VA114-input were used (for single glazing and for double glazing). Both AM's are given above.

Solar gain

It is assumed the solar gain is for 100% sensible (0% latent) and for 100% radiative (convective part Czon= 0%). There is one exception: in zone 2 the radiative part is 90 % (and so the convective part Czon= 10 %); this to take into account the effect of the lightweight air bags (light materials convert absorbed solar almost immediately into convective heat).

Properties of the constructions

The properties are as specified. However now also thermal bridges are taken into account (by increasing the thermal conductivity of the insulation layer). Table 1 gives the U-value of the several constructions (except window frame and glazing) without and with thermal bridges.

Table 1: U-value of the constructions

Construction	U-value No thermal bridges (in W/(m2.K))	U-value With thermal bridges (in W/(m2.K))
Wall 1	0,049	0,101
Wall 2	0,083	0,170
Wall 3	0,083	0,170
Roof/Ceiling	0,083	0,170
Floor (ground resistance excluded)	0,151 (0,195)	0,257 (0,417)

The constructions have an infrared emittance (emissivity) of 0,88. For the solar absorptance a distinction is made between external (0,40 - this value is estimated; a realistic value for a white surface) and internal (0,34 – from specs).

Heat loss through the floor
The heat loss through the floor (in W/m^2): the ground resistance to the heat transmission is prescribed - 1,5 m^2.K/W (according to the DS 418).
For the given floor construction this results in an overall U-value of 0,15 $W/(m^2.K)$; so a heat loss of 1,5 W/m^2 (temperature difference is 20 – 10 = 10 K)

Remark: this value is about the same as the heat loss calculated based on ISO-13370

> According to ISO-13370 (slab on ground)
> The floor has the prescribed construction and is assumed to be above a 0,50 m layer of soil. The properties of the soil are not specified. Taken is:
> - thermal conductivity = 1,75 W/(m.K)
> - Specific mass = 1500 kg/m^3
> - Specific heat = 1500 J/(kg.K)
>
> Assumption for the heat loss:
> Internal zone temperature = 20 ^oC - constant during the year
> External temperature during the year = 9,1 ^oC with minimum 0,6 ^oC and maximum 16,8 ^oC.
>
> Calculated heat loss through the floor according to ISO-13370 (slab on ground):
> $Q_{floor} = 1,76 + 0,86 \cos (arg)$
> With
> Arg = argument, that is a function of time of the year.
>
> Soil properties have some influence on this heat loss [5].

Remark: with thermal bridges included the U-value of the floor is 0,26 $W/(m^2.K)$

Heat loss from zone 2 to the back zones 3 and 4
The temperature in zone 3 and zone 4 are known from the measurement. The simulation takes the properties of the construction and a fixed temperature in zones 3 and 4 (as a mean temperature over the simulation period) into account

Heat loss by infiltration
By blow test the air tightness of the "Cube" was measured for both cases (DSF100_e – windows closed and DSF200_e – windows open).
Based on that measured air tightness the properties of cracks in the several walls were determined (under the assumption that for the DSF100_e case the leakage is uniformly distributed over all 4 facades; cracks at 0,10 m and at 5,50 m height)

Convective Surface Coefficients
The internal convective surface coefficients are constant and assumed to be 3,0 W/(m^2.K); the external convective surface coefficients are constant and assumed to be 18,0 W/(m^2.K).

Radiative Surface Coefficients
The radiative surface coefficients are calculated based on mean temperature, view factors and infrared emittance.
External sky radiation is calculated based on clouds cover, vapour pressure (location Arnhem – the Netherlands)

Pre-conditioning period
Weather files are available for a period of 2-3 weeks. VA114 works with a pre-conditioning period of 42 days. Normally 42 days before the starting date is taken. Now this is not possible, therefore 42 times the first day is taken.

Temperature control in the zones
The zones 2, 3 and 4 are equipped with a 100% convective heating and cooling device. The capacity of these devices are assumed to be infinite.

The control temperature is the air temperature.

The set point temperature for heating and cooling is the same (bang-bang), so no dead-band.

Each zone has its specific set point.

Comments/assumptions with respect to test case DSF100_e

Heat loss through the floor
Ground temperature was put at 10,0 ^{o}C.

Set points of heating/cooling device
The set points of the heating/cooling devices are:
- zone 1: no set points – free floating
- zone 2: 21,8 ^{o}C
- zone 3: 18,3 ^{o}C
- zone 4: 12,3 ^{o}C

Air tight ness
Measured relation: dP = 217,59 * (Ach)^{1,3624}; For uniformity - used relation: dP = 228 * (Ach)^{1,40}

Comments/assumptions with respect to test case DSF200

Heat loss through the floor
Ground temperature was put at 10,0 ^{o}C.

Set points of heating/cooling device
The set points of the heating/cooling devices are:
- zone 1: no set points – free floating
- zone 2: 21,8 ^{o}C
- zone 3: 18,5 ^{o}C
- zone 4: 14,7 ^{o}C

Air tight ness
Measured relation: dP = 203,14 * (Ach)^{1,3998}; For uniformity - used relation: dP = 203 * (Ach)^{1,40}

Window openings
The size of the window openings is determined by:
    3 x free opening area (0,20 m^2) + 2 x side area of opening (0,075 m^2) = 0,75 m^2
Data shown is for the comparative cases and is for both top and bottom openings.

For the empirical cases the size of the top and bottom openings are smaller and different:
    Top: 0,41 m^2
    Top: 0,49 m^2

Figure 3. Free opening area
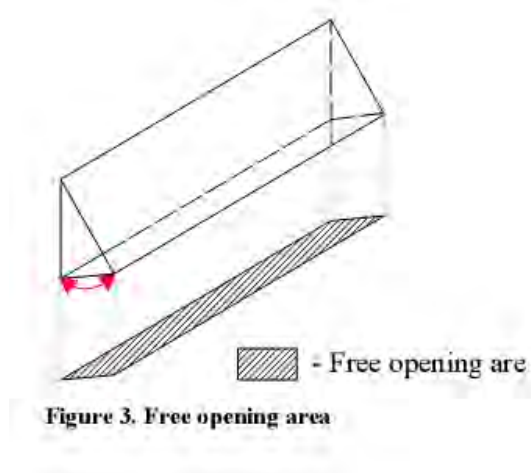
The discharge coefficient differs from the specs: VA114 uses 0,61 for both supply and exhaust openings, the specs set that coefficient to 0,65 for the supply openings and 0,35 for the exhaust openings.

Wind pressure coefficients differ from the specs: the VA114-table is applied (source AIVC) . Moreover VA114 assumes coefficients for top and bottom openings are the same (see chapter 5); the specs prescribe different coefficients for top and bottom

The internal convective surface coefficients in zone 1 (DSF has air flow through it) are unchanged: 3,0 W/(m^2.K).

Wind speed profile

The measured wind speed profile corresponds with:

$$Vh/Vh10 = 0,288 * \ln (h/0,31)$$

VA114 works with the relation of Davenport. For flat, open terrain it says:

$$Vh/Vh10 = 0,922 * (h/6,0)^{0.16}$$

These relations look very different, but at roof height (6,0 m) the specified relation gives Vh/Vh10 = 0, 853 whereas Davenport gives Vh/Vh10 = 0,922. So VA114 works with a 8 % higher wind speed. In the table below the difference is given as function of height.

Table 2: Ratio Vh/Vh10 (Windspeed at height h resp. at h= 10 m)

Height (m)	Specs	VA114
1	0,34	0,69
2	0,54	0,77
3	0,65	0,83
5	0,80	0,90
7	0,90	0,95
10	1,00	1,00
20	1,20	1,12

4. Modelling Options

Applied modelling options.

Infrared heat exchange (see chapter 2)
Infrared heat exchange within a zone works with view factors between the internal surfaces and with emittances of that internal surfaces. The view factors are calculated with a detailed Ray-tracing method, which is applicable for all shapes of zones

Heat exchange between zone by airflow - ventilation (see chapter 2)
Air exchange takes place between ambient and the zone and between neighbouring zones. This air exchange is calculated according to a network node model (model vent2). Air flow by thermal buoyancy, wind pressure and wind fluctuations. Calculation is based on properties of openings (cracks, open windows, …), actual temperatures, wind velocity and wind direction.

Solar distribution over the internal surfaces (see chapter 2)
Direct radiation and diffuse radiation are treated separately.
For the direct radiation it is calculated which internal surfaces are hit; such a surface absorbs a part of that direct radiation and reflects the rest diffusely.
The direct solar distribution is calculated with a detailed Ray-tracing method, which is applicable for all shapes of zones
The distribution of the diffuse radiation (through windows and the reflected direct radiation by internal surfaces) is calculated by the view factors (see above) and by the reflections (= 1,0 – absorptance) of the internal surfaces.

Solar shading (see chapter 2)
External façade parts, own building parts and set back of window cause both shading of the direct solar radiation and shading of the diffuse solar radiation. The direct shading is calculated by a detailed Ray-tracing method, which is again applicable for all shapes of zones.
Surrounding buildings can be submitted (input) to the program as external façade parts too. In that way both shading of the direct solar radiation and shading of the diffuse solar radiation is calculated.
For the diffuse shading a detailed Ray-tracing method is applied.

5.   Modeling Difficulties

Window modelling (all DSF-cases)

The window can be modelled in several ways:
-     as one construction (glazing and frame combined - method fg0)
-     as two constructions (glazing and frame separately); 3 ways are distinguished:
    -     frame one part, each of the 12 glazing parts separately (method fg1)
    -     frame one part, glazing one part – both height and width of glazing smaller than window dimensions (method fg2)
    -     frame one part, glazing one part – height of glazing same as window height, width of glazing smaller than window width (method fg3).

Each method has its advantages and disadvantages:
-     method fg0 is easy to model, but window surface temperature (= mix of glazing and frame temperature) differs from the glazing temperature (a required output result)
-     method fg1, fg2, fg3 require more detailed input, but give the right glazing temperatures
-     method fg3 has the window openings at the right height; important in modelling thermal buoyancy.
-     …..

Method fg3 was selected

Figure 1: : frame (f) and glazing (g) separated

```
 ---------------------------
|     |               |     |
|     |               |     |
|     |               |     |
|     |               |     |
|frame|   Glazing     |frame|
|     |               |     |
|     |               |     |
|     |               |     |
 ---------------------------
```
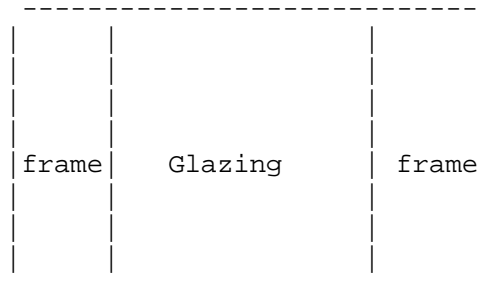
Modelling of internal window (all DSF-cases)

The internal window model used by VA114 was improved since the former tests: the real optical properties of the glazing part (the real transmission and the real absorption in the panes) are taken into account :
-     transmission of solar radiation = Trsm
-     absorption in the glazing panes = Abs,i
-     reflection of solar radiation = 1 – Trsm – Sum(Abs,i)
-     Angular Modifier (AM) = 1,0

The transmission Trsm and the absorptions Abs,i are derived from the g-value, the C_f-value and the U-value.

Modelling of window openings (DSF200-cases)

In VA114 per window 2 openings can be defined, each with their own dimensions and position within the glazing area.

Figure 2: : Window can have 2 openings

```
 _____
|   _____                  |
|  |      |                 |
|   _____                  |
|                           |
|                ____       |
|               |    |      |
|                ____       |
 _____
```
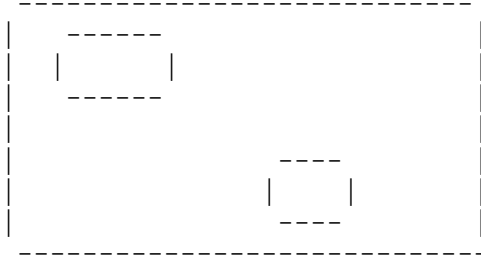
In test case DSF200 the bottom openings have not the same size as the top openings:
bottom 0,49 m^2 and top 0,41 m^2

In figure 2 the glazing dimensions and the position of both openings are given.

Figure 2: Glazing dimensions and position of both openings

```
-----.-----2,965-----.------
|    | ============ |    |
|    | | 1,37*0,30 | |    |   Height 5,060 – 5,360
|    | ============ |    |
|    |              |    |       ^
|    |              |    |       |  difference 4,990
|Frame|  Glazing    |Frame|      |
|    |              |    |       v
5,450|              |    |
|    | ============ |    |
|    | | 1,63*0,30 | |    |   Height 0,080 – 0,038
|    | ============ |    |
-----.--------------.------
<- - - - - - 3,555 - - - - - >
```
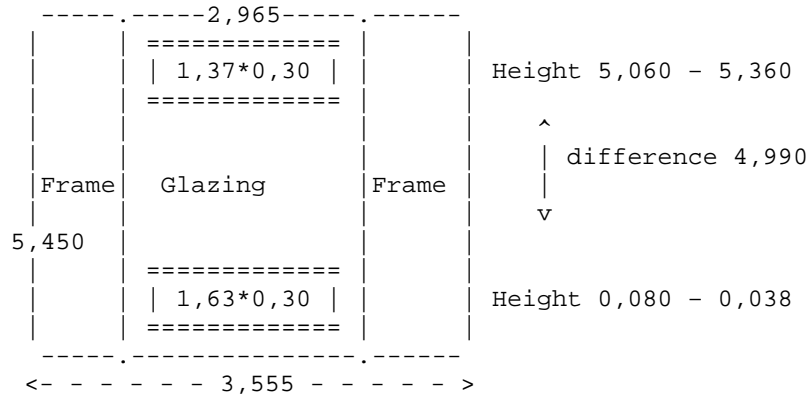
Each of the two openings is modelled by two "cracks":
Length of cracks = width of opening
Height of crack1 = 0,28 * height of opening
Height of crack2 = 0,72 * height of opening
C-value of cracks = 0,40 * height of opening
Discharge coefficient used in the determination of C-value is 0,61 (both for top and bottom openings) in stead of the prescribed 0,65 for supply openings and 0,35 for exhaust openings.

Window openings are fully open and not controlled. All restrictions (window is not allowed to open) are excluded, so the window is open 24 hours a day.

Modelling of airflow

Air flow is calculated based on actual wind speed and wind direction, the actual ambient temperature and the zone temperature of the former time step (Tzone (hour-1))

Calculation of air flow is only possible in case cracks are present in all zones. There are cracks in each zone; properties are determined from air tightness data..

Wind pressure coefficients

In the DSF-test specifications the Cp-values of the top openings are different from those of the bottom openings. VA114 have one Cp-value on a façade, so Cp-values for top and bottom openings are the same.
VA114 makes use of the AIVC-table; values in that table are different from the DSF-table (See figure 3). Cp-values are available for each 45 degrees; rather rough. Interpolation between these values was done.

Figure 3: Wind pressure coefficients according to specs and according to VA114-table

Cp-value distribution
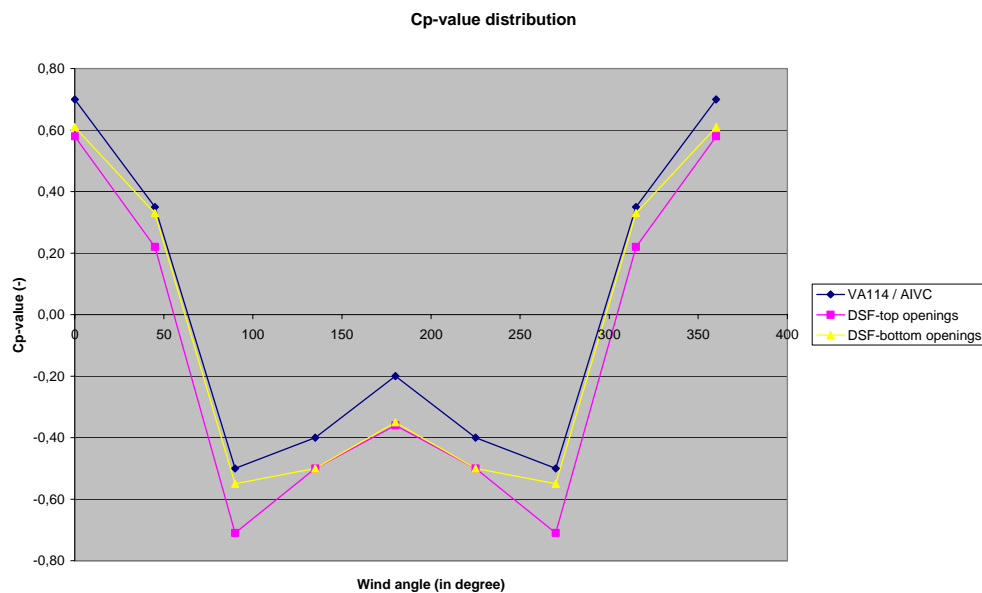
Downward and upward flow separate in the output

How to distinguish? Driving forces are buoyancy and wind. Wind by pressure drop and by wind fluctuations. In the VA114-model the wind pressure difference = 0,0: openings are on the same façade (so wind pressure coefficients are independent on the height).

Observed air flows:
- Air flow in occurs at the bottom openings (through both "cracks") and air flow out at the top openings (through both "cracks") – see figure 4a.
- In some cases in- and outflow occurs both at the bottom and top openings (one "crack" in, second "crack" out) - see figure 4b.
- It also happens air flow in occurs at the top openings and air flow out at the bottom openings – see figure 4c.

Figure 4a: In- and outflow, upward flow

```
        ------------
       |            |
     / | ← 630      |
       | ← 600      |
       |            |
       |     ^      |
       |     |  1230 |
       |            |
       |            |
     / | → 600      |
       | → 630 kg/h |
        ------------
```
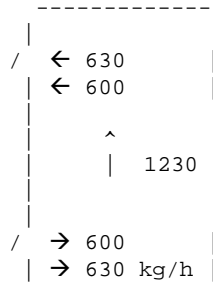
Figure 4b: In- and outflow, upward and downward flow

```
        ------------            ------------
       |            |          |            |
     / | ← 400      |        / | → 400      |
       | → 200      |          | ← 200      |
       |            |          |            |
       |    | ^     |          |    | ^     |
       |200? v | 400?|         |400? v | 200?|
       |            |          |            |
       |            |          |            |
     / | ← 200      |        / | → 200      |
       | → 400 kg/h |          | ← 400 kg/h |
        ------------            ------------
```
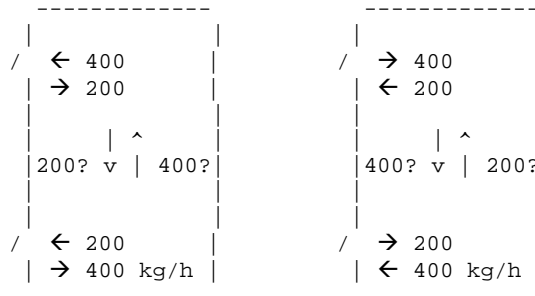
Figure 4c: In- and outflow, downward flow

```
        ------------
       |            |
     / | → 210      |
       | → 200      |
       |            |
       |    |       |
       |    v   410 |
       |            |
       |            |
     / | ← 200      |
       | ← 210 kg/h |
        ------------
```
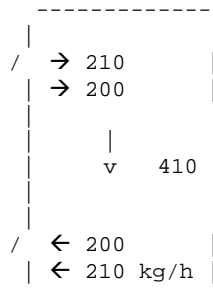
In situation 4a there is a resulting upward flow (+) and in situation 4c a resulting downward flow (-). In both situations the resulting flow is equal to the amount of fresh ambient air that is entering. In situation 4b the resulting flow is upward (+200 kg/h) in the left figure and down ward in the right figure (-200 kg/h); but both different from the amount of fresh air that is entering (600 kg/h).

In the results the fresh air amount should be given, but giving that amount with a '+' or '-' sign to indicate upward or downward flow results in a jump from + to – in the air flow plot.

So it is not easy to give upward and downward flow separately in the output.

Remark: in the DSF the real air flows can/will be higher than the fresh air amount because of recirculation in the DSF.

6. Software errors discovered and/or Comparison between different versions of the same software.

The following software errors were discovered and corrected.

The internal window model

It was found the internal window model was too simple:
- transmission = g-value
- absorption in the panes = 0,0
- reflection of the window = 1,0 – g-value
- Angular Modifier = 1,0

The internal window model used by VA114 was improved: the real optical properties of the glazing part (the real transmission and the real absorption in the panes) are taken into account :
- transmission of solar radiation = Trsm
- absorption in the glazing panes = Abs,i
- reflection of solar radiation = 1 – Trsm – Sum(Abs,i)
- Angular Modifier (AM) = 1,0

The transmission Trsm and the absorptions Abs,i are derived from the g-value, the C_f-value and the U-value.

The sub model for air flow by wind fluctuations

In Appendix AA this model is described.

In the original version the wind coefficient C_1 was 0,01 and the wind velocity was the wind velocity at roof height. The way of sheltering had no influence on the velocity in the window opening.

After studying literature it was found the C_1 is dependent on the way of sheltering (exposed $C_1=$ 0,004 , semi-exposed $C_1= 0,002$, sheltered $C_1 =0,001$) and the wind velocity should be the wind at a local weather station. The model was revised for those points.

In figure 5 a comparison is made between the original model and the revised model for October 8th, a windy day (see figure 6); the temperature difference between DSF-zone and ambient was within a few degrees (see figure 7). In figure 5 also the measured air flow is given.

Conclusions:
From figure 5 the following conclusions can be drawn:

1. The revised model gives an lower air flow than the original model.

2. The empirical data shows a strong wind dependency, which is not found from the VA114 sub model for air flow by wind fluctuations. This point to the difference in Cp-value between top and bottom opening, that is not taken into account by VA114.

It seems to be necessary to extend the VA114 model with different Cp-values for different positions on a façade.

Figure 5: Air flow by the original and the revised air flow model; measured air flow
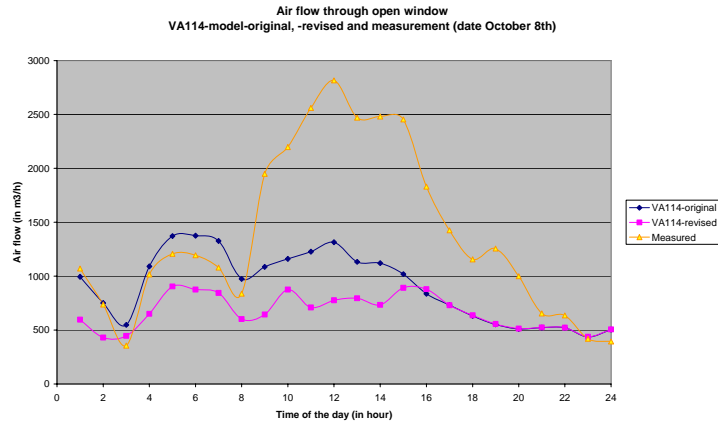
Figure 6: Wind velocity on October 8th, a windy day
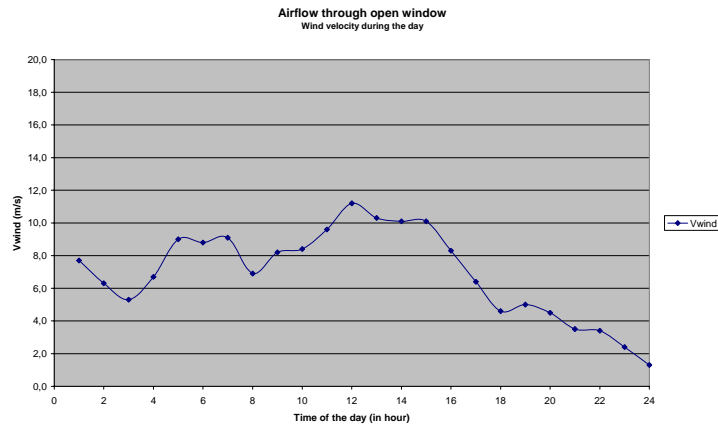
Figure 7: Temperature difference between DSF-zone and ambient – October 8th
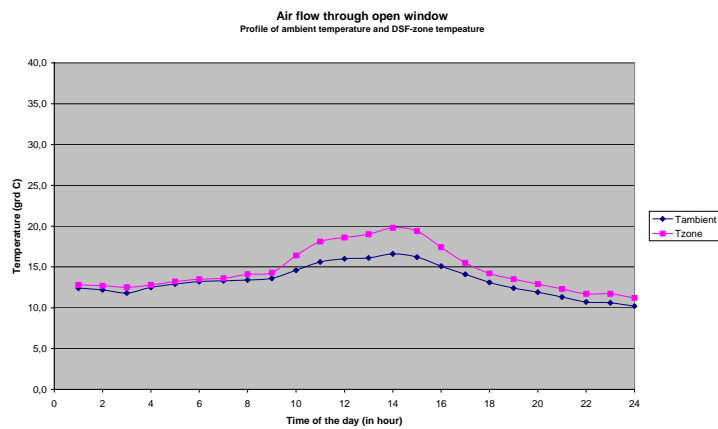
7. Results

DSF100_e

The results of test case DSF100_e are given in file "Output Results DSF100_e-20080207.xls":
19 days with hourly results for the specified output parameters.

Totals during the 19-day's period:
Heating	154 kWh
Cooling	-59 kWh

Peak power used:
Heating	0,81 kW
Cooling	-2,94 kW

Net solar gain:
Incident on the DSF	473 kWh
Solar transmitted to zone 1	342 kWh
Solar transmitted to zone 2	157 kWh
Absorption by internal window	xxx kWh (is calculated, but not in output available)

Extreme temperatures:
Maximum zone 1	29,9 °C
Minimum zone 1	3,3 °C
Mean zone 1	13,5 °C

DSF200_e

The results of test case DSF200_e are given in file "Output Results DSF200_e-20080207.xls":
15 days with hourly results for the specified output parameters.

Totals during the 15-day's period:
Heating	60 kWh
Cooling	- 128 kWh

Peak power used:
Heating	0,53 kW
Cooling	-2,61 kW

Net solar gain:
Incident on the DSF	766 kWh
Solar transmitted to zone 1	549 kWh
Solar transmitted to zone 2	238 kWh
Absorption by internal window	xxx kWh

Extreme temperatures:
Maximum zone 1	22,9 °C
Minimum zone 1	6,2 °C
Mean zone 1	14,1 °C

Discussion :

Results are presented for the specifications and assumptions mentionned in this Modeler Report.
There are still some question marks :

-   The air bags in zone 2 are modelled by a radiative part of solar is 90% (Czon= 10% ; i.e. 10% of the solar radiation goes direct as convective heat to the zone air node) instead of 100% (Czon= 0%) ; this is a default value for VA114, but this assumption requires some more background.
-   Air tightness was assumed to be uniformly distributed over the 4 facades of the Cube.
-   VA114 works with constant convective heat transfer coefficients (internal 3,0 W/(m^2.K) and external 18,0 W/(m^2.K)), so independent of air movement, air flow and wind
-   …………….

Comparison with measured data and with results of the other programs and evaluation of that comparison should lead to an answer on those points.

8.   Other

Solar on a clear sky

Solar data was checked for a clear sky: the solar intensity on the horizontal and the solar height should have their maximum at the same time (see figure 8.1).

The day selected was October 25, 2006.

As can be seen: the profiles are in very good agreement / are synchronical.

Figure 8.1:   Solar intensity on the horizontal and solar height on a clear day - normalized
Calculations for the location "The Cube", Aalborg University

Total solar radiation and solar height on October 25
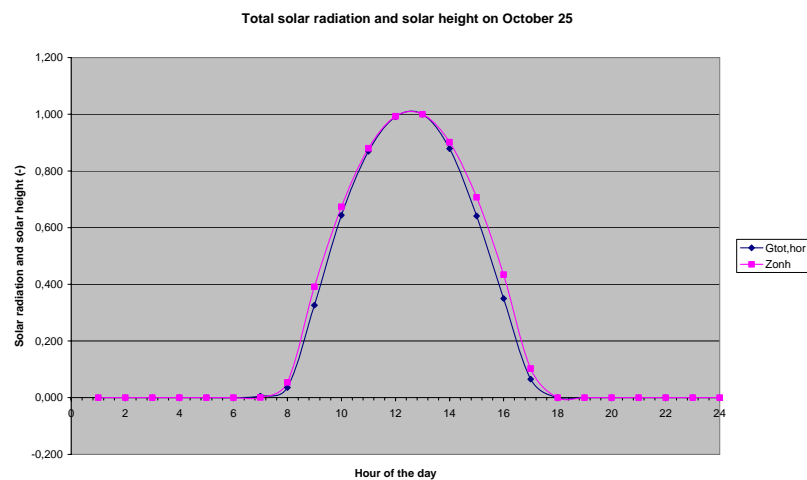
Final remark:

VA114 has an option to simulate the DSF not as separate zone, but as a single, ventilated component. Ventilation can be done in all thinkable ways. These simulations are not done yet, but can/will be done in future.

9. Conclusions and Recommendations

VABI Software bv does developments on the Building simulation program VA114. The program was subjected to the IEA34/43 DSF-Empirical-tests [6].

In this modeller report information about the program, about the tests and about the results are given.

Results are presented for the specifications and assumptions mentionned in this Modeler Report.

Remark

At the Glasgow – meeting (October 2007) the 'final' results were discussed for the first time. This lead to some extra exercises:
- Determination of the properties of the glazing with WIS
- The Steady State test

and some changes :
- U-value of the glazing of the internal window became 1,12 $W/(m^2.K)$ instead of 1,20
- The presence of cold bridges

The results in this report should be considered as final results.

10. References

[1] Judkoff, R and Neymark, J
 "International Energy Agency Building Energy Simulation Test (BESTEST) and Diagnostic Method", IEA: SHC Task 12 / ECBCS Annex 21, February 1995.

[2] Soethout, L. L.
"BESTEST Kwalificatietesten uitgevoerd aan het gebouwsimulatieprogramma VA114, versienummer 1.35". TNO-rapport 98-BBI-R0830, mei 1998.

[3] Wijsman, A.J.Th.M.; Plokker, W.
"Eerste thermische gebouwsimulatieprogramma's ondergingen de keurmerktest".
TVVL Magazine, augustus 1999.

[4] Kalyanova, O. and Heiselberg, P.
"Comparative Test Case Specification – Test cases DSF100_2, DSF200_3, DSF200_4 and DSF400_3", IEA: SHC Task 34 / ECBCS Annex 43, April 2007.

[5] Wijsman, A. J. Th. M.
"Double Skin Façade – Modeler Report; Comparative Test cases", Vabi Software bv, April 2007.

[6] Kalyanova, O. and Heiselberg, P.
"Empirical Test Case Specification – Test cases DSF100_e and DSF200_e.", IEA: SHC Task 34 / ECBCS Annex 43, April 2007.

[7] Wijsman, A. J. Th. M.
"Double Skin Façade – Modeler Report; Empirical Test cases", Vabi Software bv, April 2007.

[8] Wijsman, A. J. Th. M.
"Double Skin Façade – Modeler Report; Comparative Test cases", Vabi Software bv, June 2007.

[9] Wijsman, A. J. Th. M.
"Double Skin Façade – Modeler Report; Empirical Test cases", Vabi Software bv, June 2007.

Appendix A: Heat exchange by airflow

Model description

Air exchange takes place between ambient and the zone and between neighbouring zones. Air exchange occurs through cracks and other openings in walls. Processes that are responsible for these airflows are:
- thermal buoyancy
- wind pressure and wind fluctuations
- mechanical imbalance over a zone

In figure A.1 this is given schematically

```
                M-In            M-Out           M-In
                 |               ^               |
                 |               |               |
      ----|------------|------------|------
         |     |       |   |       |     |   |
     <-|-   v  |       |   |       v   - |  ->
         |     |       |   |       |     |   |
 Wind    |     |       |   |       |     |   |
 === >   |     |       |   |       |     |   |
         |     |     <.-     <- - - -    |   |
         |     |       |       |         |   |
     - - | - >     - - -.->      -.>      <|-
  v      |               |       |        |       vv
      -------------------------------------------------------
```
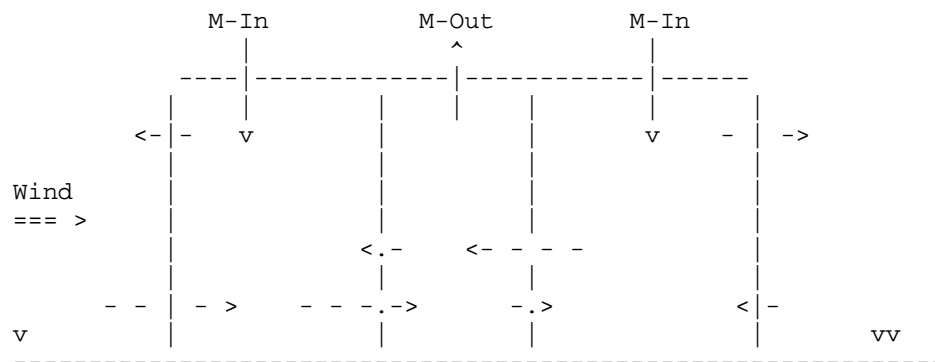
Figure A.1: Airflows in a building

In subroutine "VENT" the airflows are determined. Three models are available:
- subroutine "VENT1":
  In- and exfiltration flows are calculated based on an empirical relation for the air exchange rate. Interzonal flows are user given. In case of mechanical imbalance these in- and exfiltration flows and interzonal flows are adjusted to obtain balance.
- subroutine "VENT2":
  In- and exfiltration flows and interzonal flows are calculated with a nodal network. Thermal buoyancy, wind pressure, wind fluctuations and mechanical imbalance are taken into account.
- subroutine "VENT3":
  Airflows are calculated by interpolation between data from a database (depending on wind velocity and wind direction, ambient temperature and zone temperatures).

Some more information about the models will be given now. All models use as wind velocity the wind velocity at roof height.

Wind velocity at roof height

Available is the wind velocity from weather tape. That wind velocity is measured at a height of 10 m in a flat, open terrain. The wind velocity used in the models is the wind velocity at roof height. With the local circumstances (flat open terrain / woods, hilly terrain, villages, suburbs / town centre) and the relations of DAVENPORT the wind velocity at roof height is determined:

```
IWVELD = 1  A.    Flat, open terrain
                  Vwindh = Vwind6 * (Height/  6.)**0.16

IWVELD = 2  B.    Woods, hilly terrain, villages, suburbs
                  Vwindh = Vwind6 * (Height/ 46.)**0.28

IWVELD = 3  C.    Town centre
                  Vwindh = Vwind6 * (Height/104.)**0.40
```

In these relations is Vwind6 the wind velocity at a height of 6 m in flat, open terrain. With relation A:

```
                  Vwind6 = Vwind10 * (6./10)**0.16
                         = 0.922 * Vwind10
```

- subroutine "VENT1"

In- and exfiltration flows are calculated based on an empirical relation for the air exchange rate. Interzonal flows are user given. In case of mechanical imbalance these in- and exfiltration flows and interzonal flows are adjusted to maintain balance. The so-called SIMPLE model.

Relation for the infiltration rate Fv (in times per hour):
```
     Fv = Fva + Fvb*Vwind + Fvc*Vwind**2
```
Fva, Fvb and Fvc are given by user input. Vwind is wind velocity at roof height.

In- and exfiltration flows follow from multiplying the infiltration rate with the volume of the zone. In principle the infiltration flow is equal to the exfiltration flow

The interzonal airflows are given by user input. In principle the interzonal air flow from zone I to zone J is equal to the interzonal air flow from zone J to zone I.

In case of mechanical imbalance above mentioned airflows are adjusted based on the air balance for that zone

-   subroutine "VENT2"

In- and exfiltration flows and interzonal flows are calculated with a nodal network. Thermal buoyancy, wind pressure, wind fluctuations and mechanical imbalance are taken into account.

Method uses zone temperatures at the end of the last time step and ambient temperature, wind velocity and wind direction of the present time step. The so-called DETAILED model

In general:

The airflow through a crack is given by

```
Flow = L . C . DP^1/N
```

width

```
L  =  crack length
C  =  air leakage coefficient of crack.
N  =  1/power coefficient
DP =  pressure difference across crack
```

A crack is characterized by its C and N. Common value for $N = 1,5$

Required input parameters:
- crack length L
- characteristics (C and N) of crack
- height at which crack is positioned

Crack height is important for calculation of thermal buoyancy. For calculation of airflows because of wind pressure differences are required:
- wind pressure coeffients CD
- wind velocity at roof height
- wind direction

In general:

Wind pressure = CD * Pthrust

with

CD	= wind pressure coefficient
Pthrust	= thrust = 0.5 * Rho * (Vwind)**2
Rho	= specific mass of ambient air
Vwind	= wind velocity at roof height

The wind pressure coefficients are available in table A.1 – source AIVC.

With the local circumstances (exposed, semi-exposed, sheltered) , the building height (< 3 storeys, 4-6 storeys, > 6 storeys), building shape (ratio length/width), wind direction and orientation of the façade in which the crack is present the CD-value is determined

Remark: a window opening is modelled by 2 cracks. After calculation of the airflows through that window the flows are corrected for wind fluctuations. By these fluctuations the in- and outflow through this window opening increase.

Calculation method

From the air balances for the several zones (sum of entering air flows = sum of leaving air flows) the pressure in each zone can be determined.
The relation between flow and pressure drop across a crack is not lineair, which makes the solution not so easy. Therefore the relation between flow and pressure drop

```
Flow = L . C . DP^(1/N)
```

is made linear

```
Flow = CLP . DP
```

with

```
CLP = L . C . DP^(1/N-1)
```

The calculation process is iteratively:
- make a first estimation of the pressures in the zones
- calculate the coefficients CLP
- calculate the pressures in the zones: the air balances over the zones give N-equations (the number of zones) with N-unknowns (the pressures in each zone). By matrix solving all pressures are known.
- calculate the coefficients CLP again
- and so on

The airflow through each crack can now be calculated based on the known pressures.

Table A.1: Wind pressure coefficients CD

```
Igeval IWbw IWdim IWbst IWvlk  1    2    3    4    5    6    7    8    9
   1     1    1     1     1    .70  .53  .35 -.08 -.50 -.45 -.40 -.30 -.20
   2     1    1     1     2    .70  .53  .35 -.08 -.50 -.45 -.40 -.30 -.20
   3     1    1     1     3   -.60 -.60 -.60 -.60 -.60 -.60 -.60 -.60 -.60
   4     1    1     1     4   -.40 -.45 -.50 -.55 -.60 -.55 -.50 -.45 -.40
   5     1    1     1     5   -.10 -.25 -.40 -.50 -.60 -.50 -.40 -.25 -.10
   6     1    1     2     1    .40  .25  .10 -.10 -.30 -.33 -.35 -.28 -.20
   7     1    1     2     2    .40  .25  .10 -.10 -.30 -.33 -.35 -.28 -.20
   8     1    1     2     3   -.60 -.55 -.50 -.45 -.40 -.45 -.50 -.55 -.60
   9     1    1     2     4   -.35 -.40 -.45 -.50 -.55 -.50 -.45 -.40 -.35
  10     1    1     2     5   -.10 -.30 -.50 -.55 -.60 -.55 -.50 -.30 -.10
  11     1    1     3     1    .20  .13  .05 -.10 -.25 -.28 -.30 -.28 -.25
  12     1    1     3     2    .20  .13  .05 -.10 -.25 -.28 -.30 -.28 -.25
  13     1    1     3     3   -.50 -.50 -.50 -.45 -.40 -.45 -.50 -.50 -.50
  14     1    1     3     4   -.30 -.35 -.40 -.45 -.50 -.45 -.40 -.35 -.30
  15     1    1     3     5   -.08 -.19 -.30 -.40 -.50 -.40 -.30 -.19 -.08
  16     1    2     1     1    .50  .38  .25 -.13 -.50 -.65 -.80 -.75 -.70
  17     1    2     1     2    .60  .40  .20 -.35 -.90 -.75 -.60 -.48 -.35
  18     1    2     1     3   -.70 -.70 -.70 -.75 -.80 -.75 -.70 -.70 -.70
  19     1    2     1     4   -.60 -.63 -.65 -.68 -.70 -.68 -.65 -.63 -.60
  20     1    2     1     5   -.18 -.32 -.45 -.53 -.60 -.53 -.45 -.32 -.18
 210     1    2     2     1    .28  .18  .07 -.15 -.35 -.47 -.59 -.55 -.50
 220     1    2     2     2    .39  .29  .18 -.22 -.60 -.53 -.46 -.37 -.28
 230     1    2     2     3   -.60 -.59 -.58 -.60 -.61 -.60 -.58 -.59 -.60
 240     1    2     2     4   -.53 -.55 -.56 -.56 -.56 -.56 -.56 -.55 -.53
 250     1    2     2     5   -.18 -.31 -.43 -.43 -.42 -.43 -.43 -.31 -.18
  26     1    2     3     1    .06 -.03 -.12 -.16 -.20 -.29 -.38 -.34 -.30
  27     1    2     3     2    .18  .17  .15 -.08 -.30 -.31 -.32 -.26 -.20
  28     1    2     3     3   -.49 -.48 -.46 -.44 -.41 -.44 -.46 -.48 -.49
  29     1    2     3     4   -.45 -.46 -.46 -.44 -.41 -.44 -.46 -.46 -.45
  30     1    2     3     5   -.18 -.29 -.40 -.32 -.23 -.32 -.40 -.29 -.18
```

```
- IWbouw  = 1 : low buildings (\< 3 storeys)
            2 : middle high buildings ( 4 - 6 storeys)
            3 : high buildings (> 6 storeys)
- IWdim   = 1 : length/width   1 : 1
            2 :                2 : 1
- IWbeschut= 1 : exposed
             2 : semi-exposed
             3 : sheltered
- IWvlak  = 1 : at the long side
            2 : at the short side
            3 : roof angle < 10 degree
            4 : 10 degree < roof angle < 30
            5 : roof angle > 30 degree
- IWricht = 1 :   0.0 degree
            2 :  22.5 degree
            3 :  45.0 degree
            . :  .... degree
           17 : 360.0 degree
```

Remark: coefficients for IWbouw=2 and 3 (middle high and high buildings) are not available at the moment.. It is assumed they are equal to the coefficient for low buildings IWbouw=1

Source:

Air Infiltration and Ventilation Centre Handbook: 'Air infiltration Calculation Techniques - an Application Guide' (Liddament, 1986).

Open windows

Modelling can again be done in the simple way (air flow by open window is user given) or in the detailed way (air flow by open window is calculated).

The model user should specify each window to open in each zone. In figure A.2 this is given schematically

```
     --------------------------------------------------
    |                                                  |
    |   ---------------------------------------        |
    |  |              L9              Window   |       |
    |  |   -----------                         |       |
    |  |  | Part 2    |                         |       |
    |  |  | to open  L8                         |       |
    |  |  |           |                         |       |
    |  |   ----L7-----                          |       |
    |  |                                      L2|       |
    |  |                                        |       |
    |  |                                        |       |
    |  |   -----------                          |       |
    |  |  | Part 1    |                         |       |
    |  |  | to open  L5                         |       |
    |  |  |           |                         |       |
    |  |   ----L4-----                          |       |
    | |              L6                         |       |
    |  ----------------------L1-----------------        |
    |                                      L3  Wall     |
     --------------------------------------------------
```
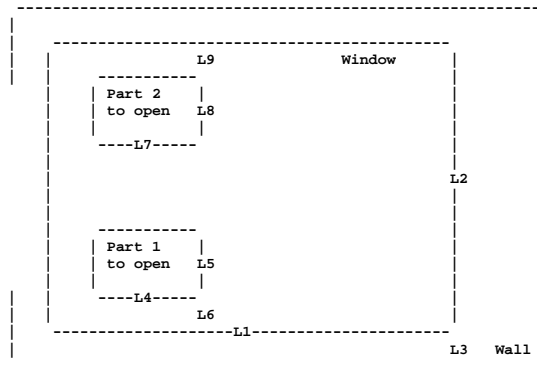
Figure A.2: Geometry of window parts to open

It should be specified what type of window opening it is:
-   open it by moving in horizontal direction
-   open it by moving in vertical direction
-   …………

For each type of window opening in the model a translation is made to above shown geometry.

Each of the two openings is modelled as two cracks. Each crack has the following specs:
-   crack length L
-   characteristics (C and N) of crack
-   height at which crack is positioned

And other …….

Control of window opening

Control of the window at day time operation and at night time operation can be selected independently.

General restrictions can be selected why windows are not allowed to be opened (danger for breaking in during weekend and night time, ambient noise during office hours). Also weather restrictions (too cold outdoors, too windy outdoors, ……) can be specified.

In case there are no restrictions windows open if indoor temperature Tzone comes above a given level (given by user input) and they close if temperature becomes below that temperature.

A window can have 5 opening positions between 0 % open (window is closed) and 100 % open (window at maximum position).

In time the position can be fixed (say for instance position 2) or variable (between position 1 and 5).

Variable window opening:
- if Tzone > Topen then window goes 1 position more open
- if Tzone < Topen then window goes 1 position more close.

Possible is for instance a fixed opening position at night time (people are not present) and a variable position at day time (people are present).

To prevent draught:
In case air velocity indoors comes above a certain level (given by user input) the window will go one position more close

Remark: Air flow by wind fluctuations through window openings is not modelled by other programs. Therefore in Appendix AA a description of the VA114-submodel is given.

Appendix AA: Air flow by wind fluctuations

Introduction
In IEA34/43 subtask E (DSF = Double Skin Facade) tests on Building Performance
Simulations programs are conducted. One process that is tested is the ventilation of
the DSF, i.e. the air flow through the DSF.

VA114's ventilation model takes 3 processes into account:
- air flow by thermal buoyancy
- air flow by wind pressure and by wind fluctuations
- air flow by mechanical imbalance over a zone

In appendix A all processes are described in short. Other participating programs take
these processes also into account except air flow by wind fluctuations.

On request a short description of the sub-model for air flow by wind fluctuations is
given in this memo.

Remark: VA114 works with one Cp-value for the entire façade, so in case there are no cracks or
openings in one of the other walls the air flow by wind pressure will be 0,0.

The model for air flow by wind fluctuations

Wind on a single sided window opening, that is part of a further air tight zone, will
cause an air flow through one half of the window opening the zone in and an air flow
through the other half of the window opening the zone out. The mean velocity of the
air is given by:

$$V_{oprm} = SQRT \ (C_1 {*} V_{wind}^2 + C_3) \tag{1}$$

With

V_{oprm} = mean velocity of the air through the window opening to inside
V_{wind} = wind velocity at a local weather station

The coefficient C1 is depending on the sheltering:
- $C_1 = 0,004$ for exposed situations
- $C_1 = 0,002$ for semi-exposed situations
- $C_1 = 0,001$ for sheltered situations

The coefficient $C_3 = 0,01$; that means that in case there is no wind there is basic mean
velocity of $V_{oprm} = 0,1$ m/s.

So at a wind of 0 m/s the $V_{oprm} = 0,1$ m/s; at a wind of 10 m/s the $V_{oprm} = 0,33$ m/s for
a sheltered situation and 0,64 m/s for an exposed situation.

During a gust of wind locally the wind will be higher: $V_{wind, max}$. And so the V_{oprm}:

$$V_{oprm,max} = \text{SQRT} (C_1 * V_{wind,max}^2 + C_3) \qquad (2)$$

Moreover it is assumed:

$$V_{wind, max} = 2,0 * V_{wind} \qquad (3)$$

With the mean velocity V_{oprm} in the window opening the inflow and outflow can be calculated and in the same way the maximum inflow and outflow. Air flows by wind fluctuations.

In practice the window is not the only opening in the zone, so there will be a flow (an inflow or an outflow) through the window opening because of buoyancy, wind pressure and/or mechanical imbalance.

The air flow by wind fluctuations and the air flow by buoyancy, wind pressure and/or mechanical imbalance interact with each other. In case the latter is large with respect to the first the effect of the first (air flow by wind fluctuations) is negligible.

The model takes both air flows into account and calculates the resulting air flows. How that is done will not be discussed here.

Remark: The model is rather empirical and was set up by TNO from measurements in a rather (wind) shielded situation [1].

$$V_{oprm} = \text{SQRT} (C_1 * V_{wind}^2 + C_2 * H * dT + C_3) \qquad (4)$$

With

       V_{oprm} = mean velocity of the air through the window opening to inside
       V_{wind} = wind velocity at a local weather station
       H   = height of window opening
       dT   = temperature difference between inside and outside
       C_1 = 0,001
       C_2 = 0,0035
       C_3 = 0,01

In VA114 the second term (buoyancy) is separately taken into account, so left out in formula.

The calculated air flow rates (by formula 4) act as 'guaranteed' minimum value for urban situations. These air flow rates will often be exceeded in more wind exposed situations. For those situations the wind coefficient $C_1 = 0,001$ will be higher. On the analogy of Awbi [2], table 3.4, page 67, it was decided to take for exposed situations $C_1 = 0,004$ and for semi-exposed situations $C_1 = 0,002$.

Resume

This appendix describes the model of air flow by wind fluctuations. The model is rather simple and should be seen as a first step to take this effect into account.

[1]   Phaff, J.C. , de Gids, W.F. et al
        The ventilation of buildings. Investigation of the consequences of opening one window on the internal climate of the room, TNO report C448, March 1980.

[2]   Awbi, H.B.
        Ventilation of buildings. Air infiltration and natural ventilation (chapter 3), E & FN Spon, ISBN 0-419-15690-9.

Appendix B: Solar gain and solar exchange between zones

Model description

In subroutine "ZONINT" the solar gain and solar exchange between zones is simulated. In figure B.1 this is given very schematically.
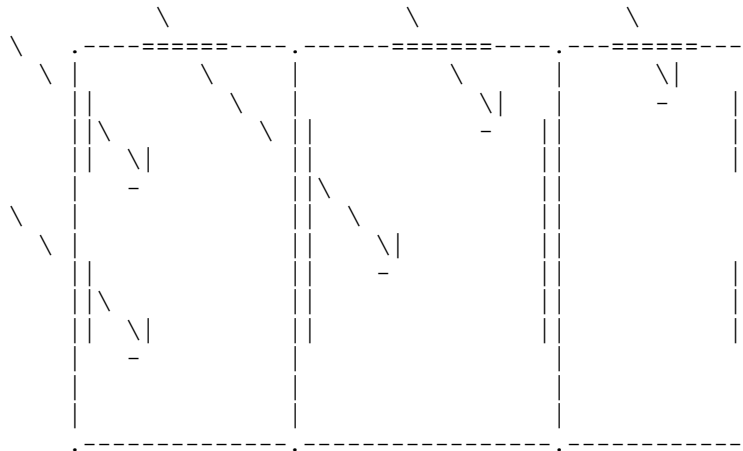
Figure B.1: Solar enters a zone by external windows and by internal windows. Windows can be present in the facades and in the roof.

It is calculated what fraction of the solar gain of a zone
- is used for the evaporation by plants
- comes sensible available to the air node
- comes sensible available to the walls; the distribution over all surfaces within the zone is calculated.

Direct and diffuse solar radiation are treated separately.

Steps in the calculation process:

.   *calculation of the solar gain of a zone*

External windows:

```
SOMZON = Σ A(IV,IVLK)*TRANS(IV,IVLK)*
            (Amdir*Gdir(IV,IVLK)+Amdif*Gdif(IV,IVLK))
```

with

```
SOMZON      = solar gain
A           = area of the window
TRANS       = transmission of the window (incident angle 45°)
Amdir       = Angular Modifier-direct radiation (=1.000 at 45°)
Gdir        = intensity direct solar radiation on the window
Amdif       = Angular Modifier-diffuse radiation (at 58°)
Gdif        = intensity diffuse solar radiation on the window
```

Internal Windows:
The solar radiation, that enters the zone by internal windows is added to the solar gain
SOMZON.

. *calculation of the latent and the sensible part of the solar gain*

Latent part (evaporation by plants)
```
SOMZONV    = VZON(IV) * SOMZON
```

Sensible part
```
SOMZONS    = (1.0 - VZON(IV)) * SOMZON
```

The fraction VZON is an input of the model.

. *calculation of the convective part and the radiative part*

Convective part (to the air node)
```
QZONL(IV) = CZON(IV)    * SOMZONS
```

Radiative part (to the wall surfaces)
```
QZONW(IV) = (1-CZON(IV)) * SOMZONS
```

The fraction CZON is an input of the model.

. *Calculation of the internal distribution of the radiative part.*

Many models are available here, from very simple ones (100% goes to the floor) to very
detailed ones.
For the calculation of the exchange between zones a detailed model, that calculates the
actual solar distribution (so each time step) is applied.

Detailed model for the internal solar distribution

The distribution of the solar radiation is separately done for direct and for diffuse radiation and is
dependent on the solar position, the geometry of the zone, the absorption / reflection of the
internal surfaces bounding that zone.

Each window is treated separately.

The solar entering the zone by a window has two components:
-       a direct component
-       a diffuse component
Remark: a fraction FDIFRM of the direct radiation is converted into diffuse when it passes
the window. The fraction FDIFRM is an input of the model (at this moment FDIFRM=0.0).
Remark: the circumsolair diffuse radiation component is treated as direct solar radiation

The internal distribution is calculated in subroutine ZABSVLK: the fraction of the radiative
part of the solar gain that is absorbed by each surface. The part absorbed by the surface of a
window is assumed to pass that window (to outdoors or to a neighbouring zone) for 100 %.

The direct component

Subroutine PZONI2 calculates, based on the solar position, what internal surface(s) receive direct radiation, that enters the zone by a specific window. A fraction (= absorption coefficient) of this direct radiation is absorbed, the rest (1-absorption) is diffuse reflected.

Remark: in case the internal surface is an internal window PZONI2 calculates also what internal surface(s) of the neighbouring zone recieve this direct radiation.

Remark: PZONI2 uses a Ray-tracing method; shading by external facade parts, by own building parts and by window setback is integrated in this method.

Remark: for simpler cases (rectangular zones; no internal window) subroutine PZONI0 (100 % of the direct radiation hits the floor) and subroutine PZONI1 (a projection method, that calculates where the direct solar radiation hits the internal surfaces) are available.

The diffuse component

The calculation of the distribution of the diffuse radiation (diffuse entered by the windows + the diffuse reflected direct radiation) happens by exchange factors. These exchange factors FUFACA(IV,I,J) are derived from the view factors and the absorption coefficients of all internal surfaces.

Remark: the absorption coefficient of the surface of an internal window is assumed to be equal to the g_{value} of that window; so (1-g_{value}) is reflected by that window surface.

Remark: in case of internal windows the exchange between zones is calculated iteratively.

The result of this calculation is the solar absorbed by each internal surface.

Final Remark: as can be seen from figure 1 the following situations can occur:

- a beam of rays hits a part of an internal window
- a beam of rays hits more than one internal window
- several beams of rays hit the same internal window.

The model is able to handle these situations.

Appendix C: Solar shading

Model description

In subroutine "ZONEXT" the solar radiation on external surfaces is simulated. Based on the orientation of each surface and the known solar radiation on each orientation. Both the unshaded direct component (Gdir(IV,IVLK)) and the unshaded diffuse components (Gdif(IV,IVLK)) are known.

For solar shading a distinction is made between direct and diffuse solar shading

Direct solar shading
Direct solar shading happens by surrounding buildings (subroutine 'schaduw1'), by external facade parts, by own building parts and by setback of the window (subroutine 'schaduw2').

Shading factors:
        Pschv1 (IV,IVLK)   surrounding buildings
        Pschv2 (IV,IVLK)   external facade parts, own building parts, setback window
Remark: Factor = 0.0 is not shaded, factor = 1.0 is fully shaded
Remark: only windows have shading, shading of opaque walls is (until further notice) not taken into account

These factors are combined to one factor
        Psch0(IV,IVLK) = 1. - (1.- Pschv1(IV,IVLK)) * (1. - Pschv2(IV,IVLK))

Diffuse solar shading
Diffuse solar shading by surrounding buildings is not taken into account; diffuse solar shading by external facade parts, by own building parts and by setback of the window is (subroutine 'schadw2d').

Shading factors:
        Pschv1d (IV,IVLK)   surrounding buildings (is not taken into account, i.e. = 0.0)
        Pschv2d (IV,IVLK)   external facade parts, own building parts, setback window
Remark: Factor = 0.0 is not shaded, factor = 1.0 is fully shaded
Remark: only windows have shading, shading of opaque walls is (until further notice) not taken into account

These factors are combined to one factor
        Psch1(IV,IVLK) = 1. - (1.- Pschv1d(IV,IVLK)) * (1. - Pschv2d(IV,IVLK))

Solar radiation, shading included
The shaded solar radiation on external surfaces is given by:
        Direct solar radiation   Gdir(IV,IVLK) = (1.0-Psch0(IV,IVLK)) * Gdir(IV,IVLK)
        Diffuse solar radiation   Gdif(IV,IVLK) = (1.0-Psch1(IV,IVLK)) * Gdif(IV,IVLK)

Remark:
The circumsolar diffuse radiation component is treated as direct solar radiation.

More details about the mentioned models (subroutine Schaduw1, Schaduw2 and Schadw2d) is given below.

Direct solar shading by surrounding buildings
Direct solar shading by surrounding buildings is simulated in subroutine 'schaduw1'.

The method
For a number of points on an external surface (see figure C.1.) the skyline is determined:
        SKYH(IGR,IV,IPUNT)
This is done once and for each external surface.

```
5.---------------.4
 |               |
 |       .1      |
 |               |
2.---------------.3
```
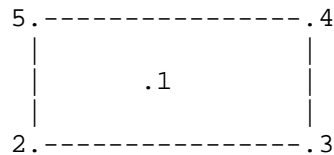
Figure C.1: External surface with 5 points to determine shading

If the solar height at the given solar azimuth is below the skyline of a point then there is shading in that point (Psch = 1.0), if it is above there is no shading (Psch = 0.0).

The shading factor for that surface is the average shading factor of the 5 points.

Direct solar shading by external façade parts, own building parts and by setback of window
Direct solar shading by external facade parts, by own building parts and by setback of the window is simulated in subroutine 'schaduw2'.

In figure C.2a and b the situation with obstructions is shown

```
     . . . . . . . . . . . . . .
    .                          .
    .        Surface IVLK      .
    .                          .
    .      4.    1.---------------------------.4  4.
    .      /|   /                   .        /    /!
    .     / |  /           Obstruction 1    /    / !
    .    /  | .---------------------------.     /  !
    .   /   ! 2              .         3  /    !
    .  /    !                .           /     !
    . 3.    !                .         3.      !
    .  !    !                .          !      !
    .  !    !                .          !      !
    .  !Obs 2!               .          !Obs 3!
    .  !    !                .          !     !
    .  !   .1                .          |    .1
    .  !   /                 .          !   /
    . .!. /. . . . . . . . . . .        !  /
       ! /                              ! /
       !/                               !/
       2.                               2.
```
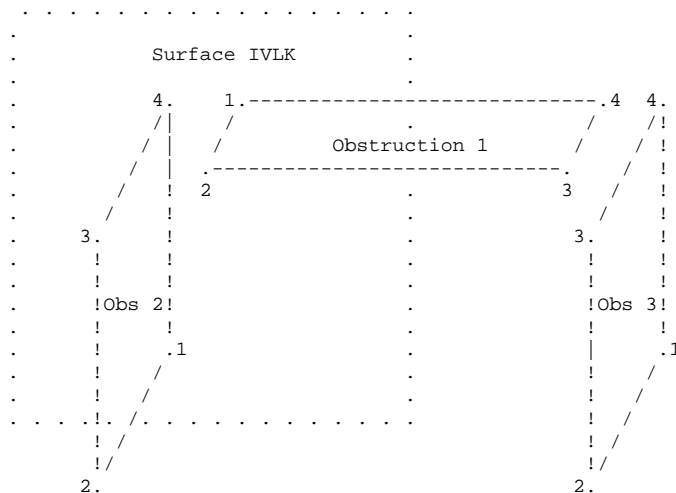
Figure C.2a: External obstructions (facade parts) – side view

```
      ---------------------------------------
      |                        .            |
      |      IV = 1            .  IV = 2     |
      |                        .            |
      |      Surface IVLK      .            |
      --------==.==.==.==.==---------. . . . . . |
          \                   |            |
           \                  |            |
            \                 |  IV = 3    |
             \                |            |
              \               |            |
    Obstruction \             ----------
```
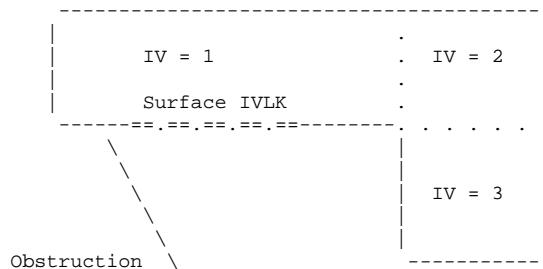
Figure C.2b: External obstructions (facade parts) – top view

The method
The projections of all obstructions and all surfaces of the building on a plane perpendicular to the solar rays are determined. The overlap between the projection of an obstruction and the projection of a surface gives information about the shading:
- 'no overlap'   means   'no shading'
- 'overlap'   means   'shading'; the size of the overlap is a measure for the shading (0.0-1.0)

Remark: another new method uses Ray-tracing to determine the shading factor; at the moment it is only in use for windows and is integrated with the calculation method for the internal solar distribution. For this method the window is divided into 10x10 points.

Diffuse solar shading
Diffuse solar shading by external facade parts, by own building parts and by setback of the window is simulated in subroutine 'schadw2d'.

To the diffuse solar radiation belong the isotropic component, the component from the horizon and the ground reflection component. The circumsolar component is treated as direct solar radiation.

In figure 2a and b the situation with obstructions is shown

The method
The shading by an obstruction on a surface is determined by the view factor between that surface and that obstruction.

The shading by setback of the window follows from the sum of the view factors between that surface and the edges around that surface: Fschzyv(IV,IVLK)

The shading by own building parts follows from the sum of the view factors between that surface and the own building parts: Fschegd(IV,IVLK)

The shading by other facade parts (obstructions) follows from the sum of the view factors between that surface and the several obstructions: Fschbel(IV,IVLK)

Total shading::
```
     Fschdif = Fschzyv(IV,IVLK) + Fschegd(IV,IVLK) + Fschbel(IV,IVLK)
```

Appendix D: Solar processor of VA114

Introduction

In IEA34/43 subtask B1 (MZ = Multi Zone-non air) and subtask E (DSF = Double
Skin Façade) tests on Building Performance Simulations programs are conducted,
where the solar radiation impinging on the façade is the most important driving force.
From first comparisons it seemed VA114 predicts a somewhat higher incident solar
radiation on the façade starting from the same solar source on the horizontal surface.
In this appendix the solar processor of VA114 is described in short to give the other
task participants inside in that model. An earlier version of this appendix was
distributed and reactions were gathered. A summary of these reactions is given. It did
not lead directly to the cause, but the comments and suggestions given will be
checked. That will be done in due time, but not as part of this IEA34/43 Task.

The description of VA114's solar processor

Solar position

Solar position is given by solar height (h) and solar azimuth (az). Both are calculated
half way the hour.

Used formulas:
- hour angle OHM
  $OHM = 2 * \pi / 24 * (12,5 – ST)$

  with solar time ST
    $ST = KL – DTIME$
  In this formula
    KL = hour of the day
    DTIME = time shift in hours
  The time shift DTIME is given by
    $DTIME = EQT/60 – (DLONGD/15 – ITIMEZ)$
  with
    EQT = equation of time (in minutes); EQT depends on day of the year
    DLONGD = longitude of site (in degrees; East = positive)
    ITIMEZ = time zone (East = positive)

- Solar height H and solar azimuth AZ
  Sinus of solar height (sinh) and cosinus of solar azimuth (cosaz) are both
  calculated based on solar declination, latitude of site and hour angle OHM.

Splitting in Direct and Diffuse radiation

For IEA-34/43 MZ (subtask Multi-Zone Non air) the GH (Global radiation on the horizontal) and GBN (Normal Beam radiation) is given on tape. With sinus of solar height (sinh) follows for the GBH (Horizontal Beam radiation):

$$GBH = GBN * sinh$$

and for the GDH (Horizontal Diffuse radiation)

$$GDH = GH - GBH$$

For IEA-34/43 DSF (subtask Double Skin Façade) the GH (Global radiation on the horizontal) and GDH (Horizontal Diffuse radiation) is given on tape. For the GBH (Horizontal Beam radiation) follows:

$$GBH = GH - GDH$$

and with sinus of solar height (sinh) the GBN (Normal Beam radiation):

$$GBN = GBH / sinh$$

Remark:
GBN should be lower than a maximum value GBN,max that is based on the outer atmospheric normal radiation G0N and the air mass AIRM. Correction:

IF (GBN > (GBN,max +55,6)) THEN GBN = GBN,max

The corrected GBN results in a corrected GBH and with GDH = GH – GBH in a corrected GDH.

Splitting Diffuse on the horizontal in 3 components

The diffuse on the horizontal surface is split into 3 components based on Perez [1]:
- Isotropic component D1
  $D1 = GDH * (1,0 - F1ACC)$
- Circumsolar component D2
  $D2 = GDH * (F1ACC / CZET)$
- Component from the horizon D3
  $D3 = GDH * F2ACC$

With

F1ACC = new circumsolar brightness coefficient
F2ACC = horizon brightness coefficient
CZET = cosinus of zenith angle

Remark:
F1ACC and F2ACC should be both between 0,0 and 1,0; circumsolar (D1) has as maximum value of 500 W/m^2.
If not values F1ACC, F2ACC or D1 are given the limit value and components are recalculated.

Calculation of total solar radiation on a tilted surface

By geometric formulas the contribution of the direct component, the 3 diffuse components and the ground reflected component to the total radiation on the tilted surface are calculated.

The used formulas:
- Direct solar radiation:
  GBT = GBN*COS(Teta)
  With
  GBN = Normal Beam radiation
  Teta = angle of incidence of solar radiation on the tilted surface

- Diffuse isotropic radiation:
  GD1 = D1 * 0,5 * (1,0 + COS(Beta))
  With
  D1 = diffuse isotropic component on horizontal
  Beta = tilt of surface

- Diffuse circumsolar radiation:
  GD2 = D2*COS(Teta)
  With
  D2 = diffuse circumsolar component
  Teta = angle of incidence of solar radiation on the tilted surface

- Diffuse radiation component from horizon:
  GD3 = D3 * SIN(Beta)
  With
  D3 = diffuse component from the horizon
  Beta = tilt of surface

- Ground reflection:
  GRT = GH * RHO * 0,5 * (1,0 - COS(Beta))
  With
  GH = total radiation on the horizontal
  RHO = ground reflectivity
  Beta = tilt of surface

Total radiation on tilted surface:
  GT = GBT + GD1 + GD2 + GD3 + GRT

Remark
VA114's solar processor is described. The big lines are given. If necessary more details can be provided, such as details about calculation of:
- equation of time EQT
- solar height and solar azimuth
- outer atmospheric normal radiation G0N
- Perez factors F1ACC and F2ACC; zenith angle ZET
- Angle of incidence of solar radiation impinging on the tilted surface
- ……..

Reactions and suggestions from participants

Valuable reactions were received from Joel Neymark (USA) and Paul Strachan (GB).

Joel Neymark

He read about the Perez 1987, 1988 anisotropic sky model in Duffie and Beckman (*Solar Engineering of Thermal Processes*, 1991) that there are a number
of disagreements that could occur with respect to how the model details are implemented ...
e.g.
- for calculating circumsolar diffuse a maximum for cos(zenith angle) of cos(85) is shown (*remark VABI: VA114 takes that into account*).
- the implementation of the brightness coefficients could easily be different among modelers (for those using a Perez model).

Duffie and Beckman note that this Perez model generally predicts slightly higher total radiation on a tilted surface, so in the MZ work the VA114 results are consistent with that. Duffie and Beckman recommend Perez for surfaces with azimuth angle far away from 0 [which is common for many building vertical surfaces]

Paul Strachan

Most of the calculations looked OK to him.

One difference is that VA114 is using Perez 1987. Paul's program ESPr was updated to the Perez 1990 model (probably also used by TRNSYS-TUD and Energy+). His experience: it does make some difference, but not a huge amount.

Paul (ESPr) supplied detailed results on direct and diffuse radiation for the comparative tests concerning solar radiation on the façade. For the period April 17 - April 30 a comparison between ESPr and VA114 was made [2]:
- concerning the solar sum over the period:
- Direct   - VA114 is 1,4% higher than ESPr
- Diffuse - VA114 is 4,2% higher than EPSr
- Total   - VA114 is 2,8% higher than EPSr
- daily plots show VA114 is somewhat higher in the peaks!!!

Paul suggested another possibility for comparisons: compare with the detailed solar processing analysis that used the EMPA data set.
It was published as:
> Loutzenhiser P G, Manz H, Felsmann C and Strachan P A, Frank T and Maxwell G M Empirical Validation of Models to Compute Solar Irradiance on Inclined Surfaces for Building Energy Simulation, Solar Energy, 81(2), Feb 2007, pp 254-267.

All the measured data and the predictions are included on the IEA34/43 FTP site. Measured were direct normal as well as global horizontal and diffuse horizontal.

Other comparisons by Vabi Software BV

The solar results of the comparative and empirical DSF-tests were studied intensively. There were a lot of observations, concerning all programs [3]. But our conclusion about the VA114 solar processor is:

> On total radiation and direct radiation VA114 is close to the other programs. On diffuse radiation two groups of programs can be distinguished, a higher group and a lower group; VA114 belongs to the higher group and is the highest in that group.

So the differences are much smaller than was found from the earlier comparisons

Remark: information about what model assumptions other solar processors are using is not available at the moment. The individual Modeler's reports should provide that information. Not all Modeler's reports are available at the moment

Resume

In this appendix VA114's solar processor is described in big lines. Valuable reactions / suggestions were received from task participants. It did not lead directly to the cause of the differences, but the suggestions given will checked. That will be done in due time, but not as part of this IEA34/43 Task. Until now it was concluded the differences between VA114 and the other programs are much smaller than was found from the first, earlier comparisons

Literature

[1]   Perez et all
        "A new simplified version of the Perez diffuse irradiation model for tilted surfaces", Solar Energy Voume 30, No. 3, pp. 221-231, 1987.

[2]   Wijsman, A
        "Solar radiation VA114 versus ESPr", Excel sheet, June 12th, 2007

[3]   Wijsman, A
        "Solar radiation predicted by the several programs", May 31st, 2007

Appendix E: Questionnaire completed for the program VA114

GENERAL

1 **Program name and version number** **VA114 – version 2.25**

2 **Name of organization performed the simulations** **VABI Software bv**

3 **Name of person performed simulations and contact information** **A. Wijsman**

 Email: a.wijsman@vabi.nl

4 **Program status**

☐ Freeware
X Commercial
☐ Other, please specify

5 **Time convention for weather data: first interval in the weather input lasts 00:00-01:00, climate is assumed constant over the sampling interval**

X Yes
☐ No, please specify

CALCULATION OF BOUNDARY CONDITIONS

6 **Please specify the solar model for calculation of incident solar radiation**
See appendix D to this Modeller report

7 **Transmission of the direct solar radiation into zone 1**

☐ Calculated with the constant solar heat gain coefficient (g-value)
☐ Calculated with the g-value as a function of incidence (function of incidence is fixed within code)
☐ Calculated with the g-value as a function of incidence (function of incidence is user defined)
X Other, please specify: Calculated with Transmission (as a function of incidence – user defined) and Absorption in the pane;

8 **Transmission of the direct solar radiation into zone 2**

☐ Treated as diffuse solar radiation and calculated with the constant g-value
☐ Calculated with the g-value as a function of incidence (function of incidence is fixed within code)
☐ Calculated with the g-value as a function of incidence (function of incidence is user defined)
X Other, please specify: Calculated with Transmission and Absorption in the panes; properties at angle of incidence of 45 degree

9 **Transmission of the diffuse solar radiation into zone 1**

☐ Calculated with the solar heat gain coefficient at the solar incidence 60°
X Other, please specify: Calculated with Transmission (at solar incidence of 58°) and Absorption in the pane.

10   Distribution of solar radiation to the surfaces in the zone 1

☐ Distributed equally to all surfaces
☐ Calculated according surface area weighting
☐ Calculated according to solar path and view factors
X Other, please specify: Different treatment for Direct and Diffuse solar radiation. Distribution of Direct solar is calculated by solar path; partly absorbed and partly diffuse reflected at surfaces that are hit. Distribution of Diffuse solar and Diffuse reflected Direct solar is calculated by absorption factors (based on view factors and absorption coefficients of the surfaces that are hit)

11   Distribution of solar radiation to the surfaces in the zone 2

☐ Distributed equally to all surfaces
☐ Calculated according surface area weighting
☐ Calculated according to solar path and view factors
X Other, please specify: same as distribution in zone 1

MODEL DEFINITIONS

12   Air temperature in the zone 1 is calculated as:

X One node temperature
☐ Few zones are stacked on the top of each other and the air temperature in each of zones is calculated, please specify number of stacked zones
☐ Other, please specify

13   Air temperature in the zone 2 is calculated as:

X One node temperature
☐ Few zones are stacked on the top of each other and the air temperature in each of zones is calculated, please specify number of stacked zones
☐ Other, please specify

HEAT EXCHANGE WITH EXTERIOR

14   External heat transfer coefficents

X Split radiative/convective
☐ Combined radiative/ convective
☐ Other, please specify

15   External heat transfer coefficents are calculated with identical assumptions for all surfaces (window frame, window glazing, walls etc.)

☐ Yes
X No, please specify : External heat transfer coefficients are not calculated (see external convection and external radiative heat exchange)

16   External convection

☐ Constant coefficients fixed within code
X User-specified constant coefficients
☐ Calculated within code as a function of orientation
☐ Calculated within code as a function of wind speed
☐ Calculated within code as a function of wind speed and direction
☐ Other, please specify

17   External radiative heat exchange

☐ Assumed to be ambient temperature
X   Assumed to be sky temperature
☐ Other, please specify

HEAT TRANSFER WITHIN ZONES

18   Internal heat transfer coefficients

X   Split radiative/convection
☐ Combined radiative/ convective
☐ Other, please specify

19   Internal heat transfer coefficients are calculated with identical assumptions in all zones and for all surfaces (window frame, window glazing, walls etc.)

☐ Yes
☐ No, please specify : Ixternal heat transfer coefficients are not calculated (see internal convection and internal radiative heat exchange)

20   Internal convection

☐ Constant coefficients fixed within code
X   User-specified constant coefficients
☐ Calculated within code as a function of orientation (vertical/horizontal)
☐ Calculated within code as a function of temperature difference
☐ Calculated within code as a function of air velocity in the zone
☐ Calculated within code as a function of surface finishes
☐ Other, please specify

21   Longwave radiation exchange within zone

☐ Constant linearized coefficients
☐ Linearized coefficients based on view factors
X   Linearized coefficients based on view factors and surface emissivities
☐ Nonlinear treatment of radiation heat exchange
☐ Other, please specify

WINDOW

22   Window

X Window frame and glazing are modelled as separate elements of construction; properties are user defined
☐ Window frame and glazing are modelled as separate elements of construction, but   the total U-value is calculated within the code
☐ Window frame and glazing are modelled as separate elements of construction, but   the total U-value and g-value are calculated within the code
☐ Other, please specify

23   Glazing temperature

☐ Calculated for 1 nodal point on the basis of fixed resistance
X Calculated dynamically, using the same scheme as for opaque elements
☐ Other, please specify

AIRFLOW MODEL

24   Discharge coefficient

X Fixed within the code
☐ User-specified fixed value
☐ Calculated by code, please specify what are the parameters involved in code calculations

☐ Other, please specify

25   Pressure difference coefficients

☐ Fixed within the code, identical for all openings sharing the same surface
X User-specified, identical for all openings sharing the same surface
☐ User-specified for every opening
☐ Other, please specify

26   Calculated mass flow rate in the model is a function of

X Buoyancy force
X Wind pressure
X Wind fluctuations
☐ Other, please specify

ESRU

Report

University of
Strathclyde
Glasgow

IEA SHC Task 34 / ECBCS Annex 43

Subtask E: Double Skin Facade

ESP-r Modeller Report

Empirical Test Cases

Paul Strachan

23rd July 2007

Energy Systems Research Unit
Dept. of Mechanical Engineering
James Weir Building
75 Montrose Street
Glasgow G1 1XJ
Scotland, UK

Email: paul@esru.strath.ac.uk
Tel: +44 (0)141 548 2041
Fax: +44 (0)141 552 5105

http://www.esru.strath.ac.uk

1. Introduction

ESP-r, Version 11.3 of April 2007, was used for the modelling.

ESP-r is Open Source software. Authors are Energy Systems Research Unit, University of Strathclyde, Scotland, UK; Natural Resources Canada; and other groups and individuals.

The program is based on a finite volume approach, with user-selectable timesteps.

The tests reported here are based on the revised Empirical Test Specifications of June 2007.

2. Modelling Assumptions

DSF100_e and DSF200_e cases:

Modelling of the floor of zone 1 (double façade): it is clear in the pictures that the floor is covered with wiring. An assumption was made that this was equivalent to 3mm of insulation on the floor, and surface temperatures on top of this were reported. It is not clear how representative this is of the actual temperatures recorded by the floor sensors. Comparisons are likely to be unreliable.

Modelling of test room floor: this is mostly shadowed from both longwave and shortwave radiation by the fabric ducts. Again, a crude approximation was made that the effect would be similar to a thin (3mm) insulation layer on the floor, and surface temperatures on top of this were reported. It is not clear how representative this is of the actual temperatures recorded by the floor sensors. Comparisons are likely to be unreliable.

Modelling of surface convection in test room: velocities were stated to be less than 0.2m/s; it was assumed that buoyancy-driven convection correlations would be most appropriate.

Test room thermal bridges: these were not included in the model. In a more detailed model, these should be included, making use of estimated linear thermal transmittances calculated for the test room edges. This assumption will lead to an underestimate of the heating load at night time in the test room.

Test room infiltration: this was simply modelled as the measured value at 50Pa pressure difference divided by 20 – a reasonably common approximation. However, a better infiltration model based on wind speed may improve the modelling of air movement.

Test room surface properties: spectral data could not be used. Internal emissivity was set to 0.88 for all opaque surfaces; internal absorptivity for solar radiation was set to 0.34 for opaque surfaces.

Ground reflectivity: Spectral data could not be utilised, so a value of 0.1 was used.

DSF100_e case:
The double façade was modelled as a single zone: it was therefore assumed that the air was fully mixed. Given the likely complex flows that may exist in the façade, the alternative was to use CFD to model the temperature and air velocity distribution. This can be done in ESP-r, and a preliminary model was established, but results have not yet been submitted.

It was assumed that the double façade was perfectly sealed. This is unlikely in practice, but no information on its air tightness was available. It is likely to lead to an overestimate of the internal temperatures.

DSF200_e case:
The double façade was modelled as 3 stacked zones to represent the temperature stratification. Tests in previous projects had indicated that 3 stacked zones were usually sufficient to represent the temperature gradient. Boundaries between the stacked zones were assumed to be essentially massless and fully transparent.

The given pressure coefficients were used (these are likely to lead to the greatest source of uncertainty). A wind speed correction was based on the roof height of 6 m. For open country, the reduction factor was calculated as 0.922.

A discharge coefficient of 0.65 was used for the lower opening (usually supply air) and 0.72 for the upper opening (usually extract air), based on the specification.

3. Modelling algorithms

Solar radiation
ESP-r uses the Perez 1990 anisotropic diffuse sky model for calculating diffuse radiation. Direct and diffuse transmission, glazing absorption and internal zone distribution are calculated separately. Ray tracing is used to allocate the direct solar transmittance to the appropriate internal surface for both the double façade and test room. Diffuse radiation passing through the window is allocated to surfaces not in the same plane as the window based on surface area and absorptivity. After the first bounce, direct radiation is treated as diffuse and added to the reflected diffuse radiation. This is iteratively spread to all internal zone surfaces based on the area and absorptivity (in the case of opaque surfaces) or the absorptances and transmittances (in the case of transparent constructions) until all radiation is accounted for.

Airflow
For the DSF200_e case, the airflow is modelled using an airflow network approach, which is integrated with the thermal model so that the calculated airflows are based on nodal temperatures from the thermal model (as well as wind-driven pressures), and the resulting predicted airflows are used in the energy balances of the thermal simulation.

The network model is simple in this case – an internal node for each of the 3 stacked zones in the double façade and two external nodes at the top and bottom openings. The top and bottom openings were modelled using the orifice equation with user specified discharge coefficients (0.65 for the inlet at the bottom and 0.72 for the outlet at the top). Opening areas were given as $0.33m^2$ for the bottom and $0.39m^2$ for the top. Pressure coefficients were included as boundary conditions for the openings as given in the specifications. A wind speed reduction factor of 0.922 was included from the 10m wind speed to bring it down to the wind speed at the height of the double façade, which is the reference height for the specified pressure coefficients.

Convection and longwave radiation
These were calculated explicitly both internally and externally for all surfaces. In the case of convection, buoyancy correlations were used for the internal surfaces and an algorithm based on correlations with wind speed and direction was used for external surfaces. For longwave radiation, external radiation was calculated based on estimates of sky and ground temperature, with all vertical surfaces assumed to have viewfactors of 50% to sky and 50% to ground. Internal viewfactors were explicitly calculated for the time-varying internal longwave radiation exchanges for both the double façade and test room.

4. Modelling Options

The building model for the DSF200_e case is shown below. The double façade was modelled as 3 stacked zones to represent temperature stratification.
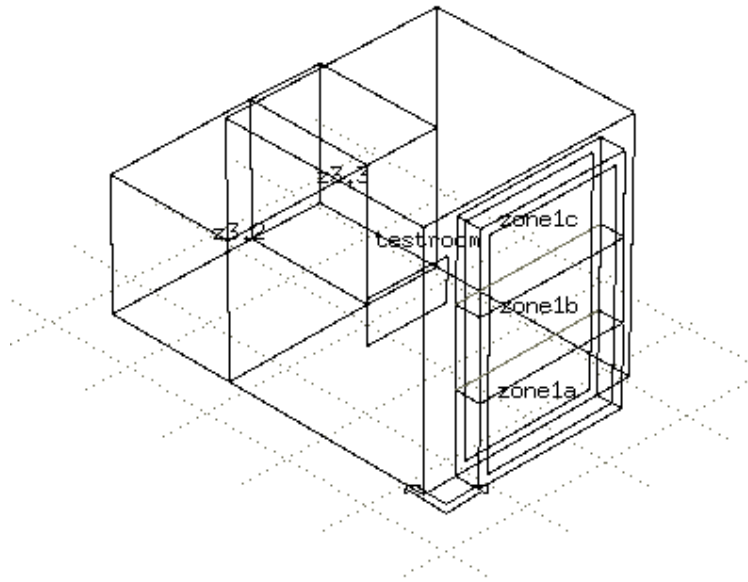
For the DSF100_e case, the double façade was only modelled as a single zone, with the resulting assumption that the air inside is fully mixed.

Glazing properties: as input, ESP-r requires the optical properties (transmittance and layer absorptances) at angles of incidence of 0, 40, 55, 70 and 80 degrees. For the single and double glazed units in the double façade, these were obtained using WIS for the glazings given in the specification, using the supplied spectral values. The normal incidence values were essentially the same as those given in the specifications. For the single glazing the following values were used:

Angle	0	40	55	70	80
Solar transmission	0.763	0.741	0.690	0.550	0.323
Solar absorption	0.161	0.175	0.184	0.191	0.180

For the double glazed unit, values were as follows:

Angle	0	40	55	70	80
Solar transmission	0.532	0.513	0.462	0.331	0.163
Solar absorption outer	0.103	0.111	0.117	0.119	0.110
Solar absorption inner	0.114	0.119	0.120	0.114	0.089

Framing: this was lumped and modelled as a separate surface.

Thermal mass: this was represented as additional surfaces inside the test room. The ventilation system has a stated mass of 750 kg mass. Not all this is directly linked to internal

air (e.g. internal fans in ductwork etc). In the absence of other information, it was assumed that 375 kg is "accessible" to the room air.

Rooms to rear of testroom: measured 10 minutely temperatures were used as set points for these rooms so the air temperature in the simulation corresponded to the measured values.

Simulation timestep: 10 minutes, to coincide with the provided climate and temperature data which was used for the boundary conditions. Results data were post-processed to provide hourly averages.

5. Modelling Difficulties

ESP-r does not output the incident direct and diffuse or the solar altitude in the results file. Instead, the simulation trace facility was turned on, and the required data extracted by processing the output.

6. Software Errors Discovered and/or Comparison Between Different Versions of the Same Software

None.

7. Conclusions and Recommendations

Results indicate that the night time heating load is under-predicted for the test room. This may be due to the fact that thermal bridges were ignored. Further simulations should be run to check this. It may be a good idea to model the thermal bridges with specialist software and provide the information to all participants (as was done with the test cell experiments at EMPA for the subtask C on shading/daylight/solar interaction). A sensitivity study could also be done on the infiltration in the test room to see if this has a significant

8. References

WIS: Window Information System, available from http://www.windat.org/wis/html/index.html.

Clemens Felsmann
Technical University of Dresden
Institute of Thermodynamics and Building Systems Engineering
July 24, 2007

Building Energy Simulation Software and Version(s):
The software tool of TRNSYS-TUD is a research code that was developed at the Institute of Thermodynamics and Building Systems Engineering of Technical University of Dresden (TUD) based on the frame of the former TRNSYS version 14.2. Modifications and developments at the original source code were necessary to stabilize calculation processes, to improve both user-friendliness as well as handling of the software and to extend fields of software application. In this context some new features have been added especially to the building model, as detailed long-wave radiation exchange, under-floor heating and thermally activated building systems, detailed solar distribution, internal windows, simple day lighting, etc. Also the ability to run with very little simulation time steps (seconds) was implemented. The realization of some of these features has been initialized by the IEA Task34/Annex43 software validation tests. The air flow model of TRNSYS-TUD originally based on COMIS but was also upgraded with some new features as for instance air flow model through large openings.

Building Model
The building model was built by dividing both Zone 1 (double skin façade) and Zone 2 (Cube) into 4 sub-zones each. Each of the sub-zones is represented by a single air temperature node. Sub-zones are stacked upon each other and are separated by fictitious walls. Due to this configuration temperature stratification could be modeled. The air temperature inside DSF reported in the output file is calculated based on the air temperatures of each of the stacked zones which have been weighted according to the specific air volumes of four sub-zones using the following equation:

$$\vartheta_{air,DSF} = \frac{0.94\text{m}^3 \times \vartheta_{air,DSF,1} + 4.66\text{m}^3 \times \vartheta_{air,DSF,2} + 4.66\text{m}^3 \times \vartheta_{air,DSF,3} + 0.94\text{m}^3 \times \vartheta_{air,DSF,4}}{0.94\text{m}^3 + 4.66\text{m}^3 + 4.66\text{m}^3 + 0.94\text{m}^3}$$

The fictitious walls between stacked sub-zones are dimensionless, without any mass, and fully transparent. They also allow vertical air flow. The vertical airflow is calculated by the program depending on temperature and pressure conditions at the

nodes of the airflow network assuming a large opening. A c_D-value of 0.5 was used for the simulations.

Figure 1 shows a grid of the building model.
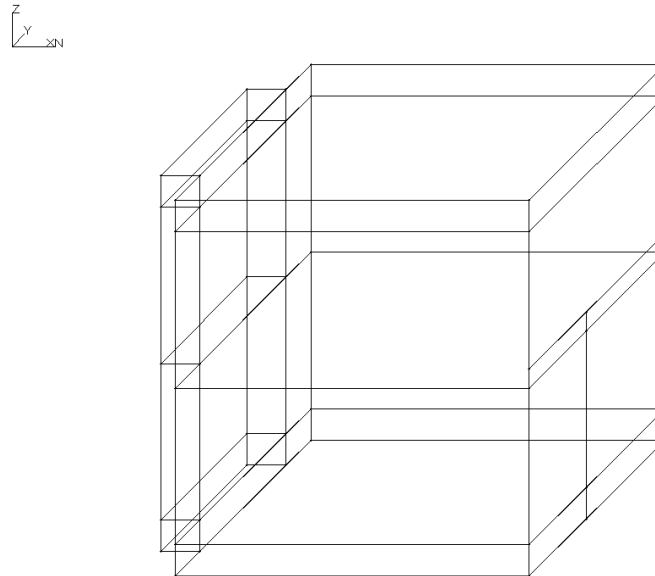
Figure 1: Building grid model

Optical and thermal properties of the glass (external and internal windows) have been calculated using WINDOWS 5.2a [1] and OPTICS 5.1[2]. IGDB identifiers were given in the specification. Figure 2 shows optical glazing properties as used for simulation in dependency on solar incident angle. This angle again depends on the sun's position at the sky and varies with time.
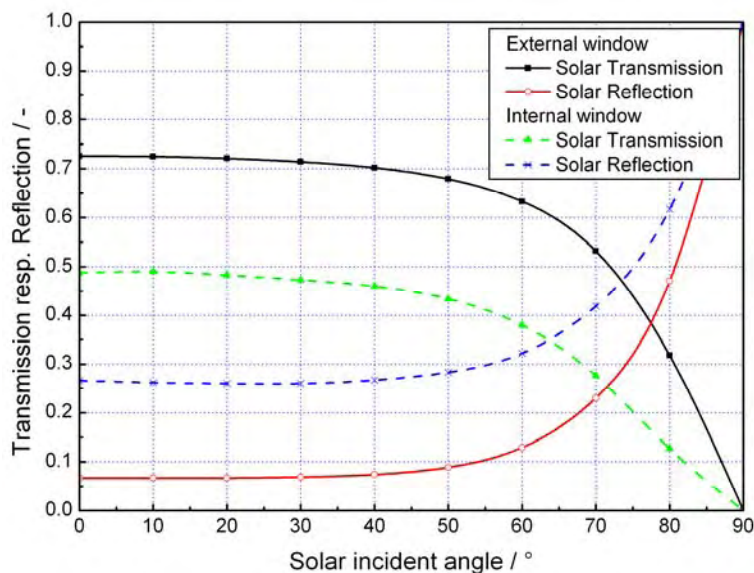
Figure 2: Optical glazing properties

Distribution of solar radiation within the zones is calculated in two steps:

1. At first direct solar radiation is distributed according to an algorithm that accounts for geometric relations between the sun's position and different locations of surfaces. Reflected parts of direct solar radiation were treated as diffuse.

2. Afterwards all diffuse radiation is distributed by an area weighted method.

Solar reflectance properties of surfaces have been calculated based on given spectral data. The normalized relative spectral distribution of solar radiation defined in prEN410 [3] and ISO9050 [4] was used to calculate a uniform reflectance value for all surfaces. Figure 3 shows spectral distribution defined in the relevant standards.
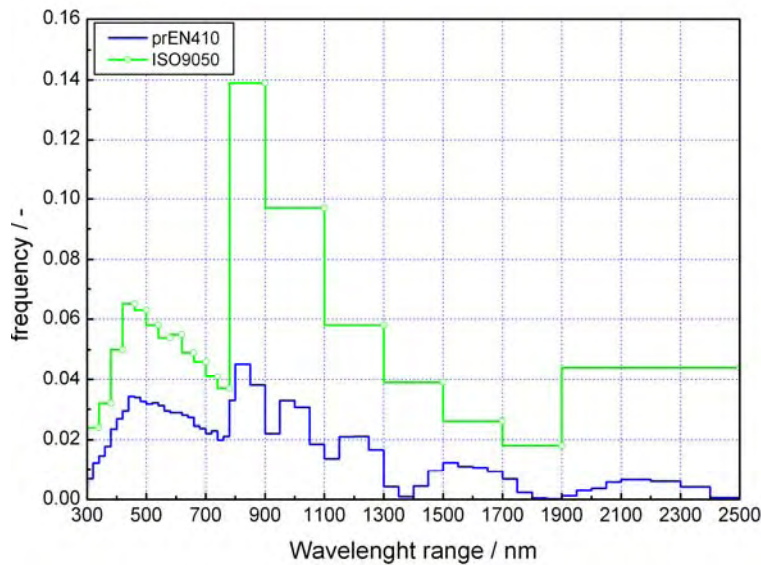
Figure 3: Frequency of solar radiation spectrum

The solar properties used in empirical simulations are as follows:

	Zone 1 (DSF)	Zone 2 (Cubus)
Solar Reflectance	78%	76 %
Solar Absorptance	22 %	24 %

Convective film coefficients have been fixed. Different values were chosen to model the impact of air flow on heat transfer.

External walls: 4.4 W/m²K (inside) 25 W/m²K (outside)

Roof / external window: 3 W/m²K (inside)   25 W/m²K (outside)

Floor: 3 W/m²K

Internal walls / internal window: 4.4 W/m²K (both sides)

Radiative heat transfer depends on view factors, emission properties and surface temperatures.

Test Case 100_2
All openings were closed. This test case was easily to simulate. The simulation time step was 0.1 hr = 6 min.

Test Cases 200_3 and 200_4
Free area of the openings had to be 0.6m² for both external and internal windows. The air flow model of TRNSYS TUD calculates area A of the openings in dependency on the angle α windows are opened as follows:

$$A = B \times H \times f(\alpha)$$

Here the function $f(\alpha)$ again depends on window construction. For these software validation exercises a function as depicted in Figure 4 was used. This function was found from a literature review.
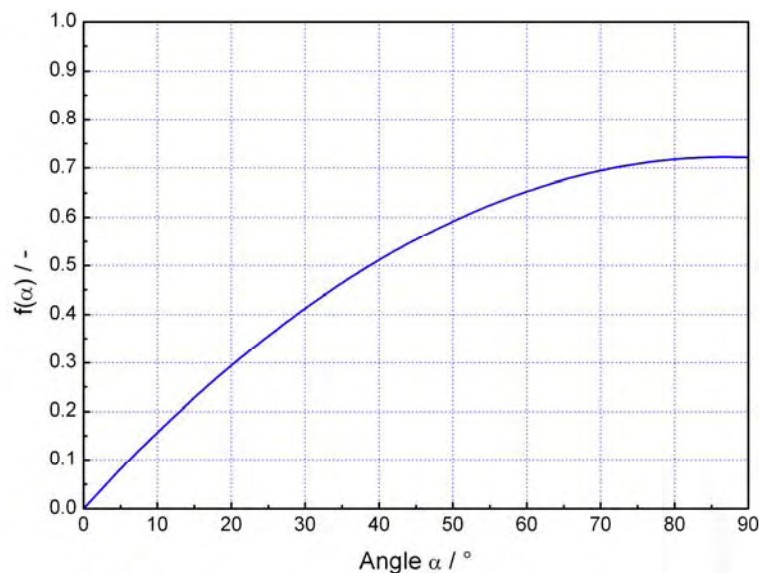
Figure 4: Correction of free area of openings

Using the curve above both external and internal openings have been assumed to be opened with an angle of about 26° to realize a free area as requested.

The simulation time step was 0.1 hr = 6 min.

Test Case 200_e

The simulation time step was 0.1667 hr = 10 min. A 24 hr period for preconditioning was defined. Detailed boundary conditions as provided for the ground and the adjacent zones have been used for simulation but no surface spectral data could be taken into account. Different from the wind profile described in the empirical test case specification a wind profile power law was used. Figure 5 shows a comparison between measure wind profile values and the power law approximation. The wind profile exponent was set to 0.34.

Due to the specified free area of openings windows were assumed to be opened at an angle of 16° (bottom opening) and 13.3° (top openings), respectively.
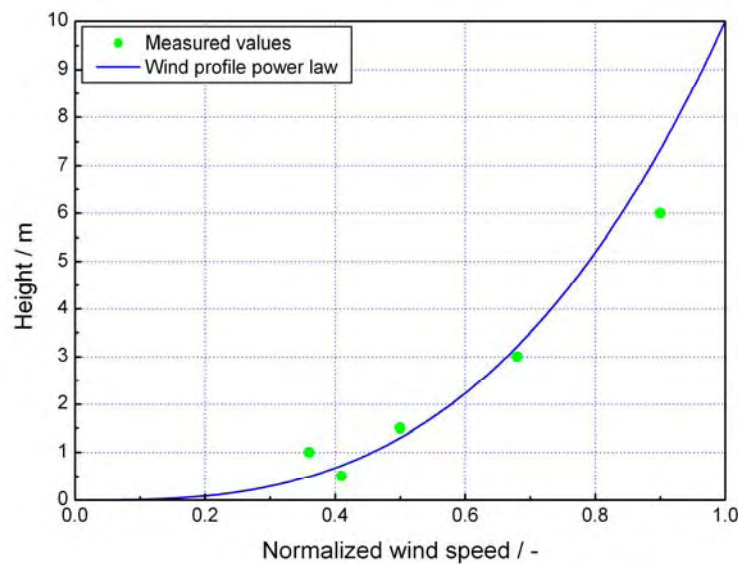
Figure 5: Comparison between measured values and wind profile power law

Test Case 400_3
Openings were assumed to be opened with an angle of 45°. Independent from this the air flow through the building was nearly fixed by defining a constant fan air flow.

The simulation time step was 0.1 hr = 6 min.

References
[1]   WINDOWS   5.2a,   2005,   Lawrence   Berkeley   National Laboratory (LBNL)
[2]   OPTICS   5.1,   2003,   Lawrence   Berkeley   National Laboratory (LBNL)
[3] prEN410: Glass in building – Determination of luminous and solar   characteristics   of   glazing;   German   version EN 410:1998

[4] ISO9050: Glass in building – Determination of light transmittance, solar direct transmittance, total solar energy transmittance, ultraviolet transmittance and related glazing factors

APPENDIX VII. Experimental set-up and full-scale measurements in 'the Cube'.

Experimental Set-up and Full-scale measurements in 'the Cube'

Technical Report

O. Kalyanova
P. Heiselberg

AALBORG UNIVERSITY

Department of Civil Engineering

Aalborg University
Department of Civil Engineering
Indoor Environmental Engineering Research Group

DCE Technical Report No. 034

Experimental Set-up and Full-scale measurements in the 'Cube'

by

O. Kalyanova
P. Heiselberg

May 2008

Scientific Publications at the Department of Civil Engineering

Technical Reports are published for timely dissemination of research results and scientific work carried out at the Department of Civil Engineering (DCE) at Aalborg University. This medium allows publication of more detailed explanations and results than typically allowed in scientific journals.

Technical Memoranda are produced to enable the preliminary dissemination of scientific work by the personnel of the DCE where such release is deemed to be appropriate. Documents of this kind may be incomplete or temporary versions of papers—or part of continuing work. This should be kept in mind when references are given to publications of this kind.

Contract Reports are produced to report scientific work carried out under contract. Publications of this kind contain confidential matter and are reserved for the sponsors and the DCE. Therefore, Contract Reports are generally not available for public circulation.

Lecture Notes contain material produced by the lecturers at the DCE for educational purposes. This may be scientific notes, lecture books, example problems or manuals for laboratory work, or computer programs developed at the DCE.

Theses are monograms or collections of papers published to report the scientific work carried out at the DCE to obtain a degree as either PhD or Doctor of Technology. The thesis is publicly available after the defence of the degree.

Latest News is published to enable rapid communication of information about scientific work carried out at the DCE. This includes the status of research projects, developments in the laboratories, information about collaborative work and recent research results.

INDEX

1. AN OUTDOOR TEST FACILITY 'THE CUBE'

1.1 FOREWORD

'The Cube' is an outdoor test facility located at the main campus of Aalborg University. It has been built in the fall of 2005 with the purpose of detailed investigations of the DSF performance, development of the empirical test cases for validation and further improvements of various building simulation software for the modelling of buildings with double skin facades in the frame of IEA ECBCS ANNEX 43/SHC Task 34, Subtask E-Double Skin Facade.

The test facility is designed to be flexible for a choice of the DSF operational modes, natural or mechanical flow conditions, different types of shading devices etc. Moreover, the superior control of the thermal conditions in the room adjacent to the DSF and the opening control allow to investigate the DSF both as a part of complete ventilation system and as a separate element of building construction.

The test facility is equipped to allow measurements of any power supplied to the experimental zone in order to maintain the necessary thermal conditions. An accuracy of these measurements is justified by the quality of the facility construction: 'the Cube' is very well insulated and tight.

1.2 GEOGRAPHY AND SITE LOCATION

The experimental test facility 'the Cube' is located in the suburban area, in a neighbourhood of a few company buildings and farms (Figure 1). Windows of the double skin façade face to the South.

The following coordinates define its' geographical location:

Time zone	+1 hr MGT
Degrees of longitude	9.93 East
Degrees of latitude	57.05 North
Altitude	19 m

Table 1.Geographical and site parameters of 'the Cube'.

Figure 1. Site location of 'the Cube'. A – three storeys company building, B – one storey farm, C- 'the Cube'.

1.3 'THE CUBE', THE MAIN PRINCIPLES OF OPERATION

Figure 2. 'The Cube'.

The Cube consists of four domains, which are named as:
- Double Skin Façade (DSF)
- Experiment room
- Instrument room
- Engine room
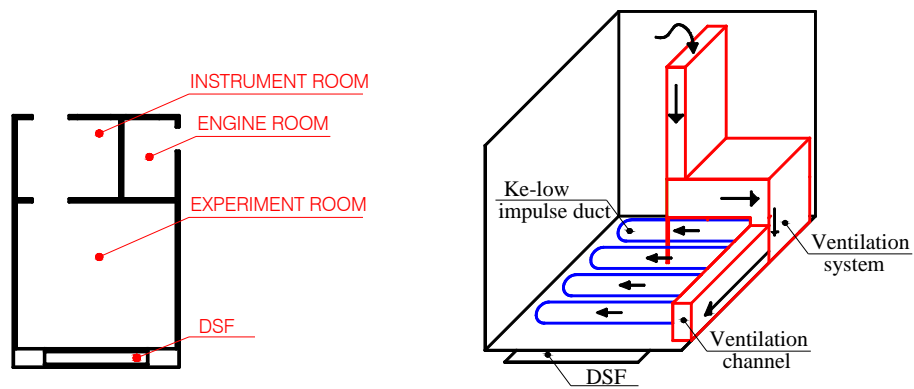
Figure 3. Plan of 'the Cube' (left), schema of the ventilation system in the experiment room (right).

All openings of the double skin façade are controlled and can be operated separately, a combination of the openings open defines an operative strategy of the DSF, see (Loncour, et al., 2004). Depending on the mode of DSF performance it can function as a barrier for the solar heat gains, as an additional insulation, can preheat the air incoming into the occupied zone, etc. In any of the above cases, the DSF affects the thermal conditions in the experiment room.

The temperature in the experiment room can be kept constant, as there is a cooling machine installed in the engine room and a ventilation system with the heating and cooling unit is installed in the experiment room (Figure 3). In order to avoid temperature gradients in the experiment room, the air is mixed by recirculation. The air intake for recirculation is at the top of the room, after the intake the air passes through the preconditioning units of the ventilation system and then it is exhausted at the bottom of the room through the fabric ke-low impulse ducts. Maximum power on cooling and heating unit is 10 kW and 2 kW correspondingly. The air motion caused by the ventilation system results in an air velocity of approximately 0.2 m/s.

Figure 4. Ke-low impulse ducts (left, centre). Ventilation system in the experiment room (right).

The instrument room contains all measuring equipment: data loggers, computers, flowmeter etc. (Figure 5).

8

Figure 5. Equipment in the instrument room.

1.4 GEOMETRY AND CONSTRUCTIONS OF 'THE CUBE'

The name of the test facility *cube* is originated from its shape, as the main building (Experimental room and DSF) is 6x6x6 m in external dimensions. The instrument room and the engine room are built as an extension to the main building attached to the northern wall of the experiment room. The extension building is only 3 m height and 3 m depth.
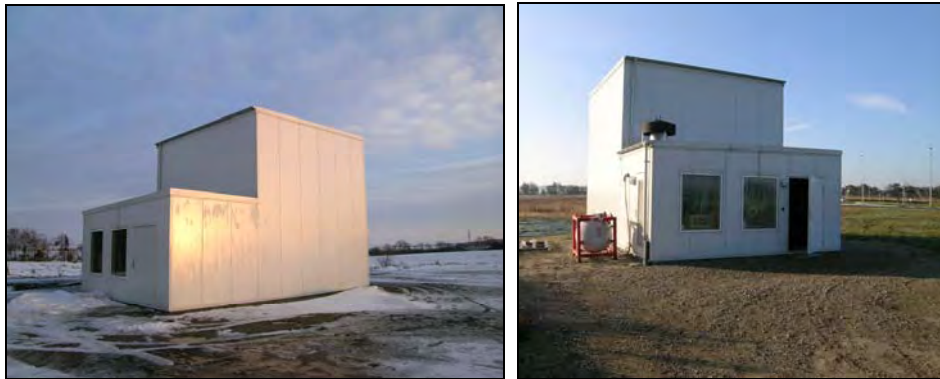
Figure 6. View to the extension part of the facility. 'The Cube' from the North-West view (left), from the North view (right).

The DSF and the experiment room are very well insulated and tight. There is approximately 40cm-layer of Rockwool insulation in the each wall. Detailed information about the construction and insulation of the test facility can be found in Appendix. The internal dimensions of the experiment room and DSF are given in Table 2.

EXPERIMENT ROOM

DSF
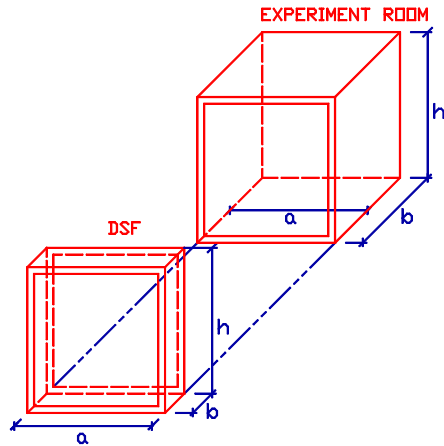
Room	a, mm	b, mm	h, mm	Volume*, m^3
DSF	3555	580	5450	11.24*
Experiment room	5168	4959	5584	143.11*

*Volume of Zone 1 and Zone 2 is calculated to the glass surfaces of the windows and NOT to the window frame or the walls
Table 2. Internal dimensions of 'the Cube'.

Window partitions of the double skin façade visually subdivide the DSF into three sections. The definition of the sections is given in the following figure and will be used in the further discussions (Figure 7). Major part of air temperature measurements in the DSF cavity and all measurements of velocity profiles were conducted in the section 2 of the DSF cavity. Analogous to the definition of sections, there is a definition made for the windows in Figure 8.
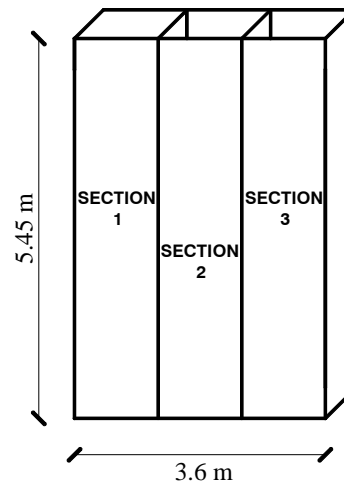
Figure 7. Definition of sections in DSF.

10

SOH 1	SOH 2	SOH 3
BOH 1	BOH 2	BOH 3
BOL 1	BOL 2	BOL 3
SOL 1	SOL 2	SOL 3

SIH 1	SIH 2	SIH 3
BIH 1	BIH 2	BIH 3
BIL 1	BIL 2	BIL 3
SIL 1	SIL 2	SIL 3

Transcription:

1st letter stands for   "B" – big
         "S" – small
2nd letter stands for   "O" – outside
         "I" – inside
3rd letter stands for   "H" –high
         "L" – low
Number stands for   "1,2,3"– number
         of DSF section
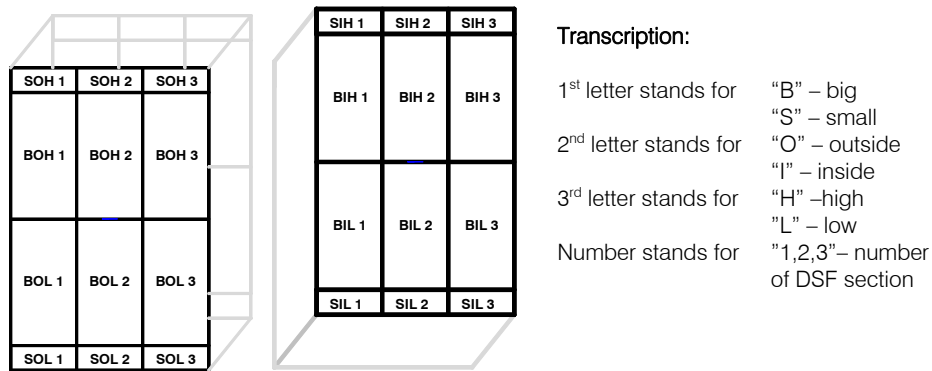
Example:
SOH3 – **S**mall **O**uter window, located **H**igher than the middle plane in the DSF section **3**.
BIL2 – Large (**B**ig) **I**nner window, located **L**ower than the middle plane in the DSF section **2**.

Figure 8. Definition of DSF windows.

The SOH, SOL, SIH and SIL windows are operated and can function as openings, depending on DSF operational mode. The opening angle is controlled and expressed in percent from the maximal opening angle of 75.5°, direction of opening of all windows is the same, as shown on the Figure 9.

a)   b)   c)   d)
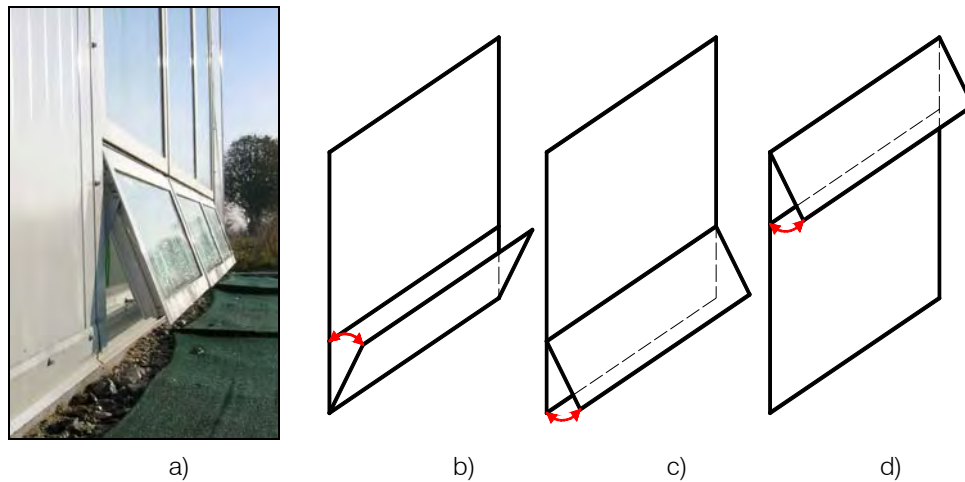
Figure 9. Direction of opening the windows, a) photo, b) SIL-openings, c) SOL-openings, d) SOH- and SIH-openings.

All windows at the test facility produced by VELFAC, the outer part of the window frame is made of aluminum and the inner part is wooden. The windows of the outer shell of the DSF construction consist of 8mm thick, clear single glazing. The windows of the inner shell of the DSF construction are low energy double glazing filled with argon (4-16Ar-4).

There is no shading device used for the experiments, but it is possible to install one, if necessary.

In the MODE 2 all openings were closed, while in the MODE 1 only the external top and bottom openings were open. The definition of modes is given in 3.1 and the definition of free opening area is given below.
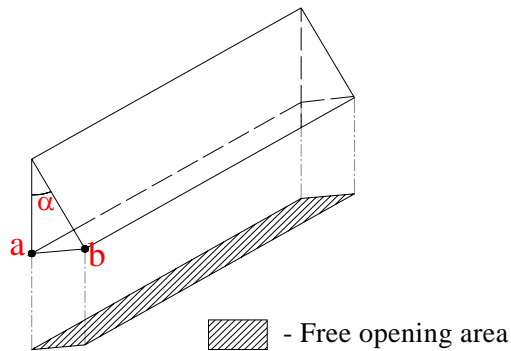
☒ - Free opening area

Figure 10. Free opening area.

	Top opening	Bottom opening
Free opening area *of one operable opening*, m^2	0.11	0.13
Distance 'ab', m	0.09	0.110
Angle α, deg	11.5	14

Table 3. Free opening area for MODE 1

	Internal top opening	External bottom opening
Free opening area *of one operable opening*, m^2	0.08	0.08
Distance 'ab', m	0.068	0.068
Angle α, deg	8.5	8.5

Table 4. Free opening area for MODE 3

Following is the definition of the glazed surfaces of the DSF, used for further discussions:

io   – internal surface of the outer window glass pane
eo   – external surface of the outer window glass pane
ii   – internal surface of the inner window, inner glass pane
ei   – external surface of the inner window, outer glass pane

1.5   GROUND REFLECTION

Knowledge of solar radiation is crucial for the task of these experiments. However, in non-laboratory conditions the ground reflected solar radiation depends on the surrounding of the test facility and therefore it can vary a lot. A large carpet was fixed on the ground from the side of the southern façade of 'the Cube' to achieve uniform and relatively known reflection from the ground (Figure 11). The size of the carpet is estimated to ensure that façade sees 50% of the covered ground. Increase of this value would require double-up the carpet size.

Fabric of the carpet was chosen so that it does not change the reflectance property when is wet and close to the generally assumed reflectance property of the ground.

Figure 11. Illustration of the ground carpet in front of 'the Cube'.

1.6   OPTICAL PROPERTIES OF THE SURFACES IN THE TEST FACILITY

Absorption, reflection and transmission properties of the most exposed to solar radiation surfaces in the DSF and experiment room were tested at the EMPA Materials Science & Technology Laboratory. Available information about the optical properties of surfaces can be found in Appendix as a function of the wave length. The spectral data in the wave length interval 250-2500nm is given there for the following surfaces:

- Glazing
- Ceiling and wall surface finishing in the DSF
- Ceiling and wall surface finishing in the experiment room
- Carpet in front of 'the Cube'

2.   PRELIMINARY EXPERIMENTS

A number of preliminary experiments had to be completed before the final experimental set-up. Preliminary experiments were focused on improvements and "calibration" of the test facility (air tightness and thermal insulation properties), improvements of measurement techniques and on positioning of equipment.

This preliminary experiment program was divided into a sequence of tests, where each test gives information on a limited number of parameters and the set of "calibration" test together gives a complete characterization of the entire test facility.

2.1   "CALIBRATION" OF THE TEST FACILITY

2.1.1   Tightness of 'the Cube'

The air tightness of 'the Cube' was measured a few times, during the construction, insulation and air tightening of the test facility, before and after installation of the experimental setup to ensure the tightness. These tests were completed with the blower door technique, with an overpressure in the tested domain. In addition, a control test with the underpressure conditions in the domain was repeated and lead to the same results as for the overpressure.

The overall tightness of the test facility is characterized by air tightness of:

1. Experiment room when all windows are closed
2. Experiment room when the outer openings are open and the inner openings are closed
3. Experiment room when the outer openings are closed and the inner openings are open
4. Double skin facade when all windows are closed

Following figure demonstrates results of the air tightness tests after completing the experimental set-up.

14
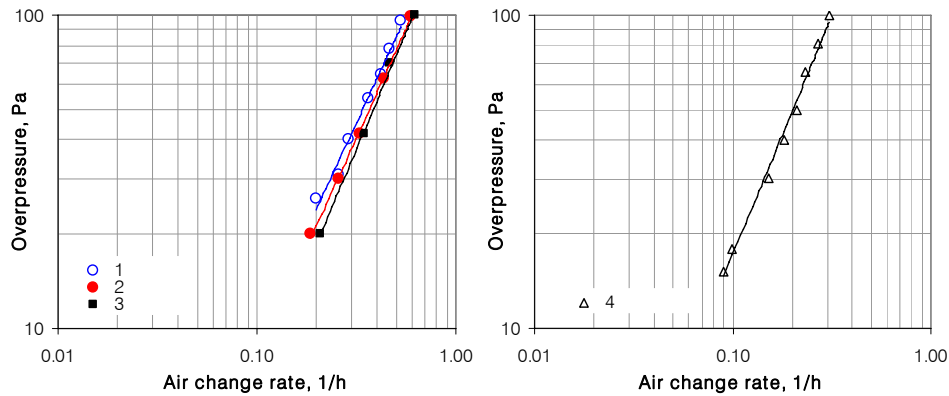
1. Experiment room when all windows are closed V=143m^3
2. Experiment room when the outer openings are open and the inner openings are closed V=143m^3
3. Experiment room when the outer openings are closed and the inner openings are open V=154.2m^3
4. Double skin facade when all windows are closed V=11.2m^3

Figure 12. Air tightness characteristics of 'the Cube'.

Results in the Figure 12 are plotted for the air change rate, which is calculated for the actual volumes and only the case 1 and case 2 are comparable.

2.1.2 Transmission heat losses of 'the Cube'

Normally, the investigation of the transmission heat loss is done by the stepwise increase of temperature difference between two environments. In a laboratory conditions, as a rule, one of the environments imitates the indoor and another one the outdoor conditions. In this kind of tests, it is wise to keep the imitated indoor temperature range close to usual and allow stepwise variation of imitated outdoor temperature.

Preliminary it was agreed on indoor air temperature of 22°C for the final experimental set-up in the outdoor test facility 'the Cube'. Accordingly, the preferred indoor air temperature for the evaluation of the heat losses in the 'Cube' was the same 22°C. However, it is not possible to imitate the outdoor air temperature in the real building and the experiment had to be adapted to the actual outdoor conditions.

For an accurate transmission heat loss measurement in an actual outdoor environment, it is necessary to find a period with the relatively constant outdoor temperature, low wind velocity, minimum or zero solar radiation intensity, and maximum cloudiness, no snow or rain. It is very difficult to fulfill these conditions. However there were two periods of measurements able to come near the requirements. The outer openings of the DSF were open.

A statistical analysis of data from the two periods of measurements is performed for quality assurance and suitability of the data chosen for the transmission heat loss evaluation (Table 5). The indoor and outdoor air temperatures were measured as explained in (section 3.2.1) and collected with 1 minute interval. The assembled data was processed and the statistical analysis was made for 10min intervals.

The measurements were conducted to characterize the experiment room independently from the double-skin façade. Therefore all of the external openings of the DSF were fully open to near the conditions in the DSF to an outdoor environment, while the internal openings were tight closed (external air curtain mode – MODE1).

Table 5, confirms good stability of the external weather conditions, the indoor thermal conditions were stable as well, with STD from 0.01 to 0.02°C.

ΔT=15.98 °C

Statistical parameter	Temperature, °C		Heating load, kW	Solar gains, kW
	Indoors	Outdoors		
Average for the measurement period	22.00	6.03	0.72	0.01
Min for the measurement period	21.97	4.98	0.64	0.01
Max for the measurement period	22.04	6.68	0.81	0.02
STD	0.02	0.44	0.04	0.00

Number of measurement points   90
Duration of measurement interval, h   15

ΔT=21.28 °C

Statistical parameter	Temperature, °C		Heating load, kW	Solar gains, kW
	Indoors	Outdoors		
Average for the measurement period	21.95	0.67	0.88	0.03
Min for the measurement period	21.93	0.38	0.79	0.01
Max for the measurement period	21.98	1.49	0.98	0.15
STD	0.01	0.19	0.04	0.04

Number of measurement points   228
Duration of measurement interval, h   38

Table 5. Statistical analysis of data in the transmission heat loss experiments.

Results of these tests are plotted in the Figure 13 and compared with the results of manual calculations. Unfortunately, it was possible to find only two periods suitable for empirical estimation of the transmission heat loss, however, the third point can be obtained theoretically for conditions when no transmission heat losses exist ($\Delta t=0$).

The manual calculations were conducted using the overall thermal resistances, counting on for gains from the equipment and solar gains into the experiment room. Finally, it can be observed from Figure 13 that the thermal bridges are present in the test facility and must be included into the simulations.
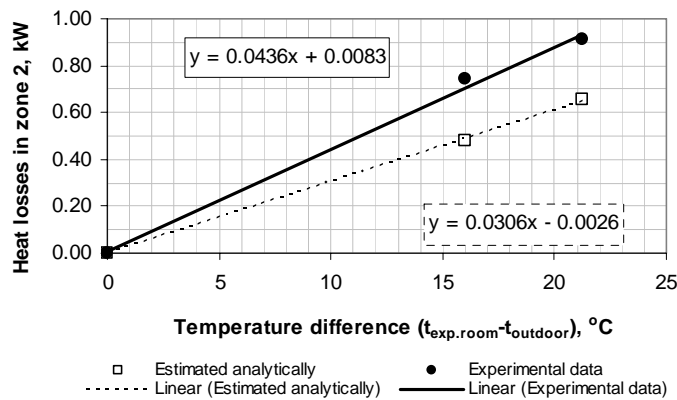
Figure 13. Transmission heat losses of 'the Cube' as a function of temperature difference.

It is essential to mention that the external shell of the DSF was open to the outdoor (openings were fully open and the conditions in the DSF were similar, but not identical to the outdoor environment). Furthermore, the experimental conditions do differ from the

ideal situation and there is a risk of rim or snow layer on the roof of the test facility during the measurement with Δt=21.28°C.

2.2 MEASUREMENT TECHNIQUES

Since a long time ago, experiments became a common practice for a scientist. Nowadays, there is a lot of literature exists and the principles of the various measurement techniques are well developed, characterized and in most of the cases their application is already evaluated and rated. However, the situation is different when unusual experimental conditions are applied.

Measurements in a real building are different from the measurement in the laboratory. One must adapt the measurement program to the outdoor conditions, to disturbances of experiments and to possible limits in a number of test sequences.

Detailed measurement in a full-size building is also different from the scale-models, as it requires large amount of equipment. Besides, the reliable experimental data obtained in outdoor conditions often implies high sampling frequencies; otherwise an essential data can be lost. All of this together, results in a vast amount of data to be processed and analyzed.

And, finally, measurements in a DSF building or in the DSF itself aren't an easy matter, most of the measurement techniques are developed for the conventional buildings and can't be directly applied in DSF, as even the air temperature can become difficult to measure accurately in the DSF cavity.

On account of these concerns, a set of tests was completed to improve a quality of measurements in 'the Cube'.

2.2.1 Measurements of the air temperature under the direct solar irradiation

The presence of the direct solar radiation is an essential element for the façade operation, but it can heavily affect measurements of air temperature and may lead to errors of high magnitude using bare thermocouples and even adopting shielding devices. An accurate air temperature measurement is crucial for prediction, evaluation and control of the dynamic performance of the façade, as a significant part of the complete ventilation system.

Another distinctive element of the double skin facades is application of shading devices in the cavity in order to prevent glare and penetration of solar heat gains into the occupied zone. Depending on type of shading in the ventilated cavity, the surface of the shading device is heated up to 65°C. Location of the temperature sensor nearby the shading device may lead to serious measurement errors if the temperature sensor is unprotected.

In the field of meteorology the problem of accuracy in temperature measurements was recognized over 150 years ago (Erell, et al. 2005), a screen, designed by Stevenson, is now widely used to measure air temperature in the field. Moreover, some meteorologists even suggest a standard methodology for dealing with this sort of errors. It is essential that the experts dealing with the issues of occupants' thermal comfort consider developing of similar guidance for measurements of air temperature under the shortwave or long-wave radiation loads.

This section describes the experimental setup to find the best suitable technique for accurate measurements of air temperature when exposed to solar radiation.

2.2.1.1 METHODS

The experimental setup included 11 thermocouples, placed in a row 15 cm away from each other, as shown in Figure 14.

Thermocouples type K (Chromel/Alumel) with the junction of approximately 2.5 mm in the diameter were used in the experimental setup. Thermocouples were calibrated in three points: 10, 20 and 35°C. The measurement results collected by a data logger HBM 334 measured at a frequency 0.2 Hz. Experimental results are reported as 10 minutes average values.

a)   b)   c)
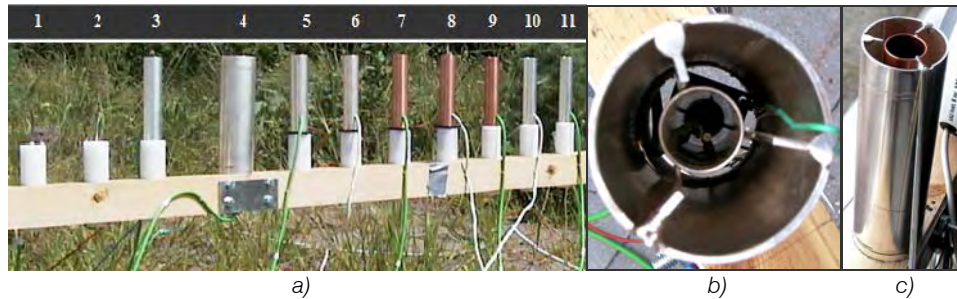
Figure 14.a) Experimental setup. Test cases are numbered according to their position in the experimental setup. b) Test case 4 - Thermocouple coated with silver and shielded with two silver coated tubes (photo from above). c) Visualization of double shielding.

After completing preliminary tests of shielding strategies the test cases in the Table 6 and Figure 14, were chosen for the final experiments. The experimental setup includes bare thermocouples, thermocouples shielded differently from the direct solar access, shielded and ventilated thermocouples and differently shielded silver coated thermocouples.

K – thermocouple type K without silver coating
KS – thermocouple type K with silver coating
T – copper shielding tube
TS – copper shielding tube coated with silver (both inner and outer surfaces)
2TS – two copper shielding tubes coated with silver (both inner and outer surfaces)
F – ventilated with a mini fan
- – no ventilation or no shielding tube

Test case	1	2	3	4	5	6	7*	8	9*	10	11
Thermocouple	K	KS	KS	KS	KS	K	KS	K	KS	K	KS
Shielding tube	-	-	TS	2TS	TS	TS	T	T	T	TS	TS
Fan	-	-	-	F	F	F	F	F	-	-	-

*- Results are not available due to a measurement error
Table 6. Test cases in the experimental set-up.

If a thermocouple is shielded with a copper tube (K+T), it is most likely that the shielding tube becomes overheated due to the solar radiation and readings from the temperature sensor become affected by the strong radiative heat exchange. In the case (8) it is assumed that the fan increases convection at the surface of the tube, removes heated air from the cavity and finally reduces the effect of radiation heat flux. However, the radiative heat exchange between the sensor and the heated surface of the tube exists and still causes some errors. In order to fight the radiative heat flux, silver, the metal which has the most superior reflectivity of visible light rays, is considered for the test cases. Thus besides the traditional thermocouples and copper tubes, the test cases include silver coated thermocouple, silver coated shielding tubes and a combination of both (2,3,4,5,6,7,9,10,11).

In the experimental setup shown in Figure 14 the mini fans are located at the bottom of a shielding tube and the air is sucked in the direction from the top to the bottom of the tubes. In a case of double shielding, Figure 14, one mini fan ventilates both of the cavities. Shielding tubes have the following dimensions: for the inner tube Ø25mm and length 100mm, tubes of the same dimensions were used in the other test cases. The outer tube in the test case 4: Ø60mm and length 130mm.

The experimental setup was placed outdoors, in the open flat country facing south. Due to necessity to run the fans connected to the electricity the experiments were run only at the day time.

2.2.1.2   RESULTS

In order to verify equal intensity of solar radiation to all sensors in the setup, two pyranometers were located at the left and at the right hand side of the temperature sensors. The results of the preliminary investigation show that in a day with the small or medium cloudiness the distribution of the solar radiation to the temperature sensors can be estimated as uniform, due to the comparably small size of the experimental setup. There are no experiments performed in the cloudy days with the dominating diffuse solar radiation.

In order to investigate the best suitable way to measure the air temperature, eleven cases were tested in the final experimental setup (Table 6). The challenging part of the experiments is the lack of knowledge about the true air temperature and that an evaluation of the results in absolute terms is not possible. As a result, the best approximation to the true air temperature is the measured air temperature in the test case which shows the minimal values in the presence of solar radiation. The same approach was used by Sonne, et al. (1993) to investigate outdoor air temperature measurements. On the contrary in the clear night unprotected sensors have a tendency to show lower temperature due to night time long-wave radiation.

Experimental results show that there is a wide spread in the temperature readings between protected and unprotected sensors. In a day with a medium intensity of solar radiation the difference between minimum and maximum air temperature measured with differently protected thermocouples is 4°C (mean values are compared), but this temperature difference can increase up to 10°C for a day with a stronger direct solar radiation.
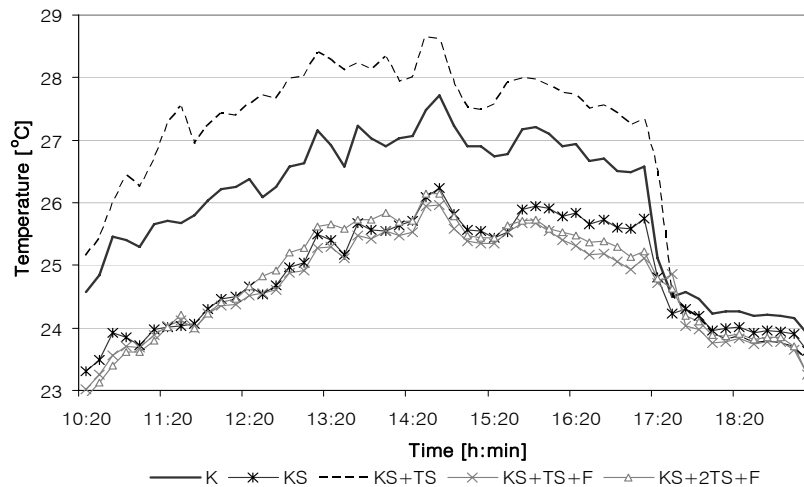
Figure 15.Measured air temperature for the test cases 1, 2, 3, 4, 5.

Air temperature readings show three different levels in Figure 15. The figure includes stepwise increase in implemented shielding devices starting from a bare thermocouple. Improvement of the bare thermocouple with the silver coating gives a remarkable result, as the temperature readings decrease almost to the minimal values (mean value 24.86°C). Moving forward shading a silver coated thermocouple with the silver coated tube (both inner and outer surfaces), the measured air temperature increases drastically due to the thermal mass of the tube, which gets heated and subsequently heats air in the tube, the radiative heat exchange in this case should be minimized due to silver coating of the thermocouple and tube. The situation is improved with increase of the convective coefficient by application of a mini fan (test case $KS+TS+F$) and the minimum measured air temperatures are distinctive for this test case (mean value 24.67°C).
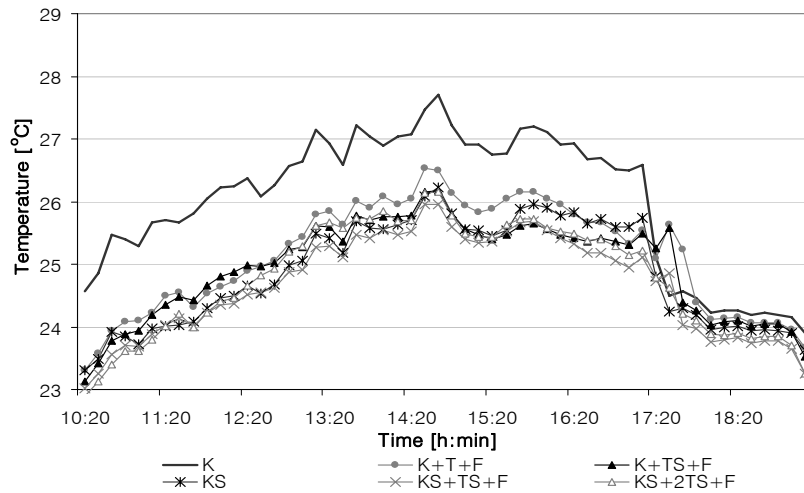
Figure 16.Measured air temperature for the test cases 1, 2, 4, 5, 6, 8.

Additionally, one more enhancement was developed for protecting a temperature sensor: a double shielding of the temperature sensor with two silver coated tubes ($KS+2TS+F$) as explained earlier. Experimental results show that application of double shielding is not efficient (mean value 24.79°C), as it requires larger size of the external shield and thus the thermal mass is increased. Otherwise the reason for the inefficiency is the fan which in this case might be not strong enough to ensure the necessary flow motion through the two cavities (the external cavity between the shields and internal cavity in the internal shielding tube). Hence, the test case 4 requires further investigations.

One can find intricate dealing with silver due to its oxidation feature and cost. The results for uncoated thermocouples in comparison to the experimental results are discussed above. It is evident that avoiding silver coating will lead to higher readings than in the case with the coating, but the improvement is still very good when compared with application of bare thermocouple (Figure 16).

Test case	1	2	3	4	5	6	7*	8	9*	10	11
Test case	K	KS	KS TS	KS $2TS$ F	KS TS F	K TS F	KS T F	K T F	KS T	K TS	KS TS
Mean measured temperature, [°C]	26.02	24.86	26.87	24.79	24.67	24.94	-	25.12	-	28.43	27.06
STD [°C]	1.17	0.89	1.64	0.90	0.82	0.79	-	0.90	-	2.16	1.70

Min of mean measured temperature,   24.67°C
Max of mean measured temperature,   28.43°C

* Results are not available due to measurement errors
Table 7. Mean measured air temperature.

On the basis of the investigations the shielding type of test case 5 (*KS+TS+F*) was chosen as the most suitable for the accurate measurements of air temperature. The silver coated shielding tube and a mini fan (test case 5, *KS+TS+F*) and silver coated thermocouples (test case 2, *KS*) were applied for measurement of the air temperature in 'the Cube', in the experiment room. Readings from the sensors with the shielding technique from the test case 5 and test case 2 are compared in Figure 17, results are remarkable, as according to one sensor the air temperature kept by ventilation system was relatively constant (shielding approach of test case 5), while another temperature sensor (shielding approach of test case 2) shows a swing in the periods with the direct solar access to the sensors.
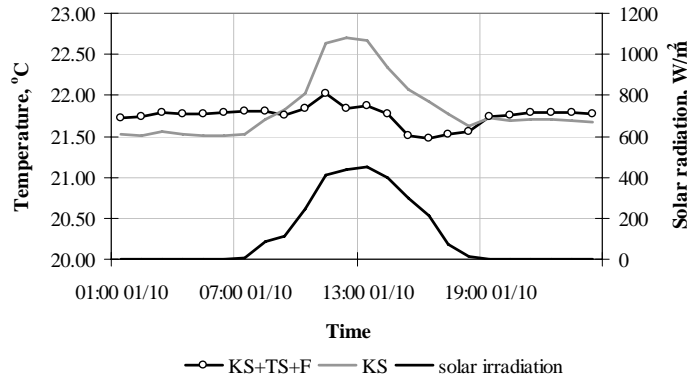
Figure 17.Results of application shielding technique from test case 2 and 5.

2.2.2 Measurements of the air speed with the hot-sphere anemometer under the direct solar irradiation

Application of the hot-sphere anemometer is defined by its ability to measure the air speed in the range of the low velocities typically found within buildings. Therefore, the measurements of the air speed in an occupied zone became the widest area for application of the hot-spheres. As a rule, the air speed in the occupied zone varies 0-0.2 m/s and frequently this is the velocity range for application of hot-spheres. However, the hot-spheres capability is much higher, as they allow measuring of air velocity in the range 0-5 m/s.

Regarding the air flow in the naturally ventilated Double Skin Façade (DSF) cavity following aspects are defined as distinguishing for the DSF operation and thus for the air motion in the cavity space. Naturally driven air flow in the DSF cavity is highly transient due to highly fluctuating wind character and, as a result, the variation of the air flow magnitude in the DSF cavity is huge. Moreover the velocity profile in the DSF cavity varies depending on the flow regime, defined by the ambient temperature, glazing temperature (solar radiation absorbed by glazing), etc. Solar irradiation is the necessary parameter for the DSF performance and thus in most of the cases equipment installed in the DSF cavity is exposed to the high solar fluxes.

Due to the fluctuations, the instant values of the air velocity in the DSF can vary 0-5 m/s. As a consequence, the detailed measurements of the air flow in the cavity require equipment able to perform measurements of the velocity with a highly varying velocity magnitude. Large number of equipment is necessary for the measurements of the velocity profile in the cavity and at the same time it is essential to have equipment of a small size to minimize the disturbances to the flow pattern in the cavity. Moreover, the

equipment must be able to respond adequately to the fluctuations and also to be able to coup with the high solar loads.

The described conditions in the DSF cavity are very different from the conditions in an occupied zone, but still, according to the tests described in this section the hot-sphere anemometers are an excellent choice for the measurements in the DSF cavity. It is demonstrated, how the hot sphere anemometer respond to fluctuations, to exposure to the high solar fluxes and how the hot-sphere anemometers can be used for distinguishing of the flow direction in the DSF cavity. Results of these tests were applied for measurements in 'the Cube'.

2.2.2.1 Testing the dynamic properties of the hot-sphere anemometers

In the DSF the airflow is highly transient, especially when the DSF is naturally ventilated. When using hot-sphere anemometers in a double façade cavity it is vital that the anemometer is able to measure the air velocity, responding adequately to the flow dynamics.

To ensure this a test method following the requirements in EN 13182 aimed at measuring the mean velocity and turbulence intensity in the occupied zone in connection with thermal comfort was applied.

The principle of the test method was to place the anemometer in the laminar air flow generated by a jet-wind tunnel and then oscillate the censor back and forth in the air flow by means of a crank movement, hereby overlaying the laminar flow with an almost pure sine wave. The principle is shown on Figure 18.
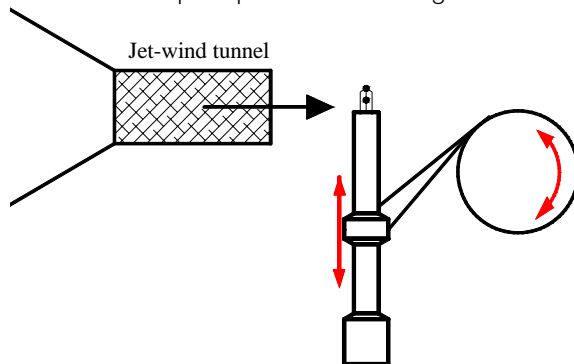
Figure 18.Principle of dynamical test of hot-sphere anemometer.
The results of the tests proved that the hot-sphere anemometers responds very well to the fluctuations up to 1Hz.

2.2.2.2 Testing of the hot-sphere performance when exposed to the solar radiation

Temperature compensation is the working principle of the hot-sphere anemometer. It is designed with two spheres: the heated and unheated one. The unheated, so called 'cold' sphere measures the temperature of the flow, while the heated 'hot' sphere measures convection at the surface of the heated sensor. The air speed is determined as a result of compensation between readings from the 'cold' and 'hot' sphere. Accordingly, an accurate measurement of the air temperature with the 'cold' sphere is crucial for the acceptable temperature compensation and thus for the reliable measurement of the air speed.

The presence of direct solar radiation is an essential and distinctive element in the DSF operation. Consequently, the hot-sphere anemometer is exposed to sun when measuring in the double façade cavity, the 'cold' and 'hot' spheres heated by solar radiation and, as a result, the sensor's ability to compensate for temperature become doubtful. The following experiments were performed in order to evaluate influence of solar radiation on performance of hot-sphere anemometer measuring the upward and downward flow.

The experiments took place in the isothermal conditions in the laboratory. A hot-sphere anemometer was located in the jet wind tunnel, affect of solar radiation was imitated by a strong lamp, producing 800 W/m^2 of radiative heat flux (Figure 19).
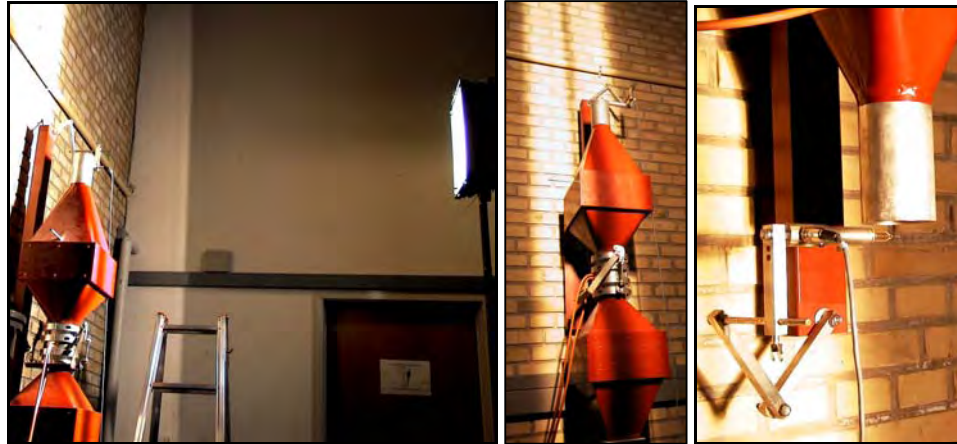
Figure 19. Hot-sphere anemometer in the jet-wind tunnel lit with the lamp imitating solar radiation.

First the air speed was measured on the exit from the jet-wind tunnel without the radiative heat flux. The true mass flow rate was determined from the pressure difference registered by micro manometer at the orifice in the wind tunnel. Afterwards the same measurement was repeated with the solar flux. All in all the experiment is conducted for eight different mass flow rates.
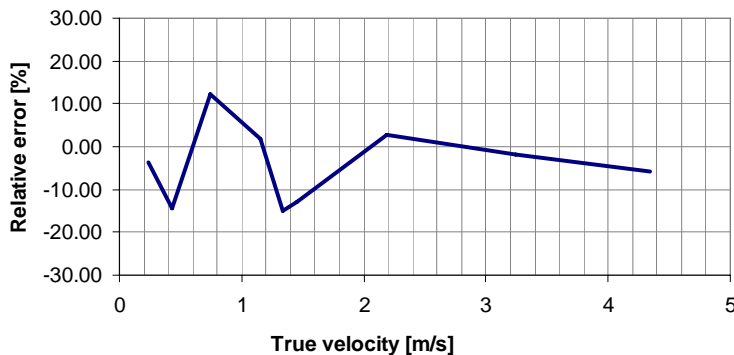
Figure 20. Relative error measured by a hot-sphere anemometer measured when exposed to a strong radiative heat flux.

The relative error is calculated as:

Equation 2-1

$$E_r = \frac{V_{rhv} - V}{V_t} \cdot 100\%$$

Where,

E_r - relative error
V_{rhf} - velocity measured with the radiation heat flux
V - velocity measured without radiation heat flux
V_t - true air velocity in the jet-wind tunnel calculated from orifice

If there is any influence of radiation on the performance of the anemometer then it ought to be strongest in the range of low velocities. According to the Figure 20, there is no consistency in the measured relative error. The magnitude of the error varies a lot, and even in the range of the low velocities it is not possible to identify any regularity. One can conclude that the hot-sphere anemometer doesn't change the performance when exposed to direct solar radiation. This can be explained by two factors. The first one is the surface of the spheres which has very high reflectance property and it is possible that the major part of solar radiation approaching the sphere is reflected. Moreover, the 'cold' and 'hot' spheres must be heated up equally as both of them are equally exposed, and, as the main principle of the hot-sphere anemometer is the temperature compensation, then equally heated spheres would not affect the temperature compensation.

According to the above conclusion the hot-sphere anemometers were used for measurements of the velocity profile in the double façade cavity in the outdoor test facility 'The Cube'.

2.2.2.3   Testing of the hot-spheres for measurements of the flow direction

In the double skin façade both upward and downward flow will occur and therefore it is important to determine the direction of the flow, meanwhile the exact angle of flow direction is insignificant. From this point of view, any simple method that doesn't require advanced equipment could be useful. A simple method to register a flow direction using two hot-sphere anemometers separated by a small plate is tested, as explained below.

It is suggested that two hot-sphere anemometers are placed in the flow filed separated by a plate perpendicularly to the main flow, as shown in the Figure 21. As a consequence, readings from these two sensors will be different and the flow direction is possible to determine depending on readings from the sensors. Sensor measuring highest velocity denotes flow direction from the sensor to the plate.
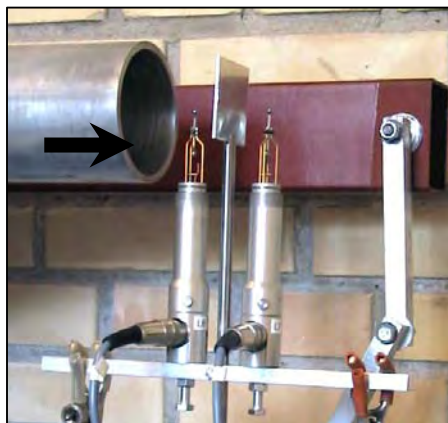
Figure 21. Experimental setup: Measurement of flow direction with two hot-sphere anemometers.

The challenging part of this method was to choose an appropriate size of the shielding plate and distance between the plate and the hot-sphere anemometers. These questions were solved according to the results of the experiments described below.

The experiments were conducted in order to test the method in the upward flow and downward flow. Two hot-sphere anemometers, separated by a plate were placed in the centre at the exit plane of the jet-wind tunnel (Figure 21). Hereafter, the anemometer located closer to the exit plane of the jet-wind tunnel is regarded as the 'front' anemometer and the one located behind the plate as the 'back' anemometer. A shielding plate of a square form was used for the experiments and tested for three different sizes: 1x1cm, 5x5cm and 7x7cm. The distance between the anemometers and the shielding plate were also investigated. Velocity was measured as one minute average values, with a 10Hz sampling rate.

Experimental results, aimed to explore influence of the size of the shielding plate are presented in the following Figure 22. The difference between velocity measured by the front (V_f) and the back (V_b) anemometer compared in relation to the true air velocity calculated from the pressure difference at the orifice in the jet-wind tunnel (V). The front and back anemometers were placed 3cm away from the plate. Obtained results are similar for the upward and downward flow.
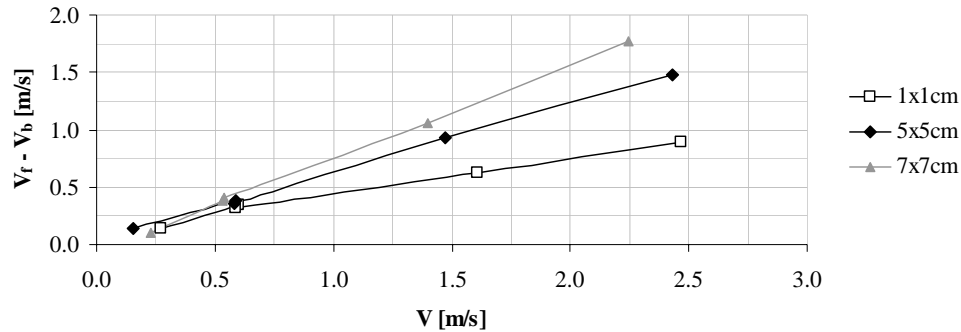
Figure 22. Investigation of size of shielding plate for downwards flow.

It is obvious that with increase of the plate size the difference between readings from the front and back anemometer becomes much more noticeable and it turns out to be much easier to distinguish between the flow directions.

The importance of distance between the plate and anemometers is investigated with the plate of 7x7cm dimensions. The distance between front anemometer and the plate is marked as (*f*) and the distance between the back anemometer and plate regarded as (*b*). Results are similar for the upward flow and downward flow (Figure 23).
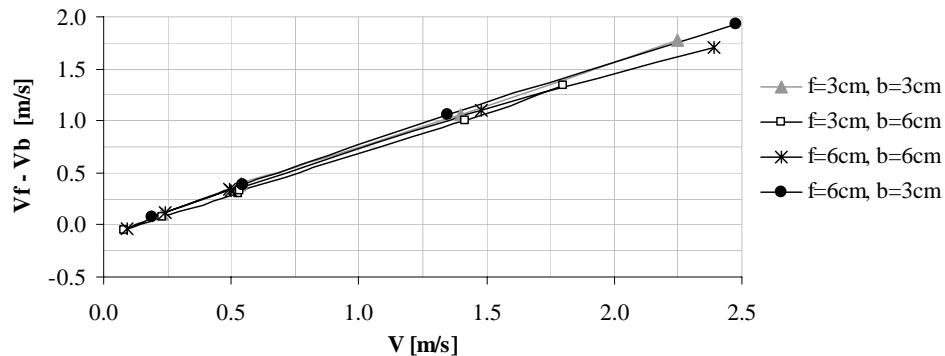
Figure 23. Investigation location of hot-sphere anemometers in relation to the shielding plate for downward flow.

Apparently the distance between the plate and anemometers is not as crucial as the size of the plate, but in reasonable range. Tested distances between 3 and 6 cm appear to be applicable for this sort of measurements, but still the location of the back anemometer too far from the shielding surface can be damaging because of disturbance from the turbulent vortexes after the plate. Meanwhile, for the measurements performed in the jet-wind tunnel the location of the front sensor is less sensitive to the disturbances. Still it is necessary to keep it closer to the plate as it acts as the reference measure.

If method is used for the measurements in the DSF cavity then due to the wind fluctuation the flow direction changes rapidly and the described subdivision of anemometers to the front and back one doesn't exist any more, as both of them share these functions. That's why, both of them must be placed on same distances from the plate and in order to avoid turbulent vortexes a distance of 3 cm from the plate to the anemometers is the better one.

Because of DSF exposure to the solar radiation, as explained before, the plate will be heated up by the sun and will cause a convective heat flux from the surface, and can become a reason for a measurement fault. In order to avoid this situation, it is recommended that the plate is made of material with the low absorption property.

2.2.2.4 Summary

There are three different test cases described in the testing of the hot-sphere anemometers for their further application in the DSF cavity. Although the hot-spheres are mainly used for the measurements in the occupied zone and the conditions in the double façade cavity are very different from the ones in the occupied zone, the obtained results show that the hot-sphere anemometers are a good solution when necessary to investigate the air flow element in the DSF cavity. It is investigated that the hot-spheres respond well to the fluctuations, with up to 1Hz frequency. Higher frequency of fluctuations results mainly in over prediction of the low velocities. Solar irradiation does not influence readings from the hot-sphere anemometers, and they can be used for the velocity measurements in the DSF cavity. Finally, it is possible to distinguish the flow direction in the DSF cavity when using hot-spheres and the procedure for that is also described. Unfortunately the last proposal about the distinguishing of the flow direction wasn't tested in the DSF, but it is planned to do so in the next set of DSF-experiments.

2.2.3 Calibration of openings

The pressure difference method is a technique, which is still in the testing and validation stage. It takes roots in preliminary testing of the openings, which are calibrated to achieve a relation between the airflow rate and the pressure difference between the surface pressure at the opening and inside pressure of the double skin façade. As a result, when the pressure difference is measured during the experiments, the airflow can be calculated from the estimated relation. This chapter describes the stage of opening calibration; the final experimental setup for measurements of air flow is described in paragraph 3.2.2.

The air flow through an opening is caused by the pressure differences in the separated environments. If the correlation between the pressure difference and air flow is known then the knowledge of one parameter indicates a possibility for calculation of another one.

Since the variation of pressure at the window surface is the reflection of the pressure induced by wind, then the pressure difference had to be measured between pressure at the external window surface and the reference internal pressure.

A window of the same geometry as in the test facility 'the Cube' was installed in a wooden well sealed box that was connected to a fan and an orifice where the airflow was measured. The window was tested for two cases with 15 different opening angles each. The first case tested is when the window works as an inlet opening and the other case is when it functions as an exhaust. With the purpose of finding the best location for the pressure difference measurements and at the same time to minimize disturbance from the flow turbulence a few points on the window surface and on the wall surface next to the window were tested (Figure 24). A relation between the pressure difference and the airflow passing through the opening can be expressed as in the Equation 2-2, *a* and *b* depend on the opening degree of the window.
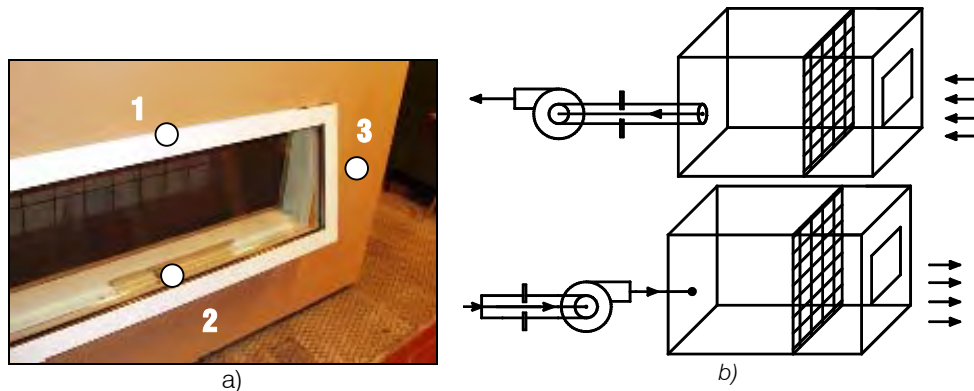
Figure 24. a)Location of the pressure measurements points. b)Top- air supplied through the opening, bottom – air exhausted through the opening.

Equation 2-2

$$Q = a \cdot \Delta P^b$$

Q - air flow, m³/h
ΔP - pressure difference, [Pa]
a,b   - empirically obtained coefficients

The isothermal conditions were kept during the tests. A micro manometer FCO510 measured the pressure difference.

Figure 25. Experimental setup for preliminary opening calibration. a) Front side view. b) Back side view. c) Opening angle is estimated in millimeters.

According to the experimental results, the pressure measurement in the point 2 (Figure 24) is disturbed by a turbulence at the edge of window and, as a result, it is difficult to find the correlation between the pressure difference and the air flow. Results obtained for the point 3 (Figure 24) are valid and can be applied, the weakness of this point is an additional measurement uncertainty when exactly the same location for the pressure measurement is to be found in the final experimental setup. Finally, the measurements completed for the point 1 showed the best results and the linear correlation between the pressure difference and air flow was obtained for the log-log plot, Figure 26. These results further referred as the 'calibration' of an opening and applied for calculation of an air flow in the DSF cavity on a basis of measured pressure differences, as explained in 3.2.2.
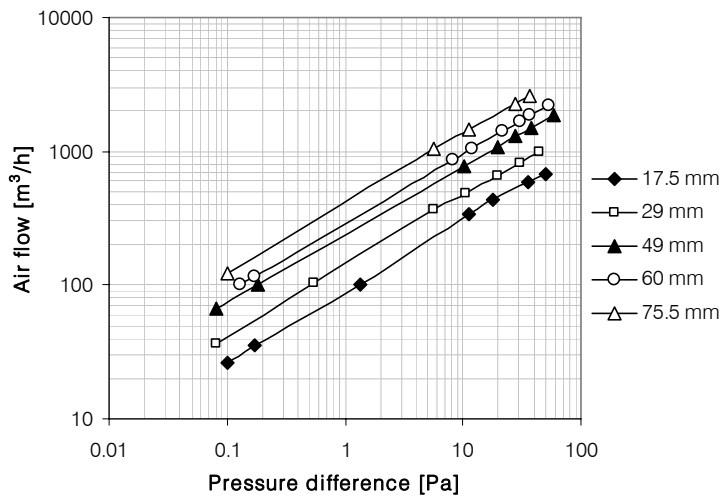
Figure 26. Correlation between pressure difference and air flow rate through the window for different opening angles obtained for point 1.

2.2.3.1   The discharge coefficient

The discharge coefficient represents a ratio between the actual and ideal discharge of fluid through an opening and thus it is heavily related to the flow rate. The difference between the actual and ideal discharge is caused by the friction forces at the edges of an opening and the jet contraction.

According to By og Byg (2002), consider an opening with the uniform pressure difference distribution, then there will appear an air stream across the opening and the air speed in the contracted part of the jet can be described as:

Equation 2-3

$$V_c = C_V \cdot V_{teo} = C_V \cdot \left(\frac{2 \cdot |\Delta P|}{\rho} \right)^{\frac{1}{2}}$$

V_c - air velocity in the contracted part of the jet, m/s
V_{teo} - ideal, or theoretical velocity in the jet (without friction), m/s
C_V - velocity coefficient, which depends on friction in the opening
ρ - air density, kg/m³

$\varDelta P$ - pressure difference across the opening, Pa

The contracted volume flow through the opening is then described as following:

Equation 2-4

$$q_V = A_c \cdot V_c = \left(C_c \cdot A\right) \cdot \left(C_V \cdot V_{teo}\right) = C_d \cdot A \cdot \left(\frac{2 \cdot |\varDelta P|}{\rho}\right)^{\frac{1}{2}}$$

Then:

Equation 2-5

$$C_d = C_V \cdot C_c$$

Where,
q_v - volume flow, m³/s
A_c - contracted area of the jet, m²
A - geometry correct area of the opening, m²
C_c - contraction coefficient of the jet for the particular opening
C_d - discharge coefficient of the particular opening

Considering the experimental data available from the above section 2.2.3, one is able to calculate the discharge coefficient for every opening degree, as following:

Equation 2-6

$$C_d = \frac{q_V}{A \cdot \sqrt{\dfrac{2 \cdot |\Delta P|}{\rho}}}$$

The discharge coefficients in the experimental set-up were calculated, according to the above expression and the results of calculations were further used in the empirical test case specification, see Kalyanova & Heiselberg (2007).

3.   THE FULL-SCALE MEASUREMENTS

The content of this section is addressed to the full-scale experiments conducted in the experimental test facility 'the Cube', in a period September-December, 2006.

Experimental results contain of three modes of the DSF performance:
- MODE 1: External air curtain mode (01.10.2006 – 15.10.2006)
- MODE 2: Transparent insulation mode (19.10.2006 - 06.11.2006)
- MODE 3: Preheating mode (09-11-2006 - 30-11-2006)

Certainly, the application of the results set the main constrains in a design of the experimental setup. Besides the measurements in the DSF, both the weather conditions and the conditions in the experiment room as a reflection of the DSF performance were registered.

3.1   MODES OF THE DSF PERFORMANCE IN THE EXPERIMENTS

There are five main operational modes of the double skin performance if the classification is made according to the flow path in the cavity, see (Loncour, et al., 2004). The full-scale measurements were conducted for the following three operational modes.

- MODE 1: External air curtain mode. The external operable windows (SOL and SOH) open, the air enters the DSF at the bottom of the cavity, gets heated while passing through the DSF cavity and then, released to the external environment, carrying away some amount of the solar heat gains. The flow motion in the cavity is naturally driven.
- MODE 2: Transparent insulation mode. All the openings closed. The principle of this mode is the same as of the conventional window. Air in the DSF cavity is heated to the temperature higher than the outside temperature, this decreases the radiant heat exchange between the internal window surface and the adjacent room.
- MODE 3: Preheating mode. External bottom openings (SOL) and the internal top openings (SIH) open. The air enters from the outside at the bottom of the DSF, the air passes through the DSF cavity and then it is released to the experiment room at the top of DSF cavity. The flow motion is mechanically driven.

Figure 27. Operational modes of the DSF. External air curtain (left). Transparent insulation (centre). Preheating mode (right).

In the MODE 3 a fan, creating underpressure in the experiment room was controlled to keep the air change rate constant. The airflow rate was set to 143 m³/h that corresponds to an air change rate in the experiment room of 1 and apx.13 in the DSF, 1/h.

3.2 THE EXPERIMENTAL SET-UP

From the beginning the focus of these experiments was twofold, since the results had to be applied for the empirical validation of building simulation software in IEA ECBCS ANNEX 43/SHC Task 34, Subtask E- Double Skin Façade and, at the same time, the detailed investigation of the DSF performance had to be carried out. Because of that the experimental set-up and the measurement programme were arranged to satisfy both objectives.

The air temperature, air flow rate in the cavity and, correspondingly, the amount of surplus heat gains removed with the cavity air are the main measures of the double skin façade performance. The air temperature in the experiment room of 'the Cube' was kept uniform and constant at apx.22°C to minimize the influence of the interior environment.

Both, the interior and exterior environment define the boundary conditions for the DSF, and the detailed knowledge of those was essential for further application of the experimental results and evaluation of the DSF performance.

The surplus solar gains into the experiment room were measured indirectly, by assessment of the total cooling power delivered to the experiment room in order to keep the air temperature constant. All of equipment in the experiment room which function as a heat source was connected to the wattmeter to keep a track of all loads and losses in the room.

Information about the experiments is given in the next sections. It is divided into the groups, according to the matter that was measured, as following:

- Temperature
- Air flow rate
- Solar irradiation
- Wind velocity and direction (wind profile)
- Air humidity
- Atmospheric pressure
- Power loads

3.2.1 Temperature

The temperature was measured with the thermocouples type K, silver coated, in order to reduce radiation heat exchange of the sensor (chapter 2.2.1). Depending on location of the sensor, the temperature was registered with two frequencies: every 0.2 second and every 60 seconds. High frequencies were used for the measurement of air temperature in the DSF cavity and outlet air temperatures only.

The air temperature was measured in the engine room (tc 11, where *tc xx – is a sign for a thermocouple with the number xx*), instrument room (tc 4), DSF, experiment room. The outside air temperature was measured in 2 points (tc 67, tc 77), at the height 2 m above the ground (thermocouples). The ground temperature, underneath of foundation in the experiment room (tc 51, tc 52).

3.2.1.1 Temperature measurements in the Experiment room

In order to assess an existence of the vertical temperature gradients, the air temperature in the room was measured with the bare thermocouples, which were placed at the different heights in four locations in the room:
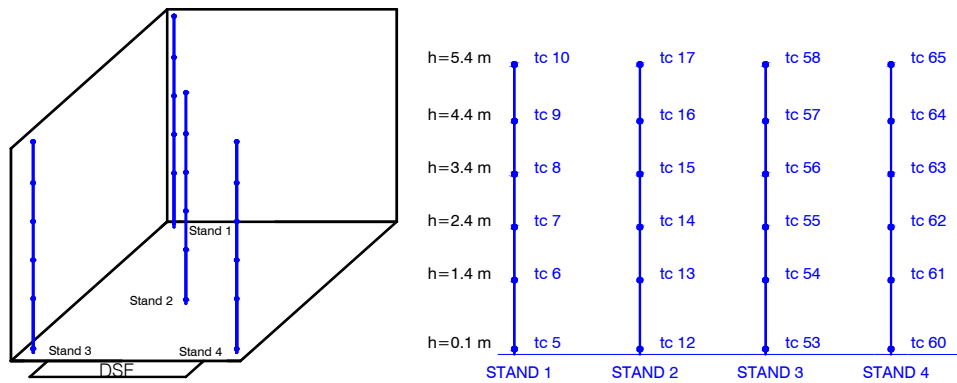
tc – number of a thermocouple

Figure 28. Measurements of the air temperature in the experiment room.

A thermocouple shaded with the silver tube and ventilated by the minifan was installed in the middle of the room, on the stand 2, h=2.5 m

The surface temperatures in the room were measured according to the Figure 29, the sensors were glued to the surfaces with the paste of high heat transmitting property.
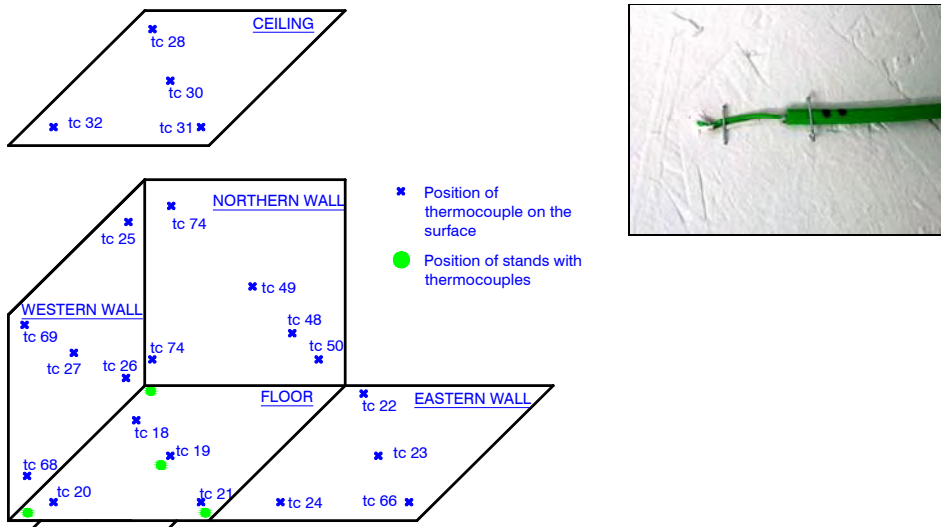
Figure 29. Measurements of surface temperatures in the experiment room. Positioning of equipment (left). Photo of thermocouple glued to a wall surface (right).

3.2.1.2   Temperature measurements in the DSF

According to the previous investigations (see chapter 2.2.1) the thermocouples in the DSF cavity were protected from the influence of direct solar radiation by a silver coated and ventilated tube, the air flow through the tube was ensured by a minifan. Thermocouples were placed in each DSF section in several heights (Figure 30).
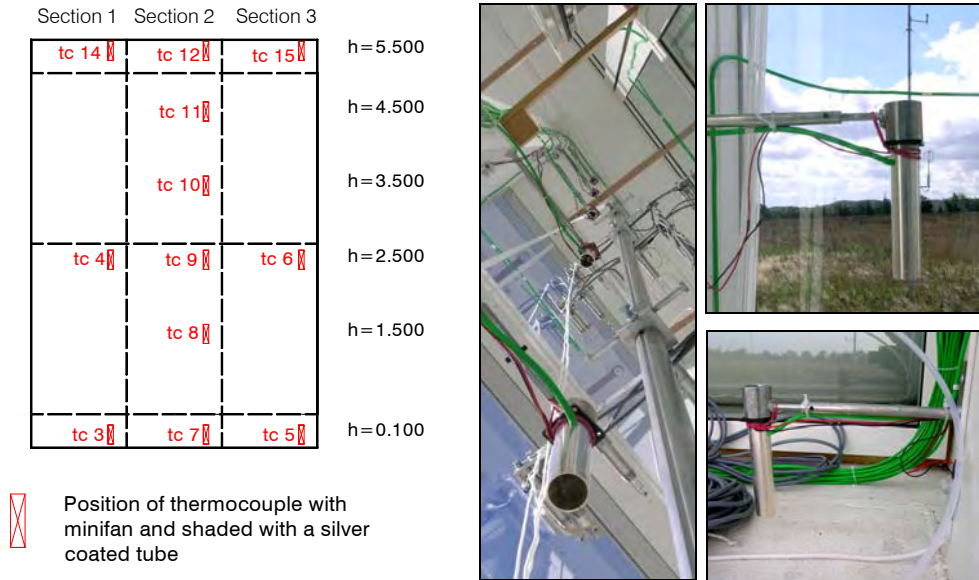
Figure 30. Measurements of air temperature in the DSF cavity. Positioning of sensors, view from outside (left). Photo of experimental setup (right), thermocouple is shielded with silver coated ventilated tube.

Wall surface temperatures in the DSF were measured in 1 point each, the thermocouples were glued to the surfaces with the paste of high heat transmission property.

Measurement of glazing surface temperature was performed in the centre of the glazing pane for each large window section (BOL, BIL, BOH and BIH windows). The temperature was measured of:
- The internal surface of the inner window (ii)
- The external surface of the inner window (ei)
- The internal surface of the outer window pane (ie)

This measurement was conducted with sensors shaded form direct solar access (Figure 31, Figure 32). Continuous shading of the thermocouple sensor at the inner pain was ensured by a thin aluminium foil fixed around the sensor at the external surface. As a result the foil shaded both a sensor at the external and internal surfaces. The thermocouple at the internal surface of the outer pane was shaded in a similar way by a piece of aluminium sticky tape on the external surface of the outer pain.
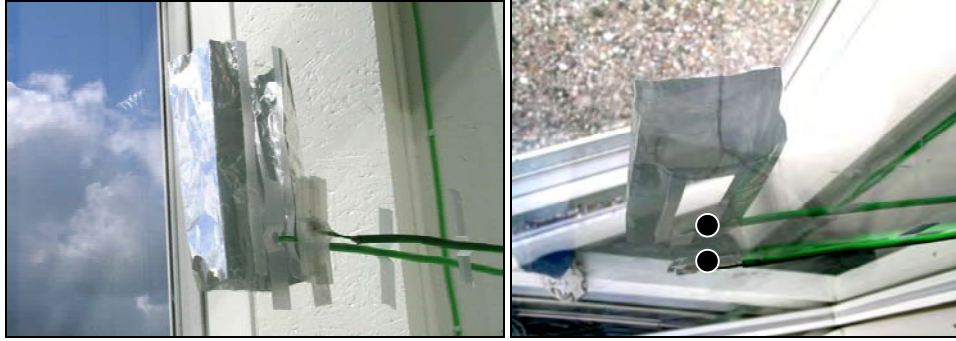
Figure 31. Glass surface temperature measurements. Thermocouples are shielded by silver foil.

NORTHERN WALL

WESTERN WALL

FLOOR

EASTERN WALL

SOUTHERN WALL

tc 36 | tc 29 | tc 40

tc 37 | tc 39 | tc 41

tc 72 | tc 70 | tc 43

tc 71 | tc 44 | tc 42

tc 76 | tc 73 | tc 46

tc 75 | tc 47 | tc 45

⊗ Thermocouple shaded from the direct solar irradiation
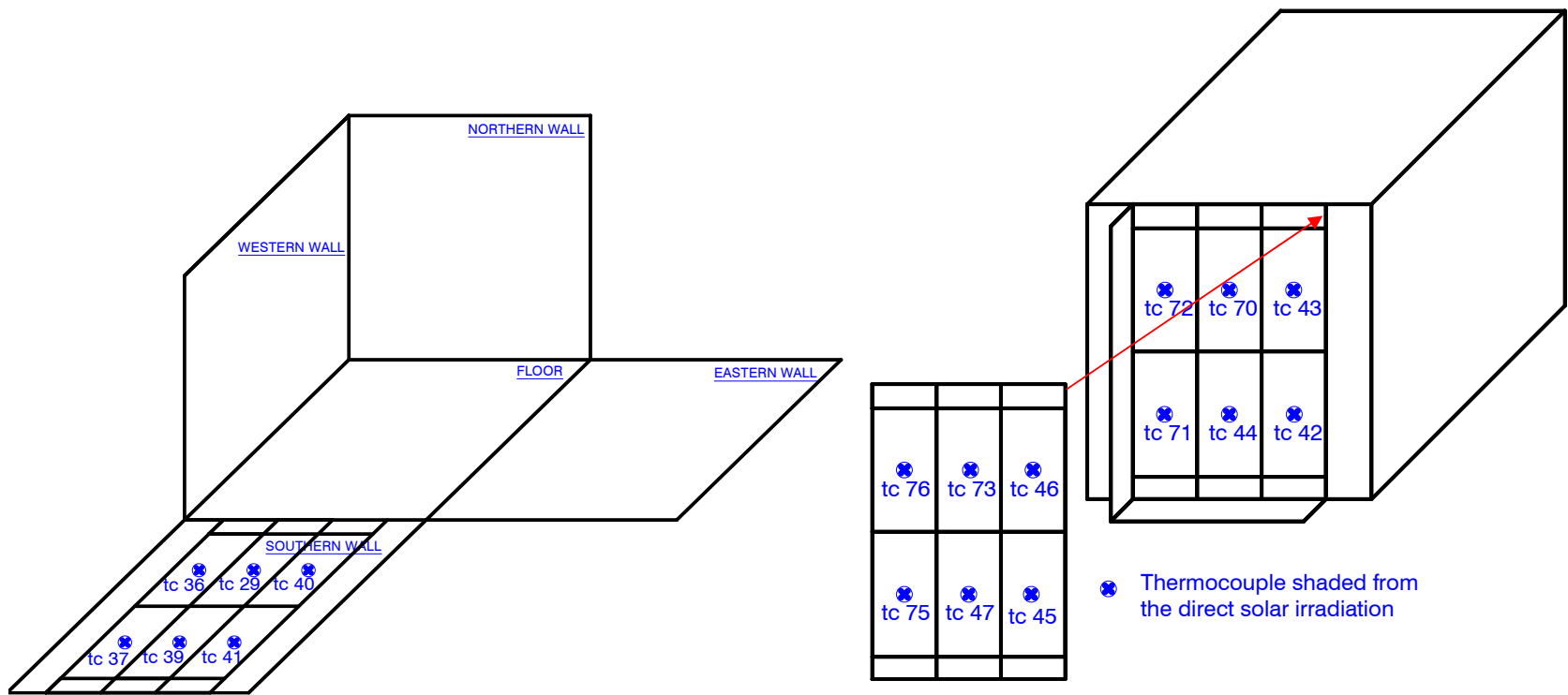
Figure 32. Measurement of glass surface temperature. ii-surfaces (left). ie-,ei-surfaces (right).

3.2.1.3 Measurement of inlet and outlet air temperature

In the MODE 1 and MODE 3 the inlet air temperature into the DSF was assumed to be the same as the outside air temperature. The temperature of the air leaving the DSF cavity was measured directly in the opening.

Normally in the MODE 1, the air leaves the cavity through the SOH-openings, the temperature of the leaving air was measured in every SOH-opening. In order to avoid the influence of solar radiation, the thermocouples were shaded by the silver coated tube and ventilated with a minifan. Location of the temperature sensor in relation to the opening area can be seen in the Figure 33, for different window sections.

SECTION 1,3   SECTION 2

0.6 m

0.25 m

0.95 m

0.6 m

Position of thermocouple with minifan and shaded with a silver coated tube
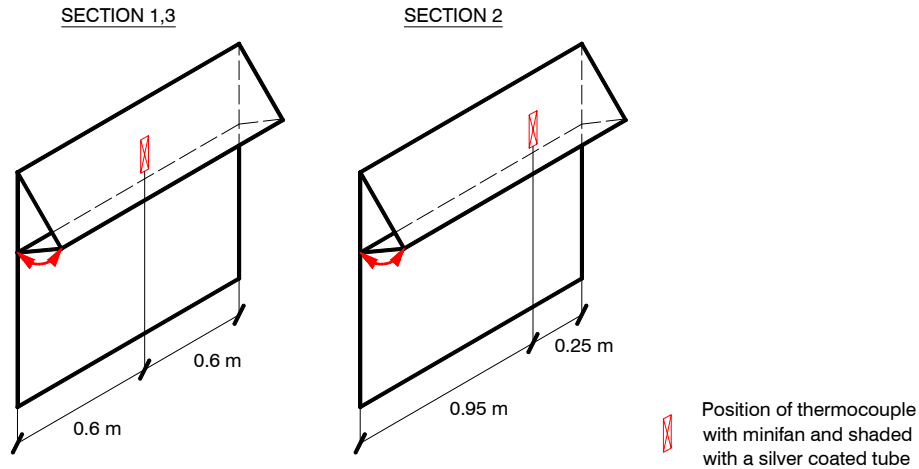
Figure 33. Temperature measurement of the outlet temperature. Positioning of the equipment

Figure 34. Measurement of outlet air temperature from the DSF.

In the MODE 2, all the openings were closed, consequently no inlet or outlet air temperature was measured.

In the MODE 3 same as in the MODE 1, the inlet air temperature was assumed to be the same as the outside air temperature, while the outlet air temperature was measured in each SIH-opening by thermocouples shaded with the silver coated tube and ventilated with a minifan. Positioning of the sensors in relation to the opening area is as in Figure 33 and Figure 34.

3.2.2 Air flow rate in the DSF cavity

Assessment of the air change rate is crucial for the evaluation of indoor climate and the performance of a double skin façade. As a result, the air change rate repeatedly becomes a target for measurement, prediction and simulation. In the meantime, the air

flow occurred in the naturally ventilated spaces is very intricate and extremely difficult to measure. The stochastic nature of wind and as a consequence non-uniform and dynamic flow conditions in combination with the assisting or opposing buoyancy force cause the main difficulties.

In the literature, there are three methods used for estimation of the air change rate in a naturally ventilated space. These are the tracer gas method, method of calculating the air flow from the measured velocity profiles in an opening or calculated from the expressions for the natural ventilation or scale modelling, see (Larsen, 2006 and Hitchin & Wilson, 1967), which involves measurements of air temperature, wind speed, wind direction, wind pressure coefficients on the surfaces and pressure drop across the opening.

Experimental investigation of the airflow rate requires measurement of many highly fluctuating parameters. The fluctuation frequency implies the high sampling frequency for the measurements. For example according to Larsen (2006), the wind speed has to be measured at least at the frequency of 5 Hz, otherwise peaks in the wind velocity can be lost when averaged in time. As a consequence, measurements of the airflow rate are limited to time and costs. When measured with the tracer gas method the limitations are extended to the airflow rates, as with the high airflow rate the amount of injected tracer gas will be enormous. Because of these, the investigation of the natural air flow often is carried out in the controlled environment of the wind tunnel or scale models.

This section addresses the experimental setup for measurements of the air flow rate in the DSF cavity of 'the Cube'. There are three techniques used for the air flow measurements, these are:

- Velocity profile method
- Tracer gas method
- Pressure difference method

Velocity profile method
This method requires a set of anemometers to measure a velocity profile in the opening, and then the shape of the determined velocity profile depends on amount of anemometers installed. At the same time, the equipment located directly in the opening can become an obstruction for the flow appearance. Thus, the method becomes a trade off between the maximum desired amount of anemometers and the minimum desired flow obstruction. Instead of placing equipment directly in the opening in the case of the double skin façade, it can be placed in the DSF cavity, where the velocity profile can be measured in a few levels instead for one.

For the double skin façade, the negative aspect of this method is explained by airflow variation, as the instantaneous air velocity in the cavity may vary from 0 to 5 m/s. This velocity range is challenging, as the equipment must be suitable for measurements of both low and higher velocities, moreover, it is necessary to be able to detect the reverse flow appearance and follow the flow fluctuations. As explained earlier in 2.2.2.2, the hot-sphere anemometers have proved to be suitable for the task.

Temperature compensation is the main working principle of the hot sphere anemometers, therefore measurements of air velocity under the direct solar radiation access can be an issue for the accuracy of the experiments. In order to prevent this kind of error the hot sphere anemometers were preliminary tested and calibrated under the artificial sun conditions, in the wind tunnel, see chapter 2.2.2.

Accuracy of the velocity profile method depends on many factors. Therefore it is common to express it in accuracy of the measuring equipment. The hot sphere anemometers have been calibrated and had an accuracy of 0.01m/s.

Tracer gas method
This method requires the minimum amount of measurements and equipment, but it is characterized with frequent difficulties to obtain uniform concentration of the tracer gas, disturbances from the wind wash-out effects and finally with the time delay of signal caused by the time constant of gas analyzer. The constant injection method (Etheridge, 1996) is used in the experiments described in following sections.

Talking about the accuracy of these measurements, one can speak only of accuracy of equipment used for the measurement, as it is not possible to give estimation for the dataset accuracy for the whole measurement period. This is partly caused by the dynamics of the measured air flow, where the measurement accuracy will change along with the changes of boundary conditions. Another reason is simply the lack of information and experience for this kind of measurement in outdoor test facilities. Still, one can refer to the literature about the accuracy of the experimental method used. According to McWilliams (2002), the tracer gas theory assumes that the tracer gas concentration is constant throughout the measured zone. The expected error of tracer gas results is in the range of 5-10%, what greatly depends on the tracer gas mixing with the air in the DSF cavity.

Pressure difference method
The pressure difference method is a technique, which is still in the testing and validation stage. It takes roots in preliminary testing of the openings, which calibrated to achieve a relation between the airflow rate and the pressure difference between the surface pressure at the opening and inside pressure of the double skin façade. As a result, when the pressure difference is measured during the experiments, the airflow can be calculated from the estimated relation. The procedure for calibration of openings is described in chapter 2.2.3.

3.2.2.1 Experimental setup

The velocity profile method
During the experiments in 'the Cube' all of the velocity measurements were conducted in the section 2 (Figure 7), the velocity profiles were measured in 3-6 levels, with the various number of anemometers in different levels. Different amount of levels was used for different DSF operational modes. Levels are numbered with the Roman numbers in the Figure 35. All in all 46 of hot-sphere anemometers were installed in the experimental setup (Figure 36), 34 of them were engaged in the measurements of the velocity profiles in different levels of the DSF cavity. The measurement frequency of the hot-sphere anemometers is 10Hz.

External

h= 5.15 m VI

h= 4.70 m V

h= 4.36 m IV

h= 2.50 m III

h= 1.91 m II

h= 0.95 m I
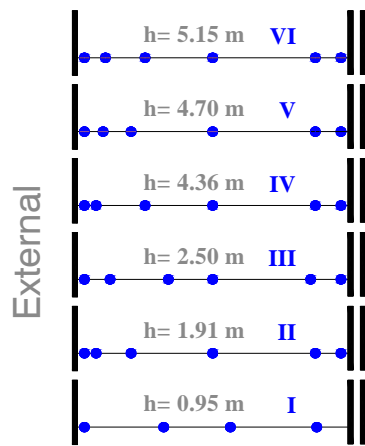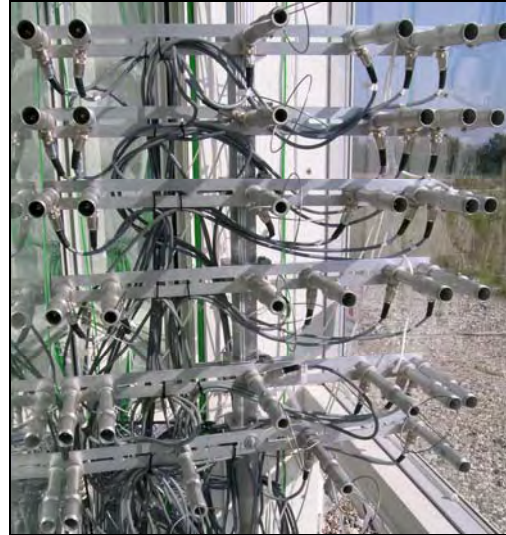
● - Anemometer

Figure 35. Positioning of anemometers in the DSF cavity (left). Anemometers in the DSF cavity before they were moved up to their heights (right).

Figure 36. View to the final positioning of anemometers in the cavity (view from the bottom of DSF).

The tracer gas method

Carbon dioxide (CO_2) is the tracer gas used during the whole period of experiments. Carbon dioxide was released in the lower part of the double skin façade cavity, but above the SOL- and SIL-openings. Even distribution of the tracer gas along the DSF cavity was ensured by its injection through a perforated tube of internal diameter 3.5 mm, perforation distance 4mm and 0.5mm diameter of perforations (Figure 37). Samples of the tracer gas dilution were taken in 12 points Figure 38 (4 samples per section) at the top of the DSF cavity, but below the SOH- openings. All the samples were blended together in the collector (Figure 37) and then the concentration of the diluted tracer gas was measured by a gas analyzer BINOS (Figure 37).

a)   *b)*
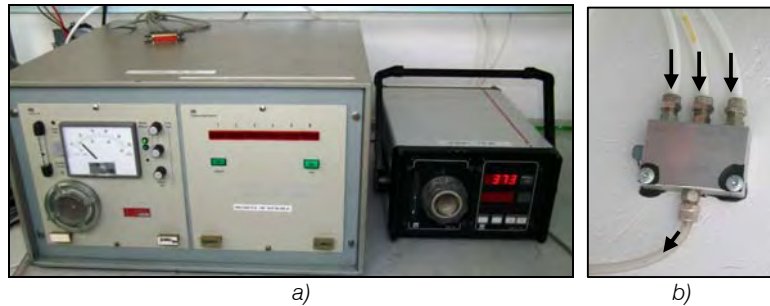
Figure 37. a) URAS and BINOS gas analyzers in the experiment room (correspondingly from left to right). b) Air collector of the samples.

Concentration of carbon dioxide in the outdoor (incoming) air was measured continuously, by a gas analyzer URAS. Both of the devices were preliminary calibrated and had an accuracy of 10ppm. During the experiments the gas analyzers were located in the experiment room in order to avoid any kind of the ambient temperature variations which are harmful for the measurement accuracy. The Helios data logger collected the measurement data from the gas analyzers with the frequency 0.1Hz. The constant injection method was used during the experiments and the quantity of the released tracer gas was kept constant (3-5 l/min).

to BINOS

CO_2

a)   *b)*

— - release of tracer gas

— - to tracer gas collector
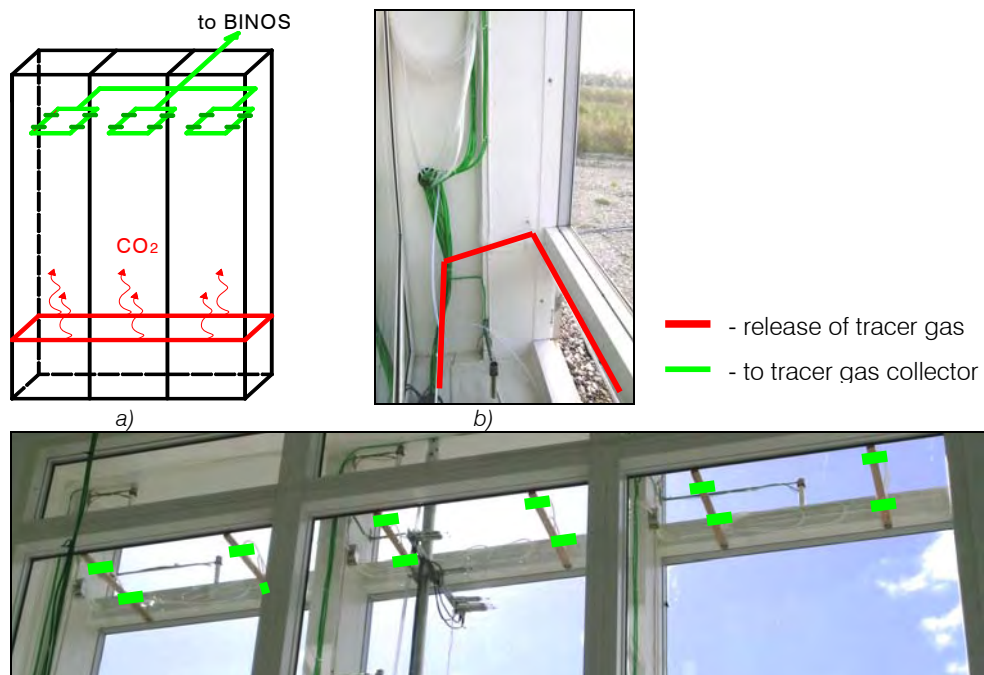
Figure 38. a) Experimental setup for the tracer gas method. b) Positioning of the perforated tube for the release of the tracer gas at the bottom of the DSF cavity. c) Positioning of the air intakes for samples of tracer gas polluted air, at the top of the DSF cavity.

Pressure difference method

This method gives an inspiration for finding a way to cope with the extremely high wind fluctuations. It includes two stages: a stage of calibration the opening and the stage of actual measurements, the latter one took part along with the other two techniques described above, while the former one was completed in the laboratory in advance, as described in (chapter 2.2.3). Next, the actual measurements of the air flow in the double skin façade cavity took place. This time the pressure difference was measured with six pressure transducers Furness Controls Ltd. FC044 (Figure 39, number of pressure transducers corresponds to the number of open windows in the 'Cube').

Figure 39. Pressure transducers Furness Controls Ltd. FC044 (left). Location of the pressure measurements at the window surfaces, SOL-openings (right).

The pressure difference was measured between the surface pressure at the opening and the reference pressure in the double façade cavity. The pressure on the external window surface was measured separately for each window while the reference pressure in the DSF cavity was only separated for the bottom openings SOL and top openings SOH and was measured at the corresponding height of the openings. Location of pressure measurements on the window external surface can be seen in the Figure 39 for the bottom openings SOL, corresponding positions were used for top openings SOH.

3.2.3 Solar radiation

In this experimental study solar radiation is measured for assembling the climate data (as boundary conditions).

For purpose of weather data assembling two pyranometers were placed horizontally on the roof of 'the Cube' (Figure 40). BF3 pyranometer measures Global and Diffuse solar irradiation on the horizontal surface. Another pyranometer, Wilhelm Lambrecht, measures only Global solar irradiation on the horizontal surface and was placed on the roof for control of BF3-readings.

Figure 40. Photo of pyranometers on the roof of 'the Cube', Wilhelm Lambrecht pyranometer at the left and BF3 at the right.

Correlation between total solar radiation, received on the external surface of the DSF and, afterwards, total solar radiation transmitted into the DSF and into the experiment room is regarded as one of the measures of the DSF performance. For that reason, three more pyranometers were used for measurements of the solar radiation received on the DSF surface (Wilhelm Lambrecht-pyranometer), solar radiation transmitted into the DSF (CM11-pyranometer, from Kipp&Zonen) and into the experiment room(CM21-pyranometer, from Kipp&Zonen). Positioning of these pyranometers in relation to the DSF surface can be seen in Figure 41 and Figure 42.
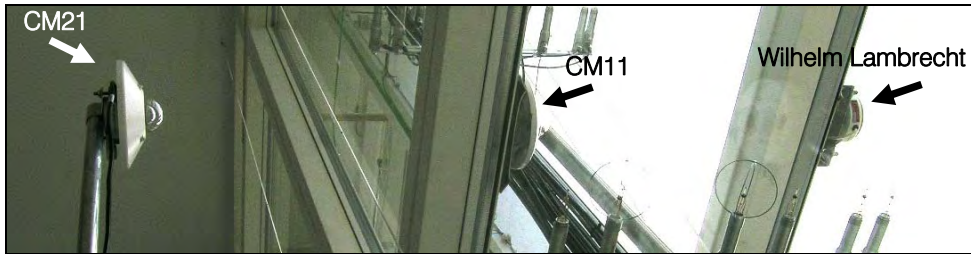
Figure 41. Photo of pyranometers in 'the Cube'.

Pyranometers were installed on the same horizontal distance from each other, in the centre of the DSF surface. However, in order to apply the results assembled by pyranometer CM21 and CM11, this data has to be adjusted to the view factors calculated for the complex geometry in the DSF, as the window frames cover a weighty part of the pyranometers' 'view'.

43
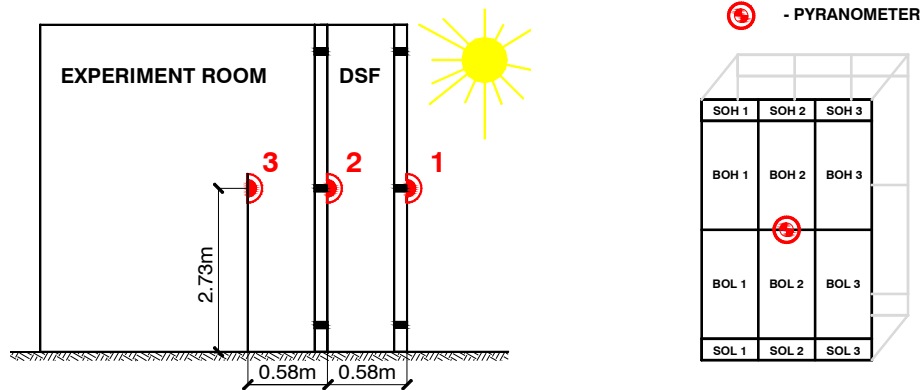
Figure 42. Positioning of pyranometers in the experimental set-up (left). Positioning of the pyranometer in relation to the DSF window sections (right).

All of the pyranometers were connected to HELIOS data logger and the measurements results were assembled with the frequency 0.1Hz. Primary to the installation all of the pyranometers were calibrated in reference with CM21, which is calibrated in sunsimulator and corrected by Kipp&Zonen B.V. The max errors appear at the small angles of incidence, that means that for most of the time the error is much less.

Equipment	Max error:
BF3 (total)	6%
BF3(diffuse)	10%
Wilhelm Lambercht (horizontal)	3%
Wilhelm Lambercht (vertical)	5%
CM11	0.01%

Table 8. Maximal error of pyranometers in the experimental set-up.

3.2.4 Wind velocity profile

Wind velocity and wind direction was measured in six points above the ground in order to build a vertical wind velocity profile. Both 2D and 3D ultrasonic anemometers (Figure 44) were placed on the mast in the centre line of the building, 2m away from it's South façade (Figure 43).
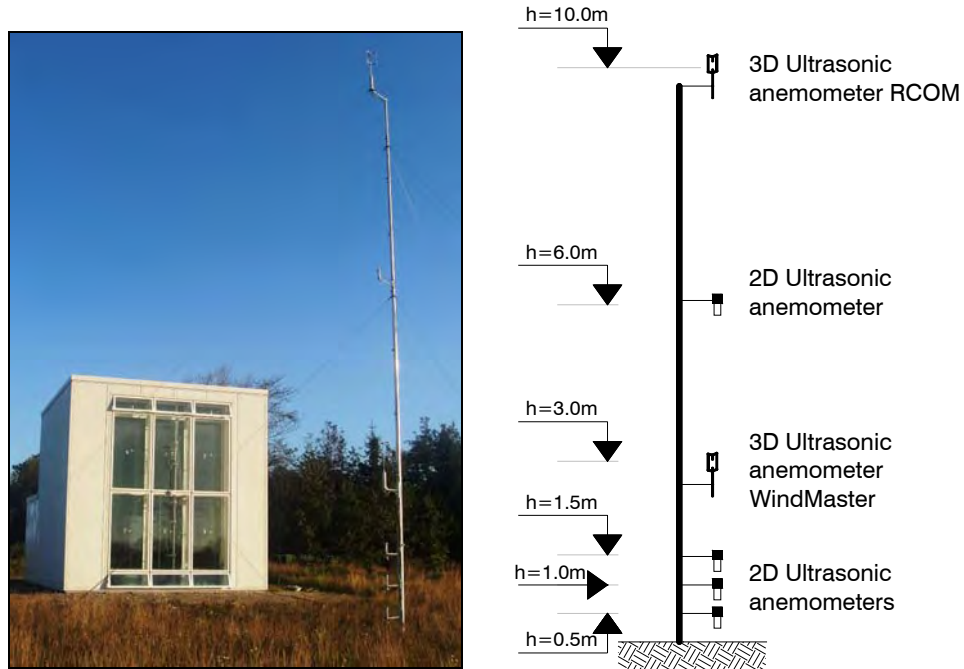
Figure 43. Photo of wind profile mast (left). Positioning of equipment on the mast (right).

The 2D anemometers were from FT Technologies Ltd., type FT702 of range from 0 to 30m/s. The 3D ultrasonic anemometers were RCOM Research R3, type 1210+1189 PCA and WindMaster, type 1086M from Gill producer and had range from 0 to 30m/s and from 0 to 50m/s correspondingly. The frequency of the sampling rate was 5 Hz.

Figure 44. The 3D (left) and 2D(right) ultrasonic anemometer.

3.2.5 Air humidity

Air humidity of the outside air was measured continuously for completing the list of required climate data parameters for building simulation tools. Outside air humidity was measured every 10 minutes, using portable COMARK data logger N2003 from Comark Instruments Inc (Figure 45).

Figure 45. COMARK data logger N2003.

3.2.6 Climate data from the Danish Meteorological Institute (DMI)

The measurement procedure described in this report is complex and required a lot of the devices to measure and record the data simultaneously. Thus the measurement pauses were necessary to offload the data recorded at the high frequencies to release the memory capacity and prolong the long lasting experiments.

Since the complete set of the climate data was required for the empirical validation of the building simulation software, than the measurement pauses had to be filled in with the reliable data. This has been purchased for a weather station located near by the experimental test facility, from the Danish Meteorological Institute (DMI), which is responsible for planning, establishing and operating DMI's operational observation network and measurement stations at several hundred locations in Denmark.

The atmospheric pressure wasn't measured at the 'Cube', but the data from DMI was used instead for.

3.2.7 Power loads to the experiment room

One of the main targets of this experimental work was to accurately estimate solar gains and heat losses by the room adjacent to the double skin façade, as these parameters independently reflect the performance of the DSF cavity. Their independence is assured by the minimized influence of the experiment room on the DSF performance, as the thermal conditions in the room were kept constant, no regulation of the window openings used and no shading devices installed, building is very well insulated and air tight, the air tightness of the building, the transmission heat losses are known (see chapter 2.1.1 and 2.1.2) and all influencing climate parameters were measured.

3.2.7.1 Cooling load

Water was used in the cooling unit of the ventilation system. With the purpose to avoid the condensation on the surface of the surface of the cooling unit the minimum water temperature was set to 12°C, this resulted in a large area of the cooling surface and size of the whole system.

The difference between the supply and return water temperature from the cooling unit in the experiment room was measured as voltage in mV, the maximum error of this measurement was 0.1°C. The mass flow of the water supplied to the cooling unit was measured with a water flow meter MULTICAL from Kamstrup, which measures in a range from 0 to 1kg/s and can have a total error of ±0.2% of the range. Both the temperature difference and the water mass flow were collected by Helios data logger at a frequency 0.1Hz.

3.2.7.2   Heating load

The heating unit in the ventilation system was rarely activated, as in the most of cases an additional heating load was created by a fan of the running ventilation system in the experiment room ensured an additional load. Moreover, some equipment had to be installed in the experiment room and resulted in additional loads. For keeping a track on all loads to the experiment room, including the heating unit, all equipment in the room was connected to a wattmeter D5255S from producer Norma. The accuracy of the device was 0.1% of the range. Readings from the wattmeter were assembled at a frequency 0.1Hz by a data logger Helios.

3.3   EXPERIMENTAL DATA TREATMENT

The experiments described in the above chapters have resulted in a vast amount of data. This section is prepared to get an overview of the results available. Here, it is also explained the data treatment to compile the final set of empirical data for validation purposes of building simulation software. Results are available in the file *Exp_results.xls,* as an hour-averaged values:

1	Month	
2	Date	
3	Hour	
4	Experiment room, surface temperature, °C	Floor
5		Ceiling
6		East Wall
7		West Wall
8		North Wall
9	DSF, surface temperatures, °C	Floor
10		Ceiling
11		East Wall
12		West Wall
13	Glass surf. temperature, °C	ei
14		ie
15		ii
16	Volume averaged air temperature in the DSF, °C	
17	Air temp in the section 2, DSF, °C	h= 0.1m
18		h= 1.5m
19		h= 2.5m
20		h= 3.5m
21		h= 4.5m
22		h= 5.5m
23	Cooling/heating load, kW	
24	Solar irradiation on DSF, W/m²	
25-31	Mass flow in DSF, kg/h	

Table 9. Overview of the results in Exp_results.xls.

The surface temperatures in the experiment room are given as an average value for all measurement points on a surface. A great care must be taken when using these values for the validations, as in the periods with the solar radiation a part of the surface is lighted and will have higher temperature than the surfaces in the shadow. Therefore the authors advise not to use this parameter for validation, but only for evaluation of thermal conditions in the room.

Surface temperatures in the DSF were measured only in the center-point of each surface and the results of these measurements are available in the file. Please note, that the measurement of the floor surface temperature may be inaccurate as explained in the earlier chapters.

Glass surface temperature was measured in the center of the pane, in every big window (6 measurement points). According to the studies of the experimental results the surface temperature of the glazing was nearly identical for the corresponding glass surfaces. In view of that, an average value for all corresponding surfaces is reported as the main result (average for ei-, average for ie-, average for ii-surfaces).

Volume averaged air temperature is calculated for the section 2 of the DSF, using measurements of the air temperature gradient in the cavity at 6 heights above the floor. Results for the section 2 of the DSF cavity are used as representative for the whole cavity, as according to studies of experimental data, the temperature gradient existed the same in all three sections of the cavity.

Cooling load in the experiment room is calculated according to Equation 3-1.

Equation 3-1

$$Q_c = \overset{\bullet}{m} \cdot c_p \cdot \Delta t$$

Where,
Q_c - cooling load, kW
$\overset{\bullet}{m}$ - water mass flow rate, kg/s
c_p - thermal heat capacity of the water, kJ/kg°K
Δt - temperature difference of the supply and return water, °K

Equation 3-2

$$Q_{c,h} = Q_c + Q_h$$

Where,
$Q_{c,h}$ - cooling/heating load to the experiment room, kW
Q_c - cooling load to the experiment room, kW
Q_h - heating load to the experiment room, kW

The cooling system was activated for the most of the time, as the equipment in the experiment room had a significant contribution to the thermal balance of the room in a form additional heat load. This contribution was measured with the Wattmeter and has been removed from the experimental data set as described in the Equation 3-2. In this equation the cooling load is always negative and heating load is always positive, so the sign of the cooling/heating load in the data file tells whether the cooling or heating power has been delivered to the room to keep the air temperature constant to a given value.

Solar irradiation on the external surface of DSF was measured and included into the set of experimental results.

The air flow rate was measured in the DSF cavity, this was then converted to the mass flow rate, using the atmospheric pressure, volume averaged air temperature in the cavity and outdoor air relative humidity.

REFERENCES

By og Byg (2002)   By og Byg, 2002 : Andersen, K T, Heiselberg, P K, Aggerholm, S. / Naturlig ventilation i erhvervsbygninger : beregning og dimensionering. Kbh. :. 118 s.

Erell, et al. (2005)   Erell, E, Leal, V, and Maldonado, E. 2005, Measurement of air temperature in the presence of a large radiant flux: an assessment of passively ventilated thermometer screens, Boundary-Layer Meteorology, vol. 114, pp. 205-231.

Etheridge (1996)   Etheridge, D. 1996. Building ventilation: theory and measurement. - Chichester : John Wiley, 1996. - 724 s.

EN13182   European Standard EN 13182, Ventilation for buildings - Instrumentation requirements for air velocity measurements in ventilated spaces, CEN 2002

Hitchin & Wilson (1967)   Hitchin, E R and Wilson, C B. 1967. A review of experimental techniques for the investigation of natural ventilation in buildings. Building Sciences Vol. **2** (1967), pp. 59–82.

Kalyanova & Heiselberg (2007)   Kalyanova, O and Heiselberg, P. 2007. Empirical Test Case Specification: Test Cases DSF100_e and DSF200_e : IEA ECBCS Annex43/SHC Task 34 : Validation of Building Energy Simulation Tools. Aalborg: Aalborg University : Department of Civil Engineering. ISSN 1901-726X DCE Tiechnical Report No.033

Larsen (2006)   Larsen, T S. 2006. Natural Ventilation Driven by Wind and Temperature Difference. Ph.D Thesis. Aalborg : Department of Civil Engineering : Aalborg University, 2006. 140 p.

Loncour, et al. (2004)   Loncour, X, Deneyer, A, Blasco, et al. 2004. Ventilated Double Facades. Classification & Illustration of façade concepts. Belgian Building Research Institute: Department of Building Physics, Indoor Climate & Building Services. October 2004. http://www.bbri.be/activefacades/new/index.cfm?cat=7_documents&sub=1_download

Sonne, et al. (1993)   Sonne, J K, Vieira, R K, and Rudd, A F. 1993. Limiting solar radiation effects on outdoor air temperature measurements, ASHRAE Transactions, vol. 99 (I), pp. 231-240.

McWilliams (2002)   McWilliams J., (2002). Review of Airflow Measurement Techniques. Lawrence Berkeley National Laboratory, December 1, 2002

APPENDIX

Detailed plan and section of the test facility, 'the Cube

PLAN

N

WALL 3

416   416
416

WALL 2   WALL 2

ZONE 2

6000
4848

WALL 1   WALL 1
3555
1185 1185 1185

ZONE 1

736*

5168

6000

SECTION 1-1

736*   ROOF   416
416

454 134

DSF   WALL 3

2271

ZONE 1   ZONE 2

5584   6000

2271

124

124

FLOOR

454

370

720   4864

6000
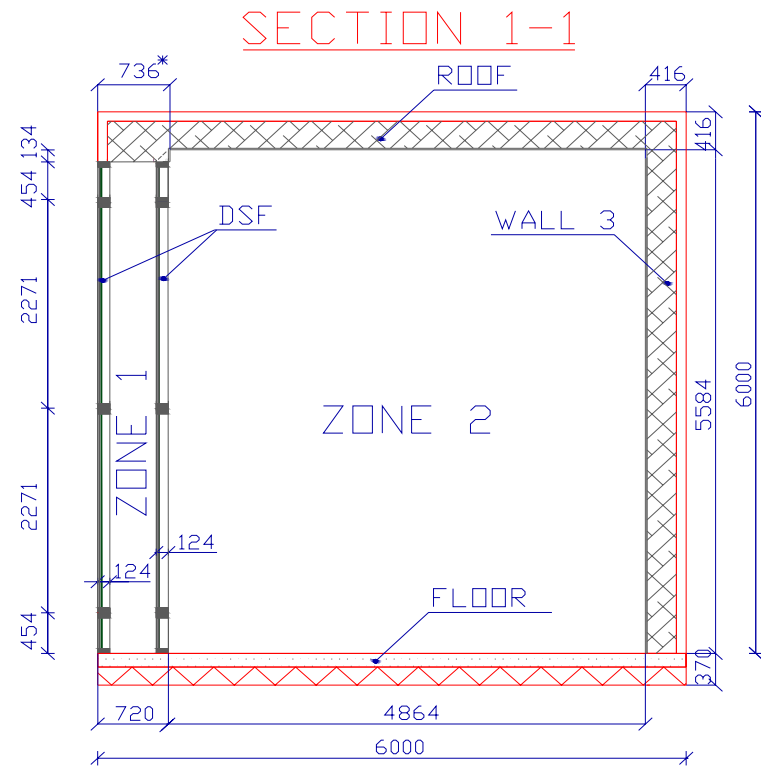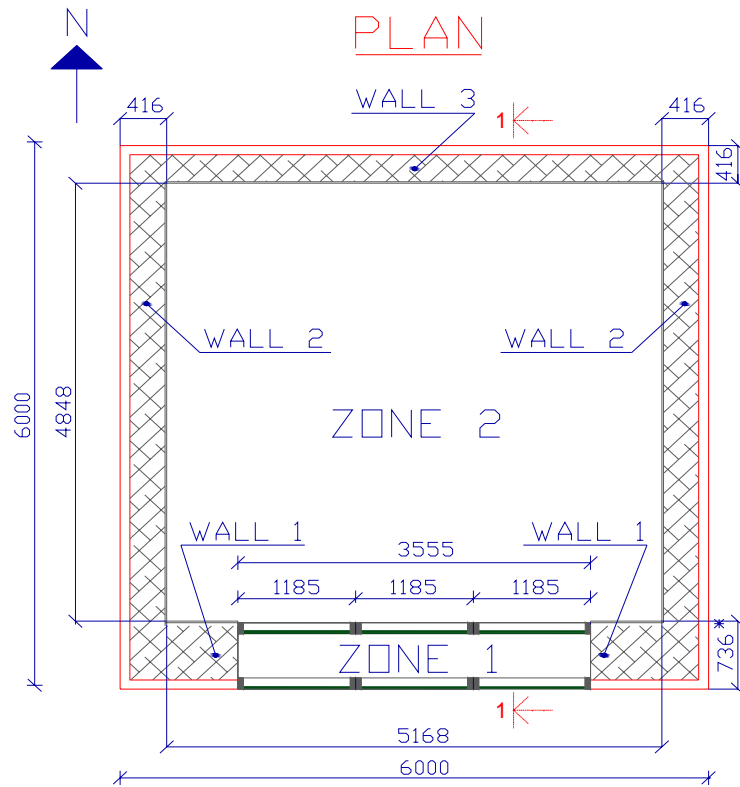
736* – The external dimension of the DSF is 720 mm.
    Additional 16 mm for the layer of Plywood are
    attached to the wall.

Physical properties of the constructions

All constructions in the building are very well insulated. Constructions are subdivided into groups, which are:

- Wall 1- the South façade wall, comprise of external and internal windows
- Wall 2- the East and West façade walls, consist of the same materials.
- Wall 3- the North wall
- Roof
- Floor

This grouping of the constructions is also depicted in the detailed plan of the test facility.

The material properties are prescribed in the following tables. The data is given in separate tables for each of previously defined construction. The first layer in the table always denotes layer facing the internal environment of the model.

Walls' properties

Wall 1:

Material layer number	Material	Layer thickness, mm	Material density, kg/m³	Thermal conductivity, W/mK	Specific heat capacity, J/kgK	Thermal resistance, m²K/W
1	Plywood	16	544	0.115	1213	0.139
2	Rockwool M39	620	32	0.039	711	15.897
3	Isowand Vario	100	142	0.025	500	4

Wall 2:

Material layer number	Material	Layer thickness, mm	Material density, kg/m³	Thermal conductivity, W/mK	Specific heat capacity, J/kgK	Thermal resistance, m²K/W
1	Plywood	16	544	0.115	1213	0.139
2	Rockwool M39	300	32	0.039	711	7.692
3	Isowand Vario	100	142	0.025	500	4

Wall 3:

Material layer number	Material	Layer thickness, mm	Material density, kg/m³	Thermal conductivity, W/mK	Specific heat capacity, J/kgK	Thermal resistance, m²K/W
1	Plywood	16	544	0.115	1213	0.139
2	Rockwool M39	300	32	0.039	711	7.692
3	Isowand Vario	100	142	0.025	500	4

Roof:

Material layer number	Material	Layer thickness, mm	Material density, kg/m³	Thermal conductivity, W/mK	Specific heat capacity, J/kgK	Thermal resistance, m²K/W
1	Plywood	16	544	0.115	1213	0.139
2	Rockwool M39	300	32	0.039	711	7.692
3	Isowand Vario	100	142	0.025	500	4

Floor:
According to the DS 418, the ground resistance to the heat transmission is 1.5 m²K/W.

Material layer number	Material	Layer thickness, mm	Material density, kg/m³	Thermal conductivity, W/mK	Specific heat capacity, J/kgK	Thermal resistance, m²K/W
1	Reinforced concrete, levelled and smoothed	150	2400	1.800	1000	0.639
2	Expanded Polystyrene	220	17	0.045	750	4.889

Windows' properties

Grouping of window partitions and their dimensions were specified in the geometry-part. The physical properties of the windows are prescribed for the same groups.

Window	U-value of window W/m²K	U-value of glazing W/m²K	U-value of frame W/m²K
V1,V2- External window partition	5.36	5.70	3.63
V3-V6 Internal window partition	1.60	1.20	3.63

Optical properties of the surfaces in the test facility

Windows of the DSF consist of glazing, which has been tested and spectral properties are available for every sample. Samples are defined in the table:

Window	Sample number	
	Glass layer facing outside	Glass layer facing inside
External window sections	Clear glass *Sample 1*	
Internal window sections, filled with Argon, 90 %	Clear glass *Sample 2.1*	Glass with the coating attached to the front* surface. *Sample 2.2*
DSF wall and ceiling surface finish	Wooden piece, painted white *Sample 3*	
Experiment room wall and ceiling surface finish	Wooden piece, painted white[1] *Sample 4*	
Ground carpet in front of 'the Cube'	*Sample 5*	

*The definition of front and back is given below
Table. Definition of samples for the glazing spectral data.

Front side always turned towards exterior, while back is turned towards the interior (experiment room).

---

[1] Sample 3 and 4 are painted with different painting
   Floor surface finishes were not tested.

Transcattance

Reflectance

Reflectance
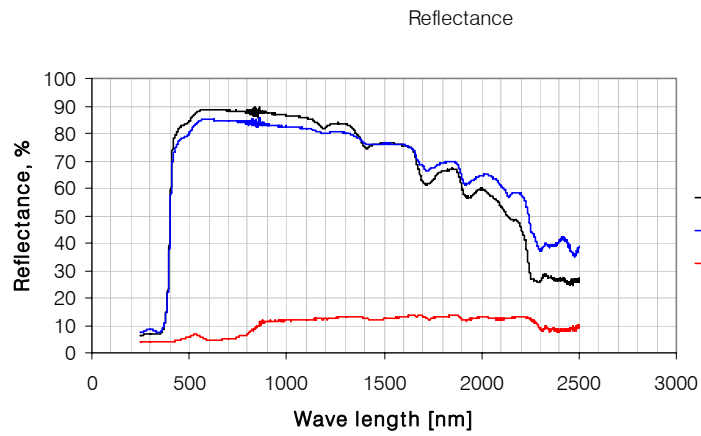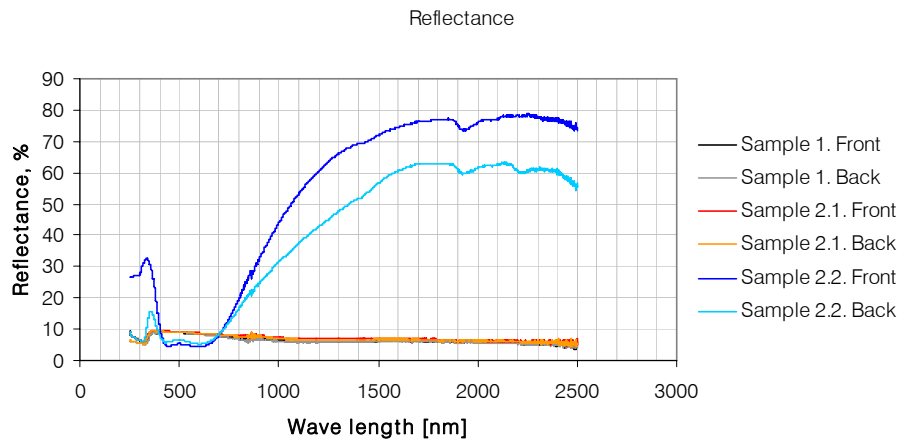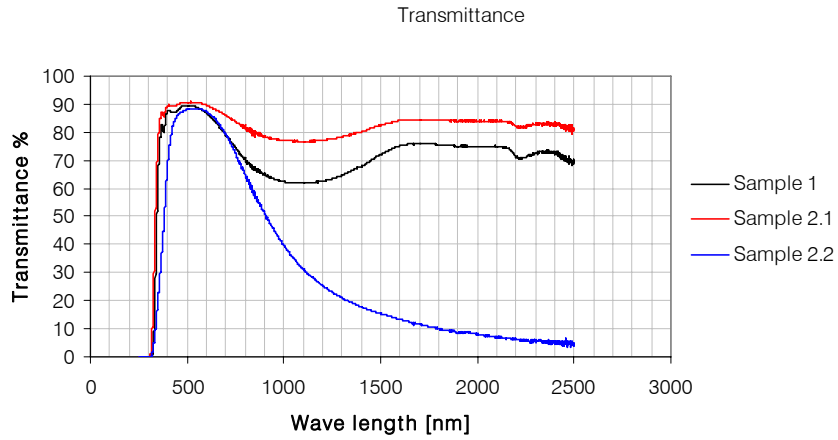
APPENDIX VIII. Experimental data for the full-scale measurements in 'the Cube'.

Experimental results from Test Case DSF100_e

1	2	3	4	5	6	7	8	9	10	11	12	13	14	15	16	17	18	19	20	21	22	23	24
			Exp.room, surface temperature, oC					DSF, surface temperatures oC				Glass surf. temperature, oC			Volume averaged air temperature in the DSF oC	Air temp in the section 2, DSF, oC							Solar irradiation on DSF, W/m2
Month	Date	Hour	Floor	Ceiling	East Wall	West Wall	North Wall	Floor	Ceiling	East Wall	West Wall	ei	ie	ii		h= 0.1m	h= 1.5m	h= 2.5m	h= 3.5m	h= 4.5m	h= 5.5m	Cooling/heating load, kW	
													AVERAGE										
10	19	1	21.1	21.2	21.1	21.5	21.7	12.8	12.2	12.3	12.2	11.5	13.4	20.0	11.8	11.7	11.4	11.9	11.9	12.1	12.2	0.527	0
10	19	2	21.1	21.2	21.1	21.5	21.7	12.8	12.4	12.4	12.3	11.7	13.4	20.0	11.8	11.6	11.3	11.8	11.8	12.0	12.4	0.551	0
10	19	3	21.1	21.2	21.1	21.5	21.7	12.8	12.6	12.4	12.4	11.8	13.5	20.0	11.9	11.7	11.4	11.9	11.9	12.2	12.4	0.558	0
10	19	4	21.1	21.2	21.1	21.5	21.7	12.8	12.8	12.5	12.5	11.8	13.5	20.0	11.9	11.8	11.4	11.9	11.9	12.2	12.5	0.532	0
10	19	5	21.1	21.2	21.2	21.5	21.7	12.9	12.8	12.6	12.5	11.9	13.6	20.0	12.0	11.8	11.5	12.0	12.0	12.3	12.5	0.515	0
10	19	6	21.1	21.2	21.2	21.5	21.7	12.9	12.9	12.6	12.6	11.9	13.6	20.1	12.0	11.9	11.5	12.0	11.9	12.2	12.6	0.532	0
10	19	7	21.1	21.2	21.2	21.5	21.7	12.9	12.9	12.6	12.6	11.9	13.6	20.1	12.1	11.9	11.6	12.0	12.1	12.4	12.5	0.537	0
10	19	8	21.1	21.2	21.2	21.5	21.7	12.9	12.8	12.7	12.7	11.9	13.6	20.1								0.504	1
10	19	9	21.1	21.2	21.2	21.5	21.7	13.3	13.4	12.9	13.0	12.6	14.3	20.2								0.618	11
10	19	10	21.1	21.2	21.2	21.5	21.7	13.8	14.3	13.7	13.6	13.2	15.4	20.4	14.1	13.3	13.8	14.2	14.2	14.4	14.8	0.461	16
10	19	11	21.1	21.3	21.2	21.5	21.7	14.1	14.6	14.0	14.0	13.6	15.6	20.5	14.5	13.7	14.2	14.6	14.5	14.7	15.1	0.409	21
10	19	12	21.1	21.3	21.3	21.6	21.7	14.3	15.0	14.4	14.3	14.0	15.9	20.6	14.8	14.0	14.6	15.0	14.8	15.1	15.4	0.389	21
10	19	13	21.1	21.3	21.3	21.6	21.7	14.7	15.3	14.8	14.7	14.3	16.3	20.7	15.2	14.5	14.9	15.4	15.2	15.5	15.8	0.350	29
10	19	14	21.1	21.4	21.3	21.6	21.7	14.9	15.6	15.1	15.0	14.4	16.5	20.8	15.4	14.7	15.1	15.6	15.4	15.6	16.0	0.321	26
10	19	15	21.1	21.4	21.3	21.6	21.7	15.0	15.8	15.3	15.2	14.7	16.7	20.8	15.6	14.9	15.3	15.8	15.6	15.8	16.1	0.358	22
10	19	16	21.1	21.4	21.3	21.6	21.7	15.0	15.9	15.4	15.4	14.5	16.6	20.7	15.5	14.8	15.2	15.7	15.6	15.8	16.1	0.341	15
10	19	17	21.1	21.3	21.3	21.6	21.7	14.8	15.7	15.4	15.3	13.8	16.2	20.6	15.2	14.5	14.8	15.2	15.1	15.4	15.9	0.384	4
10	19	18	21.1	21.3	21.3	21.6	21.7	14.6	15.5	15.2	15.1	13.7	15.9	20.5	15.0	14.4	14.6	15.0	14.9	15.1	15.7	0.415	0
10	19	19	21.1	21.3	21.3	21.6	21.7	14.6	15.4	15.1	15.1	13.9	15.9	20.5	15.0	14.4	14.6	15.1	14.9	15.1	15.6	0.417	0
10	19	20	21.1	21.3	21.3	21.6	21.7	14.6	15.4	15.1	15.1	14.1	16.0	20.5	15.0	14.5	14.7	15.1	15.0	15.2	15.7	0.416	0
10	19	21	21.1	21.3	21.3	21.6	21.7	14.7	15.5	15.2	15.1	14.2	16.0	20.5	15.1	14.6	14.8	15.2	15.1	15.3	15.8	0.391	0
10	19	22	21.1	21.3	21.3	21.6	21.7	14.7	15.5	15.2	15.1	14.1	16.0	20.5	15.1	14.6	14.8	15.2	15.1	15.3	15.8	0.382	0
10	19	23	21.1	21.3	21.3	21.6	21.7	14.7	15.5	15.2	15.1	13.9	16.0	20.5	14.9	14.4	14.6	15.0	14.9	15.1	15.6	0.372	0
10	19	24	21.1	21.3	21.3	21.6	21.7	14.5	15.3	15.1	15.0	13.1	15.6	20.5	14.5	14.1	14.1	14.5	14.5	14.7	15.4	0.373	0
10	20	1	21.1	21.3	21.3	21.6	21.7	14.4	15.0	14.8	14.8	12.6	15.2	20.4	14.2	13.7	13.7	14.1	14.1	14.4	15.1	0.361	0
10	20	2	21.1	21.3	21.3	21.6	21.7	14.3	14.7	14.6	14.5	12.5	15.0	20.3	14.0	13.6	13.6	14.0	13.9	14.2	14.9	0.347	0
10	20	3	21.1	21.3	21.3	21.6	21.7	14.2	14.6	14.4	14.4	12.4	14.9	20.3	13.9	13.5	13.4	13.8	13.8	14.1	14.8	0.346	0

1	2	3	4	5	6	7	8	9	10	11	12	13	14	15	16	17	18	19	20	21	22	23	24
10	20	4	21.1	21.3	21.3	21.6	21.7	14.1	14.5	14.3	14.2	12.3	14.8	20.3	13.8	13.4	13.3	13.7	13.7	14.0	14.7	0.358	0
10	20	5	21.1	21.3	21.2	21.6	21.7	14.1	14.4	14.2	14.1	12.5	14.8	20.3	13.9	13.5	13.4	13.8	13.8	14.1	14.7	0.358	0
10	20	6	21.1	21.3	21.2	21.6	21.7	14.1	14.5	14.2	14.1	12.8	15.0	20.3	14.0	13.6	13.6	14.0	13.9	14.2	14.8	0.341	0
10	20	7	21.1	21.3	21.2	21.6	21.7	14.2	14.5	14.2	14.2	12.9	15.1	20.3	14.1	13.7	13.7	14.1	14.0	14.3	14.9	0.357	0
10	20	8	21.1	21.3	21.3	21.6	21.7	14.3	14.6	14.3	14.2	13.0	15.2	20.4								0.360	6
10	20	9	21.1	21.5	21.5	21.6	21.8	15.4	16.1	15.4	15.3	14.8	17.4	21.0								0.623	112
10	20	10	21.2	21.7	21.6	21.9	21.9	16.5	17.9	17.2	16.7	16.4	19.2	21.8	17.3	16.4	17.0	17.5	17.5	17.7	18.0	0.061	62
10	20	11	21.2	21.6	21.5	21.8	21.8	16.3	17.6	17.0	16.7	15.7	18.2	21.3	17.1	16.4	16.8	17.3	17.2	17.4	17.7	0.136	54
10	20	12	21.2	21.5	21.5	21.8	21.8	16.4	17.5	17.0	16.9	15.8	18.2	21.3	17.1	16.4	16.8	17.2	17.2	17.4	17.7	0.144	43
10	20	13	21.2	21.5	21.5	21.7	21.7	16.5	17.4	17.1	17.0	15.7	18.1	21.2	17.1	16.5	16.8	17.3	17.1	17.3	17.6	0.168	47
10	20	14	21.2	21.5	21.5	21.8	21.7	16.8	17.6	17.3	17.2	16.0	18.4	21.3	17.4	16.8	17.1	17.6	17.4	17.6	17.9	0.136	60
10	20	15	21.2	21.5	21.5	21.7	21.7	16.5	17.5	17.3	17.2	15.8	18.1	21.2	17.1	16.5	16.8	17.2	17.1	17.3	17.6	0.201	24
10	20	16	21.2	21.5	21.4	21.7	21.7	16.1	17.2	17.0	16.9	15.1	17.5	21.0	16.5	16.0	16.2	16.6	16.5	16.7	17.2	0.284	12
10	20	17	21.2	21.4	21.4	21.6	21.7	15.8	16.8	16.6	16.6	14.5	16.9	20.8	16.0	15.5	15.6	16.0	15.9	16.2	16.7	0.334	3
10	20	18	21.2	21.4	21.3	21.6	21.7	15.5	16.3	16.3	16.2	14.1	16.4	20.6	15.6	15.2	15.2	15.6	15.5	15.7	16.3	0.335	0
10	20	19	21.2	21.4	21.3	21.6	21.7	15.4	16.0	16.0	15.9	13.8	16.2	20.6	15.3	14.9	14.9	15.3	15.1	15.4	16.0	0.376	0
10	20	20	21.1	21.4	21.3	21.6	21.7	15.2	15.6	15.6	15.6	13.1	15.8	20.5	14.8	14.6	14.4	14.8	14.7	15.0	15.6	0.383	0
10	20	21	21.1	21.4	21.3	21.6	21.7	15.0	15.3	15.4	15.3	13.1	15.5	20.5	14.7	14.4	14.3	14.6	14.6	14.8	15.4	0.391	0
10	20	22	21.1	21.3	21.3	21.6	21.7	15.0	15.2	15.2	15.2	13.3	15.5	20.4	14.7	14.4	14.3	14.6	14.6	14.8	15.4	0.410	0
10	20	23	21.1	21.3	21.3	21.6	21.7	14.9	15.2	15.1	15.1	13.3	15.5	20.4	14.6	14.4	14.2	14.6	14.5	14.8	15.4	0.398	0
10	20	24	21.1	21.3	21.3	21.6	21.7	14.8	15.1	15.0	14.9	12.9	15.4	20.4	14.5	14.2	14.0	14.4	14.3	14.6	15.2	0.421	0
10	21	1	21.1	21.3	21.3	21.6	21.7	14.7	14.9	14.8	14.8	12.8	15.3	20.4	14.3	14.1	13.9	14.3	14.2	14.4	15.1	0.404	0
10	21	2	21.1	21.3	21.3	21.6	21.7	14.6	14.8	14.6	14.6	12.4	15.1	20.4	14.1	13.8	13.6	14.0	13.9	14.2	14.9	0.414	0
10	21	3	21.1	21.3	21.3	21.6	21.7	14.5	14.6	14.5	14.5	12.6	15.0	20.3	14.1	13.8	13.7	14.0	14.0	14.2	14.9	0.411	0
10	21	4	21.1	21.3	21.3	21.6	21.7	14.5	14.7	14.4	14.4	12.8	15.1	20.4	14.2	13.9	13.8	14.1	14.1	14.3	14.9	0.403	0
10	21	5	21.1	21.3	21.3	21.6	21.7	14.5	14.7	14.4	14.4	12.8	15.1	20.4	14.2	13.9	13.8	14.2	14.1	14.4	15.0	0.430	0
10	21	6	21.1	21.3	21.3	21.6	21.7	14.5	14.7	14.4	14.4	12.9	15.2	20.4	14.2	13.9	13.8	14.2	14.2	14.4	15.0	0.409	0
10	21	7	21.1	21.3	21.3	21.6	21.7	14.5	14.7	14.4	14.4	13.1	15.2	20.4	14.3	14.0	13.9	14.3	14.2	14.5	15.0	0.418	0
10	21	8	21.1	21.3	21.3	21.6	21.7	14.6	14.8	14.5	14.4	13.2	15.3	20.4	14.4	14.1	14.1	14.4	14.4	14.6	15.1	0.417	2
10	21	9	21.1	21.3	21.3	21.6	21.7	14.8	15.0	14.6	14.6	13.7	15.6	20.5	14.8	14.4	14.4	14.8	14.7	14.9	15.3	0.374	13
10	21	10	21.1	21.4	21.3	21.6	21.7	15.1	15.3	15.0	15.0	14.2	16.2	20.7	15.2	14.9	14.9	15.3	15.2	15.4	15.7	0.350	20
10	21	11	21.2	21.4	21.4	21.6	21.8	15.4	15.6	15.3	15.3	14.2	16.5	20.8	15.5	15.2	15.2	15.6	15.5	15.7	16.0	0.300	30
10	21	12	21.2	21.5	21.5	21.8	21.8	16.5	16.4	15.9	16.0	15.9	17.7	21.3	17.1	16.7	17.0	17.3	17.2	17.3	17.5	0.072	110

1	2	3	4	5	6	7	8	9	10	11	12	13	14	15	16	17	18	19	20	21	22	23	24
10	21	13	21.2	21.6	21.6	21.9	21.8	17.1	17.7	17.0	17.1	16.9	19.1	21.7	18.0	17.2	17.8	18.2	18.1	18.3	18.5	0.095	68
10	21	14	21.3	21.7	21.7	21.9	21.8	18.1	18.7	17.9	18.1	18.2	20.1	22.0	19.5	18.6	19.5	19.8	19.6	19.7	19.9	-0.110	146
10	21	15	21.4	22.0	21.9	22.2	21.9	19.9	21.1	19.7	20.4	20.9	23.3	23.2	22.5	21.0	22.8	22.9	22.6	22.7	23.0	-0.440	208
10	21	16	21.3	21.9	21.8	22.1	21.8	18.8	21.6	20.2	20.8	19.1	22.2	22.4	20.6	19.4	20.3	20.9	20.7	20.9	21.3	-0.063	42
10	21	17	21.3	21.7	21.6	21.9	21.8	17.6	20.1	19.3	19.7	16.7	19.6	21.5	18.5	17.7	18.1	18.5	18.5	18.8	19.4	0.137	10
10	21	18	21.2	21.6	21.5	21.8	21.8	16.8	18.7	18.3	18.6	15.1	18.0	21.1	17.1	16.5	16.6	17.1	17.0	17.3	18.1	0.242	1
10	21	19	21.2	21.5	21.4	21.7	21.8	16.3	17.6	17.5	17.7	14.1	17.0	20.8	16.1	15.6	15.6	16.0	15.9	16.3	17.1	0.292	0
10	21	20	21.2	21.5	21.4	21.7	21.7	15.9	16.8	16.8	17.0	13.9	16.4	20.7	15.7	15.2	15.2	15.6	15.5	15.8	16.6	0.323	0
10	21	21	21.2	21.4	21.4	21.7	21.7	15.8	16.4	16.4	16.6	14.2	16.4	20.6	15.6	15.3	15.2	15.6	15.5	15.7	16.4	0.365	0
10	21	22	21.2	21.4	21.4	21.6	21.7	15.6	16.1	16.1	16.2	13.7	16.2	20.6	15.3	15.0	14.9	15.3	15.2	15.4	16.1	0.348	0
10	21	23	21.2	21.4	21.4	21.6	21.7	15.5	15.9	15.8	15.9	13.7	16.0	20.6	15.2	14.9	14.8	15.2	15.1	15.3	15.9	0.384	0
10	21	24	21.2	21.4	21.3	21.6	21.7	15.4	15.7	15.6	15.7	13.5	15.9	20.5	15.0	14.7	14.6	15.0	14.9	15.1	15.8	0.388	0
10	22	1	21.2	21.4	21.3	21.6	21.7	15.3	15.6	15.4	15.5	13.7	15.8	20.5	15.0	14.7	14.6	15.0	14.9	15.1	15.7	0.387	0
10	22	2	21.2	21.4	21.3	21.6	21.7	15.2	15.4	15.2	15.3	13.1	15.6	20.5	14.7	14.4	14.2	14.6	14.5	14.8	15.5	0.380	0
10	22	3	21.2	21.4	21.3	21.6	21.7	15.0	15.2	15.0	15.1	13.0	15.4	20.4	14.5	14.3	14.1	14.5	14.4	14.6	15.3	0.416	0
10	22	4	21.2	21.4	21.3	21.6	21.7	14.9	15.0	14.8	14.9	12.6	15.3	20.4	14.3	14.1	13.8	14.2	14.1	14.4	15.1	0.400	0
10	22	5	21.2	21.3	21.3	21.6	21.7	14.7	14.8	14.6	14.7	12.5	15.0	20.4	14.1	13.9	13.7	14.1	14.0	14.2	15.0	0.416	0
10	22	6	21.2	21.3	21.3	21.6	21.7	14.7	14.7	14.5	14.5	12.5	15.0	20.3	14.1	13.8	13.6	14.0	13.9	14.2	14.9	0.413	0
10	22	7	21.2	21.3	21.3	21.6	21.7	14.6	14.7	14.4	14.4	12.7	15.0	20.3	14.2	13.9	13.7	14.1	14.0	14.3	14.9	0.415	0
10	22	8	21.2	21.3	21.3	21.6	21.7	14.7	14.8	14.4	14.5	13.2	15.3	20.4	14.4	14.2	14.0	14.4	14.3	14.5	15.1	0.422	5
10	22	9	21.2	21.3	21.3	21.6	21.7	14.7	14.7	14.5	14.5	12.2	15.2	20.5	14.1	13.8	13.6	14.0	13.9	14.2	14.9	0.384	16
10	22	10	21.2	21.4	21.4	21.7	21.8	15.2	14.8	14.6	14.6	12.5	15.5	20.7	15.2	14.9	14.8	15.3	15.2	15.5	15.8	0.256	80
10	22	11	21.4	21.8	21.7	22.2	21.8	17.6	17.1	16.8	16.5	16.4	19.6	22.5	18.5	17.6	18.1	18.7	18.5	18.9	19.1	-0.251	192
10	22	12	21.7	22.4	22.2	22.7	22.1	21.1	20.2	19.2	18.8	20.9	23.6	24.4	25.3	24.0	25.1	25.9	25.5	25.7	25.7	-1.555	542
10	22	13	22.0	23.6	23.2	23.6	22.6	26.8	27.7	24.3	24.5	27.9	32.9	28.5	31.7	29.0	32.0	32.5	32.1	32.1	32.7	-3.031	693
10	22	14	22.0	23.7	23.5	23.6	22.6	27.8	32.0	27.7	29.2	27.9	35.3	28.5	30.5	27.5	30.3	31.0	30.8	31.2	32.1	-2.512	430
10	22	15	21.6	22.7	22.4	22.7	22.1	21.8	28.2	25.5	26.1	19.1	25.6	23.5	23.2	21.5	22.4	23.0	23.2	23.7	25.5	-0.585	31
10	22	16	21.6	22.3	22.1	22.3	21.9	20.3	24.3	22.7	23.7	16.6	21.5	22.4	21.2	19.9	20.5	21.1	21.0	21.5	22.8	-0.397	139
10	22	17	21.5	22.0	21.9	22.1	21.8	19.4	22.4	21.6	22.8	16.7	20.9	22.0	19.7	18.5	19.1	19.6	19.7	20.1	21.2	-0.077	34
10	22	18	21.5	21.8	21.7	21.9	21.8	17.8	19.9	19.4	20.2	13.4	17.8	21.1	16.9	16.1	16.2	16.6	16.6	17.1	18.6	0.133	0
10	22	19	21.4	21.6	21.5	21.8	21.8	17.0	18.1	17.7	18.4	13.1	16.5	20.8	15.8	15.2	15.2	15.6	15.6	16.0	17.2	0.249	0
10	22	20	21.4	21.5	21.5	21.7	21.8	16.4	16.9	16.6	17.2	12.8	15.9	20.6	15.2	14.7	14.6	15.0	14.9	15.3	16.3	0.287	0
10	22	21	21.4	21.5	21.4	21.7	21.8	16.0	16.1	15.9	16.4	12.7	15.6	20.5	14.9	14.6	14.4	14.8	14.7	15.0	15.8	0.338	0

1	2	3	4	5	6	7	8	9	10	11	12	13	14	15	16	17	18	19	20	21	22	23	24
10	22	22	21.4	21.4	21.4	21.7	21.8	15.9	15.7	15.5	15.9	13.1	15.6	20.5	14.9	14.6	14.5	14.9	14.7	15.0	15.7	0.334	0
10	22	23	21.3	21.4	21.4	21.7	21.7	15.7	15.6	15.3	15.6	13.5	15.7	20.5	14.9	14.7	14.5	14.9	14.8	15.0	15.6	0.380	0
10	22	24	21.3	21.4	21.4	21.6	21.7	15.6	15.5	15.2	15.4	13.3	15.7	20.5	14.8	14.6	14.4	14.8	14.6	14.9	15.5	0.373	0
10	23	1	21.3	21.4	21.4	21.6	21.7	15.4	15.2	14.9	15.1	12.7	15.4	20.5	14.4	14.3	14.0	14.4	14.2	14.5	15.2	0.388	0
10	23	2	21.3	21.4	21.3	21.6	21.7	15.2	15.0	14.7	14.8	12.5	15.1	20.4	14.2	14.1	13.8	14.2	14.1	14.3	15.0	0.394	0
10	23	3	21.3	21.4	21.3	21.6	21.7	15.0	14.8	14.5	14.6	12.3	15.0	20.4	14.1	13.9	13.6	14.0	13.9	14.2	14.9	0.408	0
10	23	4	21.3	21.3	21.3	21.6	21.7	14.9	14.6	14.4	14.4	12.3	14.9	20.4	14.0	13.9	13.6	13.9	13.8	14.1	14.8	0.408	0
10	23	5	21.3	21.3	21.3	21.6	21.7	14.9	14.6	14.3	14.4	12.7	15.0	20.3	14.2	14.1	13.8	14.1	14.0	14.3	14.9	0.431	0
10	23	6	21.2	21.3	21.3	21.6	21.7	15.0	14.7	14.4	14.4	13.2	15.3	20.4	14.5	14.3	14.1	14.4	14.3	14.5	15.1	0.430	0
10	23	7	21.2	21.3	21.3	21.6	21.7	15.0	14.9	14.5	14.6	13.5	15.5	20.4	14.6	14.5	14.3	14.7	14.5	14.7	15.3	0.410	0
10	23	8	21.2	21.3	21.3	21.6	21.7	15.1	15.1	14.7	14.7	13.8	15.7	20.5								0.406	1
10	23	9	21.2	21.4	21.3	21.6	21.7	15.2	15.3	14.9	14.9	14.3	16.0	20.6	15.3	15.0	14.9	15.4	15.1	15.3	15.7	0.390	8
10	23	10	21.3	21.4	21.4	21.7	21.8	16.1	16.0	15.6	15.6	15.5	17.1	20.9	16.5	16.2	16.3	16.6	16.4	16.6	16.8	0.261	58
10	23	11	21.3	21.5	21.5	21.7	21.8	16.5	16.9	16.4	16.4	16.3	18.1	21.2	17.2	16.6	16.9	17.3	17.2	17.4	17.6	0.230	35
10	23	12	21.3	21.5	21.5	21.8	21.8	16.7	17.3	16.8	16.8	16.0	18.2	21.3	17.3	16.8	17.1	17.5	17.3	17.5	17.7	0.179	48
10	23	13	21.3	21.6	21.5	21.8	21.8	17.0	17.6	17.2	17.2	16.3	18.5	21.4	17.6	17.0	17.4	17.7	17.6	17.8	18.1	0.164	46
10	23	14	21.4	21.7	21.7	22.0	21.8	18.1	18.5	17.9	18.1	17.8	19.9	22.0	19.3	18.4	19.3	19.5	19.3	19.4	19.6	-0.101	126
10	23	15	21.3	21.8	21.7	22.0	21.8	17.9	19.1	18.4	18.7	17.4	20.0	21.9	19.1	18.3	19.1	19.4	19.2	19.3	19.6	0.007	77
10	23	16	21.4	21.8	21.8	22.0	21.8	18.4	19.8	19.0	19.6	18.0	20.6	22.0	19.9	18.9	19.8	20.2	20.0	20.1	20.5	-0.049	92
10	23	17	21.3	21.7	21.6	21.9	21.8	17.6	19.4	18.8	19.3	16.7	19.4	21.5	18.4	17.6	18.0	18.4	18.4	18.6	19.1	0.122	27
10	23	18	21.3	21.6	21.5	21.8	21.8	16.8	18.3	18.0	18.3	15.4	17.9	21.0	17.1	16.6	16.6	17.0	17.0	17.3	17.9	0.245	0
10	23	19	21.3	21.5	21.5	21.8	21.8	16.4	17.4	17.3	17.5	14.4	17.1	20.8	16.2	15.8	15.8	16.2	16.1	16.4	17.1	0.281	0
10	23	20	21.2	21.5	21.4	21.7	21.8	16.0	16.7	16.7	16.8	13.6	16.4	20.7	15.5	15.1	15.0	15.4	15.3	15.6	16.4	0.330	0
10	23	21	21.2	21.5	21.4	21.7	21.8	15.6	16.0	16.1	16.2	12.9	15.8	20.6	14.9	14.6	14.4	14.8	14.7	15.0	15.9	0.345	0
10	23	22	21.2	21.4	21.4	21.7	21.8	15.3	15.4	15.6	15.7	12.0	15.2	20.5	14.2	13.8	13.7	14.0	14.0	14.4	15.3	0.369	0
10	23	23	21.2	21.4	21.4	21.7	21.7	14.9	14.9	15.0	15.1	11.4	14.6	20.3	13.7	13.4	13.1	13.5	13.4	13.8	14.8	0.385	0
10	23	24	21.2	21.4	21.3	21.6	21.7	14.6	14.4	14.5	14.5	10.8	14.2	20.2	13.1	12.8	12.5	12.9	12.9	13.3	14.3	0.405	0
10	24	1	21.2	21.4	21.3	21.6	21.7	14.2	13.9	14.0	14.0	10.4	13.7	20.1	12.7	12.4	12.2	12.5	12.5	12.9	13.9	0.432	0
10	24	2	21.2	21.3	21.3	21.6	21.7	14.0	13.6	13.6	13.6	10.4	13.5	20.1	12.6	12.4	12.1	12.4	12.4	12.8	13.7	0.457	0
10	24	3	21.2	21.3	21.3	21.6	21.7	14.0	13.4	13.3	13.4	10.8	13.6	20.1	12.7	12.5	12.2	12.5	12.5	12.9	13.7	0.446	0
10	24	4	21.2	21.3	21.3	21.6	21.7	13.9	13.4	13.2	13.2	11.0	13.7	20.1	12.8	12.6	12.3	12.6	12.6	13.0	13.8	0.456	0
10	24	5	21.2	21.3	21.3	21.6	21.7	13.9	13.4	13.2	13.2	11.2	13.8	20.1	12.9	12.7	12.4	12.7	12.7	13.1	13.8	0.460	0
10	24	6	21.2	21.3	21.2	21.5	21.7	13.9	13.5	13.1	13.1	11.2	13.9	20.1	12.9	12.6	12.4	12.7	12.7	13.0	13.8	0.467	0

1	2	3	4	5	6	7	8	9	10	11	12	13	14	15	16	17	18	19	20	21	22	23	24
10	24	7	21.2	21.3	21.2	21.5	21.7	13.8	13.4	13.1	13.1	11.1	13.8	20.1	12.9	12.6	12.4	12.7	12.7	13.0	13.8	0.457	0
10	24	8	21.1	21.3	21.2	21.5	21.7	13.8	13.4	13.0	13.0	11.0	13.8	20.1	12.8	12.6	12.3	12.6	12.6	12.9	13.7	0.473	0
10	24	9	21.1	21.3	21.2	21.5	21.7	13.8	13.4	13.0	13.0	11.0	13.8	20.1	12.9	12.7	12.4	12.7	12.7	13.0	13.8	0.455	3
10	24	10	21.3	21.3	21.4	21.7	21.9	14.2	13.8	13.3	13.3	11.9	14.4	20.4	13.4	13.3	13.0	13.4	13.3	13.5	14.2	0.455	28
10	24	11	21.3	21.4	21.4	21.6	21.9	14.8	14.2	13.8	13.8	12.7	15.2	20.7	14.1	13.8	13.7	14.1	14.0	14.2	14.7	0.430	45
10	24	12	21.3	21.4	21.5	21.6	21.9	15.1	14.7	14.2	14.2	13.2	15.7	20.8	14.6	14.3	14.2	14.6	14.5	14.7	15.1	0.770	46
10	24	13	21.3	21.5	21.5	21.7	21.9	15.4	15.1	14.7	14.7	13.5	16.2	21.0	14.9	14.6	14.6	15.0	14.9	15.1	15.5	0.257	39
10	24	14	21.4	21.5	21.5	21.8	21.9	15.3	15.3	14.8	14.8	13.2	16.0	20.9	14.8	14.4	14.4	14.8	14.7	14.9	15.4	0.318	33
10	24	15	21.4	21.6	21.6	21.9	21.9	16.4	15.9	15.4	15.6	14.9	17.3	21.4	16.6	16.1	16.5	16.7	16.6	16.7	16.9	0.086	133
10	24	16	21.4	21.8	21.8	22.0	21.9	16.9	17.5	16.6	17.1	15.8	18.9	21.9	17.8	16.9	17.7	18.1	17.9	18.0	18.4	0.052	106
10	24	17	21.4	21.7	21.7	21.9	21.9	16.2	17.6	16.8	17.3	14.6	18.1	21.4	16.6	15.8	16.2	16.6	16.6	16.9	17.5	0.215	28
10	24	18	21.3	21.6	21.6	21.8	21.9	15.3	16.5	15.9	16.2	12.6	16.1	20.8	14.8	14.2	14.3	14.7	14.6	15.0	16.0	0.331	0
10	24	19	21.3	21.5	21.5	21.8	21.9	14.7	15.4	15.0	15.2	11.2	14.9	20.5	13.6	13.1	13.0	13.4	13.4	13.8	14.9	0.400	0
10	24	20	21.3	21.5	21.4	21.7	21.9	14.3	14.5	14.3	14.4	10.4	14.1	20.3	12.8	12.4	12.2	12.6	12.6	13.0	14.2	0.423	0
10	24	21	21.3	21.4	21.4	21.7	21.9	13.9	13.8	13.7	13.8	9.8	13.5	20.2	12.3	11.8	11.7	12.0	12.0	12.5	13.6	0.464	0
10	24	22	21.3	21.4	21.4	21.7	21.8	13.6	13.2	13.2	13.2	9.3	13.1	20.1	11.8	11.4	11.2	11.5	11.5	12.0	13.1	0.491	0
10	24	23	21.3	21.4	21.4	21.7	21.9	13.4	12.8	12.8	12.8	9.3	12.8	20.1	11.5	11.2	10.9	11.3	11.3	11.8	12.8	0.492	0
10	24	24	21.3	21.4	21.4	21.7	21.9	13.1	12.5	12.4	12.4	8.8	12.5	20.0	11.2	10.8	10.5	10.9	10.9	11.4	12.5	0.512	0
10	25	1	21.3	21.4	21.3	21.6	21.9	12.9	12.2	12.0	12.1	8.5	12.2	19.9	10.9	10.6	10.3	10.6	10.7	11.1	12.2	0.527	0
10	25	2	21.3	21.3	21.3	21.6	21.9	12.8	12.0	11.8	11.8	9.0	12.3	19.9	11.0	10.8	10.4	10.7	10.8	11.3	12.2	0.538	0
10	25	3	21.3	21.3	21.3	21.6	21.9	12.7	12.0	11.7	11.7	8.9	12.3	19.9	11.0	10.7	10.4	10.7	10.8	11.2	12.2	0.544	0
10	25	4	21.3	21.3	21.3	21.6	21.9	12.6	11.9	11.6	11.6	8.7	12.2	19.9	10.8	10.5	10.2	10.5	10.6	11.1	12.1	0.549	0
10	25	5	21.2	21.3	21.3	21.6	21.8	12.4	11.7	11.4	11.3	8.4	12.0	19.9	10.7	10.3	10.0	10.4	10.5	10.9	11.9	0.547	0
10	25	6	21.2	21.3	21.3	21.6	21.8	12.4	11.7	11.3	11.3	8.9	12.1	19.9	10.9	10.5	10.3	10.6	10.7	11.1	12.0	0.556	0
10	25	7	21.2	21.3	21.2	21.5	21.8	12.4	11.7	11.3	11.3	9.0	12.3	19.9	10.9	10.6	10.3	10.6	10.8	11.2	12.1	0.548	0
10	25	8	21.3	21.3	21.3	21.6	21.9	12.4	11.8	11.4	11.3	8.9	12.4	20.0	11.2	10.8	10.7	11.0	11.1	11.5	12.4	0.524	27
10	25	9	21.4	21.7	21.7	22.2	21.9	15.1	14.5	15.0	13.8	14.3	16.5	21.5	17.6	16.0	17.1	17.9	17.7	18.3	18.5	-0.142	355
10	25	10	21.7	22.7	22.5	23.3	22.1	19.5	21.5	22.2	19.2	21.2	26.1	25.0	26.0	22.4	25.3	26.7	26.5	27.5	27.5	-1.366	591
10	25	11	22.2	23.8	23.2	24.6	22.2	24.1	29.4	28.2	24.6	27.3	34.5	28.7	32.5	28.0	31.8	33.8	33.0	34.3	34.3	-2.728	741
10	25	12	22.5	24.4	23.6	24.7	22.4	27.9	34.4	31.7	28.4	30.6	38.2	30.1	35.4	31.5	34.9	36.6	35.9	37.0	36.7	-3.740	799
10	25	13	22.5	24.7	24.0	24.5	23.0	30.8	36.8	33.0	31.5	32.2	39.8	30.7	37.4	33.8	36.9	38.5	37.8	38.7	38.9	-4.176	819
10	25	14	22.7	24.6	24.5	24.3	22.9	32.3	39.1	34.6	35.4	33.0	41.9	30.9	39.5	34.9	39.1	40.6	40.3	40.6	41.3	-3.729	748
10	25	15	22.6	24.4	24.3	24.0	22.6	31.4	40.5	36.2	38.3	32.3	42.2	30.1	39.4	34.6	39.0	40.2	40.1	40.8	41.8	-2.878	602

1	2	3	4	5	6	7	8	9	10	11	12	13	14	15	16	17	18	19	20	21	22	23	24
10	25	16	22.4	24.0	23.8	23.7	22.3	29.6	40.0	36.2	40.1	30.9	37.7	26.8	36.6	32.2	35.9	36.6	37.3	38.2	39.7	-1.838	391
10	25	17	22.1	23.2	22.8	23.0	22.0	25.8	35.9	33.1	36.4	24.3	31.2	24.5	29.6	26.3	28.0	29.1	29.8	31.0	33.3	-0.819	70
10	25	18	21.9	22.5	22.2	22.4	21.9	22.3	29.5	27.8	29.9	17.0	23.3	22.5	22.3	20.3	20.7	21.5	22.0	23.1	26.5	-0.273	0
10	25	19	21.8	22.1	21.9	22.2	21.8	20.0	24.6	23.8	25.4	13.7	19.3	21.5	18.6	16.9	17.2	17.8	18.1	19.1	22.4	0.026	0
10	25	20	21.8	21.9	21.7	22.0	21.8	18.5	21.1	21.0	22.3	11.9	17.0	21.0	16.2	15.0	15.1	15.5	15.7	16.6	19.5	0.165	0
10	25	21	21.8	21.8	21.7	21.9	21.9	17.3	18.6	18.8	20.0	10.6	15.5	20.7	14.6	13.6	13.6	14.0	14.1	14.9	17.4	0.256	0
10	25	22	21.8	21.7	21.6	21.9	21.9	16.5	16.8	17.2	18.1	9.7	14.4	20.5	13.4	12.6	12.5	12.9	12.9	13.6	15.8	0.327	0
10	25	23	21.6	21.5	21.5	21.8	21.8	15.6	15.3	15.7	16.5	9.3	13.6	20.2	12.7	12.1	11.9	12.2	12.2	12.9	14.7	0.374	0
10	25	24	21.6	21.5	21.4	21.8	21.8	15.2	14.5	14.8	15.4	9.5	13.4	20.2	12.4	12.0	11.7	12.0	12.0	12.6	14.1	0.415	0
10	26	1	21.6	21.4	21.4	21.7	21.8	14.9	13.9	14.2	14.7	9.7	13.3	20.1	12.3	12.0	11.6	11.9	12.0	12.5	13.7	0.451	0
10	26	2	21.5	21.4	21.4	21.7	21.8	14.6	13.6	13.7	14.1	10.0	13.3	20.1	12.3	12.1	11.7	12.0	12.0	12.5	13.6	0.469	0
10	26	3	21.5	21.4	21.3	21.7	21.8	14.5	13.5	13.5	13.7	10.7	13.5	20.1	12.6	12.5	12.1	12.4	12.4	12.7	13.7	0.480	0
10	26	4	21.5	21.4	21.4	21.7	21.9	14.7	13.7	13.6	13.8	11.5	14.1	20.3	13.0	12.9	12.5	12.8	12.8	13.1	13.9	0.465	0
10	26	5	21.5	21.4	21.4	21.7	21.8	14.6	13.7	13.5	13.6	11.1	14.1	20.3	12.9	12.8	12.4	12.7	12.7	12.9	13.8	0.510	0
10	26	6	21.4	21.3	21.3	21.6	21.8	14.4	13.6	13.3	13.4	11.0	13.9	20.2	12.8	12.8	12.3	12.6	12.6	12.8	13.7	0.497	0
10	26	7	21.4	21.4	21.3	21.7	21.8	14.3	13.5	13.2	13.3	10.9	13.9	20.2	12.7	12.7	12.2	12.5	12.5	12.8	13.6	0.507	0
10	26	8	21.4	21.4	21.3	21.7	21.8	14.3	13.5	13.2	13.3	11.3	14.0	20.2	12.9	12.9	12.5	12.8	12.8	13.0	13.7	0.507	0
10	26	9	21.4	21.4	21.3	21.7	21.8	14.4	13.7	13.4	13.4	11.9	14.4	20.3	13.3	13.2	12.9	13.2	13.1	13.4	14.0	0.485	4
10	26	10	21.4	21.4	21.4	21.7	21.9	14.6	14.0	13.6	13.6	12.1	14.7	20.5	13.6	13.5	13.2	13.6	13.4	13.7	14.3	0.429	18
10	26	11	21.4	21.5	21.4	21.8	21.8	15.8	14.8	14.3	14.4	14.1	16.2	21.0	15.7	15.5	15.4	15.8	15.6	15.8	16.0	0.255	87
10	26	12	21.4	21.6	21.5	21.8	21.8	16.2	16.0	15.4	15.4	15.4	17.4	21.2	16.3	15.9	16.1	16.5	16.3	16.5	16.7	0.254	49
10	26	13	21.4	21.6	21.5	21.8	21.9	16.3	16.7	16.0	15.9	16.2	17.8	21.2	16.7	16.2	16.5	16.9	16.8	16.9	17.1	0.276	32
10	26	14	21.4	21.6	21.6	21.9	21.9	17.0	17.4	16.6	16.6	17.2	18.6	21.4	18.0	17.3	17.9	18.2	18.1	18.2	18.3	0.196	72
10	26	15	21.4	21.7	21.6	21.9	21.9	17.5	18.4	17.5	17.6	18.0	19.6	21.7	18.5	17.6	18.4	18.7	18.6	18.7	18.9	0.168	57
10	26	16	21.4	21.6	21.6	21.9	21.8	17.1	18.5	17.8	17.8	17.5	19.2	21.5	18.0	17.3	17.8	18.2	18.1	18.3	18.6	0.228	25
10	26	17	21.4	21.6	21.6	21.8	21.9	16.8	18.2	17.8	17.8	16.9	18.6	21.2	17.4	16.8	17.1	17.6	17.5	17.7	18.0	0.291	4
10	26	18	21.3	21.6	21.5	21.8	21.8	16.4	17.7	17.4	17.5	15.8	17.8	21.0	16.9	16.3	16.5	16.9	16.8	17.0	17.5	0.333	0
10	26	19	21.3	21.5	21.5	21.8	21.8	16.3	17.4	17.2	17.2	15.7	17.6	20.9	16.6	16.2	16.3	16.7	16.6	16.8	17.2	0.364	0
10	26	20	21.3	21.5	21.5	21.8	21.8	16.2	17.1	16.9	17.0	15.3	17.2	20.9	16.3	15.9	16.0	16.4	16.2	16.5	16.9	0.378	0
10	26	21	21.3	21.5	21.5	21.7	21.8	16.1	16.8	16.7	16.8	15.1	17.1	20.8	16.1	15.8	15.8	16.2	16.0	16.3	16.7	0.383	0
10	26	22	21.3	21.5	21.5	21.8	21.9	15.9	16.6	16.5	16.6	14.7	16.8	20.8	15.9	15.6	15.5	15.9	15.8	16.0	16.5	0.363	0
10	26	23	21.3	21.5	21.4	21.7	21.8	15.7	16.3	16.2	16.3	13.8	16.4	20.7	15.4	15.0	14.9	15.3	15.2	15.5	16.2	0.392	0
10	26	24	21.3	21.5	21.5	21.8	21.9	15.3	15.8	15.7	15.8	12.7	15.7	20.6	14.5	14.2	14.1	14.5	14.4	14.7	15.5	0.405	0

1	2	3	4	5	6	7	8	9	10	11	12	13	14	15	16	17	18	19	20	21	22	23	24
10	27	1	21.3	21.5	21.4	21.7	21.8	15.0	15.2	15.1	15.2	12.1	15.0	20.5	14.0	13.6	13.5	13.8	13.8	14.1	15.0	0.417	0
10	27	2	21.2	21.4	21.4	21.7	21.8	14.7	14.7	14.5	14.7	11.9	14.7	20.4	13.6	13.4	13.2	13.5	13.4	13.7	14.6	0.434	0
10	27	3	21.3	21.4	21.4	21.7	21.8	14.5	14.3	14.0	14.1	11.0	14.3	20.3	13.1	13.0	12.6	13.0	12.9	13.2	14.1	0.462	0
10	27	4	21.3	21.4	21.4	21.7	21.8	14.4	14.0	13.6	13.8	11.6	14.2	20.3	13.2	13.1	12.7	13.1	13.0	13.2	14.0	0.479	0
10	27	5	21.2	21.4	21.4	21.7	21.8	14.3	13.9	13.5	13.6	11.5	14.3	20.3	13.2	13.0	12.7	13.1	13.0	13.3	14.0	0.461	0
10	27	6	21.2	21.4	21.4	21.7	21.8	14.3	13.9	13.6	13.6	12.2	14.5	20.3	13.5	13.3	13.0	13.4	13.4	13.6	14.3	0.466	0
10	27	7	21.2	21.4	21.4	21.7	21.8	14.4	14.1	13.8	13.7	12.6	14.8	20.4	13.8	13.5	13.3	13.7	13.7	13.9	14.5	0.459	0
10	27	8	21.2	21.4	21.4	21.7	21.8	14.4	14.3	14.0	13.9	12.4	14.9	20.4	13.8	13.5	13.4	13.7	13.7	14.0	14.6	0.445	3
10	27	9	21.2	21.4	21.4	21.7	21.8	14.6	14.4	14.1	14.0	12.4	15.0	20.5	14.0	13.6	13.6	13.9	13.9	14.1	14.7	0.394	19
10	27	10	21.4	21.7	21.7	22.0	21.9	16.1	15.5	15.4	15.1	14.4	17.3	21.6	17.2	16.3	16.7	17.4	17.1	17.6	17.7	-0.108	252
10	27	11	21.8	22.8	22.5	23.4	22.1	20.7	21.4	20.9	19.6	19.8	26.0	25.9	24.7	22.2	24.1	25.5	24.9	25.8	25.6	-1.690	593
10	27	12	22.2	23.8	23.2	24.1	22.4	24.4	27.1	25.6	24.0	23.3	31.7	28.3	29.0	26.3	28.4	29.9	29.1	30.2	30.1	-2.929	711
10	27	13	22.2	24.2	23.7	24.1	22.8	27.1	30.6	27.7	27.2	25.6	34.2	29.3	31.8	28.9	31.1	32.6	32.1	32.8	33.3	-3.524	764
10	27	14	22.5	24.3	24.2	24.0	22.9	29.0	34.1	29.8	31.2	27.7	37.4	30.0	34.8	30.7	34.4	35.7	35.4	35.8	36.6	-3.441	727
10	27	15	22.5	24.2	24.1	23.9	22.6	28.5	36.1	31.7	34.3	27.5	38.1	29.3	34.9	30.6	34.5	35.5	35.4	36.3	37.4	-2.596	564
10	27	16	22.2	23.6	23.3	23.3	22.2	25.8	34.4	30.6	34.1	23.5	31.9	25.6	28.5	25.2	27.2	28.2	28.7	29.8	31.9	-1.377	200
10	27	17	21.9	22.7	22.4	22.6	21.9	21.6	28.5	25.9	28.1	16.1	23.2	22.7	21.0	19.0	19.7	20.4	20.7	21.7	24.7	-0.399	13
10	27	18	21.8	22.1	21.9	22.2	21.8	19.3	23.5	22.1	23.7	13.4	18.8	21.5	17.7	16.3	16.6	17.1	17.3	18.1	20.8	0.000	0
10	27	19	21.7	21.9	21.8	22.0	21.8	18.0	20.3	19.7	21.0	12.7	17.0	21.0	16.2	15.2	15.4	15.7	15.9	16.5	18.6	0.159	0
10	27	20	21.6	21.7	21.6	21.9	21.8	17.2	18.3	18.2	19.2	12.2	16.1	20.8	15.2	14.5	14.5	14.9	14.9	15.4	17.2	0.235	0
10	27	21	21.6	21.6	21.6	21.8	21.8	16.5	16.9	17.1	17.9	11.6	15.4	20.6	14.4	13.8	13.8	14.1	14.1	14.6	16.1	0.296	0
10	27	22	21.6	21.6	21.5	21.8	21.9	15.9	15.9	16.2	16.8	10.9	14.8	20.5	13.6	13.1	13.0	13.3	13.3	13.9	15.2	0.337	0
10	27	23	21.5	21.5	21.5	21.8	21.8	15.3	14.9	15.2	15.7	9.9	14.1	20.3	12.8	12.3	12.1	12.5	12.5	13.0	14.4	0.381	0
10	27	24	21.5	21.5	21.4	21.7	21.8	14.8	14.1	14.4	14.8	9.2	13.4	20.2	12.1	11.6	11.4	11.8	11.8	12.3	13.7	0.423	0
10	28	1	21.5	21.4	21.4	21.7	21.8	14.2	13.4	13.6	13.9	8.4	12.7	20.0	11.4	11.0	10.8	11.1	11.1	11.7	13.1	0.448	0
10	28	2	21.5	21.4	21.4	21.7	21.8	13.8	12.8	12.9	13.2	8.0	12.3	19.9	11.0	10.5	10.3	10.6	10.6	11.2	12.5	0.468	0
10	28	3	21.5	21.4	21.4	21.7	21.8	13.4	12.3	12.4	12.6	7.7	12.0	19.9	10.6	10.2	9.9	10.2	10.3	10.8	12.1	0.491	0
10	28	4	21.5	21.4	21.4	21.7	21.9	13.1	11.9	11.9	12.1	7.4	11.7	19.8	10.3	9.9	9.6	9.9	9.9	10.5	11.8	0.513	0
10	28	5	21.4	21.3	21.3	21.6	21.8	12.8	11.6	11.5	11.6	7.5	11.5	19.7	10.2	9.9	9.6	9.9	10.0	10.5	11.6	0.525	0
10	28	6	21.4	21.3	21.3	21.6	21.8	12.8	11.5	11.3	11.4	8.2	11.7	19.8	10.6	10.3	9.9	10.3	10.3	10.8	11.7	0.551	0
10	28	7	21.4	21.3	21.3	21.6	21.8	12.8	11.6	11.4	11.4	8.9	12.1	19.8	11.0	10.8	10.4	10.7	10.8	11.1	12.0	0.536	0
10	28	8	21.5	21.4	21.4	21.7	21.9	13.0	11.9	11.5	11.5	9.3	12.5	20.0	11.6	11.4	11.1	11.4	11.5	11.8	12.6	0.523	
10	28	9	21.4	21.3	21.3	21.6	21.8	13.1	12.1	11.6	11.6	10.1	12.9	20.0	11.9	11.7	11.4	11.7	11.8	12.0	12.8	0.511	9

1	2	3	4	5	6	7	8	9	10	11	12	13	14	15	16	17	18	19	20	21	22	23	24
10	28	10	21.3	21.3	21.3	21.6	21.8	13.2	12.4	11.8	11.8	10.3	13.2	20.1	12.0	11.9	11.6	11.9	11.9	12.1	12.9	0.512	9
10	28	11	21.4	21.4	21.4	21.7	21.9	13.4	12.6	12.1	12.1	10.2	13.4	20.2	12.4	12.3	12.0	12.4	12.3	12.5	13.2	0.483	17
10	28	12	21.4	21.4	21.4	21.7	21.9	13.7	12.8	12.3	12.3	10.8	13.7	20.3	13.4	13.2	13.0	13.4	13.3	13.5	13.9	0.460	28
10	28	13	21.3	21.4	21.4	21.7	21.9	14.1	13.3	12.8	12.8	12.1	14.6	20.5	14.6	14.2	14.3	14.7	14.5	14.7	15.0	0.423	37
10	28	14	21.4	21.5	21.5	21.8	21.9	14.9	14.3	13.6	13.6	13.5	15.8	20.9	15.0	14.6	14.7	15.1	15.0	15.1	15.5	0.297	62
10	28	15	21.3	21.5	21.5	21.8	21.9	15.1	15.0	14.3	14.2	13.8	16.3	20.9	15.2	14.8	14.9	15.3	15.2	15.4	15.8	0.315	46
10	28	16	21.4	21.5	21.5	21.8	21.9	15.2	15.4	14.7	14.7	13.7	16.5	21.0	14.6	14.2	14.1	14.5	14.5	14.7	15.3	0.313	42
10	28	17	21.3	21.5	21.5	21.7	21.9	14.8	15.3	14.7	14.7	13.2	15.9	20.7	14.2	13.8	13.8	14.2	14.1	14.4	15.0	0.408	3
10	28	18	21.3	21.4	21.4	21.7	21.8	14.5	14.9	14.4	14.4	12.8	15.4	20.5	13.9	13.6	13.5	13.8	13.8	14.0	14.7	0.462	0
10	28	19	21.3	21.4	21.4	21.7	21.8	14.4	14.7	14.3	14.3	12.4	15.1	20.5	13.7	13.4	13.2	13.6	13.5	13.8	14.5	0.471	0
10	28	20	21.3	21.4	21.4	21.7	21.9	14.2	14.4	14.1	14.1	12.1	14.8	20.4	13.5	13.3	13.0	13.4	13.4	13.6	14.3	0.473	0
10	28	21	21.2	21.4	21.3	21.6	21.8	14.1	14.2	13.9	13.9	11.9	14.6	20.3	13.5	13.2	13.0	13.4	13.4	13.6	14.3	0.493	0
10	28	22	21.3	21.4	21.4	21.7	21.9	14.1	14.2	13.9	13.9	12.0	14.6	20.4	13.4	13.2	13.0	13.3	13.3	13.6	14.3	0.501	0
10	28	23	21.2	21.4	21.3	21.6	21.8	14.0	14.1	13.8	13.8	12.0	14.6	20.3	12.9	12.6	12.4	12.8	12.8	13.1	13.9	0.493	0
10	28	24	21.3	21.4	21.4	21.7	21.9	13.9	13.9	13.6	13.6	11.0	14.3	20.3	12.7	12.3	12.1	12.5	12.5	12.8	13.7	0.488	0
10	29	1	21.3	21.4	21.4	21.7	21.9	13.7	13.7	13.4	13.4	10.7	14.0	20.3	12.4	12.0	11.8	12.2	12.2	12.6	13.4	0.498	0
10	29	2	21.2	21.4	21.4	21.7	21.9	13.5	13.4	13.2	13.1	10.4	13.7	20.2	12.1	11.8	11.6	12.0	12.0	12.3	13.2	0.505	0
10	29	3	21.3	21.5	21.4	21.7	21.9	13.4	13.2	13.0	13.0	10.3	13.5	20.2	11.9	11.5	11.3	11.7	11.7	12.1	13.0	0.516	0
10	29	4	21.2	21.4	21.4	21.7	21.9	13.2	12.9	12.7	12.7	9.9	13.2	20.1	11.6	11.2	11.0	11.4	11.4	11.8	12.7	0.526	0
10	29	5	21.2	21.4	21.3	21.7	21.9	13.0	12.7	12.4	12.4	9.5	13.0	20.1	11.2	10.9	10.6	11.0	11.1	11.5	12.4	0.520	0
10	29	6	21.2	21.4	21.3	21.6	21.9	12.8	12.4	12.1	12.1	9.1	12.7	20.0	10.9	10.5	10.2	10.6	10.7	11.1	12.1	0.531	0
10	29	7	21.2	21.4	21.3	21.6	21.9	12.6	12.1	11.9	11.9	8.6	12.4	20.0	10.5	10.1	9.9	10.2	10.3	10.8	11.8	0.557	
10	29	8	21.3	21.4	21.3	21.6	21.9	12.4	11.8	11.5	11.5	8.0	12.0	19.9								0.555	1
10	29	9	21.3	21.4	21.4	21.7	21.9	12.3	11.6	11.3	11.3	7.8	11.8	19.9	10.3	10.0	9.7	10.0	10.1	10.6	11.6	0.561	6
10	29	10	21.3	21.4	21.3	21.6	21.9	12.5	11.5	11.2	11.2	8.3	12.0	20.0	10.6	10.4	10.1	10.4	10.5	10.8	11.8	0.509	29
10	29	11	21.3	21.5	21.4	21.8	21.9	13.6	12.1	11.8	11.9	9.6	13.4	20.5	11.9	11.6	11.4	11.8	11.9	12.1	12.7	0.332	87
10	29	12	21.5	21.7	21.7	22.1	22.0	15.1	13.5	13.0	13.1	12.0	15.6	21.5	14.7	14.3	14.3	14.7	14.6	14.9	15.1	-0.218	259
10	29	13	21.5	22.2	22.1	22.4	22.2	18.1	17.4	15.8	16.2	16.7	21.4	24.3	19.3	18.1	19.1	19.6	19.4	19.5	20.0	-1.162	352
10	29	14	21.7	22.5	22.5	22.6	22.3	19.1	20.3	18.0	18.9	17.2	23.2	24.5	20.8	19.1	20.7	21.2	21.0	21.1	21.7	-0.994	290
10	29	15	21.6	22.4	22.4	22.5	22.1	18.8	21.2	19.1	20.1	17.4	22.8	23.8	21.8	19.9	21.9	22.2	22.0	22.2	22.7	-0.751	318
10	29	16	21.7	22.5	22.6	22.7	22.0	20.4	24.1	21.4	23.8	21.3	25.6	24.0	25.1	22.4	25.0	25.3	25.3	25.8	26.5	-0.755	330
10	29	17	21.5	22.3	22.2	22.4	21.9	19.1	24.8	22.0	24.6	19.1	24.3	23.0	22.0	19.7	21.2	21.9	22.2	22.9	24.1	-0.241	85
10	29	18	21.5	22.0	21.9	22.1	21.9	17.0	21.6	19.6	21.1	13.4	19.0	21.6	16.9	15.4	15.9	16.5	16.7	17.5	19.5	0.173	1

1	2	3	4	5	6	7	8	9	10	11	12	13	14	15	16	17	18	19	20	21	22	23	24
10	29	19	21.4	21.7	21.6	21.9	21.9	15.5	18.3	17.1	18.1	10.2	15.5	20.8	14.1	12.9	13.1	13.6	13.7	14.4	16.6	0.298	0
10	29	20	21.4	21.6	21.5	21.8	21.9	14.6	16.0	15.4	16.2	9.4	14.0	20.4	12.8	11.9	12.0	12.3	12.4	13.1	15.0	0.393	0
10	29	21	21.4	21.5	21.5	21.8	21.9	14.1	14.6	14.3	15.0	9.2	13.4	20.2	12.1	11.4	11.4	11.7	11.8	12.4	14.0	0.461	0
10	29	22	21.3	21.3	21.3	21.6	21.7	13.5	13.5	13.3	13.9	8.5	12.8	20.0	11.5	10.9	10.8	11.1	11.2	11.8	13.2	0.502	0
10	29	23	21.4	21.4	21.3	21.7	21.8	13.2	12.9	12.7	13.2	8.2	12.4	20.0	11.0	10.4	10.3	10.6	10.6	11.2	12.6	0.525	0
10	29	24	21.4	21.4	21.4	21.7	21.9	12.9	12.3	12.2	12.6	7.9	12.0	20.0	10.5	10.0	9.9	10.2	10.2	10.8	12.1	0.555	0
10	30	1	21.3	21.3	21.2	21.5	21.8	12.5	11.8	11.6	11.9	7.9	11.8	19.8	10.4	10.1	9.8	10.1	10.2	10.7	11.8	0.566	0
10	30	2	21.3	21.3	21.3	21.6	21.8	12.5	11.6	11.4	11.6	8.2	11.9	19.8	10.4	10.1	9.8	10.1	10.2	10.7	11.7	0.581	0
10	30	3	21.3	21.3	21.3	21.6	21.9	12.4	11.5	11.2	11.4	8.1	11.8	19.9	10.3	10.0	9.7	10.0	10.1	10.6	11.6	0.591	0
10	30	4	21.3	21.3	21.2	21.5	21.8	12.3	11.4	10.9	11.1	8.5	11.9	19.8	10.6	10.3	10.0	10.3	10.4	10.7	11.6	0.589	0
10	30	5	21.2	21.2	21.1	21.5	21.7	12.2	11.3	10.9	11.0	8.6	12.0	19.7	10.7	10.4	10.1	10.4	10.5	10.8	11.7	0.603	0
10	30	6	21.2	21.2	21.2	21.5	21.7	12.1	11.4	10.9	11.0	8.6	12.0	19.8	10.7	10.4	10.1	10.4	10.5	10.9	11.8	0.591	0
10	30	7	21.2	21.2	21.2	21.5	21.8	12.2	11.5	11.0	11.0	9.0	12.2	19.8	10.9	10.6	10.3	10.6	10.7	11.1	11.9	0.588	0
10	30	8	21.2	21.2	21.2	21.5	21.8	12.2	11.6	11.1	11.1	9.4	12.4	19.9	11.2	10.9	10.6	10.9	11.0	11.3	12.1	0.614	3
10	30	9	21.3	21.3	21.3	21.6	21.8	12.5	12.0	11.4	11.4	9.8	12.8	20.0	11.5	11.2	11.0	11.3	11.3	11.6	12.4	0.545	10
10	30	10	21.3	21.4	21.4	21.7	21.9	12.9	12.4	11.7	11.7	10.4	13.4	20.2	12.1	11.8	11.6	12.0	12.0	12.2	12.9	0.512	27
10	30	11	21.3	21.4	21.4	21.7	21.9	13.4	12.9	12.3	12.2	11.1	14.1	20.5	12.6	12.3	12.2	12.6	12.5	12.8	13.4	0.456	33
10	30	12	21.2	21.4	21.3	21.6	21.8	13.6	13.2	12.6	12.6	11.6	14.4	20.5	13.3	13.1	13.0	13.4	13.3	13.5	13.9	0.412	50
10	30	13	21.2	21.4	21.4	21.7	21.8	14.1	13.8	13.2	13.2	11.8	15.2	20.8	13.5	13.1	13.0	13.5	13.4	13.7	14.2	0.349	49
10	30	14	21.2	21.4	21.4	21.7	21.8	13.9	13.8	13.3	13.2	10.6	14.6	20.6	13.0	12.7	12.5	12.9	12.9	13.1	13.8	0.403	35
10	30	15	21.2	21.3	21.3	21.6	21.8	13.5	13.5	13.0	13.0	10.4	14.0	20.4	12.6	12.3	12.1	12.5	12.5	12.7	13.5	0.452	16
10	30	16	21.2	21.4	21.3	21.6	21.8	13.2	13.2	12.8	12.8	10.2	13.7	20.2	12.3	12.0	11.8	12.2	12.1	12.4	13.3	0.511	7
10	30	17	21.2	21.3	21.3	21.6	21.8	12.9	12.9	12.4	12.5	9.9	13.3	20.1	12.0	11.7	11.4	11.8	11.8	12.1	13.0	0.541	2
10	30	18	21.2	21.3	21.2	21.5	21.8	12.8	12.6	12.2	12.2	9.7	13.1	20.0	11.7	11.5	11.2	11.6	11.6	11.9	12.7	0.584	0
10	30	19	21.2	21.3	21.3	21.6	21.8	12.7	12.5	12.0	12.1	9.8	13.0	20.0	11.6	11.4	11.1	11.5	11.4	11.7	12.6	0.572	0
10	30	20	21.1	21.2	21.2	21.5	21.8	12.7	12.4	11.9	12.0	10.3	13.1	20.0	11.9	11.7	11.4	11.8	11.7	12.0	12.7	0.582	0
10	30	21	21.2	21.3	21.3	21.6	21.8	12.9	12.7	12.2	12.2	11.3	13.6	20.1	12.4	12.2	12.0	12.3	12.3	12.5	13.2	0.565	0
10	30	22	21.2	21.3	21.3	21.6	21.8	13.2	13.2	12.6	12.5	12.5	14.2	20.2	13.1	12.7	12.8	13.2	13.1	13.3	13.8	0.551	0
10	30	23	21.2	21.4	21.3	21.6	21.8	13.5	13.8	13.1	13.0	13.2	15.0	20.4	13.8	13.3	13.5	13.8	13.7	13.9	14.4	0.549	0
10	30	24	21.2	21.3	21.3	21.6	21.8	13.7	14.3	13.5	13.5	13.5	15.3	20.4	14.1	13.6	13.8	14.2	14.1	14.3	14.8	0.526	0
10	31	1	21.2	21.4	21.3	21.6	21.8	13.9	14.6	13.9	13.8	13.7	15.6	20.5	14.3	13.8	14.0	14.4	14.3	14.5	15.0	0.511	0
10	31	2	21.1	21.4	21.3	21.6	21.8	13.9	14.7	14.0	14.0	13.3	15.5	20.5	14.2	13.8	13.9	14.3	14.2	14.4	14.9	0.504	0
10	31	3	21.1	21.4	21.3	21.6	21.8	14.0	14.8	14.2	14.2	13.4	15.5	20.5	14.3	13.8	14.0	14.4	14.3	14.5	15.0	0.499	0

1	2	3	4	5	6	7	8	9	10	11	12	13	14	15	16	17	18	19	20	21	22	23	24
10	31	4	21.2	21.4	21.4	21.6	21.8	14.1	14.9	14.3	14.4	13.5	15.6	20.5	14.4	13.9	14.0	14.5	14.3	14.6	15.1	0.505	0
10	31	5	21.2	21.4	21.4	21.7	21.9	14.1	14.9	14.4	14.4	13.3	15.5	20.5	14.3	13.8	13.9	14.3	14.2	14.5	15.0	0.500	0
10	31	6	21.2	21.4	21.4	21.7	21.9	14.1	14.9	14.4	14.5	13.4	15.5	20.5	14.3	13.8	13.9	14.3	14.2	14.5	15.0	0.493	0
10	31	7	21.1	21.4	21.4	21.7	21.8	14.1	14.8	14.4	14.4	12.9	15.3	20.5	14.1	13.7	13.7	14.1	14.0	14.2	14.8	0.499	0
10	31	8	21.1	21.4	21.4	21.7	21.9	14.0	14.6	14.3	14.3	12.5	15.1	20.5	13.9	13.5	13.5	13.9	13.8	14.0	14.7	0.502	0
10	31	9	21.1	21.4	21.4	21.7	21.9	13.9	14.4	14.1	14.2	11.9	14.8	20.5	13.6	13.3	13.2	13.6	13.5	13.8	14.5	0.485	8
10	31	10	21.3	21.6	21.6	21.9	21.9	15.0	15.0	14.9	14.8	13.6	16.3	21.2	16.3	15.6	15.9	16.5	16.2	16.7	16.8	0.143	163
10	31	11	21.8	22.8	22.5	23.6	22.1	20.0	21.0	20.4	19.4	21.6	26.4	26.1	25.8	23.1	25.5	26.6	26.1	27.0	26.8	-1.844	680
10	31	12	21.9	23.4	22.9	23.8	22.2	21.7	26.4	24.7	23.2	21.5	29.9	27.0	24.9	22.2	24.2	25.3	25.2	25.9	26.5	-1.804	346
10	31	13	21.6	22.6	22.3	22.8	22.1	18.9	23.5	22.2	21.3	15.7	22.1	23.1	20.6	19.1	20.0	20.7	20.6	21.0	22.0	-0.647	166
10	31	14	21.7	22.7	22.5	22.8	22.2	20.8	23.3	22.0	22.4	18.7	24.6	24.6	22.4	20.7	22.1	22.7	22.5	22.8	23.5	-1.126	291
10	31	15	21.6	22.3	22.1	22.4	22.0	18.5	21.6	20.7	21.1	14.9	20.8	22.6	18.4	17.3	17.8	18.3	18.4	18.8	20.0	-0.192	59
10	31	16	21.5	22.0	21.8	22.1	21.9	17.0	19.3	18.8	19.2	12.7	17.7	21.5	15.9	15.1	15.2	15.7	15.7	16.2	17.7	0.118	16
10	31	17	21.4	21.7	21.6	21.9	21.9	15.7	17.1	16.9	17.2	11.3	15.6	20.8	14.3	13.7	13.7	14.1	14.0	14.5	16.0	0.287	1
10	31	18	21.4	21.6	21.5	21.8	21.9	15.0	15.7	15.6	15.9	10.5	14.6	20.5	13.4	12.9	12.7	13.1	13.0	13.5	14.9	0.374	0
10	31	19	21.4	21.5	21.5	21.8	21.9	14.6	14.7	14.8	15.1	10.4	14.1	20.4	13.0	12.5	12.4	12.7	12.8	13.2	14.3	0.434	0
10	31	20	21.4	21.5	21.5	21.8	21.9	14.2	14.1	14.3	14.4	10.1	13.8	20.3	12.6	12.1	12.0	12.3	12.4	12.8	13.8	0.461	0
10	31	21	21.4	21.5	21.4	21.7	21.9	13.9	13.6	13.8	13.9	9.6	13.4	20.2	12.1	11.6	11.5	11.8	11.9	12.3	13.3	0.469	0
10	31	22	21.4	21.5	21.4	21.7	21.9	13.5	13.0	13.2	13.3	8.8	12.8	20.1	11.5	11.0	10.8	11.2	11.2	11.7	12.8	0.488	0
10	31	23	21.4	21.4	21.4	21.7	21.9	13.1	12.5	12.7	12.7	8.5	12.4	20.1	11.1	10.6	10.4	10.7	10.8	11.3	12.4	0.512	0
10	31	24	21.3	21.4	21.3	21.6	21.8	12.9	12.1	12.3	12.3	8.5	12.2	20.0	10.9	10.6	10.3	10.6	10.7	11.1	12.2	0.518	0
11	1	1	21.3	21.4	21.4	21.7	21.9	12.7	12.0	12.1	12.0	8.2	12.1	20.0	10.7	10.3	10.0	10.4	10.5	10.9	11.9	0.548	0
11	1	2	21.3	21.4	21.3	21.6	21.9	12.3	11.6	11.6	11.5	7.2	11.6	19.9	10.0	9.5	9.3	9.7	9.8	10.3	11.5	0.544	0
11	1	3	21.3	21.4	21.3	21.6	21.9	11.8	11.0	11.0	10.9	5.8	10.8	19.8	9.1	8.5	8.3	8.7	8.8	9.4	10.9	0.559	0
11	1	4	21.3	21.3	21.3	21.6	21.9	11.3	10.4	10.3	10.2	4.9	10.1	19.6	8.3	7.6	7.5	7.8	8.0	8.7	10.2	0.587	0
11	1	5	21.3	21.3	21.3	21.6	21.9	10.8	9.7	9.5	9.5	3.7	9.2	19.5	7.5	6.7	6.6	6.9	7.1	7.9	9.6	0.611	0
11	1	6	21.3	21.3	21.2	21.5	21.8	10.4	9.1	8.9	8.9	3.6	8.8	19.3	7.1	6.4	6.3	6.5	6.8	7.6	9.1	0.642	0
11	1	7	21.4	21.3	21.3	21.6	22.0	10.3	8.8	8.5	8.6	3.6	8.7	19.4	6.9	6.2	6.0	6.3	6.6	7.3	8.8	0.650	0
11	1	8	21.4	21.3	21.3	21.6	21.9	10.0	8.5	8.1	8.2	3.5	8.6	19.4	6.7	6.1	5.9	6.1	6.5	7.2	8.6	0.689	2
11	1	9	21.3	21.3	21.3	21.6	21.9	10.1	8.4	8.0	8.0	3.8	8.7	19.4								0.626	25
11	1	10	21.1	21.1	21.1	21.4	21.7	10.0	8.4	7.8	7.9	4.0	9.0	19.4								0.620	26
11	1	11	21.4	21.4	21.4	21.7	22.0	10.5	8.8	8.2	8.2	4.2	9.5	19.8								0.400	135
11	1	12	21.8	22.1	22.0	22.5	22.2	14.5	12.5	11.4	11.3	11.5	16.6	23.3								-0.719	375

1	2	3	4	5	6	7	8	9	10	11	12	13	14	15	16	17	18	19	20	21	22	23	24
11	1	13	21.7	22.6	22.5	22.8	22.4	17.3	17.2	14.7	15.0	15.0	21.8	25.3								-1.640	475
11	1	14	21.8	22.6	22.5	22.7	22.3	16.6	18.4	16.0	16.5	12.0	20.4	24.1								-1.005	321
11	1	15	21.7	22.4	22.4	22.5	22.2	16.1	18.6	16.3	17.4	11.5	19.9	23.6								-0.563	212
11	1	16	21.6	22.2	22.2	22.3	22.0	15.3	18.1	16.1	18.1	10.8	17.7	22.1								-0.246	174
11	1	17	21.5	21.8	21.7	21.9	21.9	13.1	15.6	13.9	15.0	6.3	13.4	20.6								0.305	11
11	1	18	21.5	21.5	21.4	21.7	21.9	11.8	12.9	11.8	12.5	4.4	10.9	19.9								0.484	0
11	1	19	21.4	21.3	21.2	21.5	21.8	10.9	10.9	10.2	10.7	3.3	9.4	19.4								0.606	
11	1	20	21.4	21.3	21.2	21.6	21.9	10.3	9.7	9.2	9.7	3.0	8.8	19.3								0.658	
11	1	21	21.3	21.2	21.1	21.4	21.8	9.7	8.7	8.3	8.7	2.3	8.1	19.1								0.704	
11	1	22	21.3	21.1	21.1	21.4	21.8	9.2	8.0	7.6	7.9	1.7	7.6	19.0								0.731	0
11	1	23	21.3	21.2	21.1	21.4	21.8	8.9	7.6	7.0	7.3	1.5	7.3	19.0								0.761	0
11	1	24	21.3	21.1	21.1	21.4	21.8	8.6	7.2	6.5	6.7	1.3	7.0	18.9								0.775	0
11	2	1	21.3	21.1	21.1	21.4	21.8	8.4	6.9	6.1	6.3	1.3	6.9	18.9								0.805	0
11	2	2	21.3	21.1	21.0	21.4	21.8	8.2	6.7	5.8	5.9	1.2	6.8	18.9								0.822	0
11	2	3	21.3	21.1	21.0	21.4	21.8	8.0	6.6	5.6	5.7	1.2	6.7	18.8								0.823	0
11	2	4	21.2	21.1	21.0	21.3	21.8	7.7	6.3	5.3	5.4	0.4	6.4	18.8								0.814	0
11	2	5	21.2	21.1	21.0	21.3	21.8	7.4	6.0	4.9	5.0	-0.1	6.0	18.7								0.862	0
11	2	6	21.2	21.0	21.0	21.3	21.8	7.2	5.7	4.6	4.6	-0.3	5.8	18.6								0.848	0
11	2	7	21.2	21.0	20.9	21.2	21.8	7.1	5.5	4.4	4.4	-0.1	5.7	18.6								0.885	
11	2	8	21.2	21.0	21.0	21.3	21.8	7.0	5.4	4.3	4.3	0.1	5.8	18.6								0.884	4
11	2	9	21.3	21.3	21.3	21.7	21.9	9.3	7.5	7.6	6.2	5.7	9.5	19.9								0.353	293
11	2	10	21.6	22.2	22.1	22.8	22.0	13.6	14.5	14.8	11.6	13.6	19.4	23.7								-0.771	518
11	2	11	21.7	22.6	22.4	23.1	22.1	15.2	19.2	17.7	15.0	14.7	22.3	24.6								-0.939	395
11	2	12	22.3	24.6	24.0	24.9	23.4	19.7	23.8	21.0	18.9	23.8	29.1	29.6								0.259	751
11	2	13	22.9	26.6	26.1	26.5	25.2	24.1	30.3	25.3	24.3	30.3	35.7	32.5								-3.052	821
11	2	14	22.9	26.0	25.7	25.7	24.8	25.5	34.4	28.6	29.0	29.2	37.8	31.2								-3.152	507
11	2	15	22.5	24.4	24.0	24.1	23.5	20.6	29.9	26.1	26.6	18.1	27.0	25.5								-1.475	213
11	2	16	22.3	23.4	23.2	23.3	22.7	19.5	26.6	24.1	25.8	17.5	24.1	23.8								-0.980	181
11	2	17	22.1	22.6	22.4	22.6	22.3	17.3	23.6	21.8	23.4	13.0	20.4	22.4								-0.360	27
11	2	18	22.0	22.0	21.9	22.2	22.1	15.0	19.5	18.2	19.2	8.1	15.3	21.0								0.045	0
11	2	19	21.9	21.6	21.6	21.8	21.9	13.5	16.0	15.4	16.1	6.0	12.5	20.2								0.238	
11	2	20	21.8	21.4	21.4	21.7	21.9	12.4	13.6	13.3	14.0	4.8	11.0	19.8								0.401	
11	2	21	21.7	21.3	21.3	21.6	21.8	11.6	11.8	11.8	12.3	4.0	10.0	19.5								0.492	0

1	2	3	4	5	6	7	8	9	10	11	12	13	14	15	16	17	18	19	20	21	22	23	24
11	2	22	21.7	21.3	21.3	21.6	21.9	11.0	10.6	10.6	11.1	3.6	9.4	19.4								0.552	0
11	2	23	21.7	21.3	21.2	21.6	21.9	10.5	9.8	9.7	10.1	3.2	8.8	19.3								0.632	0
11	2	24	21.6	21.3	21.2	21.6	21.9	10.1	9.1	8.9	9.2	3.1	8.5	19.3								0.653	0
11	3	1	21.6	21.2	21.2	21.5	21.9	9.7	8.6	8.2	8.5	2.7	8.2	19.2								0.676	
11	3	2	21.6	21.2	21.2	21.5	21.9	9.3	8.2	7.7	7.9	2.2	7.9	19.1								0.707	0
11	3	3	21.5	21.2	21.1	21.5	21.9	8.9	7.7	7.1	7.3	1.6	7.5	19.0								0.743	0
11	3	4	21.5	21.1	21.1	21.4	21.8	8.5	7.2	6.5	6.7	0.9	7.0	18.9								0.762	0
11	3	5	21.4	21.1	21.1	21.4	21.8	8.2	6.7	6.0	6.1	0.8	6.6	18.8								0.800	0
11	3	6	21.3	21.0	21.0	21.3	21.8	8.0	6.5	5.7	5.8	1.1	6.6	18.8								0.800	0
11	3	7	21.3	21.0	21.0	21.3	21.8	8.1	6.6	5.7	5.7	2.1	7.0	18.8								0.816	0
11	3	8	21.3	21.1	21.0	21.4	21.8	8.1	6.7	5.7	5.7	2.3	7.3	18.9								0.805	4
11	3	9	21.4	21.4	21.4	21.8	21.9	10.5	9.1	9.5	7.9	7.6	11.1	20.2	11.6	10.3	11.0	11.7	11.7	12.1	12.7		
11	3	10	21.5	21.8	21.7	22.3	21.9	12.6	13.6	13.7	11.3	11.5	16.4	21.8	13.9	12.1	13.2	13.9	14.1	14.6	15.3		
11	3	11	21.3	21.4	21.4	21.7	21.7	11.6	12.5	11.9	10.8	7.7	13.4	20.7	11.1	10.2	10.5	11.0	11.4	11.9	11.5		
11	3	12	21.3	21.3	21.4	21.6	21.8	11.7	11.7	11.3	10.7	8.0	13.0	20.5	10.9	10.3	10.4	10.8	10.9	11.3	11.9		
11	3	13	21.5	21.5	21.6	21.8	21.9	12.9	12.2	11.6	11.4	9.7	14.0	21.2	13.2	12.3	13.0	13.3	13.2	13.4	13.9		
11	3	14	21.9	22.4	22.7	22.6	22.3	17.9	18.3	15.7	16.9	17.7	23.8	25.9	21.8	19.4	22.4	22.3	21.9	22.2	22.8		
11	3	15	22.1	23.1	23.4	23.1	22.5	19.6	24.6	20.6	22.8	20.6	29.8	27.6	26.7	22.9	26.8	27.0	26.9	27.8	28.8		
11	3	16	21.9	23.1	23.2	23.1	22.3	19.5	27.5	23.1	27.3	19.8	27.6	25.0	25.5	21.6	24.8	25.3	25.8	27.0	28.4		
11	3	17	21.7	22.4	22.3	22.5	22.1	16.6	24.2	20.6	23.5	12.6	20.9	22.6	17.8	15.3	16.5	17.1	17.6	18.9	21.6		
11	3	18	21.5	21.9	21.8	22.0	21.9	14.2	19.0	16.7	18.4	8.2	15.0	20.8	13.2	11.5	11.9	12.4	12.7	13.8	16.6		
11	3	19	21.4	21.5	21.5	21.8	21.9	13.0	15.5	14.2	15.6	6.8	12.7	20.2	11.1	9.8	10.1	10.5	10.7	11.6	14.0		
11	3	20	21.4	21.4	21.3	21.7	21.8	12.2	13.3	12.7	13.8	6.2	11.6	19.9	10.0	8.8	9.1	9.4	9.6	10.4	12.4		
11	3	21	21.3	21.2	21.2	21.5	21.8	11.7	11.9	11.6	12.5	6.4	11.0	19.6	9.6	8.8	8.9	9.2	9.3	10.1	11.5		
11	3	22	21.3	21.2	21.2	21.5	21.8	11.5	11.3	11.1	11.8	6.9	11.1	19.6	9.7	9.0	9.0	9.3	9.4	10.1	11.2		
11	3	23	21.3	21.2	21.2	21.5	21.8	11.3	10.9	10.7	11.3	6.7	11.1	19.7	9.5	8.8	8.8	9.1	9.3	9.9	10.9		
11	3	24	21.3	21.2	21.1	21.5	21.8	11.1	10.7	10.4	10.8	7.0	11.0	19.6	9.4	8.8	8.8	9.1	9.3	9.8	10.8		
11	4	1	21.2	21.2	21.1	21.5	21.8	11.0	10.6	10.3	10.6	7.1	11.1	19.6	9.5	8.9	8.8	9.1	9.3	9.8	10.8		
11	4	2	21.2	21.2	21.2	21.5	21.8	11.0	10.6	10.2	10.4	7.5	11.2	19.7	9.6	9.0	9.0	9.3	9.5	10.0	10.8		
11	4	3	21.2	21.2	21.1	21.5	21.8	10.9	10.5	10.1	10.2	7.0	11.1	19.7	9.3	8.7	8.7	9.0	9.2	9.7	10.7		
11	4	4	21.2	21.2	21.2	21.5	21.8	10.8	10.4	10.0	10.1	7.1	11.0	19.7	9.4	8.8	8.7	9.0	9.2	9.7	10.7		
11	4	5	21.2	21.1	21.1	21.5	21.8	10.8	10.5	9.9	10.0	7.7	11.2	19.6	9.7	9.1	9.1	9.4	9.6	10.1	10.9		
11	4	6	21.2	21.2	21.2	21.5	21.8	10.9	10.7	10.2	10.2	8.2	11.6	19.7	10.0	9.5	9.5	9.7	9.9	10.3	11.1		

1	2	3	4	5	6	7	8	9	10	11	12	13	14	15	16	17	18	19	20	21	22	23	24
11	4	7	21.1	21.2	21.1	21.5	21.8	11.0	10.9	10.3	10.3	8.6	11.8	19.7	10.3	9.7	9.7	10.0	10.2	10.6	11.4		
11	4	8	21.1	21.2	21.1	21.5	21.8	11.1	11.1	10.4	10.4	8.7	11.9	19.8	10.4	9.8	9.9	10.2	10.4	10.7	11.5		
11	4	9	21.1	21.2	21.2	21.5	21.8	11.2	11.3	10.6	10.6	8.9	12.2	19.9	11.0	10.5	10.5	10.9	11.0	11.3	12.0		
11	4	10	21.3	21.5	21.5	22.1	21.8	13.6	13.5	13.2	12.5	12.7	16.1	21.6	15.4	14.3	15.0	15.7	15.5	16.0	16.2		
11	4	11	21.5	22.2	22.1	22.9	21.9	16.4	18.1	17.2	15.9	16.7	22.1	24.4	20.6	18.4	20.1	21.1	20.8	21.6	21.6		
11	4	12	21.5	22.3	22.1	22.7	22.0	16.6	20.1	18.7	17.6	15.6	21.8	23.6	18.3	16.6	17.7	18.4	18.5	19.0	19.6		
11	4	13	21.4	22.1	22.0	22.4	22.0	16.4	19.1	17.9	17.4	14.7	19.8	22.6	17.7	16.4	17.2	17.8	17.9	18.2	18.8		
11	4	14	21.4	22.0	22.0	22.2	21.9	16.5	18.5	17.5	17.5	14.6	19.4	22.5	18.4	17.0	18.0	18.6	18.5	18.8	19.3		
11	4	15	21.5	22.0	22.0	22.2	22.0	16.8	19.1	18.0	18.5	15.3	20.4	22.8	18.7	17.1	18.3	19.0	18.9	19.2	19.8		
11	4	16	21.4	21.9	21.8	22.1	21.9	15.8	18.5	17.5	18.2	13.3	18.5	21.8	16.6	15.2	16.0	16.6	16.7	17.1	18.0		
11	4	17	21.3	21.6	21.6	21.9	21.8	14.5	16.8	16.1	16.4	11.8	16.0	20.9	14.6	13.6	14.0	14.4	14.5	14.9	16.0		
11	4	18	21.3	21.5	21.4	21.8	21.8	13.9	15.5	15.1	15.3	11.2	14.9	20.5	13.7	12.9	13.1	13.5	13.6	14.0	15.0		
11	4	19	21.3	21.4	21.4	21.7	21.8	13.6	14.7	14.5	14.6	11.1	14.4	20.4	13.2	12.5	12.7	13.0	13.1	13.5	14.4		
11	4	20	21.2	21.3	21.3	21.6	21.8	13.4	14.1	14.0	14.1	11.2	14.2	20.2	13.1	12.5	12.6	13.0	13.0	13.4	14.2		
11	4	21	21.2	21.4	21.3	21.7	21.8	13.3	14.0	13.8	13.9	11.5	14.3	20.3	13.1	12.5	12.7	13.0	13.1	13.4	14.1		
11	4	22	21.2	21.3	21.3	21.7	21.8	13.3	13.9	13.7	13.7	11.4	14.3	20.3	13.0	12.5	12.6	12.9	13.0	13.3	14.0		
11	4	23	21.2	21.3	21.3	21.6	21.8	13.1	13.7	13.5	13.5	11.1	14.1	20.2	12.8	12.3	12.4	12.7	12.8	13.1	13.8		
11	4	24	21.1	21.3	21.3	21.6	21.8	13.1	13.6	13.4	13.4	11.1	14.1	20.2	12.8	12.3	12.4	12.7	12.8	13.1	13.8		
11	5	1	21.1	21.3	21.3	21.6	21.8	13.0	13.5	13.3	13.2	11.1	14.0	20.2	12.8	12.2	12.3	12.6	12.7	13.0	13.7		
11	5	2	21.1	21.3	21.3	21.6	21.8	13.0	13.5	13.3	13.3	11.5	14.2	20.2	13.0	12.4	12.5	12.8	12.9	13.2	13.8		
11	5	3	21.1	21.3	21.3	21.6	21.8	13.1	13.6	13.4	13.3	11.7	14.3	20.3	13.1	12.5	12.7	13.0	13.1	13.4	14.0		
11	5	4	21.1	21.3	21.3	21.6	21.8	13.1	13.7	13.4	13.3	11.8	14.3	20.3	13.2	12.6	12.7	13.1	13.1	13.4	14.0		
11	5	5	21.1	21.3	21.3	21.6	21.8	13.2	13.8	13.5	13.4	12.1	14.5	20.3	13.3	12.8	12.9	13.2	13.3	13.6	14.2		
11	5	6	21.1	21.3	21.3	21.6	21.8	13.2	13.9	13.6	13.4	12.1	14.6	20.3	13.4	12.8	13.0	13.3	13.4	13.7	14.3		
11	5	7	21.1	21.3	21.3	21.6	21.8	13.3	14.0	13.7	13.6	12.4	14.7	20.3	13.5	13.0	13.1	13.5	13.5	13.8	14.4		
11	5	8	21.1	21.3	21.3	21.6	21.8	13.3	14.1	13.7	13.6	12.4	14.8	20.3	13.6	13.0	13.2	13.6	13.6	13.8	14.5		
11	5	9	21.1	21.3	21.3	21.6	21.8	13.5	14.3	13.9	13.8	12.6	15.0	20.4	13.9	13.3	13.5	13.9	13.8	14.1	14.6		
11	5	10	21.1	21.4	21.3	21.7	21.8	13.7	14.5	14.1	14.0	13.0	15.3	20.5	14.2	13.6	13.8	14.2	14.1	14.4	14.9		
11	5	11	21.1	21.4	21.4	21.7	21.8	14.0	14.8	14.4	14.3	13.3	15.7	20.6	14.6	14.0	14.2	14.6	14.5	14.8	15.2		
11	5	12	21.1	21.5	21.4	21.8	21.8	14.5	15.2	14.8	14.7	13.9	16.3	20.9	15.2	14.6	14.8	15.3	15.2	15.4	15.7		
11	5	13	21.1	21.5	21.5	21.8	21.8	14.9	15.7	15.3	15.2	14.3	16.8	21.1	15.6	14.9	15.2	15.7	15.6	15.9	16.2		
11	5	14	21.1	21.5	21.4	21.7	21.8	14.6	15.8	15.4	15.2	13.7	16.5	20.9	15.1	14.4	14.8	15.2	15.2	15.4	15.9		
11	5	15	21.1	21.4	21.4	21.7	21.8	14.4	15.6	15.2	15.1	13.4	16.1	20.7	14.9	14.2	14.5	14.9	14.9	15.2	15.7		

1	2	3	4	5	6	7	8	9	10	11	12	13	14	15	16	17	18	19	20	21	22	23	24
11	5	16	21.1	21.4	21.4	21.7	21.8	14.2	15.4	15.1	15.0	13.1	15.8	20.6	14.6	13.9	14.2	14.6	14.5	14.8	15.4		
11	5	17	21.1	21.4	21.4	21.7	21.8	14.0	15.1	14.8	14.7	12.8	15.4	20.5	14.3	13.6	13.8	14.2	14.2	14.5	15.1		
11	5	18	21.1	21.4	21.3	21.7	21.8	13.8	14.8	14.6	14.5	12.5	15.2	20.4	14.0	13.4	13.6	13.9	13.9	14.2	14.9		
11	5	19	21.1	21.4	21.3	21.7	21.8	13.7	14.6	14.4	14.3	12.3	15.0	20.4	13.8	13.2	13.4	13.8	13.8	14.1	14.7		
11	5	20	21.0	21.4	21.3	21.6	21.8	13.6	14.4	14.3	14.2	12.1	14.8	20.3	13.7	13.1	13.2	13.6	13.6	13.9	14.6		
11	5	21	21.1	21.4	21.3	21.7	21.8	13.5	14.3	14.2	14.0	11.9	14.7	20.3	13.5	13.0	13.1	13.4	13.5	13.8	14.4		
11	5	22	21.1	21.4	21.3	21.7	21.8	13.5	14.2	14.1	13.9	11.9	14.6	20.3	13.4	12.9	13.0	13.3	13.4	13.7	14.3		
11	5	23	21.1	21.4	21.3	21.7	21.8	13.5	14.1	14.0	13.8	11.8	14.6	20.3	13.4	12.8	12.9	13.3	13.3	13.6	14.3		
11	5	24	21.1	21.4	21.3	21.7	21.8	13.4	14.0	13.9	13.8	11.9	14.5	20.3	13.4	12.8	12.9	13.3	13.4	13.6	14.3		
11	6	1	21.1	21.4	21.3	21.7	21.8	13.5	14.1	13.9	13.8	12.2	14.7	20.3	13.5	13.0	13.1	13.5	13.5	13.8	14.4		
11	6	2	21.0	21.4	21.3	21.7	21.8	13.5	14.1	14.0	13.8	12.0	14.7	20.3	13.5	12.9	13.1	13.4	13.5	13.8	14.4		
11	6	3	21.0	21.4	21.3	21.6	21.8	13.4	14.0	13.9	13.7	11.8	14.5	20.3	13.4	12.8	12.9	13.3	13.3	13.6	14.3		
11	6	4	21.1	21.4	21.3	21.7	21.8	13.4	14.0	13.9	13.7	11.9	14.6	20.3	13.4	12.9	13.0	13.3	13.4	13.7	14.3		
11	6	5	21.1	21.4	21.3	21.7	21.8	13.4	14.1	13.9	13.7	12.2	14.7	20.3	13.5	13.0	13.1	13.4	13.5	13.8	14.4		
11	6	6	21.0	21.4	21.3	21.7	21.8	13.5	14.2	14.0	13.8	12.5	14.8	20.3	13.7	13.2	13.3	13.7	13.7	14.0	14.5		
11	6	7	21.1	21.4	21.3	21.7	21.8	13.5	14.3	14.1	13.9	12.5	14.9	20.4	13.8	13.2	13.4	13.7	13.8	14.0	14.6		
11	6	8	21.0	21.4	21.3	21.6	21.8	13.5	14.3	14.1	13.9	12.4	14.9	20.3	13.8	13.2	13.4	13.7	13.7	14.0	14.6		
11	6	9	21.0	21.4	21.3	21.6	21.8	13.6	14.3	14.2	14.0	12.5	14.9	20.4	13.9	13.3	13.5	13.8	13.9	14.1	14.7		
11	6	10	21.1	21.4	21.4	21.7	21.8	13.8	14.5	14.4	14.2	13.0	15.3	20.5	14.2	13.7	13.9	14.2	14.2	14.4	14.9		
11	6	11	21.1	21.4	21.4	21.7	21.8	14.1	14.8	14.7	14.5	13.4	15.7	20.6	14.7	14.2	14.4	14.8	14.7	14.9	15.3		
11	6	12	21.1	21.5	21.5	21.8	21.9	14.9	15.5	15.3	15.1	14.2	16.7	21.0	15.6	15.1	15.3	15.8	15.6	15.9	16.1		
11	6	13	21.1	21.5	21.5	21.8	21.9	14.9	15.9	15.7	15.5	14.1	16.9	21.1	15.5	14.9	15.2	15.7	15.5	15.8	16.2		
11	6	14	21.1	21.5	21.5	21.8	21.8	14.9	15.9	15.7	15.5	14.1	16.7	20.9	15.7	15.1	15.3	15.8	15.6	15.9	16.2		
11	6	15	21.1	21.5	21.5	21.8	21.8	15.1	16.1	15.9	15.8	14.0	16.9	21.1	15.6	14.9	15.3	15.7	15.6	15.9	16.3		
11	6	16	21.1	21.5	21.5	21.8	21.8	14.7	15.9	15.8	15.6	13.5	16.3	20.8	15.1	14.4	14.7	15.1	15.0	15.3	15.8		
11	6	17	21.1	21.5	21.4	21.7	21.8	14.4	15.6	15.5	15.3	13.3	15.9	20.6	14.7	14.1	14.4	14.7	14.7	15.0	15.6		
11	6	18	21.1	21.4	21.4	21.7	21.8	14.2	15.2	15.2	15.0	12.8	15.5	20.5	14.3	13.7	13.9	14.3	14.3	14.6	15.2		
11	6	19	21.0	21.4	21.3	21.7	21.8	13.9	14.9	14.9	14.7	12.0	15.0	20.4	13.9	13.3	13.4	13.8	13.8	14.1	14.8		
11	6	20	21.1	21.4	21.3	21.7	21.8	13.8	14.6	14.6	14.4	12.0	14.8	20.3	13.7	13.1	13.2	13.6	13.6	13.9	14.6		
11	6	21	21.1	21.4	21.3	21.7	21.8	13.7	14.4	14.4	14.3	12.0	14.7	20.3	13.7	13.1	13.2	13.5	13.6	13.9	14.5		
11	6	22	21.1	21.4	21.3	21.7	21.8	13.7	14.3	14.3	14.2	11.8	14.7	20.3	13.4	12.9	13.0	13.3	13.4	13.7	14.3		
11	6	23	21.0	21.4	21.3	21.7	21.8	13.5	14.0	14.1	13.9	11.2	14.3	20.3	13.1	12.5	12.6	12.9	13.0	13.3	14.0		
11	6	24	21.0	21.4	21.3	21.6	21.8	13.3	13.8	13.9	13.7	10.9	14.0	20.2	12.9	12.4	12.4	12.7	12.8	13.1	13.9		

Experimental results from Test Case DSF200_e

1	2	3	4	5	6	7	8	9	10	11	12	13	14	15	16	17	18	19	20	21	22	23	24
			Exp. room, surface temperature, oC					DSF, surface temperatures oC				Glass surf. temperature, oC				Air temp in the section 2, DSF, oC							
												ei	ie	ii									
Month	Date	Hour	Floor	Ceiling	East Wall	West Wall	North Wall	Floor	Ceiling	East Wall	West Wall	AVERAGE			Volume averaged air temperature in the DSF oC	h= 0.1m	h= 1.5m	h= 2.5m	h= 3.5m	h= 4.5m	h= 5.5m	Cooling/heating load, kW	Solar irradiation on DSF, W/m2
10	1	1	21.5	21.5	21.4	21.8	21.9	15.5	13.6	14.6	14.8	11.3	13.9	20.2								0.425	0
10	1	2	21.5	21.5	21.4	21.8	21.9	15.2	13.2	14.1	14.3	11.0	13.6	20.2								0.439	0
10	1	3	21.5	21.5	21.4	21.8	21.9	14.8	13.0	13.6	13.8	10.4	13.1	20.1								0.464	0
10	1	4	21.5	21.4	21.4	21.8	21.9	14.6	12.7	13.2	13.4	10.2	13.0	20.1								0.485	0
10	1	5	21.5	21.4	21.4	21.8	21.9	14.4	12.4	12.8	13.0	9.9	12.7	20.0								0.497	0
10	1	6	21.5	21.4	21.4	21.7	21.9	14.1	12.1	12.4	12.6	10.0	12.4	20.0								0.491	0
10	1	7	21.5	21.4	21.4	21.8	21.9	14.2	12.0	12.4	12.6	10.6	12.8	20.0								0.507	8
10	1	8	21.5	21.5	21.5	21.9	21.9	15.1	13.1	13.4	13.4	12.8	14.4	20.7								0.262	144
10	1	9	21.5	21.7	21.7	22.2	21.9	16.2	15.5	15.9	15.3	15.7	16.9	21.7	14.1	14.4	13.1	13.8	14.1	14.5	14.9	-0.007	171
10	1	10	21.7	22.0	21.9	22.5	22.0	17.5	16.4	17.0	15.9	16.8	17.7	22.1	15.8	16.2	14.9	15.5	15.8	16.2	16.4	-0.247	284
10	1	11	22.2	22.9	22.7	23.8	22.1	24.0	21.8	23.4	20.7	26.5	26.7	26.3	22.4	21.7	21.1	22.2	23.0	23.8	22.9	-1.819	646
10	1	12	22.7	23.7	23.2	24.3	22.2	27.4	24.3	26.8	24.5	30.0	30.8	28.1	25.0	24.0	23.9	25.2	26.0	26.7	24.1	-2.902	731
10	1	13	22.6	24.1	23.6	24.2	22.3	29.4	25.9	28.0	27.3	31.6	32.4	28.9	26.3	25.4	25.0	26.5	27.2	28.0	25.5	-3.286	733
10	1	14	22.8	24.1	23.8	24.0	22.3	30.0	27.4	29.1	30.8	31.4	33.2	28.8	26.7	25.5	25.1	26.7	27.8	28.6	26.3	-2.883	620
10	1	15	22.6	23.7	23.5	23.6	22.1	28.2	26.8	29.2	31.8	28.7	30.9	26.9	26.0	25.0	24.5	26.2	27.1	27.6	25.6	-1.938	434
10	1	16	22.4	23.3	23.1	23.2	22.0	25.7	25.8	28.7	31.6	26.8	28.0	24.9	24.9	23.9	23.4	25.0	25.8	26.3	25.0	-1.266	332
10	1	17	22.2	22.7	22.5	22.8	21.9	22.6	24.3	26.7	29.0	22.6	24.5	23.4	21.4	20.7	19.9	21.2	21.9	22.4	22.1	-0.535	83
10	1	18	22.0	22.2	22.0	22.3	21.8	20.4	20.8	23.4	25.0	18.0	20.2	21.8	18.4	18.3	17.4	18.3	18.7	19.0	18.7	-0.063	7
10	1	19	22.0	22.0	21.9	22.2	21.9	19.3	18.1	21.4	22.7	16.3	18.3	21.3	17.2	17.4	16.6	17.4	17.3	17.4	17.0	0.118	0
10	1	20	21.9	21.9	21.8	22.1	21.9	18.6	16.9	20.1	21.1	16.1	17.6	21.1	16.6	17.0	16.2	16.8	16.6	16.7	16.5	0.240	0
10	1	21	21.9	21.8	21.7	22.1	21.9	18.3	16.4	19.2	20.0	15.6	17.2	21.0	16.2	16.6	15.8	16.3	16.1	16.2	16.0	0.261	0
10	1	22	21.8	21.8	21.7	22.0	21.9	17.9	16.0	18.4	19.1	15.2	16.8	20.9	16.0	16.5	15.7	16.1	15.9	16.0	15.8	0.294	0
10	1	23	21.8	21.7	21.6	22.0	21.9	17.7	16.0	18.0	18.5	15.4	17.0	20.9	15.9	16.1	15.6	16.1	15.9	15.9	15.6	0.306	0
10	1	24	21.7	21.7	21.6	22.0	21.9	17.3	15.6	17.4	17.7	14.1	16.2	20.8	14.8	14.9	14.3	14.8	14.7	15.0	15.0	0.332	0
10	2	1	21.7	21.6	21.6	22.0	21.9	16.9	15.6	16.7	17.0	13.8	15.7	20.7	14.5	15.1	13.9	14.4	14.3	14.6	14.9	0.338	0

1	2	3	4	5	6	7	8	9	10	11	12	13	14	15	16	17	18	19	20	21	22	23	24
10	2	2	21.7	21.7	21.6	22.0	22.0	16.8	15.2	16.3	16.6	13.8	15.7	20.7	14.4	14.9	13.9	14.4	14.4	14.5	14.4	0.354	0
10	2	3	21.7	21.6	21.6	21.9	21.9	16.5	14.8	16.0	16.2	13.4	15.4	20.6	14.1	14.6	13.5	14.0	14.0	14.2	14.3	0.364	0
10	2	4	21.7	21.6	21.6	22.0	21.9	16.3	14.3	15.6	15.8	13.2	15.2	20.6	13.9	14.4	13.5	14.0	13.9	14.0	13.7	0.390	0
10	2	5	21.7	21.6	21.6	21.9	21.9	16.0	13.8	15.3	15.5	12.8	15.0	20.5	13.6	14.1	13.2	13.7	13.5	13.6	13.3	0.401	0
10	2	6	21.6	21.6	21.5	21.9	21.9	15.8	13.3	14.9	15.1	12.8	14.7	20.5	13.3	13.8	13.1	13.5	13.3	13.2	12.9	0.437	0
10	2	7	21.6	21.5	21.5	21.8	21.9	15.6	13.0	14.6	14.7	12.6	14.5	20.4	13.1	13.7	12.9	13.3	13.1	13.0	12.7	0.438	3
10	2	8	21.6	21.6	21.5	21.9	21.9	15.8	13.1	14.5	14.7	12.7	14.7	20.5	13.6	14.2	13.3	13.7	13.5	13.6	13.2	0.383	28
10	2	9	21.7	21.8	21.8	22.2	21.9	17.5	14.5	16.0	15.9	16.3	17.0	21.5	16.6	16.9	16.4	17.1	16.9	16.9	15.7	-0.106	265
10	2	10	21.7	22.2	22.1	22.7	22.0	19.1	16.3	19.8	18.2	18.8	20.2	22.8	17.3	17.4	17.2	18.0	17.8	17.5	15.9	-0.440	224
10	2	11	21.9	22.4	22.3	23.0	22.0	21.3	17.3	21.1	19.4	20.6	22.1	24.0	19.4	19.3	19.3	20.1	20.1	20.0	17.8	-0.916	368
10	2	12	21.9	22.5	22.3	22.8	22.0	20.4	18.1	21.3	20.3	19.8	22.0	23.5	18.2	18.1	18.0	18.8	18.8	18.6	17.2	-0.526	138
10	2	13	21.9	22.4	22.2	22.6	22.0	20.5	17.4	20.4	20.1	18.3	20.5	23.0	18.8	19.0	18.5	19.3	19.3	19.2	17.6	-0.730	293
10	2	14	22.0	22.5	22.5	22.8	22.0	22.4	19.1	21.4	22.2	21.9	23.5	24.3	20.1	19.5	19.7	20.6	20.9	20.9	19.0	-0.908	258
10	2	15	22.1	22.7	22.6	22.8	22.0	23.1	20.4	22.4	24.1	22.3	24.3	24.5	19.9	18.6	19.1	20.2	20.7	21.1	19.5	-0.968	308
10	2	16	21.9	22.4	22.3	22.6	21.9	20.7	20.1	22.0	23.0	20.2	21.5	22.9	19.5	18.7	18.6	19.6	20.1	20.6	19.5		254
10	2	17	21.8	22.3	22.1	22.4	21.9	19.7	20.1	21.6	23.1	19.1	21.0	22.5	17.5	17.1	16.4	17.2	17.6	18.2	18.2	-0.210	72
10	2	18	21.8	22.0	21.9	22.2	21.9	18.2	17.9	19.6	20.6	15.7	18.0	21.4	15.9	15.9	15.3	16.1	16.2	16.3	15.7	0.125	7
10	2	19	21.7	21.8	21.7	22.0	21.9	17.3	16.1	18.2	18.9	14.2	16.5	20.9	15.0	15.3	14.2	14.8	14.9	15.3	15.4	0.256	0
10	2	20	21.7	21.7	21.7	22.0	21.9	16.9	15.4	17.2	17.8	13.4	15.8	20.7	14.5	14.8	13.8	14.4	14.5	14.7	14.6	0.307	0
10	2	21	21.7	21.7	21.6	21.9	21.9	16.5	14.6	16.5	17.0	13.3	15.5	20.6	14.1	14.5	13.6	14.2	14.1	14.3	13.9	0.354	0
10	2	22	21.6	21.6	21.6	21.9	21.9	16.2	14.0	15.9	16.4	12.7	15.1	20.6	13.6	14.1	12.9	13.5	13.5	13.7	13.7	0.373	0
10	2	23	21.6	21.6	21.5	21.9	21.9	15.9	14.0	15.3	15.6	12.5	14.5	20.4	13.2	13.8	12.5	12.9	12.9	13.2	13.6	0.392	0
10	2	24	21.6	21.6	21.5	21.9	21.9	15.8	14.2	15.0	15.2	12.9	14.6	20.4	13.4	13.8	12.8	13.2	13.2	13.5	13.8	0.413	0
10	3	1	21.6	21.6	21.5	21.9	21.9	15.7	14.3	14.9	15.0	13.1	14.7	20.5	13.4	13.8	12.9	13.3	13.3	13.5	13.7	0.397	0
10	3	2	21.6	21.6	21.5	21.9	21.9	15.6	14.1	14.7	14.7	13.1	14.7	20.4	13.4	13.8	13.0	13.4	13.3	13.5	13.6	0.417	0
10	3	3	21.6	21.6	21.5	21.9	21.9	15.6	14.1	14.7	14.7	13.2	14.8	20.5	13.6	13.7	13.2	13.6	13.6	13.9	13.7	0.422	0
10	3	4	21.5	21.5	21.4	21.8	21.9	15.5	14.1	14.7	14.6	13.4	15.0	20.4	13.7	13.7	13.3	13.7	13.7	13.9	13.8	0.431	0
10	3	5	21.5	21.5	21.4	21.8	21.9	15.4	13.9	14.6	14.5	12.8	14.7	20.4	13.2	13.2	12.7	13.2	13.3	13.5	13.3	0.428	0
10	3	6	21.5	21.5	21.4	21.8	21.8	15.1	13.5	14.3	14.2	12.2	14.3	20.3	12.8	13.0	12.4	12.8	12.8	13.0	12.9	0.451	0
10	3	7	21.4	21.4	21.4	21.7	21.8	14.9	13.2	14.0	13.9	12.0	14.1	20.3	12.7	12.6	12.2	12.7	12.7	13.0	12.7	0.443	11
10	3	8	21.5	21.6	21.5	21.9	21.9	15.9	13.8	15.0	14.8	13.7	15.6	21.1	13.8	13.3	13.4	13.9	14.1	14.5	13.9	0.222	165
10	3	9	21.6	21.9	21.8	22.3	22.0	16.9	15.7	16.9	16.2	15.9	17.6	21.8	15.1	14.4	14.5	15.1	15.4	16.0	15.5	0.046	124
10	3	10	21.6	21.9	21.8	22.2	21.9	17.3	16.2	17.3	16.5	16.2	17.8	21.8	15.8	15.1	15.4	16.0	16.2	16.6	15.7	-0.039	142

1	2	3	4	5	6	7	8	9	10	11	12	13	14	15	16	17	18	19	20	21	22	23	24
10	3	11	21.7	22.1	22.0	22.4	22.0	18.7	17.2	18.3	17.5	18.2	19.4	22.5	17.7	16.9	17.3	17.8	18.1	18.6	17.6	-0.382	250
10	3	12	22.0	22.5	22.4	22.9	22.1	21.2	19.5	20.6	19.6	21.4	22.6	24.2	19.2	18.6	18.7	19.3	19.6	20.1	19.1	-0.977	312
10	3	13	22.1	23.0	22.8	23.2	22.2	24.4	21.8	22.3	21.9	25.1	25.7	25.8	21.7	20.1	20.9	21.5	22.2	23.1	22.2	-1.883	522
10	3	14	21.9	22.7	22.5	22.9	22.1	21.3	22.1	22.4	22.1	21.1	23.3	24.1	19.1	18.0	18.2	19.0	19.5	20.2	19.8	-0.757	128
10	3	15	21.9	22.4	22.3	22.6	22.0	20.7	20.8	21.4	21.5	19.8	21.3	22.8	19.5	18.9	18.7	19.3	19.7	20.2	20.0	-0.449	195
10	3	16	21.9	22.6	22.8	22.8	21.9	23.1	22.7	23.0	25.1	23.3	23.4	23.5	20.6	19.3	19.4	20.1	20.9	21.8	22.1	-0.789	347
10	3	17	21.8	22.3	22.2	22.5	21.9	19.6	21.7	21.7	22.9	18.7	20.5	22.4	17.3	17.1	16.3	16.8	17.2	17.7	18.6	-0.182	60
10	3	18	21.7	22.0	21.9	22.2	21.9	18.1	19.4	19.5	20.3	15.8	17.7	21.3	15.6	16.0	14.7	15.3	15.4	15.8	16.4	0.070	8
10	3	19	21.7	21.8	21.7	22.1	21.9	17.3	17.8	18.2	18.8	14.5	16.5	20.9	14.9	15.3	14.1	14.6	14.7	15.1	15.8	0.241	0
10	3	20	21.6	21.7	21.6	22.0	21.9	16.6	16.3	17.1	17.6	13.0	15.5	20.7	13.9	14.3	13.2	13.7	13.7	14.1	14.7	0.314	0
10	3	21	21.6	21.7	21.6	21.9	21.9	16.1	15.3	16.2	16.6	12.1	14.7	20.5	13.2	13.6	12.5	13.0	13.0	13.3	13.8	0.367	0
10	3	22	21.6	21.6	21.6	21.9	21.9	15.9	14.5	15.5	15.9	12.4	14.5	20.4	13.1	13.4	12.6	13.1	13.1	13.4	13.3	0.383	0
10	3	23	21.6	21.6	21.5	21.9	21.9	15.6	14.0	15.0	15.3	11.9	14.3	20.4	12.8	13.4	12.2	12.6	12.6	12.9	13.2	0.401	0
10	3	24	21.6	21.6	21.5	21.9	21.9	15.5	13.8	14.6	14.9	12.2	14.2	20.3	12.9	13.0	12.4	12.8	12.9	13.1	13.0	0.426	0
10	4	1	21.6	21.6	21.5	21.9	21.9	15.3	13.5	14.4	14.5	11.6	14.0	20.4	12.1	12.1	11.5	12.0	12.1	12.5	12.5	0.444	0
10	4	2	21.5	21.5	21.5	21.8	21.9	14.8	12.9	13.8	13.9	10.7	13.3	20.2	11.6	11.6	11.0	11.5	11.5	11.9	12.0	0.465	0
10	4	3	21.5	21.5	21.4	21.8	21.9	14.5	12.6	13.3	13.4	10.3	12.9	20.1	11.1	11.1	10.4	10.9	11.0	11.3	11.7	0.484	0
10	4	4	21.5	21.5	21.4	21.8	21.9	14.3	12.4	12.9	12.9	10.0	12.6	20.0	10.9	11.2	10.2	10.6	10.6	10.9	11.5	0.493	0
10	4	5	21.5	21.4	21.4	21.7	21.9	14.0	12.1	12.5	12.5	9.6	12.3	19.9	10.8	11.1	10.1	10.6	10.6	10.9	11.4	0.508	0
10	4	6	21.5	21.4	21.4	21.7	21.9	13.9	12.1	12.3	12.3	10.0	12.4	20.0	11.0	11.0	10.4	10.9	10.9	11.2	11.6	0.516	0
10	4	7	21.5	21.5	21.4	21.8	21.9	14.1	12.2	12.4	12.4	10.6	12.8	20.1	11.4	11.5	10.9	11.3	11.3	11.6	11.9	0.509	11
10	4	8	21.5	21.5	21.4	21.8	21.9	14.5	12.7	12.8	12.8	11.5	13.6	20.4	12.4	12.2	11.9	12.3	12.3	12.8	13.2	0.397	81
10	4	9	21.6	21.9	21.9	22.5	21.9	17.4	16.1	16.9	15.8	18.0	18.0	22.2	16.6	15.5	15.6	16.3	16.8	17.7	17.7	-0.295	371
10	4	10	21.7	22.3	22.2	22.8	22.0	18.4	18.9	20.0	17.5	19.3	20.2	22.9	17.0	16.7	16.3	16.9	17.1	17.5	17.6	-0.417	191
10	4	11	21.8	22.3	22.2	22.8	22.0	19.4	19.3	20.0	18.0	19.5	20.7	23.3	18.3	18.1	17.5	18.1	18.3	18.8	18.8	-0.561	247
10	4	12	21.8	22.2	22.1	22.6	22.0	18.9	19.2	19.5	18.2	18.7	19.9	22.6	18.0	18.1	17.4	17.9	18.1	18.4	18.1	-0.419	200
10	4	13	21.8	22.3	22.2	22.6	22.0	19.8	19.2	19.7	18.8	19.3	20.7	23.2	17.2	17.0	16.6	17.2	17.4	17.8	17.5	-0.530	173
10	4	14	21.7	22.1	22.0	22.3	21.9	18.5	18.3	19.0	18.4	17.5	19.0	22.1	17.3	17.4	16.6	17.2	17.3	17.6	17.6	-0.125	91
10	4	15	21.7	22.0	21.9	22.2	21.9	18.6	18.2	18.8	18.6	17.7	19.1	22.0	18.2	18.3	17.6	18.1	18.2	18.5	18.3	-0.097	120
10	4	16	21.8	22.3	22.4	22.5	22.0	20.7	20.2	20.5	21.5	21.5	21.6	23.0	20.8	20.7	19.9	20.6	21.1	21.4	21.3	-0.547	363
10	4	17	21.7	22.3	22.4	22.5	21.9	19.6	21.8	21.7	24.7	21.0	22.4	23.4	18.8	18.4	17.7	18.5	19.0	19.5	19.8	-0.370	239
10	4	18	21.6	22.0	21.9	22.2	21.9	17.7	19.5	19.8	21.1	15.9	18.3	21.8	15.5	15.5	14.4	15.1	15.4	15.9	16.5	0.048	42
10	4	19	21.6	21.8	21.7	22.0	21.9	16.4	16.6	17.5	18.0	12.5	15.2	20.8	13.3	13.3	12.5	13.0	13.2	13.6	14.2	0.256	0

1	2	3	4	5	6	7	8	9	10	11	12	13	14	15	16	17	18	19	20	21	22	23	24
10	4	20	21.6	21.6	21.6	21.9	21.9	15.7	14.9	16.0	16.4	11.4	14.0	20.4	12.3	12.2	11.5	12.1	12.3	12.7	13.0	0.370	
10	4	21	21.6	21.6	21.5	21.9	21.9	15.2	13.7	15.0	15.4	10.5	13.4	20.3	11.6	11.4	10.9	11.4	11.6	12.0	12.2	0.419	
10	4	22	21.5	21.5	21.5	21.8	21.9	14.7	12.7	14.2	14.5	10.1	12.9	20.1	11.3	11.2	10.6	11.2	11.3	11.7	11.6	0.462	0
10	4	23	21.5	21.5	21.4	21.8	21.9	14.5	12.2	13.6	13.8	10.3	12.8	20.0	11.2	11.2	10.7	11.2	11.3	11.6	11.4	0.483	0
10	4	24	21.5	21.5	21.4	21.8	21.9	14.2	11.9	13.2	13.3	9.9	12.7	20.0	10.9	10.9	10.3	10.8	10.9	11.3	11.1	0.497	0
10	5	1	21.5	21.4	21.4	21.8	21.9	13.9	11.4	12.7	12.8	9.3	12.3	20.0	10.4	10.4	9.8	10.4	10.5	10.9	10.6	0.502	0
10	5	2	21.5	21.4	21.4	21.7	21.9	13.7	11.1	12.3	12.3	9.6	12.0	19.9	10.4	10.6	9.9	10.4	10.4	10.6	10.5	0.527	0
10	5	3	21.5	21.4	21.4	21.7	21.9	13.6	11.0	12.2	12.1	9.7	12.2	19.9	10.4	10.4	9.9	10.4	10.5	10.8	10.6	0.547	0
10	5	4	21.4	21.4	21.3	21.7	21.9	13.5	11.0	12.0	11.8	9.4	12.1	19.9	10.3	10.3	9.8	10.2	10.3	10.7	10.5	0.549	0
10	5	5	21.4	21.4	21.3	21.7	21.9	13.2	10.7	11.7	11.6	8.7	11.7	19.8	9.7	9.7	9.2	9.7	9.7	10.1	9.8	0.561	
10	5	6	21.4	21.3	21.3	21.7	21.9	12.9	10.0	11.2	11.2	8.1	11.3	19.7	9.2	9.4	8.8	9.3	9.4	9.6	9.1	0.574	0
10	5	7	21.4	21.3	21.3	21.7	21.9	12.7	9.6	10.9	10.9	8.0	11.1	19.7	9.2	9.4	8.7	9.2	9.3	9.6	9.2	0.588	7
10	5	8	21.4	21.4	21.4	21.8	21.9	13.4	10.3	11.6	11.4	9.8	12.4	20.3	10.7	10.3	10.2	10.8	10.9	11.3	10.8	0.443	125
10	5	9	21.6	21.8	21.8	22.4	21.9	15.8	13.6	15.4	14.2	15.7	16.4	21.8	14.6	13.0	13.8	14.5	15.1	16.0	14.8	-0.165	359
10	5	10	21.9	22.6	22.6	23.3	22.0	19.7	18.6	22.5	18.2	21.4	21.8	24.2	18.2	15.8	16.9	17.8	18.8	20.3	19.4	-1.247	599
10	5	11	22.4	23.5	23.1	24.2	22.1	23.4	22.5	26.2	20.9	24.4	26.4	27.2	20.5	19.8	19.3	20.2	20.9	21.8	21.2	-2.215	701
10	5	12	22.8	23.9	23.3	24.5	22.1	24.8	23.0	26.0	21.7	24.7	26.4	27.9	19.5	19.2	18.4	19.3	19.9	20.5	19.8	-2.808	627
10	5	13	22.2	23.2	22.8	23.4	22.0	21.1	20.9	22.8	20.2	19.2	21.8	24.7	16.9	16.4	16.1	17.0	17.4	17.8	16.9	-1.384	245
10	5	14	22.4	23.1	23.1	23.2	22.0	24.0	19.5	22.2	22.9	20.7	23.4	25.7	20.2	18.3	19.3	20.2	21.2	22.1	20.1	-2.106	669
10	5	15	22.5	23.5	23.5	23.5	22.0	26.5	23.4	25.0	28.5	24.7	28.2	27.9	20.9	18.3	19.4	20.6	21.8	23.3	21.9	-2.242	634
10	5	16	22.2	23.0	22.8	23.0	21.9	21.0	21.9	23.6	25.1	19.2	22.0	23.7	18.0	16.3	16.9	17.8	18.7	19.7	18.8	-0.837	218
10	5	17	22.1	22.6	22.5	22.7	21.9	19.7	20.6	22.7	25.2	19.1	21.2	23.1	17.0	15.8	15.8	16.7	17.5	18.4	17.9	-0.441	203
10	5	18	21.9	22.1	22.0	22.3	21.8	17.6	17.8	20.0	21.6	14.8	17.6	21.5	14.5	14.2	13.4	14.4	14.9	15.4	14.9	0.053	9
10	5	19	21.8	21.8	21.7	22.0	21.8	16.3	15.2	17.6	18.7	11.9	15.1	20.7	12.8	12.9	11.8	12.5	12.8	13.3	13.4	0.257	0
10	5	20	21.8	21.7	21.6	22.0	21.9	15.7	13.8	16.2	17.1	11.3	14.1	20.4	12.5	12.8	11.9	12.5	12.6	12.8	12.4	0.370	0
10	5	21	21.7	21.6	21.5	21.9	21.9	15.3	12.4	15.2	16.0	11.0	13.8	20.3	12.1	12.6	11.9	12.4	12.2	12.0	11.5	0.415	0
10	5	22	21.7	21.5	21.5	21.8	21.9	15.0	11.8	14.5	15.1	11.1	13.5	20.2	11.9	12.5	11.7	12.1	11.9	11.7	11.3	0.461	0
10	5	23	21.7	21.5	21.4	21.8	21.9	14.8	11.6	13.9	14.4	11.2	13.4	20.2	11.9	12.5	11.7	12.1	11.9	11.8	11.4	0.481	0
10	5	24	21.6	21.5	21.4	21.8	21.9	14.7	11.7	13.6	14.0	11.4	13.5	20.2	12.0	12.6	11.8	12.2	12.0	11.8	11.6	0.486	0
10	6	1	21.6	21.4	21.4	21.8	21.8	14.5	11.7	13.3	13.6	11.1	13.3	20.1	11.9	12.5	11.6	12.0	11.8	11.8	11.5	0.497	0
10	6	2	21.6	21.4	21.4	21.7	21.8	14.3	11.7	13.1	13.3	10.9	13.2	20.1	11.7	12.4	11.3	11.7	11.6	11.8	11.6	0.511	0
10	6	3	21.6	21.4	21.4	21.7	21.8	14.2	11.7	13.0	13.1	11.1	13.1	20.1	12.0	12.6	11.6	12.0	11.9	12.0	11.9	0.532	0
10	6	4	21.5	21.3	21.3	21.7	21.8	14.1	12.0	12.9	13.1	11.7	13.3	20.1	12.2	12.7	11.9	12.3	12.1	12.2	12.1	0.535	0

1	2	3	4	5	6	7	8	9	10	11	12	13	14	15	16	17	18	19	20	21	22	23	24
10	6	5	21.5	21.4	21.3	21.7	21.8	14.1	12.1	13.0	13.1	11.8	13.4	20.1	12.3	12.7	12.0	12.4	12.2	12.3	12.2	0.543	0
10	6	6	21.5	21.4	21.4	21.7	21.9	14.2	12.3	13.0	13.2	12.0	13.6	20.2	12.5	13.0	12.3	12.6	12.4	12.4	12.3	0.550	0
10	6	7	21.5	21.4	21.4	21.7	21.9	14.2	12.5	13.1	13.2	12.2	13.8	20.2	12.8	13.3	12.5	12.9	12.7	12.7	12.5	0.545	0
10	6	8	21.5	21.4	21.4	21.7	21.9	14.5	12.8	13.3	13.4	12.7	14.3	20.3	13.4	13.8	13.2	13.6	13.4	13.4	13.1	0.520	12
10	6	9	21.5	21.5	21.5	21.9	21.9	15.2	13.5	14.1	14.1	13.9	15.5	20.8	14.2	14.5	14.1	14.5	14.3	14.2	13.8	0.365	53
10	6	10	21.5	21.6	21.6	21.9	21.9	16.1	14.6	15.1	15.0	15.2	16.6	21.2	15.4	15.4	15.3	15.7	15.6	15.5	15.0	0.239	86
10	6	11	21.7	22.0	21.9	22.5	21.9	18.8	16.7	17.6	16.8	18.8	20.0	22.8	18.6	17.9	18.5	18.9	19.0	19.4	18.0	-0.529	365
10	6	12	21.9	22.5	22.3	22.9	22.0	20.9	19.8	20.8	19.7	22.0	23.7	24.6	19.9	18.9	19.5	20.2	20.6	21.1	19.4	-1.014	321
10	6	13	21.8	22.4	22.2	22.7	22.0	20.3	19.9	20.8	20.1	20.8	22.4	23.6	19.7	18.7	19.3	20.0	20.3	20.6	19.2	-0.750	221
10	6	14	21.8	22.5	22.4	22.7	22.0	21.6	20.4	21.5	21.9	22.1	23.7	24.1	20.8	19.9	20.7	21.4	21.6	21.6	19.7	-0.913	304
10	6	15	21.9	22.6	22.5	22.8	22.0	22.4	21.2	22.6	24.1	22.7	24.8	24.6	20.9	19.6	20.5	21.5	21.9	22.0	20.0	-0.933	283
10	6	16	21.8	22.3	22.1	22.5	21.9	19.7	19.9	21.8	22.6	19.6	21.6	22.7	19.0	18.2	18.6	19.5	19.7	19.6	18.5	-0.248	69
10	6	17	21.7	22.0	21.9	22.2	21.9	18.8	18.6	20.5	21.2	18.3	19.9	21.8	18.3	17.9	18.0	18.7	18.7	18.6	17.8	0.024	44
10	6	18	21.6	21.8	21.7	22.1	21.8	18.1	17.7	19.6	20.2	17.1	18.8	21.4	17.4	17.3	17.2	17.7	17.7	17.7	17.1	0.161	14
10	6	19	21.6	21.8	21.7	22.0	21.9	17.5	16.9	18.7	19.3	16.1	17.9	21.1	16.7	16.8	16.3	16.9	16.8	16.8	16.5	0.264	0
10	6	20	21.6	21.7	21.6	21.9	21.9	17.0	16.1	17.9	18.4	15.2	17.1	20.9	15.8	16.0	15.3	15.9	15.8	15.9	15.7	0.314	0
10	6	21	21.5	21.6	21.5	21.9	21.9	16.6	15.4	17.2	17.7	14.8	16.4	20.8	15.3	15.6	14.9	15.4	15.3	15.4	15.2	0.347	0
10	6	22	21.5	21.6	21.5	21.9	21.9	16.5	15.4	16.9	17.2	15.1	16.4	20.7	15.6	15.9	15.4	15.8	15.6	15.6	15.5	0.378	0
10	6	23	21.5	21.6	21.5	21.9	21.9	16.4	15.5	16.6	17.0	15.1	16.4	20.7	15.5	15.8	15.3	15.7	15.5	15.5	15.4	0.365	0
10	6	24	21.5	21.6	21.5	21.9	21.9	16.4	15.5	16.5	16.8	15.2	16.5	20.8	15.7	16.0	15.5	15.8	15.6	15.6	15.6	0.382	0
10	7	1	21.5	21.6	21.5	21.8	21.9	16.3	15.5	16.3	16.6	15.1	16.4	20.7	15.6	15.9	15.4	15.7	15.5	15.6	15.5	0.387	0
10	7	2	21.5	21.6	21.5	21.8	21.9	16.3	15.5	16.2	16.4	15.1	16.4	20.7	15.6	15.9	15.4	15.7	15.5	15.6	15.5	0.394	0
10	7	3	21.4	21.5	21.5	21.8	21.9	16.2	15.4	16.1	16.3	15.0	16.3	20.7	15.4	15.6	15.2	15.6	15.3	15.3	15.2	0.397	0
10	7	4	21.5	21.6	21.5	21.8	21.9	16.1	15.2	15.9	16.1	14.6	16.1	20.7	15.2	15.4	15.0	15.3	15.1	15.1	15.0	0.375	0
10	7	5	21.5	21.6	21.5	21.9	21.9	15.9	14.8	15.7	15.9	14.2	15.9	20.7	14.7	15.0	14.5	14.9	14.7	14.7	14.5	0.415	0
10	7	6	21.5	21.6	21.5	21.9	21.9	15.8	14.5	15.5	15.6	14.0	15.6	20.6	14.5	14.8	14.3	14.7	14.4	14.4	14.2	0.405	0
10	7	7	21.4	21.5	21.5	21.8	21.9	15.6	14.1	15.2	15.3	13.6	15.3	20.5	14.2	14.5	14.0	14.3	14.1	14.1	13.9	0.424	1
10	7	8	21.4	21.5	21.5	21.8	21.9	15.6	13.8	15.0	15.1	13.3	15.2	20.6	14.0	14.5	13.9	14.2	14.0	13.9	13.7	0.390	28
10	7	9	21.5	21.8	21.8	22.3	21.9	17.2	14.8	16.7	16.3	16.6	17.3	21.6	16.3	16.1	16.3	17.0	16.8	16.4	15.1	-0.052	272
10	7	10	21.7	22.4	22.3	23.0	22.0	19.6	16.9	21.2	18.9	20.4	21.3	23.3	18.2	17.4	18.3	19.2	19.2	18.8	16.6	-0.704	344
10	7	11	22.1	22.9	22.7	23.5	22.1	21.9	18.8	23.9	20.9	22.3	24.2	25.2	20.3	18.9	20.1	21.1	21.5	21.5	18.6	-1.487	530
10	7	12	22.8	23.8	23.3	24.3	22.2	26.2	22.3	26.7	24.0	27.3	29.1	28.2	22.8	20.6	22.1	23.4	24.2	25.0	21.3	-3.019	744
10	7	13	22.4	23.7	23.2	23.8	22.2	24.6	22.2	25.6	24.4	23.4	26.5	26.7	20.9	19.3	20.2	21.3	22.1	22.7	20.2	-2.448	522

1	2	3	4	5	6	7	8	9	10	11	12	13	14	15	16	17	18	19	20	21	22	23	24
10	7	14	22.4	23.6	23.3	23.6	22.2	25.0	21.7	25.1	25.4	23.2	26.0	27.0	19.8	19.3	19.2	20.1	20.5	20.5	19.0	-2.286	468
10	7	15	22.1	22.8	22.6	22.9	22.0	20.1	18.5	22.1	21.4	17.6	19.6	23.3	16.6	16.7	15.9	16.5	16.7	17.0	16.6	-0.706	116
10	7	16	22.0	22.3	22.2	22.5	21.9	18.7	16.9	19.9	19.5	16.2	17.6	21.8	15.6	15.8	15.0	15.6	15.7	16.0	15.7	-0.232	85
10	7	17	21.9	22.1	21.9	22.3	21.9	17.0	15.0	18.0	17.5	14.0	15.6	21.1	13.8	14.1	13.3	13.8	13.8	14.0	13.9	0.080	26
10	7	18	21.8	21.8	21.7	22.1	21.9	16.2	14.0	16.6	16.1	13.3	14.7	20.6	13.4	13.8	13.0	13.4	13.4	13.5	13.5	0.240	5
10	7	19	21.7	21.7	21.6	21.9	21.9	15.7	13.7	15.7	15.2	13.2	14.4	20.4	13.5	13.7	13.1	13.5	13.4	13.5	13.6	0.320	0
10	7	20	21.7	21.6	21.6	21.9	21.9	15.4	13.5	15.2	14.7	12.9	14.1	20.4	13.1	13.4	12.7	13.1	13.0	13.2	13.2	0.361	0
10	7	21	21.7	21.6	21.5	21.9	21.9	15.1	13.4	14.8	14.3	13.0	14.1	20.3	13.4	13.6	13.0	13.3	13.2	13.4	13.5	0.372	0
10	7	22	21.7	21.6	21.5	21.9	21.9	15.0	13.6	14.7	14.3	13.1	14.2	20.4	13.2	13.5	12.9	13.2	13.1	13.3	13.4	0.427	0
10	7	23	21.6	21.5	21.5	21.8	21.9	14.8	13.3	14.4	13.9	12.6	13.9	20.3	12.9	13.2	12.6	12.9	12.8	13.0	13.1	0.436	0
10	7	24	21.6	21.6	21.5	21.9	21.9	14.7	13.3	14.3	13.8	12.8	14.0	20.3	13.0	13.3	12.7	13.0	12.9	13.1	13.2	0.434	0
10	8	1	21.6	21.5	21.5	21.8	21.9	14.6	13.2	14.1	13.7	12.8	14.0	20.3	12.9	13.2	12.6	13.0	12.9	13.0	13.0	0.462	0
10	8	2	21.6	21.5	21.5	21.8	21.9	14.6	13.2	14.1	13.7	12.7	14.0	20.3	12.8	13.0	12.5	12.8	12.7	12.9	12.8	0.464	0
10	8	3	21.5	21.5	21.5	21.8	21.9	14.5	13.0	14.0	13.6	12.5	13.9	20.3	12.7	12.8	12.4	12.8	12.7	12.8	12.7	0.456	0
10	8	4	21.5	21.5	21.4	21.8	21.9	14.6	13.2	14.1	13.7	12.8	14.3	20.3	13.3	13.5	13.0	13.4	13.2	13.4	13.4	0.496	0
10	8	5	21.5	21.5	21.4	21.8	21.9	14.7	13.8	14.2	13.9	13.5	14.6	20.3	13.8	14.0	13.5	13.8	13.7	13.9	14.0	0.456	0
10	8	6	21.5	21.5	21.4	21.8	21.9	14.7	14.0	14.3	14.0	13.6	14.7	20.4	13.8	14.0	13.4	13.8	13.7	13.9	14.0	0.459	0
10	8	7	21.5	21.5	21.4	21.8	21.9	14.7	14.0	14.4	14.0	13.6	14.7	20.4	13.8	14.0	13.5	13.8	13.7	13.9	14.0	0.470	1
10	8	8	21.5	21.5	21.5	21.8	21.9	14.9	14.1	14.6	14.2	13.8	15.0	20.6	14.0	14.2	13.6	14.0	13.9	14.1	14.1	0.404	27
10	8	9	21.5	21.6	21.5	21.9	21.9	15.4	14.4	15.1	14.6	14.4	15.6	20.9	14.7	14.9	14.3	14.7	14.7	14.9	14.7	0.250	97
10	8	10	21.7	22.1	22.1	22.7	22.0	18.3	16.9	18.6	17.0	19.1	19.4	22.9	17.5	17.4	17.0	17.6	17.7	18.0	17.4	-0.600	417
10	8	11	22.3	23.1	22.9	23.8	22.2	21.5	19.6	23.0	19.7	22.2	23.5	25.9	19.5	19.4	18.7	19.5	19.8	20.2	19.3	-1.740	622
10	8	12	22.8	23.9	23.4	24.3	22.3	24.3	21.6	24.8	21.6	24.8	26.1	28.0	20.6	20.9	19.7	20.5	21.0	21.4	20.3	-2.964	744
10	8	13	22.5	24.0	23.5	24.1	22.3	24.6	21.7	23.9	22.3	24.3	25.6	27.5	21.4	21.7	20.3	21.1	21.6	22.2	21.1	-2.975	670
10	8	14	22.6	24.0	23.9	23.9	22.3	26.8	23.7	24.8	26.3	26.6	28.4	28.5	23.2	23.4	21.9	22.9	23.6	24.4	23.3	-3.084	727
10	8	15	22.5	23.9	23.8	23.8	22.2	25.9	23.8	25.4	28.3	24.8	27.4	27.8	21.5	21.4	20.2	21.3	22.0	22.6	21.5	-2.351	594
10	8	16	22.2	23.2	23.1	23.1	22.0	21.8	21.1	23.6	25.3	19.8	21.8	23.9	17.8	17.7	16.8	17.6	18.1	18.5	18.1	-1.060	210
10	8	17	22.1	22.5	22.3	22.6	22.0	18.8	17.9	20.5	20.8	15.7	17.8	21.9	15.5	15.7	14.8	15.4	15.5	15.8	15.7	-0.220	48
10	8	18	22.0	22.1	21.9	22.2	21.9	17.5	16.1	18.6	18.7	14.1	16.2	21.0	14.4	14.8	13.8	14.3	14.4	14.6	14.6	0.079	16
10	8	19	21.9	21.9	21.7	22.1	21.9	16.6	14.8	17.2	17.2	13.0	15.0	20.7	13.5	13.9	12.9	13.4	13.4	13.6	13.6	0.248	0
10	8	20	21.8	21.7	21.7	22.0	21.9	16.0	13.9	16.2	16.0	12.3	14.3	20.5	12.9	13.4	12.4	12.8	12.8	13.0	13.0	0.347	0
10	8	21	21.8	21.7	21.6	21.9	21.9	15.6	13.3	15.4	15.2	11.7	13.9	20.3	12.4	12.8	11.9	12.3	12.3	12.5	12.5	0.379	0
10	8	22	21.8	21.7	21.6	21.9	22.0	15.2	12.9	14.8	14.6	11.3	13.6	20.3	12.0	12.3	11.5	11.9	11.9	12.1	12.1	0.406	0

1	2	3	4	5	6	7	8	9	10	11	12	13	14	15	16	17	18	19	20	21	22	23	24
10	8	23	21.7	21.6	21.5	21.9	21.9	14.9	12.6	14.3	14.1	11.0	13.4	20.2	11.9	12.2	11.4	11.8	11.8	12.1	12.2	0.430	0
10	8	24	21.7	21.6	21.5	21.9	21.9	14.7	12.7	13.9	13.8	10.8	13.3	20.2	11.7	12.1	11.1	11.6	11.6	11.9	12.2	0.460	0
10	9	1	21.7	21.6	21.5	21.9	22.0	14.6	12.7	13.6	13.6	11.1	13.4	20.2	12.2	12.4	11.6	12.1	12.1	12.4	12.5	0.453	0
10	9	2	21.6	21.5	21.4	21.8	21.9	14.7	12.9	13.6	13.6	12.3	14.0	20.2	12.9	13.1	12.5	12.9	12.9	13.2	13.0	0.458	0
10	9	3	21.6	21.5	21.4	21.8	21.9	14.9	13.4	13.9	13.8	13.0	14.6	20.3	13.4	13.5	13.0	13.4	13.4	13.6	13.6	0.454	0
10	9	4	21.5	21.5	21.4	21.8	21.9	15.0	13.8	14.0	14.0	13.1	14.8	20.4	13.6	13.6	13.1	13.5	13.5	13.8	13.9	0.448	0
10	9	5	21.5	21.5	21.5	21.8	21.9	15.0	14.1	14.2	14.1	13.3	14.9	20.4	13.6	13.7	13.2	13.6	13.6	13.8	14.0	0.418	0
10	9	6	21.5	21.5	21.4	21.8	21.9	15.0	14.1	14.2	14.1	13.4	15.1	20.4	13.9	14.0	13.6	14.0	13.9	14.0	13.7	0.450	0
10	9	7	21.5	21.5	21.4	21.8	21.8	15.0	13.8	14.3	14.2	13.5	15.2	20.4	13.9	14.1	13.6	14.0	13.9	14.1	13.7	0.457	1
10	9	8						15.2	13.9	14.5	14.4				13.9	14.2	13.6	14.1	14.0	14.1	13.8	0.364	47
10	9	9						16.9	15.3	16.6	16.1				16.8	16.4	16.4	17.2	17.2	17.4	16.0	-0.099	257
10	9	10	21.8	22.3	22.3	22.8	22.0	19.6	18.1	20.9	18.9	21.4	21.9	23.4	19.0	17.9	18.2	19.3	19.8	20.3	18.6	-0.747	374
10	9	11	22.3	23.1	22.9	23.8	22.2	23.3	21.6	24.9	22.0	25.8	26.8	26.3	22.0	20.7	20.7	21.9	22.7	23.6	22.2	-1.852	621
10	9	12	22.6	23.8	23.2	24.1	22.2	26.1	24.3	26.9	24.8	29.2	30.0	27.9	24.1	23.3	22.6	24.1	25.1	25.9	23.7	-2.793	697
10	9	13	22.3	23.6	23.1	23.6	22.2	24.7	22.4	26.2	25.4	25.3	27.5	26.4	22.4	22.1	21.7	23.0	23.2	23.4	21.1	-1.963	388
10	9	14	22.1	23.0	22.7	23.0	22.0	22.8	20.4	24.6	24.8	22.0	24.4	24.5	20.6	20.5	20.1	21.2	21.3	21.2	19.5	-1.102	220
10	9	15	22.0	22.5	22.2	22.6	21.9	20.5	18.6	22.6	23.0	18.8	21.1	22.7	18.6	18.7	18.1	19.0	19.0	18.9	17.8	-0.390	96
10	9	16	21.9	22.1	22.0	22.3	21.9	19.5	17.9	21.1	21.5	17.7	19.5	21.9	17.9	18.0	17.3	18.0	18.2	18.4	17.7	-0.081	69
10	9	17	21.8	22.0	21.9	22.2	21.9	18.8	17.4	20.2	20.7	17.2	19.0	21.6	17.5	17.5	17.0	17.7	17.8	17.8	17.0	0.049	60
10	9	18	21.8	21.9	21.8	22.1	21.9	18.0	17.1	19.4	19.9	16.1	18.2	21.4	16.4	16.5	15.6	16.4	16.6	16.9	16.6	0.149	14
10	9	19	21.7	21.8	21.7	22.0	21.9	17.1	16.1	18.2	18.5	14.3	16.6	20.9	15.3	15.6	14.7	15.3	15.4	15.6	15.3	0.297	0
10	9	20	21.7	21.7	21.6	21.9	21.9	16.8	15.4	17.4	17.6	14.3	16.2	20.7	15.0	15.2	14.3	15.0	15.0	15.3	15.0	0.342	0
10	9	21	21.7	21.7	21.6	21.9	21.9	16.5	15.1	16.8	17.1	14.2	16.0	20.7	14.8	15.1	14.2	14.8	14.8	15.0	14.7	0.355	0
10	9	22	21.6	21.6	21.5	21.9	21.9	16.2	14.7	16.4	16.6	14.1	15.8	20.6	14.6	15.0	14.0	14.6	14.6	14.8	14.6	0.369	0
10	9	23	21.6	21.6	21.6	21.9	21.9	16.2	14.8	16.1	16.2	14.1	15.8	20.6	14.5	14.6	14.0	14.5	14.5	14.7	14.5	0.407	0
10	9	24	21.5	21.6	21.5	21.8	21.9	16.0	14.7	15.8	15.9	14.1	15.7	20.6	14.4	14.5	14.0	14.5	14.5	14.7	14.3	0.406	0
10	10	1	21.6	21.6	21.5	21.8	21.9	16.0	14.7	15.7	15.8	14.0	15.7	20.6	14.3	14.3	13.8	14.3	14.3	14.6	14.3	0.421	0
10	10	2	21.5	21.6	21.5	21.9	21.9	15.9	14.6	15.5	15.6	13.8	15.6	20.6	14.3	14.3	13.9	14.4	14.4	14.6	14.3	0.428	0
10	10	3	21.5	21.6	21.5	21.8	21.9	15.8	14.6	15.5	15.5	14.0	15.6	20.6	14.3	14.2	13.9	14.4	14.4	14.5	14.3	0.409	0
10	10	4	21.5	21.5	21.5	21.8	21.9	15.6	14.4	15.3	15.2	13.4	15.3	20.5	13.8	13.9	13.4	13.8	13.8	14.1	13.9	0.418	0
10	10	5	21.5	21.6	21.5	21.8	21.9	15.4	14.3	15.0	14.9	13.1	14.9	20.5	13.6	13.9	13.2	13.6	13.5	13.7	13.7	0.407	0
10	10	6	21.5	21.5	21.4	21.8	21.9	15.2	13.9	14.7	14.5	12.6	14.6	20.4	13.2	13.6	12.7	13.1	13.1	13.3	13.3	0.445	0
10	10	7	21.5	21.5	21.5	21.8	21.9	15.0	13.6	14.4	14.2	11.8	14.2	20.3	12.6	12.8	12.1	12.5	12.5	12.8	12.9	0.440	3

1	2	3	4	5	6	7	8	9	10	11	12	13	14	15	16	17	18	19	20	21	22	23	24
10	10	8	21.5	21.6	21.6	21.9	21.9	15.5	14.0	15.0	14.6	13.1	15.1	20.8	14.0	13.4	13.0	14.2	14.2	14.6	14.9		149
10	10	9	21.6	21.9	21.8	22.3	22.0	17.4	18.6	19.1	17.5	19.8	19.9	22.4	19.3	15.5	16.5	20.5	20.5	21.0	21.6		398
10	10	10	21.9	23.2	22.9	23.5	22.3	21.2	23.6	25.4	21.1	25.3	25.0	25.6	20.7	19.5	18.8	20.3	20.9	21.8	22.7	0.078	606
10	10	11	22.6	24.4	24.0	25.0	22.9	23.9	26.2	28.1	23.3	26.7	27.9	28.3	22.1	21.4	20.3	21.4	22.1	23.4	24.2	-2.293	669
10	10	12	22.8	24.5	23.8	24.8	22.6	27.3	28.2	28.3	25.1	30.1	29.8	28.5	24.7	25.1	23.1	24.0	24.6	25.6	26.1	-3.635	769
10	10	13	22.6	24.4	23.7	24.3	22.4	29.8	30.1	28.4	27.3	31.9	31.6	29.0	25.4	26.0	23.6	24.6	25.3	26.1	26.9	-4.005	754
10	10	14	22.6	24.1	24.0	23.9	22.2	30.9	30.7	28.7	30.6	31.2	32.0	28.8	26.0	26.3	24.2	25.2	25.9	26.6	27.7	-3.478	715
10	10	15	22.5	23.8	23.7	23.7	22.0	29.2	30.9	28.9	32.8	29.5	31.1	27.9	24.5	24.8	22.5	23.6	24.2	24.9	26.7	-2.493	499
10	10	16	22.2	23.3	23.3	23.2	21.8	25.8	28.7	27.8	31.5	26.7	26.1	24.6	22.8	23.3	20.9	22.0	22.4	23.0	24.9	-1.507	402
10	10	17	22.1	22.8	22.6	22.8	21.8	22.2	26.5	26.1	29.8	22.7	23.6	23.5	19.7	20.2	18.0	18.9	19.3	19.9	21.7	-0.759	155
10	10	18	22.0	22.2	22.0	22.3	21.7	19.6	22.8	22.8	25.0	16.3	18.8	21.7	16.1	16.2	14.7	15.4	15.8	16.4	17.8	-0.182	13
10	10	19	21.9	21.9	21.8	22.1	21.7	17.9	19.5	20.0	21.6	13.3	16.0	20.8	14.1	14.7	13.0	13.6	13.8	14.3	15.3	0.075	0
10	10	20	21.8	21.7	21.7	22.0	21.8	17.1	17.3	18.2	19.5	12.2	14.9	20.5	13.3	13.8	12.4	12.9	13.0	13.5	14.1	0.210	0
10	10	21	21.7	21.6	21.6	21.9	21.8	16.4	15.8	16.9	17.9	11.4	14.2	20.3	12.7	13.4	11.9	12.3	12.3	12.7	13.4	0.269	0
10	10	22	21.7	21.6	21.6	21.9	21.9	15.8	14.8	15.8	16.7	10.7	13.6	20.2	11.9	12.1	11.0	11.5	11.6	12.0	12.8	0.308	0
10	10	23	21.7	21.5	21.5	21.8	21.8	15.1	13.8	14.8	15.4	9.7	12.8	20.1	11.0	11.3	10.2	10.7	10.8	11.2	12.0	0.378	0
10	10	24	21.7	21.5	21.5	21.8	21.9	14.5	13.1	13.9	14.4	9.1	12.3	20.0	10.5	10.6	9.7	10.2	10.3	10.6	11.5	0.388	0
10	11	1	21.6	21.4	21.5	21.8	21.9	14.1	12.4	13.1	13.5	8.8	11.8	19.9	10.1	10.6	9.5	9.9	9.9	10.2	10.8	0.447	0
10	11	2	21.6	21.4	21.4	21.8	21.9	14.1	12.1	12.6	13.0	9.2	12.0	19.9	10.4	10.9	9.8	10.2	10.2	10.5	11.1	0.453	0
10	11	3	21.6	21.4	21.4	21.8	21.9	13.9	12.0	12.4	12.7	9.4	12.1	19.9	10.3	10.7	9.6	10.0	10.1	10.4	11.0	0.461	0
10	11	4	21.6	21.4	21.4	21.7	21.9	13.5	11.6	11.9	12.1	8.5	11.5	19.8	9.3	9.8	8.6	9.0	9.1	9.4	10.1	0.487	0
10	11	5	21.5	21.3	21.3	21.7	21.9	13.2	11.2	11.4	11.6	8.0	11.2	19.7	9.6	9.7	8.9	9.3	9.4	9.7	10.5	0.494	0
10	11	6	21.5	21.3	21.3	21.7	21.9	12.9	11.0	11.1	11.2	7.9	11.1	19.7	9.4	9.7	8.8	9.1	9.2	9.5	10.2	0.518	0
10	11	7	21.5	21.3	21.4	21.7	21.9	13.2	11.2	11.1	11.3	9.6	11.7	19.7	10.4	11.0	9.9	10.2	10.1	10.4	10.8	0.522	1
10	11	8	21.5	21.3	21.3	21.7	21.9	13.6	11.8	11.5	11.6	10.7	12.6	19.9	11.4	12.0	10.9	11.2	11.1	11.3	11.7	0.440	25
10	11	9	21.7	21.7	21.7	22.3	22.0	16.0	14.4	14.3	13.9	15.9	16.0	21.4	14.8	14.9	13.9	14.5	14.7	15.1	15.7	-0.092	297
10	11	10	21.7	22.1	22.1	22.7	22.0	17.5	17.5	17.9	16.4	18.7	19.6	22.8	16.8	16.4	16.0	16.7	17.0	17.5	17.4	-0.425	215
10	11	11	21.6	21.9	21.9	22.3	21.9	16.3	16.9	17.1	16.3	15.7	17.8	21.8	15.5	15.4	14.8	15.4	15.5	15.9	15.8	-0.014	51
10	11	12	21.6	21.7	21.7	22.1	21.9	16.1	15.8	16.1	15.9	15.1	16.6	21.2	15.1	15.3	14.6	15.1	15.1	15.4	15.3	0.134	51
10	11	13	21.5	21.6	21.6	22.0	21.9	16.0	15.4	15.8	15.8	14.9	16.4	21.0	14.9	15.1	14.4	14.9	14.9	15.2	15.1	0.191	43
10	11	14	21.6	21.6	21.6	21.9	21.9	15.8	15.1	15.6	15.6	14.5	16.0	20.9	14.6	14.8	14.1	14.5	14.5	14.8	14.8	0.282	28
10	11	15	21.5	21.6	21.6	21.9	21.9	15.8	15.0	15.4	15.6	14.5	15.9	20.8	14.6	14.8	14.1	14.5	14.5	14.8	14.9	0.286	26
10	11	16	21.5	21.5	21.5	21.9	21.9	15.6	15.0	15.3	15.4	14.3	15.8	20.7	14.4	14.6	13.9	14.3	14.3	14.6	14.7	0.331	15

1	2	3	4	5	6	7	8	9	10	11	12	13	14	15	16	17	18	19	20	21	22	23	24
10	11	17	21.5	21.5	21.4	21.8	21.9	15.3	14.7	15.0	15.2	13.8	15.4	20.5	14.1	14.4	13.5	14.0	14.0	14.3	14.4	0.380	6
10	11	18	21.4	21.4	21.4	21.8	21.9	15.1	14.5	14.8	15.0	13.4	15.1	20.5	13.7	14.0	13.1	13.6	13.5	13.8	14.1	0.391	4
10	11	19	21.5	21.4	21.4	21.8	21.9	14.8	14.2	14.4	14.6	12.4	14.5	20.4	12.7	13.1	12.0	12.4	12.4	12.7	13.2	0.408	0
10	11	20	21.4	21.4	21.4	21.8	21.9	14.4	13.6	13.8	14.1	11.2	13.6	20.2	12.3	12.9	11.8	12.1	12.1	12.4	12.8	0.464	0
10	11	21	21.4	21.4	21.4	21.8	21.9	14.5	13.4	13.6	13.9	12.2	13.9	20.2	13.0	13.4	12.6	12.9	12.8	13.0	13.3	0.452	0
10	11	22	21.4	21.4	21.4	21.8	21.9	14.6	13.6	13.7	14.0	12.8	14.4	20.3	13.2	13.6	12.8	13.2	13.1	13.3	13.5	0.459	0
10	11	23	21.4	21.4	21.4	21.8	21.9	14.7	13.8	13.8	14.1	13.2	14.6	20.3	13.8	14.0	13.4	13.7	13.6	13.8	14.0	0.438	0
10	11	24	21.4	21.4	21.4	21.7	21.9	14.8	14.2	14.1	14.3	13.8	15.1	20.4	14.1	14.3	13.8	14.1	14.0	14.3	14.3	0.461	0
10	12	1	21.4	21.4	21.4	21.7	21.9	14.7	14.0	14.1	14.3	13.4	14.9	20.4	13.8	14.1	13.4	13.8	13.7	14.0	14.0	0.451	0
10	12	2	21.4	21.4	21.4	21.8	21.9	14.7	13.9	14.1	14.3	13.4	14.9	20.4	13.8	14.1	13.4	13.8	13.7	13.9	13.9	0.458	0
10	12	3	21.4	21.4	21.4	21.8	21.9	14.7	14.0	14.1	14.4	13.6	15.0	20.4	13.9	14.1	13.5	13.9	13.8	14.0	14.0	0.438	0
10	12	4	21.4	21.4	21.4	21.7	21.9	14.6	13.9	14.1	14.3	13.4	14.8	20.4	13.6	13.9	13.2	13.6	13.5	13.8	13.8	0.444	0
10	12	5	21.4	21.4	21.4	21.8	21.9	14.5	13.7	13.9	14.2	13.1	14.6	20.3	13.4	13.7	13.0	13.3	13.3	13.5	13.5	0.458	0
10	12	6	21.4	21.4	21.4	21.7	21.9	14.4	13.4	13.7	14.1	12.8	14.3	20.3	13.1	13.4	12.7	13.0	13.0	13.2	13.3	0.445	0
10	12	7	21.4	21.4	21.4	21.7	21.9	14.3	13.3	13.6	14.0	12.8	14.3	20.3	13.1	13.4	12.7	13.1	13.0	13.2	13.3	0.469	0
10	12	8	21.3	21.4	21.4	21.7	21.9	14.3	13.3	13.6	13.9	12.8	14.3	20.3	13.1	13.5	12.7	13.1	13.0	13.2	13.3	0.441	3
10	12	9	21.3	21.4	21.4	21.7	21.9	14.4	13.4	13.6	14.0	13.0	14.5	20.3	13.3	13.6	12.9	13.3	13.2	13.4	13.5	0.430	9
10	12	10	21.4	21.4	21.4	21.8	21.9	14.6	13.6	13.8	14.2	13.4	14.8	20.4	13.6	13.9	13.2	13.6	13.5	13.7	13.7	0.439	16
10	12	11	21.4	21.5	21.5	21.8	21.9	14.9	13.9	14.1	14.4	13.8	15.2	20.6	14.0	14.2	13.6	14.0	13.9	14.1	14.0	0.379	33
10	12	12	21.4	21.5	21.5	21.8	21.9	15.0	14.2	14.4	14.7	14.1	15.5	20.7	14.2	14.5	13.8	14.3	14.2	14.4	14.3	0.350	33
10	12	13	21.4	21.5	21.5	21.8	21.9	15.1	14.5	14.6	14.9	14.3	15.6	20.7	14.3	14.5	13.9	14.3	14.2	14.5	14.5	0.344	27
10	12	14	21.4	21.5	21.5	21.8	21.9	15.0	14.5	14.5	14.9	14.0	15.4	20.6	14.1	14.3	13.6	14.1	14.0	14.3	14.3	0.364	18
10	12	15	21.4	21.5	21.5	21.8	21.9	15.1	14.5	14.5	14.9	14.1	15.4	20.6	14.2	14.4	13.8	14.2	14.1	14.4	14.5	0.368	23
10	12	16	21.4	21.5	21.5	21.8	21.9	15.1	14.6	14.6	15.0	14.2	15.5	20.6	14.2	14.4	13.8	14.2	14.1	14.4	14.5	0.363	14
10	12	17	21.4	21.5	21.5	21.8	21.9	15.0	14.7	14.6	14.9	14.1	15.4	20.6	14.1	14.3	13.7	14.1	14.0	14.3	14.5	0.404	7
10	12	18	21.3	21.4	21.4	21.7	21.9	14.8	14.5	14.5	14.8	13.8	15.2	20.4	14.0	14.2	13.6	14.0	13.9	14.1	14.3	0.437	1
10	12	19	21.3	21.4	21.4	21.7	21.9	14.8	14.5	14.4	14.7	13.8	15.2	20.4	14.1	14.3	13.7	14.1	14.0	14.2	14.5	0.419	0
10	12	20	21.3	21.4	21.4	21.7	21.9	14.8	14.5	14.4	14.7	13.8	15.2	20.4	14.0	14.2	13.6	14.0	13.9	14.2	14.4	0.437	0
10	12	21	21.3	21.4	21.4	21.7	21.9	14.8	14.5	14.4	14.7	13.6	15.1	20.4	13.8	14.0	13.4	13.8	13.7	14.0	14.3	0.429	0
10	12	22	21.3	21.4	21.4	21.7	21.9	14.7	14.6	14.4	14.6	13.5	15.1	20.4	13.7	13.9	13.3	13.7	13.6	13.8	14.2	0.419	0
10	12	23	21.3	21.4	21.4	21.7	21.9	14.7	14.5	14.3	14.6	13.5	15.0	20.4	13.8	14.0	13.3	13.7	13.6	13.9	14.2	0.441	0
10	12	24	21.3	21.4	21.4	21.7	21.9	14.7	14.6	14.3	14.6	13.7	15.1	20.4	13.9	14.1	13.5	13.9	13.8	14.0	14.3	0.418	0
10	13	1	21.4	21.5	21.4	21.8	21.9	14.8	14.7	14.4	14.6	13.8	15.3	20.5	14.0	14.1	13.5	13.9	13.8	14.1	14.4	0.422	0

1	2	3	4	5	6	7	8	9	10	11	12	13	14	15	16	17	18	19	20	21	22	23	24
10	13	2	21.4	21.5	21.4	21.8	21.9	14.7	14.6	14.4	14.6	13.4	15.1	20.5	13.7	13.8	13.2	13.6	13.5	13.8	14.1	0.426	0
10	13	3	21.3	21.5	21.4	21.8	21.9	14.7	14.7	14.4	14.5	13.6	15.1	20.4	13.8	13.9	13.3	13.7	13.6	13.9	14.2	0.434	0
10	13	4	21.3	21.5	21.4	21.8	21.9	14.7	14.7	14.4	14.5	13.6	15.1	20.5	13.7	13.9	13.2	13.6	13.6	13.8	14.2	0.437	0
10	13	5	21.3	21.4	21.4	21.8	21.9	14.6	14.6	14.3	14.5	13.5	15.0	20.4	13.4	13.7	12.9	13.3	13.3	13.5	13.9	0.417	0
10	13	6	21.3	21.4	21.4	21.7	21.9	14.5	14.4	14.1	14.3	13.1	14.7	20.4	13.4	13.6	12.9	13.3	13.2	13.5	13.8	0.446	0
10	13	7	21.3	21.4	21.4	21.7	21.9	14.5	14.4	14.1	14.3	13.2	14.8	20.4	13.5	13.8	13.0	13.4	13.3	13.6	13.9	0.447	0
10	13	8	21.3	21.4	21.4	21.8	21.9	14.6	14.3	14.1	14.2	13.0	14.7	20.4								0.412	10
10	13	9																					
10	13	10						17.8	19.0	19.1	18.1				17.4	17.1	16.5	17.2	17.4	17.8	18.4	-0.418	198
10	13	11	21.7	22.4	22.3	23.0	21.9	19.8	20.2	20.7	19.4	21.3	22.3	24.3	19.3	19.2	18.3	19.1	19.3	19.9	20.0	-1.269	496
10	13	12	22.2	23.2	22.8	23.7	22.1	22.7		22.7	21.9	25.2	25.9	26.7	21.0	21.1	19.8	20.6	21.0	21.6	22.2	-2.294	584
10	13	13	22.1	23.6	23.2	23.7	22.3	25.4	25.1	23.0	23.8	26.5	27.0	27.4	22.1	22.5	20.8	21.5	22.0	22.6	23.3	-3.011	709
10	13	14	22.2	23.9	23.9	23.8	22.4	27.8	27.0	24.5	28.1	28.2	29.8	28.8	23.4	23.3	21.7	22.7	23.3	24.2	25.1	-3.155	730
10	13	15	22.2	23.8	23.8	23.7	22.2	27.1	28.0	25.4	30.7	26.9	28.9	27.8	22.7	22.2	20.9	21.9	22.5	23.3	25.2	-2.400	592
10	13	16	22.0	23.4	23.5	23.3	22.0	23.2	27.2	24.8	30.1	24.3	24.4	24.6	20.6	19.9	18.9	19.8	20.4	21.0	23.4	-1.452	398
10	13	17	21.9	22.7	22.5	22.8	21.8	19.5	24.7	22.8	27.9	19.5	21.3	23.1	17.2	16.9	15.8	16.6	17.0	17.6	19.6	-0.633	169
10	13	18	21.7	22.1	21.9	22.3	21.7	17.2	20.6	19.6	22.9	13.8	16.6	21.3	13.5	14.0	12.2	12.9	13.2	13.8	15.1	-0.040	11
10	13	19	21.7	21.8	21.6	22.0	21.7	15.8	17.2	17.2	19.3	10.8	14.0	20.4	12.0	12.4	10.9	11.4	11.7	12.2	13.2	0.180	
10	13	20	21.6	21.6	21.5	21.9	21.7	15.0	15.0	15.5	17.2	9.6	12.9	20.1	11.0	11.4	10.1	10.6	10.7	11.1	12.0	0.278	0
10	13	21	21.6	21.5	21.4	21.8	21.7	14.2	13.6	14.3	15.7	8.8	12.1	19.9	10.3	10.5	9.4	9.9	10.0	10.5	11.4	0.362	0
10	13	22	21.5	21.4	21.3	21.7	21.8	13.8	12.6	13.3	14.4	8.3	11.6	19.8	9.9	10.1	9.1	9.5	9.6	10.0	10.9	0.405	0
10	13	23	21.5	21.3	21.3	21.7	21.8	13.4	11.9	12.5	13.4	7.9	11.3	19.6	9.6	9.8	8.8	9.2	9.3	9.6	10.6	0.442	0
10	13	24	21.5	21.3	21.3	21.7	21.8	13.0	11.4	11.9	12.6	7.6	11.0	19.6	9.1	9.2	8.4	8.8	8.9	9.3	10.2	0.467	0
10	14	1	21.4	21.3	21.3	21.7	21.8	12.8	11.0	11.3	11.9	7.6	10.9	19.5	9.2	9.5	8.5	8.9	9.0	9.3	10.2	0.494	0
10	14	2	21.4	21.2	21.2	21.6	21.8	12.4	10.7	10.9	11.4	7.2	10.6	19.5	8.6	8.6	7.8	8.3	8.4	8.7	9.6	0.501	0
10	14	3	21.4	21.2	21.2	21.6	21.7	12.1	10.3	10.4	10.8	6.8	10.2	19.4	8.1	8.3	7.4	7.8	7.9	8.3	9.1	0.523	0
10	14	4	21.4	21.2	21.2	21.6	21.7	12.0	10.0	10.1	10.3	6.9	10.1	19.4	8.1	8.5	7.4	7.8	7.9	8.2	9.1	0.535	0
10	14	5	21.4	21.1	21.2	21.5	21.7	11.7	9.7	9.7	9.9	6.4	9.8	19.3	7.7	7.8	6.9	7.4	7.5	7.9	8.8	0.569	0
10	14	6	21.3	21.1	21.1	21.5	21.7	11.5	9.4	9.3	9.5	5.9	9.4	19.2	7.0	7.5	6.2	6.6	6.7	7.1	8.0	0.592	0
10	14	7	21.3	21.1	21.1	21.5	21.7	11.1	8.9	8.8	8.9	5.3	8.9	19.1	6.9	7.1	6.1	6.6	6.7	7.0	8.0	0.600	1
10	14	8	21.3	21.1	21.2	21.6	21.7	11.6	9.2	9.3	9.2	7.2	9.9	19.5	7.7	8.0	6.9	7.4	7.5	7.9	8.7	0.474	105
10	14	9	21.5	21.5	21.5	22.1	21.8	13.5	11.7	12.2	11.3	12.2	12.9	20.9	11.0	10.8	9.7	10.4	10.9	11.7	12.5	-0.050	287
10	14	10	21.8	22.3	22.3	23.1	21.9	17.3	16.9	17.7	15.2	20.5	19.4	23.6	16.3	14.8	14.8	15.6	16.2	17.7	18.7	-1.130	535

1	2	3	4	5	6	7	8	9	10	11	12	13	14	15	16	17	18	19	20	21	22	23	24
10	14	11	22.2	23.2	22.9	24.1	22.0	21.6	22.8	23.8	19.3	26.9	26.4	27.1	20.3	18.6	18.6	19.3	20.1	21.8	23.2	-2.301	717
10	14	12	22.6	23.9	23.3	24.3	22.1	24.9	26.5	25.6	22.1	29.9	28.7	28.2	21.9	20.9	20.2	21.0	21.7	23.2	24.5	-3.140	741
10	14	13	22.4	23.9	23.4	24.0	22.3	25.8	27.5	25.5	23.8	28.5	28.4	28.0	22.5	22.5	20.9	21.8	22.4	23.3	24.4	-3.090	634
10	14	14	22.3	23.6	23.4	23.6	22.2	26.1	27.8	25.8	26.6	28.9	28.7	27.2	22.7	23.2	20.9	22.0	22.5	23.0	24.3	-2.425	519
10	14	15	22.1	23.1	23.0	23.2	22.0	23.6	26.7	25.2	26.5	24.4	25.8	25.4	19.5	19.0	18.0	18.8	19.4	20.2	21.6	-1.406	267
10	14	16	21.9	22.5	22.3	22.6	21.8	20.0	23.4	22.9	23.5	18.9	20.6	22.6	17.7	18.1	16.5	17.3	17.5	17.9	18.9	-0.591	146
10	14	17	21.8	22.1	22.0	22.3	21.7	18.4	21.0	21.2	22.5	17.1	18.9	21.9	15.9	16.3	14.7	15.4	15.7	16.1	17.4	-0.191	86
10	14	18	21.7	21.8	21.7	22.1	21.7	16.6	18.4	18.9	19.8	13.1	15.8	20.9	13.5	13.8	12.3	13.0	13.2	13.7	14.9	0.093	9
10	14	19	21.7	21.6	21.5	21.9	21.7	15.7	16.1	17.0	17.6	11.0	14.1	20.3	12.4	12.6	11.4	12.0	12.2	12.7	13.6	0.264	0
10	14	20	21.6	21.4	21.4	21.8	21.7	15.0	14.5	15.5	16.0	9.9	12.9	20.1	10.9	10.9	10.0	10.5	10.7	11.1	12.1	0.338	0
10	14	21	21.6	21.4	21.3	21.7	21.7	14.3	13.1	14.2	14.6	8.8	11.9	19.8	9.9	9.9	9.1	9.6	9.7	10.1	11.1	0.392	
10	14	22	21.5	21.3	21.3	21.7	21.7	13.6	12.0	13.0	13.3	7.7	11.0	19.6	9.0	9.1	8.1	8.6	8.7	9.2	10.2	0.447	0
10	14	23	21.5	21.2	21.3	21.6	21.7	13.1	11.1	12.1	12.3	7.3	10.5	19.5	8.4	8.6	7.5	8.0	8.2	8.6	9.5	0.489	0
10	14	24	21.5	21.2	21.2	21.6	21.7	12.6	10.4	11.3	11.4	6.7	10.0	19.4	7.9	8.2	7.1	7.6	7.7	8.1	9.0	0.514	0
10	15	1	21.4	21.2	21.2	21.5	21.7	12.3	9.9	10.7	10.7	6.6	9.8	19.3	7.7	7.6	6.8	7.3	7.5	7.9	8.7	0.534	0
10	15	2	21.4	21.1	21.2	21.5	21.7	12.0	9.5	10.1	10.1	6.1	9.5	19.2	7.4	7.4	6.6	7.2	7.3	7.7	8.5	0.576	
10	15	3	21.4	21.1	21.1	21.5	21.7	11.9	9.3	9.7	9.7	6.4	9.5	19.2	7.6	7.7	6.9	7.3	7.3	7.7	8.4	0.572	
10	15	4	21.4	21.1	21.1	21.4	21.7	11.6	9.1	9.4	9.4	6.2	9.4	19.2	7.3	7.4	6.6	7.1	7.2	7.6	8.2	0.584	0
10	15	5	21.3	21.1	21.1	21.4	21.7	11.4	8.9	9.2	9.0	6.3	9.3	19.2	7.2	7.4	6.6	7.0	7.0	7.4	7.9	0.609	0
10	15	6	21.3	21.1	21.1	21.4	21.7	11.3	8.7	9.0	8.8	6.1	9.3	19.2	7.2	7.2	6.5	7.0	7.2	7.6	7.9	0.601	0
10	15	7	21.3	21.1	21.1	21.4	21.7	11.1	8.6	8.9	8.6	6.2	9.3	19.2	7.2	7.4	6.5	7.0	7.1	7.5	7.8	0.631	1
10	15	8	21.3	21.1	21.1	21.5	21.7	11.5	9.1	9.5	8.9	7.2	10.0	19.5	7.9	7.6	7.1	7.7	7.9	8.5	8.9	0.506	89
10	15	9	21.5	21.5	21.5	22.1	21.8	13.6	12.1	12.6	11.4	12.8	13.6	21.0	11.4	10.0	10.3	11.0	11.5	12.6	13.1	-0.056	311
10	15	10	21.7	22.3	22.2	23.0	21.9	16.9	16.9	17.8	15.1	18.9	19.2	23.5	15.6	13.1	14.2	15.0	15.6	17.3	18.0	-1.064	549
10	15	11	22.2	23.2	22.8	24.0	22.0	20.7	22.0	23.0	18.7	24.5	25.1	26.8	18.9	16.8	17.4	18.1	18.8	20.7	21.7	-2.208	701
10	15	12	22.6	23.8	23.2	24.2	22.1	24.1	25.5	24.8	21.2	28.4	27.8	28.1	21.1	19.9	19.4	20.2	21.0	22.5	23.7	-3.162	748
10	15	13	22.3	23.8	23.3	23.9	22.2	24.2	26.6	24.7	22.7	26.8	27.4	27.6	20.6	20.2	19.0	19.9	20.6	21.4	22.5	-2.725	511
10	15	14	22.2	23.3	23.1	23.4	22.1	24.2	25.7	24.0	24.3	25.0	25.6	25.9	21.5	22.0	20.0	21.0	21.5	22.0	22.9	-2.067	525
10	15	15	22.1	23.1	23.1	23.2	22.0	23.8	25.8	24.3	26.3	24.9	26.1	25.9	20.1	20.5	18.5	19.5	19.8	20.4	21.8	-1.599	377
10	15	16	21.9	22.6	22.5	22.7	21.8	20.4	23.8	22.8	24.5	20.6	21.7	23.2	18.0	18.2	16.8	17.5	17.8	18.2	19.3	-0.742	159
10	15	17	21.8	22.1	21.9	22.3	21.7	18.0	21.0	20.6	21.6	16.7	18.4	21.7	15.6	15.9	14.6	15.2	15.4	15.8	16.6	-0.117	27
10	15	18	21.7	21.7	21.6	22.0	21.7	16.7	18.4	18.7	19.3	14.4	16.3	20.8	14.3	14.4	13.4	14.0	14.2	14.6	15.3	0.139	1
10	15	19	21.6	21.5	21.5	21.9	21.7	16.1	16.7	17.4	17.8	13.3	15.3	20.5	13.5	13.7	12.7	13.2	13.3	13.7	14.3	0.275	0

1	2	3	4	5	6	7	8	9	10	11	12	13	14	15	16	17	18	19	20	21	22	23	24
10	15	20	21.6	21.5	21.4	21.8	21.7	15.5	15.5	16.4	16.7	12.2	14.5	20.3	12.7	12.8	11.9	12.4	12.5	12.9	13.5	0.328	0
10	15	21	21.5	21.4	21.4	21.8	21.7	15.0	14.5	15.4	15.7	11.5	13.8	20.2	12.0	12.1	11.3	11.8	11.9	12.3	12.9	0.372	0
10	15	22	21.5	21.3	21.3	21.7	21.7	14.7	13.9	14.7	14.9	11.4	13.5	20.1	11.9	12.2	11.2	11.7	11.8	12.1	12.6	0.400	0
10	15	23	21.5	21.3	21.3	21.7	21.7	14.5	13.5	14.2	14.4	11.4	13.5	20.0	11.9	12.1	11.2	11.7	11.8	12.1	12.6	0.413	0
10	15	24	21.4	21.3	21.3	21.7	21.7	14.3	13.3	13.9	14.0	11.5	13.4	20.0	11.8	12.1	11.1	11.6	11.7	12.0	12.5	0.415	0

Experimental results from Test Case DSF200_e- mass flow rates

1	2	3	25	26	27	28	29	30	31
			Mass flow in DSF, kg/h						
Month	Date	Hour	from velocity profiles						from CO2
			h=0.95m	h=1.91m	h=2.5m	h=4.36m	h=4.7m	h=5.15m	
10	1	1							
10	1	2							
10	1	3							
10	1	4							
10	1	5							
10	1	6							
10	1	7							
10	1	8							
10	1	9	1078	725	633				452
10	1	10	1061	794	695				472
10	1	11	1425	1209	1266				652
10	1	12	1558	1274	1524				1067
10	1	13	1589	1254	1516				970
10	1	14	1591	1238	1450				847
10	1	15	1442	1147	1273				957
10	1	16	1280	1086	1187				1051
10	1	17	1029	707	684				953
10	1	18	949	728	516				1551
10	1	19	1058	949	804				
10	1	20	1170	1038	922				
10	1	21	1001	916	791				
10	1	22			659				
10	1	23			577				
10	1	24			478				
10	2	1			380				
10	2	2			407				
10	2	3			344				
10	2	4			493				

1	2	3	25	26	27	28	29	30	31
10	2	5			595				
10	2	6			687				
10	2	7			692				
10	2	8			667				
10	2	9							
10	2	10	1472	1149			2066	2900	
10	2	11	1669	1248			2168	3176	
10	2	12	1567	1205			1981	2629	
10	2	13	1442	1111			1872	2619	
10	2	14	1642	1260			1892	2329	1701
10	2	15	1751	1244			1904	2324	1457
10	2	16	1469	940			1436	1719	951
10	2	17	1329	834			1283	1426	697
10	2	18	871	486			1078	1381	1961
10	2	19	708	568			808	961	1257
10	2	20	665	615			719	827	818
10	2	21	888	684			863	1214	1885
10	2	22					800	967	1096
10	2	23					665	715	420
10	2	24					619	583	474
10	3	1					703	663	725
10	3	2					738	786	1191
10	3	3					581	951	668
10	3	4					632	1026	971
10	3	5					595	845	598
10	3	6					746	1098	901
10	3	7					704	1189	786
10	3	8							751
10	3	9	1237	790	660				565
10	3	10	1145	703	645				860
10	3	11	1000	600	659				743
10	3	12	1509	1101	1122				1122
10	3	13	1540	1135	1159				824

1	2	3	25	26	27	28	29	30	31
10	3	14	1366	1065	1124				691
10	3	15	1165	804	829				834
10	3	16	1269	964	1020				702
10	3	17	1053	777	925				538
10	3	18	804	511	542				447
10	3	19			377				363
10	3	20			346				321
10	3	21			431				296
10	3	22			447				993
10	3	23			378				382
10	3	24			364				819
10	4	1			340				433
10	4	2			372				382
10	4	3			390				351
10	4	4			506				326
10	4	5			428				291
10	4	6			358				312
10	4	7			342				339
10	4	8			442				352
10	4	9							704
10	4	10	1745	1336	1098	1145	1364	1341	1283
10	4	11	1813	1289	1080	1110	1338	1309	1061
10	4	12	1772	1275	1107	1095	1360	1365	1165
10	4	13	2081	1471	1225	1167	1414	1522	1053
10	4	14	1730	1196	969	962	1219	1333	858
10	4	15	1674	1131	985	914	1158	1306	862
10	4	16	2029	1450	1218	1107	1418	1688	818
10	4	17	2019	1501	1274	1210	1710	2143	845
10	4	18	1831	1229	1069	1034	1320	1454	833
10	4	19	1462	881	715	740	1004	980	724
10	4	20	951	492	478	481	630	576	582
10	4	21	739	344	368	424	557	543	371
10	4	22	512	597	368	445	604	775	436

1	2	3	25	26	27	28	29	30	31
10	4	23			368	416	631	875	635
10	4	24					633	897	531
10	5	1					663	907	562
10	5	2					865	1289	1144
10	5	3					716	1331	709
10	5	4					704	1097	594
10	5	5					732	1051	643
10	5	6					834	1345	1625
10	5	7					876	1447	1406
10	5	8					857	1374	655
10	5	9	1663	1061			898	1217	667
10	5	10	1742	1161			1204	1630	794
10	5	11	2137	1617			1445	1702	1139
10	5	12	3153	2264			2381	2498	1391
10	5	13	2803	1903			2014	2106	1318
10	5	14	2218	1394			1708	2321	1129
10	5	15	2573	1768			1988	2313	922
10	5	16	2360	1637			1743	2014	831
10	5	17	1815	1216			1365	1646	849
10	5	18	1276	727			1108	1276	803
10	5	19	530	785			936	1041	556
10	5	20	593	634			717	822	999
10	5	21	792	993			1096	1517	3528
10	5	22					1469	2364	4740
10	5	23					1490	2350	4900
10	5	24					1333	2165	5593
10	6	1					1711	2860	6166
10	6	2					1152	1665	3119
10	6	3					1403	2112	4915
10	6	4					2430	3530	
10	6	5					2777	3880	
10	6	6					2559	3593	
10	6	7					2246	3428	

1	2	3	25	26	27	28	29	30	31
10	6	8					1643	2653	
10	6	9	907	559	548	780	1165	1788	
10	6	10	1086	694	691	844	1327	2140	
10	6	11	1551	972	838	977	1501	2526	3452
10	6	12	1954	1281			1623	2463	1783
10	6	13	2266	1350			1575	2469	1514
10	6	14	1804	1113			1477	2257	3248
10	6	15	2421	1505			2121	3280	2294
10	6	16	2191	1356			1820	2754	4308
10	6	17	1734	1014			1436	2343	
10	6	18	1157	751			1172	1679	
10	6	19	804	528			1028	1358	
10	6	20	837	559			1094	1490	
10	6	21	869	511			1193	1641	
10	6	22					1556	2218	
10	6	23					1805	2580	
10	6	24					1927	2876	
10	7	1					2343	3543	
10	7	2					2623	3984	
10	7	3					2984	4505	
10	7	4					2430	4005	
10	7	5					1932	3278	
10	7	6					2042	3355	
10	7	7					2025	3346	
10	7	8							
10	7	9	1386	931	976	1111	2076	3390	
10	7	10	1520	1052	1107	1275	2059	3275	
10	7	11	1988	1357	1368	1670	2317	3541	4453
10	7	12	2516	1560	1478	1863	2409	3664	2137
10	7	13	2611	1671	1510	1945	2337	3303	1834
10	7	14	2605	1619	1378	1646	2032	2940	4218
10	7	15	3583	2319	2064	2201	2792	3716	3737
10	7	16	3641	2395	2084	1869	2332	2785	2735

1	2	3	25	26	27	28	29	30	31
10	7	17	3831	2491	2294	2037	2575	3113	3904
10	7	18	3965	2550	2302	2020	2574	3243	3874
10	7	19	4308	2725	2518	2353	3056	3753	4884
10	7	20	4496	2878	2782	2604	3284	4053	5358
10	7	21	4699	3046	2881	2769	3614	4425	4621
10	7	22			3037	2787	3538	4313	4755
10	7	23			2956	2704	3488	4234	4147
10	7	24			2565	2359	3015	3696	4435
10	8	1			2313	2137	2806	3444	4843
10	8	2			1781	2053	2696	3469	5148
10	8	3			1359				4339
10	8	4			738				4708
10	8	5			1673				4160
10	8	6			2095				3826
10	8	7			2221				3866
10	8	8			2089				2447
10	8	9			1647				2627
10	8	10	3435	2210	1961	1774	2276	2759	2445
10	8	11	3096	2031	2021	1710	2059	2379	3011
10	8	12	4029	2644	2558	2455	2936	3329	3127
10	8	13	4377	2934	2737	2618	3176	3568	2373
10	8	14	4152	2808	2403	2371	2876	3261	1909
10	8	15	3954	2658	2623	2369	2759	3096	2346
10	8	16	4136	2838	2062	2255	2958	3322	2440
10	8	17	3709	2421	1407	1773	2517	2950	2526
10	8	18	3041	1971	1101	1339	1959	2296	1712
10	8	19	2115	1298	1223	1011	1358	1532	2524
10	8	20	2128	1316	813	923	1362	1536	2523
10	8	21	2302	1429	567	977	1521	1773	2959
10	8	22	1642	1067	399	748	1200	1309	1737
10	8	23			351	599	901	1047	1248
10	8	24			272	452	739	898	593
10	9	1			276	366	636	633	419

1	2	3	25	26	27	28	29	30	31
10	9	2			348	367	557	584	1177
10	9	3			371	366	586	786	749
10	9	4			462	393	608	688	556
10	9	5			447	276	599	612	488
10	9	6					661	684	
10	9	7					925	1403	5199
10	9	8					880	1148	1798
10	9	9					925	1036	2301
10	9	10	1133	768			1325	1674	1285
10	9	11	1306	926			1622	1967	1148
10	9	12	1568	1107			1879	2107	1370
10	9	13	1814	1309			2172	2340	3251
10	9	14	1803	1364			2559	2929	3398
10	9	15	1631	1244			2445	2915	4846
10	9	16	1435	1042			2112	2660	1648
10	9	17	1071	727			1550	1888	2530
10	9	18	986	662			1274	1460	1021
10	9	19	891	550			1248	1457	1227
10	9	20	564	491			884	900	1029
10	9	21	514	778			812	996	990
10	9	22	526	491			731	824	1440
10	9	23					902	1055	938
10	9	24					736	816	1724
10	10	1					747	1058	1077
10	10	2					724	993	1779
10	10	3					721	1170	1192
10	10	4					812	1624	964
10	10	5					760	1272	1318
10	10	6					731	783	1624
10	10	7					866	858	992
10	10	8					835	845	741
10	10	9							4345
10	10	10					698	613	

1	2	3	25	26	27	28	29	30	31
10	10	11					671	637	1286
10	10	12					1853	1873	1234
10	10	13					1854	1908	1227
10	10	14					2054	2114	1195
10	10	15					2044	2277	1125
10	10	16					2127	2732	1084
10	10	17					2435	2526	867
10	10	18					2174	2170	554
10	10	19					1167	1140	439
10	10	20					693	646	380
10	10	21					550	485	376
10	10	22					576	491	322
10	10	23					556	454	310
10	10	24					596	509	250
10	11	1					573	412	324
10	11	2					639	504	302
10	11	3					717	529	292
10	11	4					682	486	400
10	11	5					770	639	229
10	11	6					674	483	239
10	11	7					655	374	338
10	11	8					649	401	389
10	11	9					722	514	679
10	11	10					811	684	1022
10	11	11					1354	1131	1073
10	11	12					1471	1935	1143
10	11	13					1259	1937	1191
10	11	14					1234	1849	1083
10	11	15					1061	1708	1064
10	11	16					1035	1411	948
10	11	17					937	1104	782
10	11	18					920	1096	625
10	11	19					803	958	823

1	2	3	25	26	27	28	29	30	31
10	11	20					766	760	624
10	11	21					766	719	1054
10	11	22					754	762	1293
10	11	23					1108	1299	1589
10	11	24					1180	1452	2107
10	12	1					1367	2694	1830
10	12	2					1497	2895	2109
10	12	3					1465	2742	1828
10	12	4					1566	2977	1516
10	12	5					1371	2282	1520
10	12	6					1409	2300	1311
10	12	7					1547	2322	1337
10	12	8							1396
10	12	9					1245	1960	1302
10	12	10					1307	2170	1429
10	12	11	1634	1017			1148	1873	1522
10	12	12	1849	1166			1379	2446	1289
10	12	13	1899	1219			1343	2482	1094
10	12	14	1545	1024			1167	1920	1129
10	12	15	1585	1054			1130	1531	1069
10	12	16	1610	1013			1120	1353	980
10	12	17	1370	846			981	1183	1002
10	12	18	1276	788			946	1017	1165
10	12	19	1146	668			908	908	913
10	12	20	1349	736			995	1072	860
10	12	21	852	640			788	868	720
10	12	22	558	802			765	730	473
10	12	23					738	652	846
10	12	24					755	665	635
10	13	1					745	676	493
10	13	2					705	613	508
10	13	3					718	624	349
10	13	4					724	600	463